(p)ppGpp AND ITS HOMOLOGS: ENZYMATIC AND MECHANISTIC DIVERSITY AMONG THE MICROBES

EDITED BY: Katarzyna Potrykus, Michael Cashel and Gert Bange
PUBLISHED IN: Frontiers in Microbiology

frontiers Research Topics

frontiers

ISSN 1664-8714
ISBN 978-2-88966-953-0
DOI 10.3389/978-2-88966-953-0

About Frontiers

Frontiers is more than just an open-access publisher of scholarly articles: it is a pioneering approach to the world of academia, radically improving the way scholarly research is managed. The grand vision of Frontiers is a world where all people have an equal opportunity to seek, share and generate knowledge. Frontiers provides immediate and permanent online open access to all its publications, but this alone is not enough to realize our grand goals.

Frontiers Journal Series

The Frontiers Journal Series is a multi-tier and interdisciplinary set of open-access, online journals, promising a paradigm shift from the current review, selection and dissemination processes in academic publishing. All Frontiers journals are driven by researchers for researchers; therefore, they constitute a service to the scholarly community. At the same time, the Frontiers Journal Series operates on a revolutionary invention, the tiered publishing system, initially addressing specific communities of scholars, and gradually climbing up to broader public understanding, thus serving the interests of the lay society, too.

Dedication to Quality

Each Frontiers article is a landmark of the highest quality, thanks to genuinely collaborative interactions between authors and review editors, who include some of the world's best academicians. Research must be certified by peers before entering a stream of knowledge that may eventually reach the public - and shape society; therefore, Frontiers only applies the most rigorous and unbiased reviews.
Frontiers revolutionizes research publishing by freely delivering the most outstanding research, evaluated with no bias from both the academic and social point of view. By applying the most advanced information technologies, Frontiers is catapulting scholarly publishing into a new generation.

What are Frontiers Research Topics?

Frontiers Research Topics are very popular trademarks of the Frontiers Journals Series: they are collections of at least ten articles, all centered on a particular subject. With their unique mix of varied contributions from Original Research to Review Articles, Frontiers Research Topics unify the most influential researchers, the latest key findings and historical advances in a hot research area! Find out more on how to host your own Frontiers Research Topic or contribute to one as an author by contacting the Frontiers Editorial Office: frontiersin.org/about/contact

(p)ppGpp AND ITS HOMOLOGS: ENZYMATIC AND MECHANISTIC DIVERSITY AMONG THE MICROBES

Topic Editors:
Katarzyna Potrykus, University of Gdansk, Poland
Michael Cashel, Eunice Kennedy Shriver National Institute of Child Health and Human Development (NICHD), United States
Gert Bange, University of Marburg, Germany

Citation: Potrykus, K., Cashel, M., Bange, G., eds. (2021). (p)ppGpp and Its Homologs: Enzymatic and Mechanistic Diversity Among the Microbes. Lausanne: Frontiers Media SA. doi: 10.3389/978-2-88966-953-0

Table of Contents

frontiers in Microbiology

EDITORIAL
published: 25 March 2021
doi: 10.3389/fmicb.2021.658282

Editorial: (p)ppGpp and Its Homologs: Enzymatic and Mechanistic Diversity Among the Microbes

Katarzyna Potrykus[1]*, *Michael Cashel*[2]* and *Gert Bange*[3]*

[1] Department of Bacterial Molecular Genetics, Faculty of Biology, University of Gdańsk, Gdańsk, Poland, [2] Intramural Program, Eunice Kennedy Shriver Institute of Child Health and Human Development, National Institutes of Health, Bethesda, MD, United States, [3] Department of Chemistry, Center for Synthetic Microbiology (SYNMIKRO), Philipps-University Marburg, Marburg, Germany

Keywords: (p)ppGpp, stringent response, (p)ppApp, (p)ppGpp synthesis and degradation, enzymatic regulation, RSH, SAH, SAS

Editorial on the Research Topic

(p)ppGpp and Its Homologs: Enzymatic and Mechanistic Diversity Among the Microbes

OPEN ACCESS

Edited by:
Kenneth C. Keiler,
Pennsylvania State University (PSU), United States

Reviewed by:
Vasili Hauryliuk,
Umeå University, Sweden

***Correspondence:**
Katarzyna Potrykus
katarzyna.potrykus@ug.edu.pl
Michael Cashel
cashelm@mail.nih.gov
Gert Bange
gert.bange@synmikro.uni-marburg.de

Specialty section:
This article was submitted to Microbial Physiology and Metabolism, a section of the journal Frontiers in Microbiology

Received: *25 January 2021*
Accepted: *22 February 2021*
Published: *25 March 2021*

Citation:
Potrykus K, Cashel M and Bange G (2021) Editorial: (p)ppGpp and Its Homologs: Enzymatic and Mechanistic Diversity Among the Microbes. Front. Microbiol. 12:658282. doi: 10.3389/fmicb.2021.658282

DR. MICHAEL CASHEL – THE ROLE OF LUCK IN THE DISCOVERY OF (p)ppGpp

The background leading to the discovery of (p)ppGpp in *E. coli* began long ago when one of the goals in microbiology was to understand the biosynthetic pathways for DNA, RNA, and protein accumulation. Amino acid (AA) auxotrophs starved for one or more amino acid stopped growth and accumulation of all macromolecules, and this was referred to as the stringent response. A puzzle arose because mutants at a single locus (*relA*) in many strains continued to accumulate rRNA and tRNA for some time after growth had stopped due to AA starvation. The name for "RelA" is because the otherwise strong stringent RNA control in response to starvation was greatly relaxed in the mutant (Stent and Brenner, 1961). In addition, comparing *valS*^{ts} *relA* vs. *valS*^{ts} *relA*$^{+}$ double mutants at restrictive temperatures suggested that limited charging of a single tRNA (valyl tRNA) can trigger the stringent response, despite the presence of an otherwise full array of charged tRNA (Neidhardt, 1966). Another puzzle was that adding chloramphenicol to non-growing AA starved cells could restore (relax) the rates of RNA accumulation (Kurland and Maaløe, 1962).

At about that time, Dr. Jon Gallant found that plasmolysis of cells in hypertonic 2M sucrose permeabilized them to actinomycin, which blocked incorporation of labeled NTP substrates by RNA polymerase (RNAP). Dr. Cashel's task for graduate training in the Gallant lab in Seattle was to ask if RNAP activity in plasmolyzed cells reflected the stringent/relaxed RNA control observed *in vivo*. The assay was to compare the RNA control response when labeling RNA with ^{3}H-UTP vs. ^{3}H-UMP and remaining cold ATP, GTP, and CTP rNTP substrates. The results suggested that all phosphotransfer might play an indirect role in the operation of the stringent response by inhibiting RNA polymerase through limiting the formation of UTP from UMP (Gallant and Cashel, 1967). Since uracil permeability was later shown to be severely inhibited by ppGpp, RNA synthesis estimates needed correction for uptake inhibition as well (Winslow and Lazzarini, 1969).

To verify the blocked phosphotransfer hypothesis, researchers asked whether phosphorylation of all ribonucleotides was similarly affected. This was probed in uniformly ^{32}P labeled cells analyzed by two-dimensional PEI-cellulose thin layer chromatography (TLC) to visualize most nucleotides. This first step was development with Na-formate (pH 3.4), followed by a methanol

wash, then developed in LiCl. Standard cell extraction was with strong acids. However, since formate was the first step, a shortcut for extraction was devised using Na-formate (pH 3.4) which allowed cell-free extracts to be spotted directly on chromatograms (Cashel and Gallant, 1969). This turned out to be an extremely lucky choice because (p)ppGpp was later found to be labile in strong acids, much more so than riboNTPs (Cashel and Kalbacher, 1971). The resulting TLC autoradiograms of ^{32}Pi labeled, AA starved *relA*+ but not *rel*A- strains revealed different labeling patterns. One spot seemed to appear almost by magic, it increased in starved *relA*$^{+}$ cells but disappeared for the starved *relA* mutant (Cashel and Gallant, 1969). Thus, it was called the "magic spot." Later at NIH, Dr. Cashel devised a TLC method that in one dimension resolved this spot into two (MS I and MS II) and separated them from the GTP and GDP pool (Cashel et al., 1969). The two spots were later identified as ppGpp (MS I) and pppGpp (MS II). The initial work at NIH on (p)ppGpp benefited from advice from Drs. Bob Lazzarini and Maxine Singer.

This devised method was used for many years to study the kinetics of induction, reversal, and AA starvation specificity of the stringent response (Cashel and Gallant, 1969, Cashel and Kalbacher, 1971, Cashel et al., 1969). However, 50 years later this method was found to be inadequate because pppApp co-migrates with ppGpp, and ppApp comigrates with GDP (Sobala et al., 2019). The amounts of (p)ppApp in (p)ppGpp samples estimated by the old method now needed close scrutiny. One example described in this Research Topic comes from Dr. Jue D Wang's lab showing, by mass spectrometry, that products of the *B. subtilis* small alarmone synthetase SasA (synonyms: RelP, SAS2, YwaC) include pGpp, ppApp, and AppppA (Fung et al.).

Studies of (p)ppGpp by many researchers over the past half century in the microbial and plant kingdoms have revealed an astonishing regulatory diversity that was viewed in the beginning with healthy skepticism that dominated the early claims of global effects. This Research Topic hosted in Frontiers in Microbiology provides a glimpse of the enormous diversity of alarmones' actions emerging for (p)ppGpp, and possibly for (p)ppApp, and unquestionably for monocyclic, homocyclic, and heterocyclic nucleotides, barely mentioned here.

ENZYMATIC AND MECHANISTIC DIVERSITY AMONG THE MICROBES–MANUSCRIPTS ACCEPTED FOR THIS RESEARCH TOPIC

Over the years, protein structures supported by biochemical studies have led to identifying specific contact points between a variety of cellular proteins and/or ribosomes needed for synthesis and or degradation of an increasingly diverse array of (p)ppGpp and other potential regulatory nucleotides. While introduction of specific mutations/deletions has been exploited to discover a trove of biochemical effects, the conflicts among different studies are of special interest. In this Research Topic Takada et al. define specific mutants and deletions of the *Escherichia coli* RelA and *B. subtilis Rel* RRM domains. The authors conclude that deletion of the RRM domain, which yields uncontrollable (p)ppGpp production is not related to the loss of the enzyme's auto-inhibition, but instead is caused by misregulation of RelA/Rel by the ribosome. On the other hand, the Kaspy and Glaser manuscript is a follow up of their earlier work (Gropp et al., 2001) that seems to validate their conclusion that oxidation of the zinc-finger domain (localized next to RRM) induces inactive oligomers that are argued to regulate cellular RelA activity (Kaspy and Glaser). Each work has strong evidence that supports each authors' interpretations.

Since the initial discovery of RelA as a key enzyme of (p)ppGpp synthesis, a striking diversity of enzymes capable of synthesizing and degrading the alarmones has been unraveled. This is best illustrated by the class of small alarmone synthetases (SAS), which consist of only the (p)ppGpp synthetase domain. SAS enzymes are found in many bacteria including many relevant pathogens, such as *Staphylococcus aureus* (Steinchen and Bange, 2016).

In this Research Topic, Wolz et al. describe their latest findings on the functional roles of the SAS enzymes, RelP and RelQ, on the biofilm formation and maintenance under conditions of cell wall stress in *S. aureus* (Salzer et al.). Besides the canonical SAS enzymes, in some bacterial species such as *Mycobacterium smegmatis*, the dual domain SAS enzyme RelZ is found. In this "third" small alarmone synthetase, the (p)ppGpp synthetase domain is N-terminally extended by an RNAseHII domain. In their review, Krishnan and Chatterji discuss the functional roles of this class of SAS enzymes and conclude ways to translate the learned knowledge into ways combating persistent infections (Krishnan and Chatterji).

On the other hand, Wang et al. provide compelling evidence that the SAS enzyme RelP (also known as SasA or SAS1) is also able to produce the ppApp nucleotides, in addition to its original role as (p)ppGpp producer. Thus, it will be amazing to learn to which extent these enzymes are involved in the regulation of alarmones outside of (p)ppGpp, such as (p)ppApp and AppppA, which also appears to be affected by RelP (Fung et al.).

An example of diversity among enzymes hydrolyzing 3′-pyrophosphorylated nucleotides is presented by Potrykus et al.. The authors have developed a rapid real-time enzymatic assay which allows determining a given enzyme's ability to hydrolyze (p)ppGpp and (p)ppApp. Enzymes capable of hydrolyzing only (p)ppGpp (*Streptococcus equisimilis* RelSeq), only (p)ppApp (*Methylobacterium extorquens* SAH), and both (*Drosophila melanogaster* MESH1) were investigated. Although very intriguing, the functional consequences of such diversity are as of yet unknown.

Another study in this Research Topic on (p)ppGpp hydrolases is reported by Sanyal et al., who investigate (p)ppGpp degradation *in vivo* in the absence of SpoT and two Nudix enzymes—NudG and MutT—were found to participate in this process. Such an approach was possible through the use of *relA* hypomorphic mutants, as normally, deletion of *spoT* in the presence of intact *relA* is lethal. The conclusions are rather intricate and future *in vitro* studies with purified enzymes seem highly warranted to further support them.

Besides the diversity of enzymes involved in synthesis and degradation of (p)ppGpp, our knowledge on the molecular targets affected by the alarmones is steadily increasing. Thus far, over 30 different protein targets have been reported to be binding partners of (p)ppGpp. Thus, Kushwaha et al. set out to further detail how these chemically simple molecules achieve this binding diversity (Kushwaha et al.). Using molecular dynamics simulation studies, they show that phosphate chains provide molecular plasticity to (p)ppGpp nucleotides, enabling its binding diversity, while its guanosine-moiety might provide further specificity for certain target families, such as GTPases.

In addition, Steinchen et al. summarize all reported (p)ppGpp-binding targets (Steinchen et al.). When sorting and ranking them according to their known binding strengths, ppGpp and/or pppGpp show not only the enormous diversity of cellular processes affected, but much more suggests a "priority scheme" of targets modulated by the alarmones. Thus, (p)ppGpp appears to continuously modulate most of the microbial biochemistry rather than being part of an all-or-nothing switch between the "relaxed" and "stringent" states, as initially assumed in the beginning of their discovery.

A similar view is reflected in three articles addressing the importance of (p)ppGpp basal levels in cell physiology and adaptation. Spira and Ospino point out that there is great variability in (p)ppGpp basal levels in various *E. coli* laboratory strains and discuss the consequences this basal level might bring for the cell, such as its effect on bacterial pathogenicity, antimicrobial resistance, overall growth rate, and nutritional competence. Based on the evaluated data, the authors make an interesting conclusion that the *relA* and *spoT* genes are continuously undergoing a microevolutionary pressure so that the cells are producing (p)ppGpp basal levels that are optimal for a given population.

On the other hand, Imholz et al., noticed the problem of using different laboratory strains and techniques to evaluate the relationship between basal (p)ppGpp levels, growth rate control, and RNA synthesis in *E. coli*. In their perspective article, the authors re-evaluate some of the literature data and compare it with the results obtained by them with an LC-MS method. Although there was some variation, the inverse correlation between (p)ppGpp concentration and growth rate was preserved when growth was varied by nutritional conditions. The authors also performed experiments with strains where RNA polymerase (RNAP) (p)ppGpp binding sites were disrupted and found that disrupting one or the other site does not abolish this correlation. This may not be surprising since Myers et al. show by using Differential Radial Capillary Action of Ligand Assay (DRaCALA) assays that ppGpp has similar affinity to both of its binding sites on RNAP. Interestingly, upon binding of the first ppGpp molecule, binding of the second ppGpp molecule seems to be greatly enhanced, regardless of which site was occupied first. It is therefore intriguing whether the same would be true for pppGpp, as it was shown that in many instances ppGpp is a stronger effector than pppGpp (Mechold et al., 2013). Still, experiments with a double site mutant should be performed to provide a definitive answer to the interesting notion raised by Imholz et al. that the (p)ppGpp—RNA level inverse relationship might be controlled by some other factors than the binding of (p)ppGpp to RNAP.

The review by Fernandez-Coll and Cashel also deals with the importance of (p)ppGpp basal levels in the cell. The authors make a very important point of differentiating between (p)ppGpp acting as a second messenger (i.e., under "normal" growth, meaning a change in basal levels of (p)ppGpp), and as an alarmone (i.e., under stress conditions, when (p)ppGpp levels abruptly increase). Many researchers do not make this distinction and use those terms interchangeably while, in fact, they involve different cellular strategies for adaptation or survival. In addition, the authors point out that when considering (p)ppGpp metabolism as a potential antibiotic target, the focus should not be solely on its synthesis; perhaps its hydrolysis should be considered instead.

In light of the studies striving to develop novel antibiotics based on the notion that (p)ppGpp is known to be responsible for bacterial pathogenicity, it must be noted that recently Nowicki et al. (2019) have demonstrated that several isothiocyanates (ITC) cause *E. coli* growth inhibition by induction of the stringent response. This discovery is especially important for STEC strains (encoding Shiga toxins), since unlike antibiotics, ITCs do not induce Shiga toxin production. Here, the authors offer a follow-up on their previous findings and demonstrate that similar effects are observed when employing aliphatic ITCs, and what is even more important, some of these compounds act in a synergistic fashion (Nowicki et al.). Whether this means that their mechanism of action is different or not remains to be investigated.

In addition, this Research Topic offers three review articles focused on the role of (p)ppGpp in pathogenicity and adaptation to changing environmental conditions by bacteria other than *E. coli*. The article by Zhang et al., provides a comprehensive evaluation of (p)ppGpp's role in streptococci. In particular, (p)ppGpp synthesis, effects on physiology (including persistence and pathogenicity), transcriptional regulation, and a link between (p)ppGpp and CodY are discussed. On the other hand, the review by Das and Bharda, centers on description of (p)ppGpp metabolism in several different bacteria, with analysis of (p)ppGpp's role in production of antibiotics and in antibiotic resistance (several different mechanisms are described). Finally, Kundra et al. provide a very comprehensive and detailed review of (p)ppGpp's role in virulence of several Gram(+) and Gram(–) bacteria, as well as in *Mycobacteria* and *Borrelia burgdorferi*. The authors also provide a timely and thorough evaluation of targeting (p)ppGpp signaling by potential therapeutic agents (examples of compounds affecting its synthesis and hydrolysis are provided), as well as highlight the necessity of exploring the nature of crosstalk between (p)ppGpp and c-di-AMP.

Finally, the manuscript by Bartoli et al., is an example illustrating diversity among closely related enteric bacteria in regulation by the same transcriptional factors, in this case—SlyA. This factor was initially reported to be regulated by (p)ppGpp in *Salmonella enterica*, and thus the authors set out to use SlyA-regulated genes as reporters of ppGpp levels in *E. coli*. Although that attempt has failed and the authors disprove direct regulation of SlyA by (p)ppGpp, they make an important

point that although SlyA may act through the same molecular mechanism in both bacteria, its physiological role in those bacteria is quite different.

AUTHOR CONTRIBUTIONS

KP, MC, and GB edited the Frontiers Research Topic on *(p)ppGpp and Its Homologs: Enzymatic and Mechanistic Diversity Among the Microbes* and wrote the editorial. All authors contributed to the article and approved the submitted version.

ACKNOWLEDGMENTS

GB thanks the priority program SPP1879 Nucleotide second messenger signaling in bacteria of the Deutsche Forschungsgemeinschaft (DFG) for support. MC would like to acknowledge Dr. Jon Gallant who made essential contributions to understanding (p)ppGpp, as well as the support of the Intramural Research Program of the NIH. KP acknowledges support from the Department of Bacterial Molecular Genetics, University of Gdańsk.

REFERENCES

Cashel, M., and Gallant, J. (1969). Two compounds implicated in the function of the RC gene of Escherichia coli Nature. doi: 10.1038/221838a0

Cashel, M., and Kalbacher, B. (1971). The Control of Ribonucleic Acid Synthesis in *E. coli* V. Characterization of a nucleotide associated with the Stringent Response. J. Biol. Chem. 245: 2309-2318. doi: 10.1016/S0021-9258(18)63153-9

Cashel, M., Lazzarini, R. A., and Kalbacher, B. (1969). An Improved Method for Thin-Layer Chromatography of Nucleotide Mixtures Containing ^{32}P-Labelled Orthophosphate. doi: 10.1016/S0021-9673(01)96624-5

Gallant, J., and Cashel, M. (1967). On the mechanism of amino acid control of ribonucleic acid biosynthesis. J Mol Biol. 25:545-53. doi: 10.1016/0022-2836(67)90205-7

Gropp, M., Strausz, Y., Gross, M., and Glaser, G. (2001). Regulation of Escherichia coli RelA requires oligomerization of the C-terminal domain. J Bacteriol. Jan;183(2):570-9. doi: 10.1128/JB.183.2.570-579.2001

Kurland, C. G., and Maaløe, O. (1962). Regulation of Ribosomal and Transfer RNA Synthesis J Mol Biol 4:193-210. doi: 10.1016/S0022-2836(62)80051-5

Mechold, U., Potrykus, K., Murphy, H., Murakami, K. S., and Cashel, M. (2013). Differential regulation by ppGpp versus pppGpp in Escherichia coli. Nucleic Acids Res. Jul;41(12):6175-89. doi: 10.1093/nar/gkt302

Neidhardt, F. C. (1966). Roles of amino acid activating enzymes in cellular physiology Bact. Rev. 30:701-719. doi: 10.1128/BR.30.4.701-719.1966

Nowicki, D., Maciag-Dorszyńska, M., Bogucka, K., Szalewska-Pałasz, A., and Herman-Antosiewiecz, A. (2019). Various modes of action of dietary phytochemicals, sulforaphane and phenethyl isothiocyanate, on pathogenic bacteria. Sci Rep 9, 13677. doi: 10.1038/s41598-019-50216-x

Sobala, M., Bruhn-Olszewska, B., and Cashel M, Potrykus, K. (2019). *Methylobacterium extorquens* RSH Enzyme Synthesizes (p)ppGpp and pppApp *in vitro* and *in vivo*, and Leads to Discovery of pppApp Synthesis in *Escherichia coli*. *Frontiers Microbiol*. doi: 10.3389/fmicb.2019.00859

Steinchen, W., and Bange, G. (2016). The magic dance of the alarmones (p)ppGpp. Mol Microbiol. Aug;101(4):531-44. doi: 10.1111/mmi.13412

Stent, G.S., and Brenner, S. (1961). PNAS 47:2005-14 A Genetic Locus for the Regulation of Ribonucleic Acid Synthesis. doi: 10.1073/pnas.47.12.2005

Winslow, R. M., and Lazzarini, R. A. (1969). Amino acid regulation of the rates of synthesis and chain elongation of ribonucleic acid in Escherichia coli J Biol *Chem* 244:3387–3382. doi: 10.1016/S0021-9258(18)93137-6

Conflict of Interest: The authors declare that the research was conducted in the absence of any commercial or financial relationships that could be construed as a potential conflict of interest.

frontiers in Microbiology

ORIGINAL RESEARCH
published: 28 February 2020
doi: 10.3389/fmicb.2020.00277

The C-Terminal RRM/ACT Domain Is Crucial for Fine-Tuning the Activation of 'Long' RelA-SpoT Homolog Enzymes by Ribosomal Complexes

Hiraku Takada[1,2], Mohammad Roghanian[1,2], Victoriia Murina[1,2], Ievgen Dzhygyr[1,2], Rikinori Murayama[3], Genki Akanuma[4], Gemma C. Atkinson[1], Abel Garcia-Pino[5,6] and Vasili Hauryliuk[1,2,7]**

[1] Department of Molecular Biology, Umeå University, Umeå, Sweden, [2] Laboratory for Molecular Infection Medicine Sweden, Umeå University, Umeå, Sweden, [3] Akita Prefectural Research Center for Public Health and Environment, Akita, Japan, [4] Department of Life Science, Graduate School of Science, Gakushuin University, Tokyo, Japan, [5] Cellular and Molecular Microbiology, Faculté des Sciences, Université Libre de Bruxelles, Brussels, Belgium, [6] WELBIO, Brussels, Belgium, [7] Institute of Technology, University of Tartu, Tartu, Estonia

OPEN ACCESS

Edited by:
Michael Cashel,
Eunice Kennedy Shriver National Institute of Child Health and Human Development (NICHD), United States

Reviewed by:
Rebecca Corrigan,
University of Sheffield, United Kingdom
Christiane Wolz,
University of Tübingen, Germany

***Correspondence:**
Hiraku Takada
hiraku.takada@umu.se
Vasili Hauryliuk
vasili.hauryliuk@umu.se

Specialty section:
This article was submitted to Microbial Physiology and Metabolism, a section of the journal Frontiers in Microbiology

Received: 21 November 2019
Accepted: 06 February 2020
Published: 28 February 2020

Citation:
Takada H, Roghanian M, Murina V, Dzhygyr I, Murayama R, Akanuma G, Atkinson GC, Garcia-Pino A and Hauryliuk V (2020) The C-Terminal RRM/ACT Domain Is Crucial for Fine-Tuning the Activation of 'Long' RelA-SpoT Homolog Enzymes by Ribosomal Complexes. Front. Microbiol. 11:277. doi: 10.3389/fmicb.2020.00277

The (p)ppGpp-mediated stringent response is a bacterial stress response implicated in virulence and antibiotic tolerance. Both synthesis and degradation of the (p)ppGpp alarmone nucleotide are mediated by RelA-SpoT Homolog (RSH) enzymes which can be broadly divided in two classes: single-domain 'short' and multi-domain 'long' RSH. The regulatory ACT (Aspartokinase, Chorismate mutase and TyrA)/RRM (RNA Recognition Motif) domain is a near-universal C-terminal domain of long RSHs. Deletion of RRM in both monofunctional (synthesis-only) RelA as well as bifunctional (i.e., capable of both degrading and synthesizing the alarmone) Rel renders the long RSH cytotoxic due to overproduction of (p)ppGpp. To probe the molecular mechanism underlying this effect we characterized *Escherichia coli* RelA and *Bacillus subtilis* Rel RSHs lacking RRM. We demonstrate that, first, the cytotoxicity caused by the removal of RRM is counteracted by secondary mutations that disrupt the interaction of the RSH with the starved ribosomal complex – the ultimate inducer of (p)ppGpp production by RelA and Rel – and, second, that the hydrolytic activity of Rel is not abrogated in the truncated mutant. Therefore, we conclude that the overproduction of (p)ppGpp by RSHs lacking the RRM domain is not explained by a lack of auto-inhibition in the absence of RRM or/and a defect in (p)ppGpp hydrolysis. Instead, we argue that it is driven by misregulation of the RSH activation by the ribosome.

Keywords: ppGpp, Rel, ACT, RRM, stringent response, ribosome

INTRODUCTION

Bacteria employ diverse mechanisms to sense and respond to stress. One such mechanism is the stringent response – a near-universal stress response orchestrated by hyper-phosphorylated derivatives of housekeeping nucleotides GDP and GTP: guanosine tetraphosphate (ppGpp) and guanosine pentaphosphate (pppGpp), collectively referred to as (p)ppGpp (Hauryliuk et al., 2015; Liu et al., 2015; Steinchen and Bange, 2016). Since the stringent response and (p)ppGpp-mediated

signaling are implicated in virulence, antibiotic resistance and tolerance (Dalebroux et al., 2010; Dalebroux and Swanson, 2012; Hauryliuk et al., 2015), this stress signaling system has been recently targeted for development of new anti-infective compounds (Kushwaha et al., 2019).

Both synthesis and degradation of (p)ppGpp is mediated by RelA/SpoT Homolog (RSH) enzymes. RSHs can be broadly divided into two classes: 'long' multi-domain and 'short' single-domain factors (Atkinson et al., 2011; Jimmy et al., 2019). In the majority of bacteria, including model Gram-positive bacterial species *Bacillus subtilis*, the long multi-domain RSHs are represented by one bifunctional enzyme, Rel (Mittenhuber, 2001; Atkinson et al., 2011). Beta- and Gammaproteobacteria, such as *Escherichia coli*, encode two long RSH factors – RelA and SpoT – which are the products of gene duplication and diversification of the ancestral *rel* stringent factor (Mittenhuber, 2001; Atkinson et al., 2011; Hauryliuk et al., 2015). *E. coli* RelA is the most well-studied long RSH. RelA is a dedicated sensor of amino acid starvation with strong (p)ppGpp synthesis activity that is induced by ribosomal complexes harboring cognate deacylated tRNA in the A-site, so-called 'starved' ribosomal complexes (Haseltine and Block, 1973). Unlike RelA, which lacks (p)ppGpp hydrolysis activity (Shyp et al., 2012), Rel and SpoT can both synthesize and degrade (p)ppGpp (Xiao et al., 1991; Avarbock et al., 2000). Similarly to RelA – and to the exclusion of SpoT – (p)ppGpp synthesis by Rel is strongly activated by starved ribosomes (Avarbock et al., 2000). In addition to long RSHs, bacteria often encode single domain RSH enzymes: Small Alarmone Synthetases (SAS) and Small Alarmone Hydrolases (SAH) (Atkinson et al., 2011; Jimmy et al., 2019), such as RelQ and RelP in the Firmicute bacterium *B. subtilis* (Nanamiya et al., 2008).

Long RSHs are universally comprised of two functional regions: the catalytic N-terminal domains (NTD) and the regulatory C-terminal domains (CTD) (**Figure 1A**) (Atkinson et al., 2011). The NTD region comprises the (p)ppGpp hydrolase domain (HD; enzymatically inactive in RelA) and the (p)ppGpp synthetase domain (SYNTH) linked by an α-helical region that regulates the allosteric crosstalk between both domains (Tamman et al., 2019). The CTD encompasses four domains: the Thr-tRNA synthetase, GTPase and SpoT domain (TGS), the Helical domain, the Zing Finger Domain (ZFD) [equivalent to Ribosome-InterSubunit domain, RIS, as per (Loveland et al., 2016), or Conserved Cysteine, CC, as per (Atkinson et al., 2011)], and, finally, the RNA Recognition Motif domain (RRM) [equivalent to Aspartokinase, Chorismate mutase and TyrA, ACT, as per (Atkinson et al., 2011)]. When Rel/RelA is bound to a starved ribosomal complex, the TGS domain inspects the deacylated tRNA in the A-site and the TGS domain interacts directly with the 3′ CCA end of the A-site tRNA (Arenz et al., 2016; Brown et al., 2016; Loveland et al., 2016). The conserved histidine 432 residue of *E. coli* RelA mediating this interaction is crucial for activation of RelA's enzymatic activity by the 3′ CCA (Winther et al., 2018). Both ZFD and RRM interact with the A-site finger (ASF) of the 23S ribosomal RNA (Arenz et al., 2016; Brown et al., 2016; Loveland et al., 2016), and in *E. coli* RelA this contact is crucial for efficient recruitment to and activation by starved ribosomal complexes (Kudrin et al., 2018).

While the NTD is responsible for the enzymatic function of RSHs, the CTD senses the starved ribosomal complex and transmits the signal to activate NTD-mediated (p)ppGpp synthesis by Rel/RelA (Agirrezabala et al., 2013; Arenz et al., 2016; Brown et al., 2016; Loveland et al., 2016). Since removal of the CTD increases the rate of (p)ppGpp production by Rel/RelA in the absence of ribosomes or starved complexes, the CTD was proposed to mediate the auto-inhibition of the NTD synthetase activity, thus precluding uncontrolled production of cytotoxic (p)ppGpp (Schreiber et al., 1991; Gropp et al., 2001; Mechold et al., 2002; Avarbock et al., 2005; Jiang et al., 2007; Yang et al., 2019).

The specific focus of this study is the C-terminal RRM/ACT domain of ribosome-associated RSH RelA and Rel. The RRM is absent in RelA enzymes from *Methylotenera mobilis, Elusimicrobium minutum*, *Francisella philomiraga,* and *Francisella tularensis* (Atkinson et al., 2011). The only experimentally characterized representative amongst these is *F. tularensis* RelA (Wilkinson et al., 2015). In a reconstituted biochemical system, the factor behaves similarly to *E. coli* RelA, i.e., it has very low synthesis activity by itself and is potently activated by the ribosome. Conversely, deletion of the RRM domain in factors that naturally possess it leads to inhibition of growth (Gratani et al., 2018; Ronneau et al., 2019; Turnbull et al., 2019) that is mediated by over-production of (p)ppGpp in the cell, as shown for *Caulobacter crescentus* Rel (Ronneau et al., 2019) and *E. coli* RelA (Turnbull et al., 2019). The exact molecular mechanism of misregulation remains unclear. Deletion of RRM in bifunctional *C. crescentus* Rel leads to compromised hydrolase activity (Ronneau et al., 2019), while overproduction of (p)ppGpp by monofunctional *E. coli* RelA$^{\Delta RRM}$ was suggested to be due to upregulated constitutive synthesis activity, conceivably due to defective auto-inhibition of the NTD synthetase domain by the CTD (Turnbull et al., 2019).

In this report, we inspected the possible role of the ribosome in overproduction of (p)ppGpp by ΔRRM variants of long RSHs in the cell. By characterizing truncated versions of *E. coli* RelA and *B. subtilis*, we demonstrate that the cytotoxicity of mutant RSH variants is strictly dependent on the interaction with the ribosome and deacylated tRNA, and, therefore, cannot be explained by defects in intra-molecular regulation alone.

MATERIALS AND METHODS

Multiple Sequence Alignment

Sequences were aligned with MAFFT v7.164b with the L-INS-i strategy (Katoh and Standley, 2013), and alignments were visualized with Jalview (Waterhouse et al., 2009).

Construction of Bacterial Strains and Plasmids

The strains and plasmids used in this study are listed in **Supplementary Tables S1–S3**. Oligonucleotides used in this study are provided in **Supplementary Table S4**.

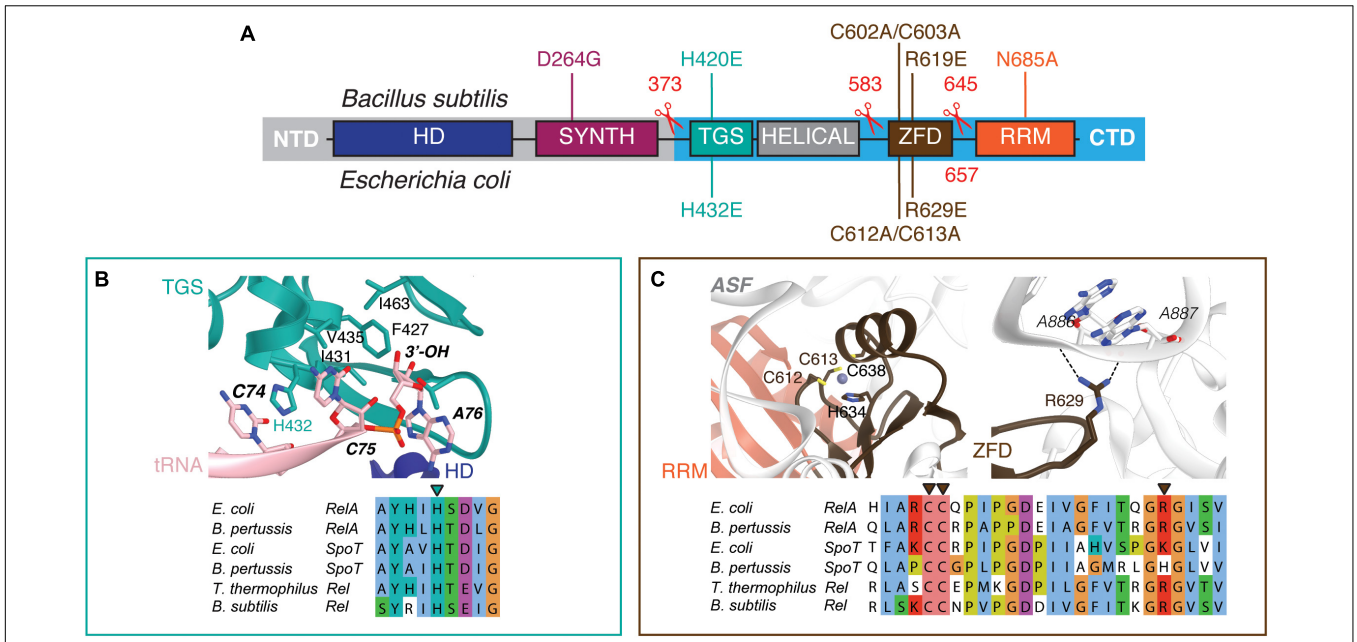

FIGURE 1 | Domain structure of 'long' ribosome-associated RSHs Rel and RelA. **(A)** The NTD region contains (p)ppGpp hydrolysis (HD) and (p)ppGpp synthesis (SYNTH) NTD domains. TGS (ThrRS, GTPase and SpoT), Helical, ZFD (Zinc Finger Domain) and RRM (RNA Recognition Motif) domains comprise the regulatory CTD region. Mutations and truncations of *B. subtilis* Rel and *E. coli* RelA used in this study are indicated above and below the domain schematics, respectively. **(B)** Conservation and structural environment of mutations in the TGS domain used in the current study. **(C)** Conservation and structural environment of mutations in the RRM domain used in the current study. The 3D structures are as per from Loveland and colleagues (Loveland et al., 2016), RDB accession number 5KPX.

A detailed description of strain construction is provided in the **Supplementary Material**.

Growth Assays

Escherichia coli BW25113 cells were transformed with expression constructs either based on a high-copy IPTG inducible vector pUC derivative pMG25 (pMG25:*relA*, Turnbull et al., 2019, pMG25:$relA^{\Delta RRM}$, pMG25:*spoR* or pMG25:$spoT^{\Delta RRM}$) or on a low-copy IPTG inducible vector, mini R1 plasmid pNDM220 which is present in one to two copies per chromosome (Molin et al., 1979) (pNDM220:*relA*, pNDM220:$relA^{\Delta RRM}$, pNDM220:$relA^{\Delta RRM-H432E}$, pNDM220:$relA^{\Delta RRM-R629E}$ or pNDM220:$relA^{\Delta RRM-C612A/C613A}$). For solid medium growth assays, ten-fold serial dilutions of overnight LB cultures were spotted onto LB agar supplemented with 30 μg/mL ampicillin and 1 mM IPTG. For liquid medium growth assays, 1000-fold dilutions of the overnight LB cultures were made in liquid LB supplemented with 30 μg/mL ampicillin and 1 mM IPTG, seeded on a 100-well honeycomb plate (Oy Growth Curves AB Ltd, Helsinki, Finland), and plates incubated in a Bioscreen C (Labsystems, Helsinki, Finland) at 37°C with continuous medium shaking.

Bacillus subtilis strains were pre-grown on LB plates lacking the IPTG inducer overnight (10 h) at 30°C. Fresh individual colonies were used to inoculate filtered LB medium in the presence of indicated concentrations of IPTG and OD_{600} adjusted to 0.01. The cultures were seeded on a 100-well honeycomb plate (Oy Growth Curves AB Ltd, Helsinki, Finland), and plates were incubated in a Bioscreen C (Labsystems, Helsinki, Finland) at 37°C with continuous medium shaking.

Growth rates (μ_2) were calculated as slopes of linear regression lines through $\log_2$-transformed OD_{600} data points.

Preparation of Polyclonal Anti-Rel Antiserum

The entire coding region of the *B. subtilis rel* gene was amplified by PCR using the synthetic oligonucleotide pQErelA_F and pQErelA_R containing a *Bam*HI site and *B. subtilis* genomic DNA as a template. The resulting PCR fragment was cut with *Bam*HI and then inserted into the *Bam*HI sites of pQE60 (Qiagen), yielding plasmid pQErelA. pOErelA was transformed into *E. coli* M15 (pREP4) (Qiagen), fresh transformants were inoculated into LB liquid culture (1000 mL) with 100 μg/mL ampicillin and grown at 37°C with vigorous shaking. At OD_{600} of 0.8 expression of Rel induced with 1 mM IPTG (final concentration). After 3 h of expression the cells were harvested by centrifugation, resuspended in buffer A (500 mM NaCl, 50 mM Tris-HCl pH 8.0) supplemented with 2 mM PMSF and lysed by sonication. Rel-His_6 inclusion bodies were collected by centrifugation, resuspended in buffer A supplemented with 8 M guanidine hydrochloride (= buffer B) and loaded onto an Ni-NTA agarose column (QIAGEN) pre-equilibrated in the same buffer. The column was washed with buffer B supplemented with 10 mM imidazole, and the protein was eluted with a 100–400 mM imidazole gradient in buffer B. The fractions containing Rel-His_6 was dialyzed against buffer A at 4°C overnight. Aggregated

Rel-His_6 protein was collected by centrifugation, resuspended in buffer A supplemented with 6 M urea and used for rabbit immunization. Rabbit serum was used as a polyclonal anti-Rel antibody.

Sucrose Gradient Fractionation and Western Blotting

Bacillus subtilis strains were pre-grown on LB plates overnight at 30°C. Fresh individual colonies were used to inoculate 200 mL LB cultures that were grown at 37°C. At OD_{600} of 0.2 amino acid starvation was induced by addition of isoleucyl tRNA synthetase inhibitor mupirocin (dissolved in DMSO, AppliChem) to final concentration of 700 nM for 20 min. As a mock control, a separate culture was treated with the same amount of DMSO. After 20 min the cells were collected by centrifugation (8,000 rpm, 5 min, JLA-16.25 Beckman Coulter rotor), dissolved in 0.5 mL of HEPES:Polymix buffer [5 mM $Mg(OAc)_2$] supplemented with 2 mM PMSF, lysed using FastPrep homogenizer (MP Biomedicals) by four 20 s pulses at speed 6.0 mp/s with chilling on ice for 1 min between the cycles), and clarified by ultracentrifugation (14,800 rpm for 20 min, Microfuge 22R centrifuge Beckman Coulter, F241.5P rotor). Clarified cell lysates were loaded onto 10-35% sucrose gradients in HEPES:Polymix buffer pH 7.5 (5 mM Mg^{2+} final concentration), subjected to centrifugation (36,000 rpm for 3 h at 4°C, SW-41Ti Beckman Coulter rotor) and analyzed using Biocomp Gradient Station (BioComp Instruments) with A_{260} as a readout.

For Western blotting 0.5 mL fractions were supplemented with 1.5 mL of 99.5% ethanol, precipitated overnight at –20°C. After centrifugation at 14,800 rpm for 30 min at 4°C the supernatants were discarded and the samples were dried. The pellets were resuspended in 40 μL of 2xSDS loading buffer [100 mM Tris-HCl pH 6.8, 4% SDS (w/v) 0.02% Bromophenol blue, 20% glycerol (w/v) 4% β-mercaptoethanol], resolved on the 8% SDS PAGE and transferred to nitrocellulose membrane (Trans-Blot Turbo Midi Nitrocellulose Transfer Pack, Bio-Rad, 0.2 μm pore size) with the use of a Trans-Blot Turbo Transfer Starter System (Bio-Rad) (10 min, 2.5 A, 25 V). Membrane blocking was done for 1 h in PBS-T (1xPBS 0.05% Tween-20) with 5% w/v non-fat dry milk at room temperature. Rel was detected using anti-Rel primary combined with goat anti-rabbit IgG-HRP secondary antibodies. All antibodies were used at 1:10,000 dilution. ECL detection was performed using WesternBright^{TM} Quantum (K-12042-D10, Advansta) Western blotting substrate and an ImageQuant LAS 4000 (GE Healthcare) imaging system.

Expression and Purification of *E. coli* RelA and *B. subtilis* Rel

Wild type and H432E mutant variants of *E. coli* RelA were expressed and purified as described earlier (Turnbull et al., 2019).

Wild type and mutant variants of *B. subtilis* Rel were overexpressed in freshly transformed *E. coli* BL21 DE3 Rosetta (Novagen). Fresh transformants were inoculated to final OD_{600} of 0.05 in the LB medium (800 mL) supplemented with 100 μg/mL kanamycin. The cultures were grown at 37°C until an OD_{600} of 0.5, induced with 1 mM IPTG (final concentration) and grown for additional 1.5 h at 30°C. The cells were harvested by centrifugation and resuspended in buffer A (750 mM KCl, 5 mM $MgCl_2$, 40 μM $MnCl_2$, 40 μM $Zn(OAc)_2$, 1 mM mellitic acid (Tokyo Kasei Kogyo Co., Ltd.), 20 mM imidazole, 10% glycerol, 4 mM β-mercaptoethanol, 25 mM HEPES:KOH pH 8) supplemented with 0.1 mM PMSF and 1 U/mL of DNase I. Cells were lysed by one passage through a high-pressure cell disrupter (Stansted Fluid Power, 150 MPa), cell debris was removed by centrifugation (25,000 rpm for 40 min, JA-25.50 Beckman Coulter rotor) and clarified lysate was taken for protein purification.

To prevent possible substitution of Zn^{2+} ions in Rel's Zn-finger domain for Ni^{2+} during purification on an Ni-NTA metal affinity chromatography column (Block et al., 2009), a 5 mL HisTrap HP column was stripped from Ni^{2+} in accordance with manufacturer's recommendations, washed with 5 column volumes (CV) of 100 mM $Zn(OAc)_2$ pH 5.0 followed by 5 CV of deionized water. Clarified cell lysate was filtered through a 0.2 μm syringe filter and loaded onto the Zn^{2+}-charged HisTrap 5 mL HP column pre-equilibrated in buffer A. The column was washed with 5 CV of buffer A, and the protein was eluted with a linear gradient (6 CV, 0-100% buffer B) of buffer B (750 mM KCl, 5 mM $MgCl_2$, 40 μM $MnCl_2$, 40 μM $Zn(OAc)_2$, 1 mM mellitic acid, 500 mM imidazole, 10% glycerol, 4 mM β-mercaptoethanol, 25 mM HEPES:KOH pH 8). Mellitic acid forms highly ordered molecular networks when dissolved in water (Inabe, 2005) and it was shown to promote the stability of *Thermus thermophilus* Rel (Van Nerom et al., 2019). Fractions most enriched in Rel (≈25–50% buffer B) were pooled, totaling approximately 5 mL. The sample was loaded on a HiLoad 16/600 Superdex 200 pg column pre-equilibrated with a high salt buffer (buffer C; 2 M NaCl, 5 mM $MgCl_2$, 10% glycerol, 4 mM β-mercaptoethanol, 25 mM HEPES:KOH pH 8). The fractions containing Rel were pooled and applied on HiPrep 10/26 desalting column (GE Healthcare) pre-equilibrated with storage buffer (buffer D; 720 mM KCl, 5 mM $MgCl_2$, 50 mM arginine, 50 mM glutamic acid, 10% glycerol, 4 mM β-mercaptoethanol, 25 mM HEPES:KOH pH 8). Arginine and glutamic acid were added to improve protein solubility and long-term stability (Golovanov et al., 2004). The fractions containing Rel were collected and concentrated in an Amicon Ultra (Millipore) centrifugal filter device (cut-off 50 kDa). To cleave off the His_{10}-SUMO tag, 35 μg of His_6-Ulp1 per 1 mg of Rel were added and the reaction mixture was incubated at room temperature for 15 min. After the His_{10}-SUMO tag was cleaved off, the protein was passed though 5 mL Zn^{2+}-charged HisTrap HP pre-equilibrated with buffer D. Fractions containing Rel in the flow-through were collected and concentrated on Amicon Ultra (Millipore) centrifugal filter device with 50 kDa cut-off. The purity of protein preparations was assessed by SDS-PAGE and spectrophotometrically [OD_{260}/OD_{280} ratio below 0.8 corresponding to less than 5% RNA contamination (Layne, 1957)]. Protein preparations were aliquoted, frozen in liquid nitrogen and stored at −80°C. Individual single-use aliquots were discarded after the experiment.

Negative Staining Electron Microscopy

3.5 μL of 2 μM Rel protein was loaded onto a glow-discharged Cu_{300} grid (TAAB Laboratories Equipment Ltd.) with manually layered 2.9 nm carbon. The sample was incubated on the grid for 1–3 min, blotted with Watman filter paper, than twice washed with water and blotted, stained with 1.5% uranyl acetate pH 4.2 for 30 s before the final blotting. Grids were dried on the bench and imaged by Talos L 120C (FEI) microscope with 92,000X magnification.

Preparation of 10X Polymix Buffer Base

The 10X Polymix base was prepared as per (Antoun et al., 2004), with minor modifications. For preparation of the putrescine solution, 100 g of putrescine (1,4-diaminobutane) was dissolved in 600 mL of ddH_2O at 90°C, and the pH adjusted with acetic acid to 8.0 (approximately 100 mL of 100% acetic acid). After cooling to room temperature, the pH was adjusted further to 7.6 and the volume was adjusted to the final of 2 L by addition of 1.134 L of ddH_2O. One 100 mL cup of activated charcoal was added and the slurry was stirred under the hood for 30 min. The slurry was filtered through, first, Whatman paper and then through a 0.45 μm BA85 membrane. The final solution was stored at 4°C in a bottle wrapped in foil since putrescine is photosensitive. The preparation of 2 L of 10X Polymix buffer base used 141.66 g KCl, 5.35 g NH_4Cl, 21.44 g $Mg(OAc)_2{\cdot}4H_2O$, 1.47 g $CaCl_2{\cdot}2H_2O$, 5.092 g spermidine, and 160 ml of putrescine solution (described above). The salts were dissolved in ddH_2O (≈1,500 mL), then the putrescine solution was added and mixed well. Spermidine was dissolved in a small volume of ddH_2O and added to the mixture. The pH was adjusted to 7.5 with concentrated acetic acid or 5 M KOH, and after that the volume was adjusted by adding ddH_2O to 2 L. The buffer was filtered through 0.2 μm nitrocellulose filter (2–3 filters are needed). The resulting 10X Polymix buffer base was aliquoted and stored at −20°C. The final working HEPES:Polymix buffer was made using the 10X Polymix buffer base, 1M DDT and 1 M HEPES:KOH pH 7.5 and contains 20 mM HEPES:KOH pH 7.5, 2 mM DTT, 5 mM $MgOAc_2$, 95 mM KCl, 5 mM NH_4Cl, 0.5 mM $CaCl_2$, 8 mM putrescine, 1 mM spermidine.

Purification of *B. subtilis* 70S Ribosomes

Bacillus subtilis strain RIK2508 (*trpC2* Δ*hpf*) strain (Akanuma et al., 2016; Brodiazhenko et al., 2018) was pre-grown on LB plates overnight at 30°C. Fresh individual colonies were used to inoculate LB liquid cultures (25 × 400 mL) to OD_{600} of 0.05 and grown at 37°C with vigorous shaking. At OD_{600} 1.2 the cells were pelleted at 4°C (TLA10.500 (Beckman), 15 min at 5,000–8,000 rcf), resuspended with ice-cold PBS buffer, pelleted again in 50 mL Falcon tubes, frozen with liquid nitrogen and stored at –80°C. Approximately 20 g of frozen *B. subtilis* cells were resuspended in 50 mL of cell opening buffer (100 mM NH_4Cl, 15 mM $Mg(OAc)_2$, 0.5 mM EDTA, 3 mM β-mercaptoethanol, 20 mM Tris:HCl pH 7.5) supplemented with 1 mU Turbo DNase (Thermo Fisher Scientific), 0.1 mM PMSF and 35 μg/mL lysozyme, incubated on ice for 1 h, and opened by three passages on a high-pressure cell disrupter (Stansted Fluid Power) at 220 MPa. Lysed cells were clarified by centrifugation for 40 min at 40,000 rpm (Ti 45 rotor, Beckman), NH_4Cl concentration was adjusted to 400 mM, and the mixture was filtered through 0.45 μm syringe filters. The filtrated lysate was loaded onto a pre-equilibrated 80 mL CIMmultus QA-80 column (BIA Separations, quaternary amine advanced composite column) at a flow rate of 20 mL/min, and the column washed with 5 CV (CV = 80 mL) of low salt buffer [400 mM NH_4Cl, 15 mM $Mg(OAc)_2$, 3 mM β-mercaptoethanol, 20 mM Tris:HCl pH 7.5]. Ribosomes were then eluted in 45 mL fractions by a step gradient to 77% high salt buffer [900 mM NH_4Cl, 15 mM $Mg(OAc)_2$, 3 mM β-mercaptoethanol, 20 mM Tris:HCl pH 7.5] for 5 CV, followed by 100% high salt buffer for 1 CV. The fractions containing ribosomes were pooled, the concentration of NH_4Cl was adjusted to 100 mM, and the ribosomes were treated with puromycin added to a final concentration of 10 μM. The resultant crude 70S preparation was resolved on a 10–40% sucrose gradient in overlay buffer [60 mM NH_4Cl, 15 mM $Mg(OAc)_2$, 0.25 mM EDTA, 3 mM β-mercaptoethanol, 20 mM Tris:HCl pH 7.5] in a zonal rotor (Ti 15, Beckman, 17 h at 21,000 rpm). The peak containing pure 70S ribosomes was pelleted by centrifugation (20 h at 35,000 rpm), and the final ribosomal preparation was dissolved in HEPES:Polymix buffer [20 mM HEPES:KOH pH 7.5, 2 mM DTT, 5 mM $Mg(OAc)_2$, 95 mM KCl, 5 mM NH_4Cl, 0.5 mM $CaCl_2$, 8 mM putrescine, 1 mM spermidine (Antoun et al., 2004)]. 70S concentration was measured spectrophotometrically (1 OD_{260} corresponds to 23 nM of 70S) and ribosomes were aliquoted (50–100 μL per aliquot), snap-frozen in liquid nitrogen and stored at –80°C.

Preparation of 70S Initiation Complexes (70S IC)

Initiation complexes were prepared by as per (Murina et al., 2018a,b), with minor modifications. The reaction mix containing *B. subtilis* 70S ribosomes (final concentration of 6 μM) with *E. coli* IF1 (4 μM), IF2 (5 μM), IF3 (4 μM), ^{3}H-fMet-$tRNA_i^{fMet}$ (8 μM), mRNA MVFStop (8 μM, 5′-GGC**AAGGAGGA**GAUAAGA<u>AUGGUUUUCUAA</u>UA-3′;
Shine-Dalgarno sequence is highlighted in bold, ORF is underlined), 1 mM GTP and 2 mM DTT in 1 × HEPES:Polymix buffer [20 mM HEPES:KOH pH 7.5, 95 mM KCl, 5 mM NH_4Cl, 5 mM $Mg(OAc)_2$, 0.5 mM $CaCl_2$, 8 mM putrescine, 1 mM spermidine, 1 mM DTT (Antoun et al., 2004)] was incubated at 37°C for 30 min. Then the ribosomes were pelleted through a sucrose cushion (1.1 M sucrose in HEPES:Polymix buffer with 15 mM Mg^{2+}) at 50,000 rpm for 2 h (TLS-55, Beckman), the pellet was dissolved in HEPES:Polymix buffer [5 mM $Mg(OAc)_2$], aliquoted, frozen in liquid nitrogen and stored at −80°C.

Preparation of ^{3}H-Labeled pppGpp

3 μM *E. faecalis* RelQ (Beljantseva et al., 2017) was incubated in reaction buffer (18 mM $MgCl_2$, 20 mM DTT, 20 mM Tris-HCl pH 8.0) together with 8 mM ATP and 5 mM ^{3}H-GTP (SA: 100 cpm/pmol) for 2 h at 37°C to produce ^{3}H-pppGpp. The resultant mixture was loaded on strong anion-exchange column (MonoQ 5/50 GL; GE Healthcare), and nucleotides were resolved

by a 0.5–1,000 mM LiCl gradient. Peak fractions containing ^{3}H-pppGpp were pooled and precipitated by addition of lithium chloride to a final concentration of 1 M followed by addition of four volumes of ethanol. The suspension was incubated at –80°C overnight and centrifuged (14,800 rpm, 30 min, 4°C). The resulting pellets were washed with absolute ethanol, dried, dissolved in 20 mM HEPES-KOH buffer (pH 7.5) and stored at –80°C.

^{3}H-pppGpp Hydrolysis Assay

The reaction mixtures contained 140–250 nM Rel, 300 μM ^{3}H-pppGpp, 1 mM $MnCl_2$, an essential cofactor for Rel's hydrolysis activity (Avarbock et al., 2000; Mechold et al., 2002;Tamman et al., 2019), all in HEPES:Polymix buffer (5 mM Mg^{2+} final concentration). After preincubation at 37°C for 3 min, the reaction was started by the addition of prewarmed Rel and 5 μL aliquots were taken throughout the time course of the reaction and quenched with 4 μL 70% formic acid supplemented with a cold nucleotide standard (4 mM GTP) for UV-shadowing.

^{3}H-pppGpp Synthesis Assay

Assays with *E. coli* RelA were performed as described earlier (Kudrin et al., 2018). In the case of *B. subtilis* Rel, the reaction mixtures typically contained 500 nM *B. subtilis* 70S IC(MVF), 140 nM Rel, guanosine nucleoside substrate (300 μM ^{3}H-GTP, PerkinElmer), 100 μM pppGpp, 2 μM *E. coli* $tRNA^{Val}$ (ChemBlock), all in HEPES:Polymix buffer (5 mM Mg^{2+} final concentration). After preincubation at 37°C for 3 min, the reaction was started by the addition of prewarmed ATP to the final concentration of 1 mM, and 5 μL aliquots were taken throughout the time course of the reaction and quenched with 4 μL 70% formic acid supplemented with a cold nucleotide standard (4 mM GTP) for UV-shadowing. Individual quenched timepoints were spotted PEI-TLC plates (Macherey-Nagel) and nucleotides were resolved in 1.5 M KH_2PO_4 pH 3.5 buffer. The TLC plates were dried, cut into sections as guided by UV-shadowing, and ^{3}H radioactivity was quantified by scintillation counting in EcoLite Liquid Scintillation Cocktail (MP Biomedicals).

RESULTS

Toxicity of *E. coli* ΔRRM RelA Is Countered by Mutations Compromising the Interaction With Starved Ribosomes

As we have shown earlier, low-level ectopic expression of $RelA^{\Delta RRM}$ from a low copy number pNDM220 plasmid under the control of a $P_{A1/O4/O3}$ promoter has a more pronounced inhibitory effect on *E. coli* growth in comparison with expression of the full-length protein (Turnbull et al., 2019). We tested whether $P_{A1/O4/O3}$-driven high-level expression of $RelA^{\Delta RRM}$ from a high-copy pUC derivative pMG25 would cause a more pronounced growth defect (**Figure 2A**). For comparison, we tested the effects of expression of the second *E. coli* RSH enzyme – SpoT – using both the full-length and the ΔRRM variants. Even in the absence of the IPTG inducer, leaky expression of $RelA^{\Delta RRM}$ has a dramatic effect on *E. coli* growth, while the full-length protein does not have an effect. In the presence of 50 μM IPTG, both full-length and $RelA^{\Delta RRM}$ inhibit the growth, although the latter has a stronger effect; induction with 500 μM IPTG completely abrogates the growth in both cases. While expression of SpoT has a detectable inhibitory effect at 500 μM IPTG, the effect is the same for full-length and $SpoT^{\Delta RRM}$. Since even leaky expression of $RelA^{\Delta RRM}$ inhibits growth, we concluded that this high-level expression system is ill-suited for follow-up microbiological investigations. Therefore, to test whether the toxicity of $RelA^{\Delta RRM}$ in *E. coli* is dependent on the interaction with starved complexes, we used the pNDM220-based low-level expression system used previously (Turnbull et al., 2019). Guided by the recent cryo-EM reconstructions of RelA (Arenz et al., 2016; Brown et al., 2016; Loveland et al., 2016), we designed a set of mutations that will specifically disrupt RelA's interaction with starved ribosomal complexes.

To disrupt the interaction between RelA and the tRNA, we adopted the H432E mutation in the TGS domain that was earlier shown to specifically abrogate the recognition of the 3′ CCA end of the A/R tRNA (Winther et al., 2018). This conserved histidine residue stacks between the two cytosine bases and hydrogen-bonds the phosphodiester backbone (**Figure 1B**). Replacing it with glutamic acid introduces a charge repulsion effect as well as a steric clash. To disrupt the interaction with the ribosome we used mutations in the ZFD: R629E as well as a double substitution C602A C603A; both mutants are expected to compromise the recognition of the 23S rRNA ASF element that is crucial for RelA recruitment (Kudrin et al., 2018). The conserved double motif docks the ZFD α-helix into the major groove of the ASF; replacement by alanine is expected to abrogate this interaction (**Figure 1C**). The conserved arginine 629 residue is in close proximity to A886-A887 and A885-A886 phosphodiester bonds (3.5 and 5 Å, respectively), and, therefore, the R629E substitution is expected to cause electrostatic repulsion.

Low-level expression of full-length RelA has a minor, but detectable growth inhibitory effect both when tested on solid LB agar media (**Figure 2B**) and in liquid LB cultures [growth rate, μ_2, decreases from 0.69 (vector) to 0.47 h^{-1}) (**Figure 2C**]. Importantly, the spotting control on solid LB media lacking IPTG shows that the size of the inoculum is not affected by potential leaky expression in the overnight culture (**Figure 2B**). Deletion of the RRM renders RelA significantly more toxic (growth rate decreases to 0.29 h^{-1}), in good agreement with the accumulation of (p)ppGpp upon expression of the construct (Turnbull et al., 2019). The effect is countered by TGS H432E, ZFD R629E and even more so by the C612A C613A substitutions (**Figures 2B,C**). $RelA^{\Delta RRM}$ expression is equally toxic in the Δ*relA* background and the effect is similarly countered by H432E, R629E and C612A C613A substitutions (**Supplementary Figure S1**), demonstrating that the growth inhibition is independent of the functionality of the endogenous RelA stringent factor. Finally, we directly confirmed the lack of activation by deacylated tRNA in the case of H432E *E. coli* RelA using biochemical assays (**Figure 2D**).

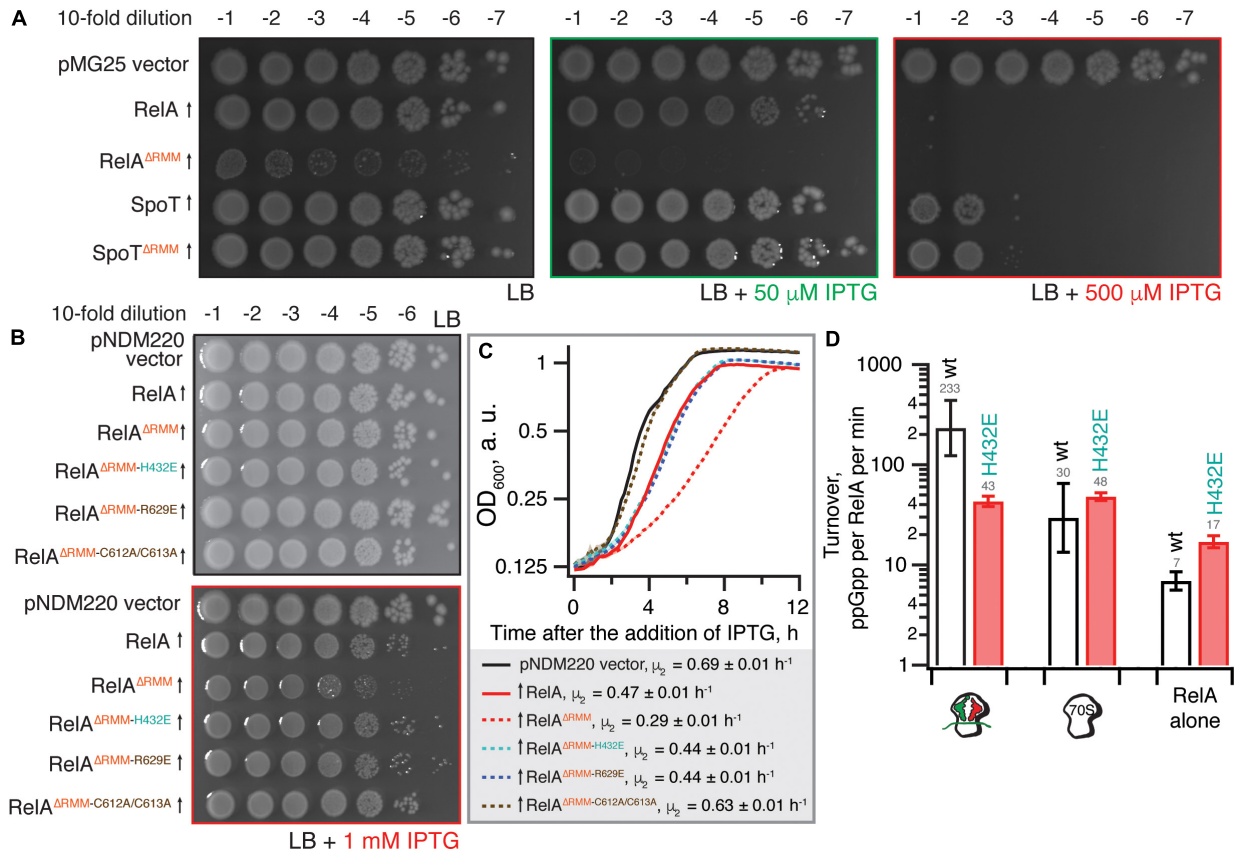

FIGURE 2 | The toxicity of ΔRRM *E. coli* RelA is mitigated by mutations compromising interactions with tRNA and the ribosome. **(A)** Wild-type *E. coli* BW25113 cells were transformed with either the empty high-copy IPTG-inducible pMG25 plasmid vector or pMG25-based constructs expressing wild-type and ΔRRM versions of *E. coli* RelA and SpoT. Up-pointing arrows indicate induction of expression. Ten-fold serial dilutions of overnight LB cultures were made and spotted onto LB agar supplemented with 100 μg/mL ampicillin and either 0, 50, or 500 μM IPTG. The plates were incubated at 37°C and scored after 18 h. **(B)** *E. coli* BW25113 cells were transformed either with the empty low-copy IPTG-inducible pNDM220 vector or pNDM220-based constructs expressing wild-type and mutant versions of *E. coli* RelA as indicated on the figure. Ten-fold serial dilutions of overnight LB cultures were made and spotted onto LB agar supplemented with 30 μg/mL ampicillin and 1 mM IPTG. As a plating control the same dilutions of the overnight cultures were spotted on LB agar supplemented with 30 μg/mL ampicillin but no IPTG. The plates were incubated at 37°C and scored after 18 h. **(C)** Thousand-fold dilutions of the same overnights were made in LB supplemented with 30 μg/mL ampicillin and 1 mM IPTG, and growth at 37°C was monitored using the Bioscreen C growth curve analysis system. The growth rates (μ^2) were calculated from three independent measurements and the error bars represent standard errors. **(D)** H432E TGS *E. coli* RelA is not activated by deacylated tRNA on the ribosome. The synthetase activity of 30 nM wild type and H432E *E. coli* RelA was assayed in the presence of 1 mM ATP, 300 μM ^{3}H GDP and 100 μM ppGpp in HEPES:Polymix buffer, pH 7.5, 37°C, 5 mM Mg^{2+}. As indicated on the figure, the reaction mixture was supplemented either with 2 μM vacant 70S ribosomes or with an *in situ* assembled starved ribosomal complex (2 μM vacant 70S combined with 2 μM mRNA(MV), 2 μM *E. coli* $tRNA_i^{fMet}$ and 2 μM *E. coli* $tRNA^{Val}$). The error bars represent standard deviations of the turnover estimates by linear regression using four data points.

Taken together, our results suggest that $RelA^{\Delta RRM}$ toxicity in *E. coli* is dependent on the functionality of the interaction with starved ribosomes. To test the generality of this hypothesis, we next characterized *B. subtilis* Rel lacking the RRM domain.

Toxicity of *B. subtilis* ΔRRM Rel Expressed in the ppGpp^0 Background Is Mediated by (p)ppGpp Synthesis and Is Countered by Mutations Compromising the Interaction With Starved Ribosomes

We expressed ΔRRM Rel under the control of an IPTG-inducible $P_{hy-spank}$ promotor (Britton et al., 2002) in ppGpp^0 (Δ*rel* Δ*relP* Δ*relQ*) (Nanamiya et al., 2008) or Δ*rel B. subtilis* strains (**Figure 3A**). In the ppGpp^0 background, inhibition of *B. subtilis* growth on LB plates is a marker of toxic (p)ppGpp overproduction. In the Δ*rel* background, (p)ppGpp is overproduced by a SAS in the absence of Rel's hydrolytic activity, causing a growth defect in *B. subtilis* (Nanamiya et al., 2008) and *S. aureus* (Geiger et al., 2014). Therefore, this experiment tests the complementation of hydrolase function of Rel that manifests in improved growth.

Unlike the full-length Rel, the $Rel^{\Delta RRM}$ truncation is toxic in the ppGpp^0 and Δ*rel* backgrounds, both when the growth is followed on plates (**Figure 3A**) and in liquid culture (**Figures 3B,C** and **Supplementary Figures S2A,B**). To probe the role of the interactions with starved ribosomes in $Rel^{\Delta RRM}$ toxicity, we used a set of substitutions in *B. subtilis* Rel

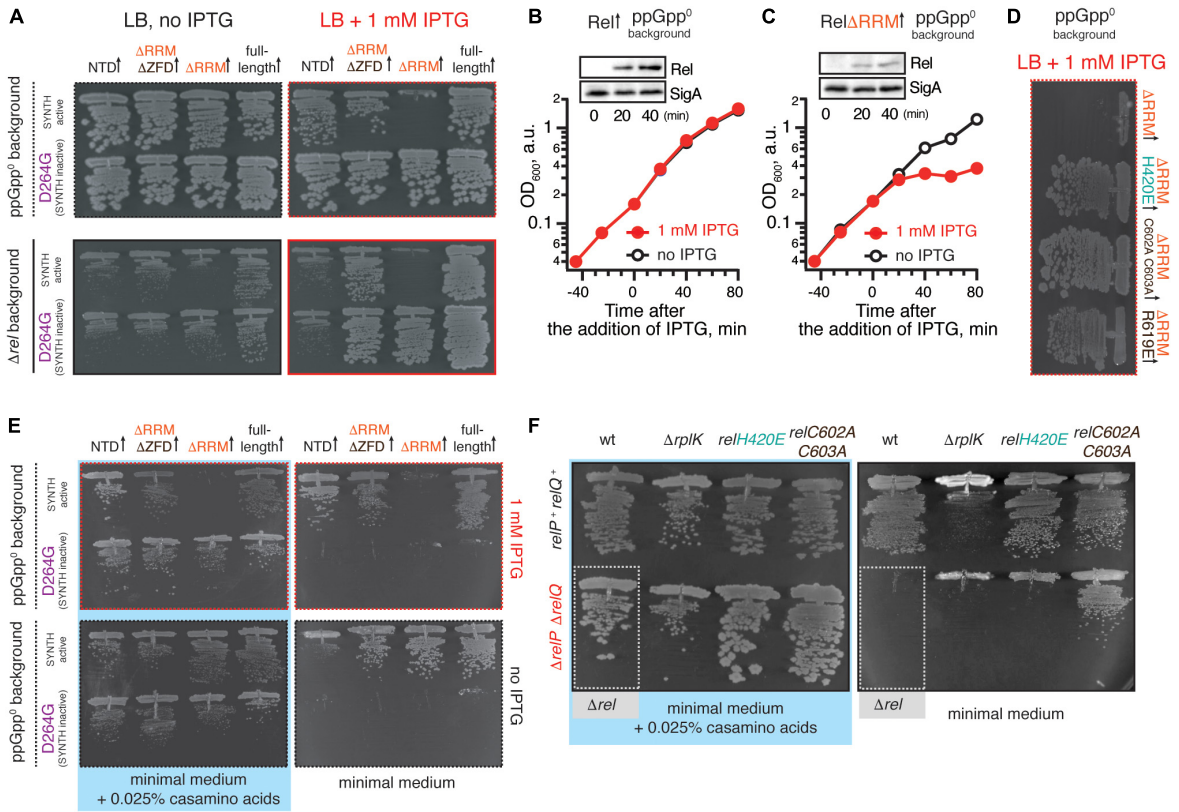

FIGURE 3 | Deletion of the regulatory RRM domain leads to *B. subtilis* Rel toxicity due to ribosome-dependent (p)ppGpp overproduction. **(A)** Full-length (VHB155 and VHB183) as well as C-terminally truncated Rel variants [synthesis-competent ΔRRM (VHB159 and VHB184), ΔRRMΔZFD (VHB160 and VHB185) and Rel^{NTD} (VHB161 and VHB186), and the corresponding synthesis-inactive D264G mutants VHB162-164; VHB187-190] were expressed in either $ppGpp^0$ (upper row; test for toxicity mediated by (p)ppGpp accumulation) or Δ*rel* (lower row; test for HD functionality) *B. subtilis* growing on solid LB medium. Up-pointing arrows (↑) indicate ectopic expression. **(B,C)** Expression of $Rel^{\Delta RRM}$ causes a growth defect in liquid culture. Either wild-type *rel* (VHB183) **(B)** or $rel^{\Delta RRM}$ mutant (VHB184) **(C)** were expressed in $ppGpp^0$ background grown in liquid LB medium at 37°C. Protein expression was induced by IPTG added to final concentration of 1 mM to exponentially growing bacterial cultures at OD_{600} 0.2. Protein expression was monitored by Western blotting using anti-Rel antibodies (see also **Supplementary Figure S2H**). **(D)** The toxicity of mutant versions of $Rel^{\Delta RRM}$ tested in $ppGpp^0$ *B. subtilis* growing on solid LB medium: wild type $Rel^{\Delta RRM}$ (VHB184), H420E (VHB231) defective in recognition of the tRNA 3' CCA end, and ZFD mutants C602A C603A (VHB233) and R619E (VHB281) defective in 70S binding. LB plates were scored after 18 h incubation at 37°C. **(E)** C-terminally truncated Rel variants (either synthesis-competent (VHB155, VHB159-161) or synthesis-inactive D264G mutant versions (VHB156, VHB162-164) were expressed in $ppGpp^0$ *B. subtilis* growing on either solid minimal medium or solid minimal medium supplemented with 0.025% casamino acids. Plates were scored after 36 h incubation at 37°C. Importantly, prior to experiment all strains were pre-cultured on solid minimal medium supplemented with 0.025% casamino acids. This was done in order to avoid the effects caused by the decreased fitness of the inoculum. **(F)** Synthesis activity of Rel mutants probed by amino acid auxotrophy assays. *B. subtilis* strains were constructed using either $relP^+$ $relQ^+$ wild-type 168 (upper row) or Δ*relP* Δ*relP* (lower row) background. The strains either expressed the indicated *rel* mutants [H420E (VHB68) and C602A C603A (VHB148), upper row, and H420E (VHB60), C602A C603A (VHB62), lower row] or contained an additional Δ*rplK* gene disruption (VHB47, $relP^+$ $relQ^+$ and VHB49, Δ*relP* Δ*relP*). The $ppGpp^0$ mutant strain (Δ*relP* Δ*relP* Δ*rel*, VHB63) was used as a control (highlighted with gray box). The strains were grown on either solid Spizizen minimal medium (right panel) or solid minimal medium supplemented with 0.025% casamino acids (left panel).

corresponding to those used to study *E. coli* RelA (**Figures 1**, **2**). The toxicity of the $Rel^{\Delta RRM}$ mutant is efficiently countered by the H420E substitution in the TGS as well as the R619E and C602A C603A substitutions in the ZFD (**Figure 3D** and **Supplementary Figures S2D–F,H**). This strongly suggests that the intact interaction with tRNA and starved ribosomes is essential for the toxicity of $Rel^{\Delta RRM}$. For comparison, we tested, full-length Rel, $Rel^{\Delta RRM\Delta ZDF}$ C-terminal truncation, as well as the NTD domain region alone. The $Rel^{\Delta RRM\Delta ZDF}$ mutant is only slightly toxic in the $ppGpp^0$ background and its expression promotes growth in the Δ*rel* background (**Figure 3A**). NTD-alone construct displays no toxicity in the $ppGpp^0$ background and does not promote the growth in the Δ*rel* background, suggesting weak – or absent – synthetase activity.

To separate the effects of (p)ppGpp production from the effects of (p)ppGpp degradation, we tested synthesis-deficient SYNTH D264G mutants (Nanamiya et al., 2008) of C-terminally truncated Rel variants (**Figure 3A** and **Supplementary Figure S2C**). The toxicity of the ΔRRM variant is abolished by the D264G mutation demonstrating that it is, indeed, mediated by (p)ppGpp production and not, for example, through inhibition of protein synthesis via competitive binding to ribosomal A-site [the latter non-enzymatic mechanism of toxicity was shown for *E. coli* $RelA^{CTD}$ (Turnbull et al., 2019)]. Both ΔRRM D264G

and ΔZFDΔRRM D264G variants promote growth in the Δ*rel* strain suggesting that neither deletion of ΔRRM alone – or both ΔZFD and ΔRRM – abrogates the hydrolysis activity of *B. subtilis* Rel (**Figure 3A**, bottom panel). At the same time expression of the synthesis-inactive D264G Rel^{NTD} has no effect, suggesting that the NTD does not efficiently hydrolyze (p)ppGpp. To test if further truncations of the NTD-only Rel (Rel^{1-373}) would induce hydrolytic activity, we tested several additional constructs of *B. subtilis* Rel – Rel^{1-336}, Rel^{1-196} and Rel^{1-155} – but neither of them could rescue the growth effect of Δ*rel B. subtilis* (**Supplementary Figure S3**). Finally, the synthesis deficiency of D264G Rel and the lack of H420E Rel activation by deacylated tRNA was confirmed using biochemical assays (**Supplementary Figure S4**).

Taken together, our results demonstrate that (i) $Rel^{\Delta RRM}$ is toxic in $ppGpp^0$ *B. subtilis*, (ii) this toxicity requires intact (p)ppGpp synthesis activity of the enzyme (iii) it is abrogated by mutations disrupting the interaction with tRNA and starved ribosomes and (iv) deletion of the RRM domain does not abrogate the hydrolysis activity of *B. subtilis* Rel.

The Synthetase Activity of $Rel^{\Delta RRM}$, $Rel^{\Delta RRM\Delta ZFD}$, and Rel^{NTD} but Not the Rel^{H420E} TGS Mutant Can Suppress Amino Acid Auxotrophy of $ppGpp^0$ *B. subtilis*

To test the low-level, non-toxic, synthesis activity of Rel mutants and to validate the effects of point mutations disrupting the interaction of Rel with starved ribosomal complexes, we took advantage of the amino acid auxotrophy phenotype of the $ppGpp^0$ *B. subtilis* (Δ*rel* Δ*relP* Δ*relQ*) (Nanamiya et al., 2008).

When $ppGpp^0$ *B. subtilis* is grown on Spizizen minimum medium (Spizizen, 1958) in the absence of casamino acids, neither of the D264G Rel mutants – either full-length or C-terminal truncations – promote growth, both whether or not expression is induced by 1 mM IPTG (**Figure 3E**, right panels). Full induction of NTD expression with 1 mM IPTG near-completely suppressed the auxotrophy phenotype (**Figure 3E**, top right panel), while the leaky expression in the absence of IPTG results in weak, but detectable suppression (**Figure 3E**, bottom right panel). This demonstrates that *B. subtilis* NTD has a weak net-synthesis activity. The $Rel^{\Delta RRM}$ is, as expected, highly toxic when expression is induced by IPTG; conversely, low-level leakage expression efficiently suppresses the amino acid auxotrophy phenotype. Removal of both RRM and ZFD domains renders the protein non-toxic. It is not trivial to reconcile this effect with the idea that removal of the RRM renders the protein toxic due to lack of auto-inhibition: one would expect that the additional removal of the ZFD domain would further compromise the CTD-mediated negative control in $Rel^{\Delta RRM}$.

We next used the auxotrophy assay to test the effects of the H420E TGS and C602A C603A ZFD substitutions on the activity of Rel expressed from the native genomic locus under the control of the native promotor (**Figure 3F**). As a positive control we used a strain lacking the genomic copy of *rplK* (*relC*) encoding ribosomal protein L11. This ribosomal element is essential for *E. coli* RelA activation by starved ribosomal complexes (Parker et al., 1976; Wendrich et al., 2002; Shyp et al., 2012) as well as for cellular functionality of *C. crescentus* Rel (Boutte and Crosson, 2011). The $ppGpp^0$ strain expressing H420E Rel fails to grow on the minimum media, reinforcing the crucial role of that this residue, while the C602A C603A can sustain the growth, suggesting that this substitution does not completely abrogate the activity.

RRM Deletion and ZFD Mutations Destabilize *B. subtilis* Rel Binding to Starved Ribosomal Complexes

Next, we probed the ribosomal association of ΔRRM and full-length Rel expressed in the $ppGpp^0$ background using a centrifugation sucrose gradient followed by Western blotting using antiserum against native, untagged *B. subtilis* Rel (**Figure 4A**). Since deacylated tRNA promotes ribosomal recruitment of *E. coli* RelA (Agirrezabala et al., 2013; Kudrin et al., 2017), we probed the association of wild type and mutant Rel variants with the ribosome both under exponential growth and upon acute isoleucine starvation induced by the isoleucyl tRNA synthetase inhibitor antibiotic mupirocin (pseudomonic acid) (Thomas et al., 2010). In good agreement with the cryo-EM structures detailing multiple contacts between the RRM and the starved complex and therefore suggesting an importance of this element in ribosomal recruitment (Arenz et al., 2016; Brown et al., 2016; Loveland et al., 2016), we do not detect a stable association of ΔRRM Rel with the ribosome upon a mupirocin challenge. This suggests that the interaction with the ribosome is significantly destabilized in $Rel^{\Delta RRM}$ and the protein dissociates during centrifugation. It is noteworthy that, despite an unstable association of $Rel^{\Delta RRM}$ with starved ribosomes, the expression of this protein strongly induces the accumulation of 100S ribosomal dimers, which is indicative of (p)ppGpp overproduction (Tagami et al., 2012). Note that the 100S formation is abrogated when the culture is treated with mupirocin (**Figure 4A** and **Supplementary Figure S5B**), most likely due to complete inhibition of translation by the antibiotic hindering expression of the 100S-promoting Hibernation Promoting Factor (HPF) which, in turn, is induced by accumulation of (p)ppGpp (Tagami et al., 2012).

Our microbiological experiments demonstrate that both the C602A and C603A double substitution and the R619E point substitution render $Rel^{\Delta RRM}$ non-toxic (**Figure 3D**), which we attribute to further destabilization of Rel's interaction with starved ribosomal complexes. To directly probe the effects of these mutations, we used centrifugation experiments with full-length Rel carrying the substitutions. As expected, both the C602A C603A double mutant and R619E full-length variants are compromised in recruitment to the ribosome upon a mupirocin challenge (**Figure 4A**).

Taken together, these results demonstrate that $Rel^{\Delta RRM}$ is significantly more toxic than the full-length protein and this toxicity is dependent on the interaction with starved ribosomes, which is, in turn, destabilized in this truncation. As a next step, we set out to test the effects of RRM deletion – either alone or in combination with mutations further compromising the

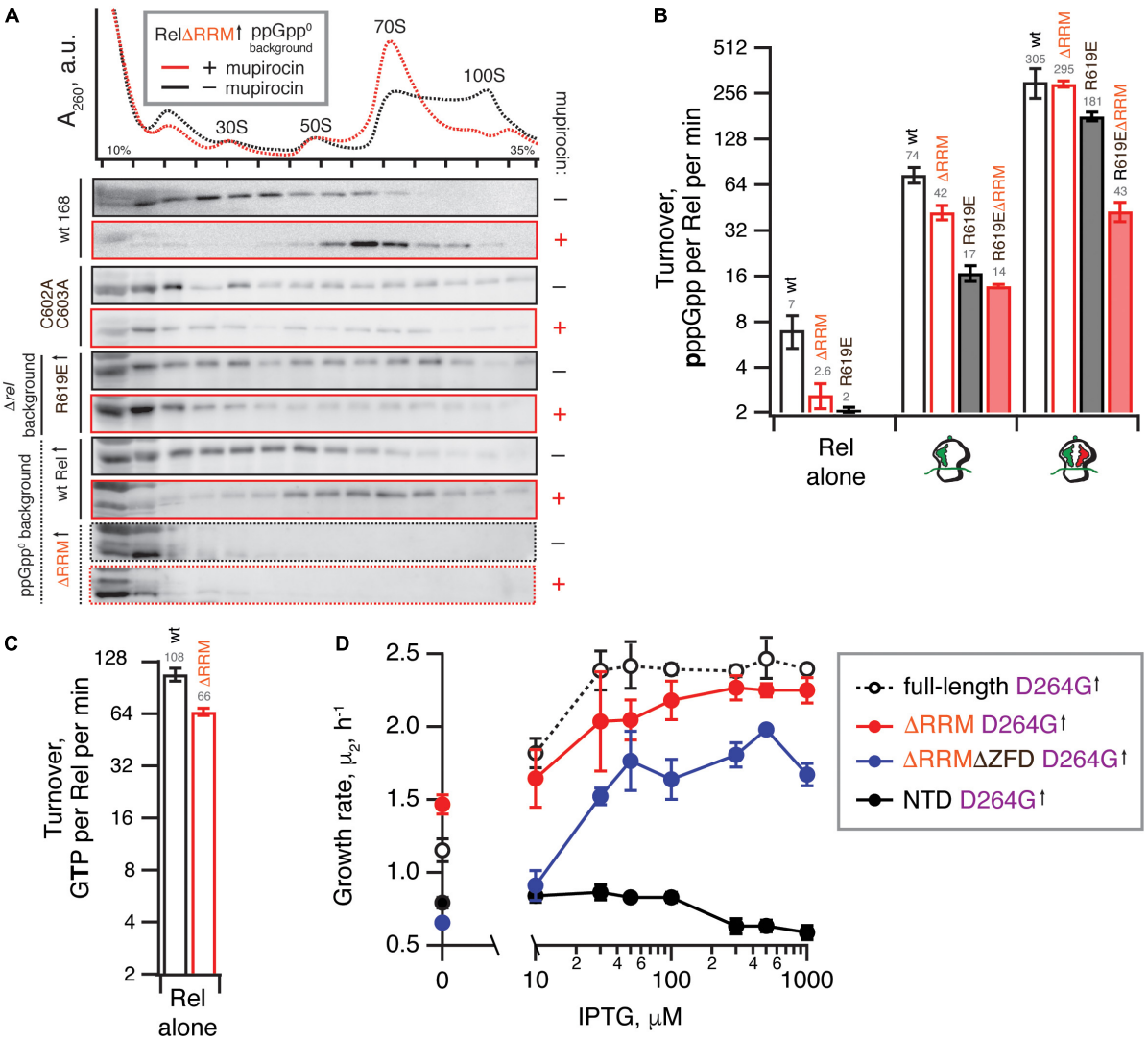

FIGURE 4 | Deletion of the regulatory RRM domain destabilizes Rel binding to starved ribosomal complexes and does not abrogate the hydrolysis activity. **(A)** Polysome profile and immunoblot analyses of Rel variants expressed either ectopically (↑) under the control of IPTG-inducible $P_{hy-spnak}$ promotor [ΔRRM Rel in ppGpp^0 *B. subtilis* (VHB184), R619E Rel in Δ*rel B. subtilis* (VHB282)] or from the native chromosomal locus [C602A C603A mutant (VHB144)]. Expression of Rel$^{\Delta RRM}$ was induced by 1 mM IPTG for 10 min followed by a 10 min challenge with 700 nM mupirocin. To drive the expression of R619E Rel, the strain was grown in LB supplemented with 1 mM IPTG. In the case of R619E and C602A C603A Rel the culture was treated with mupirocin for 20 min. Polysome profiles of all tested Rel variants are presented in **Supplementary Figure S5**, and an uncut version of a representative anti-Rel immunoblot is shown in **Supplementary Figure S2G**. **(B,C)** The effect of the RRM deletion on synthetic **(B)** and hydrolytic activity **(C)**. The effects of the RRM deletion and the R619E mutation on Rel synthetic activity were assayed either alone or in the presence of either initiation and starved ribosomal complexes. The error bars represent standard deviations of the turnover estimates by linear regression using four data points. **(D)** The effects of titratable expression of synthesis-inactive D264G mutants (full-length VHB156, ΔRRM VHB162, ΔRRMΔZFD VHB163 and Rel^{NTD} VHB164) on Δ*rel B. subtilis* growing on liquid LB medium at 37°C. The growth rates (μ^2) were calculated from three independent biological replicates and the error bars represent standard deviations.

interactions with starved ribosomes – on Rel's enzymatic activity in a reconstituted *B. subtilis* biochemical system.

Purification of RNA-Free Untagged *B. subtilis* Rel Requires Size-Exclusion Chromatography

To purify untagged *B. subtilis* Rel we combined our protocols used for purification of *E. coli* RelA (Turnbull et al., 2019) and *T. thermophilus* Rel (Van Nerom et al., 2019) (**Figure 5**). Importantly, during all of the chromatography steps we followed both absorbance at 260 and 280 nm complemented with SDS PAGE analysis of fractions. This is essential in order to identify and specifically pool the fractions containing Rel free from RNA contamination. After the initial capture using immobilized metal affinity chromatography (IMAC) in high ionic strength conditions (750 mM KCl) using HisTrap HP column charged with Zn^{2+} in order to avoid possible replacement of the Zn^{2+}

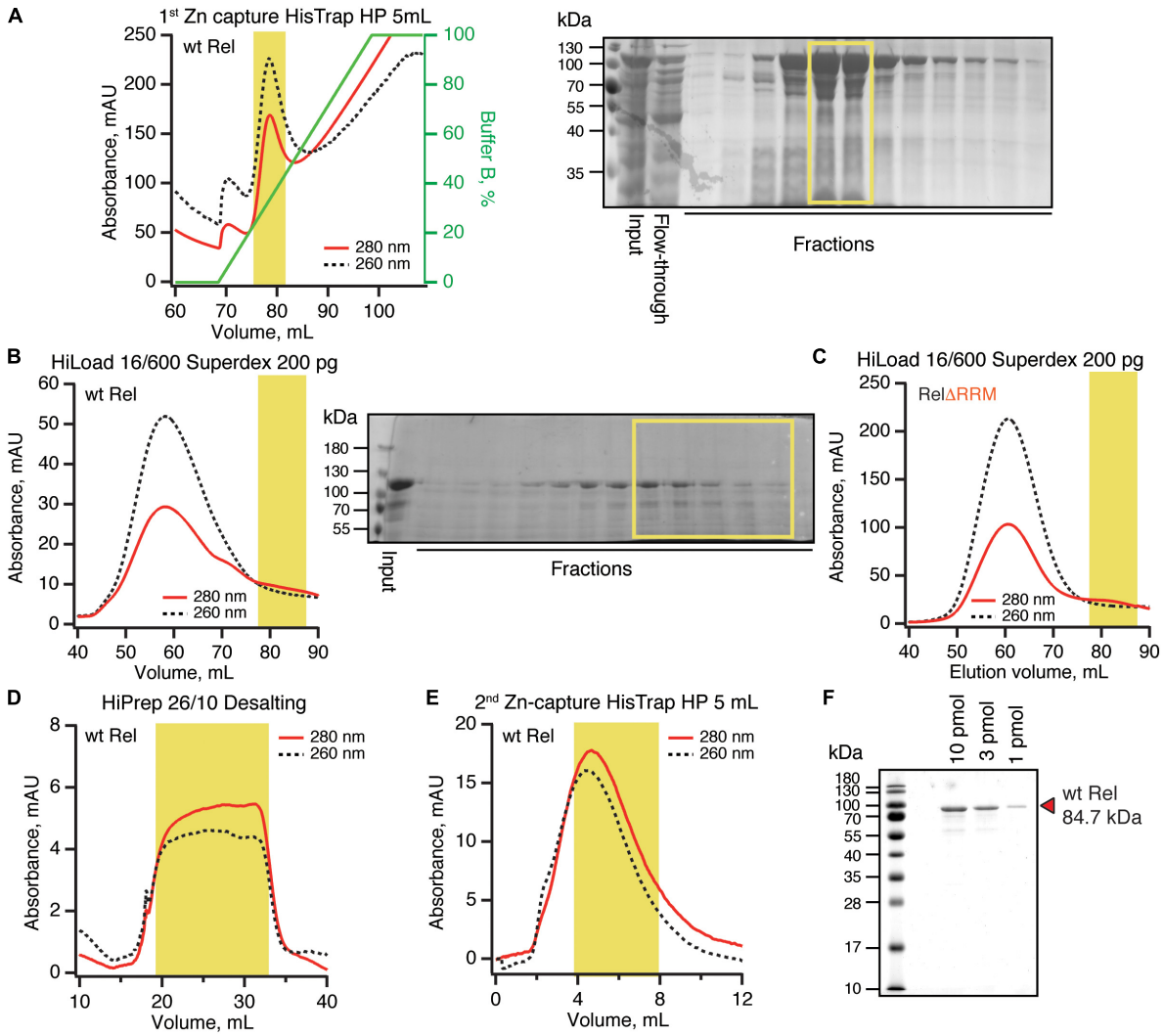

FIGURE 5 | Purification of RNA-free untagged *B. subtilis* Rel. N-terminally His_{10}-SUMO tagged RelA was overexpressed and purified as described in detail in *Materials and Methods*. **(A)** Cells were lysed and subjected to immobilized metal affinity chromatography (IMAC) using a Zn^{2+}-charged HisTrap 5 mL HP column. The fraction corresponding to Rel with the lowest contamination of nucleic acids (highlighted in yellow) was carried forward. Size-exclusion chromatography on HiLoad 16/600 Superdex 200 pg was used to further separate the RNA-free Rel fractions (**B:** full-length wild type Rel; **C:** ΔRRM Rel). Following the buffer exchange on HiPrep 10/26 desalting column **(D)**, the boxed-out fractions were pooled and the His_{10}-SUMO tag was cleaved off by the His_6-Ulp1 protease. **(E)** Native untagged Rel was separated from His_6-Ulp1 and the His_{10}-SUMO tag by the second round of IMAC. Highlighted fractions were pooled, concentrated, aliquoted, flash-frozen in liquid nitrogen and stored at –80°C. **(F)** SDS-PAGE analysis of the purified native untagged *B. subtilis* Rel.

in the ZFD domain by Ni^{2+} ions (Block et al., 2009), His_{10}-SUMO-Rel was applied on size-exclusion chromatography (SEC) on HiLoad 16/600 Superdex 200 pg column (**Figure 5D**). Both in the case of the full length (**Figure 5B**) and ΔRRM Rel (**Figure 5C**), the RNA-free fractions constitute the minority of the protein that elute considerably later than the bulk of the RNA-contaminated Rel. While the SEC step is essential for generating RNA-free Rel preparations, the majority of the protein prep is lost at this stage. After the SEC step, the buffer was exchanged to storage buffer containing arginine and glutamic acid that improve protein solubility and long-term stability (Golovanov et al., 2004) (**Figure 5D**), His_{10}-SUMO tag was cleaved off and removed by passing the protein via second IMAC (**Figure 5E**). The quality of the final preparations was assessed by SDS-PAGE (**Figure 5F** and **Supplementary Figure S6**) as well as spectrophotometrically: OD_{260}/OD_{280} ratio below 0.8 corresponding to less than 5% RNA contamination (Layne, 1957).

We have tested the effects of omission of the SEC step on the purification and activity of *B. subtilis* Rel preparations. Without the SEC step, the OD_{260}/OD_{280} ratio was dramatically higher (1.9), suggesting that, counterintuitively, the 'no SEC' Rel preparation predominantly contains not protein but RNA. We have resolved the sample on 15% SDS-PAGE (**Figure 6A**) and denaturating 1.2% agarose (2% formaldehyde) (**Figure 6B**) gels, as well as subjected the samples to negative staining electron microscopy (**Figure 6C**). While the SDS-PAGE gel revealed

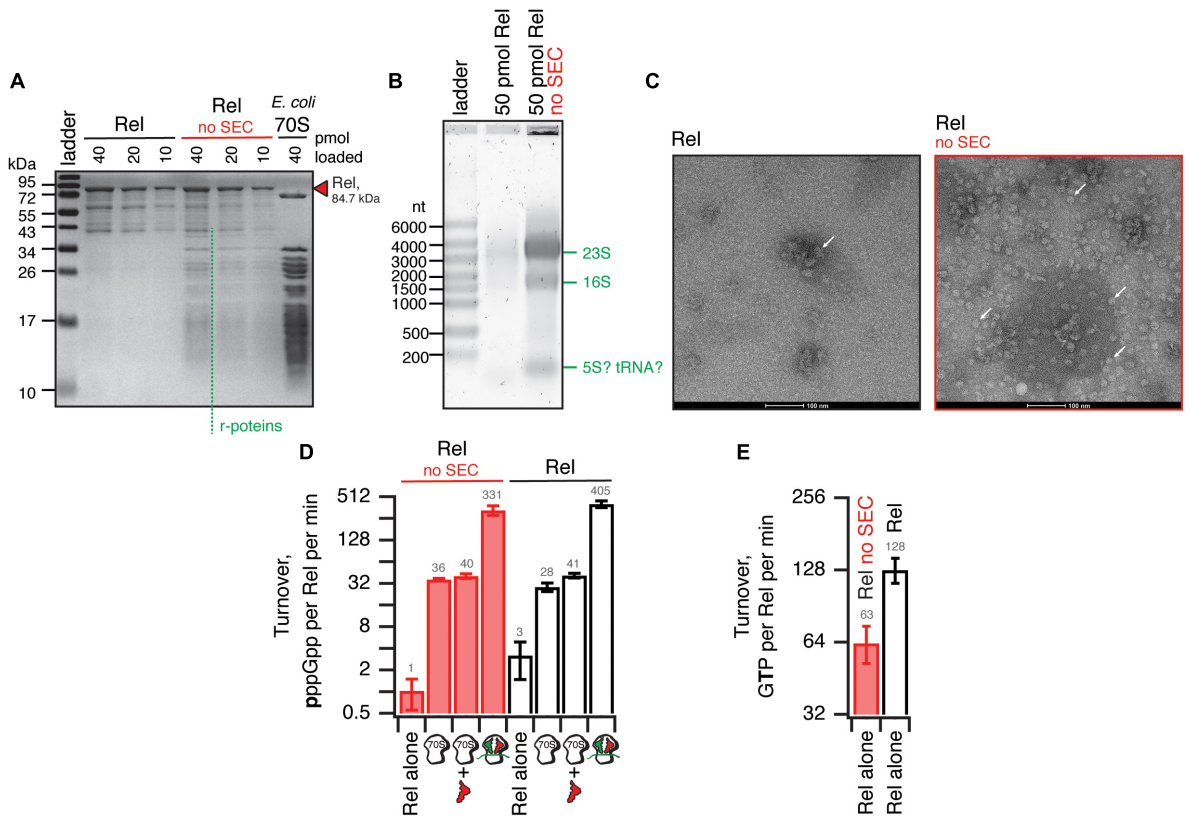

FIGURE 6 | Omission of the size-exclusion chromatography step results in sub-stoichiometric contamination of *B. subtilis* Rel preparations with *E. coli* ribosomal particles. **(A)** SDS-PAGE analysis of wild-type full-length Rel protein purified either as described in **Figure 5** or with the SEC step omitted (no SEC). Denaturing agarose gel **(B)** and negative staining electron microscopy **(C)** analyses of full-length Rel protein purified with and without the SEC step. Individual ribosomal particles are indicated with white arrows on **(C)**. Effects of the SEC omission on synthetase **(D)** and hydrolase **(E)** activity of *B. subtilis* Rel. The synthetase activity was assayed with either Rel alone or in the presence of 0.5 μM 70S, 70S supplemented with 2 μM deacylated $tRNA^{Val}$ and no mRNA or starved ribosomal complexes (0.5 μM 70S IC(MVF) supplemented with 2 μM deacylated $tRNA^{Val}$). The error bars represent standard deviations of the turnover estimates by linear regression using four data points.

multiple protein bands with Mw between 40 and 10 kDa, the agarose gel revealed that the RNA contaminant is dominated by three distinct populations of approximately 3000, 1500, and 100 nucleotides in length. Large (approximately 20 nm in diameter) particles are clearly visible on the to negative staining EM images. Collectively, this suggests that the RNA contamination is dominated by ribosomal particles, although it is unclear whether these are intact or partially degraded. Taking into account that 1 A_{260} corresponds to 23 pmol 70S particles, we estimate that our 'no SEC' preparations contain 45 nM 70S ribosomes per 1 μM Rel, which corresponds to sub-stoichiometric contamination of 5% of Rel being in complex, and 95% free. We next tested the effects of SEC omission on the enzymatic activity of Rel. The effects are exceedingly mild. The synthetase activity is virtually unaffected; importantly, activation by deacylated tRNA remains strictly mRNA-dependent, with $tRNA^{Val}$ inducing the enzymatic activity of 'no SEC' Rel only in the presence of 70S initiation complexes (70S IC) but not vacant 70S ribosomes (**Figure 6D**). Importantly, since ribosomes or starved complexes are added in our synthetase assays in excess over Rel (500 nM vs. 140 nM Rel), in the final reaction mixture purified ribosomes are in approximately 100x excess over the contaminant. Finally, the hydrolase activity of 'no SEC' Rel is approximately twofold lower (**Figure 6E**), which, however, could reflect variability in preparations.

Taken together, these results suggest that in the absence of a dedicated SEC step, Rel preparations are sub-stoichiometrically contaminated with ribosomes. While the effects of this contamination on the enzymatic activities of Rel are minor, it might interfere with other assays (see section *Discussion*).

The R619E ZFD Substitution Compromises Activation of *B. subtilis* $Rel^{\Delta RRM}$ by Starved Ribosomal Complexes

We tested the ^{3}H-pppGpp synthesis by full-length Rel as well as $Rel^{\Delta RRM}$, either alone or activated by the ribosomes or starved complexes in a reconstituted system (**Figure 4B**). When the protein is tested by itself, the $Rel^{\Delta RRM}$ mutant is less active than the full-length, suggesting that deletion of the RRM domain does not lead to the loss of auto-inhibition. While $Rel^{\Delta RRM}$ remains

less active than the full-length when activated by initiation complexes (about twofold), in the presence of starved ribosomal complexes the two proteins are equally active. This could be explained by tRNA stabilizing Rel on the ribosome and overriding the defect caused by the removal of the RRM domain.

The R619E mutation compromises activation of the full-length Rel by the initiation complexes (more than four-fold), and the effect is less pronounced in the presence of deacylated $tRNA^{Val}$ (less than twofold decrease in activity). Just as in the case of the RRM deletion, a possible explanation is that the deacylated tRNA strongly stimulates the binding of Rel to the ribosome and offsets the effect of the mutation R619E. When the R619E substitution is introduced into ΔRRM Rel, the combination of the two mutations destabilizing Rel binding to the ribosome results in compromised activation both by the initiation (five-fold) and starved (seven-fold) ribosomal complex. Despite several attempts we failed to generate sufficiently pure and soluble C602A C603A $Rel^{\Delta RRM}$, which precluded direct biochemical characterization of this mutant.

Taken together, our biochemical results demonstrate that while RRM is important in Rel recruitment to the ribosome, this domain is not absolutely essential for the activation of its (p)ppGpp synthesis activity by starved ribosomal complexes, which is consistent with the ribosome-dependent nature of the $Rel^{\Delta RRM}$ toxicity in live cells.

The RRM Deletion Moderately Decreases the Hydrolysis Activity of *B. subtilis* Rel

It was recently proposed that the RRM domain has a stimulatory effect on the hydrolysis activity of *C. crescentus* Rel, and the loss of this regulatory mechanism explains the toxicity of the ΔRRM mutant (Ronneau et al., 2019). This hypothesis does not explain the toxicity of the ΔRRM variant of the synthesis-only RSH RelA (**Figure 2** and Turnbull et al., 2019) and our microbiological experiments showing that the synthesis-defective ΔRRM D264G variant of *B. subtilis* Rel remains active as a (p)ppGpp hydrolase (**Figure 3A**). Importantly, the variant characterized by Ronneau et al. (2019) (*C. crescentus* $Rel^{\Delta 668-719}$) does not completely lack the RRM, and it is possible that the remaining beta-strand alpha-helix turn structural element was interfering with the hydrolysis activity of the construct.

Our enzymatic assays following ^{3}H-pppGpp degradation by full-length and $Rel^{\Delta RRM}$ show that the latter is approximately twice less active (**Figure 4C**). While the defect is detectable, it is quite minor. To test if the hydrolysis defect is more pronounced in the living cell, we re-tested the hydrolysis activity of synthesis-deficient SYNTH D264G full-length Rel as well as C-terminally truncated Rel variants in the Δ*rel* background using the growth rate (μ_2) as a proxy (**Figure 4D**). We modulated the expression levels by titrating the inducer, IPTG, from 10 to 1000 μM. In good agreement with the biochemical results demonstrating a minor defect in hydrolysis caused by deletion of the RRM domain, ΔRRM D264G Rel mutant promotes the growth of Δ*rel B. subtilis* only moderately less efficiently than the full-length D264G.

The Hydrolysis Activity of *B. subtilis* Rel Is Not Activated by Branched-Chain Amino Acids Binding to the RRM Domain

It was also recently reported that binding of branched-chain amino acids (BCAAs) to the ACT/RRM domain induces the hydrolysis activity of *Rhodobacter capsulatus* Rel (Fang and Bauer, 2018). The N651A substitution abrogates amino acid binding to *R. capsulatus* Rel^{CTD} and leads to (p)ppGpp accumulation in the cell, presumably due to lower hydrolysis activity of the mutant enzyme. It is, therefore, conceivable that *B. subtilis* $Rel^{\Delta RRM}$ is less hydrolytically active in the cell than the full-length protein due to the loss of BCAA-mediated activation. While the *B. subtilis* Rel^{CTD} fragment was shown to preferentially bind leucine with a K_D of 225 μM, no enzymatic assays were performed with this protein (Fang and Bauer, 2018). Notably, while the CTD region of *E. coli* RelA binds valine with high affinity (K_D of 2.85 μM) (Fang and Bauer, 2018), this interaction could not be regulating the hydrolysis activity of this synthesis-only RSH. It is, therefore, unclear whether *B. subtilis* Rel is, indeed, regulated by branched-chain amino acids similarly to *R. capsulatus* enzyme. Therefore, we tested the effect of 1 mM leucine on ^{3}H-pppGpp degradation by *B. subtilis* Rel. We detect no stimulatory effect (**Figure 7A**). Furthermore, when we introduced the N685A substitution (equivalent to N651A in *R. capsulatus*) in the chromosomal *rel* gene, we detected no growth defect in comparison to wild-type 168 *B. subtilis*, either on solid or liquid LB media (**Figures 7B–D**). Taken together, these results suggest that amino acid binding to RRM should not automatically be equated with regulation of the hydrolysis activity.

DISCUSSION

Taken together, our results demonstrate that (i) deletion of the RRM domain renders *B. subtilis* Rel and *E. coli* RelA toxic due to (p)ppGpp overproduction in a ribosome and tRNA-dependent manner, (ii) RRM deletion does not abrogate the (p)ppGpp hydrolysis activity of *B. subtilis* Rel, (iii) RRM deletion destabilizes the interaction of *B. subtilis* Rel with starved ribosomal complexes, and (iv) this destabilization renders the mutant enzyme more sensitive than the full length Rel to deactivation by additional substitutions further compromising its association with starved ribosomes. Our biochemical results do not explain why exactly ΔRRM Rel/RelA is toxic: *B. subtilis* $Rel^{\Delta RRM}$ behaves as a weaker binder of starved ribosomal complexes (**Figure 4A**) and is less enzymatically active in (p)ppGpp synthesis assays (**Figures 4B,C**) as compared to the full-length Rel. A dedicated follow-up study is necessary to clarify this question. *E. coli* $RelA^{\Delta RRM}$ displays a similar – although more pronounced – defect in activation by starved ribosomal complexes (Takada et al., 2020).

Our report expands the mutation toolbox for dissecting the molecular mechanisms of long RSH enzymes. We confirm that, as was shown for H432E *E. coli* RelA mutant (Winther et al., 2018), the corresponding H420E mutation in *B. subtilis* Rel is a useful tool for specifically abrogating activation of Rel by starved

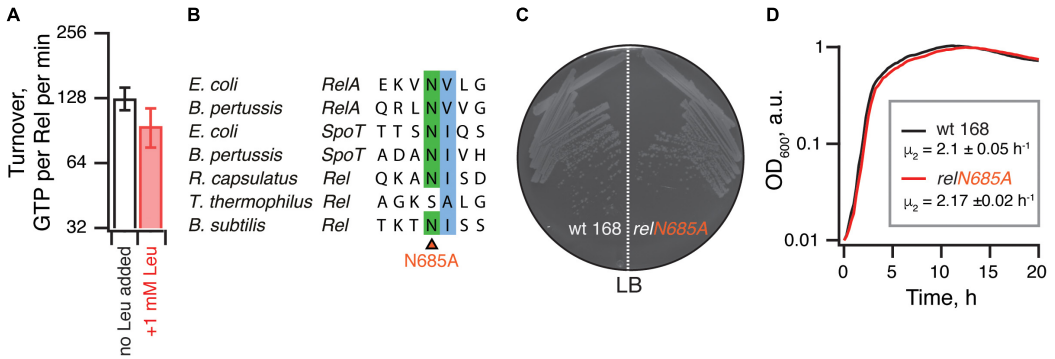

FIGURE 7 | The hydrolysis activity of *B. subtilis* Rel is not activated by branched-chain amino acids binding to the RRM domain. **(A)** Hydrolase activity of *B. subtilis* Rel is not stimulated by leucine. The experiments were performed in HEPES:Polymix buffer, pH 7.5 at 37°C in the presence of 5 mM Mg^{2+}. Error bars represent standard deviations of the turnover estimates by linear regression using four data points. **(B)** Sequence alignment of the *B. subtilis* N685 region of representative long RSHs. **(C,D)** Wild-type *B. subtilis* 168 and isogenic chromosomal *relN685A* mutant (VHB455) were grown on solid **(C)** and liquid **(D)** LB media at 37°C. The plate was scored after 12 h at 37°C. The growth rates (μ^2) were calculated from three independent biological replicates and the error bars (shown as shadows) represent standard deviations. Since the liquid media growth experiments were performed in plates format in Bioscreen C growth curve analysis system the OD_{600} is presented in arbitrary units.

ribosomal complexes. Additionally, we demonstrate the utility of two novel mutations in the ZFD domain: R619E (R629E in *E. coli* RelA) as well as a double C602A C603A substitution (C612A C613A in *E. coli* RelA). While these mutations do not completely abrogate the activation, acting in epistasis they can be employed to reveal weaker phenotypes or effects, as was shown in the current work when the mutations were combined with RRM/ACT deletion.

Finally, we would like to draw the attention of the research community working on long RSH enzymes to technical aspects of protein purification. It is common to purify Rel/RelA for biochemical experiments using a single-step purification [for example (Wood et al., 2019)]. However, both RelA (Turnbull et al., 2019) and Rel have a strong tendency for RNA contamination and multiple additional steps are necessary to remove this contaminant. Therefore, reporting the 260/280 absorbance ratio of the final preparations is essential. RNA-free protein preparations typically have a 260/280 absorbance ratio of 0.57, but this parameter can vary depending on the amino acid composition, specifically the abundance of tryptophan and phenylalanine (Layne, 1957). Without extra steps to remove RNA contamination, single-step preparations are likely to be heavily contaminated with ribosomal particles (**Figure 6**), which is likely to interfere with the estimation of the oligomerization state of Rel, since the RNA-bound protein elutes much earlier than the RNA-free fraction (**Figures 5B,C**). This contamination may explain the surprising observation that the addition of Ni-NTA purified *S. aureus* Rel inhibits the 50S assembly factor DEAD-box RNA helicase CshA (Wood et al., 2019). The unlabeled contaminating ribosomal particles could potentially be recognized by CshA, thus acting as a competitor in the helicase assay that uses a synthetic Cy3-labeled RNA duplex as a substrate. It is also plausible that formation of stable complexes of Rel with ribosomes in live *E. coli* could generate false-positive signals in bacterial two-hybrid assays, accounting for the observed protein-protein interaction between *S. aureus* Rel and the ribosome assembly factors Era and CshA (Wood et al., 2019).

DATA AVAILABILITY STATEMENT

The datasets generated for this study are available on request to the corresponding author.

AUTHOR CONTRIBUTIONS

HT conceived the study. HT, MR, and VH designed the experiments. HT performed the experiments with *B. subtilis* Rel. ID and MR performed the experiments with *E. coli* RelA. VM performed the electron microscopy. RM and GA contributed tools and reagents. GCA and AG-P performed the structure and sequence analyses. HT and VH drafted and revised the manuscript with contributions from MR, AG-P, and GCA. All authors have read and approved the final version of this manuscript.

FUNDING

This work was supported by the European Regional Development Fund through the Centre of Excellence for Molecular Cell Technology (VH), the Molecular Infection Medicine Sweden (MIMS) (VH), Swedish Research Council (Grant Nos 2017-03783 to VH and 2015-04746 to GCA), Ragnar Söderberg Foundation (VH), Umeå Centre for Microbial Research (UCMR) (postdoctoral grant 2017 to HT), MIMS Excellence by Choice Postdoctoral Fellowship Programme (MR), the Fonds National de la Recherche Scientifique (Grant Nos FRFS-WELBIO CR-2017S-03, FNRS CDR J.0068.19, and FNRS-PDR T.0066.18 to AG-P) and the Fonds Jean Brachet and the Fondation Van Buuren (AG-P).

ACKNOWLEDGMENTS

We would like to thank the Protein Expertise Platform (PEP) at Umeå University and Mikael Lindberg for constructing pET24d:*His*$_{10}$-*SUMO*-based expression constructs and purifying His$_6$-Ulp1, we would also like to thank Tetiana Brodiazhenko for construction of the pMG25-based RelA and SpoT plasmids, and Julien Caballero-Montes for comments on the manuscript. The manuscript was deposited as a preprint to bioRxiv (Takada et al., 2019). The electron microscopy data was collected at the Umeå Core Facility for Electron Microscopy, a node of the Cryo-EM Swedish National Facility, funded by the Knut and Alice Wallenberg, Family Erling Persson and Kempe Foundations, SciLifeLab, Stockholm University, and Umeå University.

SUPPLEMENTARY MATERIAL

The Supplementary Material for this article can be found online at: https://www.frontiersin.org/articles/10.3389/fmicb.2020.00277/full#supplementary-material

REFERENCES

Agirrezabala, X., Fernandez, I. S., Kelley, A. C., Carton, D. G., Ramakrishnan, V., and Valle, M. (2013). The ribosome triggers the stringent response by RelA via a highly distorted tRNA. *EMBO Rep.* 14, 811–816. doi: 10.1038/embor.2013.106

Akanuma, G., Kazo, Y., Tagami, K., Hiraoka, H., Yano, K., Suzuki, S., et al. (2016). Ribosome dimerization is essential for the efficient regrowth of *Bacillus subtilis*. *Microbiology* 162, 448–458. doi: 10.1099/mic.0.000234

Antoun, A., Pavlov, M. Y., Tenson, T., and Ehrenberg, M. M. (2004). Ribosome formation from subunits studied by stopped-flow and Rayleigh light scattering. *Biol. Proced. Online* 6, 35–54. doi: 10.1251/bpo71

Arenz, S., Abdelshahid, M., Sohmen, D., Payoe, R., Starosta, A. L., Berninghausen, O., et al. (2016). The stringent factor RelA adopts an open conformation on the ribosome to stimulate ppGpp synthesis. *Nucleic Acids Res.* 44, 6471–6481. doi: 10.1093/nar/gkw470

Atkinson, G. C., Tenson, T., and Hauryliuk, V. (2011). The RelA/SpoT homolog (RSH) superfamily: distribution and functional evolution of ppGpp synthetases and hydrolases across the tree of life. *PLoS One* 6:e23479. doi: 10.1371/journal.pone.0023479

Avarbock, A., Avarbock, D., Teh, J. S., Buckstein, M., Wang, Z. M., and Rubin, H. (2005). Functional regulation of the opposing (p)ppGpp synthetase/hydrolase activities of RelMtb from *Mycobacterium tuberculosis*. *Biochemistry* 44, 9913–9923. doi: 10.1021/bi0505316

Avarbock, D., Avarbock, A., and Rubin, H. (2000). Differential regulation of opposing RelMtb activities by the aminoacylation state of a tRNA. ribosome. mRNA. RelMtb complex. *Biochemistry* 39, 11640–11648. doi: 10.1021/bi001256k

Beljantseva, J., Kudrin, P., Andresen, L., Shingler, V., Atkinson, G. C., Tenson, T., et al. (2017). Negative allosteric regulation of *Enterococcus faecalis* small alarmone synthetase RelQ by single-stranded RNA. *Proc. Natl. Acad. Sci. U.S.A.* 114, 3726–3731. doi: 10.1073/pnas.1617868114

Block, H., Maertens, B., Spriestersbach, A., Brinker, N., Kubicek, J., Fabis, R., et al. (2009). Immobilized-metal affinity chromatography (IMAC): a review. *Methods Enzymol.* 463, 439–473. doi: 10.1016/S0076-6879(09)63027-5

Boutte, C. C., and Crosson, S. (2011). The complex logic of stringent response regulation in *Caulobacter crescentus*: starvation signalling in an oligotrophic environment. *Mol. Microbiol.* 80, 695–714. doi: 10.1111/j.1365-2958.2011.07602.x

Britton, R. A., Eichenberger, P., Gonzalez-Pastor, J. E., Fawcett, P., Monson, R., Losick, R., et al. (2002). Genome-wide analysis of the stationary-phase sigma factor (sigma-H) regulon of *Bacillus subtilis*. *J. Bacteriol.* 184, 4881–4890. doi: 10.1128/jb.184.17.4881-4890.2002

Brodiazhenko, T., Johansson, M. J. O., Takada, H., Nissan, T., Hauryliuk, V., and Murina, V. (2018). Elimination of ribosome inactivating factors improves the efficiency of *Bacillus subtilis* and *Saccharomyces cerevisiae* cell-free translation systems. *Front. Microbiol.* 9:3041. doi: 10.3389/fmicb.2018.03041

Brown, A., Fernandez, I. S., Gordiyenko, Y., and Ramakrishnan, V. (2016). Ribosome-dependent activation of stringent control. *Nature* 534, 277–280. doi: 10.1038/nature17675

Dalebroux, Z. D., Svensson, S. L., Gaynor, E. C., and Swanson, M. S. (2010). ppGpp conjures bacterial virulence. *Microbiol. Mol. Biol. Rev.* 74, 171–199. doi: 10.1128/MMBR.00046-09

Dalebroux, Z. D., and Swanson, M. S. (2012). ppGpp: magic beyond RNA polymerase. *Nat. Rev. Microbiol.* 10, 203–212. doi: 10.1038/nrmicro2720

Fang, M., and Bauer, C. E. (2018). Regulation of stringent factor by branched-chain amino acids. *Proc. Natl. Acad. Sci. U.S.A.* 115, 6446–6451. doi: 10.1073/pnas.1803220115

Geiger, T., Kastle, B., Gratani, F. L., Goerke, C., and Wolz, C. (2014). Two small (p)ppGpp synthases in *Staphylococcus aureus* mediate tolerance against cell envelope stress conditions. *J. Bacteriol.* 196, 894–902. doi: 10.1128/JB.01201-13

Golovanov, A. P., Hautbergue, G. M., Wilson, S. A., and Lian, L. Y. (2004). A simple method for improving protein solubility and long-term stability. *J. Am. Chem. Soc.* 126, 8933–8939. doi: 10.1021/ja049297h

Gratani, F. L., Horvatek, P., Geiger, T., Borisova, M., Mayer, C., Grin, I., et al. (2018). Regulation of the opposing (p)ppGpp synthetase and hydrolase activities in a bifunctional RelA/SpoT homologue from *Staphylococcus aureus*. *PLoS Genet.* 14:e1007514. doi: 10.1371/journal.pgen.1007514

Gropp, M., Strausz, Y., Gross, M., and Glaser, G. (2001). Regulation of *Escherichia coli* RelA requires oligomerization of the C-terminal domain. *J. Bacteriol.* 183, 570–579. o doi: 10.1128/jb.183.2.570-579.2001

Haseltine, W. A., and Block, R. (1973). Synthesis f guanosine tetra- and pentaphosphate requires the presence of a codon-specific, uncharged transfer ribonucleic acid in the acceptor site of ribosomes. *Proc. Natl. Acad. Sci. U.S.A.* 70, 1564–1568. doi: 10.1073/pnas.70.5.1564

Hauryliuk, V., Atkinson, G. C., Murakami, K. S., Tenson, T., and Gerdes, K. (2015). Recent functional insights into the role of (p)ppGpp in bacterial physiology. *Nat. Rev. Microbiol.* 13, 298–309. doi: 10.1038/nrmicro3448

Inabe, T. (2005). Mellitate anions: unique anionic component with supramolecular self-organizing properties. *J. Mater. Chem.* 15, 1317–1328.

Jiang, M., Sullivan, S. M., Wout, P. K., and Maddock, J. R. (2007). G-protein control of the ribosome-associated stress response protein SpoT. *J. Bacteriol.* 189, 6140–6147. doi: 10.1128/jb.00315-07

Jimmy, S., Saha, C. K., Stavropoulos, C., Garcia-Pino, A., Hauryliuk, V., and Atkinson, G. C. (2019). Discovery of small alarmone synthetases and their inhibitors as toxin-antitoxin loci. *bioXriv* [Preprint]. doi: 10.1101/575399

Katoh, K., and Standley, D. M. (2013). MAFFT multiple sequence alignment software version 7: improvements in performance and usability. *Mol. Biol. Evol.* 30, 772–780. doi: 10.1093/molbev/mst010

Kudrin, P., Dzhygyr, I., Ishiguro, K., Beljantseva, J., Maksimova, E., Oliveira, S. R. A., et al. (2018). The ribosomal A-site finger is crucial for binding and activation of the stringent factor RelA. *Nucleic Acids Res.* 46, 1973–1983. doi: 10.1093/nar/gky023

Kudrin, P., Varik, V., Oliveira, S. R., Beljantseva, J., Del Peso Santos, T., Dzhygyr, I., et al. (2017). Subinhibitory concentrations of bacteriostatic antibiotics induce *relA*-dependent and *relA*-independent tolerance to beta-Lactams. *Antimicrob. Agents Chemother.* 61:e02173-16. doi: 10.1128/AAC.02173-16

Kushwaha, G. S., Oyeyemi, B. F., and Bhavesh, N. S. (2019). Stringent response protein as a potential target to intervene persistent bacterial infection. *Biochimie* 165, 67–75. doi: 10.1016/j.biochi.2019.07.006

Layne, E. (1957). Spectrophotometric and turbidimetric methods for measuring proteins. *Methods Enzymol.* 3, 447–454. doi: 10.1016/s0076-6879(57)03413-8

Liu, K., Bittner, A. N., and Wang, J. D. (2015). Diversity in (p)ppGpp metabolism and effectors. *Curr. Opin. Microbiol.* 24, 72–79. doi: 10.1016/j.mib.2015.01.012

Loveland, A. B., Bah, E., Madireddy, R., Zhang, Y., Brilot, A. F., Grigorieff, N., et al. (2016). Ribosome*RelA structures reveal the mechanism of stringent response activation. *eLife* 5:e17029. doi: 10.7554/eLife.17029

Mechold, U., Murphy, H., Brown, L., and Cashel, M. (2002). Intramolecular regulation of the opposing (p)ppGpp catalytic activities of Rel(Seq), the Rel/Spo enzyme from *Streptococcus equisimilis*. *J. Bacteriol.* 184, 2878–2888. doi: 10.1128/jb.184.11.2878-2888.2002

Mittenhuber, G. (2001). Comparative genomics and evolution of genes encoding bacterial (p)ppGpp synthetases/hydrolases (the Rel, RelA and SpoT proteins). *J. Mol. Microbiol. Biotechnol.* 3, 585–600.

Molin, S., Stougaard, P., Uhlin, B. E., Gustafsson, P., and Nordstrom, K. (1979). Clustering of genes involved in replication, copy number control, incompatibility, and stable maintenance of the resistance plasmid R1drd-19. *J. Bacteriol.* 138, 70–79. doi: 10.1128/jb.138.1.70-79.1979

Murina, V., Kasari, M., Hauryliuk, V., and Atkinson, G. C. (2018a). Antibiotic resistance ABCF proteins reset the peptidyl transferase centre of the ribosome to counter translational arrest. *Nucleic Acids Res.* 46, 3753–3763. doi: 10.1093/nar/gky050

Murina, V., Kasari, M., Takada, H., Hinnu, M., Saha, C. K., Grimshaw, J. W., et al. (2018b). ABCF ATPases involved in protein synthesis, ribosome assembly and antibiotic resistance: structural and functional diversification across the tree of life. *J. Mol. Biol.* 431, 3568–3590. doi: 10.1016/j.jmb.2018.12.013

Nanamiya, H., Kasai, K., Nozawa, A., Yun, C. S., Narisawa, T., Murakami, K., et al. (2008). Identification and functional analysis of novel (p)ppGpp synthetase genes in *Bacillus subtilis*. *Mol. Microbiol.* 67, 291–304. doi: 10.1111/j.1365-2958.2007.06018.x

Parker, J., Watson, R. J., and Friesen, J. D. (1976). A relaxed mutant with an altered ribosomal protein L11. *Mol. Gen. Genet.* 144, 111–114. doi: 10.1007/bf00277313

Ronneau, S., Caballero-Montes, J., Coppine, J., Mayard, A., Garcia-Pino, A., and Hallez, R. (2019). Regulation of (p)ppGpp hydrolysis by a conserved archetypal regulatory domain. *Nucleic Acids Res.* 47, 843–854. doi: 10.1093/nar/gky1201

Schreiber, G., Metzger, S., Aizenman, E., Roza, S., Cashel, M., and Glaser, G. (1991). Overexpression of the relA gene in *Escherichia coli*. *J. Biol. Chem.* 266, 3760–3767.

Shyp, V., Tankov, S., Ermakov, A., Kudrin, P., English, B. P., Ehrenberg, M., et al. (2012). Positive allosteric feedback regulation of the stringent response enzyme RelA by its product. *EMBO Rep.* 13, 835–839. doi: 10.1038/embor.2012.106

Spizizen, J. (1958). Transformation of biochemically deficient strains of *Bacillus subtilis* by deoxyribonucleate. *Proc. Natl. Acad. Sci. U.S.A.* 44, 1072–1078. doi: 10.1073/pnas.44.10.1072

Steinchen, W., and Bange, G. (2016). The magic dance of the alarmones (p)ppGpp. *Mol. Microbiol.* 101, 531–544. doi: 10.1111/mmi.13412

Tagami, K., Nanamiya, H., Kazo, Y., Maehashi, M., Suzuki, S., Namba, E., et al. (2012). Expression of a small (p)ppGpp synthetase, YwaC, in the (p)ppGpp(0) mutant of *Bacillus subtilis* triggers YvyD-dependent dimerization of ribosome. *Microbiologyopen* 1, 115–134. doi: 10.1002/mbo3.16

Takada, H., Roghanian, M., Caballero-Montes, J., Van Nerom, K., Jimmy, S., Kudrin, P., et al. (2020). Ribosome association primes the stringent factor Rel for recruitment of deacylated tRNA to ribosomal A-site. *bioRxiv* [Preprint]. doi: 10.1101/2020.01.17.910273

Takada, H., Roghanian, M., Murina, V., Dzhygyr, I., Murayama, R., Akanuma, G., et al. (2019). The C-terminal RRM/ACT domain is crucial for fine-tuning the activation of 'long' RelA-SpoT Homolog enzymes by ribosomal complexes. *bioRxiv* [Preprint], doi: 10.1101/849810

Tamman, H., Van Nerom, K., Takada, H., Vandenberk, S., Polikanov, Y., Hofkens, J., et al. (2019). Nucleotide-mediated allosteric regulation of bifunctional Rel enzymes. *bioRxiv* [Preptint], doi: 10.1101/670703

Thomas, C. M., Hothersall, J., Willis, C. L., and Simpson, T. J. (2010). Resistance to and synthesis of the antibiotic mupirocin. *Nat. Rev. Microbiol.* 8, 281–289. doi: 10.1038/nrmicro2278

Turnbull, K. J., Dzhygyr, I., Lindemose, S., Hauryliuk, V., and Roghanian, M. (2019). Intramolecular interactions dominate the autoregulation of *Escherichia coli* stringent factor RelA. *Front. Microbiol.* 10:1966. doi: 10.3389/fmicb.2019.01966

Van Nerom, K., Tamman, H., Takada, H., Hauryliuk, V., and Garcia-Pino, A. (2019). The Rel stringent factor from *Thermus thermophilus*: crystallization and X-ray analysis. *Acta Crystallogr. F Struct. Biol. Commun.* 75, 561–569. doi: 10.1107/S2053230X19010628

Waterhouse, A. M., Procter, J. B., Martin, D. M., Clamp, M., and Barton, G. J. (2009). Jalview Version 2–a multiple sequence alignment editor and analysis workbench. *Bioinformatics* 25, 1189–1191. doi: 10.1093/bioinformatics/btp033

Wendrich, T. M., Blaha, G., Wilson, D. N., Marahiel, M. A., and Nierhaus, K. H. (2002). Dissection of the mechanism for the stringent factor RelA. *Mol. Cell* 10, 779–788. doi: 10.1016/s1097-2765(02)00656-1

Wilkinson, R. C., Batten, L. E., Wells, N. J., Oyston, P. C., and Roach, P. L. (2015). Biochemical studies on *Francisella tularensis* RelA in (p)ppGpp biosynthesis. *Biosci. Rep.* 35:e00268. doi: 10.1042/BSR20150229

Winther, K. S., Roghanian, M., and Gerdes, K. (2018). Activation of the stringent response by loading of RelA-tRNA complexes at the ribosomal A-site. *Mol. Cell* 70, 95–105.e4. doi: 10.1016/j.molcel.2018.02.033

Wood, A., Irving, S. E., Bennison, D. J., and Corrigan, R. M. (2019). The (p)ppGpp-binding GTPase Era promotes rRNA processing and cold adaptation in *Staphylococcus aureus*. *PLoS Genet.* 15:e1008346. doi: 10.1371/journal.pgen.1008346

Xiao, H., Kalman, M., Ikehara, K., Zemel, S., Glaser, G., and Cashel, M. (1991). Residual guanosine 3',5'-bispyrophosphate synthetic activity of *relA* null mutants can be eliminated by *spoT* null mutations. *J. Biol. Chem.* 266, 5980–5990.

Yang, N., Xie, S., Tang, N. Y., Choi, M. Y., Wang, Y., and Watt, R. M. (2019). The Ps and Qs of alarmone synthesis in *Staphylococcus aureus*. *PLoS One* 14:e0213630. doi: 10.1371/journal.pone.0213630

Conflict of Interest: The authors declare that the research was conducted in the absence of any commercial or financial relationships that could be construed as a potential conflict of interest.

frontiers in Microbiology

ORIGINAL RESEARCH
published: 04 August 2020
doi: 10.3389/fmicb.2020.01856

SlyA Transcriptional Regulator Is Not Directly Affected by ppGpp Levels

*Julia Bartoli[1], Julie Pamela Viala[1] and Emmanuelle Bouveret[2]**

[1] LISM, Institut de Microbiologie de la Méditerranée, CNRS, Aix-Marseille University, Marseille, France, [2] SAMe Unit, Microbiology Department, Pasteur Institute, Paris, France

The SlyA transcriptional regulator controls the expression of genes involved in virulence and production of surface components in *S. Typhimurium* and *E. coli*. Its mode of action is mainly explained by its antagonism with the H-NS repressor for the same DNA binding regions. Interestingly, it has been reported that the alarmone ppGpp promotes SlyA dimerization and DNA binding at the promoter of *pagC*, enhancing the expression of this gene in *Salmonella*. A recurring problem in the field of stringent response has been to find a way of following ppGpp levels *in vivo* in real time. We thought that SlyA, as a ppGpp responsive ligand, was a perfect candidate for the development of a specific ppGpp biosensor. Therefore, we decided to characterize in depth this SlyA control by ppGpp. However, using various genes whose expression is activated by SlyA, as reporters, we showed that ppGpp does not affect SlyA regulation *in vivo*. In addition, modulating ppGpp levels did not affect SlyA dimerization *in vivo*, and did not impact its binding to DNA *in vitro*. We finally showed that ppGpp is required for the expression of *hlyE* in *E. coli*, a gene also activated by SlyA, and propose that both regulators are independently required for *hlyE* expression. The initial report of ppGpp action on SlyA might be explained by a similar action of SlyA and ppGpp on *pagC* expression, and the complexity of promoters controlled by several global regulators, such as the promoters of *pagC* in *Salmonella* or *hlyE* in *E. coli*.

Keywords: SlyA, ppGpp, *Escherichia coli*, stress response, *hlyE*

OPEN ACCESS

Edited by:
Michael Cashel, Eunice Kennedy Shriver National Institute of Child Health and Human Development (NICHD), United States

Reviewed by:
William Ryan Will, University of Washington, United States
Carlos Balsalobre, University of Barcelona, Spain
Gert Bange, University of Marburg, Germany

****Correspondence:***
Emmanuelle Bouveret
emmanuelle.bouveret@pasteur.fr

Specialty section:
This article was submitted to Microbial Physiology and Metabolism, a section of the journal Frontiers in Microbiology

Received: *24 April 2020*
Accepted: *15 July 2020*
Published: *04 August 2020*

Citation:
Bartoli J, Viala JP and Bouveret E (2020) SlyA Transcriptional Regulator Is Not Directly Affected by ppGpp Levels. Front. Microbiol. 11:1856. doi: 10.3389/fmicb.2020.01856

INTRODUCTION

SlyA is a transcriptional regulator that belongs to the MarR superfamily of regulators (Will and Fang, 2020). Since its discovery as an inducer of hemolytic activity (Libby et al., 1994), several genes have been shown to be regulated by SlyA in *Salmonella enterica* and in *Escherichia coli*, however their regulons are different in these two bacteria. In *Salmonella*, SlyA controls the expression of genes required for virulence (Navarre et al., 2005; Ellison and Miller, 2006). A *slyA* mutant is impaired for growth within macrophages and is hyper susceptible to oxidative stress (Ellison and Miller, 2006). In *E. coli*, SlyA activates the expression of the cryptic hemolysin *hlyE* (*clyA*) (Wyborn et al., 2004; Lithgow et al., 2007), of Type1 fimbriae (McVicker et al., 2011), of *pagP* involved in lipid A palmitoylation in biofilm (Chalabaev et al., 2014), and of K5 capsule gene cluster (Corbett et al., 2007). In addition to these reports on specific genes, a global study has recently expanded the proposed repertoire of the SlyA regulon in *E. coli*, with cryptic genes coding for potential fimbrial-like adhesins that contribute to biofilm formation (Curran et al., 2017). Furthermore, this latter study permitted the refinement of a SlyA binding motif in *E. coli*.

Abbreviations: *E. coli*, *Escherichia coli*; GFP, green fluorescent protein; ppGpp, guanosine tetraphosphate.

SlyA binds DNA as a dimer. It functions mainly as counter-silencer by antagonizing and displacing the H-NS repressor (Stoebel et al., 2008; Will et al., 2015). Interestingly, in *E. coli*, *slyA* expression is positively autoregulated, independently of H-NS (Corbett et al., 2007). However, the majority of SlyA targets reported so far are known or predicted to be repressed by H-NS (Curran et al., 2017). The condition of induction of *slyA* itself or the potential ligand molecule of SlyA have not been elucidated. SlyA has been crystalized with a bound salicylate molecule and it was shown *in vitro* that this binding inhibited SlyA binding to DNA (Dolan et al., 2011; Will et al., 2019).

It has been reported that ppGpp nucleotide promotes SlyA dimerization and binding to its target promoters in *Salmonella*, and that ppGpp is required for SlyA activity *in vivo* (Zhao et al., 2008). ppGpp is an important nucleotide acting as a secondary messenger of the stringent response (Potrykus and Cashel, 2008). This global stress response plays a central role in the physiology of bacteria, and its main role is to slow down ribosome biosynthesis and activity while promoting survival programs. This response has been the subject of a strong and renewed interest in the last years when its importance in pathogenicity and resistance to antibiotics has been (re)discovered (Dalebroux et al., 2010; Hobbs and Boraston, 2019). There are two main modes of action of ppGpp, whose relative importances depend on bacteria:in *E. coli* and closely related bacteria, ppGpp binds RNAP in conjunction with DksA, influencing globally the transcriptome landscape of the cell (Gourse et al., 2018). In addition, ppGpp inhibits enzymes of the guanosine synthesis pathway and ribosomal GTPases (Bennison et al., 2019). The possible allosteric regulation of SlyA by ppGpp triggered high interest at the time, as shown by its highlight in an important review discussing the role of ppGpp in virulence (Dalebroux et al., 2010). If validated, this behavior might have provided a good base for the design of direct ppGpp biosensors that are still missing in the field for live detection and/or imaging of ppGpp in bacteria. However, there has been no further mention of this result or follow-up in the literature. It was only mentioned in a discussion that ppGpp was not required for *fimB* activation by SlyA in *E. coli* (McVicker et al., 2011).

Therefore, we decided to study and characterize clearly this proposed role of ppGpp in controlling SlyA mechanism. The results presented here, based on a combination of genetics, molecular, and biochemical approaches, show that ppGpp is not directly involved in the molecular mechanism of SlyA dimerization and DNA binding. However, for some SlyA regulated genes (like *hlyE* in *E. coli* or *pagCD* in *Salmonella*), complex regulation network involving H-NS and other global regulators might explain indirect ppGpp effects.

MATERIALS AND METHODS

Plasmid Constructions

Plasmid constructions are described succinctly in **Table 1**. The *slyA* ORFs from *E. coli* or *Salmonella enterica* s. Typhimurium 12023 were amplified by PCR on genomic DNA template using the indicated oligonucleotides and cloned in the pBAD24 (pEB227) and pET-6His-Tev vectors (pEB1188).

Transcriptional fusions with GFP were constructed in the pUA66 (pEB898) or pUA139 (pEB987) vector backbone (Zaslaver et al., 2006). When available, transcriptional fusions were retrieved from the Zaslaver collection (Zaslaver et al., 2006), or else the promoter regions were PCR amplified using the oligonucleotides listed in **Table 2** and cloned between XhoI and BamHI restriction sites. The Ecocyc website (Karp et al., 2018) was used for sequence retrieval.

Strain Constructions

The construction of the various strains is described succinctly in **Table 3**. Insertion of the 3Flag sequence in fusion with the *slyA* ORF on the chromosome was done by direct recombination of a PCR fragment amplified with oligonucleotides ebm1855/1856 and pJL148 plasmid (Zeghouf et al., 2004) as template, following the Datsenko and Wanner procedure (Datsenko and Wanner, 2000). Deletion mutant alleles obtained from the Keio collection (Baba et al., 2006) or tagged alleles obtained by recombination were transduced from one genetic background to another by generalized transduction with phage P1. The kanamycin resistance cassette was removed by transformation with the pCP20 plasmid (Cherepanov and Wackernagel, 1995).

Measure of Expression Using Transcriptional Fusions With GFP

Escherichia coli strains were transformed by the plasmids carrying the GFP transcriptional fusions, with or without pBAD plasmids producing SlyA proteins, and the selection plates were incubated at 37°C for 16 h. 600 μl of LB medium supplemented with the required antibiotics, and 0.05% arabinose for pBAD induction, were inoculated (three to six replicates for each assay) and grown for 16 h at 30°C in 96-well polypropylene plates of 2.2-ml wells under aeration and agitation. Fluorescent intensity measurement was performed in a Tecan infinite M200 plate reader. 150 μl of each well was transferred into a black Greiner 96-well plate for reading optical density at 600 nm (OD600) and fluorescence (excitation, 485 nm; emission, 530 nm). The expression levels were calculated by dividing the intensity of fluorescence by the OD600. After mean values were calculated, values from the control vector were subtracted. The results are given in arbitrary units, because the intensity of fluorescence is acquired with an optimal and variable gain; hence, the absolute values cannot be compared between different panels. The error bars on the figures show the standard error of the mean (SEM).

Purification of SlyA Proteins

BL21(DE3)pLysS strain was transformed with plasmids pET6HisTev-*slyA_stm* (pEB1885) or pET6HisTev-*slyA_ecoli* (pEB2004). The strains were grown in 500 ml LB at 30°C. At OD_{600nm} = 0.9, 1 mM IPTG was added and the cultures incubated during 6 h at 23°C. The proteins were then purified following the procedure described previously (Wahl et al., 2011).

Electrophoretic Mobility Shift Assay

DNA fragments containing the *pagC_stm*, *hlyE*, or *slyA* promoters were obtained by PCR using the corresponding

TABLE 1 | Plasmids.

Lab code	Name	Description	References
pEB227	pBAD24	amp^R, colE1 ori, PBAD promoter	Guzman et al., 1995
pEB1610	pBAD-SlyA_stm	PCR with primers ebm1026/1027 (EcoRI/XhoI) cloned in pBAD24 (EcoRI/SalI)	This work
pEB1609	pBAD-SlyA_eco	PCR with primers ebm1026/1189 (EcoRI/XhoI) cloned in pBAD24 (EcoRI/SalI)	This work
pEB0898	pUA66	kana^R, pSC101 ori, GFPmut2	Zaslaver et al., 2006
pEB0987	pUA139	kana^R, pSC101 ori, GFPmut2	Zaslaver et al., 2006
pEB1994	pUA-*paaA*	PCR with primers ebm1830/1831 cloned in pEB898 (XhoI/BamHI)	This work
pEB2005	pUA-*pagC*_Stm	PCR with primers ebm1847/1848 cloned in pEB898 (XhoI/BamHI)	This work
pEB2006	pUA-*pagD*_Stm	PCR with primers ebm1847/1848 cloned in pEB987 (BamHI/XhoI)	This work
pEB1937	pUA-*fimB*	PCR with primers ebm1755/1756 cloned in pEB898 (XhoI/BamHI)	This work
pEB1993	pUA-*elfA*	PCR with primers ebm1832/1833 cloned in pEB898 (XhoI/BamHI)	This work
	pUA-*slyA*	Transcriptional fusions available in the plasmid library described in the indicated reference.	Zaslaver et al., 2006
	pUA-*hlyE*		
	pUA-*pagP*		
	pUA-*agaS*		
	pUA-*ybeT*		
	pUA-*ssuE*		
	pUA-*yehD*		
	pUA-*ybeU*		
	pUA-*ygeG*		
	pUA-*agaS*		
	pUA-*ycjM*		
	pUA-*yadN*		
pEB1188	pET-6His-Tev		Wahl et al., 2011
pEB1885	pET-6His SlyA_stm	PCR with primers ebm1026/1027 cloned in pEB1188 (EcoRI/XhoI)	This work
pEB2004	pET-6His SlyA_eco	PCR with primers ebm1026/1189 cloned in pEB1188 (EcoRI/XhoI)	This work
pEB0267	pKD46	repA101(ts) Pbad-gam-bet-exo Ampi^R	Datsenko and Wanner, 2000
pEB0794	pJL148	-SPA-FRT-kana^R-FRT Ampi^R	Zeghouf et al., 2004
pEB0266	pCP20	pSC101(ts), encoding FLP gene, Ampi^R, Cam^R	Cherepanov and Wackernagel, 1995
pEB0697	pALS10	P*tac-relA,* Ampi^R	Svitil et al., 1993
pEB0698	pALS13	P*tac-relA*(1–455), Ampi^R	Svitil et al., 1993
pEB0699	pALS14	P*tac-relA*(1–331), Ampi^R	Svitil et al., 1993

transcriptional fusion plasmids as matrices, and the ebm623 and ebm629 primers that hybridize at the limit of the cloning sites. The PCR fragments were then purified using Macherey Nagel PCR purification kit. 20 nM PCR fragments were incubated with purified SlyA and ppGpp (TriLink Biotechnologies) (see legends of **Figure 4** and **Supplementary Figure S3** for the concentrations), in a 20 µl final reaction buffer containing 25 mM Tris–HCl (pH 7.2), 10 mM $MgCl_2$, 1 mM $CaCl_2$, 0.5 mM EDTA, 50 mM KCl, and 5% glycerol. The mix was incubated for 30 min at 20°C. The reactions were then analyzed by native PAGE (Acrylamide 10% 29:1). DNA was stained with GelRed (Fluo-Probes).

In vivo Crosslinking With Formaldehyde

Cells were pelleted and washed once with 10 mM potassium phosphate buffer, pH 6.8, and resuspended in the same volume, with (+F) or without (-F) formaldehyde 1%. Samples were incubated for 15 min at room temperature. The cells were then pelleted and washed again before solubilization in Laemmli loading buffer (volume normalized according to the OD_{600} of the initial cultures). Before loading on SDS-PAGE, the samples were either heated 10 min at 37°C to maintain the cross-links, or heated 20 min at 96°C to destroy them. SDS-PAGE, electrotransfer onto nitrocellulose membranes, and Western blot analyses were performed as previously described (Bouveret et al., 1995). The monoclonal anti-M2 Flag antibody used for 3Flag tag detection was purchased from Sigma.

RESULTS

We wanted to study the effect of ppGpp in the activation of gene expression by SlyA in *E. coli*. In addition to the known SlyA targets *hlyE*, *fimB*, and *slyA* itself, it was reported that SlyA might influence the expression of many genes when overexpressed (Curran et al., 2017). Based on this study, we tested a set of transcriptional fusions to select the ones that will allow us to follow the activity of SlyA. We used transcriptional fusions with GFP already available in a published *E. coli* promoter library (Zaslaver et al., 2006):*pagP*, *slyA*, *hlyE*, *agaS*, *ybeT*, *ssuE*, *yehD*, *ybeU*, *ygeG*, *agaS*, *ycjM*, and *yadN*. We completed this set by constructing transcriptional fusions missing in the library with the promoters of *elfA*, *fimB*, and *paaA* of *E. coli*, and also with

TABLE 2 | Oligonucleotides.

Lab Code	5′ –>3′ sequence	Gene
Ebm623	GCCCTTTCGTCTTCACCTCG	FW promoters
Ebm629	ATCTCCTTCTTAAATCTAGAGGATC	RV promoters
Ebm1830	CCGCTCGAGTCGCTACTCTCCAGATGTTTCAC	PpaaA FW
Ebm1831	ACGGGATCCTCAAAGCGTTCTTCTTGGGTCAC	PpaaA RV
Ebm1847	CATCTCGAGATGATGTTTCATAGCACCTCCTG	PpagC FW
Ebm1848	ACGGGATCCTAGCACGCTTTATTCCCGCTCC	PpagC RV
Ebm1755	CCGCTCGAGTGCGTTCCCCCATATCTCTAGG	PfimB FW
Ebm1756	ACGGGATCCCCATGCTCTTGCATGCTATGTACC	PfimB RV
Ebm1832	CCGCTCGAGATTCCAGCAAGGAGCTGGAGC	PelfA FW
Ebm1833	ACGGGATCCACGCTGGACGTTGCACATACC	PelfA RV
Ebm1026	ACCGAATTCTTGGAATCGCCACTAGGTTCTG	slyA FW
Ebm1189	ACGCTCGAGTCACCCTTTGGCCTGTAACTC	slyA_coli RV
Ebm1027	TTGCTCGAGTCAATCGTGAGAGTGCAATTCC	slyA_salmo RV
Ebm1855	ATCGCAAAACTTGAGCATAATATCATTGAGTTA CAGGCCAAAGGGATTCCAACTACTGCTAGC	slyA-3Flag FW
Ebm1856	TAAGTTTGCGTGTGGTCAGGTTACTGACCACA CGCCCCCTTCATTCATATGAATATCCTCCTTAG	slyA-3Flag RV

promoters of *Salmonella pagC* and *pagD*, which are regulated by the SlyA/H-NS antagonism and reported to be affected by ppGpp (Zhao et al., 2008). We then measured the expression of all these transcriptional fusions in wild type and Δ*slyA* strains (**Figure 1A** and **Supplementary Figure S1A**), as well as in the Δ*slyA* strain overproducing or not SlyA from a pBAD inducible plasmid (**Figure 1B** and **Supplementary Figure S1B**). From this, we selected 4 reporters that responded robustly to SlyA: *slyA* itself, *paaA*, *hlyE,* and *pagC*_Stm (**Figure 1** and **Supplementary Figure S1**).

The *slyA* transcriptional fusion was the only one to show a strong expression level in the wild type strain (**Figure 1A**). We therefore compared its expression in strains devoid of ppGpp (strains deleted of the *relA* and *spoT* genes). The absence of ppGpp did not modify the expression of *slyA* (**Figure 2A**). We then compared the expression of the four transcriptional fusions selected above in Δ*slyA* strains overproducing SlyA, in the presence or in the absence of ppGpp (**Figure 2B**). For the *slyA*, *paaA*, and *pagC*_Stm fusions, the absence of ppGpp did not prevent the induction by SlyA. These results indicate that *in vivo*, ppGpp is not required for the mechanism of transcription activation by SlyA.

However, the induction of the *hlyE* fusion by SlyA was strongly decreased in the absence of ppGpp (**Figure 2B**). To characterize better the specific effect of ppGpp on *hlyE*, we tested its induction by SlyA in different mutants for global regulatory factors. First, we tested the action of SlyA in the Δ*dksA* mutant. DksA is a cofactor of the RNA polymerase, required for the regulation of RNAP by ppGpp (Gourse et al., 2018). While ppGpp is still present in this mutant, *dksA* deletion mimics the global effects of a ppGpp° mutant on gene transcription due to the action of ppGpp on RNA polymerase. While SlyA still activated

TABLE 3 | Strains.

Lab code	Name	Description	References
EB072	BL21(DE3)pLys	Coli B λ(DE3) pLysS(cmR)	Studier and Moffatt, 1986
EB240	BW25113Δ*slyA*	Δ*slyA*::kana^R	Baba et al., 2006
EB126	BW25113Δ*relA*	Δ*relA*::kana^R	Baba et al., 2006
EB559	MG1655Δ*dksA*		Wahl et al., 2011
EB761	BW25113Δ*cyaA*	Δ*cyaA*::kana^R	Baba et al., 2006
EB128	BW25113Δ*fis*	Δ*fis*::kana^R	Baba et al., 2006
EB047	BW25113Δ*hns*	Δ*hns*::kana^R	Baba et al., 2006
EB944	MG1655	Wild type reference. F- λ- rph-1	Lab stock
EB425	MG1655 ppGpp°	Δ*relA*Δ*spoT*::cat	Wahl et al., 2011
EB1073	MGΔ*slyA*	P1 transduction Δ*slyA*::kana^R from EB240 to EB944. Kanamycin resistance removed with pCP20	This work
EB1076	MGΔ*slyA*Δ*relA*	P1 transduction Δ*relA*::kana^R from EB126 to EB1073. Kanamycin resistance removed with pCP20	This work
EB1077	ppGpp°_Δ*slyA*	P1 transduction Δ*spoT*::*cat* from EB425 to EB1076	This work
EB1100	Δ*dksA* Δ*slyA*	P1 transduction Δ*slyA*::kana^R from EB240 to EB559. Kanamycin resistance removed with pCP20	This work
EB781	MGΔ*cyaA*	P1 transduction Δ*cyaA*::kana^R from EB761 to EB944. Kanamycin resistance removed with pCP20	This work
EB743	MGΔ*fis*	P1 transduction Δ*fis*::kana^R from EB128 to EB944. Kanamycin resistance removed with pCP20	This work
EB951	MGΔ*hns*	P1 transduction Δ*hns*::kana^R from EB047 to EB944. Kanamycin resistance removed with pCP20	This work
EB1106	*MG_slyA*-3Flag	PCR ebm1855/1856 on pJL148, λRed recombination in EB944 followed by P1 transduction in EB944	This work
EB468	MG_ppGpp° SlyA-3Flag	P1 transduction slyA-3Flag-kana^R from EB1106 to EB425	This work

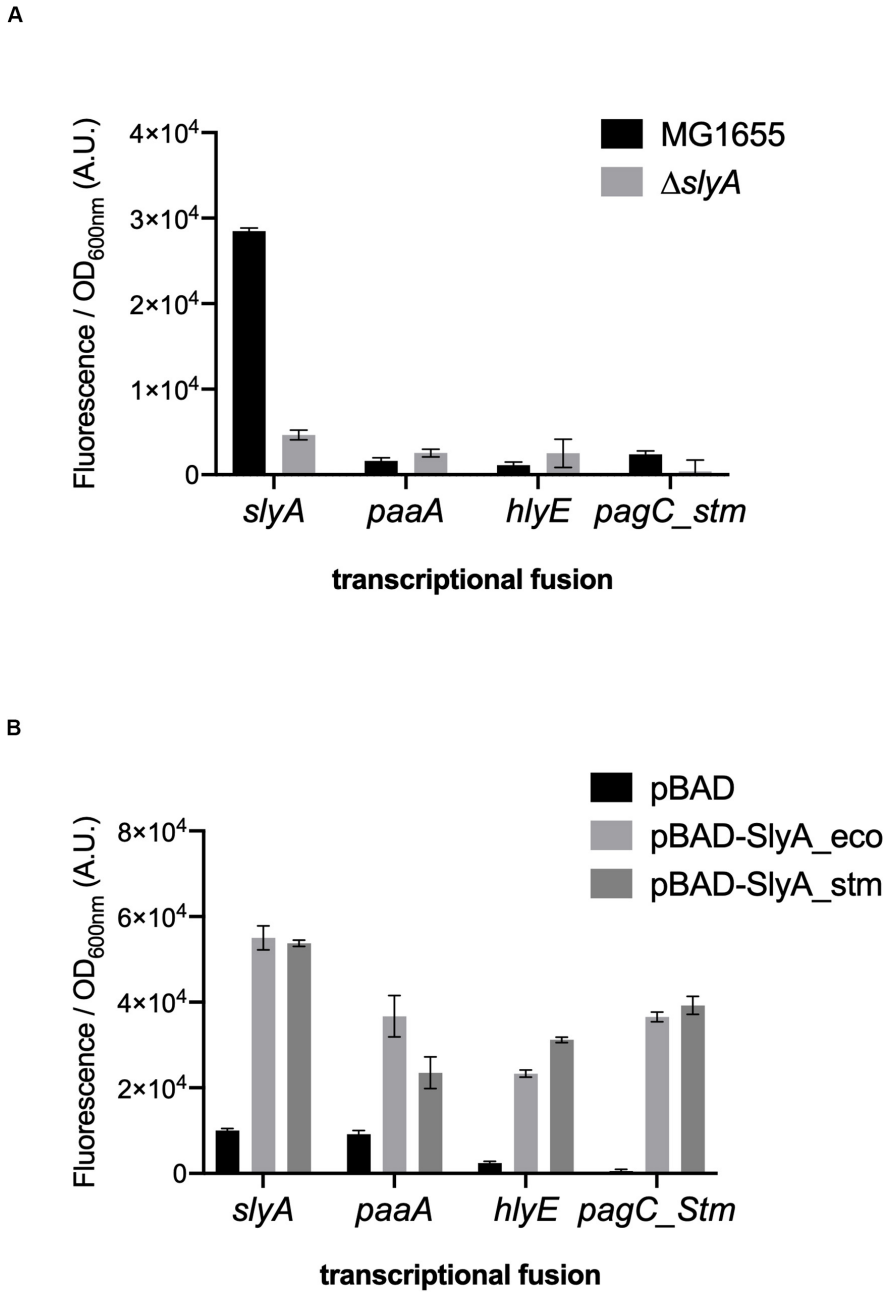

FIGURE 1 | *slyA*, *paaA*, *hlyE*, and *pagC*_stm promoters are induced by SlyA. **(A)** Comparison of transcriptional fusion activity in wild type MG1655 and in the *slyA* mutant EB1073 strains grown overnight at 30°C in LB. **(B)** Transcriptional fusion activity when SlyA protein is overproduced. MG1655 strains transformed by the indicated transcriptional fusions and the pBAD24 (pEB227), pBAD-slyA_ecoli (pEB1609), or pBAD_slyA_stm (pEB1610) plasmids were incubated overnight at 30°C in LB supplemented with 0.05% arabinose. The activities correspond to the ratio between GFP fluorescence and OD_{600nm} of 6 replicates, given in arbitrary units (A.U.). The error bars show the SEM.

the expression of the *slyA* transcriptional fusion in the Δ*dksA* mutant, as in the ppGpp° mutant (**Supplementary Figure S2**), SlyA induction of *hlyE* was strongly decreased in the Δ*dksA* mutant, similarly to what was observed in the ppGpp° mutant (**Figure 3A**). This result suggests that the effect of ppGpp on *hlyE* expression is due to its role in controlling expression through RNAP regulation (at *hlyE* promoter or others), and not to a direct control of SlyA activity. For full activation of its expression, *hlyE* would therefore need both SlyA overproduction (or activation by unknown conditions), and the presence of ppGpp.

In addition to SlyA, *hlyE* expression is controlled by a network of global regulators, such as H-NS (Wyborn et al., 2004; Lithgow et al., 2007), CRP-cAMP and FNR (Westermark et al., 2000), and it was also reported that it is

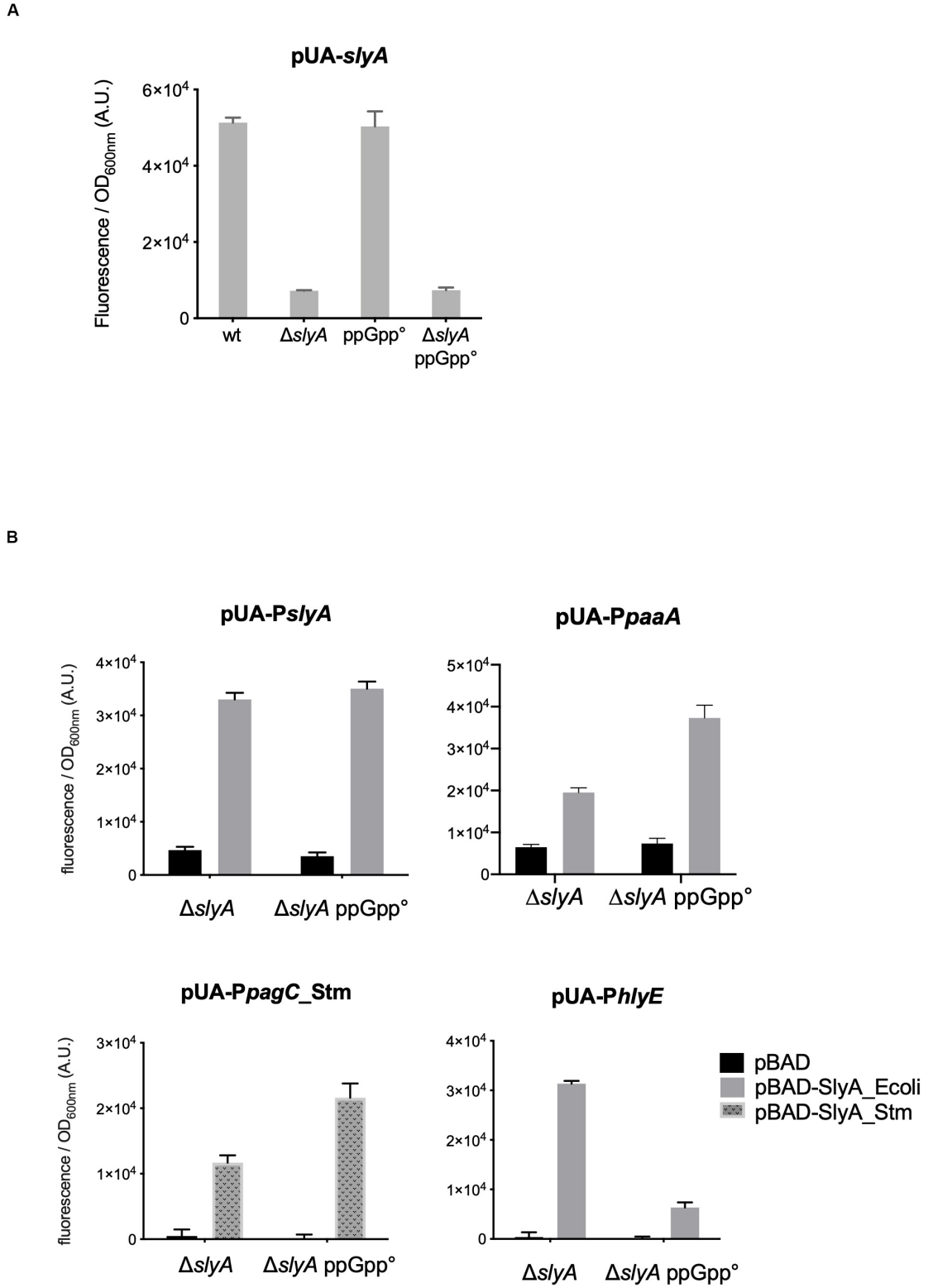

FIGURE 2 | *In vivo* induction by SlyA does not require ppGpp. **(A)** Comparison of *slyA* transcriptional fusion activity in wild type MG1655, Δ*slyA* (EB1073), ppGpp° (EB425), and Δ*slyA*_ppGpp° (EB1077) strains grown overnight at 30°C in LB. **(B)** Effect of pBAD-SlyA overproduction in Δ*slyA* or Δ*slyA*_ppGpp° strains on the expression of *slyA*, *paaA*, *pagC*_Stm, and *hlyE* transcriptional fusions, in the same conditions as in **Figure 1B**. The activities correspond to the ratio between GFP fluorescence and OD_{600nm} of six **(A)** or four **(B)** replicates, given in arbitrary units (A.U.). The error bars show the SEM.

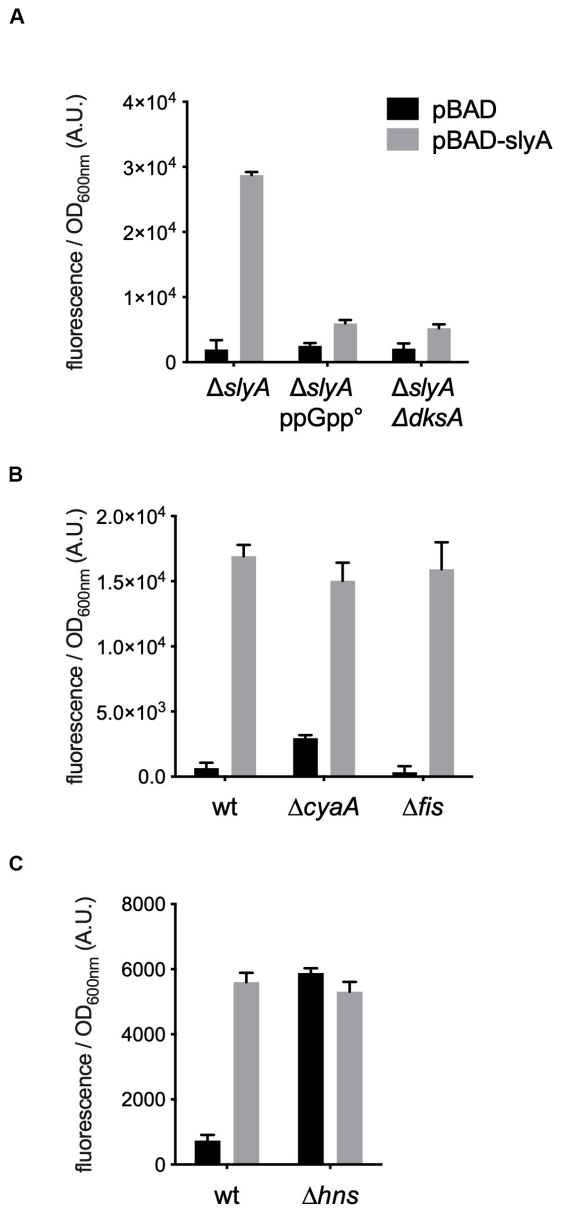

FIGURE 3 | *hlyE* activation by SlyA in global regulatory mutants. Induction of the *hlyE* transcriptional fusion by pBAD-slyA_ecoli was tested in the same conditions as in **Figure 1B**, in the indicated mutant strains: wt (MG1655), Δ*slyA* (EB1073), Δ*slyA*_ppGpp (EB1077), Δ*slyA*Δ*dksA* (EB1100), Δ*cyaA* (EB781), Δ*fis* (EB743), and Δ*hns* (EB951). The activities correspond to the ratio between GFP fluorescence and OD_{600nm} of 4 **(A,C)** or 3 **(B)** replicates, given in arbitrary units (A.U.). The error bars show the SEM.

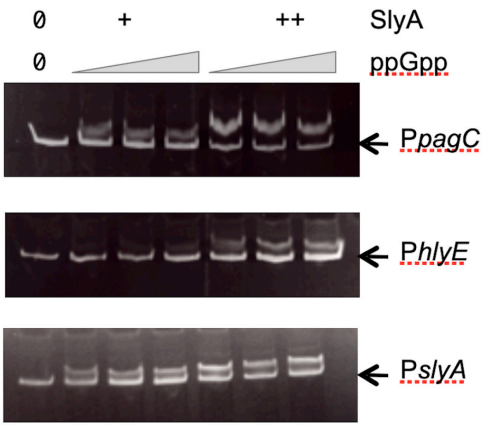

FIGURE 4 | Effect of ppGpp on SlyA binding to DNA. Electrophoretic mobility shift assays were performed using purified SlyA from *E. coli* [at 50 (+) or 100 (++) nM] or purified SlyA from *Salmonella* for the *pagC* experiment [at 200 (+) or 400 (++) nM]. For each SlyA concentration, 0, 50, or 100 μM ppGpp were added.

negatively regulated by Fis (Bradley et al., 2007). ppGpp is also a member of this complex network controlling bacterial physiology (Travers and Muskhelishvili, 2005). Therefore the ppGpp/DksA effect observed on the expression of *hlyE* might be indirect through one or several of these global regulators. We tested *hlyE* induction by SlyA in *hns*, *fis*, and *cyaA* mutants. SlyA was still able to induce *hlyE* expression in *fis* and *cyaA* mutants (**Figure 3B**). As expected, the expression of hlyE was de-repressed in the Δ*hns* mutant, and not further induced by the presence of SlyA (**Figure 3C**). This confirmed that SlyA activation of *hlyE* expression is due to the displacement of H-NS. This set of experiments suggests that ppGpp role in *hlyE* expression is not due to an indirect effect through CRP-cAMP or Fis regulators, but probably through the regulation of RNAP at the *hlyE* promoter in synergy with DksA.

Our results obtained *in vivo* suggested that ppGpp had no role in SlyA function, contrary to what was reported before (Zhao et al., 2008). Therefore, it was necessary to also test the effect of ppGpp on SlyA DNA binding *in vitro*. Using gel shift assays, we were able to detect a robust binding of SlyA on the promoter regions tested:*hlyE*, *slyA*, and *pagC_Stm* (**Supplementary Figure S3A**). We then choose for each binding assay, SlyA/DNA ratios that were just sufficient to detect a shift in order to test the effect of adding ppGpp. With addition of 50 μM or 100 μM ppGpp [the same concentrations used by Zhao et al. (2008)], the shifts were not affected (**Figure 4**). Because we used purified SlyA proteins with a 6his tag fused at the N-terminal, we also performed the same experiments after removing the tag by TEV cleavage. Also, ppGpp might have been trapped with SlyA during the purification, therefore we performed the purifications in a ppGpp null strain and obtained the same negative result (**Supplementary Figure S3B**).

The last reported effect of ppGpp on SlyA, was that it enhanced its dimerization, as shown by *in vivo* cross-linking experiments (Zhao et al., 2008). In order to detect SlyA by Western blot, we constructed wild type and ppGpp° strains producing a SlyA-3Flag tagged protein expressed from its endogenous locus. SlyA-3Flag was readily detected in the two genetic backgrounds, at the expected size of approximately 20 kDa (**Figure 5A**). To test the dimerization, we used whole cell cross-linking with formaldehyde. This cross-linker

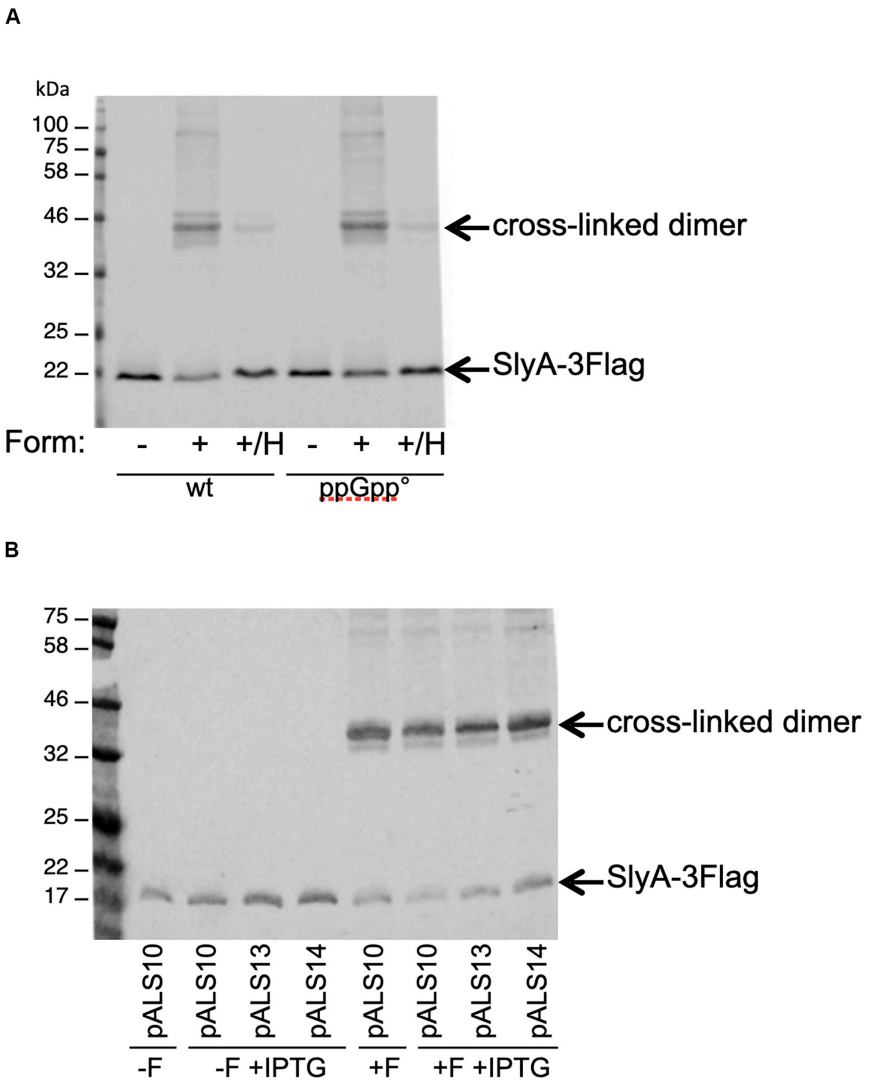

FIGURE 5 | Effect of ppGpp on SlyA dimerization *in vivo*. **(A)** MG1655_SlyA-3Flag (EB1106) and ppGpp°_SlyA-3Flag (EB1110) strains were grown to OD600 = 1.3. **(B)** Strain MG1655_SlyA-3Flag (EB1106) was transformed by plasmids pALS10, pALS13, and pALS14 (pEB0697, pEB0698, and pEB0699, respectively) (Svitil et al., 1993). These transformed strains were grown to OD600 = 1.5 and then *relA* expression was induced with 1 mM IPTG for 30 min. Then, for both panels, the cells were cross-linked with formaldehyde as described in section "Materials and Methods." +F, with formaldehyde; –F, without formaldehyde; +/H, with formaldehyde and then heated at 96°C. After SDS-PAGE and Western blot, the SlyA-3Flag tag was detected with monoclonal anti-Flag M2.

produces covalent bonds that can be destroyed by heating at 96°C. In the wild type background, dimerization of SlyA was clearly detected by cross-linking with formaldehyde (**Figure 5A**). The dimerization was identical in the ppGpp° background (**Figure 5A**). In reverse, we decided to test if an excess of ppGpp might affect SlyA dimerization, by overproducing the RelA ppGpp synthase. Plasmids pALS10, pALS13, and pALS14 code, respectively, for a full RelA protein, a constitutively active truncated RelA protein, and an inactive RelA protein (Svitil et al., 1993). We performed the cross-linking experiment in MG1655 strain transformed by these three plasmids and with induction of RelA variants expression. In the samples with induced ppGpp production (pALS10 and pALS13), SlyA dimerization was not affected, or even slightly diminished (**Figure 5B**). In conclusion, we were not able to see any positive effect of ppGpp on SlyA dimerization.

DISCUSSION

In this study, we showed that ppGpp is not required for SlyA function in *E. coli*. The expression of several reporter genes was still induced by SlyA overproduction in the absence of ppGpp *in vivo*, SlyA binding to DNA was not improved by adding ppGpp *in vitro*, and finally SlyA dimerization was not affected by ppGpp absence or increased levels *in vivo*. Even if the initial report of ppGpp effect on SlyA is now more than 10 years old (Zhao et al., 2008), we think this information is important and of public good

for the community of researchers working on ppGpp. Indeed, we are aware of several groups that were interested in developing ppGpp sensors based on this observation, including ourselves. To our knowledge, no confirmation or disproof of ppGpp effect on SlyA was reported since then, apart from a brief mention that ppGpp had no effect on SlyA control of the *fimB* promoter in *E. coli* (McVicker et al., 2011). Furthermore, SlyA was not spotted in two independent global studies aiming at identifying ppGpp binding proteins (Zhang et al., 2018; Wang et al., 2019). It is therefore still unclear what molecule can regulate SlyA activity. However, recent work provided strong evidence of SlyA control by Salicylate, which fits with SlyA belonging to the MarR family containing proteins known to respond to small aromatic carboxylate compounds (Dolan et al., 2011; Will et al., 2019).

The obvious difference that could explain the discrepancy between our work and the one reported in Zhao et al., 2008 is that we have studied the activity of SlyA in *E. coli*, while the previous study was done in *Salmonella* (Zhao et al., 2008), and that we have studied different reporter genes controlled by SlyA. In particular, the expression of *slyA* itself was a very useful reporter of SlyA action, since it is not dependent on H-NS, and permitted to observe that it was not affected in the absence of ppGpp (**Figure 2A**). Furthermore, we do not contradict the fact that *pagCD* promoters are shut down in a ppGpp° strain in *Salmonella* as shown in Zhao et al., 2008. We propose that it is in fact very similar to what we observed for the expression of *hlyE* in *E. coli*, for which SlyA overproduction can partially counteract the negative effect of ppGpp absence (**Figure 2B**), as it was observed for *pagCD* in *Salmonella* (Zhao et al., 2008). Production of SlyA_eco or SlyA_stm had identical effects when produced in *E. coli* (**Figure 1B**). Inversely, it was shown that production of SlyA_eco in *Salmonella* is able to counter silence the expression of *pagC*, similarly, to SlyA_stm (Will et al., 2019). Therefore, we think the molecular mechanism of SlyA is identical in the two bacteria. However, it is clear that the regulons and the physiological role of SlyA are very different in the two bacteria. This difference does not come from the SlyA protein itself, but from the variations in intergenic and regulatory regions of the target genes. A striking difference is for example that SlyA represses its own expression in *Salmonella* (Stapleton et al., 2002; Will et al., 2019), whereas it auto-activates its expression in *E. coli* as we showed here (**Figure 1**) and as it was demonstrated before (Corbett et al., 2007). The expression level of *slyA* might also play a role, as it has been suggested that *slyA* expression is much lower in *E. coli* than in *Salmonella* (Will et al., 2019). However, in our experiments, the P*slyA* transcriptional fusion was one of the few to display a robust basal expression level, and we were able to detect the SlyA-3Flag tagged protein expression in *E. coli* (**Figure 5**). Still, only SlyA overproduction using pBAD-SlyA plasmid permitted to detect expression of *paaA*, *hlyE*, and *pagC*_Stm, suggesting a strong excess of SlyA is necessary to overcome H-NS repression on these genes.

Concerning the effect of ppGpp on SlyA binding to DNA *in vitro*, and the dimerization of SlyA *in vivo*, the discrepancy between our results and the previous ones (Zhao et al., 2008) is more difficult to understand. Indeed, the SlyA proteins of *E. coli* and *Salmonella* are highly similar (91% identical and 95% similar over 142 amino acids), and we performed *in vitro* binding experiments with SlyA proteins purified from both *E. coli* and *Salmonella,* including a binding experiment on a similar *Salmonella pagCD* intergenic region as the one used previously (**Figure 4**). As described in the result section, we performed several control experiments to rule out any effect of the tag or the purification procedure of SlyA proteins (**Supplementary Figure S3B**). For the *in vivo* dimerization detected by cross-linking with formaldehyde, we performed the experiment in an *E. coli* strain producing a SlyA-tagged protein expressed from its endogenous locus. Zhao *et al.* performed this experiment in *Salmonella*, with a SlyA-tagged protein expressed from a plasmid. In this case, an indirect effect of ppGpp on *slyA* expression might explain the different results.

The interpretation of the experiments performed in strains mutated for global regulators (such as ppGpp) is complicated by the mode of action of SlyA, which is not a direct and classical activator, but acts mainly as a counter silencer of H-NS. It has been shown that ppGpp physiological effects are intermixed with global regulators such as Fis, CRP, or H-NS, and even DNA supercoiling state (Johansson et al., 2000; Travers and Muskhelishvili, 2005). Therefore, it is to be expected that any tinkering of ppGpp concentrations *in vivo* will affect a complex network of global regulations. Particular promoters such as *pagC* in *Salmonella* or *hlyE* in *E. coli* are controlled by an especially high numbers of specific and global factors, not only H-NS and SlyA, but also PhoPQ and EmrR in the case of *pagC* in *Salmonella* (Zhao et al., 2008; Yang et al., 2019) or CRP and FNR for *hlyE* in *E. coli* (Westermark et al., 2000; Bradley et al., 2007). Obviously, these complex regulatory networks might be affected by ppGpp levels, together with a possible direct effect of ppGpp on the RNAP depending on the nature of the promoter itself (Gourse et al., 2018), as it might be the case for *hlyE* in our study or *pagC* in *Salmonella* (Zhao et al., 2008). More generally, because ppGpp impacts global regulatory networks central to the physiology of bacteria, our study should be taken as a warning of caution in the interpretation of *in vivo* effects triggered by the modification of ppGpp levels.

DATA AVAILABILITY STATEMENT

All datasets presented in this study are included in the article/**Supplementary Material**.

AUTHOR CONTRIBUTIONS

EB and JV designed the study. EB and JB designed and performed the experiments. EB, JV, and JB discussed the results and wrote the manuscript. All authors contributed to the article and approved the submitted version.

FUNDING

This work was funded by the Centre National de la Recherche Scientifique (CNRS).

ACKNOWLEDGMENTS

We thank Laetitia My for collaborating with exploratory experiments on SlyA, preliminary to this study, and Frédéric Barras for helpful discussions.

SUPPLEMENTARY MATERIAL

The Supplementary Material for this article can be found online at: https://www.frontiersin.org/articles/10.3389/fmicb.2020.01856/full#supplementary-material

REFERENCES

Baba, T., Ara, T., Hasegawa, M., Takai, Y., Okumura, Y., Baba, M., et al. (2006). Construction of *Escherichia coli* K-12 in-frame, single-gene knockout mutants: the Keio collection. *Mol. Syst. Biol.* 2:2006.0008.

Bennison, D. J., Irving, S. E., and Corrigan, R. M. (2019). The impact of the stringent response on TRAFAC GTPases and prokaryotic ribosome assembly. *Cells* 8:1313. doi: 10.3390/cells8111313

Bouveret, E., Derouiche, R., Rigal, A., Lloubès, R., Lazdunski, C., and Bénédetti, H. (1995). Peptidoglycan-associated lipoprotein-TolB interaction. A possible key to explaining the formation of contact sites between the inner and outer membranes of *Escherichia coli*. *J. Biol. Chem.* 270, 11071–11077. doi: 10.1074/jbc.270.19.11071

Bradley, M. D., Beach, M. B., de Koning, A. P. J., Pratt, T. S., and Osuna, R. (2007). Effects of Fis on *Escherichia coli* gene expression during different growth stages. *Microbiology* 153, 2922–2940. doi: 10.1099/mic.0.2007/008565-0

Chalabaev, S., Chauhan, A., Novikov, A., Iyer, P., Szczesny, M., Beloin, C., et al. (2014). Biofilms formed by gram-negative bacteria undergo increased lipid a palmitoylation, enhancing in vivo survival. *mBio* 5:e01116-14. doi: 10.1128/mBio.01116-14

Cherepanov, P. P., and Wackernagel, W. (1995). Gene disruption in *Escherichia coli*: TcR and KmR cassettes with the option of Flp-catalyzed excision of the antibiotic-resistance determinant. *Gene* 158, 9–14. doi: 10.1016/0378-1119(95)00193-a

Corbett, D., Bennett, H. J., Askar, H., Green, J., and Roberts, I. S. (2007). SlyA and H-NS regulate transcription of the *Escherichia coli* K5 capsule gene cluster, and expression of slyA in *Escherichia coli* is temperature-dependent, positively autoregulated, and independent of H-NS. *J. Biol. Chem.* 282, 33326–33335. doi: 10.1074/jbc.m703465200

Curran, T. D., Abacha, F., Hibberd, S. P., Rolfe, M. D., Lacey, M. M., and Green, J. (2017). Identification of new members of the *Escherichia coli* K-12 MG1655 SlyA regulon. *Microbiology* 163, 400–409. doi: 10.1099/mic.0.000423

Dalebroux, Z. D., Svensson, S. L., Gaynor, E. C., and Swanson, M. S. (2010). ppGpp conjures bacterial virulence. *Microbiol. Mol. Biol. Rev.* 74, 171–199. doi: 10.1128/mmbr.00046-09

Datsenko, K. A., and Wanner, B. L. (2000). One-step inactivation of chromosomal genes in *Escherichia coli* K-12 using PCR products. *Proc. Natl. Acad. Sci. U.S.A.* 97, 6640–6645. doi: 10.1073/pnas.120163297

Dolan, K. T., Duguid, E. M., and He, C. (2011). Crystal structures of SlyA protein, a master virulence regulator of *Salmonella*, in free and DNA-bound states. *J. Biol. Chem.* 286, 22178–22185. doi: 10.1074/jbc.m111.245258

Ellison, D. W., and Miller, V. L. (2006). Regulation of virulence by members of the MarR/SlyA family. *Curr. Opin. Microbiol.* 9, 153–159. doi: 10.1016/j.mib.2006.02.003

Gourse, R. L., Chen, A. Y., Gopalkrishnan, S., Sanchez-Vazquez, P., Myers, A., and Ross, W. (2018). Transcriptional responses to ppGpp and DksA. *Annu. Rev. Microbiol.* 72, 163–184. doi: 10.1146/annurev-micro-090817-062444

Guzman, L. M., Belin, D., Carson, M. J., and Beckwith, J. (1995). Tight regulation, modulation, and high-level expression by vectors containing the arabinose PBAD promoter. *J. Bacteriol.* 177, 4121–4130. doi: 10.1128/jb.177.14.4121-4130.1995

Hobbs, J. K., and Boraston, A. B. (2019). (p)ppGpp and the stringent response: an emerging threat to antibiotic therapy. *ACS Infect. Dis.* 5, 1505–1517. doi: 10.1021/acsinfecdis.9b00204

Johansson, J., Balsalobre, C., Wang, S. Y., Urbonaviciene, J., Jin, D. J., Sondén, B., et al. (2000). Nucleoid proteins stimulate stringently controlled bacterial promoters: a link between the cAMP-CRP and the (p)ppGpp regulons in *Escherichia coli*. *Cell* 102, 475–485. doi: 10.1016/s0092-8674(00)00052-0

Karp, P. D., Ong, W. K., Paley, S., Billington, R., Caspi, R., Fulcher, C., et al. (2018). The EcoCyc database. *EcoSal Plus* 8:10.1128/ecosalplus.ESP-0009-2013. doi: 10.1128/ecosalplus.ESP-0009-2013

Libby, S. J., Goebel, W., Ludwig, A., Buchmeier, N., Bowe, F., Fang, F. C., et al. (1994). A cytolysin encoded by *Salmonella* is required for survival within macrophages. *Proc. Natl. Acad. Sci. U.S.A.* 91, 489–493. doi: 10.1073/pnas.91.2.489

Lithgow, J. K., Haider, F., Roberts, I. S., and Green, J. (2007). Alternate SlyA and H-NS nucleoprotein complexes control hlyE expression in *Escherichia coli* K-12. *Mol. Microbiol.* 66, 685–698. doi: 10.1111/j.1365-2958.2007.05950.x

McVicker, G., Sun, L., Sohanpal, B. K., Gashi, K., Williamson, R. A., Plumbridge, J., et al. (2011). SlyA protein activates fimB gene expression and type 1 fimbriation in *Escherichia coli* K-12. *J. Biol. Chem.* 286, 32026–32035. doi: 10.1074/jbc.m111.266619

Navarre, W. W., Halsey, T. A., Walthers, D., Frye, J., McClelland, M., Potter, J. L., et al. (2005). Co-regulation of *Salmonella enterica* genes required for virulence and resistance to antimicrobial peptides by SlyA and PhoP/PhoQ. *Mol. Microbiol.* 56, 492–508. doi: 10.1111/j.1365-2958.2005.04553.x

Potrykus, K., and Cashel, M. (2008). (p)ppGpp: still magical. *Annu. Rev. Microbiol.* 62, 35–51. doi: 10.1146/annurev.micro.62.081307.162903

Stapleton, M. R., Norte, V. A., Read, R. C., and Green, J. (2002). Interaction of the *Salmonella* Typhimurium transcription and virulence factor SlyA with target DNA and identification of members of the SlyA regulon. *J. Biol. Chem.* 277, 17630–17637. doi: 10.1074/jbc.m110178200

Stoebel, D. M., Free, A., and Dorman, C. J. (2008). Anti-silencing: overcoming H-NS-mediated repression of transcription in Gram-negative enteric bacteria. *Microbiology* 154, 2533–2545. doi: 10.1099/mic.0.2008/020693-0

Studier, F. W., and Moffatt, B. A. (1986). Use of bacteriophage T7 RNA polymerase to direct selective high-level expression of cloned genes. *J. Mol. Biol.* 189, 113–130. doi: 10.1016/0022-2836(86)90385-2

Svitil, A. L., Cashel, M., and Zyskind, J. W. (1993). Guanosine tetraphosphate inhibits protein synthesis in vivo. A possible protective mechanism for starvation stress in *Escherichia coli*. *J. Biol. Chem.* 268, 2307–2311.

Travers, A., and Muskhelishvili, G. (2005). DNA supercoiling - a global transcriptional regulator for enterobacterial growth. *Nat. Rev. Microbiol.* 3, 157–169. doi: 10.1038/nrmicro1088

Wahl, A., My, L., Dumoulin, R., Sturgis, J. N., and Bouveret, E. (2011). Antagonistic regulation of dgkA and plsB genes of phospholipid synthesis by multiple stress responses in *Escherichia coli*. *Mol. Microbiol.* 80, 1260–1275. doi: 10.1111/j.1365-2958.2011.07641.x

Wang, B., Dai, P., Ding, D., Del Rosario, A., Grant, R. A., Pentelute, B. L., et al. (2019). Affinity-based capture and identification of protein effectors of the growth regulator ppGpp. *Nat. Chem. Biol.* 15, 141–150. doi: 10.1038/s41589-018-0183-4

Westermark, M., Oscarsson, J., Mizunoe, Y., Urbonaviciene, J., and Uhlin, B. E. (2000). Silencing and activation of ClyA cytotoxin expression in *Escherichia coli*. *J. Bacteriol.* 182, 6347–6357. doi: 10.1128/jb.182.22.6347-6357.2000

Will, W. R., Brzovic, P., Le Trong, I., Stenkamp, R. E., Lawrenz, M. B., Karlinsey, J. E., et al. (2019). The evolution of SlyA/RovA transcription factors from repressors to countersilencers in *Enterobacteriaceae*. *mBio* 10:e00009-e19. doi: 10.1128/mBio.00009-19

Will, W. R., and Fang, F. C. (2020). The evolution of MarR family transcription factors as counter-silencers in regulatory networks. *Curr. Opin. Microbiol.* 55, 1–8. doi: 10.1016/j.mib.2020.01.002

Will, W. R., Navarre, W. W., and Fang, F. C. (2015). Integrated circuits: how transcriptional silencing and counter-silencing facilitate bacterial evolution. *Curr. Opin. Microbiol.* 23, 8–13. doi: 10.1016/j.mib.2014.10.005

Wyborn, N. R., Stapleton, M. R., Norte, V. A., Roberts, R. E., Grafton, J., and Green, J. (2004). Regulation of *Escherichia coli* hemolysin E expression by H-NS and

Salmonella SlyA. *J. Bacteriol.* 186, 1620–1628. doi: 10.1128/jb.186.6.1620-1628.2004

Yang, D., Kong, Y., Sun, W., Kong, W., and Shi, Y. (2019). A dopamine-responsive signal transduction controls transcription of *Salmonella enterica* serovar typhimurium virulence genes. *mBio* 10:e02772-18. doi: 10.1128/mBio.02772-18

Zaslaver, A., Bren, A., Ronen, M., Itzkovitz, S., Kikoin, I., Shavit, S., et al. (2006). A comprehensive library of fluorescent transcriptional reporters for *Escherichia coli*. *Nat. Methods* 3, 623–628. doi: 10.1038/nmeth895

Zeghouf, M., Li, J., Butland, G., Borkowska, A., Canadien, V., Richards, D., et al. (2004). Sequential peptide affinity (SPA) system for the identification of mammalian and bacterial protein complexes. *J. Proteome Res.* 3, 463–468. doi: 10.1021/pr034084x

Zhang, Y., Zborníková, E., Rejman, D., and Gerdes, K. (2018). Novel (p)ppGpp binding and metabolizing proteins of *Escherichia coli*. *mBio* 9:e02188-17. doi: 10.1128/mBio.02188-17

Zhao, G., Weatherspoon, N., Kong, W., Curtiss, R., and Shi, Y. (2008). A dual-signal regulatory circuit activates transcription of a set of divergent operons in *Salmonella* Typhimurium. *Proc. Natl. Acad. Sci. U.S.A.* 105, 20924–20929. doi: 10.1073/pnas.0807071106

Conflict of Interest: The authors declare that the research was conducted in the absence of any commercial or financial relationships that could be construed as a potential conflict of interest.

frontiers in Microbiology

REVIEW
published: 12 August 2020
doi: 10.3389/fmicb.2020.01759

Diversity in *E. coli* (p)ppGpp Levels and Its Consequences

Beny Spira and Katia Ospino*

Department of Microbiology, Institute of Biomedical Sciences, University of São Paulo, São Paulo, Brazil

(p)ppGpp is at the core of global bacterial regulation as it controls growth, the most important aspect of life. It would therefore be expected that at least across a species the intrinsic (basal) levels of (p)ppGpp would be reasonably constant. On the other hand, the historical contingency driven by the selective pressures on bacterial populations vary widely resulting in broad genetic polymorphism. Given that (p)ppGpp controls the expression of many genes including those involved in the bacterial response to environmental challenges, it is not surprising that the intrinsic levels of (p)ppGpp would also vary considerably. In fact, null mutations or less severe genetic polymorphisms in genes associated with (p)ppGpp synthesis and hydrolysis are common. Such variation can be observed in laboratory strains, in natural isolates as well as in evolution experiments. High (p)ppGpp levels result in low growth rate and high tolerance to environmental stresses. Other aspects such as virulence and antimicrobial resistance are also influenced by the intrinsic levels of (p)ppGpp. A case in point is the production of Shiga toxin by certain *E. coli* strains which is inversely correlated to (p)ppGpp basal level. Conversely, (p)ppGpp concentration is positively correlated to increased tolerance to different antibiotics such as β-lactams, vancomycin, and others. Here we review the variations in intrinsic (p)ppGpp levels and its consequences across the *E. coli* species.

Keywords: (p)ppGpp, polymorphism, growth rate, evolution, stress resistance, antibiotic resistance, virulence

OPEN ACCESS

Edited by:
Katarzyna Potrykus, University of Gdansk, Poland

Reviewed by:
Gemma Atkinson, Umeå University, Sweden
Marcus Persicke, Bielefeld University, Germany

****Correspondence:***
Beny Spira
benys@usp.br

Specialty section:
This article was submitted to Microbial Physiology and Metabolism, a section of the journal Frontiers in Microbiology

Received: *20 May 2020*
Accepted: *06 July 2020*
Published: *12 August 2020*

Citation:
Spira B and Ospino K (2020) Diversity in E. coli (p)ppGpp Levels and Its Consequences. Front. Microbiol. 11:1759. doi: 10.3389/fmicb.2020.01759

DIVERSITY OF (p)ppGpp CONCENTRATIONS–IMPACT ON GROWTH RATE AND BEYOND

"The study of bacterial growth is the essence of microbiology" (Jacques Monod).

The success of an organism in evolutionary terms resides in its ability to reproduce and perpetuate its genes. It would thus be expected that bacterial resources would be devoted most of the time to maximizing growth rate. This may be true under some circumstances, especially, under optimal laboratory growth conditions. However, bacteria actually keep growth rate under very tight control. At the core of growth regulation is a small nucleotide that appears in two different forms—guanosine tetra- and penta-phosphate—ppGpp and pppGpp, collectively known as (p)ppGpp. The grip of (p)ppGpp on growth rate is achieved mainly through an effective inhibition of stable RNA (rRNA and tRNA) synthesis during amino acid starvation and other nutritional stresses in a process that became known as the stringent control (Cashel and Gallant, 1968; Potrykus and Cashel, 2008; Potrykus et al., 2011). Nevertheless, the impact of (p)ppGpp on cell physiology goes far beyond stable RNA control. (p)ppGpp also inhibits DNA replication, lipid and protein synthesis and ultimately cell division (Potrykus and Cashel, 2008; Traxler et al., 2008). Whenever the growth conditions deteriorate, (p)ppGpp concentration increases, severely repressing the expression of

growth-related genes. This repression is necessary in order to promote the reallocation of resources, which are then shifted from growth promotion to the maintenance of amino acid as well as energy pools and to cell protection and survival. In fact, (p)ppGpp concentration increases stepwise according to the severity of nutrient depletion (Traxler et al., 2011).

In *E. coli* and related bacterial species, (p)ppGpp is synthesized by two different proteins—RelA and SpoT. These proteins evolved by duplication from a bifunctional ancestral RelA/SpoT Homolog (RSH) possessing both (p)ppGpp synthetic and hydrolytic capabilities, resulting in two proteins with overlapping functionalities (Mittenhuber, 2001; Atkinson et al., 2011). The RelA and SpoT proteins contain 744 and 702 amino acids, respectively. Both proteins can be divided in two parts of similar size (**Figure 1**). The NTD half of the protein harbors the catalytic HD (hydrolytic) and Synth (Synthetic) domains. In RelA, the HD domain is not active. The CTD portion of the protein contains four regulatory domains: TGS (ThrRS, GTPase, SpoT/RelA domain), AH (α-helical domain), RIS (Ribosome-InterSubunit domain) and ACT (Aspartate kinase-Chorismate mutase-TyrA domain) (Atkinson et al., 2011; Loveland et al., 2016). RelA responds to intracellular amino acid imbalancies, such as amino acid starvation, by synthesizing large amounts of (p)ppGpp (Cashel, 1969). RelA carries an inactive (p)ppGpp-hydrolytic domain and does not hydrolyze the alarmone under any conditions. SpoT is a bifunctional enzyme that contains functional (p)ppGpp-synthetic and hydrolytic domains, but displays weak (p)ppGpp-synthetic activity and strong ppGpp hydrolytic activity. The *relA* knockout accumulates ppGpp in response to several environmental stresses, such as carbon and nitrogen (Edlin and Donini, 1971), phosphate (Spira et al., 1995), iron (Vinella et al., 2005), and fatty acid (Battesti and Bouveret, 2006) starvation.

Early in (p)ppGpp research different spontaneous alleles of *relA* and *spoT* have been isolated. For instance, the *spoT*1 allele (Laffler and Gallant, 1974), that confers a spotless phenotype (absence of pppGpp under amino acid starvation), was isolated from the old 58-161 strain and is now common in many K-12 derivatives (Alföldi et al., 1962). Bacteria that carry the *spoT*1 allele overproduce (p)ppGpp both under nutrient starvation and under normal growth conditions. The *spoT*1 allele contains two different mutations - a H255Y substitution in the synthetase domain (Synth) and a two-amino acid insertion between residues 82 and 83 (+QD) in the hydrolytic domain (HD), both at the NTD portion of SpoT (**Figure 1**). The two amino acid insertions in the HD domain are likely to negatively affect the ppGpp-hydrolytic activity of SpoT resulting in high (p)ppGpp basal levels, while the H255Y substitution hits a conserved residue (Atkinson et al., 2011), but its effect on the (p)ppGpp-synthetic activity of SpoT is hard to predict. Interestingly, *spoT*1 is usually accompanied in many strains by the defective *relA*1 allele, consisting of an IS2 insertion in the HD domain that is likely to disrupt RelA (p)ppGpp-synthetic activity (Metzger et al., 1989). The *relA*1 mutant displays lower ppGpp basal level than the *relA*$^+$ strain (Lagosky and Chang, 1980) and does not accumulate (p)ppGpp in response to amino acid starvation. Apparently, the high ppGpp basal level caused by the *spoT*1 allele is compensated by the defect in (p)ppGpp synthesis caused by the presence of *relA*1. It is therefore no wonder that both alleles often appear together in the same genome.

Later on, other *spoT* alleles, such as *spoT*201, *spoT*202 an *spoT*203 were isolated by selection on amino-triazole plates (Sarubbi et al., 1988). Amino-triazole is a herbicide that inhibits the synthesis of histidine. Bacteria that synthesize high levels of (p)ppGpp overcome histidine starvation by inducing the expression of the *his* operon (Rudd et al., 1985). A critical difference between *spoT*201 and the other three alleles was that the former confers an almost normal growth rate. The other alleles (*spoT*202-203) considerably reduced growth rate and for that reason could be transferred only to a *relA*1 background, but not to a bacterium that carries a wild-type *relA* allele. The *spoT* alleles *spoT*202 and *spoT*203 consist, respectively, of T78I and R140C substitutions, both in the HD domain (Potrykus et al., 2011). The molecular nature of the *spoT*201 mutation has not been published. Given the high (p)ppGpp level in strains bearing these alleles, the *spoT*201-203 mutations have probably compromised the ppGppase activity of SpoT.

It became evident that an inverse linear correlation exists between the intrinsic level of (p)ppGpp in a bacterium (basal level under unrestricted growth conditions) and the bacterial growth rate (Sarubbi et al., 1988). This negative correlation was confirmed when *spoT* mutant alleles were transferred to other genetic backgrounds (Spira et al., 2008). The recombinant strains displayed all the hallmarks of the previously analyzed *spoT* mutations, namely slower growth rate, high levels of the sigma factor RpoS (coordinator of the general stress response) and high resistance to environmental stresses (see below).

The above mentioned *relA* and *spoT* alleles and most data on (p)ppGpp physiology and homeostasis were obtained by studying laboratory strains derived from the ancestral K-12 strain. To date very few attempts have been made to analyze (p)ppGpp homeostasis in natural isolates of *E. coli*. In two of these studies, the basal level and starvation-induced levels of (p)ppGpp were assessed in a set of strains derived from the ECOR collection (Ferenci et al., 2011) and in a collection of Shiga toxin-producing *E. coli* (STEC) strains (Stella et al., 2017). The ECOR collection contains 72 strains from various locations and environments and from five phylogenetic groups (A, B1, B2, D, and E) that supposedly represents the variability in the *E. coli* species (Ochman and Selander, 1984). Most ECOR isolates are commensal, but some are pathogenic. The levels of (p)ppGpp in non-limited minimal medium, in response to amino acid starvation or carbon starvation were reported for 33 strains of the ECOR collection. ppGpp concentrations in the ECOR strains treated with serine hydroxamate, an inhibitor of seryl-tRNA synthetase that induces amino acid starvation, were quite similar in all tested strains. However, (p)ppGpp response to carbon starvation was less homogeneous, consistent with the variation in SpoT observed in those strains. A T13N amino acid substitution was common in strains that showed low (p)ppGpp accumulation in response to carbon starvation and was absent in strains presenting high levels of ppGpp (Ferenci et al., 2011). These data suggested that *spoT* is being subjected to microevolutionary pressures.

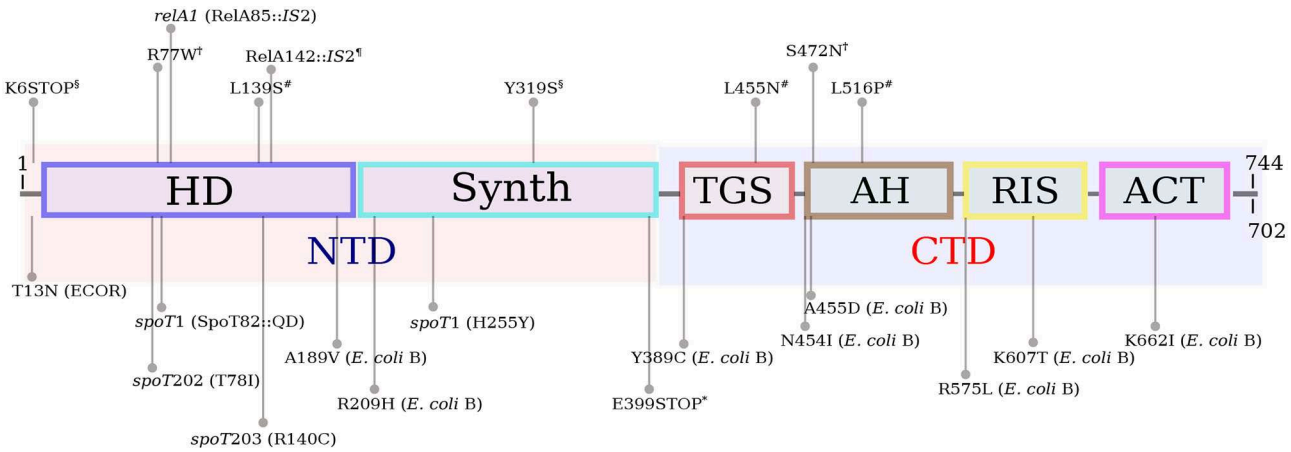

FIGURE 1 | Schematic representation of the long RSH (RelA/SpoT) architecture, as per Atkinson et al. (2011) and Loveland et al. (2016). The RelA and SpoT proteins contain 744 and 702 amino acids, respectively. The NTD half of RSH proteins harbors the catalytic HD (hydrolytic) and Synth (Synthetic) domains. In RelA, the HD domain is not active. The CTD portion of the protein contains four regulatory domains: TGS (ThrRS, GTPase, SpoT/RelA domain), AH (α-helical domain), RIS (Ribosome-InterSubunit domain) and ACT (Aspartate kinase-Chorismate mutase-TyrA domain). The mutations in RelA and SpoT mentioned in the main text are shown above and below the protein diagram, respectively. *relA*1, *spoT*1, *spoT*202 and *spoT*203 are known mutations present in many *E. coli* K-12 derivatives. The *spoT*1 allele consists of two mutations. All mutations, with the exception of those that are followed by *E. coli* B or ECOR (in parentheses) were found in K-12 strains. The T13N substitution is common in strains of the ECOR collection (Ferenci et al., 2011). The SpoT mutations in *E. coli* B were selected in an evolution experiment in glucose-limited minimal medium (Cooper et al., 2003). Mutations ending with "*" were selected during adaptation to high temperature (Kishimoto et al., 2010); "¶" labels indicate RelA mutations selected for n-butanol tolerance (Reyes et al., 2012); "#" labels point to mutations in RelA selected under high ethanol concentration (Horinouchi et al., 2015); RelA mutations ending with "†" were selected for isopropanol tolerance (Horinouchi et al., 2017) and "§" labels indicate RelA mutations selected under growth with lactate (Conrad et al., 2009).

It is well-established that the intrinsic concentration of (p)ppGpp is inversely correlated with growth rate (Ryals et al., 1982; Sarubbi et al., 1988; Potrykus et al., 2011; Jin et al., 2012). In fact, gratuitous induction of (p)ppGpp synthesis mediated by *relA* overexpression causes an almost instantaneous growth arrest (Schreiber et al., 1991; Svitil et al., 1993; Cruvinel et al., 2019). However, the vast majority of studies that analyzed this correlation used isogenic *E. coli* laboratory strains harboring different *relA* or *spoT* alleles. If growth rate is mainly regulated by (p)ppGpp a good correlation between (p)ppGpp levels and growth rate, even in a set of non-isogenic strains, would be expected. Indeed, when the intrinsic ppGpp concentrations of the ECOR isolates growing under non-limited growth conditions are plotted against their respective growth rates, an inverse correlation is observed (**Figure 2A**), with a Pearson's correlation coefficient= −0.58. Though not perfect, the inverse correlation between ppGpp concentration and growth rate in these strains validates the central role of (p)ppGpp in governing growth rates across the *E. coli* species, even in strains that come from very different genetic backgrounds as is the case of the ECOR collection. It is worth mentioning that in this as well as in other studies that analyzed (p)ppGpp in exponentially growing bacteria or in response to stresses other than amino acid starvation, pppGpp was below the detection level (Varik et al., 2017; Cruvinel et al., 2019).

In another analysis of (p)ppGpp fluctuation in natural isolates, ppGpp concentration was measured in 50 STEC strains growing under two different culture conditions—non-limited growth medium and phosphate starvation (Stella et al., 2017). A significant variability in ppGpp levels was observed among the STEC isolates (**Figure 2B**). On average, ppGpp values were twice as high in bacteria submitted to Pi starvation than in the same bacteria growing exponentially in minimal medium. ppGpp values in this set of strains went from 0.08 to 0.30 units for bacteria growing exponentially and from 0.17 to 0.42 units for phosphate-starved bacteria (units correspond to the ratio of ppGpp over GTP+ppGpp). Though this study did not evaluate the variability of ppGpp with growth rate, it correlated the levels of this alarmone with STEC cytotoxicity, as described below.

Altogether, the data presented here highlight the existence of variability in intrinsic ppGpp concentrations across the *E. coli* species and that this variability has a substantial impact on growth rate. However, in addition to growth rate control (p)ppGpp directly and indirectly affects many important bacterial characteristics, such as stress responses, virulence, antibiotic resistance and persistence, biofilm formation, genome stability, and more (Potrykus and Cashel, 2008; Dalebroux et al., 2010; Martin-Rodriguez and Romling, 2017; Rasouly et al., 2017; Hobbs and Boraston, 2019). Variability in (p)ppGpp basal levels is thus likely to affect these traits as well.

It is important to notice that in the studies mentioned above that compared (p)ppGpp values in isogenic and non-isogenic strains, (p)ppGpp was assessed using the classical method of formic acid extraction of ^{32}P-labeled bacterial nucleotide pools. These studies did not provide absolute values of (p)ppGpp concentration, but instead presented the level of ppGpp relative to that of GTP+ppGpp as detailed in Cashel (1994). The most relevant limitations of this method is the lack of absolute

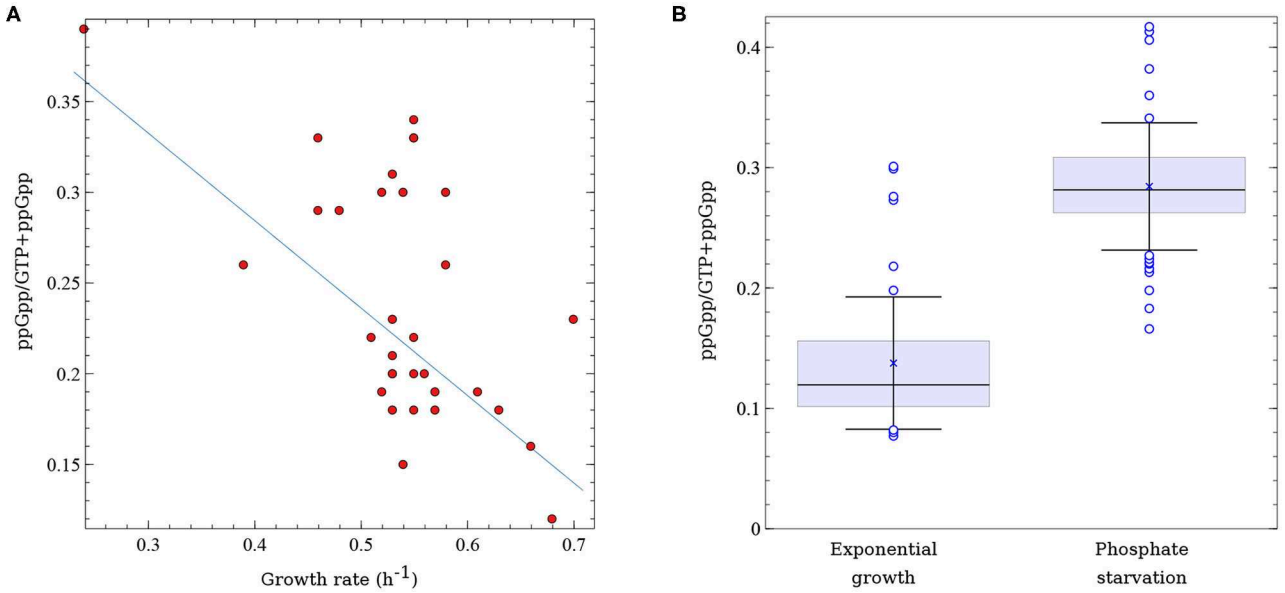

FIGURE 2 | Variability in (p)ppGpp levels across *E. coli* natural isolates. **(A)** Correlation between (p)ppGpp basal levels and growth rate (h^{-1}) in 33 strains of the ECOR collection growing exponentially in glucose minimal medium. ppGpp levels correspond to the ratio between ppGpp and GTP + ppGpp. Data was extracted from Ferenci et al. (2011). **(B)** Distribution of ppGpp levels (ppGpp/GTP+ppGpp) in 50 STEC isolates growing exponentially in non-limited (glucose) minimal medium or under phosphate starvation. x corresponds to the mean values, horizontal lines represent the median and the error bars correspond to 1 standard deviation; ○ represent outliers. Data was extracted from Stella et al. (2017).

numerical estimates of (p)ppGpp concentrations and that it leaves out GDP, which constitutes 7.7–15% of the total pool of guanosine nucleotides (Varik et al., 2017), as the resolution of the ^{32}P-labeled nucleotides on the TLC plate is not usually good enough to identify GDP spots on the autoradiogram. Because of these limitations, the ppGpp values obtained in those studies cannot be easily compared to the ones found in other reports. However, the relative values of (p)ppGpp obtained by the classical method are reproducible and give a reasonable estimate of (p)ppGpp status in a particular set of strains. More recent techniques for evaluating (p)ppGpp, based on Ion Chromatography-High-Resolution MS (Patacq et al., 2018), HPLC (Varik et al., 2017), or UPLC (Ihara et al., 2015) largely overcome the disadvantages of the ^{32}P-classical method.

ROLE OF (p)ppGpp IN STRESS RESISTANCE AND NUTRITIONAL COMPETENCE

(p)ppGpp supports survival by either directly or indirectly stimulating the expression of genes involved in stress protection. The cell response to environmental stresses such as extreme pH and osmolarity, dehydration or oxidative stress is coordinated by the sigma factor RpoS (Landini et al., 2014; Schellhorn, 2014), whose synthesis and stability is enhanced by (p)ppGpp (Gentry et al., 1993; Battesti et al., 2011). The culture history of a bacterial population determines its overall physiology, and more specifically, the strength of its response to environmental challenges (Ryall et al., 2012). The specific hurdles that a bacterial lineage experiences throughout its existence would eventually leave their imprints in its genome. For instance, alleles that maintain high levels of RpoS and other stress-related genes would be selected in a population that is being often exposed to environmental stresses Conversely, bacteria growing in a stress-free environment accumulates mutations in genes that downregulate RpoS synthesis, promotes its proteolysis or even acquire null mutations in the *rpoS* gene itself (King et al., 2004; Spira and Ferenci, 2008; Wang et al., 2010). Likewise, genes involved in (p)ppGpp metabolism are under selective pressures driven by culture conditions (Spira et al., 2008; Ferenci et al., 2011). ppGpp pleiotropy indicates that variations in intrinsic (p)ppGpp levels might have broad consequences on bacterial physiology and genotypic characteristics of bacterial populations. Bacteria that display intrinsic high levels of (p)ppGpp are more resistant to environmental stresses either because they express high levels of RpoS or because (p)ppGpp directly stimulates the transcription of other genes related to stress protection. However, the correlation between (p)ppGpp and RpoS is not as straightforward as would be expected from extrapolating data on K-12 strains (Gentry et al., 1993; Spira et al., 2008; Battesti et al., 2011). Analysis of *E. coli* natural isolates does not give a simple relationship in which RpoS concentration is proportional to (p)ppGpp concentration. While some strains exhibit a proportionality between the two measured entities, others display mediocre levels of RpoS but high (p)ppGpp levels (Ferenci et al., 2011). Surely, there are other inputs, other than (p)ppGpp that modulate the levels of RpoS.

Both (p)ppGpp and RpoS directly affect the transcription of dozens of genes and indirectly the transcription of many others (Peano et al., 2015; Wong et al., 2017). RpoS competes with other sigma factors, particularly with σ^{70} for binding to the core RNA polymerase. The outcome of this competition is that under nutrient limitation or in the stationary phase (circumstances that cause the accumulation of RpoS), the transcription of σ^{70}-dependent genes, i.e., the majority of bacterial genes, is considerably diminished. Hence, the stimulatory effect of (p)ppGpp on RpoS adds another layer of growth control in addition to the already discussed inhibition of stable RNA. Bacterial strains that accumulate high levels of (p)ppGpp or RpoS are less fit for growing on poor carbon sources or under nutrient limitation (King et al., 2004). A trade-off is thus characterized in which a certain bacterial strain cannot simultaneously be nutritionally competent and highly stress resistant (Ferenci, 2016). **Figure 3** shows how bacteria with high or low intrinsic (p)ppGpp concentrations deal with environmental challenges.

INTRINSIC (p)ppGpp CONCENTRATION AS A TARGET IN EVOLUTION EXPERIMENTS

Given that (p)ppGpp is the most important source of growth rate control (Potrykus et al., 2011), polymorphism in *relA* and *spoT* are likely to occur throughout the course of bacterial evolution and adaptation to different environments, especially in those limited in one or more nutrients, a situation that suppresses normal growth. Several evolution experiments, which resulted in the emergence of mutants related to (p)ppGpp both in batch and in continuous cultures, have been conducted to date. The mutations observed in these studies are summarized in **Figure 1**.

In one of them, 12 *E. coli* populations have been daily diluted in glucose limited minimal medium and grown for 20,000 generations. Different non-synonymous mutations in *spoT* have been observed in 8 out of 12 evolved populations (Cooper et al., 2003). The first one, A189V is located at the very end of the HD domain; R209H is at the ∼45-residues region between the HD and Synth domains; Y389C is at the regulatory TGS domain; N454I and A455D are located at the beginning of the α-helical domain; the mutations R575L and R607L are in the RIS domain and K662I is at the ACT domain. Although (p)ppGpp levels were not measured in this study, the expression of aminoacyl-tRNA synthetases and ribosomal proteins were shown to be upregulated in one of these *spoT* mutants (K662I), suggesting that the mutation caused a reduction in (p)ppGpp intrinsic concentration that led to an increase in growth rate. The ACT domain interacts with the ribosome A site in order to activate the (p)ppGpp synthetic activity (Loveland et al., 2016), thus the K662I substitution is likely to interfere with Synth activation resulting in low (p)ppGpp. A non-sense mutation in the TGS domain of *spoT* (E399*) was observed in another case of adaptive evolution of *E. coli* growing at 43.2° (Kishimoto et al., 2010). This mutant displayed high growth rate at the high temperature, possibly due to a reduction in intrinsic (p)ppGpp levels. This finding is puzzling, once it has been shown that the truncation of the CTD leads to an upshift in (p)ppGpp synthesis (Mechold et al., 2002; Battesti and Bouveret, 2006). However, this particular evolved strain carried additional mutations in *lrp* and *rho* that might have strengthened the observed phenotype.

In another experiment, *E. coli* subjected to adaptive evolution under high ethanol concentrations acquired different mutations in *relA* (L139S, L455N, and L519P) that contributed to an increased tolerance in the presence of 5% ethanol (Horinouchi et al., 2015). According to these authors, the *relA* mutations enabled a relaxed response to ethanol, by diminishing (p)ppGpp concentration, thereby increasing growth rate. The L139S mutation occurred in the pseudo-hydrolytic domain of RelA and is therefore unlikely to affect (p)ppGpp synthesis. The other two mutations—L455N and L516P, were in the TGS and AH domains, respectively. These mutations might have affected the regulation of (p)ppGpp synthesis by RelA as both TGS and AH subunits form the elbow of the boomerang-shaped RelA that interacts with the 30S ribosome and with the deacyl-tRNA (Loveland et al., 2016). A similar study with bacteria growing with increasing concentrations of isopropanol (up to 450 mM) for 210 generations showed that the evolved isolates acquired mutations in *relA* (Horinouchi et al., 2017). Again, the suggested mechanism was that the *relA* mutants expressed RelA proteins that synthesized reduced levels of (p)ppGpp in response to isopropanol, resulting in higher growth rates. The mutations—R77W and S472N, were, as before, in the pseudo-HD and AH domains, respectively.

In another experiment of guided evolution, bacteria grown in a chemostat with increasing butanol concentrations (up to 1.3%) for 144 generations acquired mutations in several genes (Reyes et al., 2012). One of the evolved isolates presented an IS2 insertion at the end of the HD domain of RelA, which has probably compromised the integrity of the entire protein, resulting in a RelA-negative phenotype. Mutations in *relA* also appeared in 2 out of 11 populations growing in lactate minimal medium (Conrad et al., 2009). One mutation—K6*, caused a frameshift at the very beginning of the gene, while the other mutation, Y319S, occurred in the Synth domain of RelA.

In addition to the direct effect of (p)ppGpp on growth, low concentrations of this alarmone also results in reduced levels of RpoS (Gentry et al., 1993; Battesti et al., 2011). Due to the competition between σ^S and σ^{70}, the former negatively affects the expression of growth-related genes, especially those involved in the uptake and assimilation of alternative carbon sources with a consequent reduction in growth rate (Gentry et al., 1993; King et al., 2004; Magnusson et al., 2005; Spira et al., 2008; Ferenci et al., 2011). Thus, mutations in *relA* would also improve growth by diminishing RpoS concentration in the cell. **Figure 3** summarizes the outcomes of bacterial evolution experiments in which mutations in (p)ppGpp-related genes have been observed.

In conclusion, selection of different *relA* and *spoT* alleles in evolution experiments is not uncommon. In fact, in most of these experiments regulatory genes are the primary targets of adaptive selection (Maharjan et al., 2006; Wang et al., 2010). Given the central role that (p)ppGpp plays in the regulation of gene transcription, protein synthesis and growth, it is not

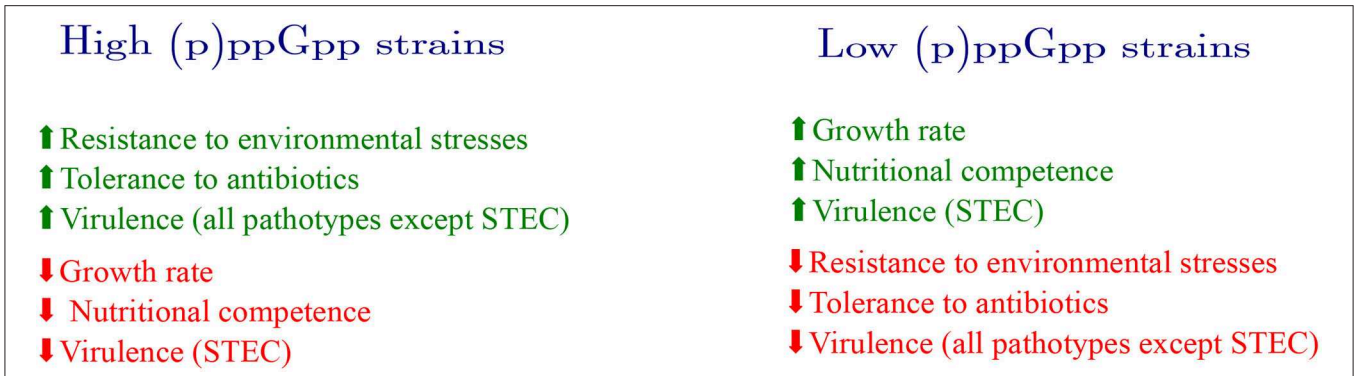

FIGURE 3 | Diversity in (p)ppGpp levels and its consequences. (p)ppGpp intrinsic concentrations are not constant across *E. coli* strains. *E. coli* isolates displaying high (p)ppGpp are benefited under environmental challenges. For instance, these bacteria tolerate higher concentrations of antibiotics and display a higher survival rate when challenged with environmental stresses. Most high-(p)ppGpp pathotypes also show increased ability to colonize host tissues (higher virulence). On the other hand, these strains display lower growth rates and less nutritional competence (ability to utilize alternative carbon sources) than other strains with intrinsically lower (p)ppGpp values. Strains displaying high (p)ppGpp usually carry mutations in the HD domain of SpoT. Mutations in the Synth domain of both RelA or SpoT or in the regulatory domains often cause a reduction in (p)ppGpp levels. The resulting strains display an increased growth rate and higher nutritional competence, but are more sensitive to environmental stresses and antibiotics. STEC is the only known *E. coli* pathotype whose virulence capability benefits from low (p)ppGpp levels.

surprising that modulation of (p)ppGpp is a primary target for evolution.

VARIABILITY IN (p)ppGpp LEVELS AND ITS INFLUENCE ON ANTIBIOTIC SUSCEPTIBILITY

The stringent response has been linked to bacterial tolerance to β-lactam antibiotics in *E. coli*. Tolerance to antibiotics is defined as the ability of microorganisms to survive transient exposure to high concentrations of an antibiotic without a change in the minimum inhibitory concentration (MIC) (Brauner et al., 2016). When both the wild-type strain and *relA* null mutants were exposed to penicillin under amino acid starvation, only the former was able to avoid cell lysis triggered by the presence of the antibiotic (Goodell and Tomasz, 1980; Kusser and Ishiguro, 1985). Moreover, the protective effect of the stringent response against β-lactam antibiotics was reverted by the addition of chloramphenicol (Kusser and Ishiguro, 1985), a well-known inhibitor of the stringent response (Cortay and Cozzone, 1983). In the aforementioned studies (p)ppGpp levels were not directly measured, however, it has been subsequently shown that mecillinam-tolerant mutants accumulated more (p)ppGpp than mecillinam-sensitive strains (Vinella et al., 1992). It became thus evident that high concentrations of (p)ppGpp increase the level of mecillinam tolerance (Joseleau-Petit et al., 1994). The mechanism by which (p)ppGpp confers tolerance to β-lactams was not entirely elucidated. One possibility is that (p)ppGpp acts by inhibiting the biosynthesis of phospholipids. In fact, treatment with cerulenin, an inhibitor of fatty acid biosynthesis, induced β-lactam resistance in the Δ*relA* mutant (Rodionov et al., 1995). In addition, the gratuitous induction of (p)ppGpp accumulation by overexpression of *relA* resulted in the inhibition of phospholipid and peptidoglycan synthesis and in penicillin tolerance (Rodionov and Ishiguro, 1995) supporting the idea that (p)ppGpp mediates penicillin tolerance through the inhibition of phospholipid synthesis (Rodionov and Ishiguro, 1996). However, a more recent study has demonstrated that antibiotic tolerance to β-lactams occurs even in the absence of RelA (Kudrin et al., 2017). *E. coli* cells treated with mupirocin, an isoleucyl-tRNA syntethase inhibitor, displayed increased ampicillin tolerance in the wild-type but not in the relaxed strain. In contrast, the combination of trimethoprim with mupirocin, tetracycline or chloramphenicol significantly increased tolerance to ampicillin in both strains. These data indicate that growth arrest/protein synthesis inhibition can, at least in some cases, increase bacterial tolerance to antibiotics in a (p)ppGpp-independent fashion.

The positive relation between antibiotic tolerance and intrinsic (p)ppGpp concentrations is not restricted to β-lactam antibiotics. The wild-type strain of *E. coli* displayed higher MIC values for trimethoprim, gentamicin and polymixin when compared to the Δ*relA* or Δ*relA* Δ*spoT* mutants (Greenway and England, 1999). The increase in MIC values characterizes an augment in bacterial resistance to these antibiotics (Brauner et al., 2016). Likewise, it has been shown that mutations in the aminoacyl-tRNA synthetase genes *leuS* and *aspS* reduced susceptibility to ciprofloxacin, chloramphenicol, rifampicin, mecillinam, ampicillin, and trimethoprim. Deletion of the *relA* gene in these mutants restored the original MIC values of these antibiotics (Garoff et al., 2018). In another instance bacteria expressing high levels of (p)ppGpp displayed resistance to microcin J25, while strains unable to produce (p)ppGpp were completely sensitive to this antibiotic. In addition, overexpression of *relA* in a strain naturally susceptible to microcin J25 resulted in high MIC values and higher survival rates in killing curves (Pomares et al., 2008).

Several studies have shown a positive correlation between the expression of *hipA*, that encodes a serine/threonine-protein kinase that belongs to a type-II toxin/anti-toxin module,

(p)ppGpp production and the formation of persisters (Korch et al., 2003; Bokinsky et al., 2013; Germain et al., 2013; Kaspy et al., 2013). Persistence is the ability of a subpopulation of an antibiotic-sensitive strain to survive for longer periods of time in the presence of high concentrations of an antibiotic than the majority of the population (Brauner et al., 2016). Some strains are able to form a higher percentage of persisters than others. For instance, strains carrying the *hipA*7 allele formed 100-fold more persistent cells than the wild-type strain when exposed to ampicillin. In the absence of (p)ppGpp (Δ*relA* Δ*spoT* double mutant) the *hipA*7 allele did not confer any advantage regarding antibiotic persistence, suggesting that the high-persistence phenotype elicited by *hipA*7 is (p)ppGpp-dependent. Accordingly, overexpression of *relA* in the *hipA*7 strain increased the frequency of persisters (Korch et al., 2003). On the other hand, overexpression of *hipA* granted resistance to ampicillin, but only in *relA*$^+$ bacteria, as bacteria overexpressing *hipA* but lacking *relA* were considerably more sensitive to ampicillin. Interestingly, the level of (p)ppGpp in the *relA*$^+$ strain overexpressing *hipA* was as high as under amino acid starvation (Bokinsky et al., 2013). Two other studies confirmed the findings of Bokinsky et al. and extended their observations to fluoroquinolone antibiotics (Germain et al., 2013; Kaspy et al., 2013). In addition, these studies suggested a mechanism for *hipA* stimulation of persistence via (p)ppGpp. In their model *hipA* inactivates the glutamyl-tRNA synthetase GltX resulting in the accumulation of uncharged tRNAs which ultimately leads to the activation of RelA and (p)ppGpp synthesis.

Formation of persister cells in bacteria exposed to ofloxacin and ampicillin was also observed upon carbon source transitions, a situation that causes the accumulation of (p)ppGpp (Amato et al., 2013; Amato and Brynildsen, 2015). Deletion of *relA* abolished the formation of ampicillin, but not of ofloxacin persistence, which required the deletion of both *relA* and *spoT*. Furthermore, by controlling the level of (p)ppGpp it has been shown that formation of ampicillin persisters required higher concentrations of (p)ppGpp than formation of ofloxacin persisters. It has also been shown that under conditions of nitrogen starvation *E. coli* accumulates high levels of (p)ppGpp and forms high percentages of persisters when treated with ciprofloxacin, but only in a *relA*$^+$ strain (Brown, 2019).

Integrons are important elements in the dissemination of antibiotic resistance genes. It has been shown that (p)ppGpp plays a role in the regulation of *intI*1, which encodes an integrase protein found in class 1 integrons (Strugeon et al., 2016). Accumulation of (p)ppGpp causes the stalling of RNA-polymerase and the formation of R-loops, which in turn activates the SOS response. The autoproteolysis of the *intI*1 repressor, LexA, ensues resulting in the transcription of *intI*1. *In trans* expression of this gene in the Δ*relA* Δ*spoT* double mutant resulted in reduced *intI*1 promoter activity when compared to the parental strains. Overall, these data indicate that (p)ppGpp helps propagating antibiotic resistance genes through activation of integrase in class 1 integrons.

VARIABILITY IN (p)ppGpp–EFFECT ON BACTERIAL PATHOGENICITY

The expression of virulence-related genes in pathogenic *E. coli* is very well-integrated with (p)ppGpp homeostasis Dalebroux et al. (2010). For instance, (p)ppGpp influences the ability of enterohemorrhagic *E. coli* (EHEC) to colonize the host intestine (Nakanishi et al., 2006). This *E. coli* pathotype secretes a potent cytotoxin—Shiga toxin, that causes serious diseases in humans—bloody diarrhea and HUS (hemolytic uremic syndrome). In addition, bacteria of this pathotype harbor a 35 Kb pathogenicity island known as the Locus of Enterocyte Effacement (LEE), which carries most genes implicated in EHEC intimate adherence (Nguyen and Sperandio, 2012). The passage from the nutrient-rich higher intestine to the nutrient-limited lower intestine triggers the accumulation of (p)ppGpp, which in turn stimulates the transcription of the LEE operons. The EHEC Δ*relA* mutant was unable to induce bacterial adherence or expression of the LEE (Nakanishi et al., 2006). Overexpression of *relA* greatly stimulated the expression of EspB and Tir, two proteins encoded by the LEE and increased the transcription of several LEE genes, implying a positive correlation between (p)ppGpp concentration and EHEC virulence. EPEC (Enteropathogenic *E. coli*) is another diarrheogenic pathotype that carries the LEE, but unlike EHEC it does not produce Shiga toxin. EPEC strains harbor a plasmid (EAF) that encodes both the BFP fimbria associated with bacterial adherence to the intestine cells and the *perABC* operon whose products control the transcription of the chromosomal LEE region (Pearson et al., 2016; Serapio-Palacios and Finlay, 2020). Deletion of *relA* partially impaired EPEC adherence to epithelial cells by diminishing the transcription of the *perABC* operon that controls the expression of the adhesins BFP and intimin (Spira et al., 2014). However, gratuitous overproduction of (p)ppGpp slightly inhibited the expression of *perABC*. The antagonistic effects of (p)ppGpp on *perABC* expression suggests that a fine-tuned concentration of (p)ppGpp is required to maximize EPEC adherence. Even though (p)ppGpp concentrations were not assessed in different EHEC and EPEC isolates the data presented in these studies suggest that the expression of virulence genes and virulence traits are modulated by this alarmone.

Shiga toxin-producing *E. coli* (STEC) is another diarrheogenic pathotype that secretes Shiga toxin, but unlike EHEC, does not harbors a LEE and, consequently, does not display intimate adherence to intestinal cells (Bryan et al., 2015; Joseph et al., 2020). The role of (p)ppGpp in STEC virulence and particularly in toxin production and secretion has been examined in detail. The *stx* genes that encode Shiga toxin were introduced in the STEC genome by means of lambdoid bacteriophages, a phenomenon known as phage lysogenic conversion (Harrison and Brockhurst, 2017). The synthesis and release of Shiga toxin is preceded by the induction of the bacteriophage, a development that eventually results in cell lysis (Waldor and Friedman, 2005; Nowicki et al., 2013). Therefore, the level of Shiga-toxin production and release is directly related to the number of STEC bacteria in a population undergoing phage induction. On the other hand, (p)ppGpp has been shown to inhibit stx phage replication, as the Δ*relA* Δ*spoT* double

mutant displayed a higher degree of phage DNA replication and formed larger plaques on Δ*relA* Δ*spoT* lawns (Nowicki et al., 2013). A subsequent report has shown that intrinsic (p)ppGpp concentration is indeed inversely correlated with Stx toxin production, as STEC strains showing higher cytotoxicity toward Vero cells (the golden standard method for measuring toxin production and STEC virulence) usually contained lower levels of (p)ppGpp (Stella et al., 2017).

The extraintestinal uropathogenic *E. coli* (UPEC) causes recurrent infections in the urinary tract. A critical mechanism of UPEC infection is the ability to invade the bladder cells by means of Type-I fimbriae. The expression of fimbrial genes is controlled by (p)ppGpp and DksA (Aberg et al., 2008). DksA is a transcription factor that binds to RNA polymerase and greatly enhances the effect of (p)ppGpp on transcription regulation (Gourse et al., 2018). (p)ppGpp activates the promoter of *fimB* that encodes a recombinase that specifically inverts the promoter of the *fimAICDFGH* operon. This operon codes for the structural components of the type-I fimbria. By inverting the promoter orientation FimB allows the transcription of the *fimAICDFGH* operon switching the promoter from "off" to "on" state (Eisenstein, 1981). Amino acid starvation or growth arrest caused by bacteria entering the stationary phase increase (p)ppGpp which activates the *fimB* and *fimA* promoters (Aberg et al., 2006). Likewise, *relA* overexpression also induces the transcription from these promoters resulting in the synthesis of Type-I fimbria and the invasion and colonization of bladder cells. Altogether, the data suggest that UPEC strains with high (p)ppGpp intrinsic levels present higher levels of virulence toward the host.

Lastly, (p)ppGpp is directly associated with the pathogenicity of many bacterial species and is required for the full expression of virulence genes (Dalebroux et al., 2010; Kalia et al., 2013). Interestingly, STEC, the only *E. coli* pathotype in which a populational study correlating (p)ppGpp and pathogenicity has been performed stands out as an outlier. STEC toxin production is coupled to phage induction, which is inhibited by (p)ppGpp. By inhibiting phage replication (p)ppGpp acts as a legitimate promoter of bacterial survival.

CONCLUSIONS

The intrinsic concentration of (p)ppGpp in strains of the species *Escherichia coli* is not constant. Rather, the level of (p)ppGpp is been shaped by the historical contingency of bacterial populations. There are two types of evidence that support this assertion: direct assessment of (p)ppGpp in *E. coli* natural isolates and the selection of *relA* and *spoT* mutant alleles in evolution experiments. These data indicate that the genes that govern (p)ppGpp synthesis and degradation are subjected to frequent microevolutionary pressures that will eventually determine the optimal concentration of (p)ppGpp in a population. Given the pleiotropic effects of (p)ppGpp in the cell, adjustments of (p)ppGpp intrinsic concentration should have broad implications on bacterial physiology (**Figure 3**). In fact, intrinsic variations in (p)ppGpp levels differentially affect growth, stress response, virulence and antibiotic resistance. However, the intrinsic levels of (p)ppGpp in *E. coli* natural isolates do not perfectly correlate with the expected phenotypes. For instance, growth rate and (p)ppGpp inverse correlation across the ECOR strains was significant but not perfect, which suggests that the role of this alarmone in growth is intertwined with other regulatory circuits and that bacterial physiology is always more complex than firstly assumed.

AUTHOR CONTRIBUTIONS

BS and KO drafted the manuscript. All authors contributed to the article and approved the submitted version.

FUNDING

This work was supported by FAPESP grant number 2018/1629-5. BS is a recipient of a CNPq productivity scholarship. KO is a recipient of a CAPES scholarship.

REFERENCES

Aberg, A., Shingler, V., and Balsalobre, C. (2006). (p)ppGpp regulates type 1 fimBriation of *Escherichia coli* by modulating the expression of the site-specific recombinase fimB. *Mol. Microbiol.* 60, 1520–1533. doi: 10.1111/j.1365-2958.2006.05191.x

Aberg, A., Shingler, V., and Balsalobre, C. (2008). Regulation of the fimB promoter: a case of differential regulation by ppGpp and DksA *in vivo*. *Mol. Microbiol.* 67, 1223–1241. doi: 10.1111/j.1365-2958.2008.06115.x

Alföldi, L., Stent, G. S., and Clowes, R. C. (1962). The chromosomal site of the RNA control (RC) locus in *Escherichia coli*. *J. Mol. Biol.* 5, 348–355. doi: 10.1016/S0022-2836(62)80077-1

Amato, S. M., and Brynildsen, M. P. (2015). Persister heterogeneity arising from a single metabolic stress. *Curr. Biol.* 25, 2090–2098. doi: 10.1016/j.cub.2015.06.034

Amato, S. M., Orman, M. A., and Brynildsen, M. P. (2013). Metabolic control of persister formation in *Escherichia coli*. *Mol. Cell* 50, 475–487. doi: 10.1016/j.molcel.2013.04.002

Atkinson, G. C., Tenson, T., and Hauryliuk, V. (2011). The RelA/spot homolog (RSH) superfamily: distribution and functional evolution of ppGpp synthetases and hydrolases across the tree of life. *PLoS ONE* 6:e23479. doi: 10.1371/journal.pone.0023479

Battesti, A., and Bouveret, E. (2006). Acyl carrier protein/spot interaction, the switch linking spot-dependent stress response to fatty acid metabolism. *Mol. Microbiol.* 62, 1048–1063. doi: 10.1111/j.1365-2958.2006.05442.x

Battesti, A., Majdalani, N., and Gottesman, S. (2011). The RpoS-mediated general stress response in *Escherichia coli*. *Annu. Rev. Microbiol.* 65, 189–213. doi: 10.1146/annurev-micro-090110-102946

Bokinsky, G., Baidoo, E. E., Akella, S., Burd, H., Weaver, D., Alonso-Gutierrez, J., et al. (2013). HipA-triggered growth arrest and β-lactam tolerance in *Escherichia coli* are mediated by RelA-dependent ppGpp synthesis. *J. Bacteriol.* 195, 3173–3182. doi: 10.1128/JB.02210-12

Brauner, A., Fridman, O., Gefen, O., and Balaban, N. Q. (2016). Distinguishing between resistance, tolerance and persistence to antibiotic treatment. *Nat. Rev. Microbiol.* 14, 320–330. doi: 10.1038/nrmicro.2016.34

Brown, D. R. (2019). Nitrogen starvation induces persister cell formation in *Escherichia coli*. *J. Bacteriol.* 201:e00622-18. doi: 10.1128/JB.00622-18

Bryan, A., Youngster, I., and McAdam, A. J. (2015). Shiga toxin producing *Escherichia coli*. *Clin. Lab. Med*. 35, 247–272. doi: 10.1016/j.cll.2015.02.004

Cashel, M. (1969). The control of ribonucleic acid synthesis in *Escherichia coli* IV. relevance of unusual phosphorylated compounds from amino acid-starved stringent strains. *J. Biol. Chem*. 244, 3133–3141.

Cashel, M. (1994). Detection of (p)ppGpp accumulation patterns in *Escherichia coli* mutants. *Methods Mol. Genet*. 3, 341–356.

Cashel, M., and Gallant, J. (1968). Control of RNA synthesis in *Escherichia coli*. I. amino acid dependence of the synthesis of the substrates of RNA polymerase. *J. Mol. Biol*. 34, 317–330. doi: 10.1016/0022-2836(68)90256-8

Conrad, T. M., Joyce, A. R., Applebee, M. K., Barrett, C. L., Xie, B., Gao, Y., et al. (2009). Whole-genome resequencing of *Escherichia coli* K-12 mg1655 undergoing short-term laboratory evolution in lactate minimal media reveals flexible selection of adaptive mutations. *Genome Biol*. 10:R118. doi: 10.1186/gb-2009-10-10-r118

Cooper, T. F., Rozen, D. E., and Lenski, R. E. (2003). Parallel changes in gene expression after 20,000 generations of evolution in *Escherichia coli*. *Proc. Natl. Acad. Sci. U.S.A*. 100, 1072–1077. doi: 10.1073/pnas.0334340100

Cortay, J., and Cozzone, A. (1983). Effects of aminoglycoside antibiotics on the coupling of protein and rna syntheses in *Escherichia coli*. *Biochem. Biophys. Res. Commun*. 112, 801–808. doi: 10.1016/0006-291X(83)91688-1

Cruvinel, G. T., Neves, H. I., and Spira, B. (2019). Glyphosate induces the synthesis of ppGpp. *Mol. Genet. Genome* 294, 191–198. doi: 10.1007/s00438-018-1499-1

Dalebroux, Z. D., Svensson, S. L., Gaynor, E. C., and Swanson, M. S. (2010). ppGpp conjures bacterial virulence. *Micro Mol. Biol. Rev*. 74, 171–199. doi: 10.1128/MMBR.00046-09

Edlin, G., and Donini, P. (1971). Synthesis of guanosine 5'-diphosphate, 2'-(or 3'-) diphosphate and related nucleotides in a variety of physiological conditions. *J. Biol. Chem*. 246, 4371–4373.

Eisenstein, B. I. (1981). Phase variation of type 1 Fimbriae in *Escherichia coli* is under transcriptional control. *Science* 214, 337–339. doi: 10.1126/science.6116279

Ferenci, T. (2016). Trade-off mechanisms shaping the diversity of bacteria. *Trends Microbiol*. 24, 209–223. doi: 10.1016/j.tim.2015.11.009

Ferenci, T., Galbiati, H. F., Betteridge, T., Phan, K., and Spira, B. (2011). The constancy of global regulation across a species: the concentrations of ppGpp and rpos are strain-specific in *Escherichia coli*. *BMC Microbiol*. 11:62. doi: 10.1186/1471-2180-11-62

Garoff, L., Huseby, D. L., Praski Alzrigat, L., and Hughes, D. (2018). Effect of aminoacyl-trna synthetase mutations on susceptibility to ciprofloxacin in *Escherichia coli*. *J. Antimicrob. Chemother*. 73, 3285–3292. doi: 10.1093/jac/dky356

Gentry, D. R., HeRNAndez, V. J., Nguyen, L. H., Jensen, D. B., and Cashel, M. (1993). Synthesis of the stationary-phase sigma factor sigma s is positively regulated by ppGpp. *J. Bacteriol*. 175, 7982–7989. doi: 10.1128/JB.175.24.7982-7989.1993

Germain, E., Castro-Roa, D., Zenkin, N., and Gerdes, K. (2013). Molecular mechanism of bacterial persistence by HipA. *Mol. Cell* 52, 248–254. doi: 10.1016/j.molcel.2013.08.045

Goodell, W., and Tomasz, A. (1980). Alteration of *Escherichia coli* murein during amino acid starvation. *J. Bacteriol*. 144, 1009–1016. doi: 10.1128/JB.144.3.1009-1016.1980

Gourse, R. L., Chen, A. Y., Gopalkrishnan, S., Sanchez-Vazquez, P., Myers, A., and Ross, W. (2018). Transcriptional responses to ppGpp and DksA. *Annu. Rev. Microbiol*. 72, 163–184. doi: 10.1146/annurev-micro-090817-062444

Greenway, D. L., and England, R. R. (1999). The intrinsic resistance of *Escherichia coli* to various antimicrobial agents requires ppGpp and sigma s. *Lett. Appl. Microbiol*. 29, 323–326. doi: 10.1046/j.1472-765X.1999.00642.x

Harrison, E., and Brockhurst, M. A. (2017). Ecological and evolutionary benefits of temperate phage: what does or doesn't kill you makes you stronger. *Bioessays* 39:1700112. doi: 10.1002/bies.201700112

Hobbs, J. K., and Boraston, A. B. (2019). (p)ppGpp and the stringent response: an emerging threat to antibiotic therapy. *ACS Infect. Dis*. 5, 1505–1517. doi: 10.1021/acsinfecdis.9b00204

Horinouchi, T., Sakai, A., Kotani, H., Tanabe, K., and Furusawa, C. (2017). Improvement of isopropanol tolerance of *Escherichia coli* using adaptive laboratory evolution and omics technologies. *J. Biotechnol*. 255, 47–56. doi: 10.1016/j.jbiotec.2017.06.408

Horinouchi, T., Suzuki, S., Hirasawa, T., Ono, N., Yomo, T., Shimizu, H., et al. (2015). Phenotypic convergence in bacterial adaptive evolution to ethanol stress. *BMC Evol. Biol*. 15:180. doi: 10.1186/s12862-015-0454-6

Ihara, Y., Ohta, H., and Masuda, S. (2015). A highly sensitive quantification method for the accumulation of alarmone ppGpp in *Arabidopsis thaliana* using UPLC-ESI-qMS/MS. *J. Plant Res*. 128, 511–518. doi: 10.1007/s10265-015-0711-1

Jin, D. J., Cagliero, C., and Zhou, Y. N. (2012). Growth rate regulation in *Escherichia coli*. *FEMS Microbiol. Rev*. 36, 269–287. doi: 10.1111/j.1574-6976.2011.00279.x

Joseleau-Petit, D., Thévenet, D., and D'Arl, R. (1994). ppGpp concentration, growth without pbp2 activity, and growth-rate control in *Escherichia coli*. *Mol. Microbiol*. 13, 911–917. doi: 10.1111/j.1365-2958.1994.tb00482.x

Joseph, A., Cointe, A., Mariani Kurkdjian, P., Rafat, C., and Hertig, A. (2020). Shiga toxin-associated hemolytic uremic syndrome: a narrative review. *Toxins* 12:67. doi: 10.3390/toxins12020067

Kalia, D., Merey, G., Nakayama, S., Zheng, Y., Zhou, J., Luo, Y., et al. (2013). Nucleotide, c-di-GMP, c-di-AMP, cGMP, cAMP, (p)ppGpp signaling in bacteria and implications in pathogenesis. *Chem. Soc. Rev*. 42, 305–341. doi: 10.1039/C2CS35206K

Kaspy, I., Rotem, E., Weiss, N., Ronin, I., Balaban, N. Q., and Glaser, G. (2013). HipA-mediated antibiotic persistence via phosphorylation of the glutamyl-tRNA-synthetase. *Nat. Commun*. 4, 1–7. doi: 10.1038/ncomms4001

King, T., Ishihama, A., Kori, A., and Ferenci, T. (2004). A regulatory trade-off as a source of strain variation in the species *Escherichia coli*. *J. Bacteriol*. 186, 5614–5620. doi: 10.1128/JB.186.17.5614-5620.2004

Kishimoto, T., Iijima, L., Tatsumi, M., Ono, N., Oyake, A., Hashimoto, T., et al. (2010). Transition from positive to neutral in mutation fixation along with continuing rising fitness in thermal adaptive evolution. *PLoS Genet*. 6:e1001164. doi: 10.1371/journal.pgen.1001164

Korch, S. B., Henderson, T. A., and Hill, T. M. (2003). Characterization of the HipA7 allele of *Escherichia coli* and evidence that high persistence is governed by (p)ppGpp synthesis. *Mol. Microbiol*. 50, 1199–1213. doi: 10.1046/j.1365-2958.2003.03779.x

Kudrin, P., Varik, V., Oliveira, S. R. A., Beljantseva, J., Del Peso Santos, T., Dzhygyr, I., et al. (2017). Subinhibitory concentrations of bacteriostatic antibiotics induce *RelA*-dependent and *RelA*-independent tolerance to β-lactams. *Antimicrob. Agents Chemother*. 61:e02173–16. doi: 10.1128/AAC.02173-16

Kusser, W., and Ishiguro, E. E. (1985). Involvement of the *RelA* gene in the autolysis of *Escherichia coli* induced by inhibitors of peptidoglycan biosynthesis. *J. Bacteriol*. 164, 861–865. doi: 10.1128/JB.164.2.861-865.1985

Laffler, T., and Gallant, J. (1974). *spoT*, a new genetic locus involved in the stringent response in *E. coli*. *Cell* 1, 27–30. doi: 10.1016/0092-8674(74)90151-2

Lagosky, P. A., and Chang, F. N. (1980). Influence of amino acid starvation on guanosine 5'-diphosphate 3'-diphosphate basal-level synthesis in *Escherichia coli*. *J. Bacteriol*. 144, 499–508. doi: 10.1128/JB.144.2.499-508.1980

Landini, P., Egli, T., Wolf, J., and Lacour, S. (2014). sigmaS, a major player in the response to environmental stresses in *Escherichia coli*: role, regulation and mechanisms of promoter recognition. *Environ. Microbiol. Rep*. 6, 1–13. doi: 10.1111/1758-2229.12112

Loveland, A. B., Bah, E., Madireddy, R., Zhang, Y., Brilot, A. F., Grigorieff, N., et al. (2016). Ribosome●RelA structures reveal the mechanism of stringent response activation. *eLife* 5:e17029. doi: 10.7554/eLife.17029

Magnusson, L. U., Farewell, A., and Nyström, T. (2005). ppGpp: a global regulator in *Escherichia coli*. *Trends Microbiol*. 13, 236–242. doi: 10.1016/j.tim.2005.03.008

Maharjan, R., Seeto, S., Notley-McRobb, L., and Ferenci, T. (2006). Clonal adaptive radiation in a constant environment. *Science*. 313, 514–517. doi: 10.1126/science.1129865

Martin-Rodriguez, A. J., and Romling, U. (2017). Nucleotide second messenger signaling as a target for the control of bacterial biofilm formation. *Curr. Top. Med. Chem*. 17:1928–1944 doi: 10.2174/1568026617666170105144424

Mechold, U., Murphy, H., Brown, L., and Cashel, M. (2002). Intramolecular regulation of the opposing (p)ppGpp catalytic activities of Rel_{Seq}, the Rel/Spo enzyme from *Streptococcus equisimilis*. *J. Bacteriol*. 184, 2878–2888. doi: 10.1128/JB.184.11.2878-2888.2002

Metzger, S., Schreiber, G., Aizenman, E., Cashel, M., and Glaser, G. (1989). Characterization of the *RelA1* mutation and a comparison of *RelA1*

with new *RelA* null alleles in *Escherichia coli*. *J. Biol. Chem*. 264, 21146–21152.

Mittenhuber, G. (2001). Comparative genomics and evolution of genes encoding bacterial (p)ppGpp synthetases/hydrolases (the Rel, RelA and SpoT proteins). *J. Mol. Microbiol. Biotechnol*. 3, 585–600.

Nakanishi, N., Abe, H., Ogura, Y., Hayashi, T., Tashiro, K., Kuhara, S., et al. (2006). ppGpp with DksA controls gene expression in the locus of enterocyte effacement (LEE) pathogenicity island of enterohaemorrhagic *Escherichia coli* through activation of two virulence regulatory genes. *Mol. Microbiol*. 61, 194–205. doi: 10.1111/j.1365-2958.2006.05217.x

Nguyen, Y., and Sperandio, V. (2012). Enterohemorrhagic *E. coli* (EHEC) pathogenesis. *Front. Cell. Infect. Microbiol*. 2:90. doi: 10.3389/fcimb.2012.00090

Nowicki, D., Kobiela, W., Węgrzyn, A., Wegrzyn, G., and Szalewska-Pałasz, A. (2013). ppGpp-dependent negative control of DNA replication of Shiga toxin-converting bacteriophages in *Escherichia coli*. *J. Bacteriol*. 195, 5007–5015. doi: 10.1128/JB.00592-13

Ochman, H., and Selander, R. K. (1984). Standard reference strains of *Escherichia coli* from natural populations. *J. Bacteriol*. 157, 690–693. doi: 10.1128/JB.157.2.690-693.1984

Patacq, C., Chaudet, N., and Létisse, F. (2018). Absolute quantification of ppGpp and pppGpp by double-spike isotope dilution ion chromatography-high-resolution mass spectrometry. *Anal. Chem*. 90, 10715–10723. doi: 10.1021/acs.analchem.8b00829

Peano, C., Wolf, J., Demol, J., Rossi, E., Petiti, L., De Bellis, G., et al. (2015). Characterization of the *Escherichia coli* σ(s) core regulon by chromatin immunoprecipitation-sequencing (ChiP-seq) analysis. *Sci. Rep*. 5:10469. doi: 10.1038/srep10469

Pearson, J. S., Giogha, C., Wong Fok Lung, T., and Hartland, E. L. (2016). The genetics of enteropathogenic *Escherichia coli* virulence. *Annu. Rev. Genet*. 50, 493–513. doi: 10.1146/annurev-genet-120215-035138

Pomares, M. F., Vincent, P. A., Farías, R. N., and Salomón, R. A. (2008). Protective action of ppGpp in microcin j25-sensitive strains. *J. Bacteriol*. 190, 4328–4334. doi: 10.1128/JB.00183-08

Potrykus, K., and Cashel, M. (2008). (p)ppGpp: still magical? *Annu. Rev. Microbiol*. 62, 35–51. doi: 10.1146/annurev.micro.62.081307.162903

Potrykus, K., Murphy, H., Philippe, N., and Cashel, M. (2011). ppGpp is the major source of growth rate control in *E. coli*. *Environ. Microbiol*. 13, 563–575. doi: 10.1111/j.1462-2920.2010.02357.x

Rasouly, A., Pani, B., and Nudler, E. (2017). A magic spot in genome maintenance. *Trends Genet*. 33, 58–67. doi: 10.1016/j.tig.2016.11.002

Reyes, L. H., Almario, M. P., Winkler, J., Orozco, M. M., and Kao, K. C. (2012). Visualizing evolution in real time to determine the molecular mechanisms of n-butanol tolerance in *Escherichia coli*. *Metab. Eng*. 14, 579–590. doi: 10.1016/j.ymben.2012.05.002

Rodionov, D. G., and Ishiguro, E. E. (1995). Direct correlation between overproduction of guanosine 3', 5'-bispyrophosphate (ppGpp) and penicillin tolerance in *Escherichia coli*. *J. Bacteriol*. 177, 4224–4229. doi: 10.1128/JB.177.15.4224-4229.1995

Rodionov, D. G., and Ishiguro, E. E. (1996). Dependence of peptidoglycan metabolism on phospholipid synthesis during growth of *Escherichia coli*. *Microbiology* 142, 2871–2877. doi: 10.1099/13500872-142-10-2871

Rodionov, D. G., Pisabarro, A. G., de Pedro, M. A., Kusser, W., and Ishiguro, E. E. (1995). Beta-lactam-induced bacteriolysis of amino acid-deprived *Escherichia coli* is dependent on phospholipid synthesis. *J. Bacteriol*. 177, 992–997. doi: 10.1128/JB.177.4.992-997.1995

Rudd, K. E., Bochner, B. R., Cashel, M., and Roth, J. R. (1985). Mutations in the *spoT* gene of *Salmonella typhimurium*: effects on his operon expression. *J. Bacteriol*. 163, 534–542. doi: 10.1128/JB.163.2.534-542.1985

Ryall, B., Eydallin, G., and Ferenci, T. (2012). Culture history and population heterogeneity as determinants of bacterial adaptation: the adaptomics of a single environmental transition. *Microbiol. Mol. Biol. Rev*. 76, 597–625. doi: 10.1128/MMBR.05028-11

Ryals, J., Little, R., and Bremer, H. (1982). Control of rRNA and tRNA syntheses in *Escherichia coli* by guanosine tetraphosphate. *J. Bacteriol*. 151, 1261–1268. doi: 10.1128/JB.151.3.1261-1268.1982

Sarubbi, E., Rudd, K. E., and Cashel, M. (1988). Basal ppGpp level adjustment shown by new *spoT* mutants affect steady state growth rates and *rRNA* ribosomal promoter regulation in *Escherichia coli*. *Mol. Genet. Genome* 213, 214–222. doi: 10.1007/BF00339584

Schellhorn, H. E. (2014). Elucidating the function of the RpoS regulon. *Future Microbiol*. 9, 497–507. doi: 10.2217/fmb.14.9

Schreiber, G., Metzger, S., Aizenman, E., Roza, S., Cashel, M., and Glaser, G. (1991). Overexpression of the *RelA* gene in *Escherichia coli*. *J. Biol. Chem*. 266, 3760–3767.

Serapio-Palacios, A., and Finlay, B. B. (2020). Dynamics of expression, secretion and translocation of type III effectors during enteropathogenic *Escherichia coli* infection. *Curr. Opin. Microbiol*. 54, 67–76. doi: 10.1016/j.mib.2019.12.001

Spira, B., and Ferenci, T. (2008). Alkaline phosphatase as a reporter of sigma(s) levels and *RpoS* polymorphisms in different *E. coli* strains. *Arch. Microbiol*. 189, 43–47. doi: 10.1007/s00203-007-0291-0

Spira, B., Ferreira, G. M., and de Almeida, L. G. (2014). *RelA* enhances the adherence of enteropathogenic *Escherichia coli*. *PLoS ONE* 9:e91703. doi: 10.1371/journal.pone.0091703

Spira, B., Hu, X., and Ferenci, T. (2008). Strain variation in ppGpp concentration and RpoS levels in laboratory strains of *Escherichia coli* K-12. *Microbiology* 154, 2887–2895. doi: 10.1099/mic.0.2008/018457-0

Spira, B., Silberstein, N., and Yagil, E. (1995). Guanosine 3',5'-bispyrophosphate (ppGpp) synthesis in cells of *Escherichia coli* starved for pi. *J. Bacteriol*. 177, 4053–4058. doi: 10.1128/JB.177.14.4053-4058.1995

Stella, A., Luz, D., Piazza, R., and Spira, B. (2017). ppGpp and cytotoxicity diversity in Shiga toxin-producing *Escherichia coli* (STEC) isolates. *Epidemiol. Infect*. 145, 2204–2211. doi: 10.1017/S0950268817001091

Strugeon, E., Tilloy, V., Ploy, M.-C., and Da Re, S. (2016). The stringent response promotes antibiotic resistance dissemination by regulating integron integrase expression in biofilms. *mBio* 7:e00868-16. doi: 10.1128/mBio.00868-16

Svitil, A. L., Cashel, M., and Zyskind, J. W. (1993). Guanosine tetraphosphate inhibits protein synthesis *in vivo*. a possible protective mechanism for starvation stress in *Escherichia coli*. *J. Biol. Chem*. 268, 2307–2311.

Traxler, M. F., Summers, S. M., Nguyen, H.-T., Zacharia, V. M., Hightower, G. A., Smith, J. T., et al. (2008). The global, ppGpp-mediated stringent response to amino acid starvation in *Escherichia coli*. *Mol. Microbiol*. 68, 1128–1148. doi: 10.1111/j.1365-2958.2008.06229.x

Traxler, M. F., Zacharia, V. M., Marquardt, S., Summers, S. M., Nguyen, H.-T., Stark, S. E., et al. (2011). Discretely calibrated regulatory loops controlled by ppGpp partition gene induction across the 'feast to famine' gradient in *Escherichia coli*. *Mol. Microbiol*. 79, 830–845. doi: 10.1111/j.1365-2958.2010.07498.x

Varik, V., Oliveira, S. R. A., Hauryliuk, V., and Tenson, T. (2017). HPLC-based quantification of bacterial housekeeping nucleotides and alarmone messengers ppGpp and (p)ppGpp. *Sci. Rep*. 7:11022. doi: 10.1038/s41598-017-10988-6

Vinella, D., Albrecht, C., Cashel, M., and d'Ari, R. (2005). Iron limitation induces spot-dependent accumulation of ppGpp in *Escherichia coli*. *Mol. Microbiol*. 56, 958–970. doi: 10.1111/j.1365-2958.2005.04601.x

Vinella, D., D'Ari, R., Jaffe, A., and Bouloc, P. (1992). Penicillin binding protein 2 is dispensable in *Escherichia coli* when ppGpp synthesis is induced. *EMBO J*. 11, 1493–1501. doi: 10.1002/j.1460-2075.1992.tb05194.x

Waldor, M. K., and Friedman, D. I. (2005). Phage regulatory circuits and virulence gene expression. *Curr. Opin. Microbiol*. 8, 459–465. doi: 10.1016/j.mib.2005.06.001

Wang, L., Spira, B., Zhou, Z., Feng, L., Maharjan, R. P., Li, X., et al. (2010). Divergence involving global regulatory gene mutations in an *Escherichia coli* population evolving under phosphate limitation. *Genome Biol. Evol*. 2, 478–487. doi: 10.1093/gbe/evq035

Wong, G. T., Bonocora, R. P., Schep, A. N., Beeler, S. M., Lee Fong, A. J., Shull, L. M., et al. (2017). Genome-wide transcriptional response to varying RpoS levels in *Escherichia coli* K-12. *J. Bacteriol*. 199:e00755–16. doi: 10.1128/JB.00755-16

Conflict of Interest: The authors declare that the research was conducted in the absence of any commercial or financial relationships that could be construed as a potential conflict of interest.

frontiers in Microbiology

ORIGINAL RESEARCH
published: 02 September 2020
doi: 10.3389/fmicb.2020.02083

Small Alarmone Synthetase SasA Expression Leads to Concomitant Accumulation of pGpp, ppApp, and AppppA in *Bacillus subtilis*

Danny K. Fung†, Jin Yang†, David M. Stevenson, Daniel Amador-Noguez and Jue D. Wang**

Department of Bacteriology, University of Wisconsin-Madison, Madison, WI, United States

OPEN ACCESS

Edited by:
Katarzyna Potrykus, University of Gdańsk, Poland

Reviewed by:
Jörg Stülke, University of Göttingen, Germany
Juan Carlos Alonso, National Center for Biotechnology (CNB), Spain

***Correspondence:**
Danny K. Fung
kfung6@wisc.edu
Jue D. Wang
wang@bact.wisc.edu

†These authors have contributed equally to this work

Specialty section:
This article was submitted to Microbial Physiology and Metabolism, a section of the journal Frontiers in Microbiology

Received: *04 June 2020*
Accepted: *07 August 2020*
Published: *02 September 2020*

Citation:
Fung DK, Yang J, Stevenson DM, Amador-Noguez D and Wang JD (2020) Small Alarmone Synthetase SasA Expression Leads to Concomitant Accumulation of pGpp, ppApp, and AppppA in Bacillus subtilis. Front. Microbiol. 11:2083. doi: 10.3389/fmicb.2020.02083

(p)ppGpp is a highly conserved bacterial alarmone which regulates many aspects of cellular physiology and metabolism. In Gram-positive bacteria such as *B. subtilis*, cellular (p)ppGpp level is determined by the bifunctional (p)ppGpp synthetase/hydrolase RelA and two small alarmone synthetases (SASs) YjbM (SasB) and YwaC (SasA). However, it is less clear whether these enzymes are also involved in regulation of alarmones outside of (p)ppGpp. Here we developed an improved LC-MS-based method to detect a broad spectrum of metabolites and alarmones from bacterial cultures with high efficiency. By characterizing the metabolomic signatures of SasA expressing *B. subtilis*, we identified strong accumulation of the (p)ppGpp analog pGpp, as well as accumulation of ppApp and AppppA. The induced accumulation of these alarmones is abolished in the catalytically dead *sasA* mutant, suggesting that it is a consequence of SasA synthetase activity. In addition, we also identified depletion of specific purine nucleotides and their precursors including IMP precursors FGAR, SAICAR and AICAR (ZMP), as well as GTP and GDP. Furthermore, we also revealed depletion of multiple pyrimidine precursors such as orotate and orotidine 5′-phosphate. Taken together, our work shows that induction of a single (p)ppGpp synthetase can cause concomitant accumulation and potential regulatory interplay of multiple alarmones.

Keywords: SasA, RelP, YwaC, pGpp, ppGpp, ppApp, AppppA, alarmone

INTRODUCTION

Survival of bacteria as single-cell organisms relies on their ability to adjust growth and cellular metabolism according to changes in the environment. A well-conserved mechanism to achieve such coordination is through the synthesis and degradation of the nucleotide alarmones ppGpp and pppGpp, collectively known as (p)ppGpp (Cashel and Gallant, 1969). (p)ppGpp regulates a repertoire of essential cellular processes including transcription, translation, ribosome synthesis, DNA replication, and nucleotide metabolism (Potrykus and Cashel, 2008; Liu et al., 2015a; Gourse et al., 2018), which altogether promotes stress adaptation and survival. In addition to (p)ppGpp, bacteria can produce a variety of other nucleotide alarmones such as pGpp, ppApp and AppppA (Bochner and Ames, 1982). However, the synthetases of these other alarmones and their roles in

stress protection are less well understood. In addition, characterizing alarmones *in vivo* has been limited by the difficulty of profiling multiple alarmones in cell extracts.

In Firmicutes such as the pathogens *Enterococcus faecalis* and *Staphylococcus aureus,* or the soil bacterium *Bacillus subtilis*, (p)ppGpp can be produced by three different synthetases: the bifunctional synthetase/hydrolase Rel (traditionally called RelA in *B. subtilis*) (Wendrich and Marahiel, 1997), and two small alarmone synthetases YjbM (also known as SasB, RelQ, or SAS1) and YwaC (also known as SasA, RelP, or SAS2) (Nanamiya et al., 2008; Srivatsan et al., 2008; Geiger et al., 2014; Gaca et al., 2015). RelA is constitutively expressed and synthesizes (p)ppGpp by sensing starved ribosomes. SasB is also constitutively expressed but its (p)ppGpp synthesis activity is determined by allosteric activation by pppGpp (Steinchen et al., 2015) or single stranded RNA (Beljantseva et al., 2017).

In contrast to RelA and SasB, SasA expression is conditional and is regulated by the envelope stress sigma factors σ^M and σ^W (Cao et al., 2002). Unlike SasB, SasA from *S. aureus* does not require pppGpp binding for activation (Steinchen et al., 2018) but can be activated by low concentrations and inhibited by high concentrations of metal ions such as Zn^{2+} (Manav et al., 2018). Importantly, SasA expression can be induced by cell wall antibiotics to promote survival in response to drug treatment in *B. subtilis* and *S. aureus* (Geiger et al., 2014; Fung et al., 2020). However, the effect of SasA expression, without cell wall stress, on cellular alarmone and metabolome composition has not been characterized.

With the aim to investigate the characteristics of alarmone regulation by the cell wall stress induced (p)ppGpp synthetase SasA, we developed a LC-MS-based method to detect and measure an expanded set of metabolites and alarmones in *B. subtilis* cells with high efficiency. We found that SasA expression leads to strong accumulation of the (p)ppGpp analog pGpp, as well as accumulation of ppApp and AppppA to ∼10% of the level of pGpp. Furthermore, we also detected depletion of specific purine nucleotides and their precursors including GTP and GDP, and IMP precursors FGAR (Phosphoribosyl-N-formylglycineamide), SAICAR (Phosphoribosyl-aminoimidazolesuccinocarboxamide), and AICAR (5-Aminoimidazole-4-carboxamide ribonucleotide). Intriguingly, we revealed that SasA expression also leads to strong depletion of pyrimidine pathway precursors such as orotate and orotidine 5′-phosphate. Our work highlights that expression of SasA can cause concomitant accumulation of alarmones beyond (p)ppGpp, suggesting that regulation mediated by SasA involves multiple alarmones.

MATERIALS AND METHODS

Bacterial Strains and Strain Construction

All bacterial strains, plasmids and oligonucleotides used in this study are listed in **Table 1**. LB and LB-agar were used for cloning and propagation of strains. For selection in *B. subtilis*, media was supplemented with the following antibiotics when necessary: spectinomycin (80 μg/mL), chloramphenicol (5 μg/mL), kanamycin (10 μg/mL), and a combination of lincomycin (12.5 μg/mL) and erythromycin (0.5 μg/mL) for MLS resistance. Carbenicillin (100 μg/mL) was used for selection in *E. coli*.

Construction of pJW731 and pJW733 was done by PCR amplification of *ywaC* and $ywaC^{D87G}$ fragments with primers oJW3495/3496 using pJW512 and pJW516 as templates, followed by *Sal*I/*Sph*I digestion and ligation into pDR110. The resulting plasmid is transformed into *E. coli* DH5α for propagation and verified by sequencing with oJW1519.

Construction of JDW3014 was done by sequential transformations of integration plasmids containing an I-sceI endonuclease cut site and regions of homology upstream and downstream of synthetase genes (pJW300 for Δ*yjbM* and pJW306 for Δ*ywaC*) followed by transformation of pSS4332 for marker-less recombination (Janes and Stibitz, 2006). Successful removal of the synthetase genes was verified by PCR and sequencing (oJW358/359 for *yjbM* and oJW904/905 for *ywaC*).

Construction of JDW4017 and JDW4019 was done by integration of JDW3014 at *amyE* with pJW731 and pJW733, followed by selection for spectinomycin resistance. The resulting strain was then transformed with Δ*relA*::*mls* PCR product synthesized from genomic DNA using oligos oJW902/oJW903, followed by selection for MLS resistance (Kriel et al., 2012). Disruption of *relA* was verified by PCR and sequencing (oJW418/419).

Construction of JDW4064 and JDW4066 was done by integration of JDW3014 at *amyE* with pJW731 and pJW733, followed by selection for spectinomycin resistance. The resulting strain was transformed with Δ*nahA*::kan^R PCR product synthesized from genomic DNA of BKK34780 (BGSC) using oligos oJW3382/oJW3383, followed by selection for kanamycin resistance. The resulting strain was further transformed with Δ*relA*::erm^R PCR product synthesized from genomic DNA using oligos oJW902/oJW903, followed by selection for MLS resistance (Kriel et al., 2012). Disruption of *nahA* and *relA* was verified by PCR and sequencing (oJW3382/oJW3383 for *nahA* and oJW418/419 for *relA*).

Growth Conditions

Bacillus subtilis strains were grown in S7 defined medium (Harwood and Cutting, 1990); MOPS was used at 50 mM rather than 100 mM, supplemented with 0.1% glutamate, 1% glucose, and 20 amino acids (50 μg/mL alanine, 50 μg/mL arginine, 50 μg/mL asparagine, 50 μg/mL glutamine, 50 μg/mL histidine, 50 μg/mL lysine, 50 μg/mL proline, 50 μg/mL serine, 50 μg/mL threonine, 50 μg/mL glycine, 50 μg/mL isoleucine, 50 μg/mL leucine, 50 μg/mL methionine, 50 μg/mL valine, 50 μg/mL phenylalanine, 500 μg/mL aspartic acid, 500 μg/mL glutamic acid, 20 μg/mL tryptophan, 20 μg/mL tyrosine, and 40 μg/mL cysteine). Cells were harvested from young, overnight LB-agar plates (< 12 h), back-diluted into fresh S7 defined media at OD_{600} = 0.005, and grown at 37°C with vigorous shaking to logarithmic phase (OD_{600} ≈ 0.1–0.3). Induction of SasA expression was done by addition of 1 mM IPTG at final concentration. Cell viability assay was done by serial dilution and

TABLE 1 | Bacterial strains, plasmids, and oligonucleotides used in this study.

Bacterial strains used in this study

Strain	Organism	Genotype	Source
JDW2901	*B. subtilis*	3610 Δ*zpdN* ΔSPβ ΔPBSX Δ*comI*	Daniel Kearns
BKK34780	*B. subtilis*	168 Δ*nahA*::*kan*^{R}	BGSC
JDW3014	*B. subtilis*	JDW2901 Δ*ywaC*Δ*yjbM*	This work
JDW4009	*E. coli*	DH5α/pDR110-*ywaC*	This work
JDW4011	*E. coli*	DH5α/pDR110-*ywaC*^{D87G}	This work
JDW4017	*B. subtilis*	JDW2901 Δ*ywaC*Δ*yjbM*Δ*relA::mls amyE::Pspank-ywaC*	This work
JDW4019	*B. subtilis*	JDW2901 Δ*ywaC*Δ*yjbM*Δ*relA::mls amyE::Pspank-ywaC*^{D87G}	This work
JDW4064	*B. subtilis*	JDW2901 Δ*ywaC*Δ*yjbM*Δ*relA::mls amyE::Pspank-ywaC*Δ*nahA::kan*^{R}	This work
JDW4066	*B. subtilis*	JDW2901 Δ*ywaC*Δ*yjbM*Δ*relA::mls amyE::Pspank-ywaC*^{D87G} Δ*nahA::kan*^{R}	This work

Plasmids used in this study

Plasmid	Genotype	Source
pDR110	*amyE*::P$_{spank}$ *amp spc*	David Rudner
pJW300	pJW239/Δ*yjbM* I-SceI site *amp cat*	Lab stock
pJW306	pJW299/Δ*ywaC* I-SceI site *amp cat*	Lab stock
pJW512	pDR154/*amyE*::P$_{xyl}$-*ywaC*	Lab stock
pJW516	pDR154/*amyE*::P$_{xyl}$-*ywaC*^{D87G}	Lab stock
pJW731	pDR110/*amyE*::P$_{spank}$-*ywaC*	This work
pJW733	pDR110/*amyE*::P$_{spank}$-*ywaC*^{D87G}	This work
pSS4332	*oriU* P$_{amy}$-I-sceI *kan*	Scott Stibitz

Oligonucleotides used in this study

Oligo	Sequence (5′ 3′)
oJW358	ATGTATGGCCGGAACTGAAG
oJW359	CGGTCGCTGTATCTGTGAAA
oJW902	AAAGAGGCGCTTTTGACGTG
oJW903	TTGTTGACCCGGGACATGGA
oJW904	CGTCCTCATACGTTAACCGC
oJW905	GGGCTATCAAAAGGACTTTACCG
oJW1519	TCATCCATCATACATCCTCCTTCTGTCGACTTAATTAAACCACTTTG
oJW3382	GCTCAAAGTATTCTTCAAGCGAGAG
oJW3383	CATTCCACTTCATGACGTAAGAGG
oJW3495	ACATGCATGCAAAGGAGGTGTACATATGGATTTATCTGTAACACATATGGACG
oJW3496	ACATGTCGACTTAATCCACTTCTTTCTTAATCCCCAGC

plating on LB plates, followed by colony counting after overnight incubation at 37°C.

Sample Collection and LC-MS Quantification of Nucleotides

LC-MS quantification of nucleotides was performed as described (Liu et al., 2015b) with modifications (Yang et al., 2020). Cells were grown in S7 defined medium to OD_{600} ∼0.3 followed by addition of 1 mM IPTG. For sample collection, 10 mL cultures were sampled by filtering through PTFE membrane (Sartorius) before and after 30-min IPTG induction. Filtered membranes with harvested cells were immediately submerged in 3 mL extraction solvent mix [on ice 50:50 (v/v) chloroform/water] to quench metabolism. This process also enables efficient cell lysis and extraction of soluble metabolites. Mixture of cell extracts were centrifuged at 5000 × g for 10 min to remove organic phase, then centrifuged at 20,000 × g for 10 min to remove cell debris. Samples were frozen at −80°C if not analyzed immediately. Samples were analyzed using HPLC-MS system consisting of a Vanquish UHPLC system linked to electrospray ionization (ESI, negative mode) to a Q Exactive Orbitrap mass spectrometer (Thermo Scientific) operated in full-scan mode to detect targeted metabolites based on their accurate masses. LC was performed on an Acquity UPLC BEH C18 column (1.7 μm, 2.1 × 100 mm; Waters). Total run time was 30 min with a flow rate of 0.2 mL/min, using Solvent A [97:3 (v/v) water/methanol, 10 mM tributylamine and 10 mM acetic acid] and acetonitrile as Solvent B. The gradient was as follows: 0 min, 5% B; 2.5 min, 5% B; 19 min, 100% B; 23.5 min 100% B; 24 min, 5% B; 30 min, 5% B.

Data Analysis

Quantification of metabolites from raw LC-MS data were performed by using the MAVEN software (Clasquin et al., 2012).

Metabolite levels of different samples were normalized to their respective OD_{600} to the same sample volumes (10 mL). Prism 7 (GraphPad) was used for statistical analysis and generation of figures.

Calculation of Metabolite Concentrations

We use the estimation that cell volume is 0.475 μL in 1 mL culture at an OD_{600} of 1.0. We adopt a cell density of 2.0×10^8 CFU/mL/OD_{600} and the shape of cytoplasm as a cylinder of 4 μm in height and 0.435 μm in radius in the calculation. This estimation corresponds to an average cell volume of 2.38 fL.

The detection efficiency of pGpp in LC-MS is around 2.4e8 ion counts/μM in 25 μL sample. Normalized ion count can be converted into intracellular concentration of pGpp by $C_{P3G} = \frac{NI_{P3G}}{E_{LC-MS} \times V_{Culture,\ N} \times OD_{600nm,\ N} \times F_{cell}}$, where NI_{P3G} is the normalized ion count of pGpp, E_{LC-MS} is the detection efficiency of pGpp in LC-MS (2.4e8 ion counts/μM), $V_{Culture,\ N}$ is the normalized culture volume (5.0 mL), $OD_{600nm,\ N}$ is the normalized optical density (1.0) and F_{cell} is the fraction of cell volume in the culture (0.000475 mL/1 mL culture/OD).

The detection efficiency of other nucleotides in LC-MS is around 2.0e8 ion counts/μM in 25 μL sample. Normalized ion count can be converted into intracellular concentration of nucleotide by $C_{nt} = \frac{NI_{nt}}{E_{LC-MS} \times V_{Culture,\ N} \times OD_{600nm,\ N} \times F_{cell}}$, where NI_{nt} is the normalized ion count of nucleotide, E_{LC-MS} is the detection efficiency of nucleotide in LC-MS (2.0e8 ion counts/μM), $V_{Culture,\ N}$ is the normalized culture volume (5.0 mL), $OD_{600nm,\ N}$ is the normalized optical density (1.0) and F_{cell} is the fraction of cell volume in the culture (0.000475 mL/1 mL culture/OD).

RESULTS

Development of an Improved LC-MS Method for Alarmone Detection in *B. subtilis*

Our previous metabolite extraction and LC-MS analysis method allowed us to efficiently detect and quantitate high abundance metabolites such as GTP in *B. subtilis* (Liu et al., 2015b), however, we were unable to detect alarmones such as (p)ppGpp even in starvation-induced *B. subtilis*. Upon revisiting our LC-MS analysis protocol, we found that pure (p)ppGpp can be sensitively detected by LC-MS at concentrations > 10 nM with 100% acetonitrile as the buffer B, but not from *B. subtilis* cell extracts using the same method (data not shown). This suggests that the lack of (p)ppGpp signals from bacterial samples was due to inefficient metabolite extraction procedures. To this end, we optimized the method to increase the breadth of detectable metabolites from cell extracts. We improved our metabolite extraction procedures (**Figure 1A**) by replacing hydrophilic nylon filtration filters with hydrophobic PTFE filters, as well as using 1:1 (v/v) chloroform: water for lysis and extraction instead of 40:20:20 (v/v/v) acetonitrile/methanol/water. These modifications allowed improved recovery of alarmones by preventing adsorption of (p)ppGpp by the nylon membrane and increasing (p)ppGpp solubility in the extraction solvent. Furthermore, we used acetonitrile instead of methanol for solvent B in liquid chromatography which improved the resolution of low abundance metabolites such as alarmones. We found that our improved LC-MS protocol allowed us to sensitively detect alarmones such as pGpp, ppGpp, pppGpp, ppApp, pppApp, and AppppA from cell extracts, while retaining detection capability for other nucleotides such as ATP and GTP (**Figure 1B**). While we detect significant amount of ppGpp in mid log phase *B. subtilis* grown in minimal media, we found that (p)ppGpp in mid log phase *B. subtilis* grown in rich media is below detection limit, likely due to the extremely low concentration of (p)ppGpp in this condition.

Expression of SasA Leads to Accumulation of Multiple Alarmones

Next, we applied our improved LC-MS detection method to investigate the metabolomic signatures upon SasA expression. It is known that SasA is transcriptionally induced by cell envelope perturbations due to alkaline stress (Nanamiya et al., 2008) or antibiotics (Cao et al., 2002). To understand the primary effects of SasA expression and to avoid alarmone synthesis by other (p)ppGpp synthetases, we constructed a strain that ectopically expresses an IPTG-inducible SasA or $SasA^{D87G}$ (synthetase-dead SasA) in the absence of the other two (p)ppGpp synthetases RelA and SasB. Because *B. subtilis* without (p)ppGpp production is auxotrophic for multiple amino acids (Kriel et al., 2014), we grew the strains in rich media to minimize growth defect and suppressors. Both strains grew at similar rates prior to induction (**Figure 2A**), implying little basal activity from potential leaky expression. Upon induction, the SasA over-expression strain stopped growth in ∼30 min while the $sasA^{D87G}$ mutant was unaffected (**Figure 2A**), confirming accumulation of alarmones in the SasA over-expression strain. The induction also had no effect on cell viability even after prolonged induction (**Supplementary Figure S1**), excluding confounding effects due to cell death.

Using metabolomics analysis, we found that SasA expression alone can cause profound changes in cellular levels of alarmones, nucleotides and their precursors (**Figure 2B** and **Supplementary Figure S2**). We found that expression of SasA resulted in strong increase in the levels of alarmones pGpp, ppApp and AppppA (**Figure 2C**). These increases are abolished in $SasA^{D87G}$ cells (**Figure 2C**), indicating that they are dependent on the (p)ppGpp synthetase activity of SasA. The most strongly induced alarmone is pGpp, a (p)ppGpp analog, reaching up to $\sim 2.5 \times 10^8$ normalized LC-MS counts (**Figure 2D**) which roughly converts to ∼0.3 mM in the cell. The high level of pGpp is also due to failure of its hydrolysis by RelA due to RelA deletion.

Intriguingly, the level of pppGpp and ppGpp were both below the detectable range. However, this is not unexpected, because ppGpp synthesized by SasA can be rapidly converted to pGpp by the newly discovered (p)ppGpp hydrolyzing enzyme NahA (Yang et al., 2020). To test this hypothesis, we measured ppGpp, pGpp and GTP levels in SasA and $SasA^{D87G}$-expressing cells in

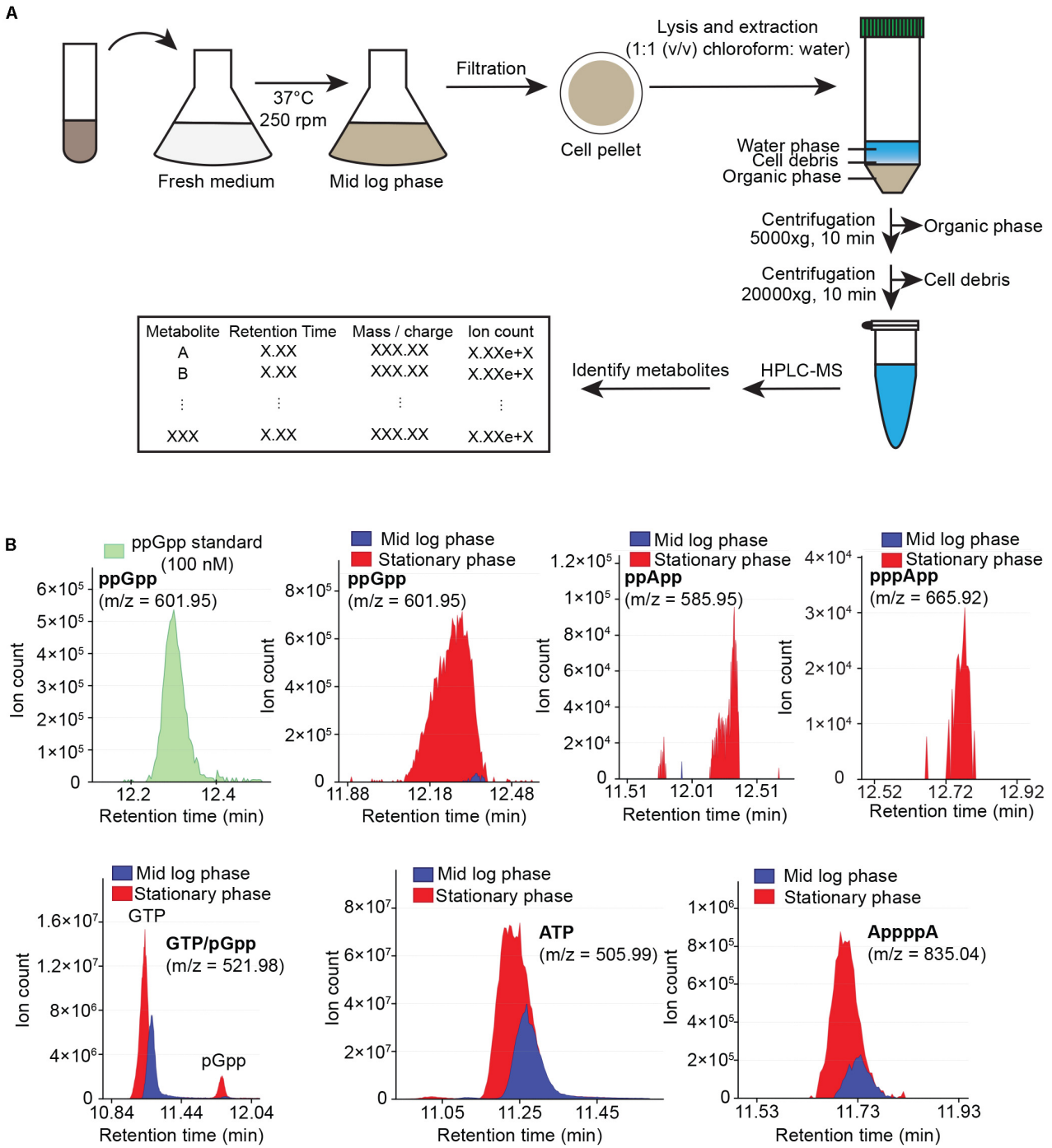

FIGURE 1 | Cellular metabolites extraction and analysis using HPLC-coupled mass spectrometry (HPLC-MS). **(A)** Flow chart of sample preparation, metabolite extraction and analysis. **(B)** HPLC-MS profile of ppGpp standard (green), and sample HPLC-MS profiles of ppGpp, ppApp, pppApp, GTP, pGpp, ATP, and AppppA detected in mid log phase (blue) and stationary phase (red) *B. subtilis* grown in minimal media. Data shown are raw ion counts.

the *nahA* mutant (**Figure 3**). We found that deletion of *nahA* led to a significant decrease (∼80%) in pGpp (**Figure 3A**) along with a strong increase in ppGpp (**Figure 3B**). This demonstrates that ppGpp is a major product of SasA but is efficiently converted to pGpp by NahA. On the other hand, changes in other metabolites such as GTP were unaffected (**Figure 3C**). In addition, we found that there is a low level of pGpp detected even in the Δ*nahA* mutant, suggesting that some pGpp can be directly produced by SasA, or there is another hydrolase which can convert ppGpp to pGpp in *B. subtilis*.

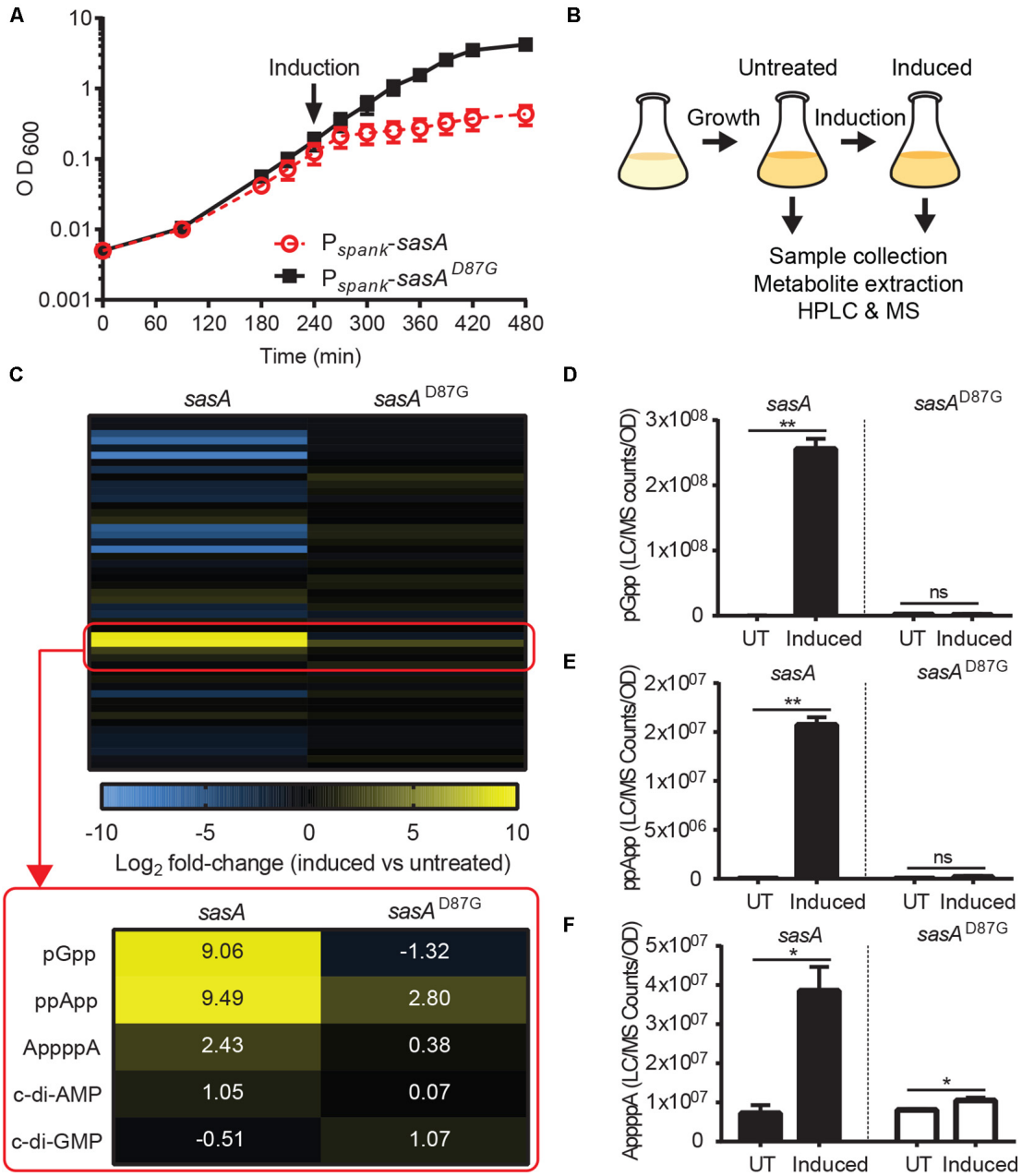

FIGURE 2 | SasA expression leads to accumulation of pGpp, ppApp, and AppppA. **(A)** Growth of *sasA* (solid square) and *sasA*^{D87G} (open circle) expression strains measured by OD_{600}. *sasA*^{D87G} encodes a synthetase-dead variant of SasA. Arrow indicates induction with 1 mM IPTG. **(B)** Schematic of metabolome profiling experiment. Cultures were grown to OD_{600}~0.3 followed by 30 min IPTG induction. Cells before and after 30 min IPTG induction were immediately harvested for metabolite extraction and HPLC-MS analysis as described in **Figure 1**. **(C)** Heat map of metabolite changes in cells after *sasA* or *sasA*^{D87G} expression. Red box highlights the increases in the level of alarmones and other detected signaling molecules. Numbers indicate mean fold-change in binary logarithm relative to untreated cells. **(D–F)** Levels of **(D)** pGpp, **(E)** ppApp and **(F)** AppppA in cells before and after *sasA* expression. UT: untreated, Induced: after induction. Data shown are LC-MS ion counts normalized to OD_{600}. Error bars indicate SD. $n = 2$. $^{**}p < 0.01$, $^{*}p < 0.05$, ns, not significant (Student's *t*-test).

In addition to pGpp, we detected strong accumulation of another nucleotide alarmone ppApp to a level ~10% of that of pGpp (**Figure 2E**). Unlike pGpp, ppApp level was unaffected by NahA (**Figure 3D**). Intriguingly, *in vitro* evidence suggest that SasA from *S. aureus* can directly produce ppApp and pppApp (Wieland Steinchen & Gert Bange, personal communication). Therefore, it is likely that SasA can synthesize ppApp as an alternative product in *B. subtilis*.

Furthermore, we detected a ~4-fold increase in AppppA upon SasA induction (**Figure 2F**) to a level similar to that of ppApp. AppppA is not known to be a product of SasA, thus its accumulation can be due to indirect effects

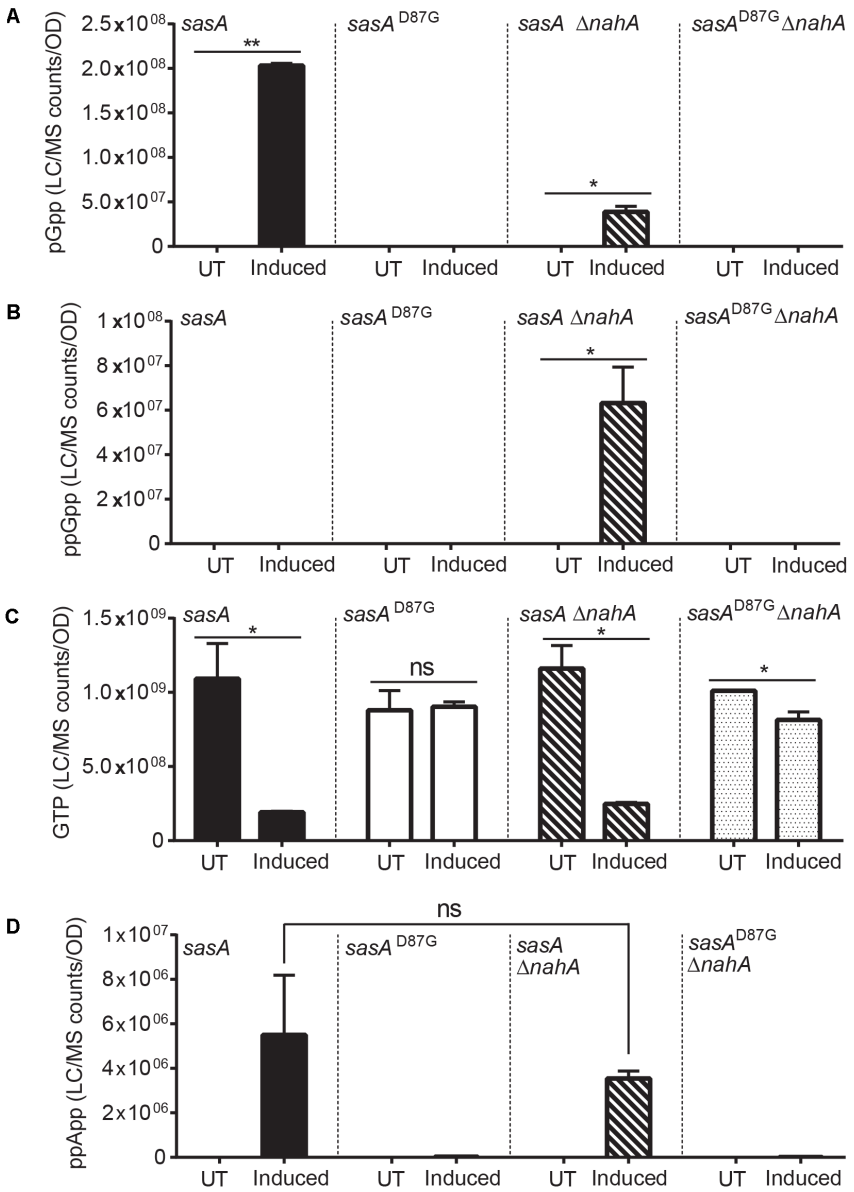

FIGURE 3 | Production of pGpp after induction of SasA is largely mediated by NahA. Bar plots of **(A)** pGpp, **(B)** ppGpp, **(C)** GTP, and **(D)** ppApp levels before and after *sasA* expression in cells with or without *nahA*. UT: untreated, Induced: after induction. Data shown are LC-MS ion counts normalized to OD_{600}. Error bars indicate *SD*. $n = 2$. $^{**}p < 0.01$, $^{*}p < 0.05$, ns, not significant (Student's *t*-test).

resulting from increased availability of its precursors (see below and "Discussion"). Taken together, these results suggest that expression of SasA can lead to accumulation of multiple alarmones in addition to its expected product.

Alarmone Synthesis by SasA Results in Reduction of Guanine Nucleotides and Accumulation of Adenine Nucleotides in *B. subtilis*

In addition to accumulation of alarmones, we identified changes in the levels of purine nucleotides upon SasA expression (**Figure 4A**). We detected significant decreases of GDP (∼4-fold) and GTP (∼4-fold), while the level of GMP remain unchanged (**Figure 4B**). These changes were attenuated or reversed in the $SasA^{D87G}$-expressing cells (**Figure 4B**). For adenine nucleotides, while AMP remained largely unchanged, we detected significant increases in ADP (∼1.8-fold) and ATP (∼3-fold) upon SasA expression. In contrast, no significant changes in AMP, ADP or ATP were observed in the *sasA*^{D87G} mutant (**Figure 4C**). The changes in GTP and ATP pools correspond to an estimated decrease in GTP from ∼1.7 mM to ∼0.4 mM and an estimated increase in ATP from ∼4.3 to ∼12.5 mM. In summary, we

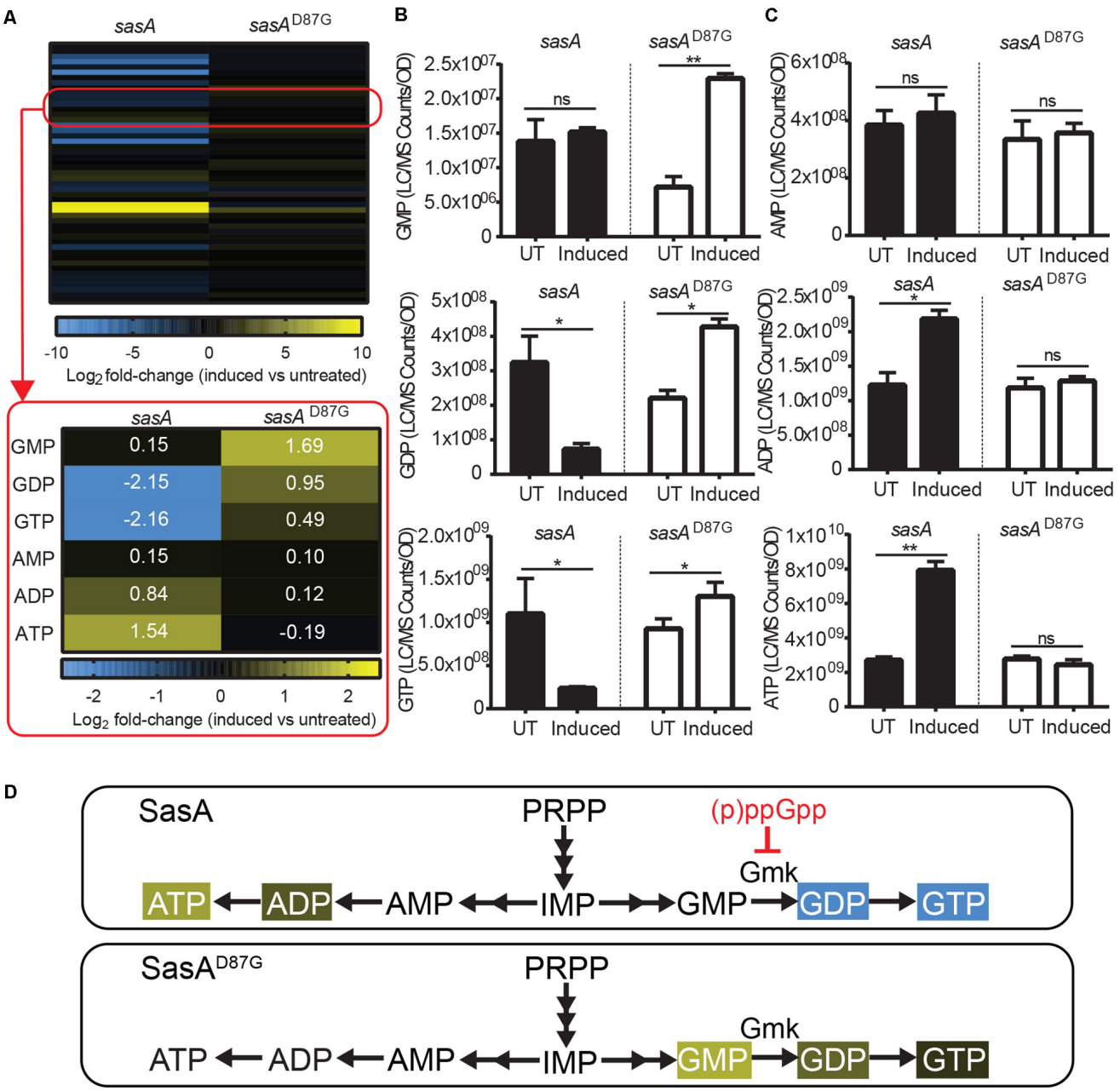

FIGURE 4 | Expression of SasA leads to depletion of guanine nucleotides and accumulation of adenine nucleotides. **(A)** Heat map of metabolite changes in cells after *sasA* or *sasA*^{D87G} expression. Red box highlights the changes in the level of guanine and adenine nucleotides. GMP, Guanosine monophosphate; GDP, Guanosine diphosphate; GTP, Guanosine triphosphate; AMP, Adenosine monophosphate; ADP, Adenosine diphosphate; ATP, Adenosine triphosphate. Numbers indicate mean fold-change in binary logarithm relative to untreated cells. **(B)** Levels of GMP, GDP, and GTP in cells before and after *sasA* or *sasA*^{D87G} expression. **(C)** Levels of AMP, ADP, and ATP in cells before and after *sasA* or *sasA*^{D87G} expression. UT: untreated, Induced: after induction. Data shown are LC-MS ion counts normalized to OD_{600}. Error bars indicate *SD*. $n = 2$. $^{**}p < 0.01$, $^{*}p < 0.05$, ns, not significant (Student's *t*-test). **(D)** Summary of nucleotide changes in cells expressing *sasA* or *sasA*^{D87G}. Color-shaded are metabolites with $\log_2$ fold-change ≥ 0.5 (yellow) or $= -0.5$ (blue) as shown in **(A)**. Red blunt arrow indicates direct inhibition by (p)ppGpp. Gmk: Guanylate kinase.

observed an overall reduction of guanine nucleotides and accumulation of adenine nucleotides during SasA-mediated alarmone accumulation (**Figure 4D**).

AMP and GMP are synthesized from S-AMP (adenylosuccinate) and XMP respectively using IMP as a common precursor (**Figure 5B**). We found that the level of IMP and its salvage pathway precursor HPX were only mildly reduced by ∼30–40% (**Figure 5B** and **Supplementary Figure S3**) after induced wild type SasA expression. However, we detected strong reductions of

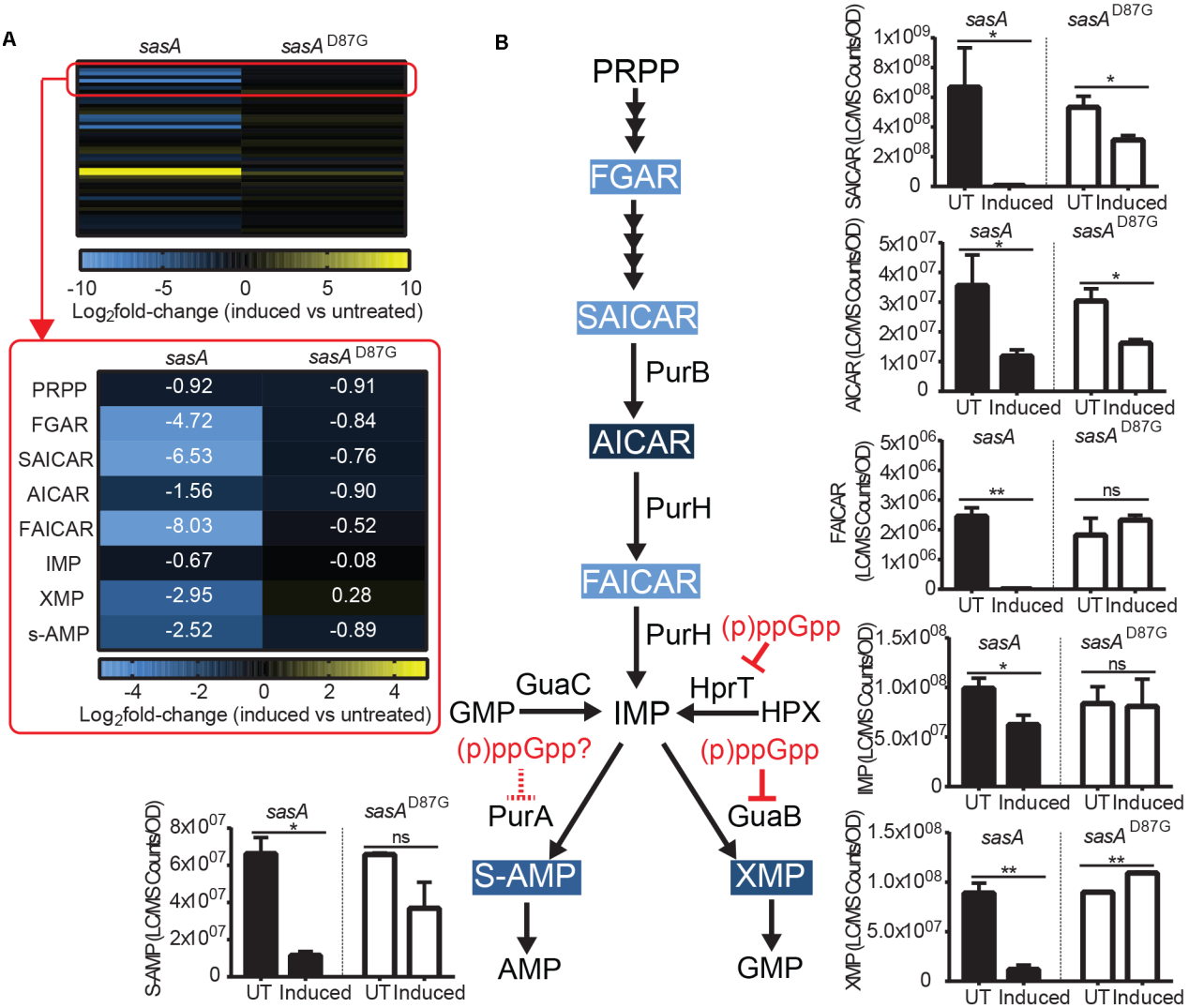

FIGURE 5 | Purine precursors are depleted during SasA expression. **(A)** Heat map of metabolite changes in cells after *sasA* or *sasA*^{D87G} expression. Red box highlights the changes in the level of PRPP-IMP pathway metabolites in addition to adenylosuccinate (S-AMP) and xanthosine monophosphate (XMP). PRPP, Phosphoribosyl pyrophosphate; FGAR, Phosphoribosyl-N-formylglycineamide; SAICAR, Phosphoribosylaminoimidazolesuccinocarboxamide; AICAR, 5-Aminoimidazole-4-carboxamide ribonucleotide; FAICAR, 5-Formamidoimidazole-4-carboxamide ribotide; IMP, Inosine monophosphate. Numbers indicate mean fold-change in binary logarithm relative to untreated cells. **(B)** Summary of metabolite changes in the *de novo* purine biosynthesis pathway in SasA-expressing cells. Bar plots shown are levels of SAICAR, AICAR, FAICAR, IMP, S-AMP, and XMP before and after *sasA* or *sasA*^{D87G} expression. PurB, Adenylsuccinate lyase; PurH, Phosphoribosylaminoimidazole carboxamide formyltransferaseand inosine-monophosphate cyclohydrolase; GuaC, GMP reductase; HprT, Hypoxanthine phosphoribosyltransferase; PurA, Adenylosuccinate synthetase; GuaB, IMP dehydrogenase. UT: untreated, Induced: after induction. Data shown are LC-MS ion counts normalized to OD_{600}. Error bars indicate *SD*. $n = 2$. $^{**}p < 0.01$, $^{*}p < 0.05$, ns: not significant (Student's *t*-test). Color-shaded are metabolites with $\log_2$ fold-change > 2 as shown in **(A)**. Solid and dashed red arrows indicate known and speculated inhibition by (p)ppGpp respectively.

both S-AMP (∼5-fold) and XMP (∼7-fold) (**Figure 5B**), possibly due to direct enzymatic inhibition of PurA (adenylosuccinate synthetase) and GuaB (IMP dehydrogenase) by the alarmones.

De novo IMP Synthesis Pathway Intermediates Are Depleted During SasA Expression

The most drastic changes in metabolites we observed upon SasA expression are in the *de novo* IMP biosynthesis pathway (**Figure 5A**). Although we found no detectable difference in PRPP levels upon SasA expression (**Figure 5A**), we found profound changes in IMP precursors phosphoribosyl-N-formylglycineamide (FGAR), phosphoribosyl-aminoimidazolesuccinocarboxamide (SAICAR), 5-Aminoimidazole-4-carboxamide ribonucleotide (AICAR) and 5-Formamidoimidazole-4-carboxamide ribotide (FAICAR) which are produced at different steps in the PRPP-IMP pathway. In the SasA^{D87G} expression strain, we detected only mild changes (< 2-fold) in these metabolites before and after induction (**Figure 5A**). In contrast, expression of SasA resulted in strong

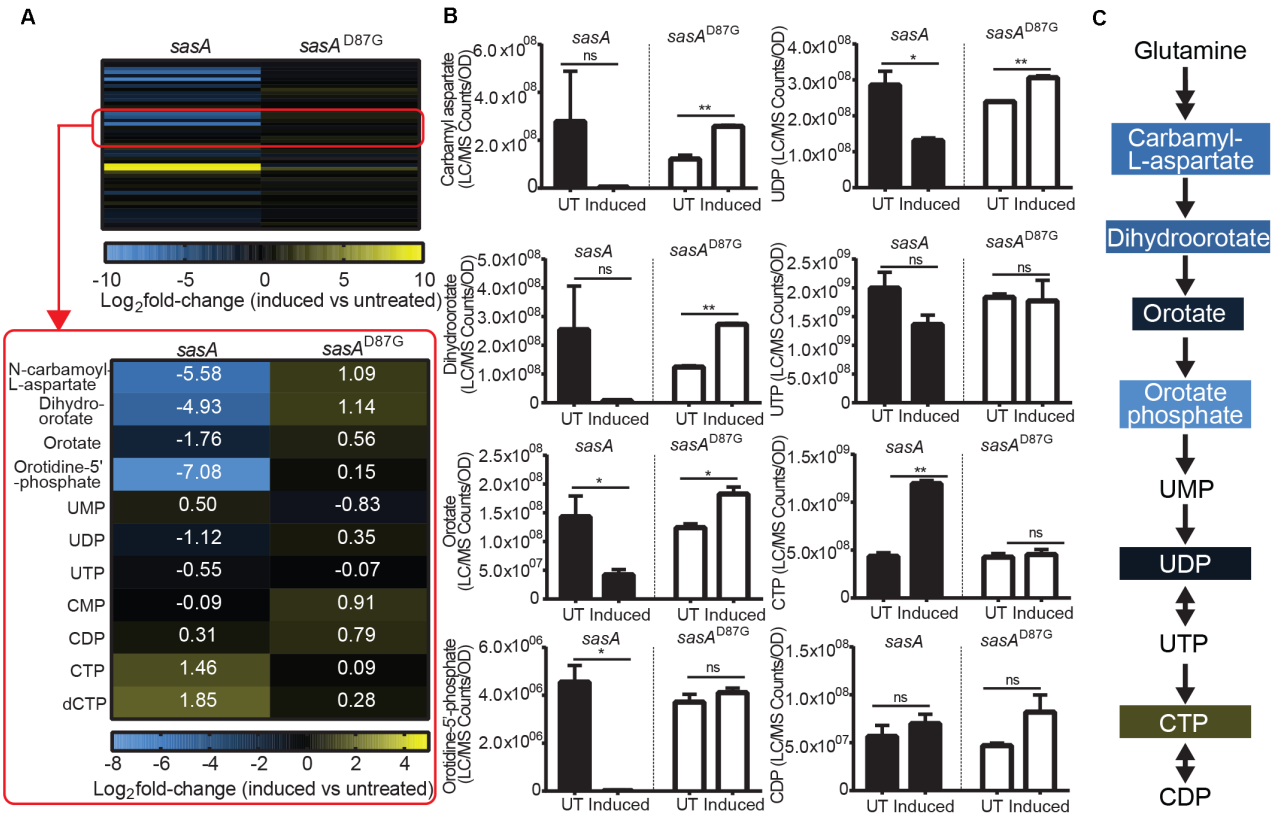

FIGURE 6 | SasA expression leads to depletion of pyrimidine precursors and increase in CTP. **(A)** Heat map of metabolite changes in cells after *sasA* or *sasA*^{D87G} expression. Red box highlights the changes in the level of pyrimidine pathway metabolites. UMP, Uridine monophosphate; UDP, Uridine diphosphate; UTP, Uridine triphosphate; CMP, Cytidine monophosphate; CDP, Cytidine diphosphate; CTP, Cytidine triphosphate; dCTP, Deoxycytidine triphosphate. Numbers indicate mean fold-change in binary logarithm relative to untreated cells. **(B)** Bar plots of pyrimidine pathway metabolites before and after *sasA* or *sasA*^{D87G} expression. UT: untreated, Induced: after induction. Data shown are LC-MS ion counts normalized to OD_{600}. Error bars indicate *SD*. $n = 2$. $^{**}p < 0.01$, $^{*}p < 0.05$, ns, not significant (Student's *t*-test). **(C)** Summary of metabolite changes in the pyrimidine pathway in *sasA*-expressing cells. Color-shaded are metabolites with $\log_2$ fold-change > 1 as shown in **(A)**.

depletion of FAICAR (> 100-fold), SAICAR (> 100-fold) and FGAR (∼30-fold), as well as ∼3-fold reduction in AICAR (**Figures 5A,B**). This suggests a strong inhibitory effect of alarmones on the synthesis of multiple PRPP-IMP pathway intermediates. However, enzymes in the PRPP-IMP pathway have not been found to be direct targets of (p)ppGpp in *B. subtilis*, suggesting the inhibition can be mediated by other alarmones or through modulation of their expression. Taken together, our data showed that SasA expression resulted in overall depletion of IMP synthesis precursors (**Figure 5B**).

De novo Pyrimidine Nucleotide Synthesis Pathway Intermediates Are Drastically Changed During SasA Expression

In addition to changes in the levels of purine nucleotides and its precursors, we also observed perturbations of the *de novo* pyrimidine synthesis pathway during SasA expression (**Figure 6A**). We found drastic changes in the levels of pyrimidine nucleotide precursors (**Figure 6A**). Apart from the undetectable carbamoyl-phosphate and glutamine which is supplied in growth media, all other four intermediates including N-carbamoyl-L-aspartate, dihydroorotate, orotate, and orotidine-5′-phosphate were depleted by ∼3.4-fold (orotate) to ∼135-fold (orotidine-5′-phosphate) after the induction of SasA expression (**Figure 6B**). In addition, we identified higher CTP (∼2.7 fold), dCTP (∼3.6-fold), and UMP (∼1.8 fold) levels after SasA induction (**Figure 6A**). UDP was slightly decreased by ∼2.2-fold (**Figure 6B**). These changes were abolished or reversed in the *sasA*^{D87G} mutant (**Figures 6A,B**). These data showed that SasA expression resulted in remodeled pyrimidine nucleotide abundance and depletion of *de novo* pyrimidine synthesis precursors (**Figure 6C**).

DISCUSSION

Understanding the breadth of alarmone regulation by (p)ppGpp synthetases is important to understand their roles in cellular physiology. However, precise detection and quantitation of alarmones in bacteria has been challenging until recent advances

in MS-based detection methods (Varik et al., 2017; Zbornikova et al., 2019). Here we documented an improved LC-MS protocol that allows efficient detection and quantitation of multiple alarmones and metabolites in *B. subtilis* cells. Using this method, we studied the metabolic signatures of stringent response mediated by the small alarmone synthetase SasA which is transcriptionally induced in response to cell wall stresses. Apart from increased level of the (p)ppGpp derivative pGpp, we detected unexpected accumulations of ppApp, AppppA and a mild increase of other signaling molecules such as c-di-AMP, as well as changes in *de novo* purine and pyrimidine biosynthesis metabolites (**Figure 7**). Our findings suggest that expression of (p)ppGpp synthetase can affect the levels of alarmones outside of (p)ppGpp, implying complex multi-alarmone regulations during the stringent response.

Accumulation of Multiple Alarmones From SasA Expression

The increase in multiple alarmones and second messengers upon SasA expression is likely due to both direct and indirect mechanisms. First, SasA may produce ppApp and pGpp in addition to (p)ppGpp. Although it was showed that SasA from *S. aureus* can efficiently synthesize ppGpp *in vitro* (Steinchen et al., 2018), it is possible that the enzyme can produce other (p)ppGpp analogs such as pGpp and ppApp depending on substrate availability. For example, another small alarmone synthetase SasB in *Enterococcus faecalis* can produce pGpp *in vitro* (Gaca et al., 2015). On the other hand, Rel from *Methylobacterium extorquens* can synthesize pppApp both *in vitro* and when expressed in *E. coli* (Sobala et al., 2019), and the secreted toxin Tas1 from *Pseudomonas aeruginosa* can produce pppApp, ppApp, and pApp in target *E. coli* cells to mediate contact dependent inhibition (Ahmad et al., 2019). These findings suggest that stress responses mediated by (p)ppGpp synthetases may not be strictly limited to the alarmones pppGpp and ppGpp.

Second, pGpp can be produced efficiently from (p)ppGpp through the NuDiX hydrolase NahA (Yang et al., 2020). We found that under SasA expression the majority of accumulated pGpp was due to NahA-mediated conversion of ppGpp produced by SasA (**Figures 3A,B**). On the other hand, we could also detect a low level of pGpp in the *nahA* mutant, suggesting that SasA may directly produce pGpp (**Figures 3A,B**). However, we cannot rule out the presence of another hydrolase in *B. subtilis* which can convert ppGpp to pGpp.

AppppA is known to be produced from ATP through distinct mechanisms catalyzed by aminoacyl-tRNA synthetases (**Supplementary Figure S4**; Bochner et al., 1984). Due to the disparity between these enzymes and (p)ppGpp synthetases, the possibility that SasA can directly synthesize AppppA is low. Instead, one plausible explanation to its accumulation is through indirect increases of ATP (**Figure 4C**) which is the initiating substrate for its synthesis. Our characterization thus supports the interconnected nature of purine nucleotides, not just for guanine, but also for adenine nucleotides.

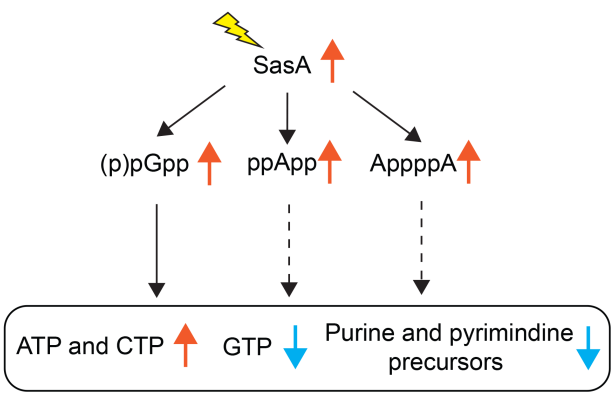

FIGURE 7 | Effects of SasA expression on alarmones and nucleotide synthesis. Expression of SasA in the absence of other (p)ppGpp synthetases leads to concomitant accumulations of (p)ppGpp analogs pGpp, ppApp and AppppA, as well as depletions in GTP and purine precursors. To the contrary, ATP level is increased. Furthermore, pyrimidine precursors are also depleted along with increases in CTP. Our recent findings on pGpp binding targets (Yang et al., 2020) suggest that pGpp targets are largely similar to that of (p)ppGpp. Thus, the depletion of GTP and inhibition of purine precursor biosynthesis is likely a downstream effect of pGpp (solid arrows). The roles of ppApp or AppppA on nucleotide biosynthesis regulation (dashed arrows) remains to be determined.

Depletion of GTP and Purine Precursors by Alarmone Accumulation

Apart from alarmone accumulation, we found that SasA expression also resulted in depletion of GTP and accumulation of ATP. This characteristic metabolic change resembles the metabolic changes during amino acid starvation (Kriel et al., 2012) which is primarily mediated by the (p)ppGpp synthetase-hydrolase RelA. Although we detected pGpp and ppApp instead of (p)ppGpp as the predominant alarmones synthesized by SasA, the drop in GTP is at least contributed by direct inhibition of the GMP kinase Gmk by pGpp, similarly to that of (p)ppGpp (Liu et al., 2015b). This is supported by recent finding that pGpp, ppGpp, and pppGpp share similar binding properties to *de novo* purine biosynthesis enzymes (Yang et al., 2020). Whether the other (p)ppGpp analog ppApp can directly regulate GTP synthesis is under investigation.

In addition, we also identified depletion of both S-AMP (adenylosuccinate) and XMP which are products of IMP. Synthesis of XMP from IMP is catalyzed by GuaB which has been reported to interact with ppGpp in *E. coli* (Zhang et al., 2018) but is only weakly inhibited by (p)ppGpp in *B. subtilis* (Kriel et al., 2012). The strong inhibition of XMP synthesis observed here suggests that the inhibition can potentially be mediated by alternative mechanisms, such as through other induced alarmones or by repression of *guaB* expression. On the other hand, S-AMP synthesis from IMP is catalyzed by PurA (Saxild and Nygaard, 1991) which is also a ppGpp-binding target

in *E. coli* (Pao and Dyess, 1981). Consistently, we have recently identified PurA as a target of (p)ppGpp and pGpp in *B. anthracis* (Yang et al., 2020), suggesting that the inhibition of S-AMP synthesis is at least partially attributed to pGpp.

Interestingly, we revealed that intermediates (e.g., FGAR, SAICAR, and FAICAR) in the upstream PRPP-IMP pathway are also depleted in response to SasA expression. Since PRPP level was similar, the inhibition is likely specific to the catalytic steps between PRPP and IMP which are catalyzed by the gene products of the *pur* operon. While none of the enzymes from this operon have been found to be a (p)ppGpp target in *B. subtilis*, we have previously found that transcription of the *pur* operon is strongly downregulated during starvation in a (p)ppGpp-dependent manner (Kriel et al., 2014). This is supported by our recent finding that the *pur* operon repressor PurR can bind to pGpp and (p)ppGpp (Yang et al., 2020). Thus, it is possible that regulation of purine synthesis by (p)ppGpp in *B. subtilis* involves two distinct components: transcription control for upstream intermediates and direct interaction for downstream precursors. This is in contrast to regulation in *E. coli* where a number of PRPP-IMP pathway enzymes such as PurF, PurB, and PurC have been recently identified as targets of (p)ppGpp (Wang et al., 2019), which highlights the disparity of purine synthesis control between evolutionarily distant species.

Physiological Implications of SasA-Mediated Growth Control

Unlike (p)ppGpp synthesis triggered by nutrient starvation through the (p)ppGpp synthetase RelA, (p)ppGpp synthesis by SasA is induced in response to cell wall stresses (Nanamiya et al., 2008; Geiger et al., 2014). The physiological benefit of SasA induction is likely multifold. First, damages to the cell wall is highly detrimental during growth since it can lead to cell lysis. Since (p)ppGpp accumulation and its associated depletion of GTP allows rapid and coordinated control of growth-determining processes such as ribosome synthesis (Liu et al., 2015a), connecting cell wall status to the stringent response likely increases survival in response to cell wall damages. Secondly, SasA expression is under the regulation of σ^M/σ^W regulon along with a repertoire of other genes responsible for cell wall synthesis and division (Cao et al., 2002; Libby et al., 2019), thus allowing complementary response to cell wall stresses. Thirdly, many naturally existing antibiotics target the bacterial cell wall and can be produced by microbes occupying the same physiological niche. An example is the soil bacterium *B. subtilis* which co-exist with other cell wall antibiotic-producing *Bacillus* species. The presence of SasA-mediated response likely enables the bacteria to sense and survive emerging antibiotic assault to increase their competitive fitness.

DATA AVAILABILITY STATEMENT

The raw data supporting the conclusions of this article will be made available by the authors, without undue reservation.

AUTHOR CONTRIBUTIONS

DF and JW designed the study. DF and JY performed the experiments and data analysis. DS and DA-N provided the operation and technical assistance of the LC and MS instrument. DF, JY, and JW discussed the findings and wrote the manuscript. All authors contributed to the article and approved the submitted version.

FUNDING

This work was supported by an R35 GM127088 from NIGMS (to JW) and the National Science Foundation (NSF) Grant award no. 1715710 (to DA-N).

ACKNOWLEDGMENTS

We thank the members of the Wang lab for their comments on the manuscript.

SUPPLEMENTARY MATERIAL

The Supplementary Material for this article can be found online at: https://www.frontiersin.org/articles/10.3389/fmicb.2020.02083/full#supplementary-material

FIGURE S1 | Induction of SasA expression does not result in loss of cell viability. Culture aliquots were taken over time after IPTG induction and plated on LB plates without IPTG for colony counts to monitor cell viability. Data shown are mean CFU/mL. Error bars represent SD. $n = 2$.

FIGURE S2 | Metabolomic changes mediated by SasA. Heat map of metabolite changes in cells after *sasA* or $sasA^{D87G}$ expression. Numbers indicate mean fold-change in binary logarithm relative to untreated cells. $n = 2$.

FIGURE S3 | Hypoxanthine levels before and after *sasA* or $sasA^{D87G}$ expression. Levels of hypoxanthine (HPX) before and after induction of *sasA* or $sasA^{D87G}$ expression. UT: untreated, Induced: after induction. Data shown are LC/MS ion counts normalized to OD_{600}. Error bars indicate SD. $n = 2$. $^{**}p < 0.01$, $^{*}p < 0.05$, ns: not significant (Student's *t*-test).

FIGURE S4 | Biosynthesis pathway of AppppA. AppppA is synthesized by a two-step reaction catalyzed by aminoacyl-tRNA syntheatse (AA-tRNA synthetase) using ATP as substrates. In the presence of ATP, amino acid (AA) is first adenylated by AA-tRNA synthetase to generate amino acid-AMP (AA-AMP). The AMP moiety in AA-AMP is then transferred to another ATP molecule to generate AppppA.

REFERENCES

Ahmad, S., Wang, B., Walker, M. D., Tran, H. R., Stogios, P. J., Savchenko, A., et al. (2019). An interbacterial toxin inhibits target cell growth by synthesizing (p)ppApp. *Nature* 575, 674–678. doi: 10.1038/s41586-019-1735-9

Beljantseva, J., Kudrin, P., Andresen, L., Shingler, V., Atkinson, G. C., Tenson, T., et al. (2017). Negative allosteric regulation of *Enterococcus faecalis* small alarmone synthetase RelQ by single-stranded RNA. *Proc. Natl. Acad. Sci. U.S.A.* 114, 3726–3731. doi: 10.1073/pnas.1617868114

Bochner, B. R., and Ames, B. N. (1982). Complete analysis of cellular nucleotides by two-dimensional thin layer chromatography. *J. Biol. Chem.* 257, 9759–9769.

Bochner, B. R., Lee, P. C., Wilson, S. W., Cutler, C. W., and Ames, B. N. (1984). AppppA and related adenylylated nucleotides are synthesized as a consequence of oxidation stress. *Cell* 37, 225–232. doi: 10.1016/0092-8674(84)90318-0

Cao, M., Wang, T., Ye, R., and Helmann, J. D. (2002). Antibiotics that inhibit cell wall biosynthesis induce expression of the *Bacillus subtilis* sigma(W) and sigma(M) regulons. *Mol. Microbiol.* 45, 1267–1276. doi: 10.1046/j.1365-2958.2002.03050.x

Cashel, M., and Gallant, J. (1969). Two compounds implicated in the function of the RC gene of *Escherichia coli*. *Nature* 221, 838–841. doi: 10.1038/221838a0

Clasquin, M. F., Melamud, E., and Rabinowitz, J. D. (2012). LC-MS data processing with MAVEN: a metabolomic analysis and visualization engine. *Curr. Protoc. Bioinformatics* 37, 14.11.1–14.11.23.

Fung, D. K., Barra, J. T., Schroeder, J. W., Ying, D., and Wang, J. D. (2020). A shared alarmone-GTP switch underlies triggered and spontaneous persistence. *BioRxiv* [Preprint]. doi: 10.1101/2020.03.22.002139v1

Gaca, A. O., Kudrin, P., Colomer-Winter, C., Beljantseva, J., Liu, K., Anderson, B., et al. (2015). From (p)ppGpp to (pp)pGpp: characterization of regulatory effects of pGpp synthesized by the small alarmone synthetase of *Enterococcus faecalis*. *J. Bacteriol.* 197, 2908–2919. doi: 10.1128/jb.00324-15

Geiger, T., Kastle, B., Gratani, F. L., Goerke, C., and Wolz, C. (2014). Two small (p)ppGpp synthases in *Staphylococcus aureus* mediate tolerance against cell envelope stress conditions. *J. Bacteriol.* 196, 894–902. doi: 10.1128/jb.01201-13

Gourse, R. L., Chen, A. Y., Gopalkrishnan, S., Sanchez-Vazquez, P., Myers, A., and Ross, W. (2018). Transcriptional responses to ppGpp and DksA. *Annu. Rev. Microbiol.* 72, 163–184. doi: 10.1146/annurev-micro-090817-062444

Harwood, C. R., and Cutting, S. M. (1990). *Molecular Biological Methods for Bacillus (Chichester*. New York: Wiley.

Janes, B. K., and Stibitz, S. (2006). Routine markerless gene replacement in *Bacillus anthracis*. *Infect. Immun.* 74, 1949–1953. doi: 10.1128/iai.74.3.1949-1953.2006

Kriel, A., Bittner, A. N., Kim, S. H., Liu, K., Tehranchi, A. K., Zou, W. Y., et al. (2012). Direct regulation of GTP homeostasis by (p)ppGpp: a critical component of viability and stress resistance. *Mol. Cell.* 48, 231–241. doi: 10.1016/j.molcel.2012.08.009

Kriel, A., Brinsmade, S. R., Tse, J. L., Tehranchi, A. K., Bittner, A. N., Sonenshein, A. L., et al. (2014). GTP dysregulation in *Bacillus subtilis* cells lacking (p)ppGpp results in phenotypic amino acid auxotrophy and failure to adapt to nutrient downshift and regulate biosynthesis genes. *J. Bacteriol.* 196, 189–201. doi: 10.1128/jb.00918-13

Libby, E. A., Reuveni, S., and Dworkin, J. (2019). Multisite phosphorylation drives phenotypic variation in (p)ppGpp synthetase-dependent antibiotic tolerance. *Nat. Commun.* 10:5133.

Liu, K., Bittner, A. N., and Wang, J. D. (2015a). Diversity in (p)ppGpp metabolism and effectors. *Curr. Opin. Microbiol.* 24, 72–79. doi: 10.1016/j.mib.2015.01.012

Liu, K., Myers, A. R., Pisithkul, T., Claas, K. R., Satyshur, K. A., Amador-Noguez, D., et al. (2015b). Molecular mechanism and evolution of guanylate kinase regulation by (p)ppGpp. *Mol. Cell.* 57, 735–749. doi: 10.1016/j.molcel.2014.12.037

Manav, M. C., Beljantseva, J., Bojer, M. S., Tenson, T., Ingmer, H., Hauryliuk, V., et al. (2018). Structural basis for (p)ppGpp synthesis by the *Staphylococcus aureus* small alarmone synthetase RelP. *J. Biol. Chem.* 293, 3254–3264. doi: 10.1074/jbc.ra117.001374

Nanamiya, H., Kasai, K., Nozawa, A., Yun, C. S., Narisawa, T., Murakami, K., et al. (2008). Identification and functional analysis of novel (p)ppGpp synthetase genes in *Bacillus subtilis*. *Mol. Microbiol.* 67, 291–304. doi: 10.1111/j.1365-2958.2007.06018.x

Pao, C. C., and Dyess, B. T. (1981). Effect of unusual guanosine nucleotides on the activities of some *Escherichia coli* cellular enzymes. *Biochim. Biophys. Acta* 677, 358–362. doi: 10.1016/0304-4165(81)90247-6

Potrykus, K., and Cashel, M. (2008). (p)ppGpp: still magical? *Annu. Rev. Microbiol.* 62, 35–51. doi: 10.1146/annurev.micro.62.081307.162903

Saxild, H. H., and Nygaard, P. (1991). Regulation of levels of purine biosynthetic enzymes in *Bacillus subtilis*: effects of changing purine nucleotide pools. *J. Gen. Microbiol.* 137, 2387–2394. doi: 10.1099/00221287-137-10-2387

Sobala, M., Bruhn-Olszewska, B., Cashel, M., and Potrykus, K. (2019). Methylobacterium extorquens RSH enzyme synthesizes (p)ppGpp and pppApp *in vitro* and *in vivo*, and leads to discovery of pppApp synthesis in *Escherichia coli*. *Front. Microbiol.* 10:859. doi: 10.3389/fmicb.2019.00859

Srivatsan, A., Han, Y., Peng, J., Tehranchi, A. K., Gibbs, R., Wang, J. D., et al. (2008). High-precision, whole-genome sequencing of laboratory strains facilitates genetic studies. *PLoS Genet.* 4:e1000139. doi: 10.1371/journal.pgen.1000139

Steinchen, W., Schuhmacher, J. S., Altegoer, F., Fage, C. D., Srinivasan, V., Linne, U., et al. (2015). Catalytic mechanism and allosteric regulation of an oligomeric (p)ppGpp synthetase by an alarmone. *Proc. Natl. Acad. Sci. U.S.A.* 112, 13348–13353. doi: 10.1073/pnas.1505271112

Steinchen, W., Vogt, M. S., Altegoer, F., Giammarinaro, P. I., Horvatek, P., Wolz, C., et al. (2018). Structural and mechanistic divergence of the small (p)ppGpp synthetases RelP and RelQ. *Sci. Rep.* 8:2195.

Varik, V., Oliveira, S. R. A., Hauryliuk, V., and Tenson, T. (2017). HPLC-based quantification of bacterial housekeeping nucleotides and alarmone messengers ppGpp and pppGpp. *Sci. Rep.* 7:11022.

Wang, B., Dai, P., Ding, D., Del Rosario, A., Grant, R. A., Pentelute, B. L., et al. (2019). Affinity-based capture and identification of protein effectors of the growth regulator ppGpp. *Nat. Chem. Biol.* 15, 141–150. doi: 10.1038/s41589-018-0183-4

Wendrich, T. M., and Marahiel, M. A. (1997). Cloning and characterization of a relA/spoT homologue from *Bacillus subtilis*. *Mol. Microbiol.* 26, 65–79. doi: 10.1046/j.1365-2958.1997.5511919.x

Yang, J., Anderson, B. W., Turdiev, A., Turdiev, H., Stevenson, D. M., Amador-Noguez, D., et al. (2020). Systemic characterization of pppGpp, ppGpp and pGpp targets in *Bacillus* reveals NahA converts (p)ppGpp to pGpp to regulate alarmone composition and signaling. *bioRxiv* [Preprint]. doi: 10.1101/2020.03.23.003749

Zbornikova, E., Knejzlik, Z., Hauryliuk, V., Krasny, L., and Rejman, D. (2019). Analysis of nucleotide pools in bacteria using HPLC-MS in HILIC mode. *Talanta* 205:120161. doi: 10.1016/j.talanta.2019.120161

Zhang, Y., Zbornikova, E., Rejman, D., and Gerdes, K. (2018). Novel (p)ppGpp Binding and Metabolizing Proteins of *Escherichia coli*. *mBio* 9:e02188-17.

Conflict of Interest: The authors declare that the research was conducted in the absence of any commercial or financial relationships that could be construed as a potential conflict of interest.

frontiers in Microbiology

HYPOTHESIS AND THEORY
published: 07 September 2020
doi: 10.3389/fmicb.2020.02072

(p)ppGpp: Magic Modulators of Bacterial Physiology and Metabolism

Wieland Steinchen, Victor Zegarra and Gert Bange**

Department of Chemistry, Center for Synthetic Microbiology (SYNMIKRO), Philipps-University Marburg, Marburg, Germany

When bacteria experience growth-limiting environmental conditions, the synthesis of the hyperphosphorylated guanosine derivatives (p)ppGpp is induced by enzymes of the RelA/SpoT homology (RSH)-type protein family. High levels of (p)ppGpp induce a process called "stringent response", a major cellular reprogramming during which ribosomal RNA (rRNA) and transfer RNA (tRNA) synthesis is downregulated, stress-related genes upregulated, messenger RNA (mRNA) stability and translation altered, and allocation of scarce resources optimized. The (p)ppGpp-mediated stringent response is thus often regarded as an all-or-nothing paradigm induced by stress. Over the past decades, several binding partners of (p)ppGpp have been uncovered displaying dissociation constants from below one micromolar to more than one millimolar and thus coincide with the accepted intracellular concentrations of (p)ppGpp under non-stringent (basal levels) and stringent conditions. This suggests that the ability of (p)ppGpp to modulate target proteins or processes would be better characterized as an unceasing continuum over a concentration range instead of being an abrupt switch of biochemical processes under specific conditions. We analyzed the reported binding affinities of (p)ppGpp targets and depicted a scheme for prioritization of modulation by (p)ppGpp. In this ranking, many enzymes of e.g., nucleotide metabolism are among the first targets to be affected by rising (p)ppGpp while more fundamental processes such as DNA replication are among the last. This preference should be part of (p)ppGpp's "magic" in the adaptation of microorganisms while still maintaining their potential for outgrowth once a stressful condition is overcome.

Keywords: stringent response, (p)ppGpp, alarmones, metabolism, physiology

OPEN ACCESS

Edited by:
Haike Antelmann,
Freie Universität Berlin, Germany

Reviewed by:
Vasili Hauryliuk,
Umeå University, Sweden
Fabian M. Commichau,
Brandenburg University of Technology Cottbus-Senftenberg, Germany

****Correspondence:***
Wieland Steinchen
wieland.steinchen@synmikro.uni-marburg.de
Gert Bange
gert.bange@synmikro.uni-marburg.de

Specialty section:
This article was submitted to Microbial Physiology and Metabolism, a section of the journal Frontiers in Microbiology

Received: *22 June 2020*
Accepted: *06 August 2020*
Published: *07 September 2020*

Citation:
Steinchen W, Zegarra V and Bange G (2020) (p)ppGpp: Magic Modulators of Bacterial Physiology and Metabolism. Front. Microbiol. 11:2072. doi: 10.3389/fmicb.2020.02072

THE METABOLISM OF (p)ppGpp

Bacteria must adapt to fluctuations in their ever-changing surroundings to survive. In order to accomplish optimal resource allocation upon facing environmental shifts, the pathways through which microorganisms rewire their metabolism need to be finely and promptly tuned. An efficient control of metabolism senses stress, adjusts growth accordingly, mandates which genes – and to which extent – are expressed, and ultimately provides a fitness advantage over poorly-adapted microbial competitors. The second messenger molecules (p)ppGpp are compounds that can accomplish all this.

More than 50 years ago, the "magic spots", which were identified as guanosine 5'-diphosphate 3'-diphosphate (ppGpp) and guanosine 5'-triphosphate 3'-diphosphate (pppGpp) and collectively referred to as (p)ppGpp or "alarmones", were discovered by Cashel and Gallant (1969). Since then, the synthesis and degradation of (p)ppGpp as well as the (p)ppGpp-mediated response

to nutrient limitations, a phenomenon known as the "stringent response", have been subject of extensive studies. Central in the metabolism of (p)ppGpp are members of the RelA/SpoT homology (RSH)-type protein family (Atkinson et al., 2011). Briefly, when bacteria encounter nutrient-limiting conditions, RSH proteins utilize ATP as a donor substrate and, through transfer of its β- and γ-phosphates onto the 3'-hydroxy group of the acceptor substrate guanosine 5'-diphosphate (GDP) or guanosine 5'-triphosphate (GTP), generate ppGpp or pppGpp, respectively (Sy and Lipmann, 1973). RSH proteins also degrade (p)ppGpp through removal of the 3'-pyrophosphate moiety of (p)ppGpp, thereby regenerating GDP/GTP (Hogg et al., 2004). "Long" RSH proteins harbor (p)ppGpp hydrolase and synthetase domains whose reciprocal activities are controlled by further regulatory domains (Atkinson et al., 2011). "Short" RSH proteins consisting only of a (p)ppGpp synthetase or hydrolase domain constitute the class of small alarmone synthetases (SAS) and hydrolases (SAH), respectively (Atkinson et al., 2011). Enzymes of the GppA/PPX family are able to convert pppGpp to ppGpp opening the avenue for more intricate differential regulation by the two alarmone species (Keasling et al., 1993; Kuroda et al., 1997; Kristensen et al., 2008).

The activity of RSH proteins is subject to regulation by various mechanisms, and (p)ppGpp-inducing conditions include, e.g., the presence of stalled ribosomes (Rel/RelA; Haseltine and Block, 1973; Wendrich et al., 2002), fatty acid starvation, and carbon downshifts (SpoT; Battesti and Bouveret, 2006, 2009), enhanced transcription of (p)ppGpp synthetases through cell wall stress stimuli (SAS2/RelP; Zweers et al., 2012; Geiger et al., 2014) or allosteric stimulation through the alarmone pppGpp itself (SAS1/RelQ; Gaca et al., 2015; Steinchen et al., 2015). The intracellular concentrations of (p)ppGpp during growth of *Escherichia coli* amount approximately 10–40 μM during logarithmic growth – unfortunately those basal levels are still not robustly determined because they typically fall beneath or close to the limit of quantification as in two recent studies (Varik et al., 2017; Zbornikova et al., 2019) – and peak at 800 μM at the onset of stationary phase. Full induction of the stringent response during acute amino acid starvation [e.g., induced by a transfer RNA (tRNA) synthetase inhibitor] gives rise to an increase of the intracellular (p)ppGpp concentrations to approximately 1 mM (Haseltine and Block, 1973; Kuroda et al., 1997; Kriel et al., 2012; Varik et al., 2017), ultimately causing growth arrest (Schreiber et al., 1991; Svitil et al., 1993; Potrykus and Cashel, 2008).

A PRIORITY PROGRAM OF (p)ppGpp SHUTDOWN IS ADVISED BY ITS BINDING AFFINITIES

Substantial progress has been made in the identification and characterization of (p)ppGpp binding targets (reviewed in: Kanjee et al., 2012; Steinchen and Bange, 2016; recent original works: Corrigan et al., 2016; Zhang et al., 2018; Wang et al., 2019), which fall into different cellular processes such as DNA replication, transcription, translation, ribosome biogenesis, or nucleotide metabolism (Srivatsan et al., 2008; Liu et al., 2015a; Corrigan et al., 2016; Bennison et al., 2019). Firstly, these studies provide insights as to how (p)ppGpp affect virulence, pathogenicity, persister cell and biofilm formation, heat shock response, and cell growth (Dalebroux and Swanson, 2012; He et al., 2012; Bager et al., 2016; Strugeon et al., 2016; Schafer et al., 2020). Secondly, they supply a wealth of biochemical data that quantitatively describe (p)ppGpp/protein interactions.

We were wondering whether any prioritization in the order of regulation between those targets/processes would exist. We collected and analyzed binding affinities (exemplified by the dissociation constants, K_d, of the (p)ppGpp/protein complexes), inhibitory constants (K_i) and EC_{50}/IC_{50} values for the targets of (p)ppGpp and depicted a scheme of prioritization in (p)ppGpp modulation (**Figure 1** and **Supplementary Table S1**). Proteins involved in the metabolism of amines and amino acids exhibit very high-affine (p)ppGpp binding with K_d's as low as 0.01 μM (*E. coli* LdcI, Kanjee et al., 2011a,b). They are followed by a multitude of enzymes involved in the metabolism of nucleotides featuring K_d values below 10 μM (Zhang et al., 2018; Wang et al., 2019), the tRNA modification GTPase TrmE and riboswitches of the YkkC type 2a (Peselis and Serganov, 2018; Sherlock et al., 2018). Notably, their K_d values below the assumed basal levels of (p)ppGpp imply a certain degree of regulation by (p)ppGpp even under non-stringent conditions (see below). (p)ppGpp binding to targets involved in transcription [i.e., *E. coli* RNA polymerase (RNAP); Bhardwaj et al., 2018] and *Francisella tularensis* MglA-SspA (Cuthbert et al., 2017) proceeds between 2 and 25 μM. It shall be noted that (p)ppGpp elicit control over *E. coli* RNAP through modulation of relative transcription rates from different promoters instead of a general reduction or induction of RNAP activity (Gourse et al., 2018). These targets are succeeded by further enzymes of nucleotide metabolism with K_d values ranging between 30 and 80 μM. Except for GpmA exhibiting a K_d of 52 μM, proteins associated with carbon metabolism feature dissociation constants/IC_{50} values of 132–800 μM (Dietzler and Leckie, 1977; Taguchi et al., 1977; Fujita and Freese, 1979; Wang et al., 2019). In a similar range falls the inhibition of DNA replication *via* (p)ppGpp binding to DnaG (Wang et al., 2007; Maciag et al., 2010; Rymer et al., 2012). Enzymes of fatty acid metabolism exhibit weak binding affinities (Polakis et al., 1973; Stein and Bloch, 1976), suggesting regulation by (p)ppGpp only to take place under full stringent control (i.e., 1,000 μM (p)ppGpp). Some enzymes partaking in (p)ppGpp metabolism, i.e., the (p)ppGpp synthetases RelQ (Gaca et al., 2015; Steinchen et al., 2015) and Rel/RelA (Shyp et al., 2012; Kudrin et al., 2018; Takada et al., 2020a), are stimulated in their activity by pppGpp and to a lesser extent by ppGpp. Furthermore, the enzymes GdpP, Pde2, and PgpH involved in the degradation pathway of the second messenger cyclic-diadenosine-monophosphate (c-di-AMP) display K_i values for inhibition by ppGpp between 35 and 400 μM.

Importantly, in proteins where (p)ppGpp bind competitively to another compound (**Figure 1** and **Supplementary Table S1**),

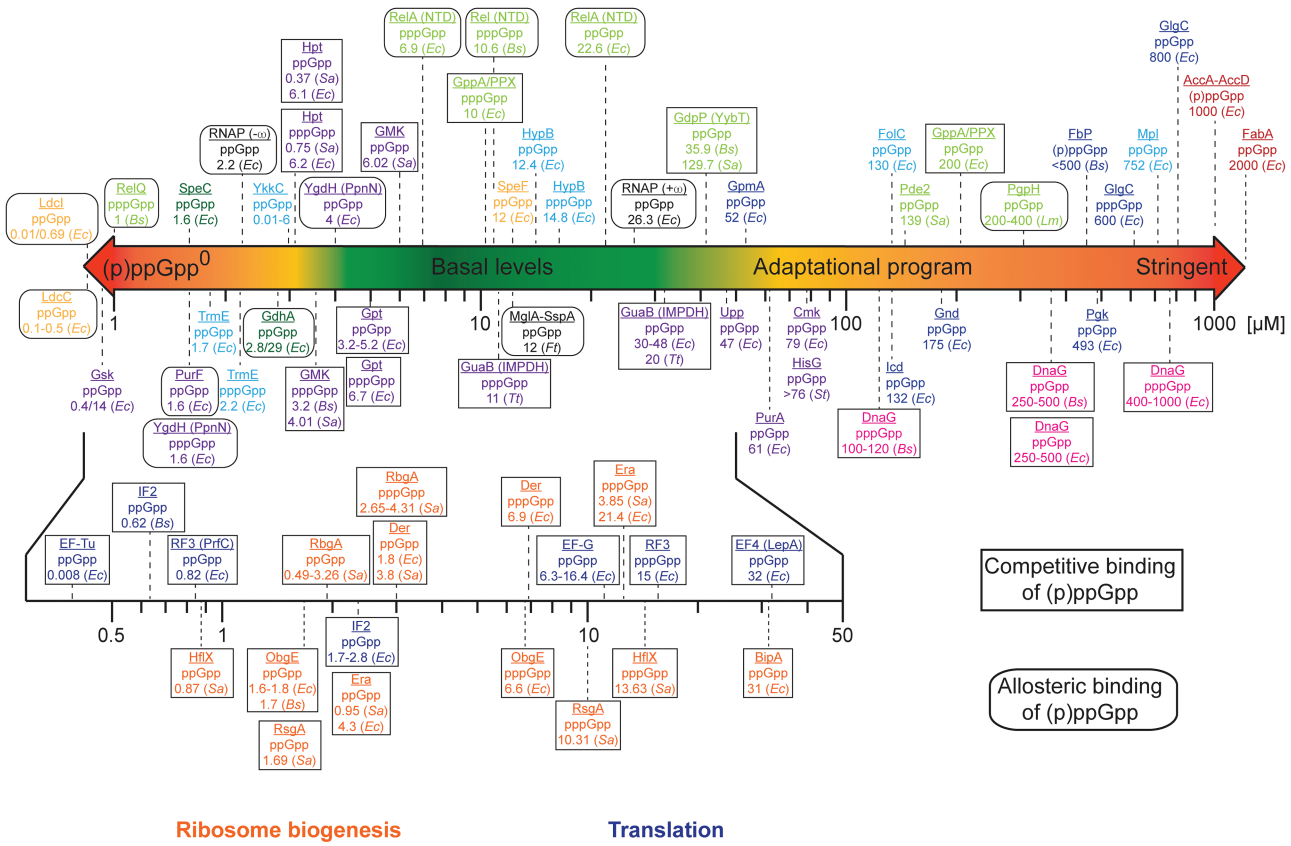

FIGURE 1 | Scheme of prioritization of (p)ppGpp-mediated adaptation. The colored bar denotes the approximate intracellular concentrations (in μM) of (p)ppGpp in bacteria. Binding targets of (p)ppGpp were sorted according to their dissociation constants (K_d). For DnaG, "enzymes" and proteins of carbon metabolism and fatty acid synthesis, K_i or EC_{50}/IC_{50} values are depicted. Proteins are color-coded according to their belonging to different groups/biochemical processes. Rectangles and rounded rectangles indicate whether (p)ppGpp binding to the target molecule is competitive or allosteric. Bacterial species are abbreviated as follows: *Escherichia coli* (*Ec*), *Bacillus subtilis* (*Bs*), *Staphylococcus aureus* (*Sa*), *Listeria monocytogenes* (*Lm*), *Francisella tularensis* (*Ft*), *Thermus thermophilus* (*Tt*), and *Salmonella typhimurium* (*St*). Further details can be found in **Supplementary Table S1**.

the intracellular concentration of this compound also affects the fraction of the (p)ppGpp-bound protein. The influence of this other compound rises with its intracellular concentration. For example, the concentration of GTP under non-stringent conditions is assumed to fall between approximately 1 (Varik et al., 2017; Zbornikova et al., 2019) and 5 mM (Bennett et al., 2009) but may drop heavily due to (p)ppGpp-dependent inhibition of GTP anabolism (Kriel et al., 2012; Liu et al., 2015b). Thereby, inhibition of GTPases is governed by the (p)ppGpp to GTP ratio that is indicative for the metabolic state of the cell. Assuming, for example, similar K_d values for (p)ppGpp and GTP binding, only approximately 1% of a protein would be inhibited at 10 μM (p)ppGpp/1 mM GTP while this fraction rises to 50% at equal concentrations of both nucleotides. In fact, the K_i for the inhibition of the GTPase RbgA of 300 and 800 μM (ppGpp and pppGpp in presence of 50S ribosomal subunits determined at 1 mM GTP; Pausch et al., 2018; **Supplementary Table S1**) is a better estimate than the K_d value. Similar considerations apply to some enzymes of nucleotide metabolism, e.g., GMK (Nomura et al., 2014) with its substrate GMP or Gpt (Hochstadt-Ozer and Cashel, 1972) with the substrate guanine. In contrast to GTP, however, the intracellular concentrations of those nucleotides are lower, i.e., 24 μM GMP and 19 μM guanine (Bennett et al., 2009), suggesting 90% inhibition at (p)ppGpp concentrations of approximately 200 μM. In contrast, the enzymes YgdH (PpnN; Zhang et al., 2019), PurF (Wang et al., 2019), and LdcI are allosterically inhibited by (p)ppGpp, rendering inhibition by (p)ppGpp independent of the substrate concentration. Summarized, the kinetic parameters of (p)ppGpp interaction with target proteins indicate the following hierarchy of adaptation: amine and amino acid metabolism, nucleotide metabolism, translational and ribosome biogenesis GTPases, DNA replication, carbon metabolism, and fatty acid synthesis (**Figure 1**).

IMPORTANCE OF BASAL (p)ppGpp LEVELS FOR BACTERIAL PHYSIOLOGY

Increasing evidence recommends that bacteria require basal (p)ppGpp levels to maintain homeostasis (Sokawa et al., 1975; Sarubbi et al., 1988; Silva and Benitez, 2006; Lemos et al., 2008; Gaca et al., 2013; Stott et al., 2015; Li et al., 2020) and strains that are completely devoid of any (p)ppGpp (known as (p)ppGpp^0) reveal multiple disabilities in cell division, transcription, translation, GTP homeostasis, and antibiotic tolerance. In *Bacillus subtilis*, the lack of (p)ppGpp causes elevated GTP levels, which through dysregulation of the GTP-dependent transcriptional repressor CodY result in auxotrophies for branched-chain amino acids (Kriel et al., 2014). Similar CodY-mediated detrimental effects of ppGpp^0-strains were observed for *Enterococcus faecalis* (Gaca et al., 2013) and *Staphylococcus aureus* (Pohl et al., 2009). In a *rel*-deletion strain of *Synechococcus elongatus*, the transcript levels of 52–67% of all genes were upregulated at least 3-fold and the levels of rRNA elevated indicating a "transcriptionally relaxed" state (Puszynska and O'Shea, 2017). Furthermore, cell size and volume increased but could be restored by synthetic compensation of (p)ppGpp (Puszynska and O'Shea, 2017). In *Vibrio cholera* basal (p)ppGpp has been linked to the expression of virulence factors and cell motility (Silva and Benitez, 2006). Basal (p)ppGpp was also required for the tolerance of *E. faecalis* against vancomycin (Abranches et al., 2009). These reports emphasize the importance of basal (p)ppGpp levels, which through high-affine binding of the alarmones (K_d < 10 μM; **Figure 1**) exert a regulatory function in the absence of a (p)ppGpp-stimulating trigger.

TOXIC OVER-ACCUMULATION OF (p)ppGpp

Intuitively, a prolonged mismatch of (p)ppGpp synthesis and degradation resulting in over-accumulation of (p)ppGpp, is detrimental for the cell. In *E. coli*, RelA and SpoT are responsible for the synthesis of (p)ppGpp, with only SpoT being able to hydrolyze the alarmones. As such, the role of SpoT is pivotal for preventing toxic (p)ppGpp accumulation as exemplified by SpoT-deletion strains being characterized by reduced growth rates and distorted amino acid requirements (Xiao et al., 1991). Bacteria of the Firmicutes phylum, instead of possessing RelA and SpoT, harbor the bifunctional enzyme Rel (Atkinson et al., 2011). The hydrolase activity of Rel is required to prevent toxic concentrations of (p)ppGpp, which results in severe growth defects (Gratani et al., 2018; Takada et al., 2020b). This effect appears more notorious in the presence of the two small alarmone synthetases, RelP and RelQ, the (p)ppGpp synthetase activity of which is not properly contained in absence of the (p)ppGpp-degrading Rel (Geiger et al., 2014). In *Mycobacterium tuberculosis*, (p)ppGpp degradation is equally essential since deletion of (p)ppGpp hydrolase activity, while retaining (p)ppGpp synthesis, lead to lethal toxicity evidenced by irregularities in colony formation irrespective of the nutritional environment (Weiss and Stallings, 2013). Notably, these *M. tuberculosis* strains were also impaired in their virulence in a mouse model during both acute and chronic infection, highlighting the interference with (p)ppGpp metabolism as a potential antimicrobial therapeutic strategy. Taken together, a tight regulation of the antagonistic (p)ppGpp producing and degrading activities is indispensable for many, if not all bacteria for (i) correctly adjusting (p)ppGpp levels in response to environmental cues, (ii) coordinating various cellular processes in an orchestrated manner, and (iii) avoiding lethal consequences due to (p)ppGpp over-accumulation.

CROSSTALK BETWEEN (p)ppGpp AND c-di-AMP

Bacteria possess a thorough toolbox of nucleotide-based second messengers to efficiently respond to diverse external cues (Pesavento and Hengge, 2009; Kalia et al., 2013; Hengge et al., 2016). Among those, c-di-AMP is a signaling molecule mainly synthetized by Gram-positive bacteria (Romling, 2008; da Aline Dias et al., 2020; He et al., 2020; Yin et al., 2020), which fulfills a pivotal role in the osmotic homeostasis (Stulke and Kruger, 2020). The dynamic range of intracellular c-di-AMP is much lower than for (p)ppGpp and lies in the one-digit μM range (in *B. subtilis* 1.7 μM during vegetative growth to 5.1 μM 2 h after sporulation; Oppenheimer-Shaanan et al., 2011). The importance of c-di-AMP for bacterial physiology is also highlighted by the observation that both the complete absence and over-accumulation of c-di-AMP impede growth of *B. subtilis* (Mehne et al., 2013; Gundlach et al., 2015). Comparison of the transcriptional profiles of *S. aureus* cells at high c-di-AMP or (p)ppGpp concentrations revealed an overlap of 27.9% between the two regulons (Corrigan et al., 2015). Intriguingly, (p)ppGpp inhibit the activity of the *S. aureus* c-di-AMP phosphodiesterase GdpP with a K_i of 129.7 ± 42.8 μM *in vitro* correlating with higher levels of c-di-AMP observed *in vivo* (Corrigan et al., 2015). Inhibition by ppGpp with an IC_{50} of 139 ± 5.6 μM was also reported for the second *S. aureus* c-di-AMP phosphodiesterase Pde2 (Bowman et al., 2016). Similar observations made for the c-di-AMP hydrolases YybT (GdpP) from *B. subtilis* (Rao et al., 2010) and PgpH from *Listeria monocytogenes* (Huynh et al., 2015). These K_i/IC_{50} values suggest that (p)ppGpp concentrations must rise above their basal levels to inhibit c-di-AMP degradation. Deletion of *S. aureus* GdpP with concomitant increase of c-di-AMP evokes elevated (p)ppGpp (Corrigan et al., 2015), thus implying that induction of one second messenger, (p)ppGpp or c-di-AMP, augments the other. Conversely, the depletion of the only c-di-AMP synthetase, *dacA*, in *L. monocytogenes* also induced a toxic accumulation of (p)ppGpp (Whiteley et al., 2015). This apparent twist might be caused in the narrow dynamic range of c-di-AMP whereby deflection in either direction triggers (p)ppGpp synthesis or indicate species-specific differences in the regulatory circuits. Nevertheless, the functional connection of c-di-AMP and (p)ppGpp is further substantiated by the observation that the essentiality of *dacA* in *L. monocytogenes* during growth in rich medium was abrogated in a (p)ppGpp^0-strain or in the wild-type strain grown in minimal medium (Whiteley et al., 2015). Hereby, the activity of the

GTP-dependent transcriptional regulator CodY appears critical to *dacA* essentiality in rich media in that mutation of *codY* in the (p)ppGpp^0-strain renders *dacA* again essential. This implies that elements of the CodY regulon may be toxic in the absence of c-di-AMP-producing DacA (Whiteley et al., 2015). The GTP-loading state and activity of CodY (Sonenshein, 2007) are in turn linked to (p)ppGpp through the inhibition of GTP anabolic enzymes involved in nucleotide metabolism by the alarmones (see above). Thus, as a whole, the interdependencies between c-di-AMP and (p)ppGpp conceivably require a high degree of coordination and involve a number of different cellular processes.

THE EMERGING HYPERPHOSPHORYLATED NUCLEOTIDES (p)ppApp

In the 1970s, the accumulation of two further magic spots designated as (p)ppApp was observed in *B. subtilis* during the early stages of sporulation (Rhaese and Groscurth, 1976; Rhaese et al., 1977; Nishino et al., 1979) and the (p)ppApp synthetic activity retrieved from the ribosomal fraction, which indicates the contribution of an RSH. The first RSH to catalyze (p)ppApp formation was recently identified in *Methylobacterium extorquens* (Sobala et al., 2019), however, (p)ppApp-producing activity was not evidenced for the *E. coli* RelA enzyme (Jimmy et al., 2020). Another source of (p)ppApp is the nucleoside 5'-diphosphate kinase from *Streptomyces morookaensis* although the enzyme being secreted raises the question of its physiological relevance for this organism (Oki et al., 1975). The high similarity of (p)ppGpp and (p)ppApp – they only differ in their nucleobase – advises a putative overlap of their target spectra. Recent studies evidence that *E. coli* PurF and RNAP, both of which are validated targets of (p)ppGpp, also bind (p)ppApp (Bruhn-Olszewska et al., 2018; Ahmad et al., 2019). However, while in PurF both second messengers bind in similar fashion at the same site and inhibit the enzyme with equal potency (Ahmad et al., 2019; Wang et al., 2019), the binding sites on RNAP are discrete and (p)ppApp enhance transcription from, e.g., the *rrnB* P1 promoter as opposed to (p)ppGpp (Bruhn-Olszewska et al., 2018). In one study, ppApp also inhibited the (p)ppGpp synthetic activity of *E. coli* RelA with an IC_{50} of 24.5 ± 3.5 μM (Beljantseva et al., 2017) raising the possibility that, in fact, (p)ppApp and (p)ppGpp are antagonists. Besides potentially fulfilling regulatory functions in their host cell, (p)ppApp also serve as toxins during interbacterial warfare (Ahmad et al., 2019). Hereby, the type VI secretion system (T6SS) effector protein Tas1 of *Pseudomonas aeruginosa* PA14, a (p)ppApp synthetase, is injected into the target cell and depletes the cellular ATP pools, resulting in dysregulation of the metabolome and, ultimately, cell death. Endogenous ppApp, the metabolism of which is embedded in toxin-antitoxin systems, might represent an intricate pathway to control growth (Jimmy et al., 2020). Whether the (p)ppApp molecules exert growth control independent from (p)ppGpp *via* a separated protein target spectrum or in a competitive manner to (p)ppGpp remains to be investigated.

CONCLUDING REMARKS

The functions of (p)ppGpp are often simplistically portrayed as a biphasic switch between relaxed and stringent environmental conditions, the latter triggering a major metabolic rearrangement through induction of (p)ppGpp synthesis. The presence of gradation in (p)ppGpp-dependent regulation of transcription is an approved mechanism (Traxler et al., 2008; Balsalobre, 2011; Traxler et al., 2011). However, the wide range of binding affinities among the (p)ppGpp-affected protein targets covering four orders of magnitude furthermore suggests a post-translational adaptational program activated hierarchically by increasing (p)ppGpp. The depicted scheme illustrates the importance of high-affine (p)ppGpp targets that explicitly require regulation, thus suggesting a protagonism of the alarmones on cell homeostasis. We believe that the post-translational sequential "dimming" of protein activities by (p)ppGpp, a conception potentially also true for related second messengers like (p)ppApp and c-di-AMP, plays a major role in successful adaptation of microorganisms.

DATA AVAILABILITY STATEMENT

The original contributions presented in the study are included in the article/**Supplementary Material**, further inquiries can be directed to the corresponding authors.

AUTHOR CONTRIBUTIONS

WS and GB conceived the study. WS and VZ performed the analysis. WS, VZ, and GB wrote the manuscript. All authors contributed to the article and approved the submitted version.

FUNDING

GB receives support through the SPP1879 priority program of the Deutsche Forschungsgemeinschaft (DFG).

ACKNOWLEDGMENTS

GB thanks the SPP1879 priority program of the Deutsche Forschungsgemeinschaft (DFG) for financial support.

SUPPLEMENTARY MATERIAL

The Supplementary Material for this article can be found online at: https://www.frontiersin.org/articles/10.3389/fmicb.2020.02072/full#supplementary-material

REFERENCES

Abranches, J., Martinez, A. R., Kajfasz, J. K., Chavez, V., Garsin, D. A., and Lemos, J. A. (2009). The molecular alarmone (p)ppGpp mediates stress responses, vancomycin tolerance, and virulence in *Enterococcus faecalis*. *J. Bacteriol.* 191, 2248–2256. doi: 10.1128/JB.01726-08

Ahmad, S., Wang, B., Walker, M. D., Tran, H. R., Stogios, P. J., Savchenko, A., et al. (2019). An interbacterial toxin inhibits target cell growth by synthesizing (p)ppApp. *Nature* 575, 674–678. doi: 10.1038/s41586-019-1735-9

Atkinson, G. C., Tenson, T., and Hauryliuk, V. (2011). The RelA/SpoT homolog (RSH) superfamily: distribution and functional evolution of ppGpp synthetases and hydrolases across the tree of life. *PLoS One* 6:e23479. doi: 10.1371/journal.pone.0023479

Bager, R., Roghanian, M., Gerdes, K., and Clarke, D. J. (2016). Alarmone (p)ppGpp regulates the transition from pathogenicity to mutualism in *Photorhabdus luminescens*. *Mol. Microbiol.* 100, 735–747. doi: 10.1111/mmi.13345

Balsalobre, C. (2011). Concentration matters!! ppGpp, from a whispering to a strident alarmone. *Mol. Microbiol.* 79, 827–829. doi: 10.1111/j.1365-2958.2010.07521.x

Battesti, A., and Bouveret, E. (2006). Acyl carrier protein/SpoT interaction, the switch linking SpoT-dependent stress response to fatty acid metabolism. *Mol. Microbiol.* 62, 1048–1063. doi: 10.1111/j.1365-2958.2006.05442.x

Battesti, A., and Bouveret, E. (2009). Bacteria possessing two RelA/SpoT-like proteins have evolved a specific stringent response involving the acyl carrier protein-SpoT interaction. *J. Bacteriol.* 191, 616–624. doi: 10.1128/JB.01195-08

Beljantseva, J., Kudrin, P., Jimmy, S., Ehn, M., Pohl, R., Varik, V., et al. (2017). Molecular mutagenesis of ppGpp: turning a RelA activator into an inhibitor. *Sci. Rep.* 7:41839. doi: 10.1038/srep41839

Bennett, B. D., Kimball, E. H., Gao, M., Osterhout, R., Van Dien, S. J., and Rabinowitz, J. D. (2009). Absolute metabolite concentrations and implied enzyme active site occupancy in *Escherichia coli*. *Nat. Chem. Biol.* 5, 593–599. doi: 10.1038/nchembio.186

Bennison, D. J., Irving, S. E., and Corrigan, R. M. (2019). The impact of the stringent response on TRAFAC GTPases and prokaryotic ribosome assembly. *Cell* 8:1313. doi: 10.3390/cells8111313

Bhardwaj, N., Syal, K., and Chatterji, D. (2018). The role of omega-subunit of *Escherichia coli* RNA polymerase in stress response. *Genes Cells* 23, 357–369. doi: 10.1111/gtc.12577

Bowman, L., Zeden, M. S., Schuster, C. F., Kaever, V., and Grundling, A. (2016). New insights into the cyclic di-adenosine monophosphate (c-di-AMP) degradation pathway and the requirement of the cyclic dinucleotide for acid stress resistance in *Staphylococcus aureus*. *J. Biol. Chem.* 291, 26970–26986. doi: 10.1074/jbc.M116.747709

Bruhn-Olszewska, B., Molodtsov, V., Sobala, M., Dylewski, M., Murakami, K. S., Cashel, M., et al. (2018). Structure-function comparisons of (p)ppApp vs (p)ppGpp for *Escherichia coli* RNA polymerase binding sites and for rrnB P1 promoter regulatory responses in vitro. *Biochim. Biophys. Acta Gene Regul. Mech.* 1861, 731–742. doi: 10.1016/j.bbagrm.2018.07.005

Cashel, M., and Gallant, J. (1969). Two compounds implicated in the function of the RC gene of *Escherichia coli*. *Nature* 221, 838–841. doi: 10.1038/221838a0

Corrigan, R. M., Bellows, L. E., Wood, A., and Grundling, A. (2016). ppGpp negatively impacts ribosome assembly affecting growth and antimicrobial tolerance in gram-positive bacteria. *Proc. Natl. Acad. Sci. U. S. A.* 113, E1710–E1719. doi: 10.1073/pnas.1522179113

Corrigan, R. M., Bowman, L., Willis, A. R., Kaever, V., and Grundling, A. (2015). Cross-talk between two nucleotide-signaling pathways in *Staphylococcus aureus*. *J. Biol. Chem.* 290, 5826–5839. doi: 10.1074/jbc.M114.598300

Cuthbert, B. J., Ross, W., Rohlfing, A. E., Dove, S. L., Gourse, R. L., Brennan, R. G., et al. (2017). Dissection of the molecular circuitry controlling virulence in *Francisella tularensis*. *Genes Dev.* 31, 1549–1560. doi: 10.1101/gad.303701.117

da Aline Dias, P., de Nathalia Marins, A., de Gabriel Guarany, A., de Robson Francisco, S., and Cristiane Rodrigues, G. (2020). The world of cyclic dinucleotides in bacterial behavior. *Molecules* 25:2462. doi: 10.3390/molecules25102462

Dalebroux, Z. D., and Swanson, M. S. (2012). ppGpp: magic beyond RNA polymerase. *Nat. Rev. Microbiol.* 10, 203–212. doi: 10.1038/nrmicro2720

Dietzler, D. N., and Leckie, M. P. (1977). Regulation of ADP-glucose synthetase, the rate-limiting enzyme of bacterial glycogen synthesis, by the pleiotropic nucleotides ppGpp and pppGpp. *Biochem. Biophys. Res. Commun.* 77, 1459–1467. doi: 10.1016/S0006-291X(77)80143-5

Fujita, Y., and Freese, E. (1979). Purification and properties of fructose-1,6-bisphosphatase of *Bacillus subtilis*. *J. Biol. Chem.* 254, 5340–5349.

Gaca, A. O., Kajfasz, J. K., Miller, J. H., Liu, K., Wang, J. D., Abranches, J., et al. (2013). Basal levels of (p)ppGpp in *Enterococcus faecalis*: the magic beyond the stringent response. *mBio* 4, e00646–e00613. doi: 10.1128/mBio.00646-13

Gaca, A. O., Kudrin, P., Colomer-Winter, C., Beljantseva, J., Liu, K., Anderson, B., et al. (2015). From (p)ppGpp to (pp)pGpp: characterization of regulatory effects of pGpp synthesized by the small alarmone synthetase of *Enterococcus faecalis*. *J. Bacteriol.* 197, 2908–2919. doi: 10.1128/JB.00324-15

Geiger, T., Kastle, B., Gratani, F. L., Goerke, C., and Wolz, C. (2014). Two small (p)ppGpp synthases in *Staphylococcus aureus* mediate tolerance against cell envelope stress conditions. *J. Bacteriol.* 196, 894–902. doi: 10.1128/JB.01201-13

Gourse, R. L., Chen, A. Y., Gopalkrishnan, S., Sanchez-Vazquez, P., Myers, A., and Ross, W. (2018). Transcriptional responses to ppGpp and DksA. *Annu. Rev. Microbiol.* 72, 163–184. doi: 10.1146/annurev-micro-090817-062444

Gratani, F. L., Horvatek, P., Geiger, T., Borisova, M., Mayer, C., Grin, I., et al. (2018). Regulation of the opposing (p)ppGpp synthetase and hydrolase activities in a bifunctional RelA/SpoT homologue from *Staphylococcus aureus*. *PLoS Genet.* 14:e1007514. doi: 10.1371/journal.pgen.1007514

Gundlach, J., Mehne, F. M., Herzberg, C., Kampf, J., Valerius, O., Kaever, V., et al. (2015). An essential poison: synthesis and degradation of cyclic di-AMP in *Bacillus subtilis*. *J. Bacteriol.* 197, 3265–3274. doi: 10.1128/JB.00564-15

Haseltine, W. A., and Block, R. (1973). Synthesis of guanosine tetra- and pentaphosphate requires the presence of a codon-specific, uncharged transfer ribonucleic acid in the acceptor site of ribosomes. *Proc. Natl. Acad. Sci. U. S. A.* 70, 1564–1568. doi: 10.1073/pnas.70.5.1564

He, H., Cooper, J. N., Mishra, A., and Raskin, D. M. (2012). Stringent response regulation of biofilm formation in *Vibrio cholerae*. *J. Bacteriol.* 194, 2962–2972. doi: 10.1128/JB.00014-12

He, J., Yin, W., Galperin, M. Y., and Chou, S. H. (2020). Cyclic di-AMP, a second messenger of primary importance: tertiary structures and binding mechanisms. *Nucleic Acids Res.* 48, 2807–2829. doi: 10.1093/nar/gkaa112

Hengge, R., Grundling, A., Jenal, U., Ryan, R., and Yildiz, F. (2016). Bacterial signal transduction by cyclic di-GMP and other nucleotide second messengers. *J. Bacteriol.* 198, 15–26. doi: 10.1128/JB.00331-15

Hochstadt-Ozer, J., and Cashel, M. (1972). The regulation of purine utilization in bacteria. V. Inhibition of purine phosphoribosyltransferase activities and purine uptake in isolated membrane vesicles by guanosine tetraphosphate. *J. Biol. Chem.* 247, 7067–7072.

Hogg, T., Mechold, U., Malke, H., Cashel, M., and Hilgenfeld, R. (2004). Conformational antagonism between opposing active sites in a bifunctional RelA/SpoT homolog modulates (p)ppGpp metabolism during the stringent response. *Cell* 117, 57–68. doi: 10.1016/S0092-8674(04)00260-0

Huynh, T. N., Luo, S., Pensinger, D., Sauer, J. D., Tong, L., and Woodward, J. J. (2015). An HD-domain phosphodiesterase mediates cooperative hydrolysis of c-di-AMP to affect bacterial growth and virulence. *Proc. Natl. Acad. Sci. U. S. A.* 112, E747–E756. doi: 10.1073/pnas.1416485112

Jimmy, S., Saha, C. K., Kurata, T., Stavropoulos, C., Oliveira, S. R. A., Koh, A., et al. (2020). A widespread toxin-antitoxin system exploiting growth control via alarmone signaling. *Proc. Natl. Acad. Sci. U. S. A.* 117, 10500–10510. doi: 10.1073/pnas.1916617117

Kalia, D., Merey, G., Nakayama, S., Zheng, Y., Zhou, J., Luo, Y., et al. (2013). Nucleotide, c-di-GMP, c-di-AMP, cGMP, cAMP, (p)ppGpp signaling in bacteria and implications in pathogenesis. *Chem. Soc. Rev.* 42, 305–341. doi: 10.1039/C2CS35206K

Kanjee, U., Gutsche, I., Alexopoulos, E., Zhao, B., El Bakkouri, M., Thibault, G., et al. (2011a). Linkage between the bacterial acid stress and stringent responses: the structure of the inducible lysine decarboxylase. *EMBO J.* 30, 931–944. doi: 10.1038/emboj.2011.5

Kanjee, U., Gutsche, I., Ramachandran, S., and Houry, W. A. (2011b). The enzymatic activities of the *Escherichia coli* basic aliphatic amino acid decarboxylases exhibit a pH zone of inhibition. *Biochemistry* 50, 9388–9398. doi: 10.1021/bi201161k

Kanjee, U., Ogata, K., and Houry, W. A. (2012). Direct binding targets of the stringent response alarmone (p)ppGpp. *Mol. Microbiol.* 85, 1029–1043. doi: 10.1111/j.1365-2958.2012.08177.x

Keasling, J. D., Bertsch, L., and Kornberg, A. (1993). Guanosine pentaphosphate phosphohydrolase of *Escherichia coli* is a long-chain exopolyphosphatase. *Proc. Natl. Acad. Sci. U. S. A.* 90, 7029–7033. doi: 10.1073/pnas.90.15.7029

Kriel, A., Bittner, A. N., Kim, S. H., Liu, K., Tehranchi, A. K., Zou, W. Y., et al. (2012). Direct regulation of GTP homeostasis by (p)ppGpp: a critical component of viability and stress resistance. *Mol. Cell* 48, 231–241. doi: 10.1016/j.molcel.2012.08.009

Kriel, A., Brinsmade, S. R., Tse, J. L., Tehranchi, A. K., Bittner, A. N., Sonenshein, A. L., et al. (2014). GTP dysregulation in *Bacillus subtilis* cells lacking (p)ppGpp results in phenotypic amino acid auxotrophy and failure to adapt to nutrient downshift and regulate biosynthesis genes. *J. Bacteriol.* 196, 189–201. doi: 10.1128/JB.00918-13

Kristensen, O., Ross, B., and Gajhede, M. (2008). Structure of the PPX/GPPA phosphatase from *Aquifex aeolicus* in complex with the alarmone ppGpp. *J. Mol. Biol.* 375, 1469–1476. doi: 10.1016/j.jmb.2007.11.073

Kudrin, P., Dzhygyr, I., Ishiguro, K., Beljantseva, J., Maksimova, E., Oliveira, S. R. A., et al. (2018). The ribosomal A-site finger is crucial for binding and activation of the stringent factor RelA. *Nucleic Acids Res.* 46, 1973–1983. doi: 10.1093/nar/gky023

Kuroda, A., Murphy, H., Cashel, M., and Kornberg, A. (1997). Guanosine tetra- and pentaphosphate promote accumulation of inorganic polyphosphate in *Escherichia coli*. *J. Biol. Chem.* 272, 21240–21243. doi: 10.1074/jbc.272.34.21240

Lemos, J. A., Nascimento, M. M., Lin, V. K., Abranches, J., and Burne, R. A. (2008). Global regulation by (p)ppGpp and CodY in *Streptococcus mutans*. *J. Bacteriol.* 190, 5291–5299. doi: 10.1128/JB.00288-08

Li, G., Zhao, Q., Luan, T., Hu, Y., Zhang, Y., Li, T., et al. (2020). Basal-level effects of (p)ppGpp in the absence of branched-chain amino acids in *Actinobacillus pleuropneumoniae*. *J. Bacteriol.* 202, e00640–e00719. doi: 10.1128/JB.00640-19

Liu, K., Bittner, A. N., and Wang, J. D. (2015a). Diversity in (p)ppGpp metabolism and effectors. *Curr. Opin. Microbiol.* 24, 72–79. doi: 10.1016/j.mib.2015.01.012

Liu, K., Myers, A. R., Pisithkul, T., Claas, K. R., Satyshur, K. A., Amador-Noguez, D., et al. (2015b). Molecular mechanism and evolution of guanylate kinase regulation by (p)ppGpp. *Mol. Cell* 57, 735–749. doi: 10.1016/j.molcel.2014.12.037

Maciag, M., Kochanowska, M., Lyzen, R., Wegrzyn, G., and Szalewska-Palasz, A. (2010). ppGpp inhibits the activity of *Escherichia coli* DnaG primase. *Plasmid* 63, 61–67. doi: 10.1016/j.plasmid.2009.11.002

Mehne, F. M., Gunka, K., Eilers, H., Herzberg, C., Kaever, V., and Stulke, J. (2013). Cyclic di-AMP homeostasis in *Bacillus subtilis*: both lack and high level accumulation of the nucleotide are detrimental for cell growth. *J. Biol. Chem.* 288, 2004–2017. doi: 10.1074/jbc.M112.395491

Nishino, T., Gallant, J., Shalit, P., Palmer, L., and Wehr, T. (1979). Regulatory nucleotides involved in the Rel function of *Bacillus subtilis*. *J. Bacteriol.* 140, 671–679. doi: 10.1128/JB.140.2.671-679.1979

Nomura, Y., Izumi, A., Fukunaga, Y., Kusumi, K., Iba, K., Watanabe, S., et al. (2014). Diversity in guanosine 3',5'-bisdiphosphate (ppGpp) sensitivity among guanylate kinases of bacteria and plants. *J. Biol. Chem.* 289, 15631–15641. doi: 10.1074/jbc.M113.534768

Oki, T., Yoshimoto, A., Sato, S., and Takamatsu, A. (1975). Purine nucleotide pyrophosphotransferase from *Streptomyces morookaensis*, capable of synthesizing pppApp and pppGpp. *Biochim. Biophys. Acta* 410, 262–272. doi: 10.1016/0005-2744(75)90228-4

Oppenheimer-Shaanan, Y., Wexselblatt, E., Katzhendler, J., Yavin, E., and Ben-Yehuda, S. (2011). c-di-AMP reports DNA integrity during sporulation in *Bacillus subtilis*. *EMBO Rep.* 12, 594–601. doi: 10.1038/embor.2011.77

Pausch, P., Steinchen, W., Wieland, M., Klaus, T., Freibert, S. A., Altegoer, F., et al. (2018). Structural basis for (p)ppGpp-mediated inhibition of the GTPase RbgA. *J. Biol. Chem.* 293, 19699–19709. doi: 10.1074/jbc.RA118.003070

Pesavento, C., and Hengge, R. (2009). Bacterial nucleotide-based second messengers. *Curr. Opin. Microbiol.* 12, 170–176. doi: 10.1016/j.mib.2009.01.007

Peselis, A., and Serganov, A. (2018). ykkC riboswitches employ an add-on helix to adjust specificity for polyanionic ligands. *Nat. Chem. Biol.* 14, 887–894. doi: 10.1038/s41589-018-0114-4

Pohl, K., Francois, P., Stenz, L., Schlink, F., Geiger, T., Herbert, S., et al. (2009). CodY in *Staphylococcus aureus*: a regulatory link between metabolism and virulence gene expression. *J. Bacteriol.* 191, 2953–2963. doi: 10.1128/JB.01492-08

Polakis, S. E., Guchhait, R. B., and Lane, M. D. (1973). Stringent control of fatty acid synthesis in *Escherichia coli*. Possible regulation of acetyl coenzyme a carboxylase by ppGpp. *J. Biol. Chem.* 248, 7957–7966.

Potrykus, K., and Cashel, M. (2008). (p)ppGpp: still magical? *Annu. Rev. Microbiol.* 62, 35–51. doi: 10.1146/annurev.micro.62.081307.162903

Puszynska, A. M., and O'Shea, E. K. (2017). ppGpp controls global gene expression in light and in darkness in *S. elongatus*. *Cell Rep.* 21, 3155–3165. doi: 10.1016/j.celrep.2017.11.067

Rao, F., See, R. Y., Zhang, D., Toh, D. C., Ji, Q., and Liang, Z. X. (2010). YybT is a signaling protein that contains a cyclic dinucleotide phosphodiesterase domain and a GGDEF domain with ATPase activity. *J. Biol. Chem.* 285, 473–482. doi: 10.1074/jbc.M109.040238

Rhaese, H. J., and Groscurth, R. (1976). Control of development: role of regulatory nucleotides synthesized by membranes of *Bacillus subtilis* in initiation of sporulation. *Proc. Natl. Acad. Sci. U. S. A.* 73, 331–335. doi: 10.1073/pnas.73.2.331

Rhaese, H. J., Hoch, J. A., and Groscurth, R. (1977). Studies on the control of development: isolation of *Bacillus subtilis* mutants blocked early in sporulation and defective in synthesis of highly phosphorylated nucleotides. *Proc. Natl. Acad. Sci. U. S. A.* 74, 1125–1129. doi: 10.1073/pnas.74.3.1125

Romling, U. (2008). Great times for small molecules: c-di-AMP, a second messenger candidate in bacteria and archaea. *Sci. Signal.* 1:pe39. doi: 10.1126/scisignal.133pe39

Rymer, R. U., Solorio, F. A., Tehranchi, A. K., Chu, C., Corn, J. E., Keck, J. L., et al. (2012). Binding mechanism of metalNTP substrates and stringent-response alarmones to bacterial DnaG-type primases. *Structure* 20, 1478–1489. doi: 10.1016/j.str.2012.05.017

Sarubbi, E., Rudd, K. E., and Cashel, M. (1988). Basal ppGpp level adjustment shown by new spoT mutants affect steady state growth rates and rrnA ribosomal promoter regulation in *Escherichia coli*. *Mol. Gen. Genet.* 213, 214–222. doi: 10.1007/BF00339584

Schafer, H., Beckert, B., Frese, C. K., Steinchen, W., Nuss, A. M., Beckstette, M., et al. (2020). The alarmones (p)ppGpp are part of the heat shock response of *Bacillus subtilis*. *PLoS Genet.* 16:e1008275. doi: 10.1371/journal.pgen.1008275

Schreiber, G., Metzger, S., Aizenman, E., Roza, S., Cashel, M., and Glaser, G. (1991). Overexpression of the relA gene in *Escherichia coli*. *J. Biol. Chem.* 266, 3760–3767.

Sherlock, M. E., Sudarsan, N., and Breaker, R. R. (2018). Riboswitches for the alarmone ppGpp expand the collection of RNA-based signaling systems. *Proc. Natl. Acad. Sci. U. S. A.* 115, 6052–6057. doi: 10.1073/pnas.1720406115

Shyp, V., Tankov, S., Ermakov, A., Kudrin, P., English, B. P., Ehrenberg, M., et al. (2012). Positive allosteric feedback regulation of the stringent response enzyme RelA by its product. *EMBO Rep.* 13, 835–839. doi: 10.1038/embor.2012.106

Silva, A. J., and Benitez, J. A. (2006). A *Vibrio cholerae* relaxed (relA) mutant expresses major virulence factors, exhibits biofilm formation and motility, and colonizes the suckling mouse intestine. *J. Bacteriol.* 188, 794–800. doi: 10.1128/JB.188.2.794-800.2006

Sobala, M., Bruhn-Olszewska, B., Cashel, M., and Potrykus, K. (2019). Methylobacterium extorquens RSH enzyme synthesizes (p)ppGpp and pppApp in vitro and in vivo, and leads to discovery of pppApp synthesis in *Escherichia coli*. *Front. Microbiol.* 10:859. doi: 10.3389/fmicb.2019.00859

Sokawa, Y., Sokawa, J., and Kaziro, Y. (1975). Regulation of stable RNA synthesis and ppGpp levels in growing cells of *Escherichia coli*. *Cell* 5, 69–74. doi: 10.1016/0092-8674(75)90093-8

Sonenshein, A. L. (2007). Control of key metabolic intersections in *Bacillus subtilis*. *Nat. Rev. Microbiol.* 5, 917–927. doi: 10.1038/nrmicro1772

Srivatsan, A., Han, Y., Peng, J., Tehranchi, A. K., Gibbs, R., Wang, J. D., et al. (2008). High-precision, whole-genome sequencing of laboratory strains facilitates genetic studies. *PLoS Genet.* 4:e1000139. doi: 10.1371/journal.pgen.1000139

Stein, J. P. Jr., and Bloch, K. E. (1976). Inhibition of *E. coli* beta-hydroxydecanoyl thioester dehydrase by ppGpp. *Biochem. Biophys. Res. Commun.* 73, 881–884. doi: 10.1016/0006-291X(76)90204-7

Steinchen, W., and Bange, G. (2016). The magic dance of the alarmones (p)ppGpp. *Mol. Microbiol.* 101, 531–544. doi: 10.1111/mmi.13412

Steinchen, W., Schuhmacher, J. S., Altegoer, F., Fage, C. D., Srinivasan, V., Linne, U., et al. (2015). Catalytic mechanism and allosteric regulation of an oligomeric (p)ppGpp synthetase by an alarmone. *Proc. Natl. Acad. Sci. U. S. A.* 112, 13348–13353. doi: 10.1073/pnas.1505271112

Stott, K. V., Wood, S. M., Blair, J. A., Nguyen, B. T., Herrera, A., Mora, Y. G., et al. (2015). (p)ppGpp modulates cell size and the initiation of DNA replication in *Caulobacter crescentus* in response to a block in lipid biosynthesis. *Microbiology* 161, 553–564. doi: 10.1099/mic.0.000032

Strugeon, E., Tilloy, V., Ploy, M. C., and Da Re, S. (2016). The stringent response promotes antibiotic resistance dissemination by regulating integron integrase expression in biofilms. *mBio* 7, e00868–e00916. doi: 10.1128/mBio.00868-16

Stulke, J., and Kruger, L. (2020). Cyclic di-AMP signaling in bacteria. *Annu. Rev. Microbiol.* doi: 10.1146/annurev-micro-020518-115943 [Epub ahead of print]

Svitil, A. L., Cashel, M., and Zyskind, J. W. (1993). Guanosine tetraphosphate inhibits protein synthesis in vivo. A possible protective mechanism for starvation stress in *Escherichia coli*. *J. Biol. Chem.* 268, 2307–2311.

Sy, J., and Lipmann, F. (1973). Identification of the synthesis of guanosine tetraphosphate (MS I) as insertion of a pyrophosphoryl group into the 3'-position in guanosine 5'-diphosphate. *Proc. Natl. Acad. Sci. U. S. A.* 70, 306–309. doi: 10.1073/pnas.70.2.306

Taguchi, M., Izui, K., and Katsuki, H. (1977). Activation of *Escherichia coli* phosphoenolpyruvate carboxylase by guanosine-5'-diphosphate-3'-diphosphate. *FEBS Lett.* 77, 270–272. doi: 10.1016/0014-5793(77)80249-4

Takada, H., Roghanian, M., Caballero-Montes, J., Van Nerom, K., Jimmy, S., Kudrin, P., et al. (2020a). Ribosome association primes the stringent factor Rel for recruitment of deacylated tRNA to ribosomal A-site. *bioRxiv* [Preprint]. doi: 10.1101/2020.01.17.910273

Takada, H., Roghanian, M., Murina, V., Dzhygyr, I., Murayama, R., Akanuma, G., et al. (2020b). The C-terminal RRM/ACT domain is crucial for fine-tuning the activation of 'Long' RelA-SpoT homolog enzymes by ribosomal complexes. *Front. Microbiol.* 11:277. doi: 10.3389/fmicb.2020.00277

Traxler, M. F., Summers, S. M., Nguyen, H. T., Zacharia, V. M., Hightower, G. A., Smith, J. T., et al. (2008). The global, ppGpp-mediated stringent response to amino acid starvation in *Escherichia coli*. *Mol. Microbiol.* 68, 1128–1148. doi: 10.1111/j.1365-2958.2008.06229.x

Traxler, M. F., Zacharia, V. M., Marquardt, S., Summers, S. M., Nguyen, H. T., Stark, S. E., et al. (2011). Discretely calibrated regulatory loops controlled by ppGpp partition gene induction across the 'feast to famine' gradient in *Escherichia coli*. *Mol. Microbiol.* 79, 830–845. doi: 10.1111/j.1365-2958.2010.07498.x

Varik, V., Oliveira, S. R. A., Hauryliuk, V., and Tenson, T. (2017). HPLC-based quantification of bacterial housekeeping nucleotides and alarmone messengers ppGpp and pppGpp. *Sci. Rep.* 7:11022. doi: 10.1038/s41598-017-10988-6

Wang, B., Dai, P., Ding, D., Del Rosario, A., Grant, R. A., Pentelute, B. L., et al. (2019). Affinity-based capture and identification of protein effectors of the growth regulator ppGpp. *Nat. Chem. Biol.* 15, 141–150. doi: 10.1038/s41589-018-0183-4

Wang, J. D., Sanders, G. M., and Grossman, A. D. (2007). Nutritional control of elongation of DNA replication by (p)ppGpp. *Cell* 128, 865–875. doi: 10.1016/j.cell.2006.12.043

Weiss, L. A., and Stallings, C. L. (2013). Essential roles for *Mycobacterium tuberculosis* Rel beyond the production of (p)ppGpp. *J. Bacteriol.* 195, 5629–5638. doi: 10.1128/JB.00759-13

Wendrich, T. M., Blaha, G., Wilson, D. N., Marahiel, M. A., and Nierhaus, K. H. (2002). Dissection of the mechanism for the stringent factor RelA. *Mol. Cell* 10, 779–788. doi: 10.1016/S1097-2765(02)00656-1

Whiteley, A. T., Pollock, A. J., and Portnoy, D. A. (2015). The PAMP c-di-AMP is essential for *Listeria monocytogenes* growth in rich but not minimal media due to a toxic increase in (p)ppGpp. *Cell Host Microbe* 17, 788–798. doi: 10.1016/j.chom.2015.05.006

Xiao, H., Kalman, M., Ikehara, K., Zemel, S., Glaser, G., and Cashel, M. (1991). Residual guanosine 3',5'-bispyrophosphate synthetic activity of relA null mutants can be eliminated by spoT null mutations. *J. Biol. Chem.* 266, 5980–5990.

Yin, W., Cai, X., Ma, H., Zhu, L., Zhang, Y., Chou, S. H., et al. (2020). A decade of research on the second messenger c-di-AMP. *FEMS Microbiol. Rev.* doi: 10.1093/femsre/fuaa019 [Epub ahead of print]

Zbornikova, E., Knejzlik, Z., Hauryliuk, V., Krasny, L., and Rejman, D. (2019). Analysis of nucleotide pools in bacteria using HPLC-MS in HILIC mode. *Talanta* 205:120161. doi: 10.1016/j.talanta.2019.120161

Zhang, Y. E., Baerentsen, R. L., Fuhrer, T., Sauer, U., Gerdes, K., and Brodersen, D. E. (2019). (p)ppGpp regulates a bacterial nucleosidase by an allosteric two-domain switch. *Mol. Cell* 74, 1239.e4–1249.e4. doi: 10.1016/j.molcel.2019.03.035

Zhang, Y., Zbornikova, E., Rejman, D., and Gerdes, K. (2018). Novel (p)ppGpp binding and metabolizing proteins of *Escherichia coli*. *mBio* 9, e02188–e02217. doi: 10.1128/mBio.02188-17

Zweers, J. C., Nicolas, P., Wiegert, T., van Dijl, J. M., and Denham, E. L. (2012). Definition of the sigma(W) regulon of *Bacillus subtilis* in the absence of stress. *PLoS One* 7:e48471. doi: 10.1371/journal.pone.0048471

Conflict of Interest: The authors declare that the research was conducted in the absence of any commercial or financial relationships that could be construed as a potential conflict of interest.

frontiers in Microbiology

PERSPECTIVE
published: 17 September 2020
doi: 10.3389/fmicb.2020.574872

Calibrating the Bacterial Growth Rate Speedometer: A Re-evaluation of the Relationship Between Basal ppGpp, Growth, and RNA Synthesis in *Escherichia coli*

Nicole C. E. Imholz*†, Marek J. Noga†, Niels J. F. van den Broek† and Gregory Bokinsky*

Department of Bionanoscience, Kavli Institute of Nanoscience, Delft University of Technology, Delft, Netherlands

The molecule guanosine tetraphophosphate (ppGpp) is most commonly considered an alarmone produced during acute stress. However, ppGpp is also present at low concentrations during steady-state growth. Whether ppGpp controls the same cellular targets at both low and high concentrations remains an open question and is vital for understanding growth rate regulation. It is widely assumed that basal ppGpp concentrations vary inversely with growth rate, and that the main function of basal ppGpp is to regulate transcription of ribosomal RNA in response to environmental conditions. Unfortunately, studies to confirm this relationship and to define regulatory targets of basal ppGpp are limited by difficulties in quantifying basal ppGpp. In this Perspective we compare reported concentrations of basal ppGpp in *E. coli* and quantify ppGpp within several strains using a recently developed analytical method. We find that although the inverse correlation between ppGpp and growth rate is robust across strains and analytical methods, absolute ppGpp concentrations do not absolutely determine RNA synthesis rates. In addition, we investigated the consequences of two separate RNA polymerase mutations that each individually reduce (but do not abolish) sensitivity to ppGpp and find that the relationship between ppGpp, growth rate, and RNA content of single-site mutants remains unaffected. Both literature and our new data suggest that environmental conditions may be communicated to RNA polymerase via an additional regulator. We conclude that basal ppGpp is one of potentially several agents controlling ribosome abundance and DNA replication initiation, but that evidence for additional roles in controlling macromolecular synthesis requires further study.

Keywords: ppGpp, growth rate, RNA polymerase, RNA synthesis, *Escherichia coli*

Edited by:
Katarzyna Potrykus,
University of Gdańsk, Poland

Reviewed by:
Johannes Geiselmann,
Université Grenoble Alpes, France
Regis Hallez,
University of Namur, Belgium
Llorenc Fernandez-Coll,
Eunice Kennedy Shriver National Institute of Child Health and Human Development (NICHD), United States

****Correspondence:***
Nicole C. E. Imholz
N.C.E.Imholz@rug.nl
Gregory Bokinsky
G.E.Bokinsky@tudelft.nl

†Present address:
Nicole C. E. Imholz,
Stratingh Institute for Chemistry, University of Groningen, Groningen, Netherlands
Marek J. Noga,
Translational Metabolic Laboratory, Department of Laboratory Medicine, Radboudumc, Nijmegen, Netherlands
Niels J. F. van den Broek,
Vaccine Process & Analytical Development, Janssen Vaccines & Prevention B.V., Leiden, Netherlands

Specialty section:
This article was submitted to Microbial Physiology and Metabolism, a section of the journal Frontiers in Microbiology

Received: *21 June 2020*
Accepted: *25 August 2020*
Published: *17 September 2020*

INTRODUCTION

How might a bacteria cell measure its own growth rate? In the model bacterium *Escherichia coli*, the small molecule guanosine tetraphosphate (ppGpp) is closely tied to growth rate control. However, due to the circumstances of its discovery, ppGpp is more familiar as a stress or starvation signal. ppGpp and guanosine pentaphosphate (pppGpp), collectively called (p)ppGpp, were first identified in *E. coli* as compounds produced in strains that inhibit stable RNA synthesis upon amino acid starvation, a phenomenon known as the stringent response (Cashel and Gallant, 1969). The source of (p)ppGpp during the stringent response is the enzyme RelA, which synthesizes (p)ppGpp in response to uncharged (non-aminoacyl) tRNA binding the acceptor site of an actively translating ribosome (Haseltine and Block, 1973). The high concentrations of (p)ppGpp observed during acute starvation (600–1000 pmol OD^{-1} for ppGpp) (Harshman and Yamazaki, 1971; Lazzarini et al., 1971) drive profound responses via both transcriptional and post-translational mechanisms (Traxler et al., 2008; Kanjee et al., 2012). The overall result of the stringent response is strong inhibition of all macromolecule synthesis (rRNA, DNA, proteins, phospholipids, and peptidoglycan), leading to growth arrest. (p)ppGpp is hydrolyzed by the essential enzyme SpoT. SpoT also carries an active (p)ppGpp synthase domain, although the specific biochemical trigger of (p)ppGpp synthesis by SpoT has not yet been identified. As a recent study suggests that ppGpp is more potent than pppGpp in mediating growth rate control in *E. coli* (Mechold et al., 2013) we focus exclusively upon ppGpp.

Comparatively less well-understood are the functions of "basal ppGpp": the ppGpp concentrations observed during steady-state growth in *E. coli* in the absence of stress (between 10 and 90 pmol OD^{-1}). When growth rate is varied by nutritional quality, basal ppGpp correlates inversely with growth rate. Basal ppGpp is essential in minimal media as it is required to activate transcription of amino acid pathways (Traxler et al., 2011). Just as ppGpp strongly inhibits stable RNA synthesis at high concentrations, basal ppGpp mildly inhibits transcriptional initiation from ribosomal RNA (rRNA) promoters, thus at least partly determining ribosome abundance during steady-state growth (Ryals et al., 1982). The inverse relationship between ppGpp and growth rate is thought to reflect the rheostat-like function of ppGpp as a regulator of ribosomal biosynthesis in response to nutrient availability. If ppGpp is artificially deviated from natural basal concentrations, growth is slowed, suggesting that ppGpp finds a growth-optimum level and adjusts rRNA expression accordingly (Zhu and Dai, 2019). The rate of DNA replication initiation also adjusts to small increases in basal ppGpp (Schreiber et al., 1995), and a strain entirely lacking ppGpp [$relA^-$ $spoT^-$, or $(p)ppGpp^0$] does not vary DNA replication initiation in response to growth rate, suggesting that ppGpp participates in regulating the DNA-biomass ratio (Fernández-Coll et al., 2020). As ribosome abundance is one of the factors determining the global protein synthesis rate, ppGpp may act as a growth rate-reporting signal that smoothly adjusts the steady-state rate of overall biomass synthesis (Hui et al., 2015). ppGpp should be thus considered a growth rate speedometer as well as a stress signal.

The observation that high ppGpp concentrations inhibit biomass synthesis suggests that basal ppGpp concentrations might also directly regulate all biomass synthesis pathways during steady-state growth, in addition to regulating stable RNA synthesis. This hypothetical layer of regulation would complement control of rRNA transcription, which determines the maximum rate of *steady-state* protein synthesis. For example, studies suggest that basal ppGpp might also regulate the *instantaneous* rate of protein synthesis by limiting purine synthesis (PurF, Wang et al., 2018) or translation cofactor activities (e.g., IF2, Dai et al., 2016) or the fraction of active ribosomes (Zhang et al., 2018). Basal ppGpp might also regulate cell envelope biosynthesis (Noga et al., 2020), as high ppGpp inhibits phospholipid synthesis, and inhibition of phospholipid synthesis arrests peptidoglycan synthesis (Ishiguro et al., 1980; Heath et al., 1994). In this extreme "orchestra conductor" model, ppGpp would not only regulate ribosome abundance, but would also tightly synchronize the synthesis rates of each macromolecule. This model expands the role of ppGpp beyond its better-established role, which is to inhibit general biomass synthesis at starvation-induced concentrations (>600 pmol OD^{-1}) like an emergency brake.

Defining the targets of basal ppGpp and identifying how basal ppGpp is maintained are two goals essential to understand how *E. coli* controls growth. To further encourage the recent revival of interest in the mechanisms of steady-state growth regulation and homeostasis (Scott et al., 2010, 2014; Dai et al., 2016), we contribute this Perspective on basal ppGpp in *E. coli* to evaluate the widely assumed notion that ppGpp is always inversely proportional to growth rate.

QUANTIFYING BASAL ppGpp IS DIFFICULT BUT ESSENTIAL

Actual ppGpp measurements are essential for determining which cellular processes are watching the growth rate speedometer. The rarity of basal ppGpp measurements is understandable as basal ppGpp is difficult to accurately quantify. The main challenges in measuring basal ppGpp *in vivo* are (1) its low abundance; (2) its chemical instability; (3) the presence of environmentally sensitive enzymes that rapidly hydrolyze and synthesize ppGpp. This means the analytical method must both chemically stabilize ppGpp and immediately denature all enzymes that synthesize or hydrolyze ppGpp. Moreover, in order to study ppGpp dynamics relevant to the rapid ppGpp response (<5 s), the method must enable fast sampling.

Despite these difficulties, several (p)ppGpp measurement methods have been developed, including thin layer chromatography (TLC) (Bochners and Ames, 1982; Sarubbi et al., 1988; Fernández-Coll and Cashel, 2018), high performance liquid chromatography (HPLC) (Ryals et al., 1982; Buckstein et al., 2008; Bokinsky et al., 2013; Varik et al., 2017; Jin et al., 2018) and liquid chromatography mass spectrometry

(LC-MS) (Ihara et al., 2015; Patacq et al., 2018). The advantages and disadvantages of each method have summarized in **Supplementary Table 1**. Whichever method is used, rapid quenching of metabolism during sampling (i.e., no centrifuging of live cells) is required.

ppGpp IS A RELIABLE GROWTH RATE SPEEDOMETER: MOST BASAL ppGpp MEASUREMENTS INDICATE THAT THE INVERSE CORRELATION BETWEEN ppGpp AND GROWTH RATE TRENDS IS ROBUST

A survey of reported basal ppGpp concentrations combined with our own measurements (**Figure 1**) indicates that despite apparent variability in absolute concentrations, the inverse correlation with growth rate is robust. We do not include pppGpp measurements, which are less-often reported. All data can be found in the **Supplementary Material**.

ppGpp Is an Accurate Growth Rate Speedometer in Wild-Type *E. coli* When Growth Rate Is Varied by Nutrient Source

Previously Reported Measurements

Measurements in laboratory-adapted *E. coli* show an inverse correlation between growth rate and basal ppGpp (15–90 pmol OD^{-1}) (**Figure 1A**). Early studies connected basal ppGpp, growth rate, and stable RNA abundance (Lazzarini et al., 1971; Sokawa et al., 1975; Ryals et al., 1982). Khan and Yamazaki (1974) measured basal ppGpp in an *E. coli* patient isolate and found several conditions in which ppGpp concentrations do not align smoothly with the expected trend (**Figure 1A**). However, RNA/DNA ratios in the outlier cultures followed the expected trend with growth rate (Khan and Yamazaki, 1974).

Reported ppGpp concentrations may differ perhaps due to differences in strains, turbidimeter calibration, or sampling method (Baracchini et al., 1988; Buckstein et al., 2008). Interestingly, even biological replicates show substantial variability (Ryals et al., 1982). Using an assay that exhibited less than 10% variation between individual measurements, Murray and Bremer (1996) report that ppGpp concentrations show 20% variations between biological replicates.

New Measurements (This Study)

We measured basal ppGpp concentrations in three *E. coli* K-12 strains using LC-MS (**Figure 1A**). Concentrations in MG1655 have been reported in Buckstein et al. (2008) for only three conditions (**Figure 1A**). NCM3722 is becoming increasingly popular as it lacks several genetic defects of MG1655 (Soupene et al., 2003; Brown and Jun, 2015). CF7968 (MG1655 rph^+ but not isogenic with the MG1655 reported here) has been used to demonstrate correlation between the RNA/protein ratio and the growth rate (Potrykus et al., 2011). All three strains exhibit the expected inverse correlation between ppGpp and growth rate. We observed 20% variation in technical replicates from a single culture and 23% average variation between biological replicates, similar to previous reports (Murray and Bremer, 1996).

RelA Is Not Required to Establish the Correlation Between Basal ppGpp and Growth Rate

At least three studies have compared basal ppGpp concentrations of isogenic $relA^+$ and $relA^-$ strains (Lazzarini et al., 1971; Sokawa et al., 1975; Ryals et al., 1982). Each study observed no significant difference in ppGpp concentrations and growth rates in $relA^+$ and $relA^-$, indicating that SpoT alone is able to establish an inverse correlation between ppGpp and growth rate (**Figure 1A**).

What Metabolic Process Sets Basal ppGpp Concentrations?

The observation that SpoT is able to maintain the ppGpp-growth rate correlation on its own does not necessarily indicate that RelA activity plays no role in maintaining basal ppGpp. As deacylated tRNA stimulates RelA activity (Haseltine and Block, 1973), one might presume that deacyl-tRNA abundance also correlates inversely with growth rate. However, the aminoacylated fraction of at least six tRNA species remains constant across growth rates. As total tRNA increases in parallel with rRNA, the absolute concentration of deacylated tRNA should also *increase* with growth rate (Dai et al., 2016). There are 43 different tRNA species in *E. coli*, and currently it is not known whether the acylation of each individual tRNA species varies. However, we surmise that RelA may contribute to basal ppGpp as $relA^-$ mutants exhibit different ribosome pausing behavior than wild-type (Li et al., 2018).

Identifying how SpoT maintains basal ppGpp is essential to understand the metabolic cues that lead to the inverse ppGpp-growth rate correlation. As hydrolysis and synthesis activities of a SpoT homolog are mutually exclusive (Hogg et al., 2004), basal ppGpp is likely set by a balance between the fraction of SpoT proteins engaged in either ppGpp synthesis or ppGpp hydrolysis. Environmental triggers that bias SpoT toward ppGpp synthesis were explored by Murray and Bremer (1996), and included carbon starvation, azide exposure, and simultaneous removal of all 20 amino acids. Although potential regulators have been identified [acyl carrier protein (Battesti and Bouveret, 2006), anti-sigma factor Rsd (Lee et al., 2018) and the small protein YtfK (Germain et al., 2019)], it is unclear how these regulate SpoT.

TRICKING THE GROWTH RATE SPEEDOMETER: ARTIFICIAL VARIATIONS OF ppGpp WITHIN FIXED NUTRITIONAL CONDITIONS

Mutation and overexpression of the *relA* and *spoT* genes enable different ppGpp concentrations in identical nutritional conditions. This also leads to an inverse relationship between ppGpp and growth rate.

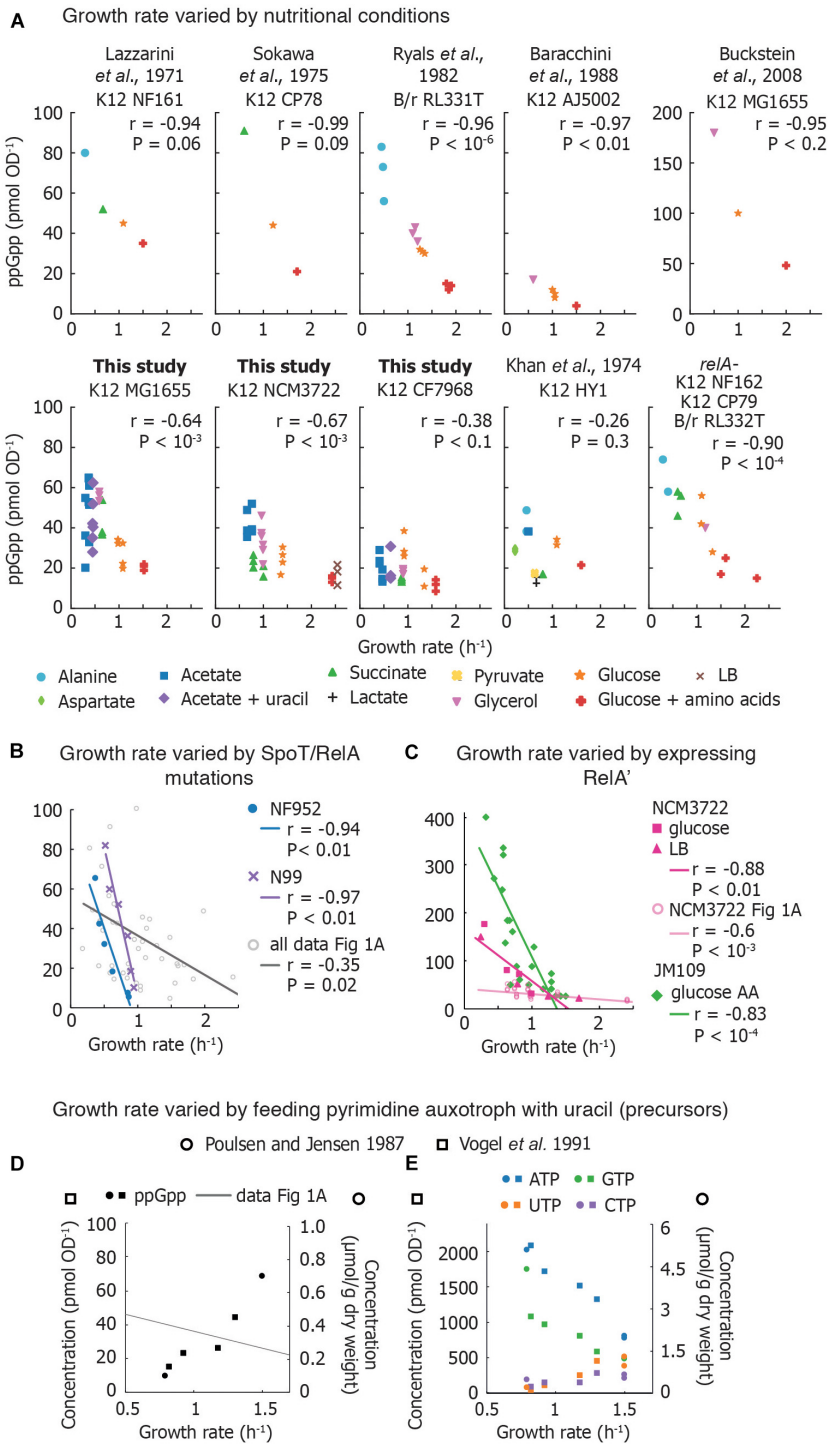

FIGURE 1 | Compilation of measurements of basal ppGpp vs. growth rate. **(A)** Basal ppGpp concentrations measured in *E. coli* strains that generally follow an inverse correlation with growth rate. Both literature data and data obtained for this study are shown (**Supplementary Section 3**). For data from this study, three technical replicates per biological replicate are shown. For data taken from the literature, the number of biological replicates varies and can be found in **Supplementary Material**. **(B)** Trends obtained by several *E. coli* strains bearing various mutations in ppGpp synthase/hydrolase enzyme SpoT grown in glucose minimal medium. Each point represents values obtained from one strain. This is compared to compiled data from A. The genotype of each strain used can be found in **Supplementary Material**. **(C)** Basal ppGpp measured during overexpression of RelA in *E. coli* JM109 (in glucose amino acids without Gln, Glu) and in *E. coli* NCM3722 in LB and glucose minimal medium. **(D,E)** Ribonucleotide concentrations in *E. coli* strains defective in pyrimidine synthesis. **(D)** ppGpp concentrations as a function of growth rate, overlaid with the compiled ppGpp vs. growth rate data of **(A)**, and **(E)** intracellular ATP, GTP, UTP, and CTP concentrations. References to data sets are provided in the **Supplementary Material**. For **(A–D)**, the Pearson correlation coefficient *r* and significance figure P (from a two-tailed significance test) is shown.

Point Mutations in RelA and SpoT Change Basal ppGpp by Rebalancing Rates of ppGpp Synthesis and Hydrolysis

Non-disabling mutations in *spoT* and *relA* perturb the balance between ppGpp synthesis and hydrolysis, resulting in varied basal ppGpp levels while retaining viability (Sarubbi et al., 1988). Two sets of mutations in different *E. coli* strains (**Supplementary Material**) exhibited inverse relationships between ppGpp and growth rate that appear to be steeper than the majority of basal level trends observed in various media (**Figure 1B**). However, as the ppGpp-growth rate relationship was not determined in the parental strains from which these mutants were obtained, direct comparisons with wild-type behaviors are not possible. rRNA decreases as basal ppGpp increases in *spoT* mutant strains as expected (Sarubbi et al., 1988; Hernandez and Bremer, 1990).

Ectopic Overexpression of RelA Generates a Steep ppGpp-Growth Rate Trendline

Overexpressing the catalytic domain of RelA (referred to as RelA′ or RelA*) artificially elevates ppGpp, inhibits rRNA synthesis and decreases growth rate. Data from ppGpp titrations using RelA′ are compared in **Figure 1C**. Schreiber et al. (1991) titrated ppGpp concentrations using RelA′ and obtained a ppGpp-growth rate trend that appears steeper than curves obtained for other strains. Two groups recently observed that RelA′ overexpression leads to higher basal ppGpp than expected for a given growth rate. RelA′ overexpression in *E. coli* NCM3722 in both LB medium and glucose minimal medium yields a ppGpp-growth rate curve steeper than the curve obtained in nutrient-limited NCM3722 (confirmed using a Chi-squared test, $P < 10^{-6}$) (Zhu et al., 2019; Noga et al., 2020). However, the RNA/protein ratio vs. growth rate trends measured in ppGpp- and carbon-limited cultures closely overlap. This suggests that in the absence of stress, growth rate and RNA synthesis control can be decoupled from *absolute* ppGpp concentrations while still obeying an inverse relationship.

BREAKING THE GROWTH RATE SPEEDOMETER: WHEN ppGpp IS NOT INVERSELY CORRELATED WITH GROWTH RATE

Nucleotide Starvation Causes a Positive Correlation Between Growth Rate and ppGpp

The most dramatic departure from the canonical ppGpp-growth rate trend has been accomplished by disrupting nucleotide metabolism. When the growth rates of nucleotide auxotrophs are titrated by adding limiting nucleotides or nucleotide precursors, ppGpp *increases* in parallel with growth rate. Poulsen and Jensen (1987) first observed this phenomenon in *E. coli* mutants unable to synthesize specific nucleotides [*carAB- guaB*(ts)]. When growth rate was titrated with pyrimidine and purine sources, the authors inverted the correlation between ppGpp and growth rate (**Figure 1D**). Vogel et al. (1991) also found that ppGpp concentrations increased from 15 to 44 pmol OD^{-1} in parallel with growth rate and total RNA in a pyrimidine auxotroph (**Figure 1D**).

Why does ppGpp correlate positively with growth rate when growth is limited by pyrimidine (uracil) supply? First, uracil limitation does not activate ppGpp synthesis in wild-type strains (Cashel and Gallant, 1969), indicating that RelA and SpoT do not detect all forms of starvation. Second, these auxotrophs exhibit low concentrations of UTP and CTP (**Figure 1E**) suggesting that ribosome abundance – and thus translation rate – is controlled by substrate concentrations in these mutants (NTP) rather than by inhibitor concentrations (ppGpp). As NTP limitation is relieved, other metabolites likely become limiting for growth, triggering ppGpp synthesis.

Growth Rate and RNA Content Do Not Strictly Follow ppGpp Concentrations During Out-of-Steady-State Growth Transitions

Steady-state correlations such as the correlation between ppGpp and growth rate imply but do not establish regulatory connections. Hypotheses inspired by correlations must be tested by environmental perturbations. Baracchini and Bremer (1988) monitored growth and rRNA synthesis while adjusting basal ppGpp by adding pseudomonic acid to *E. coli* glucose cultures. Pseudomonic acid causes accumulation of uncharged tRNA and increases ppGpp. High concentrations of pseudomonic acid abruptly increased ppGpp and rapidly arrested growth, consistent with the stringent response. Low concentrations of pseudomonic acid also triggered ppGpp synthesis (up to 60–100 pmol OD^{-1}) and an immediate but smaller decrease in rRNA synthesis. However, the instantaneous growth rate (monitored by optical density) was not perturbed in the short term by small increases in ppGpp concentrations.

These out-of-steady-state experiments reveal several important limitations of basal ppGpp regulation. First, the correlation between basal ppGpp and growth rate is broken when growth is out of steady state: were the relationship between growth rate and ppGpp to be as strict during growth transitions as during steady-state growth, a tripling in basal ppGpp would cause an immediate corresponding reduction in growth. Second, unlike the rapid protein synthesis inhibition caused by high ppGpp concentrations (Svitil et al., 1993), small increases of ppGpp (<100 pmol OD^{-1}) do not seem to immediately inhibit biomass synthesis (with the exception of stable RNA). This undermines any notion that basal ppGpp directly regulates the instantaneous translation rate. Finally, two additional studies demonstrate that ppGpp and the rate of stable RNA synthesis can be transiently decoupled during nutritional upshifts, suggesting that additional signals may regulate rRNA synthesis (Friesen et al., 1975; Hansen et al., 1975).

MEASUREMENTS OF BASAL ppGpp REVEAL THAT DISRUPTION OF ppGpp BINDING SITES ON RNA POLYMERASE DOES NOT ABOLISH CORRELATION BETWEEN BASAL ppGpp, RNA, AND GROWTH RATE

To determine whether RNA polymerase (RNAP) retains regulation by basal ppGpp if its two ppGpp binding sites are disrupted, we measured basal ppGpp levels, growth rates and cellular RNA in *E. coli* strains expressing RNAP mutants (Ross et al., 2013, 2016). Although we did not test a strain bearing both mutations together, we reasoned that mutations in either individual binding site might nevertheless strongly affect RNA synthesis control by basal ppGpp and weaken the relationship between RNA and growth rate, as observed in a ppGpp^0 strain by Potrykus et al. (2011).

We transferred mutations that disrupt ppGpp binding site 1 [*rpoZ*(wt) *rpoC* R362A R417A K615A; Ross et al., 2013] or that disrupt ppGpp binding site 2 (*rpoC* N680A K681A; Ross et al., 2016) from MG1655 to NCM3722. We confirmed that the stringent response does not arrest RNA synthesis in our mutant strains as strongly as in wild-type (**Supplementary Figure 1**), qualitatively consistent with results previously observed (Ross et al., 2016). We sampled cultures that had been grown directly from fresh colonies (i.e., without dilution from overnight cultures) to reduce the outgrowth of cells bearing additional RNAP mutations (Murphy and Cashel, 2003).

ppGpp concentrations remain inversely correlated with growth rate in both mutants. However, both mutants grow more slowly and have correspondingly higher ppGpp concentrations in most growth media than wild-type NCM3722 (**Figures 2A–C**). Furthermore, the RNA content of both mutants correlates positively with growth rate, as it does for the wild-type strain (**Figure 2D**), with exception of the lower RNA concentration for the *rpoC*2- mutant in LB medium. At first glance, this is consistent with the notion that the RNAP mutants are less sensitive to ppGpp, as apparent from the slopes of cellular RNA content vs. ppGpp (**Figure 2E**). A chi-squared

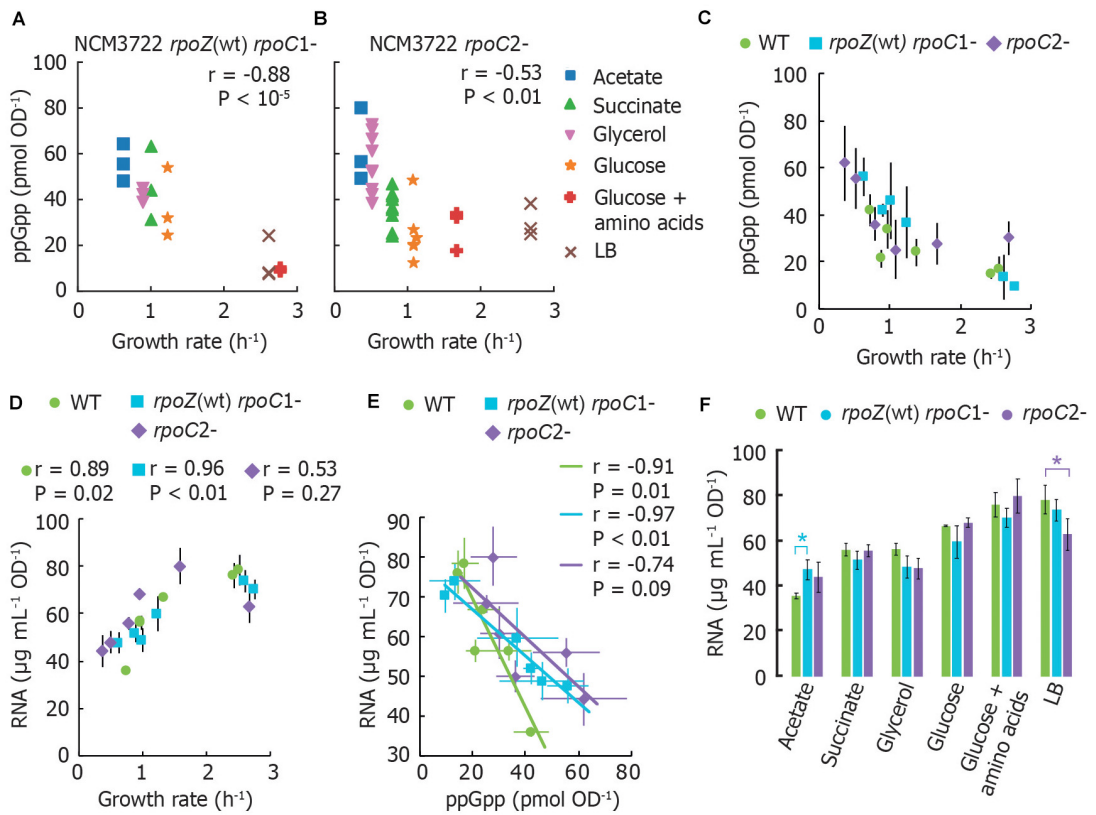

FIGURE 2 | RNA polymerase mutants without ppGpp binding site 1 or 2 still exhibit the typical ppGpp and RNA vs. growth rate trends. **(A)** Basal ppGpp in NCM3722 *rpoZ*(WT) *rpoC*1- and in **(B)** NCM3722 *rpoC*2- (showing technical replicates, 3 per culture). **(C)** Averaged data of A and B overlapped with average NCM3722 wild type data from **Figure 1A**. **(D–F)** The total RNA concentration of NCM3722 wild type and *rpoC* mutants in various growth media. Error bars represent standard deviations. **(D)** Total RNA concentration plotted as a function of growth rate. **(E)** Data of D plotted as a function of ppGpp concentrations with a linear fit. The average or each condition is shown. See **Supplementary Section 3** for materials and methods. **(F)** Data of D plotted to compare RNA content between strains grown in identical media. Bars represent the average of three technical replicates of one culture, with exception of *rpoC*2- in glycerol (2 cultures, 6 replicates) and succinate (3 cultures, 9 replicates). *$P < 0.05$ for a two-tailed student's *t*-test. For **(A,B,D,E)**, the Pearson correlation coefficient *r* and significance figure P (from a two-tailed significance test) is shown.

goodness-of-fit test verified that the mutants do not fit the wild-type pattern ($P < 10^{-6}$). In other words, higher ppGpp concentrations may be required to inhibit RNA synthesis in these strains. While it might be expected that the cultures expressing ppGpp-insensitive RNAP thus contain a higher RNA abundance than wild-type, we found that for every medium aside from MOPS/acetate, both mutant strains exhibit equivalent or even less RNA per OD unit than does the wild-type (**Figure 2F**). This is inconsistent with the abolition of growth rate control of RNA content observed in ppGpp^0 strains (Potrykus et al., 2011).

While our results indicate that neither ppGpp binding site on RNAP is *individually* sufficient to mediate ppGpp control over RNA content, we cannot exclude the possibility that the simultaneous removal of both ppGpp binding sites is required to fully eliminate the ppGpp-RNA content relationship. Other factors may also be implicated in RNA synthesis control in the NCM3722 strain. For instance, TraR, a transcription factor encoded on the F plasmid carried by NCM3722 is known to mimic the action of DksA and ppGpp (Gopalkrishnan et al., 2017).

CONCLUSION

We find that the inverse correlation between ppGpp and growth rate during steady-state growth is quite robust, even against removal of the ppGpp synthesis enzyme RelA. Deviations from the trend (e.g., RelA′ overexpression, pyrimidine starvation, and growth transitions) deserve fuller exploration as they likely hint at poorly understood facets of ppGpp biology. Disrupting either individual ppGpp binding site of RNAP did not eliminate the correlation between growth rate, RNA content, and basal ppGpp concentrations. Despite compelling evidence for basal ppGpp control of rRNA synthesis, incorporating ppGpp into quantitative models of cell behavior requires a better understanding of both transcriptional and post-translational targets. In order to advance this goal, we suggest several questions for the field:

1. *What targets are responsive to basal ppGpp concentrations?* As basal ppGpp varies with growth rate in parallel with all biosynthetic fluxes during balanced growth, it is tempting to overextend models of ppGpp control. Targets thought to be regulated during the stringent response may prove insensitive to basal ppGpp. Experiments that monitor ppGpp during growth transitions already suggest that small changes in basal ppGpp do not immediately affect instantaneous protein synthesis or total biomass production. Studies of basal ppGpp concentrations during growth transitions are essential for distinguishing what is influenced by ppGpp. We suggest experiments that monitor protein synthesis during small controlled variations in basal ppGpp ($\pm$50 pmol OD^{-1}).
2. *What establishes basal ppGpp concentrations?* It is unknown which metabolic cues drive RelA and SpoT to generate basal ppGpp.
3. *What regulates stable RNA synthesis during steady-state growth, aside from basal ppGpp?* Our observation that RNA polymerase mutants lacking either one of the two ppGpp binding sites still exhibit an inverse relationship between RNA content and ppGpp concentrations implies that other factors also regulate RNA content, as has been suggested (Fernández-Coll and Cashel, 2018). However, experiments in a strain simultaneously bearing both RNAP mutations will be necessary to confirm this.
4. *Does basal ppGpp vary inversely with growth rate when growth rate is varied by other nutrients than carbon source?* Measuring basal ppGpp vs. growth rate in conditions that have not yet been tested (e.g., nitrogen source) would also determine whether basal ppGpp is an accurate growth rate speedometer.
5. *Do all species with RSH proteins also maintain basal concentrations of ppGpp (or pppGpp) during steady-state growth?* As RSH proteins are widely distributed (Atkinson et al., 2011), basal ppGpp may be a defining feature of bacterial growth.

We further recommend the use of common reference strains (preferably *E. coli* NCM3722) and defined media to enable comparisons between labs.

DATA AVAILABILITY STATEMENT

All datasets generated for this study are included in the article/**Supplementary Material**.

AUTHOR CONTRIBUTIONS

NI and GB conceived and designed the experiments and wrote the manuscript. NI performed experiments and data analysis. NI, NB, and MN developed the LC-MS method. All authors contributed to the article and approved the submitted version.

FUNDING

NI was supported by a grant to GB from the Frontiers of Nanoscience program. MN was supported by a grant to GB from the Netherlands Organisation for Scientific Research (ALW Open 824.15.018). GB and NB were supported by startup funds provided by the Department of Bionanoscience of TU Delft.

ACKNOWLEDGMENTS

We thank Michael Cashel and Richard L. Gourse for providing strains.

SUPPLEMENTARY MATERIAL

The Supplementary Material for this article can be found online at: https://www.frontiersin.org/articles/10.3389/fmicb.2020.574872/full#supplementary-material

REFERENCES

Atkinson, G. C., Tenson, T., and Hauryliuk, V. (2011). The RelA/SpoT Homolog (RSH) superfamily: distribution and functional evolution of ppGpp Synthetases and hydrolases across the tree of life. *PLoS One* 6:e23479. doi: 10.1371/journal.pone.0023479

Baracchini, E., and Bremer, H. (1988). Stringent and growth control of rRNA synthesis in *Escherichia coli* are both mediated by ppGpp. *J. Biol. Chem.* 263, 2597–2602.

Baracchini, E., Glass, R., and Bremer, H. (1988). Studies *in vivo* on *Escherichia coli* RNA polymerase mutants altered in the stringent response. *Mol. Gen. Genet.* 213, 379–387. doi: 10.1007/bf00339606

Battesti, A., and Bouveret, E. (2006). Acyl carrier protein/SpoT interaction, the switch linking SpoT-dependent stress response to fatty acid metabolism. *Mol. Microbiol.* 62, 1048–1063. doi: 10.1111/j.1365-2958.2006.05442.x

Bochners, B. R., and Ames, B. N. (1982). Complete analysis of cellular nucleotides by two-dimensional thin layer chromatography. *J. Biol. Chem.* 257, 9759–9769.

Bokinsky, G., Baidoo, E. E. K., Akella, S., Burd, H., Weaver, D., Alonso-Gutierrez, J., et al. (2013). HipA-triggered growth arrest and β-lactam tolerance in *Escherichia coli* are mediated by RelA-dependent ppGpp synthesis. *J. Bacteriol.* 195, 3173–3182. doi: 10.1128/JB.02210-12

Brown, S. D., and Jun, S. (2015). Complete genome sequence of *Escherichia coli* NCM3722. *Genome Announc.* 3:e00879-15. doi: 10.1128/genomea.00879-15

Buckstein, M. H., He, J., and Rubin, H. (2008). Characterization of nucleotide pools as a function of physiological state in *Escherichia coli*. *J. Bacteriol.* 190, 718–726. doi: 10.1128/jb.01020-07

Cashel, M., and Gallant, J. (1969). Two compounds implicated in the function of the RC gene of *Escherichia coli*. *Nature* 221, 838–841. doi: 10.1038/221838a0

Dai, X. F., Zhu, M. L., Warren, M., Balakrishnan, R., Patsalo, V., Okano, H., et al. (2016). Reduction of translating ribosomes enables *Escherichia coli* to maintain elongation rates during slow growth. *Nat. Microbiol.* 2:16231. doi: 10.1038/nmicrobiol.2016.231

Fernández-Coll, L., and Cashel, M. (2018). Contributions of SpoT hydrolase, SpoT synthetase, and RelA synthetase to carbon source diauxic growth transitions in *Escherichia coli*. *Front. Microbiol.* 9:1802. doi: 10.3389/fmicb.2018.01802

Fernández-Coll, L., Maciag-Dorszynska, M., Tailor, K., Vadia, S., Levin, P. A., Szalewska-Palasz, A., et al. (2020). The absence of (p)ppGpp renders initiation of *Escherichia coli* chromosomal DNA synthesis independent of growth rates. *mBio* 11:e03223-19. doi: 10.1128/mBio.03223-19

Friesen, J., Fiil, N., and von Meyenburg, K. (1975). Synthesis and turnover of basal level guanosine tetraphosphate in *Escherichia coli*. *J. Biol. Chem.* 250, 304–309.

Germain, E., Guiraud, P., Byrne, D., Douzi, B., Djendli, M., and Maisonneuve, E. (2019). YtfK activates the stringent response by triggering the alarmone synthetase SpoT in *Escherichia coli*. *Nat. Commun.* 10:5763. doi: 10.1038/s41467-019-13764-4

Gopalkrishnan, S., Ross, W., Chen, A. Y., and Gourse, R. L. (2017). TraR directly regulates transcription initiation by mimicking the combined effects of the global regulators DksA and ppGpp. *Proc. Natl. Acad. Sci. U.S.A.* 114, E5539–E5548. doi: 10.1073/pnas.1704105114

Hansen, M. T., Pato, M. L., Molin, S., and Fiil, N. P. (1975). Simple downshift and resulting lack of correlation between ppGpp pool size and ribonucleic acid accumulation. *J. Bacteriol.* 122, 585–591. doi: 10.1128/jb.122.2.585-591.1975

Harshman, R. B., and Yamazaki, H. (1971). Formation of ppGpp in a Relaxed and Stringent Strain of *E. coli* during diauxie lag. *Biochemistry* 10, 3980–3982. doi: 10.1021/bi00797a027

Haseltine, W. A., and Block, R. (1973). Synthesis of guanosine tetra- and pentaphosphate requires the presence of a codon-specific, uncharged transfer ribonucleic acid in the acceptor site of ribosomes. *Proc. Natl. Acad. Sci. U.S.A.* 70, 1564–1568. doi: 10.1073/pnas.70.5.1564

Heath, R. J., Jackowski, S., and Rock, C. O. (1994). Guanosine tetraphosphate inhibition of fatty acid and phospholipid synthesis in *Escherichia coli* is relieved by overexpression of glycerol-3-phosphate acyltransferase (*plsB*). *J. Bacteriol.* 269, 26584–26590.

Hernandez, V. J., and Bremer, H. (1990). Guanosine tetraphosphate (ppGpp) dependence of the growth rate control of *rrnB* P1 promoter activity in *Escherichia coli*. *J. Biol. Chem.* 265, 11605–11614.

Hogg, T., Mechold, U., Malke, H., Cashel, M., and Hilgenfeld, R. (2004). Conformational antagonism between opposing active sites in a bifunctional Re1A/SpoT homolog modulates (p)ppGpp metabolism during the stringent response. *Cell* 117, 57–68. doi: 10.1016/S0092-8674(04)00260-0

Hui, S., Silverman, J. M., Chen, S. S., Erickson, D. W., Basan, M., Wang, J., et al. (2015). Quantitative proteomic analysis reveals a simple strategy of global resource allocation in bacteria. *Mol. Syst. Biol.* 11:784. doi: 10.15252/msb.20145697

Ihara, Y., Ohta, H., and Masuda, S. (2015). A highly sensitive quantification method for the accumulation of alarmone ppGpp in Arabidopsis thaliana using UPLC-ESI-qMS/MS. *J. Plant Res.* 128, 511–518. doi: 10.1007/s10265-015-0711-1

Ishiguro, E. E., Mirelman, D., and Harkness, R. E. (1980). Regulation of the terminal steps in peptidoglycan biosynthesis in ether-treated cells of *Escherichia coli*. *FEBS Lett.* 120, 175–178. doi: 10.1016/0014-5793(80)80291-2

Jin, H., Lao, Y. M., Zhou, J., Zhang, H. J., and Cai, Z. H. (2018). A rapid UHPLC-HILIC method for algal guanosine 5′-diphosphate 3′-diphosphate (ppGpp) and the potential separation mechanism. *J. Chromatogr. B Anal. Technol. Biomed. Life Sci.* 1096, 143–153. doi: 10.1016/j.jchromb.2018.08.009

Kanjee, U., Ogata, K., and Houry, W. A. (2012). Direct binding targets of the stringent response alarmone (p)ppGpp. *Mol. Microbiol.* 85, 1029–1043. doi: 10.1111/j.1365-2958.2012.08177.x

Khan, S. R., and Yamazaki, H. (1974). Inapparent correlation between guanosine tetraphosphate levels and RNA contents in *Escherichia coli*. *Biochem. Biophys. Res. Commun.* 59, 125–132. doi: 10.1016/s0006-291x(74)80183-x

Lazzarini, R. A., Cashel, M., and Gallant, J. (1971). On the regulation of guanosine tetraphosphate levels in stringent and relaxed strains of *Escherichia coli*. *J. Biol. Chem.* 246, 4381–4385.

Lee, J. W., Park, Y. H., and Seok, Y. J. (2018). Rsd balances (p)ppGpp level by stimulating the hydrolase activity of SpoT during carbon source downshift in *Escherichia coli*. *Proc. Natl. Acad. Sci. U.S.A.* 115, E6845–E6854. doi: 10.1073/pnas.1722514115

Li, S. H., Li, Z., Park, J. O., King, C. G., Rabinowitz, J. D., Wingreen, N. S., et al. (2018). *Escherichia coli* translation strategies differ across carbon, nitrogen and phosphorus limitation conditions. *Nat. Microbiol.* 3, 939–947. doi: 10.1038/s41564-018-0199-2

Mechold, U., Potrykus, K., Murphy, H., Murakami, K. S., and Cashel, M. (2013). Differential regulation by ppGpp versus pppGpp in *Escherichia coli*. *Nucleic Acids Res.* 41, 6175–6189. doi: 10.1093/nar/gkt302

Murphy, H., and Cashel, M. (2003). Isolation of RNA polymerase suppressors of a (p)ppGpp deficiency. *Methods Enzymol.* 371, 596–601. doi: 10.1016/s0076-6879(03)71044-1

Murray, K. D., and Bremer, H. (1996). Control of *spoT*-dependent ppGpp synthesis and degradation in *Escherichia coli*. *J. Mol. Biol.* 259, 41–57. doi: 10.1006/jmbi.1996.0300

Noga, M. J., Buke, F., van den Broek, N. J. F., Imholz, N., Scherer, N., and Bokinsky, G. (2020). Post-translational control is sufficient to coordinate membrane synthesis with growth in *Escherichia coli*. *mBio* 11:e02703-19. doi: 10.1101/728451

Patacq, C., Chaudet, N., and Létisse, F. (2018). Absolute quantification of ppGpp and pppGpp by double-spike isotope dilution ion chromatography-high-resolution mass spectrometry. *Anal. Chem.* 90, 10715–10723. doi: 10.1021/acs.analchem.8b00829

Potrykus, K., Murphy, H., Philippe, N., and Cashel, M. (2011). ppGpp is the major source of growth rate control in *E. coli*. *Environ. Microbiol.* 13, 563–575. doi: 10.1111/j.1462-2920.2010.02357.x

Poulsen, P., and Jensen, K. F. (1987). Effect of UTP and GTP pools on attenuation at the *pyrE* gene of *Escherichia coli*. *Mol. Gen. Genet.* 208, 152–158. doi: 10.1007/bf00330436

Ross, W., Sanchez-Vazquez, P., Chen, A. Y., Lee, J. H., Burgos, H. L., and Gourse, R. L. (2016). ppGpp binding to a site at the RNAP-DksA interface accounts for its dramatic effects on transcription initiation during the stringent response. *Mol. Cell* 62, 811–823. doi: 10.1016/j.molcel.2016.04.029

Ross, W., Vrentas, C. E., Sanchez-Vazquez, P., Gaal, T., and Gourse, R. L. (2013). The magic spot: a ppGpp binding site on *E. coli* RNA polymerase responsible for regulation of transcription initiation. *Mol. Cell* 50, 420–429. doi: 10.1016/j.molcel.2013.03.021

Ryals, J., Little, R., and Bremer, H. (1982). Control of ribosomal-RNA and transfer-RNA syntheses in *Escherichia coli* by guanosine tetraphosphate. *J. Bacteriol.* 151, 1261–1268. doi: 10.1128/jb.151.3.1261-1268.1982

Sarubbi, E., Rudd, K. E., and Cashel, M. (1988). Basal ppGpp level adjustment shown by new *spoT* mutants affect steady state growth rates and *rrnA* ribosomal promoter regulation in *Escherichia coli*. *MGG Mol. Gen. Genet.* 213, 214–222. doi: 10.1007/BF00339584

Schreiber, G., Metzger, S., Aizenman, E., Roza, S., Cashel, M., and Glaser, G. (1991). Overexpression of the *relA* gene in *Escherichia coli*. *J. Biol. Chem.* 266, 3760–3767.

Schreiber, G., Ron, E. Z., and Glaser, G. (1995). ppGpp-mediated regulation of DNA replication and cell division in *Escherichia coli*. *Curr. Microbiol.* 30, 27–32. doi: 10.1007/BF00294520

Scott, M., Gunderson, C. W., Mateescu, E. M., Zhang, Z., and Hwa, T. (2010). Interdependence of cell growth and gene expression: origins and consequences. *Science* 330, 1099–1102. doi: 10.1126/science.1192588

Scott, M., Klumpp, S., Mateescu, E. M., and Hwa, T. (2014). Emergence of robust growth laws from optimal regulation of ribosome synthesis. *Mol. Syst. Biol.* 10:747. doi: 10.15252/msb.20145379

Sokawa, Y., Sokawa, J., and Kaziro, Y. (1975). Regulation of stable RNA synthesis and ppGpp levels in growing cells of *Escherichia coli*. *Cell* 5, 69–74. doi: 10.1016/0092-8674(75)90093-8

Soupene, E., Van Heeswijk, W. C., Plumbridge, J., Stewart, V., Bertenthal, D., Lee, H., et al. (2003). Physiological studies of *Escherichia coli* strain MG1655: growth defects and apparent cross-regulation of gene expression. *J. Bacteriol.* 185, 5611–5626. doi: 10.1128/JB.185.18.5611-5626.2003

Svitil, A. L., Cashel, M., and Zyskind, J. W. (1993). Guanosine tetraphosphate inhibits protein synthesis *in vivo*. *J. Biol. Chem.* 268, 2307–2311.

Traxler, M. F., Summers, S. M., Nguyen, H. T., Zacharia, V. M., Hightower, G. A., Smith, J. T., et al. (2008). The global, ppGpp-mediated stringent response to amino acid starvation in *Escherichia coli*. *Mol. Microbiol.* 68, 1128–1148. doi: 10.1111/j.1365-2958.2008.06229.x

Traxler, M. F., Zacharia, V. M., Marquardt, S., Summers, S. M., Nguyen, H. T., Stark, S. E., et al. (2011). Discretely calibrated regulatory loops controlled by ppGpp partition gene induction across the "feast to famine" gradient in *Escherichia coli*. *Mol. Microbiol.* 79, 830–845. doi: 10.1111/j.1365-2958.2010.07498.x

Varik, V., Oliveira, S. R. A., Hauryliuk, V., and Tenson, T. (2017). HPLC-based quantification of bacterial housekeeping nucleotides and alarmone messengers ppGpp and pppGpp. *Sci. Rep.* 7:11022. doi: 10.1038/s41598-017-10988-6

Vogel, U., Pedersen, S., and Jensen, K. F. (1991). An unusual correlation between ppGpp pool size and rate of ribosome synthesis during partial pyrimidine starvation of *Escherichia coli*. *J. Bacteriol.* 173, 1168–1174. doi: 10.1128/jb.173.3.1168-1174.1991

Wang, B., Dai, P., Ding, D., Del Rosario, A., Grant, R. A., Pentelute, B. L., et al. (2018). Affinity-based capture and identification of protein effectors of the growth regulator ppGpp. *Nat. Chem. Biol.* 15, 141–150. doi: 10.1038/s41589-018-0183-4

Zhang, Y., Zbornikova, E., Rejman, D., and Gerdes, K. (2018). Novel (p)ppGpp binding and metabolizing proteins of *Escherichia coli*. *mBio* 9, 1–20. doi: 10.1128/mBio.02188-17

Zhu, M., and Dai, X. (2019). Growth suppression by altered (p)ppGpp levels results from non-optimal resource allocation in *Escherichia coli*. *Nucleic Acids Res.* 47, 4684–4693. doi: 10.1093/nar/gkz211

Zhu, M., Mori, M., Hwa, T., and Dai, X. (2019). Disruption of transcription–translation coordination in *Escherichia coli* leads to premature transcriptional termination. *Nat. Microbiol.* 4, 2347–2356. doi: 10.1038/s41564-019-0543-1

Conflict of Interest: The authors declare that the research was conducted in the absence of any commercial or financial relationships that could be construed as a potential conflict of interest.

Citation: Imholz NCE, Noga MJ, van den Broek NJF and Bokinsky G (2020) Calibrating the Bacterial Growth Rate Speedometer: A Re-evaluation of the Relationship Between Basal ppGpp, Growth, and RNA Synthesis in Escherichia coli. Front. Microbiol. 11:574872. doi: 10.3389/fmicb.2020.574872

frontiers in Microbiology

ORIGINAL RESEARCH
published: 18 September 2020
doi: 10.3389/fmicb.2020.575882

Small Alarmone Synthetases RelP and RelQ of *Staphylococcus aureus* Are Involved in Biofilm Formation and Maintenance Under Cell Wall Stress Conditions

*Andrea Salzer, Daniela Keinhörster, Christina Kästle, Benjamin Kästle and Christiane Wolz**

Interfaculty Institute of Microbiology and Infection Medicine, University of Tübingen, Tübingen, Germany

The stringent response is characterized by the synthesis of the alarmone (p)ppGpp. The phenotypic consequences resulting from (p)ppGpp accumulation vary among species, and for several pathogenic bacteria, it has been shown that the activation of the stringent response strongly affects biofilm formation and maintenance. In *Staphylococcus aureus,* (p)ppGpp can be synthesized by the RelA/SpoT homolog Rel upon amino acid deprivation or by the two small alarmone synthetases RelP and RelQ under cell wall stress. We found that *relP* and *relQ* increase biofilm formation under cell wall stress conditions induced by a subinhibitory vancomycin concentration. However, the effect of (p)ppGpp on biofilm formation is independent of the regulators CodY and Agr. Biofilms formed by the strain HG001 or its (p)ppGpp-defective mutants are mainly composed of extracellular DNA and proteins. Furthermore, the induction of the RelPQ-mediated stringent response contributes to biofilm-related antibiotic tolerance. The proposed (p)ppGpp-inhibiting peptide DJK-5 shows bactericidal and biofilm-inhibitory activity. However, a non-(p)ppGpp-producing strain is even more vulnerable to DJK-5. This strongly argues against the assumption that DJK-5 acts via (p)ppGpp inhibition. In summary, RelP and RelQ play a major role in biofilm formation and maintenance under cell wall stress conditions.

Keywords: stringent response, (p)ppGpp, biofilm, *Staphylococcus aureus*, cell wall stress

OPEN ACCESS

Edited by:
Katarzyna Potrykus,
University of Gdańsk, Poland

Reviewed by:
Frederico Gueiros Filho,
University of São Paulo, Brazil
David Raskin,
University of Houston, United States

****Correspondence:***
Christiane Wolz
christiane.wolz@uni-tuebingen.de

Specialty section:
This article was submitted to Microbial Physiology and Metabolism, a section of the journal Frontiers in Microbiology

Received: *24 June 2020*
Accepted: *25 August 2020*
Published: *18 September 2020*

Citation:
Salzer A, Keinhörster D, Kästle C, Kästle B and Wolz C (2020) Small Alarmone Synthetases RelP and RelQ of Staphylococcus aureus Are Involved in Biofilm Formation and Maintenance Under Cell Wall Stress Conditions. Front. Microbiol. 11:575882. doi: 10.3389/fmicb.2020.575882

INTRODUCTION

Biofilms are sessile microbial communities attached to surfaces and embedded in an extracellular matrix. Biofilm-forming staphylococci cause many device-related or chronic infections (Kong et al., 2006; O'Gara, 2007; Speziale et al., 2014; Mccarthy et al., 2015; Paharik and Horswill, 2016; Figueiredo et al., 2017; Moormeier and Bayles, 2017; Arciola et al., 2018; Otto, 2018). Depending on the composition of the biofilm matrix, staphylococcal biofilms are classified as *ica*-dependent or *ica*-independent (O'Gara, 2007). *Ica*-dependent biofilms are characterized by polysaccharide intercellular adhesin (PIA) also known as poly-N-acetyl glucosamine (PNAG), which is synthesized by enzymes encoded by the *icaADBC* operon (Götz, 2002). In *ica*-independent biofilms, proteins

(Speziale et al., 2014) and extracellular nucleic acids (eDNA) (Moormeier and Bayles, 2017) are the main matrix components. Biofilm formation is a three-step process that includes initial attachment to the surface, biofilm maturation due to intercellular aggregation and bacterial cell detachment. Detachment is mediated by the enzymatic degradation of matrix components by proteases, nucleases or a group of small amphiphilic α-helical peptides, known as phenol-soluble modulins (PSMs) (Otto, 2018).

The nature and extent of biofilms are highly variable between different strains and growth conditions. Mounting evidence suggests that subinhibitory antibiotic concentrations can promote biofilm formation (Rachid et al., 2000; Kaplan et al., 2012; Liu et al., 2018; Ranieri et al., 2018; Jin et al., 2020) by inducing eDNA release and thus shifting the composition of the biofilm matrix toward a higher eDNA content (Brunskill and Bayles, 1996; Mlynek et al., 2016; Schilcher et al., 2016). Multiple regulatory mechanisms are involved in the molecular switch from a planktonic to a biofilm lifestyle, such as transcriptional regulation via SarA, SaeRS, CodY or the quorum-sensing system Agr (Kong et al., 2006; Boles and Horswill, 2008; Beenken et al., 2010; Stenz et al., 2011; Cue et al., 2012; Mrak et al., 2012; Abdelhady et al., 2014; Atwood et al., 2015; Paharik and Horswill, 2016).

For several bacterial species, it has been demonstrated that the activation of the stringent response also affects biofilm formation (Balzer and Mclean, 2002; Taylor et al., 2002; Lemos et al., 2004; Aberg et al., 2006; Chavez De Paz et al., 2012; He et al., 2012; Sugisaki et al., 2013; De La Fuente-Nunez et al., 2014; Azriel et al., 2016; Xu et al., 2016; Diaz-Salazar et al., 2017; Liu et al., 2017; Colomer-Winter et al., 2018, 2019). The stringent response is characterized by the synthesis of guanosine-tetra-phosphate (ppGpp) and guanosine-penta-phosphate (pppGpp), collectively referred to as (p)ppGpp. The accumulation of (p)ppGpp affects gene expression, protein translation, enzyme activation and replication (Wu and Xie, 2009; Liu et al., 2015; Steinchen and Bange, 2016; Bennison et al., 2019). In many pathogenic bacteria, (p)ppGpp determines virulence or antibiotic tolerance/persistence (Dalebroux et al., 2010; Hauryliuk et al., 2015; Harms et al., 2016; Wood and Song, 2020). *Staphylococcus aureus* harbors three genes encoding (p)ppGpp synthetases, Rel, RelP, and RelQ (Wolz et al., 2010). The (p)ppGpp synthetase activity of the bifunctional Rel enzyme can be induced by tRNA-synthetase inhibitors such as mupirocin or serine-hydroxamate or by amino acid deprivation (Geiger et al., 2010). Rel usually shows strong hydrolase activity, which is essential to detoxify (p)ppGpp produced by RelP or RelQ (Gratani et al., 2018). RelP and RelQ only contain a synthase domain (Geiger et al., 2014) and are part of the VraRS cell wall stress regulon (Kuroda et al., 2003). Thus, they are transcriptionally induced (e.g., after vancomycin treatment) and contribute to tolerance toward cell wall-active antibiotics such as ampicillin or vancomycin (Geiger et al., 2014).

There is some evidence that the stringent response might trigger biofilm formation in *S. aureus* based on the observation that treatment with mupirocin (Sritharadol et al., 2018; Jin et al., 2020) or serine hydroxamate (De La Fuente-Nunez et al., 2014) results in increased biofilm formation. Moreover, the anti-biofilm peptides IDR-1018 and DJK-5 have been suggested to directly interact with (p)ppGpp, preventing its signaling effects and, thus, biofilm formation (De La Fuente-Nunez et al., 2014, 2015).

Here, we aimed to investigate the role of the stringent response mediated by the two small alarmone synthetases RelP and RelQ in biofilm formation. Under cell wall stress conditions induced by a subinhibitory vancomycin concentration, both RelP and RelQ are crucial for biofilm development. Moreover, (p)ppGpp synthesis prevents biofilm eradication by vancomycin. (p)ppGpp-mediated biofilm formation was shown to be independent of the major stringent response mediator CodY and the main biofilm regulator Agr. The anti-biofilm peptide DJK-5 could prevent biofilm formation of wild type and (p)ppGpp-defective mutants. However, the (p)ppGpp^0 strain is even more vulnerable to DJK-5. Thus, DKJ-5 does not act on biofilm formation via (p)ppGpp inhibition.

EXPERIMENTAL PROCEDURES

Bacterial Strains and Growth Conditions

The strains and plasmids used in this study are listed in **Supplementary Table S1**. For overnight cultures, the strains were grown with appropriate antibiotics (10 μg/ml erythromycin, 100 μg/ml spectinomycin) at 37°C and 200 rpm. For biofilm analyses, the following media were used: chemically defined medium (CDM; Pohl et al., 2009), tryptic soy broth (TSB, Oxoid) with 3% NaCl and 0.5% glucose, and BM2 glucose [0.4% (w/v) glucose, 62 mM potassium phosphate buffer, pH 7.0, 7 mM $(NH_4)_2SO_4$, 2 mM $MgSO_4$, 10 mM $FeSO_4$, 0.5% casamino acids] (De La Fuente-Nunez et al., 2014).

Strain Construction

For *relP* complementation, the pCG833 plasmid was constructed. The complete *relP* operon with its native promoter was amplified by PCR using the primers pCG833gibfor and pCG833gibrev and cloned via Gibson assembly into the BamHI-digested integration vector pCG3. The oligonucleotides used in these procedures are listed in **Supplementary Table S2**. Due to showing toxicity in *E. coli,* the plasmid was directly transformed into *S. aureus* Cyl316 by electroporation. The integration of the plasmid into the genome was verified by PCR using the scv1, scv21, pCG3intfor and pCG3intrev oligonucleotides followed by sequencing. The integrated plasmid was transduced into the target strains using Φ11 phage.

For *relQ* complementation, the pCG216 plasmid was constructed. *relQ* with its native promoter was amplified by PCR with the primers BamHrelQkompl-for and BamHrelQkomp-rev and ligated with the BamHI-digested pCG3 vector backbone. The plasmid was verified by PCR with relQdigfor and relQdigrev. The plasmid was transformed into Cyl316 and verified by PCR using the primers relQfor and relQrev for integration of the plasmid. The integrated plasmid was then transduced via phage Φ11 in the target strains.

codY and *agr* mutations were transduced into the (p)ppGpp strain using the lysates of RN4220-21 (Pohl et al., 2009) and RN6911 (Kornblum et al., 1990), respectively.

Colony-Forming Unit (CFU) and Minimal Inhibitory Concentration (MIC) Determination

For CFU measurements, biofilm-grown bacteria (24 h, 37°C) were resuspended by thorough pipetting. The bacterial suspension (biofilm resolved and planktonic) was serially diluted in phosphate-buffered saline (PBS), and 10 µl aliquots were spotted onto TSA plates for CFU determination. The MIC was determined by serial microdilution and *E*-tests.

Biofilm Assay

For the static biofilm assay, 1 ml medium was inoculated in a 24-well polystyrene cell culture plate (Greiner) to obtain an OD_{600} of 0.05. After 24 h of static incubation at 37°C, the wells were washed twice with 1 ml phosphate-buffered saline (PBS, pH 7.4, Gibco). The biofilm was dried at 40°C for 30 min. For biofilm staining, 200 µl of crystal violet (80 µg/ml in distilled water) was added to the wells, followed by incubation at RT for 5 min. The wells were then washed twice with 1 ml distilled water and dried at 40°C for 30 min. Biofilm quantification was performed by A_{600} determination (microplate reader, Tecan Infinite 200 and Tecan Spark). To account for the different distributions of biofilms within a single well, measurements were performed 100 times within one well, and the average was calculated. If required, a sub-inhibitory concentration of vancomycin (0.78 µg/ml) or 5 µg/ml of the anti-biofilm peptide DJK-5 (De La Fuente-Nunez et al., 2015) were added. To test the biofilm eradication capacity, preformed biofilms (37°C, 8 h) were incubated for an additional 16 h in the presence of vancomycin at concentrations ranging from 1 to 100 µg/ml. Biofilm staining and CFU determination were performed as described above.

Biofilm Composition

Biofilms were washed twice with PBS and treated with 1 mg/ml proteinase K (AppliChem, 37°C, 4 h), 0.1 mg/ml DNase (Sigma-Aldrich, 37°C, 4 h) or with 40 mM sodium periodate ($NaIO_4$) (24 h, 4°C). The biofilms were then washed twice with PBS, dried and stained as described above.

RESULTS

(p)ppGpp Synthetases Show no Significant Effect on Biofilm Formation Under Non-stress Conditions

Recently, it was proposed that the stringent response facilitates biofilm formation in several pathogens, including *S. aureus* (De La Fuente-Nunez et al., 2014). However, basal medium 2 (BM2) used in this study allowed hardly any *S. aureus* growth, resulting in a final OD_{600} below 1 after overnight growth. Therefore, we first analyzed the impact of (p)ppGpp on biofilm formation using different media. These media included tryptic soy broth (TSB) with the addition of 0.5% glucose and 3% NaCl, which is widely used for *S. aureus* biofilm analyses (Lade et al., 2019), and CDM (Pohl et al., 2009), used to define the stringent response phenotype in *S. aureus*. For discrimination between the Rel- and RelP/RelQ-mediated stringent response, a rel_{syn} mutant (mutation in the synthetase domain, leaving hydrolase activity unaltered), a *relP, relQ* double mutant and a $(p)ppGpp^0$ mutant in which all three synthetases were non-functional were included in the analysis. Independent of the (p)ppGpp synthetases, all strains showed the strongest biofilm formation in CDM. Interestingly, in the prototypic biofilm medium TSB, biofilm formation was lower than in CDM (**Figure 1A**). However, no significant difference in biofilm formation was observed between the different strains in either medium. In BM2, a trend toward a slightly higher biofilm-forming capacity in the wild type compared to the mutant strains was observed, indicating that under these nutrient-limited conditions, the stringent response might be slightly activated. Thus, (p)ppGpp synthetases have no or little influence on the biofilm formation ability under non-stressed conditions.

RelP and RelQ Regulate Biofilm Formation Under Cell Wall Stress

Subinhibitory concentrations of vancomycin were shown to transcriptionally activate *relP* and *relQ* (Geiger et al., 2014). We thus speculated that the vancomycin-induced stringent response may interfere with biofilm formation. The minimal inhibitory concentration (MIC) (1 µg/ml) of vancomycin in planktonically grown bacteria did not differ between the analyzed strains. At a subinhibitory concentration of vancomycin (0.78 µg/ml), the *relPQ* double mutant and the $(p)ppGpp^0$ mutant showed significantly reduced biofilm formation compared to the wild type and the rel_{syn} mutant (**Figures 1B,C**). Under vancomycin treatment, the wild type formed an almost uniform thick layer of biofilm. In contrast, the *relPQ* mutant and the $(p)ppGpp^0$ strain showed significantly decreased biofilm formation, with some cell aggregates remaining after the washing procedure (**Figures 1B,C**). The bacterial survival of the tested strains was not impaired by the subinhibitory concentrations of vancomycin (**Figure 1D**). Thus, the RelP- and/or RelQ-dependent changes in biofilm formation were not due to growth inhibition or bacterial killing.

RelP and RelQ Synergistically Affect Biofilm Formation

To determine which of the synthetases impacts biofilm formation under vancomycin conditions, single *relP* and *relQ* mutants were analyzed. Both *relP* and *relQ* contributed to biofilm formation in the presence of vancomycin. They act synergistically, since the *relPQ* double mutant showed the lowest biofilm formation (**Figure 2**). The *relPQ* double mutant phenotype could be complemented by the integration of either *relP* or *relQ* into the chromosome (**Figure 2**). Thus, the vancomycin-dependent induction of either *relP* or *relQ* is sufficient to sustain *S. aureus* biofilm formation under cell wall stress conditions.

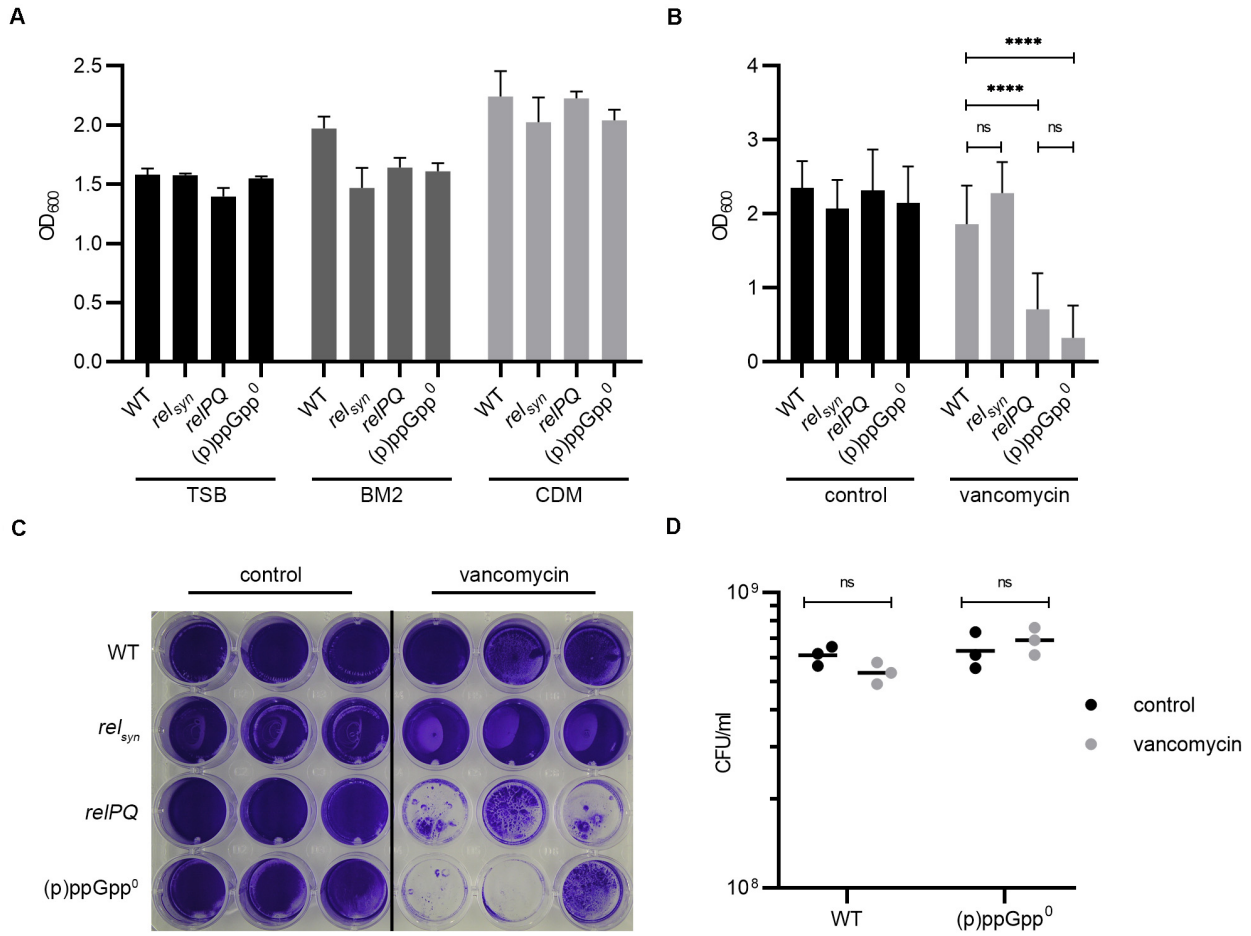

FIGURE 1 | (p)ppGpp synthases effect biofilm formation under cell wall stress conditions. **(A)** Biofilm formation in TSB (+3% NaCl, +0.5% glucose), BM2 and CDM after 24 h. **(B)** Biofilm formation under uninduced and vancomycin-stress (subinhibitory vancomycin 0.78 μg/ml) conditions in CDM after 24 h. Three separate experiments were performed with biological triplicates each. Error bars represent the standard deviation, statistical significance based on ordinary one-way ANOVA (ns: not significant, ****: $P < 0.0001$). **(C)** Representative plate stained with crystal violet. **(D)** CFU was determined from resolved biofilm and planktonic bacteria after 24 h of static incubation.

The Biofilm Composition Is Not Affected by the Stringent Response

The biofilm matrix is composed of PIA, proteins or eDNA (O'Gara, 2007; Paharik and Horswill, 2016). We analyzed which matrix components were involved in the observed RelP/Q-dependent biofilm alterations under vancomycin treatment. Preformed biofilms were treated with sodium periodate, proteinase K or DNase to selectively degrade PIA, proteins or eDNA matrix components, respectively (Seidl et al., 2008). Without vancomycin, the biofilms formed by the wild type or (p)ppGpp^0 stain were almost completely degraded by proteinase K and DNase treatment, whereas sodium periodate had no effect on the biofilm matrix (**Figures 3A,B**). To ensure that vancomycin does not impact the biofilm composition, we additionally examined the matrix components after vancomycin treatment. Again, the biofilms consisted almost exclusively of proteins, and eDNA and sodium periodate treatment did not degrade the biofilm matrix. Thus, under the conditions applied here, HG001 forms *ica*-independent biofilms, and the biofilm composition is not altered by the stringent response.

The Stringent Response Induces Biofilm Formation Independent of Agr and CodY

The quorum-sensing system Agr (especially the target genes *psm*) (Otto, 2018) and the transcriptional regulator CodY (Stenz et al., 2011) have been identified as key controllers of biofilm structure and detachment. (p)ppGpp synthesis results in the derepression of the CodY regulon and upregulation of Agr-dependent *psm* genes (Geiger et al., 2012). Thus, we hypothesized that Agr and/or CodY activity could interfere with the observed (p)ppGpp-dependent biofilm. However, the mutation of *agr* or *codY* did not impact biofilm formation (**Figure 4**). Thus, under our assay conditions, biofilm formation occurs independent of CodY or Agr. Strain specific effects of Agr (Yarwood et al., 2004) or CodY (Stenz et al., 2011) on biofilm formation were described previously.

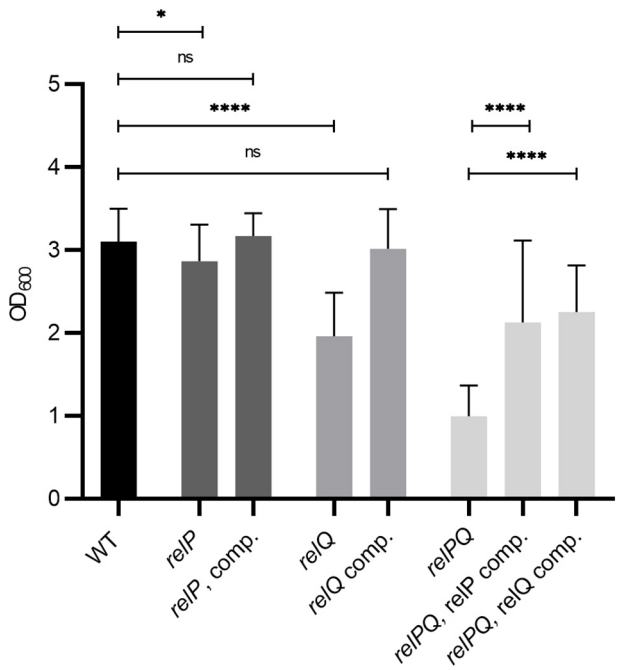

FIGURE 2 | RelP and RelQ affect biofilm formation synergistically. Biofilm formation under vancomycin-stress (0.78 μg/ml vancomycin) in CDM. Strains: HG001 wild type, *relP* and *relQ* single mutants, *relPQ* double mutant and complemented strains. Three separate experiments were performed with biological triplicates each. Error bars represent the standard deviation, statistical significance based on ordinary one-way ANOVA (ns: not significant, *: $P < 0.1$, ****: $P < 0.0001$).

(p)ppGpp Contributes to Biofilm Antibiotic Tolerance

Biofilms are normally more tolerant to high concentrations of antibiotics than planktonic cultures. We hypothesized that the stringent response contributes to biofilm antibiotic tolerance in *S. aureus*. Therefore, biofilm antibiotic tolerance was compared between the wild type and the isogenic (p)ppGpp^0 mutant. Preformed biofilms were exposed to increasing concentrations of vancomycin for 16 h. At the MIC (1 μg/ml for planktonically grown bacteria), vancomycin did not result in biofilm dispersal. However, at concentrations 10- and 100-fold higher than the MIC, the biofilm produced by the (p)ppGpp^0 strain was significantly reduced, whereas the biofilm produced by the wild type was more resistant to vancomycin treatment (**Figures 5A,B**). Thus, (p)ppGpp contributes to biofilm-related antibiotic tolerance.

The Anti-Biofilm Peptide DJK-5 Exerts Its Effects Independent of (p)ppGpp

Recently, the peptides IDR-1018 (De La Fuente-Nunez et al., 2014) and DJK-5 (De La Fuente-Nunez et al., 2015) were proposed to prevent biofilms due to the specific targeting of intracellular (p)ppGpp. If correct, the peptides are expected to inhibit biofilm formation under stringent conditions in the wild type but not in the pppGpp^0 background. We confirmed that DJK-5 interferes with biofilm formation in *S. aureus* (**Figures 6A,B**). However, without vancomycin treatment, biofilm formation by the wild type and pppGpp^0 strains was equally affected by DJK-5, indicating that the effect was independent of (p)ppGpp. The combination of a subinhibitory vancomycin concentration and DJK-5 resulted in the complete inhibition of biofilm formation in the pppGpp^0 strain. This can be explained by bacterial killing of the pppGpp^0 strain through the synergistic action of vancomycin and DJK-5 (**Figure 6C**). Thus, (p)ppGpp synthesis in the wild type obviously protects the strain from the action of DJK-5. These findings are in contrast to the assumption that the biofilm-inhibiting activity of DJK-5 is exerted via (p)ppGpp inhibition, as proposed by De La Fuente-Nunez et al. (2014, 2015).

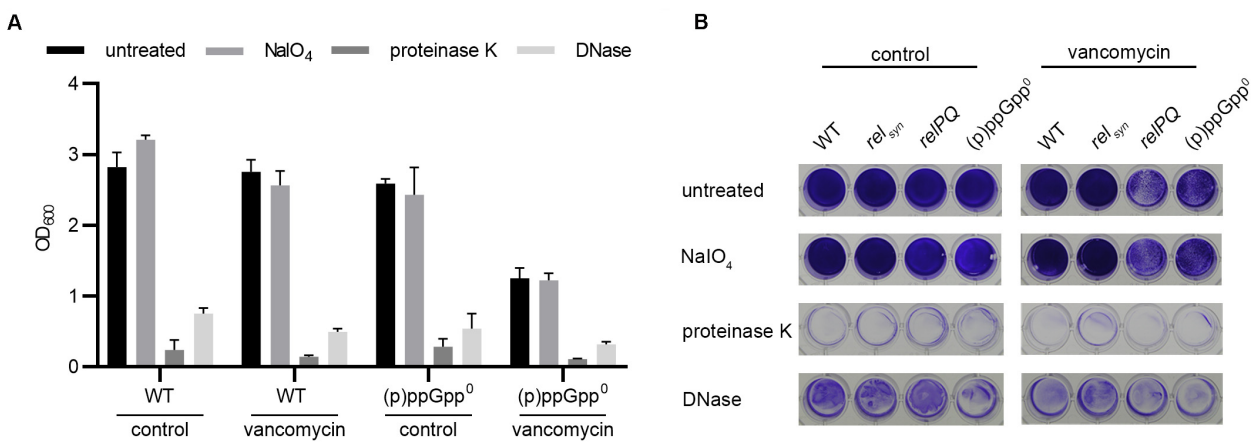

FIGURE 3 | Biofilm composition is not affected by (p)ppGpp. **(A)** Preformed biofilms of the wild type and the isogenic (p)ppGpp^0 strain were treated with either DNase or proteinase K for 4 h at 37°C or with sodium periodate for 24 h at 4°C. The remaining biofilm was stained with crystal violet and quantified by OD_{600} measurement. Three separate experiments were performed with biological triplicates each. Error bars represent the standard deviation. **(B)** Representative plate with wild type, *rel*$_{syn}$, *relPQ* and the (p)ppGpp^0 strain stained with crystal violet.

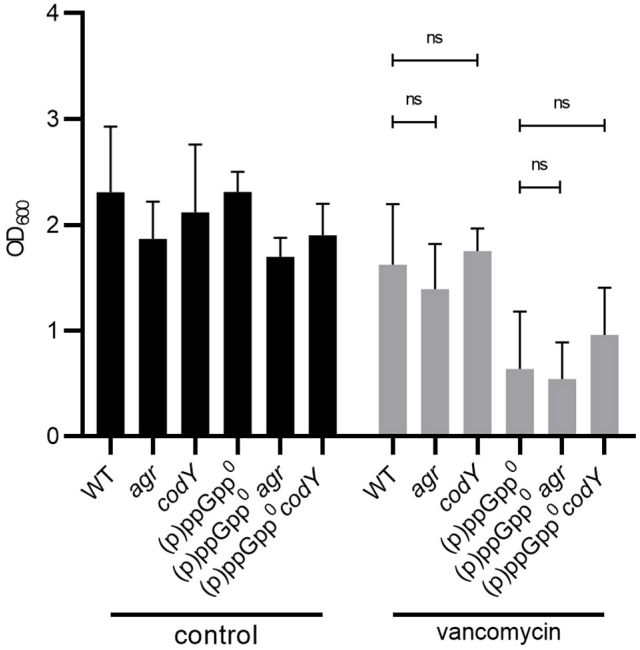

FIGURE 4 | Biofilm formation under stringent conditions is independent of CodY and Agr. Biofilm formation under non-stressed and vancomycin-stress (0.78 μg/ml vancomycin) in CDM, 24 h. Three separate experiments were performed with biological triplicates each. Error bars represent the standard deviation, statistical significance based on ordinary one-way ANOVA (ns: $P > 0.05$).

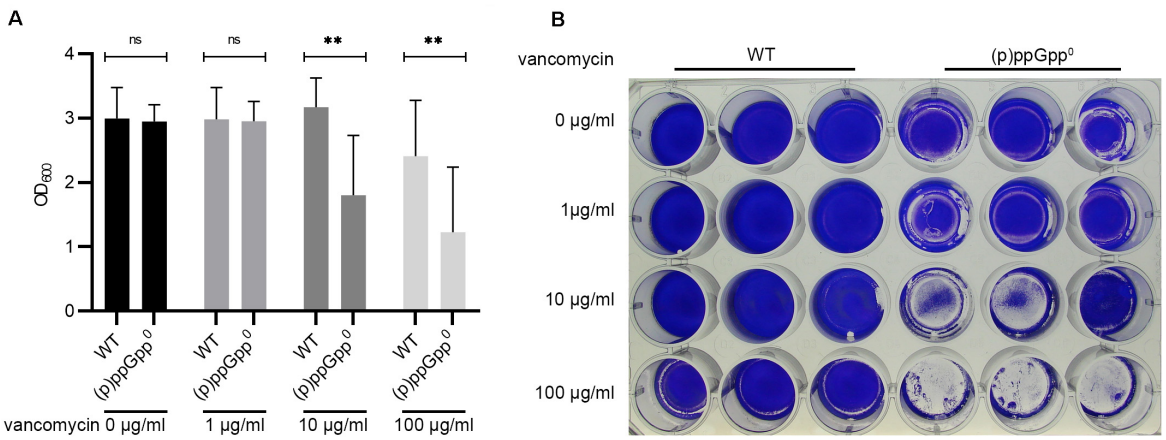

FIGURE 5 | (p)ppGpp contributes to biofilm related antibiotic tolerance. **(A)** Preformed biofilms (8 h) were exposed to increasing concentrations of vancomycin for 16 h. Three separate experiments were performed with biological triplicates each. Error bars represent the standard deviation, statistical significance based on ordinary one-way ANOVA (ns: not significant, **: $P < 0.01$). **(B)** Representative plate stained with crystal violet.

DISCUSSION

Here, we show that the small alarmone synthetases RelP and RelQ maintain the biofilm-forming capacity of *S. aureus* when exposed to subinhibitory concentrations of vancomycin. Both enzymes are part of the cell wall stress regulon and are transcriptionally induced by vancomycin (Geiger et al., 2014). They act synergistically, and the *relPQ* double mutant can be complemented via the chromosomal integration of either *relP* or *relQ*. Thus, the (p)ppGpp synthesis expected to occur upon vancomycin treatment supports biofilm growth, whereas without (p)ppGpp, no biofilms are formed in the presence of vancomycin. How (p)ppGpp promotes biofilm formation remains to be elucidated. (p)ppGpp results in an immediate decrease in intracellular GTP and derepression of the CodY regulon (Geiger et al., 2010). When CodY is loaded with GTP and/or branched-chain amino acids, it represses many metabolism-related genes, the Agr system and *ica* gene expression (Majerczyk et al., 2008; Pohl et al., 2009). The impact of CodY on biofilm formation is probably multifactorial and strain dependent

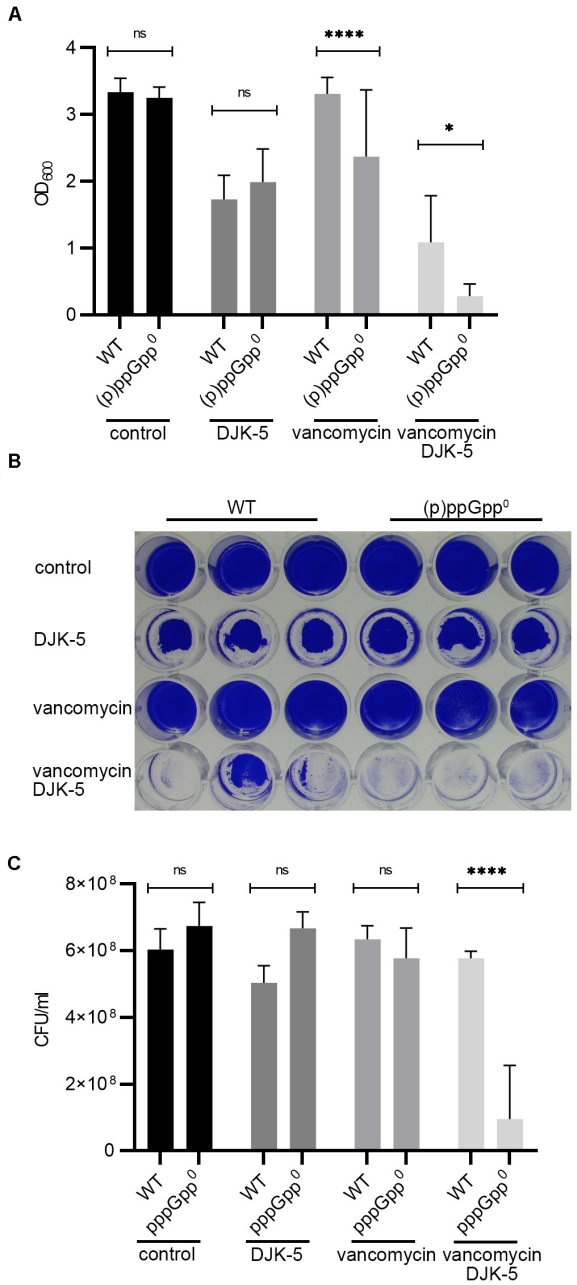

FIGURE 6 | DJK-5 interferes with biofilm formation under relaxed and stringent conditions. **(A)** Biofilms grown with or without vancomycin (0.78 μg/ml) and/or the anti-biofilm peptide DJK-5 (5 μg/ml) in CDM for 24 h. **(B)** Representative plate stained with crystal violet. **(C)** CFU of planktonic and biofilm bacteria determined in parallel after static growth for 24 h. Three separate experiments were performed with biological triplicates each. Error bars represent the standard deviation, statistical significance based on ordinary one-way ANOVA (ns: not significant, *: $P < 0.1$, ****: $P < 0.0001$).

(Stenz et al., 2011; Atwood et al., 2015). *codY* mutants have also been reported to aggregate, which can be linked with the interaction of PIA and eDNA on the bacterial surface (Mlynek et al., 2020). However, we can exclude the involvement of CodY regulation in the observed biofilm maintenance, since biofilm formation was not altered in a *codY*-negative background. Additionally, the Agr quorum-sensing system and, thus PSMs (which are strongly dependent on Agr activity), were excluded as mediators of the biofilm phenotype. Thus, the main mechanism for biofilm formation under vancomycin stress remains to be elucidated. (p)ppGpp dependent DNA-release by any of the lytic processes (e.g., autolysins, phages) likely contributes to biofilm formation. Recently, it was shown that mupirocin, a strong inducer of Rel-dependent (p)ppGpp synthesis, causes increased biofilm formation (Jin et al., 2020). Similar to our results, the mupirocin-induced biofilm forms independent of PIA and PSMs and is largely composed of eDNA. Thus, it is likely that the observed biofilm-inducing phenotype induced by mupirocin is similar to the vancomycin-dependent biofilm observed in our study. Jin et al. (2020) found that mupirocin upregulates *cidA*, encoding a holin-like protein, and that a *cidA* mutant shows reduced eDNA release. Thus, one may speculate that under our assay conditions, the (p)ppGpp-mediated activation of *cidA* may also contribute to (p)ppGpp-promoted biofilm formation.

The subinhibitory concentration of vancomycin applied in our standard biofilm assay did not affect bacterial viability, and the MIC in planktonically grown strains did not differ between the analyzed strains. When vancomycin was added to preformed biofilms, the biofilms were protected even at up to a concentration 100-fold higher than the MIC. It has been proposed that antibiotic tolerance and persister formation share common characteristics such as a slow- or non-growing phenotype (Waters et al., 2016). Here, we showed that biofilm tolerance is at least partly (p)ppGpp dependent, since biofilms of the pppGpp^0 strain were significantly better resolved in the presence of high vancomycin concentrations. This seems to contrast with recent results indicating that (p)ppGpp is not involved in persister formation in *S. aureus* (Conlon et al., 2016). However, the persister assays were performed under relaxed conditions, and thus, the role of (p)ppGpp might have been missed. Nevertheless, (p)ppGpp synthesis was previously shown to contribute to antibiotic tolerance in *S. aureus* (Geiger et al., 2014; Bryson et al., 2020) and other pathogens (Nguyen et al., 2011; Bernier et al., 2013). Nguyen et al. (2011) suggested that in *Pseudomonas aeruginosa,* the stringent response contributes to antimicrobial tolerance in biofilms by reducing oxidative stress. We recently showed that (p)ppGpp in *S. aureus* activates ROS-detoxifying systems (Horvatek et al., 2020), which might contribute to protection against vancomycin.

Due to the role of (p)ppGpp in biofilm formation and antibiotic tolerance, the (p)ppGpp synthesis pathway is thought to be a promising antimicrobial target. Anti-biofilm peptides have been reported to exert their activity via their ability to reduce (p)ppGpp levels in live bacterial cells (De La Fuente-Nunez et al., 2014, 2015). A direct mechanism of action involving the binding of (p)ppGpp and promotion of its intracellular degradation was suggested (De La Fuente-Nunez et al., 2015). We confirmed the biofilm-dissolving effect of DJK-5. However, this was clearly not due to the proposed interaction of the peptides with (p)ppGpp because an even stronger inhibitory effect of DJK-5 was observed in the (p)ppGpp^0 mutant. Interestingly, treatment

with DJK-5 and a subinhibitory vancomycin concentration resulted in significantly higher bacterial killing activity and biofilm inhibition in the (p)ppGpp^0 mutant than the wild type. Thus, (p)ppGpp protects against bactericidal DJK-5 activity. These findings are in good agreement with a recent re-analysis of the proposed antibiofilm peptide IDR-1018 in *E. coli* and *P. aeruginosa* (Andresen et al., 2016). Genetic disruption of the *relA* and *spoT* genes responsible for (p)ppGpp synthesis moderately sensitizes *E. coli* to IDR-1018, rather than protecting the bacterium (Andresen et al., 2016). While the IDR-1018 and DJK-5 peptides are potent antimicrobials, they do not specifically disrupt biofilms via a direct and specific interaction with the intracellular messenger nucleotide (p)ppGpp. Their alternative mode of action remains to be elucidated.

CONCLUSION

In conclusion, in *S. aureus,* (p)ppGpp supports biofilm formation under cell wall stress conditions and increases tolerance against vancomycin and the anti-biofilm peptide DJK-5.

DATA AVAILABILITY STATEMENT

The original contributions presented in the study are included in the article/**Supplementary Material**, further inquiries can be directed to the corresponding author.

AUTHOR CONTRIBUTIONS

All authors listed have made a substantial, direct and intellectual contribution to the work, and approved it for publication.

FUNDING

This work was supported by Grants from the "Deutsche Forschungsgemeinschaft": TR34/B1 and SPP1879 to CW; stipend from the "Deutsches Zentrum für Infektionsforschung" to CK and Infrastructural funding from Cluster of Excellence EXC 2124 "Controlling Microbes to Fight Infections".

ACKNOWLEDGMENTS

We thank Isabell Samp and Natalya Korn for excellent technical assistance. We also thank Robert Hancock for providing DJK5.

SUPPLEMENTARY MATERIAL

The Supplementary Material for this article can be found online at: https://www.frontiersin.org/articles/10.3389/fmicb.2020.575882/full#supplementary-material

REFERENCES

Abdelhady, W., Bayer, A. S., Seidl, K., Moormeier, D. E., Bayles, K. W., Cheung, A., et al. (2014). Impact of vancomycin on sarA-mediated biofilm formation: role in persistent endovascular infections due to methicillin-resistant *Staphylococcus aureus*. *J. Infect. Dis.* 209, 1231–1240. doi: 10.1093/infdis/jiu007

Aberg, A., Shingler, V., and Balsalobre, C. (2006). (p)ppGpp regulates type 1 fimbriation of *Escherichia coli* by modulating the expression of the site-specific recombinase FimB. *Mol. Microbiol.* 60, 1520–1533. doi: 10.1111/j.1365-2958.2006.05191.x

Andresen, L., Tenson, T., and Hauryliuk, V. (2016). Cationic bactericidal peptide 1018 does not specifically target the stringent response alarmone (p)ppGpp. *Sci. Rep.* 6:36549.

Arciola, C. R., Campoccia, D., and Montanaro, L. (2018). Implant infections: adhesion, biofilm formation and immune evasion. *Nat. Rev. Microbiol.* 16, 397–409. doi: 10.1038/s41579-018-0019-y

Atwood, D. N., Loughran, A. J., Courtney, A. P., Anthony, A. C., Meeker, D. G., Spencer, H. J., et al. (2015). Comparative impact of diverse regulatory loci on *Staphylococcus aureus* biofilm formation. *Microbiologyopen* 4, 436–451. doi: 10.1002/mbo3.250

Azriel, S., Goren, A., Rahav, G., and Gal-Mor, O. (2016). The stringent response regulator DksA is required for *Salmonella enterica* serovar Typhimurium growth in minimal medium, motility, biofilm formation, and intestinal colonization. *Infect. Immun.* 84, 375–384. doi: 10.1128/iai.01135-15

Balzer, G. J., and Mclean, R. J. (2002). The stringent response genes relA and spoT are important for *Escherichia* coil biofilms under slow-growth conditions. *Can. J. Microbiol.* 48, 675–680. doi: 10.1139/w02-060

Beenken, K. E., Mrak, L. N., Griffin, L. M., Zielinska, A. K., Shaw, L. N., Rice, K. C., et al. (2010). Epistatic relationships between sarA and agr in *Staphylococcus aureus* biofilm formation. *PLoS One* 5:e10790. doi: 10.1371/journal.pone.0010790

Bennison, J. B., Irving, S. E., and Corrigan, R. M. (2019). The impact of the stringent response on TRAFAC GTPases and prokaryotic ribosome assembly. *Cells* 8:1313. doi: 10.3390/cells8111313

Bernier, S. P., Lebeaux, D., Defrancesco, A. S., Valomon, A., Soubigou, G., Coppee, J. Y., et al. (2013). Starvation, together with the SOS response, mediates high biofilm-specific tolerance to the fluoroquinolone ofloxacin. *PLoS Genet.* 9:e1003144. doi: 10.1371/journal.pgen.1003144

Boles, B. R., and Horswill, A. R. (2008). Agr-mediated dispersal of *Staphylococcus aureus* biofilms. *PLoS Pathog.* 4:e1000052. doi: 10.1371/journal.ppat.1000052

Brunskill, E. W., and Bayles, K. W. (1996). Identification and molecular characterization of a putative regulatory locus that affects autolysis in *Staphylococcus aureus*. *J. Bacteriol.* 178, 611–618. doi: 10.1128/jb.178.3.611-618.1996

Bryson, D., Hettle, A. G., Boraston, A. B., and Hobbs, J. K. (2020). Clinical mutations that partially activate the stringent response confer multidrug tolerance in *Staphylococcus aureus*. *Antimicrob. Agents Chemother.* 64, e02103-19.

Chavez De Paz, L. E., Lemos, J. A., Wickstrom, C., and Sedgley, C. M. (2012). Role of (p)ppGpp in biofilm formation by *Enterococcus faecalis*. *Appl. Environ. Microbiol.* 78, 1627–1630. doi: 10.1128/aem.07036-11

Colomer-Winter, C., Flores-Mireles, A. L., Kundra, S., Hultgren, S. J., and Lemos, J. A. (2019). (p)ppGpp and CodY promote *Enterococcus faecalis* virulence in a murine model of catheter-associated urinary tract infection. *mSphere* 4, e00392-19.

Colomer-Winter, C., Gaca, A. O., Chuang-Smith, O. N., Lemos, J. A., and Frank, K. L. (2018). Basal levels of (p)ppGpp differentially affect the pathogenesis of infective endocarditis in *Enterococcus faecalis*. *Microbiology* 164, 1254–1265. doi: 10.1099/mic.0.000703

Conlon, B. P., Rowe, S. E., Gandt, A. B., Nuxoll, A. S., Donegan, N. P., Zalis, E. A., et al. (2016). Persister formation in *Staphylococcus aureus* is associated with ATP depletion. *Nat. Microbiol.* 1:16051.

Cue, D., Lei, M. G., and Lee, C. Y. (2012). Genetic regulation of the intercellular adhesion locus in staphylococci. *Front. Cell. Infect. Microbiol.* 2:38. doi: 10.3389/fcimb.2012.00038

Dalebroux, Z. D., Svensson, S. L., Gaynor, E. C., and Swanson, M. S. (2010). ppGpp conjures bacterial virulence. *Microbiol. Mol. Biol. Rev.* 74, 171–199. doi: 10.1128/mmbr.00046-09

De La Fuente-Nunez, C., Reffuveille, F., Haney, E. F., Straus, S. K., and Hancock, R. E. (2014). Broad-spectrum anti-biofilm peptide that targets a cellular stress response. *PLoS Pathog.* 10:e1004152. doi: 10.1371/journal.ppat.1004152

De La Fuente-Nunez, C., Reffuveille, F., Mansour, S. C., Reckseidler-Zenteno, S. L., Hernandez, D., Brackman, G., et al. (2015). D-enantiomeric peptides that eradicate wild-type and multidrug-resistant biofilms and protect against lethal *Pseudomonas aeruginosa* infections. *Chem. Biol.* 22, 196–205. doi: 10.1016/j.chembiol.2015.01.002

Diaz-Salazar, C., Calero, P., Espinosa-Portero, R., Jimenez-Fernandez, A., Wirebrand, L., Velasco-Dominguez, M. G., et al. (2017). The stringent response promotes biofilm dispersal in *Pseudomonas putida*. *Sci. Rep.* 7:18055.

Figueiredo, A. M. S., Ferreira, F. A., Beltrame, C. O., and Cortes, M. F. (2017). The role of biofilms in persistent infections and factors involved in ica-independent biofilm development and gene regulation in *Staphylococcus aureus*. *Crit. Rev. Microbiol.* 43, 602–620. doi: 10.1080/1040841x.2017.1282941

Geiger, T., Francois, P., Liebeke, M., Fraunholz, M., Goerke, C., Krismer, B., et al. (2012). The stringent response of *Staphylococcus aureus* and its impact on survival after phagocytosis through the induction of intracellular PSMs expression. *PLoS Pathog.* 8:e1003016. doi: 10.1371/journal.ppat.1003016

Geiger, T., Goerke, C., Fritz, M., Schafer, T., Ohlsen, K., Liebeke, M., et al. (2010). Role of the (p)ppGpp synthase RSH, a RelA/SpoT homolog, in stringent response and virulence of *Staphylococcus aureus*. *Infect. Immun.* 78, 1873–1883. doi: 10.1128/iai.01439-09

Geiger, T., Kastle, B., Gratani, F. L., Goerke, C., and Wolz, C. (2014). Two small (p)ppGpp synthases in *Staphylococcus aureus* mediate tolerance against cell envelope stress conditions. *J. Bacteriol.* 196, 894–902. doi: 10.1128/jb.01201-13

Götz, F. (2002). Staphylococcus and biofilms. *Mol. Microbiol.* 43, 1367–1378.

Gratani, F. L., Horvatek, P., Geiger, T., Borisova, M., Mayer, C., Grin, I., et al. (2018). Regulation of the opposing (p)ppGpp synthetase and hydrolase activities in a bifunctional RelA/SpoT homologue from *Staphylococcus aureus*. *PLoS Genet.* 14:e1007514. doi: 10.1371/journal.pgen.1007514

Harms, A., Maisonneuve, E., and Gerdes, K. (2016). Mechanisms of bacterial persistence during stress and antibiotic exposure. *Science* 354:aaf4268. doi: 10.1126/science.aaf4268

Hauryliuk, V., Atkinson, G. C., Murakami, K. S., Tenson, T., and Gerdes, K. (2015). Recent functional insights into the role of (p)ppGpp in bacterial physiology. *Nat. Rev. Microbiol.* 13, 298–309. doi: 10.1038/nrmicro3448

He, H., Cooper, J. N., Mishra, A., and Raskin, D. M. (2012). Stringent response regulation of biofilm formation in *Vibrio cholerae*. *J. Bacteriol.* 194, 2962–2972. doi: 10.1128/jb.00014-12

Horvatek, P., Hanna, A. M. F., Gratani, F. L., Keinhörster, D., Korn, N., Borisova, M., et al. (2020). Inducible expression of (pp) pGpp synthetases in *Staphylococcus aureus* is associated with activation of stress response genes. *biorxiv* [preprint]. doi: 10.1101/2020.04.25.059725

Jin, Y., Guo, Y., Zhan, Q., Shang, Y., Qu, D., and Yu, F. (2020). Sub-inhibitory concentrations of mupirocin stimulate *Staphylococcus aureus* biofilm formation by up-regulating cidA. *Antimicrob. Agents Chemother.* 64, e01912-19.

Kaplan, J. B., Izano, E. A., Gopal, P., Karwacki, M. T., Kim, S., Bose, J. L., et al. (2012). Low levels of beta-lactam antibiotics induce extracellular DNA release and biofilm formation in *Staphylococcus aureus*. *MBio* 3, e00198-12.

Kong, K. F., Vuong, C., and Otto, M. (2006). *Staphylococcus* quorum sensing in biofilm formation and infection. *Int. J. Med. Microbiol.* 296, 133–139. doi: 10.1016/j.ijmm.2006.01.042

Kornblum, J., Kreiswirth, B. N., Projan, S. J., Ross, H. F., and Novick, R. P. (1990). "Agr: a polycistronic locus regulating exoprotein synthesis in *Staphylococcus aureus*," in *Molecular Biology of the Staphylococci*, ed. R. P. Novick (New York, NY: VCH Publishers).

Kuroda, M., Kuroda, H., Oshima, T., Takeuchi, F., Mori, H., and Hiramatsu, K. (2003). Two-component system VraSR positively modulates the regulation of cell wall biosynthesis pathway in *Staphylococcus aureus*. *Mol. Microbiol.* 49, 807–821. doi: 10.1046/j.1365-2958.2003.03599.x

Lade, H., Park, J. H., Chung, S. H., Kim, I. H., Kim, J. M., Joo, H. S., et al. (2019). Biofilm formation by *Staphylococcus aureus* clinical isolates is differentially affected by glucose and sodium chloride supplemented culture media. *J. Clin. Med.* 8:1853. doi: 10.3390/jcm8111853

Lemos, J. A., Brown, T. A. Jr., and Burne, R. A. (2004). Effects of RelA on key virulence properties of planktonic and biofilm populations of *Streptococcus mutans*. *Infect. Immun.* 72, 1431–1440. doi: 10.1128/iai.72.3.1431-1440.2004

Liu, H., Xiao, Y., Nie, H., Huang, Q., and Chen, W. (2017). Influence of (p)ppGpp on biofilm regulation in *Pseudomonas putida* KT2440. *Microbiol. Res.* 204, 1–8. doi: 10.1016/j.micres.2017.07.003

Liu, J., Yang, L., Hou, Y., Soteyome, T., Zeng, B., Su, J., et al. (2018). Transcriptomics study on *Staphylococcus aureus* biofilm under low concentration of ampicillin. *Front. Microbiol.* 9:2413. doi: 10.3389/fmicb.2018.02413

Liu, K., Bittner, A. N., and Wang, J. D. (2015). Diversity in (p)ppGpp metabolism and effectors. *Curr. Opin. Microbiol.* 24, 72–79. doi: 10.1016/j.mib.2015.01.012

Majerczyk, C. D., Sadykov, M. R., Luong, T. T., Lee, C., Somerville, G. A., and Sonenshein, A. L. (2008). *Staphylococcus aureus* CodY negatively regulates virulence gene expression. *J. Bacteriol.* 190, 2257–2265. doi: 10.1128/jb.01545-07

Mccarthy, H., Rudkin, J. K., Black, N. S., Gallagher, L., O'neill, E., and O'gara, J. P. (2015). Methicillin resistance and the biofilm phenotype in *Staphylococcus aureus*. *Front. Cell Infect. Microbiol.* 5:1. doi: 10.3389/fcimb.2015.00001

Mlynek, K. D., Bulock, L. L., Stone, C. J., Curran, L. J., Sadykov, M. R., Bayles, K. W., et al. (2020). Genetic and biochemical analysis of CodY-mediated cell aggregation in *Staphylococcus aureus* reveals an interaction between extracellular DNA and polysaccharide in the extracellular matrix. *J. Bacteriol.* 202, e00593-19.

Mlynek, K. D., Callahan, M. T., Shimkevitch, A. V., Farmer, J. T., Endres, J. L., Marchand, M., et al. (2016). Effects of low-dose amoxicillin on *Staphylococcus aureus* USA300 biofilms. *Antimicrob. Agents Chemother.* 60, 2639–2651. doi: 10.1128/aac.02070-15

Moormeier, D. E., and Bayles, K. W. (2017). *Staphylococcus aureus* biofilm: a complex developmental organism. *Mol. Microbiol.* 104, 365–376.

Mrak, L. N., Zielinska, A. K., Beenken, K. E., Mrak, I. N., Atwood, D. N., Griffin, L. M., et al. (2012). saeRS and sarA act synergistically to repress protease production and promote biofilm formation in *Staphylococcus aureus*. *PLoS One* 7:e38453. doi: 10.1371/journal.pone.0038453

Nguyen, D., Joshi-Datar, A., Lepine, F., Bauerle, E., Olakanmi, O., Beer, K., et al. (2011). Active starvation responses mediate antibiotic tolerance in biofilms and nutrient-limited bacteria. *Science* 334, 982–986. doi: 10.1126/science.1211037

O'Gara, J. P. (2007). ica and beyond: biofilm mechanisms and regulation in *Staphylococcus epidermidis* and *Staphylococcus aureus*. *FEMS Microbiol. Lett.* 270, 179–188.

Otto, M. (2018). Staphylococcal biofilms. *Microbiol. Spectr.* 6:10.1128.

Paharik, A. E., and Horswill, A. R. (2016). The staphylococcal biofilm: adhesins, regulation, and host response. *Microbiol. Spectr.* 4:10.1128.

Pohl, K., Francois, P., Stenz, L., Schlink, F., Geiger, T., Herbert, S., et al. (2009). CodY in *Staphylococcus aureus*: a regulatory link between metabolism and virulence gene expression. *J. Bacteriol.* 191, 2953–2963. doi: 10.1128/jb.01492-08

Rachid, S., Ohlsen, K., Witte, W., Hacker, J., and Ziebuhr, W. (2000). Effect of subinhibitory antibiotic concentrations on polysaccharide intercellular adhesin expression in biofilm-forming *Staphylococcus epidermidis*. *Antimicrob. Agents Chemother.* 44, 3357–3363. doi: 10.1128/aac.44.12.3357-3363.2000

Ranieri, M. R., Whitchurch, C. B., and Burrows, L. L. (2018). Mechanisms of biofilm stimulation by subinhibitory concentrations of antimicrobials. *Curr. Opin. Microbiol.* 45, 164–169. doi: 10.1016/j.mib.2018.07.006

Schilcher, K., Andreoni, F., Dengler Haunreiter, V., Seidl, K., Hasse, B., and Zinkernagel, A. S. (2016). Modulation of *Staphylococcus aureus* biofilm matrix by subinhibitory concentrations of clindamycin. *Antimicrob. Agents Chemother.* 60, 5957–5967. doi: 10.1128/aac.00463-16

Seidl, K., Goerke, C., Wolz, C., Mack, D., Berger-Bachi, B., and Bischoff, M. (2008). *Staphylococcus aureus* CcpA affects biofilm formation. *Infect. Immun.* 76, 2044–2050. doi: 10.1128/iai.00035-08

Speziale, P., Pietrocola, G., Foster, T. J., and Geoghegan, J. A. (2014). Protein-based biofilm matrices in Staphylococci. *Front. Cell Infect. Microbiol.* 4:171. doi: 10.3389/fcimb.2014.00171

Sritharadol, R., Hamada, M., Kimura, S., Ishii, Y., Srichana, T., and Tateda, K. (2018). Mupirocin at subinhibitory concentrations induces biofilm formation in *Staphylococcus aureus*. *Microb. Drug Resist.* 24, 1249–1258. doi: 10.1089/mdr.2017.0290

Steinchen, W., and Bange, G. (2016). The magic dance of the alarmones (p)ppGpp. *Mol. Microbiol.* 101, 531–544. doi: 10.1111/mmi.13412

Stenz, L., Francois, P., Whiteson, K., Wolz, C., Linder, P., and Schrenzel, J. (2011). The CodY pleiotropic repressor controls virulence in gram-positive pathogens. *FEMS Immunol. Med. Microbiol.* 62, 123–139. doi: 10.1111/j.1574-695x.2011.00812.x

Sugisaki, K., Hanawa, T., Yonezawa, H., Osaki, T., Fukutomi, T., Kawakami, H., et al. (2013). Role of (p)ppGpp in biofilm formation and expression of filamentous structures in *Bordetella pertussis*. *Microbiology* 159, 1379–1389. doi: 10.1099/mic.0.066597-0

Taylor, C. M., Beresford, M., Epton, H. A., Sigee, D. C., Shama, G., Andrew, P. W., et al. (2002). *Listeria monocytogenes rel*A and *hpt* mutants are impaired in surface-attached growth and virulence. *J. Bacteriol.* 184, 621–628. doi: 10.1128/jb.184.3.621-628.2002

Waters, E. M., Rowe, S. E., O'gara, J. P., and Conlon, B. P. (2016). Convergence of *Staphylococcus aureus* persister and biofilm research: can biofilms be defined as communities of adherent persister cells? *PLoS Pathog.* 12:e1006012. doi: 10.1371/journal.ppat.1006012

Wolz, C., Geiger, T., and Goerke, C. (2010). The synthesis and function of the alarmone (p)ppGpp in firmicutes. *Int. J. Med. Microbiol.* 300, 142–147. doi: 10.1016/j.ijmm.2009.08.017

Wood, T. K., and Song, S. (2020). Forming and waking dormant cells: the ppGpp ribosome dimerization persister model. *Biofilm* 2:100018. doi: 10.1016/j.bioflm.2019.100018

Wu, J., and Xie, J. (2009). Magic spot: (p) ppGpp. *J. Cell Physiol.* 220, 297–302. doi: 10.1002/jcp.21797

Xu, X., Yu, H., Zhang, D., Xiong, J., Qiu, J., Xin, R., et al. (2016). Role of ppGpp in *Pseudomonas aeruginosa* acute pulmonary infection and virulence regulation. *Microbiol. Res.* 192, 84–95. doi: 10.1016/j.micres.2016.06.005

Yarwood, J. M., Bartels, D. J., Volper, E. M., and Greenberg, E. P. (2004). Quorum sensing in *Staphylococcus aureus* biofilms. *J. Bacteriol.* 186, 1838–1850. doi: 10.1128/jb.186.6.1838-1850.2004

Conflict of Interest: The authors declare that the research was conducted in the absence of any commercial or financial relationships that could be construed as a potential conflict of interest.

frontiers in Microbiology

MINI REVIEW
published: 25 September 2020
doi: 10.3389/fmicb.2020.01842

Regulation of (p)ppGpp and Its Homologs on Environmental Adaptation, Survival, and Pathogenicity of Streptococci

*Tengfei Zhang[1,2], Jiawen Zhu[1,3], Jiajia Xu[1], Huabin Shao[2] and Rui Zhou[1,4,5]**

[1]State Key Laboratory of Agricultural Microbiology, College of Veterinary Medicine, Huazhong Agricultural University, Wuhan, China, [2]Key Laboratory of Prevention and Control Agents for Animal Bacteriosis (Ministry of Agriculture and Rural Affairs), Institute of Animal and Veterinary Science, Hubei Academy of Agricultural Sciences, Wuhan, China, [3]Institute of Animal Sciences, Chengdu Academy of Agricultural and Forestry Sciences, Chengdu, China, [4]International Research Center for Animal Disease (Ministry of Science & Technology of China), Wuhan, China, [5]Cooperative Innovation Center of Sustainable Pig Production, Wuhan, China

Most streptococci are commensals, pathogens, or opportunistic pathogens for humans and animals. Therefore, it is important for streptococci to adapt to the various challenging environments of the host during the processes of infection or colonization, as well as to *in vitro* conditions for transmission. Stringent response (SR) is a special class of adaptive response induced by the signal molecules (p)ppGpp, which regulate several physiological aspects, such as long-term persistence, virulence, biofilm formation, and quorum sensing in bacteria. To understand the roles of SR in streptococci, the current mini-review gives a general overview on: (1) (p)ppGpp synthetases in the genus of *Streptococcus*, (2) the effects of (p)ppGpp on the physiological phenotypes, persistence, and pathogenicity of streptococci, (3) the transcriptional regulation induced by (p)ppGpp in streptococci, and (4) the link between (p)ppGpp and another nutrient regulatory protein CodY in streptococci.

Keywords: streptococci, (p)ppGpp synthetase, physiology, pathogenicity, regulation

OPEN ACCESS

Edited by:
Michael Cashel, Eunice Kennedy Shriver National Institute of Child Health and Human Development (NICHD), United States

Reviewed by:
Gert Bange, University of Marburg, Germany
Xiuzhu Dong, Chinese Academy of Sciences, China

***Correspondence:**
Rui Zhou
rzhou@mail.hzau.edu.cn

Specialty section:
This article was submitted to Microbial Physiology and Metabolism, a section of the journal Frontiers in Microbiology

Received: *26 May 2020*
Accepted: *14 July 2020*
Published: *25 September 2020*

Citation:
Zhang T, Zhu J, Xu J, Shao H and Zhou R (2020) Regulation of (p)ppGpp and Its Homologs on Environmental Adaptation, Survival, and Pathogenicity of Streptococci. Front. Microbiol. 11:1842. doi: 10.3389/fmicb.2020.01842

INTRODUCTION

Bacteria in the genus *Streptococcus* are Gram-positive cocci-shaped organisms organized in chains, and include *Streptococcus pyogenes*, *Streptococcus pneumoniae*, *Streptococcus mutans*, *Streptococcus suis*, *Streptococcus equisimilis*, *Streptococcus agalactiae*, and others. Most *Streptococcus* bacteria are human or animal commensals, pathogens, or opportunistic pathogens (Sader et al., 2006; Palmieri et al., 2011). During the processes of infection or colonization, bacteria suffer various challenges in stress and nutrient insufficiency in the host environment (Cotter and Hill, 2003; Kaspar et al., 2016). Typically, the blood plasma of the host provides abundant nutrients; in contrast, the interstitial tissue fluid contains much lower concentrations of free amino acids, glucose, free inorganic phosphates, and metal ions, which are required for the growth and persistence of streptococci (Zhang et al., 2012). In addition, streptococci may encounter more severe nutrient shortages when initially contacting the epidermal tissues or when persisting at a high cell density in the nidi of infection or inside host cells (Steiner and Malke, 2000). The stresses from the host also include high temperatures, an acidic environment, reactive oxygen species (ROS) stimulation, and other factors (Zeng et al., 2011; Abranches et al., 2018; Korir et al., 2018). Therefore, responses to these environmental cues are important factors with respect to colonization and disease progression.

Bacteria have evolved efficient stress response mechanisms to adapt to challenging environments. Among these responses, a special class of adaptive response induced by (p)ppGpp is called "stringent response (SR)" (Potrykus and Cashel, 2008). A wide array of physiological aspects, such as long-term persistence, virulence, biofilm formation, and quorum sensing, have been reported to be affected by (p)ppGpp (Taylor et al., 2002; Dahl et al., 2003; Kazmierczak et al., 2009; Geiger et al., 2010). Species of the *Streptococcus* genus are associated with public health and veterinary medicine concerns. An understanding of the SR of streptococci will facilitate the development of tools and means of controlling these pathogens. In this review, we provide information on (p)ppGpp synthetases and (p)ppGpp-mediated adaptation responses on the physiological phenotypes, persistence, and pathogenesis, as well as the global regulation in streptococci.

THE (p)ppGpp SYNTHETASES IN STREPTOCOCCI

Nearly 50 years ago, (p)ppGpp was discovered in *Escherichia coli* as two "magic spots." The (p)ppGpp is synthesized by RelA/SpoT homologous proteins (RSH) through transferring a pyrophosphate moiety from adenosine triphosphate (ATP) to guanosine diphosphate (GDP) or guanosine triphosphate (GTP; Cashel, 1974, 1975; Avarbock et al., 2000). Two RSH enzymes, RelA, and SpoT, are involved in (p)ppGpp synthesis in *E. coli*. The RelA has (p)ppGpp synthetic activity and is recognized to respond to amino acid starvation, and the SpoT has both synthetic and hydrolytic activities, and senses many other environmental stressors such as starvation of carbon, iron, phosphate, and fatty acids (Seyfzadeh et al., 1993; Vinella et al., 2005; Potrykus and Cashel, 2008).

In streptococci, the RSH protein is firstly characterized in *S. equisimilis* (Mechold et al., 1996), and subsequently identified in *Streptococcus rattus*, *S. pyogenes*, *S. mutans*, *S. pneumoniae*, *S. agalactiae*, and *S. suis* (Mechold et al., 1996; Whitehead et al., 1998; Lemos et al., 2007; Nascimento et al., 2008; Kazmierczak et al., 2009; Zhang et al., 2016). Different from *E. coli*, which encodes two long RSH-type synthetases (Steinchen and Bange, 2016), streptococci only contain a single long RSH-type synthetase, usually named Rel, such as Rel_{Smu} in *S. mutans* (Lemos et al., 2007), Rel_{Spn} in *S. pneumoniae* (Kazmierczak et al., 2009), Rel_{Spy} in *S. pyogenes*, Rel_{Ss} in *S. suis* (Whitehead et al., 1998; Zhang et al., 2016), and Rel_{Seq} in *S. equisimilis* (Mechold et al., 2002). The long RSH-type synthetase in streptococci contains four main domains (**Figure 1A**). The N-terminal region is the catalytic part acting as both hydrolysis and synthesis domains of (p)ppGpp, and the C-terminus is recognized as the regulatory region including TGS and ACT domains. According to the amino acid sequences, the long RSH-type synthetase in streptococci contains a RXKD motif, which is a conserved basic motif found in the bi-functional RSH proteins, and shows higher similarity with SpoT rather than the RelA of *E. coli* (**Figure 1B**; Sajish et al., 2007; Zhang et al., 2016). According to the function, the long RSH-type synthetase in streptococci has a strong (p)ppGpp hydrolytic activity and a weaker (p)ppGpp synthetic activity, also much like the SpoT in *E. coli* (Lemos et al., 2007; Sajish et al., 2007). Similar to the RelA in *E. coli*, (p)ppGpp synthetic activity of RSH in Gram-positive bacteria can be activated by interacting with idling ribosomes during amino acid starvation (Avarbock et al., 2000). However, the mechanisms of stringent responses induced by various stressors are different, but not well-characterized (Potrykus and Cashel, 2008).

Compared to *E. coli*, although one long RSH-type synthetase (like RelA in *E. coli*) which mainly has the (p)ppGpp synthetic activity is absent, some small/short proteins with only (p)ppGpp synthetic activity (Small Alarmone Synthetases, SASs) have been identified in *Firmicutes*, including most species of streptococci (**Figures 1A,C**; Lemos et al., 2007; Nanamiya et al., 2008). The numbers of SASs in streptococci vary in different species. For example, two SASs, RelP, and RelQ, are encoded in the genome of *S. mutans* (Lemos et al., 2007), and among them, RelP is the primary enzyme to synthesize (p)ppGpp during exponential growth and co-transcribed with a two-component signal transduction system (TCS) RelRS (Lemos et al., 2007), while *relQ* is in a four-gene operon, which is essential for persistence and pathogenesis of *S. mutans* (Kim et al., 2012). In contrast, we only found one SAS, RelQ, encoded in the genome of *S. suis*, and we verified that it can synthesize (p)ppGpp under amino acid starvation, but it is non-functional under glucose starvation (Zhang et al., 2016). A previous study has reported that the SAS of *Enterococcus faecalis* synthesizes a ppGpp molecule with more efficient function than pppGpp (Gaca et al., 2015), but this differentiation has not been studied in streptococci yet.

THE EFFECTS OF (p)ppGpp AND ITS HOMOLOGS ON STREPTOCOCCAL PHYSIOLOGY

(p)ppGpp, which acts as a signaling molecule to cause a stringent response, plays an important role in its environmental adaptation. This response is involved in several physiological phenotypes in streptococci, including growth and cell morphology (**Figure 2**). Usually, although the growth of *rsh* mutants is a little slower compared with wild-type strains, RSH is not essential under nutrient replete conditions in most of the streptococci (Lemos et al., 2007; Kazmierczak et al., 2009; Zhu et al., 2016). In contrast, (p)ppGpp is accumulated in wild-type cells under amino acid or glucose starvation, leading to the arrest of growth or slow growth, while RSH inactivated strains show a higher growth rate than wild-type strains at the beginning of starvation, but then evolve more quickly into the stationary phase (Kazmierczak et al., 2009; Zhu et al., 2016). These results suggest an energy saving process for long-term survival under starvation stress through a (p)ppGpp dependent regulation. In particular, the rel_{Spn} mutant of *S. pneumoniae* requires copper and manganese for growth, due to the lack of metabolic adjustment caused by (p)ppGpp (Kazmierczak et al., 2009). The rel_{Ss} is also identified as an upregulated gene under iron-restricted conditions using selective capture of transcribed sequences (SCOTS) in *S. suis* in our lab, which suggests the role of Rel_{Ss}/(p)ppGpp in iron regulation (Li et al., 2009).

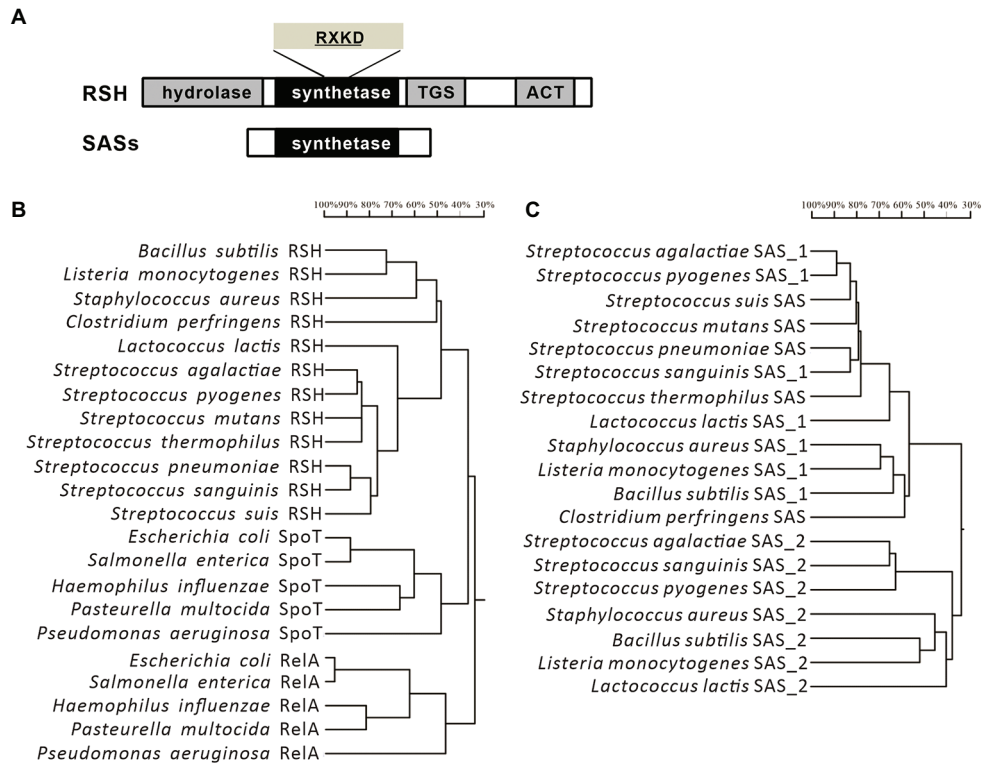

FIGURE 1 | Domain structures and phylogenetic trees of the long RelA/SpoT homologous proteins (RSH)-type synthetases and SASs from streptococci. **(A)** Domain structures of the long RSH-type synthetases and SASs from streptococci. **(B,C)** Phylogenetic trees of the long RSH-type synthetases and SASs from streptococci and other species of bacteria.

The chain arrangement of cells is the typical characteristic of streptococci, and we found that the chain length of *S. suis* becomes longer in the Δrel_{Ss}Δ*relQ* mutant (Zhu et al., 2016). The chain length of Δ*cpsA* is observed to be longer than the wild-type strain in *S. agalactiae* (Hanson et al., 2012). The increased chain length of Δrel_{Ss}Δ*relQ* mutant in *S. suis* may be attributed to the regulation of (p)ppGpp in the capsular biosynthesis cluster (*cps*) cluster, according to our transcriptome result (Zhang et al., 2016).

THE EFFECTS OF (p)ppGpp AND ITS HOMOLOGS ON PERSISTENCE AND PATHOGENICITY

Most species in streptococci are pathogens for animals and/or humans. Resistance to the unfavorable environment as well as innate and acquired immunity is the key point of persistence for pathogens. As a cariogenic bacterium, adaptation to acid stress is important for the persistence of *S. mutans* in the oral cavity, and biofilm formation is a major factor in this process (Wang et al., 2017). Biofilm formation of the Δrel_{Smu} mutant is reduced in *S. mutans*, and it is interesting that, although there is no difference in the acid sensitivities between the wild-type and Δrel_{Smu} strains grown in planktonic cultures, when cells are grown in biofilms, the Δrel_{Smu} mutants become more acid resistant than the wild-type strain, and it is directly related to increased glycolytic capacities (Lemos et al., 2004). We have confirmed that the survival of Δrel_{Ss}Δ*relQ* mutant of *S. suis* is also reduced in whole blood and it is more sensitive to phagocytosis of THP-1 monocytic leukemia cells (Zhu et al., 2016). One of the reasons may be that the increasing chain-length of the Δrel_{Ss}Δ*relQ* mutant make it more sensitive to complement deposition, and then to uptake by immune cells (Dalia and Weiser, 2011). Variation of RSH in *S. pneumoniae* is found to be associated with phenotypic differences based on a genomic diversity analysis, and researchers further confirmed that RSH confers higher resistance to neutrophil-killing (Li et al., 2015). In *S. agalactiae*, Rel_{Sag} is also essential to its survival in blood (Hooven et al., 2018). These results suggest the important roles of Rel_{Sag}/(p)ppGpp in the resistance to immune killing by the host.

As described above, (p)ppGpp/RSH confers a high resistance ability to streptococci, which aids in host persistence, and further facilitates the expression of virulence factors, as well as infection and pathogenesis. The rel_{Spn} of *S. pneumoniae* is proven to be a major virulence factor in a murine pneumonia/bacteremia model of infection (Hava and Camilli, 2002), and researchers further confirmed that Rel_{Spn} confers a higher competitiveness in mouse colonization (Li et al., 2015). It is noteworthy that the Δrel_{Spn} mutant is not only attenuated, but also the progression of infection

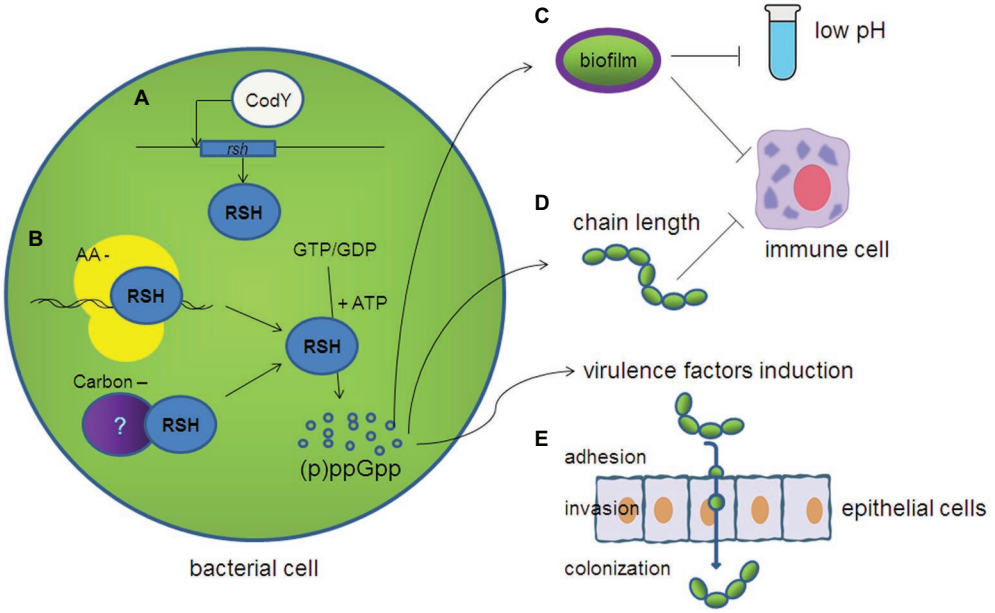

FIGURE 2 | Diagram depicting the various roles in streptococci affected by (p)ppGpp. **(A)** CodY can positively regulate the expression of *relSs* in *Streptococcus suis*. **(B)** (p)ppGpp synthesis can be triggered by the interaction of ribosomes and (p)ppGpp synthetase during amino acid starvation, but the trigger mechanisms under carbon starvation and other stress conditions are still unknown in streptococci. **(C)** (p)ppGpp contributes to the biofilm formation and confers the resistance to acid stress and immunocyte killing. **(D)** (p)ppGpp is essential for maintaining its chain length, which make it less likely to be uptaken by immune cells. **(E)** (p)ppGpp contributes to adhesion and invasion to the epithelial cells by regulating the expression of various virulence factors.

is dramatically altered. The first sign of disease is changed from lung to groin or in the abdomen and caused by the Δrel_{Spn} mutant. The change in infection progression may be due to the lack of stringent response, which plays an important role in the adaptation to the host's internal environment, including metabolic changes and the availability of metal ions (Kazmierczak et al., 2009). The intercellular communication between the ComX inducing peptide (XIP) and (p)ppGpp is also identified in *S. mutans*, and this cross-communication is involved in the virulence-related phenotypes, including modulated competence signaling and development (Kaspar et al., 2016). In our tests in *S. suis*, disruption of rel_{Ss} and *relQ* leads to decreased adhesive and invasive abilities to Hep-2 cells, and mouse infection experiments show that the Δrel_{Ss}Δ*relQ* mutant is attenuated and becomes easier to be cleaned up by the host (Zhu et al., 2016). In *S. agalactiae*, Rel_{Sag} is essential to its survival in blood, and the rel_{Sag} knockout strains demonstrated a decreased expression of beta-hemolysin, which is implicated in invasion of this pathogen (Hooven et al., 2018).

TRANSCRIPTIONAL REGULATION *VIA* (p)ppGpp DURING STRESS RESPONSE

In *E. coli*, accumulation of (p)ppGpp in concert with DksA, results in alterations in gene expression, owing to changes in RNAP activity during stress conditions (Potrykus and Cashel, 2008). In contrast to *E. coli*, the effect of (p)ppGpp on rRNA transcription is independent of DksA homologs in Gram-positive bacteria including streptococci (Kazmierczak et al., 2009). The (p)ppGpp synthesis seems to decrease rRNA transcription indirectly through depletion of the GTP pool, which is the initiating nucleotide in rRNA transcripts (Krasny and Gourse, 2004; Kazmierczak et al., 2009). The global regulation of RSH/(p)ppGpp has been investigated through the transcriptome analysis under amino acid and/or glucose starvation in some species of streptococci. The common and typical transcriptome feature is adjusting bio-macromolecular synthesis and transport in response to nutrient availability (Nascimento et al., 2008; Zhang et al., 2016). For example, during glucose starvation, lots of genes associated with protein synthesis, DNA replication and cell division were repressed, while carbohydrate transporters were upregulated under the control of Rel_{Ss}/(p)ppGpp in *S. suis* (Zhang et al., 2016). In *S. pneumoniae*, the majority of rel_{Spn}-dependent genes were associated with translation and ribosome structure, amino acid metabolism and transport, and DNA replication and repair (Kazmierczak et al., 2009). These regulations match the classical stringent response in *E. coli* and other bacteria (Potrykus and Cashel, 2008).

At the same time, the transcriptome of each *streptococcus* also shows their unique characteristics, which are associated with their adaptation and/or pathogenesis (**Figure 2**). In *S. pneumoniae*, Rel_{Spn} and (p)ppGpp amounts play wide-ranging homeostatic roles in pneumococcal physiology, and the operon encoding the major exotoxin pneumolysin is also under the regulation of (p)ppGpp/Rel_{Spn} (Kazmierczak et al., 2009). In *S. agalactiae*, the transcription levels of the arginine deiminase (*arcA*) pathway are decreased during stringent response, while arginine availability modulates the expression of cytotoxicity, which is important for virulence (Hooven et al., 2018).

During glucose starvation, besides the classic stringent response including inhibition of growth and related bio-macromolecular synthesis, the extended adaptive response includes inhibited glycolysis, and carbon catabolite repression (CCR)-mediated carbohydrate dependent metabolic switches in *S. suis* in our tests (Zhang et al., 2016). In addition, the expression of some virulence-related genes of *S. suis*, such as *cps*, glyceraldehyde-3-phosphate dehydrogenase (*gapdh*), fibronectin-binding protein (*fbps*), enolase (*eno*), *arcA*, VicR response regulator, type IV-like secretion system component (*virD*4), superoxide dismutase (*sod*), muramidase-released protein (*mrp*), extracellular protein factor (*epf*), and suilysin (*sly*) are downregulated in the Δrel_{Ss}Δ*relQ* mutant (Zhu et al., 2016). In *S. mutans*, Rel_{Smu} also plays a major role in the regulation of phenotypic traits, which are required for persistence and virulence expression of this oral pathogen (Nascimento et al., 2008). In addition, a 5-fold downregulation of *luxS* gene in the rel_{Smu} mutants suggests a link between the AI-2 quorum sensing and stringent response in *S. mutans* (Lemos et al., 2004).

Although (p)ppGpp is critical for the adaptation of starvation, a specific subset of genes involved in pathogenesis and metabolism were both modulated in the RSH mutants as well as in wild-type streptococci, suggesting the important roles of RSH-independent responses during stress conditions. For example, the regulation of a TCS *covRS*, exotoxin B regulator *ropB*, oligopeptide (*opp*), and dipeptide (*dpp*) permease systems, and *pepB* involved in the intracellular processing of oligopeptides, are RSH-independent during amino acid starvation in *S. pyogenes* (Steiner and Malke, 2000). In *S. mutans*, the expression of 50 genes involved in functions including energy metabolism and TCSs and others, is commonly affected in wild-type and Δrel_{Smu} mutant strains after Mupirocin treatment (Nascimento et al., 2008).

LINKAGE BETWEEN (p)ppGpp AND CODY IN STREPTOCOCCI

Amino acid starvation not only induces a stringent response but also CodY mediated regulation. Many common phenotypes can be regulated by both (p)ppGpp and CodY, suggesting their potential coordinated regulation (Geiger et al., 2010). GTP is not only the substrate of (p)ppGpp synthetases, but also acts as a ligand to enhance the affinity of CodY and its target DNA in lots of bacteria, like *Listeria monocytogenes*. Therefore, RelA-dependent (p)ppGpp accumulation reduces the GTP pool, and further leads to a reduction of DNA binding ability of CodY in cells (Geiger and Wolz, 2014). In the Δ*relA* mutant of *L. monocytogenes*, the increase in the GTP pool can reduce the expression of the CodY regulon and virulence, but deletion of *codY* from the Δ*relA* strain can restore its virulence (Bennett et al., 2007). In *Bacillus subtilis*, the lower GTP level imposed by stringent response also results in the de-repression of CodY target genes (Handke et al., 2008).

According to prior studies of *S. pyogenes* and *S. mutans*, GTP is not a co-factor for CodY. This may suggest that the linkage between (p)ppGpp and CodY is particularly different in streptococci (Malke et al., 2006; Lemos et al., 2008). We further confirmed this point in *S. suis* (Zhu et al., 2019). Of note, CodY can interact with the rel_{Ss} promoter in a GTP-independent manner and act as a transcriptional activator to positively regulate the rel_{Ss} expression in *S. suis* (**Figure 2**; Zhu et al., 2019). Real-time RT-PCR showed that the deletion of the *codY* gene in the Δrel_{Ss} strain further reduced the expression of virulence factors of *S. suis* compared to Δrel_{Ss}, and the lethality and colonization of the Δrel_{Ss}Δ*relQ*Δ*codY* strain in mice were significantly reduced as well. This may suggest a new interplay between the (p)ppGpp synthetase and CodY in *S. suis* (Zhu et al., 2019).

PERSPECTIVES

As the (p)ppGpp-mediated stringent response is critical in the adaptation, survival, and pathogenesis of streptococci, the (p)ppGpp related pathways are potential targets to control pathogens and their infections. To understand the mechanism of that, it is important to understand how the (p)ppGpp synthetase control the levels of (p)ppGpp pools in cells. This has been partly revealed in the model microorganism *E. coli*. The SpoT in *E. coli* interacts with the acyl carrier protein (ACP), the central cofactor of fatty acid synthesis, which is involved in sensing the signals of fatty acid starvation and carbon starvation (Battesti and Bouveret, 2006). Another study found that Rsd directly interacts with SpoT and stimulates its (p)ppGpp hydrolase activity (Lee et al., 2018). However, the stringent response in streptococci is sometimes different from that in *E. coli*, and largely unknown. For example, the interaction between RSH and ACP did not occur in *S. pneumoniae* (Battesti and Bouveret, 2009). Therefore, the sensing mechanisms of the stringent response during fatty acid and carbon starvation are still unknown in streptococci. Discovering the interactions between (p)ppGpp synthetases and stress receptors are key research points for future studies of streptococci. Another strategy for discovering antibacterial agents based on stringent response is the use of a (p)ppGpp analogue, such as Relacin, which can reduce (p)ppGpp production (Wexselblatt et al., 2012, 2013). The inhibition function of Relacin has been verified in *Bacillus* (Wexselblatt et al., 2012); whether it is functional in streptococci is still unknown.

AUTHOR CONTRIBUTIONS

TZ and RZ conceived the study and wrote the manuscript. JZ and JX provided the figures. HS revised the manuscript. All authors contributed to the article and approved the submitted version.

FUNDING

This work was supported by the National Key Research and Development Plans (2017YFD0500201), National Natural Science Foundation of China (31502094), and Hubei Province Natural Science Foundation for Innovative Research Groups (2016CFA015).

REFERENCES

Abranches, J., Zeng, L., Kajfasz, J. K., Palmer, S. R., Chakraborty, B., Wen, Z. T., et al. (2018). Biology of oral streptococci. *Microbiol. Spectr.* 6, 426–434. doi: 10.1128/microbiolspec.GPP3-0042-2018

Avarbock, D., Avarbock, A., and Rubin, H. (2000). Differential regulation of opposing RelMtb activities by the aminoacylation state of a tRNA.ribosome. mRNA.RelMtb complex. *Biochemistry* 39, 11640–11648. doi: 10.1021/bi001256k

Battesti, A., and Bouveret, E. (2006). Acyl carrier protein/SpoT interaction, the switch linking SpoT-dependent stress response to fatty acid metabolism. *Mol. Microbiol.* 62, 1048–1063. doi: 10.1111/j.1365-2958.2006.05442.x

Battesti, A., and Bouveret, E. (2009). Bacteria possessing two RelA/SpoT-like proteins have evolved a specific stringent response involving the acyl carrier protein-SpoT interaction. *J. Bacteriol.* 191, 616–624. doi: 10.1128/JB.01195-08

Bennett, H. J., Pearce, D. M., Glenn, S., Taylor, C. M., Kuhn, M., Sonenshein, A. L., et al. (2007). Characterization of relA and codY mutants of *Listeria monocytogenes*: identification of the CodY regulon and its role in virulence. *Mol. Microbiol.* 63, 1453–1467. doi: 10.1111/j.1365-2958.2007.05597.x

Cashel, M. (1974). Preparation of guanosine tetraphosphate (ppGpp) and guanosine pentaphosphate (pppGpp) from *Escherichia coli* ribosomes. *Anal. Biochem.* 57, 100–107. doi: 10.1016/0003-2697(74)90056-6

Cashel, M. (1975). Regulation of bacterial ppGpp and pppGpp. *Annu. Rev. Microbiol.* 29, 301–318. doi: 10.1146/annurev.mi.29.100175.001505

Cotter, P. D., and Hill, C. (2003). Surviving the acid test: responses of gram-positive bacteria to low pH. *Microbiol. Mol. Biol. Rev.* 67, 429–453. doi: 10.1128/mmbr.67.3.429-453.2003

Dahl, J. L., Kraus, C. N., Boshoff, H. I., Doan, B., Foley, K., Avarbock, D., et al. (2003). The role of RelMtb-mediated adaptation to stationary phase in long-term persistence of *Mycobacterium tuberculosis* in mice. *Proc. Natl. Acad. Sci. U. S. A.* 100, 10026–10031. doi: 10.1073/pnas.1631248100

Dalia, A. B., and Weiser, J. N. (2011). Minimization of bacterial size allows for complement evasion and is overcome by the agglutinating effect of antibody. *Cell Host Microbe* 10, 486–496. doi: 10.1016/j.chom.2011.09.009

Gaca, A. O., Kudrin, P., Colomer-Winter, C., Beljantseva, J., Liu, K., Anderson, B., et al. (2015). From (p)ppGpp to (pp)pGpp: characterization of regulatory effects of pGpp synthesized by the small alarmone synthetase of *Enterococcus faecalis*. *J. Bacteriol.* 197, 2908–2919. doi: 10.1128/JB.00324-15

Geiger, T., Goerke, C., Fritz, M., Schafer, T., Ohlsen, K., Liebeke, M., et al. (2010). Role of the (p)ppGpp synthase RSH, a RelA/SpoT homolog, in stringent response and virulence of *Staphylococcus aureus*. *Infect. Immun.* 78, 1873–1883. doi: 10.1128/IAI.01439-09

Geiger, T., and Wolz, C. (2014). Intersection of the stringent response and the CodY regulon in low GC Gram-positive bacteria. *Int. J. Med. Microbiol.* 304, 150–155. doi: 10.1016/j.ijmm.2013.11.013

Handke, L. D., Shivers, R. P., and Sonenshein, A. L. (2008). Interaction of *Bacillus subtilis* CodY with GTP. *J. Bacteriol.* 190, 798–806. doi: 10.1128/JB.01115-07

Hanson, B. R., Runft, D. L., Streeter, C., Kumar, A., Carion, T. W., and Neely, M. N. (2012). Functional analysis of the CpsA protein of *Streptococcus agalactiae*. *J. Bacteriol.* 194, 1668–1678. doi: 10.1128/JB.06373-11

Hava, D. L., and Camilli, A. (2002). Large-scale identification of serotype 4 *Streptococcus pneumoniae* virulence factors. *Mol. Microbiol.* 45, 1389–1406. doi: 10.1046/j.1365-2958.2002.t01-1-03106.x

Hooven, T. A., Catomeris, A. J., Bonakdar, M., Tallon, L. J., Santana-Cruz, I., Ott, S., et al. (2018). The *Streptococcus agalactiae* stringent response enhances virulence and persistence in human blood. *Infect. Immun.* 86, e00612–e00617. doi: 10.1128/IAI.00612-17

Kaspar, J., Kim, J. N., Ahn, S. J., and Burne, R. A. (2016). An essential role for (p)ppGpp in the integration of stress tolerance, peptide signaling, and competence development in *Streptococcus mutans*. *Front. Microbiol.* 7:1162. doi: 10.3389/fmicb.2016.01162

Kazmierczak, K. M., Wayne, K. J., Rechtsteiner, A., and Winkler, M. E. (2009). Roles of rel(Spn) in stringent response, global regulation and virulence of serotype 2 *Streptococcus pneumoniae* D39. *Mol. Microbiol.* 72, 590–611. doi: 10.1111/j.1365-2958.2009.06669.x

Kim, J. N., Ahn, S. J., Seaton, K., Garrett, S., and Burne, R. A. (2012). Transcriptional organization and physiological contributions of the relQ operon of *Streptococcus mutans*. *J. Bacteriol.* 194, 1968–1978. doi: 10.1128/JB.00037-12

Korir, M. L., Flaherty, R. A., Rogers, L. M., Gaddy, J. A., Aronoff, D. M., and Manning, S. D. (2018). Investigation of the role that NADH peroxidase plays in oxidative stress survival in Group B *Streptococcus*. *Front. Microbiol.* 9:2786. doi: 10.3389/fmicb.2018.02786

Krasny, L., and Gourse, R. L. (2004). An alternative strategy for bacterial ribosome synthesis: *Bacillus subtilis* rRNA transcription regulation. *EMBO J.* 23, 4473–4483. doi: 10.1038/sj.emboj.7600423

Lee, J. W., Park, Y. H., and Seok, Y. J. (2018). Rsd balances (p)ppGpp level by stimulating the hydrolase activity of SpoT during carbon source downshift in *Escherichia coli*. *Proc. Natl. Acad. Sci. U. S. A.* 115, E6845–E6854. doi: 10.1073/pnas.1722514115

Lemos, J. A., Brown, T. A. Jr., and Burne, R. A. (2004). Effects of RelA on key virulence properties of planktonic and biofilm populations of *Streptococcus mutans*. *Infect. Immun.* 72, 1431–1440. doi: 10.1128/iai.72.3.1431-1440.2004

Lemos, J. A., Lin, V. K., Nascimento, M. M., Abranches, J., and Burne, R. A. (2007). Three gene products govern (p)ppGpp production by *Streptococcus mutans*. *Mol. Microbiol.* 65, 1568–1581. doi: 10.1111/j.1365-2958.2007.05897.x

Lemos, J. A., Nascimento, M. M., Lin, V. K., Abranches, J., and Burne, R. A. (2008). Global regulation by (p)ppGpp and CodY in *Streptococcus mutans*. *J. Bacteriol.* 190, 5291–5299. doi: 10.1128/JB.00288-08

Li, Y., Croucher, N. J., Thompson, C. M., Trzcinski, K., Hanage, W. P., and Lipsitch, M. (2015). Identification of pneumococcal colonization determinants in the stringent response pathway facilitated by genomic diversity. *BMC Genomics* 16:369. doi: 10.1186/s12864-015-1573-6

Li, W., Liu, L., Chen, H., and Zhou, R. (2009). Identification of *Streptococcus suis* genes preferentially expressed under iron starvation by selective capture of transcribed sequences. *FEMS Microbiol. Lett.* 292, 123–133. doi: 10.1111/j.1574-6968.2008.01476.x

Malke, H., Steiner, K., Mcshan, W. M., and Ferretti, J. J. (2006). Linking the nutritional status of *Streptococcus pyogenes* to alteration of transcriptional gene expression: the action of CodY and RelA. *Int. J. Med. Microbiol.* 296, 259–275. doi: 10.1016/j.ijmm.2005.11.008

Mechold, U., Cashel, M., Steiner, K., Gentry, D., and Malke, H. (1996). Functional analysis of a relA/spoT gene homolog from *Streptococcus equisimilis*. *J. Bacteriol.* 178, 1401–1411. doi: 10.1128/jb.178.5.1401-1411.1996

Mechold, U., Murphy, H., Brown, L., and Cashel, M. (2002). Intramolecular regulation of the opposing (p)ppGpp catalytic activities of Rel(Seq), the Rel/Spo enzyme from *Streptococcus equisimilis*. *J. Bacteriol.* 184, 2878–2888. doi: 10.1128/jb.184.11.2878-2888.2002

Nanamiya, H., Kasai, K., Nozawa, A., Yun, C. S., Narisawa, T., Murakami, K., et al. (2008). Identification and functional analysis of novel (p)ppGpp synthetase genes in *Bacillus subtilis*. *Mol. Microbiol.* 67, 291–304. doi: 10.1111/j.1365-2958.2007.06018.x

Nascimento, M. M., Lemos, J. A., Abranches, J., Lin, V. K., and Burne, R. A. (2008). Role of RelA of *Streptococcus mutans* in global control of gene expression. *J. Bacteriol.* 190, 28–36. doi: 10.1128/JB.01395-07

Palmieri, C., Varaldo, P. E., and Facinelli, B. (2011). *Streptococcus suis*, an emerging drug-resistant animal and human pathogen. *Front. Microbiol.* 2:235. doi: 10.3389/fmicb.2011.00235

Potrykus, K., and Cashel, M. (2008). (p)ppGpp: still magical? *Annu. Rev. Microbiol.* 62, 35–51. doi: 10.1146/annurev.micro.62.081307.162903

Sader, H. S., Streit, J. M., Fritsche, T. R., and Jones, R. N. (2006). Antimicrobial susceptibility of gram-positive bacteria isolated from European medical centres: results of the Daptomycin surveillance programme (2002-2004). *Clin. Microbiol. Infect.* 12, 844–852. doi: 10.1111/j.1469-0691.2006.01550.x

Sajish, M., Tiwari, D., Rananaware, D., Nandicoori, V. K., and Prakash, B. (2007). A charge reversal differentiates (p)ppGpp synthesis by monofunctional and bifunctional Rel proteins. *J. Biol. Chem.* 282, 34977–34983. doi: 10.1074/jbc.M704828200

Seyfzadeh, M., Keener, J., and Nomura, M. (1993). spoT-dependent accumulation of guanosine tetraphosphate in response to fatty acid starvation in *Escherichia coli*. *Proc. Natl. Acad. Sci. U. S. A.* 90, 11004–11008. doi: 10.1073/pnas.90.23.11004

Steinchen, W., and Bange, G. (2016). The magic dance of the alarmones (p)ppGpp. *Mol. Microbiol.* 101, 531–544. doi: 10.1111/mmi.13412

Steiner, K., and Malke, H. (2000). Life in protein-rich environments: the relA-independent response of *Streptococcus pyogenes* to amino acid starvation. *Mol. Microbiol.* 38, 1004–1016. doi: 10.1046/j.1365-2958.2000.02203.x

Taylor, C. M., Beresford, M., Epton, H. A., Sigee, D. C., Shama, G., Andrew, P. W., et al. (2002). *Listeria monocytogenes* relA and hpt mutants are impaired in surface-attached growth and virulence. *J. Bacteriol.* 184, 621–628. doi: 10.1128/jb.184.3.621-628.2002

Vinella, D., Albrecht, C., Cashel, M., and D'ari, R. (2005). Iron limitation induces SpoT-dependent accumulation of ppGpp in *Escherichia coli*. *Mol. Microbiol.* 56, 958–970. doi: 10.1111/j.1365-2958.2005.04601.x

Wang, X., Li, X., and Ling, J. (2017). *Streptococcus gordonii* LuxS/autoinducer-2 quorum-sensing system modulates the dual-species biofilm formation with *Streptococcus mutans*. *J. Basic Microbiol.* 57, 605–616. doi: 10.1002/jobm.201700010

Wexselblatt, E., Kaspy, I., Glaser, G., Katzhendler, J., and Yavin, E. (2013). Design, synthesis and structure-activity relationship of novel Relacin analogs as inhibitors of Rel proteins. *Eur. J. Med. Chem.* 70, 497–504. doi: 10.1016/j.ejmech.2013.10.036

Wexselblatt, E., Oppenheimer-Shaanan, Y., Kaspy, I., London, N., Schueler-Furman, O., Yavin, E., et al. (2012). Relacin, a novel antibacterial agent targeting the stringent response. *PLoS Pathog.* 8:e1002925. doi: 10.1371/journal.ppat.1002925

Whitehead, K. E., Webber, G. M., and England, R. R. (1998). Accumulation of ppGpp in *Streptococcus pyogenes* and *Streptococcus rattus* following amino acid starvation. *FEMS Microbiol. Lett.* 159, 21–26. doi: 10.1111/j.1574-6968.1998.tb12836.x

Zeng, X., Yuan, Y., Wei, Y., Jiang, H., Zheng, Y., Guo, Z., et al. (2011). Microarray analysis of temperature-induced transcriptome of *Streptococcus suis* serotype 2. *Vector Borne Zoonotic Dis.* 11, 215–221. doi: 10.1089/vbz.2009.0225

Zhang, T., Ding, Y., Li, T., Wan, Y., Li, W., Chen, H., et al. (2012). A fur-like protein PerR regulates two oxidative stress response related operons dpr and metQIN in *Streptococcus suis*. *BMC Microbiol.* 12:85. doi: 10.1186/1471-2180-12-85

Zhang, T., Zhu, J., Wei, S., Luo, Q., Li, L., Li, S., et al. (2016). The roles of RelA/(p)ppGpp in glucose-starvation induced adaptive response in the zoonotic *Streptococcus suis*. *Sci. Rep.* 6:27169. doi: 10.1038/srep27169

Zhu, J., Zhang, T., Su, Z., Feng, L., Liu, H., Xu, Z., et al. (2019). Co-regulation of CodY and (p)ppGpp synthetases on morphology and pathogenesis of *Streptococcus suis*. *Microbiol. Res.* 223-225, 88–98. doi: 10.1016/j.micres.2019.04.001

Zhu, J., Zhang, T., Su, Z., Li, L., Wang, D., Xiao, R., et al. (2016). (p)ppGpp synthetases regulate the pathogenesis of zoonotic *Streptococcus suis*. *Microbiol. Res.* 191, 1–11. doi: 10.1016/j.micres.2016.05.007

Conflict of Interest: The authors declare that the research was conducted in the absence of any commercial or financial relationships that could be construed as a potential conflict of interest.

frontiers in Microbiology

REVIEW
published: 09 October 2020
doi: 10.3389/fmicb.2020.592718

Possible Roles for Basal Levels of (p)ppGpp: Growth Efficiency Vs. Surviving Stress

*Llorenç Fernández-Coll and Michael Cashel**

Intramural Research Program, Eunice Kennedy Shriver NICHD, NIH, Bethesda, MD, United States

Two (p)ppGpp nucleotide analogs, sometimes abbreviated simply as ppGpp, are widespread in bacteria and plants. Their name alarmone reflects a view of their function as intracellular hormone-like protective alarms that can increase a 100-fold when sensing any of an array of physical or nutritional dangers, such as abrupt starvation, that trigger lifesaving adjustments of global gene expression and physiology. The diversity of mechanisms for stress-specific adjustments of this sort is large and further compounded by almost infinite microbial diversity. The central question raised by this review is whether the small basal levels of (p)ppGpp functioning during balanced growth serve very different roles than alarmone-like functions. Recent discoveries that abrupt amino acid starvation of *Escherichia coli*, accompanied by very high levels of ppGpp, occasion surprising instabilities of transfer RNA (tRNA), ribosomal RNA (rRNA), and ribosomes raises new questions. Is this destabilization, a mode of regulation linearly related to (p)ppGpp over the entire continuum of (p)ppGpp levels, including balanced growth? Are regulatory mechanisms exerted by basal (p)ppGpp levels fundamentally different than for high levels? There is evidence from studies of other organisms suggesting special regulatory features of basal levels compared to burst of (p)ppGpp. Those differences seem to be important even during bacterial infection, suggesting that unbalancing the basal levels of (p)ppGpp may become a future antibacterial treatment. A simile for this possible functional duality is that (p)ppGpp acts like a car's brake, able to stop to avoid crashes as well as to slow down to drive safely.

Keywords: (p)ppGpp, balanced growth, overt starvation, basal levels, destabilized stable RNA

OPEN ACCESS

Edited by:
Hans-Georg Koch,
University of Freiburg, Germany

Reviewed by:
Mohammad Roghanian,
Umeå University, Sweden
Christiane Wolz,
University of Tübingen, Germany
Kürşad Turgay,
Max-Planck-Gesellschaft (MPG), Germany

***Correspondence:**
Michael Cashel
cashelm@mail.nih.gov

Specialty section:
This article was submitted to Microbial Physiology and Metabolism, a section of the journal Frontiers in Microbiology

Received: *07 August 2020*
Accepted: *16 September 2020*
Published: *09 October 2020*

Citation:
Fernández-Coll L and Cashel M (2020) Possible Roles for Basal Levels of (p)ppGpp: Growth Efficiency Vs. Surviving Stress. Front. Microbiol. 11:592718. doi: 10.3389/fmicb.2020.592718

(p)ppGpp, MANY WAYS TO TRANSFER A PYROPHOSPHATE GROUP BACK AND FORTH

Synthetases of (p)ppGpp transfer the intact 5'-βγ pyrophosphate group from ATP to the ribose 3' hydroxyl group of GTP or GDP, while (p)ppGpp hydrolases regenerate the GDP and GTP substrates by removal of the same pyrophosphate (Cashel and Kalbacher, 1970; Que et al., 1973; Sy and Lipmann, 1973; Kari et al., 1977). Many combinations of synthetase and hydrolase proteins are found throughout bacterial and plant kingdoms, along with uncertainty of functional implications or even the identities of the alarmone produced (Atkinson et al., 2011; Avilan et al., 2019; Ronneau and Hallez, 2019; Sobala et al., 2019; Jimmy et al., 2020).

No synthetases of (p)ppGpp have been yet found in animal cells, but an enzyme capable of hydrolysis of (p)ppGpp, called Mesh1 has been detected in worms, flies, and humans (Sun et al., 2010). The human version of Mesh1 has been found to hydrolyze (p)ppApp and NADPH as well as (p)ppGpp (Ding et al., 2020; Jimmy et al., 2020). Whether NADPH is the *bona fide* substrate of Mesh1 is still a matter of debate, considering that the Drosophila version did not reduce the cellular pools of NADPH when expressed in *Escherichia coli* (Zhu and Dai, 2019).

Many proteins with (p)ppGpp synthetase and/or hydrolase activity are found among diverse bacteria (Atkinson et al., 2011; Jimmy et al., 2020). Long RelA/SpoT Homologue (RSH) enzymes (**Figure 1A**), often about 750 residues, contain domains responsible for both activities, hydrolysis and synthesis, followed by regulatory domains. Although all bacteria have bifunctional long RSH enzymes, some can also have monofunctional enzymes (Atkinson et al., 2011; Avilan et al., 2019). To avoid futile cycles of synthesis and hydrolysis, this bifunctional enzyme balances both activities by undergoing conformational changes that activate one activity while inhibiting the other, as shown by structural studies made with the RSH catalytic region of *Streptococcus equisimilis* or *Thermus thermophilus* (Mechold et al., 2002; Hogg et al., 2004; Tamman et al., 2020). Binding of other proteins to the RSH enzyme seems to promote those conformational changes in response to environmental changes (Battesti and Bouveret, 2006; Chen et al., 2014; Lee et al., 2018; Germain et al., 2019; Ronneau et al., 2019; Peterson et al., 2020). Also, RSH enzymes seem to be subject to positive allosteric regulation by their products (Shyp et al., 2012; Kudrin et al., 2018).

In addition, single domain, small alarmone synthetases (SASs), and small alarmone hydrolases (SAHs) are also encountered, sometimes with multiple or additional domains. It has been shown that SAS examples can also synthesize pGpp using GMP as a substrate, with putative physiological roles (Gaca et al., 2015b; Ruwe et al., 2017; Yang et al., 2019; Petchiappan et al., 2020).

After accumulation, (p)ppGpp will change gene expression patterns by binding to RNA polymerase (RNAP) in Gram-negative bacteria or in Gram positives by lowering GTP levels, which is sensed by the transcription factor CodY (reviewed by Gaca et al., 2015a). Alternatively, (p)ppGpp can directly bind to some proteins and alter their synthetic activities (Zhang et al., 2018; Anderson et al., 2019; Wang et al., 2019, 2020).

Synthesis and Hydrolysis of (p)ppGpp in *Escherichia coli* and Downstream Effects

Escherichia coli contain two long RSH enzymes: RelA and SpoT (**Figure 1A**). While SpoT is a bifunctional enzyme, RelA is a monofunctional enzyme with a non-functional hydrolase domain, making SpoT the only source of hydrolysis (Xiao et al., 1991). Apart from the N-terminal catalytic region of the protein, RelA and SpoT contain a C-terminal regulatory region, displaying highly conserved domains (**Figure 1A**). Although several C-terminal domains are important for binding to ribosomes or synthesis fine-tuning (Loveland et al., 2016; Takada et al., 2020), the ThrRS, GTPase, SpoT/RelA domain (TGS) domain seems to often be important for controlling the conformational change that these proteins endure to control (p)ppGpp synthesis.

RelA binds to the ribosome by burying its C-terminal region inside the ribosome, just exposing the catalytic region to the cytoplasm. RelA will synthesize (p)ppGpp in response to amino acid starvation (**Figure 1B**) thorough first sensing cognate binding of uncharged transfer RNA (tRNA) to the ribosomal A-site followed by binding of RelA C-terminal region to the ribosome that leads to fixing the position of the TGS domain such that it can fit the uncharged, but not charged, CCA bases of the 3' end of the tRNA in a pocket (Arenz et al., 2016; Brown et al., 2016; Loveland et al., 2016). The final stabilizing contact between the RelA N-terminus region and Ribosome is viewed as a final lock. While the RelA synthetase domain contacts the tip of the 16S ribosomal RNA (rRNA) spur, the non-functional RelA hydrolase domain will bind near the sarcin-ricin loop of the 23S rRNA (Loveland et al., 2016; Winther et al., 2018). Loveland et al. (2016) note that this model is consistent with a stable tRNA-ribosome idling reaction rather than the extended hopping model that hypothesizes that RelA can dissociate from ribosomes after being activated and remain capable of multiple rounds of (p)ppGpp synthesis after dissociation (Haseltine et al., 1972; Haseltine and Block, 1973; Wendrich et al., 2002). Alternatively, conflicting evidences show that free RelA can stably bind uncharged tRNA and then bind to ribosomes (Winther et al., 2018). The description of the complex mechanisms at play is an extremely active field at the moment but it is not the main topic of this review.

In contrast to RelA, the N-terminal region of SpoT in *E. coli* encodes a strong hydrolase along with a weak synthetase, and the C-terminal region of SpoT that has four domains similar to

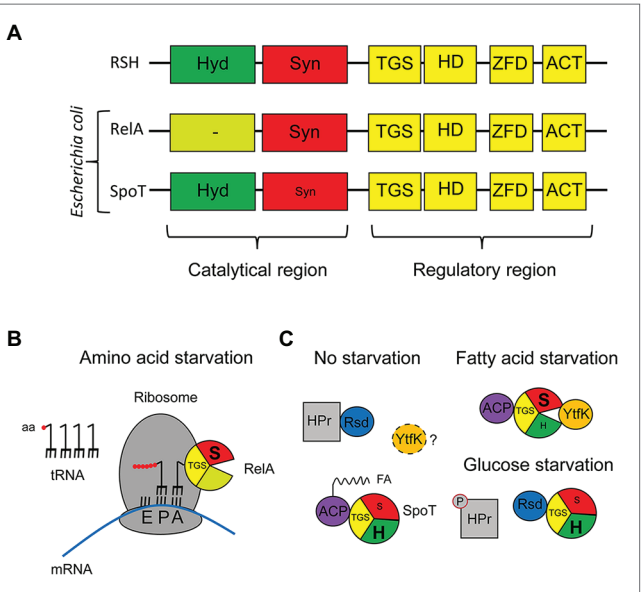

FIGURE 1 | Long RSH enzymes in *Escherichia coli*. **(A)** Cartoon of the domain distribution of a general RSH enzyme as described by Atkinson et al. (2011), as well as for the two RSH enzymes of *E. coli*, RelA and SpoT. **(B)** Schematic representation of the binding of RelA to the ribosome and its activation during amino acid starvation. **(C)** Illustration of the different proteins that bind to SpoT from *E. coli* under non-starvation conditions, fatty acid starvation, or glucose starvation.

those in RelA. It is still uncertain if SpoT interacts with ribosomes. So far, two proteins have been found to bind to the TGS domain of SpoT in response to starvation (**Figure 1C**). They are acyl carrier protein (ACP; fatty acid limitation) and Rsd (glucose limitation). While the acylated form of ACP (in presence of fatty acids) binding to SpoT will tilt the balance against synthesis and toward hydrolysis, the binding of the unacylated form (starvation) will promote synthesis (Battesti and Bouveret, 2006). The binding of Rsd to SpoT will tilt the balance toward hydrolysis, but it will only occur during glucose starvation, when Rsd is released from the phosphorylated form of HPr, a key component of the glucose phosphotransferase system (PTS; Lee et al., 2018).

Other interactions not involving the TGS has been described for SpoT. During phosphate and fatty acid starvation, YtfK binds to the catalytic region and tilts the balance toward synthesis (Germain et al., 2019). Structural studies with the *Thermus thermophilus* RSH protein, mentioned earlier, show that the hydrolysis and synthesis domains are in an open conformation during synthesis but closed during hydrolysis (Tamman et al., 2020). Therefore, considering that YtfK binds to both the hydrolase and synthetase domains (Germain et al., 2019); one could speculate that YtfK could bind between both domains to hold SpoT in the open conformation (**Figure 1C**). Further studies are required to integrate the various signaling systems together, like a possible synergy between ACP and YtfK to activate SpoT synthetase during fatty acid starvation or a possible competition between ACP and Rsd. Moreover, not much is known about YtfK activation: does it sense the presence of certain nutrients like ACP? Is it sequestered as Rsd? or does its gene expression change under certain conditions? These interactions for SpoT again raise mirror image questions to those raised for RelA. What are the functions of the C-terminal domains beyond TGS if SpoT does not require ribosomal binding for activity? Is it to preserve the weak but constitutive synthetase catalytic activity allowing non-RelA regulation to occur through metabolic signals other than uncharged tRNA? Again, structural studies seem needed for SpoT binding proteins. Another example of existing regulatory intricacies comes from the finding that starvation for either glucose or lipids can deplete amino acid precursors and activate RelA in addition of SpoT (Fernández-Coll and Cashel, 2018; Sinha et al., 2019).

In *E. coli*, as mentioned above, it has been thought for many years that (p)ppGpp exerts its effects mainly by binding to RNAP and changing gene expression by either stimulating or inhibiting transcription of separate sets of genes. Structural studies have shown that (p)ppGpp binds to two different sites in RNAP. Site 1 binding of (p)ppGpp is between the ω and β' subunits (Mechold et al., 2013). For site 2, (p)ppGpp binds inside the secondary channel of the RNAP, between the β' subunit and the cofactor DksA (Ross et al., 2016; Molodtsov et al., 2018). Both (p)ppGpp and DksA can act as cofactors for regulation of many genes, but they can also have independent or even opposite effects on gene expression (Magnusson et al., 2007; Aberg et al., 2008, 2009). This co-regulation of genes by (p)ppGpp and DksA is consistent with binding at site 2, but the effects involving site 1 are not so clear. Antagonistic effects have been attributed to other proteins that, like DksA, can also bind to the secondary channel, such as GreA (Aberg et al., 2009), suggesting that the competition of proteins for the secondary channel can change the nature of site 2 (Potrykus et al., 2006; Vinella et al., 2012; Yuzenkova et al., 2012; Zenkin and Yuzenkova, 2015; Fernández-Coll et al., 2018).

EFFECTS OF BASAL LEVELS OF (p)ppGpp IN *ESCHERICHIA COLI*

(p)ppGpp seems to have different roles depending on its abundance in the cell. While sudden burst of (p)ppGpp during stress, starvation, or stationary phase, will stop cellular growth, and cells will go into survival mode (alarmone); the low basal levels, during exponential phase, in absence of starvation, (p)ppGpp will meld the external conditions with the bacterial growth, maintaining the homeostasis of cellular components and macromolecules, acting as a secondary messenger (**Figure 2**). It is because of this duality between basal levels and stressful spikes of (p)ppGpp, and more particularly in the effect of basal levels, that we decided on the focus of this review.

When bacteria grow at constant temperature without starvation, all cellular components are synthesized exponentially. The subtle intricacies of the balanced exponential growth have long been fascinating (Neidhardt, 1999). As originally defined by Schaechter M., Maaloe O., and Kjeldgaard N.O. in 1958, balanced growth rates were determined not by limiting nutrient abundance but by the ability of the cell to use different nutrients in excess. Using those conditions, an inverse correlation is found between the levels of (p)ppGpp and growth rate, where higher levels of (p)ppGpp correlate with lower growth rates (Imholz et al., 2020).

The exponential phase of growth transits into stationary phase, which is associated with regulation often directly or indirectly due to elevated (p)ppGpp as well as a myriad of additional mechanisms that include recruitment of alternative sigma factors and ribosome

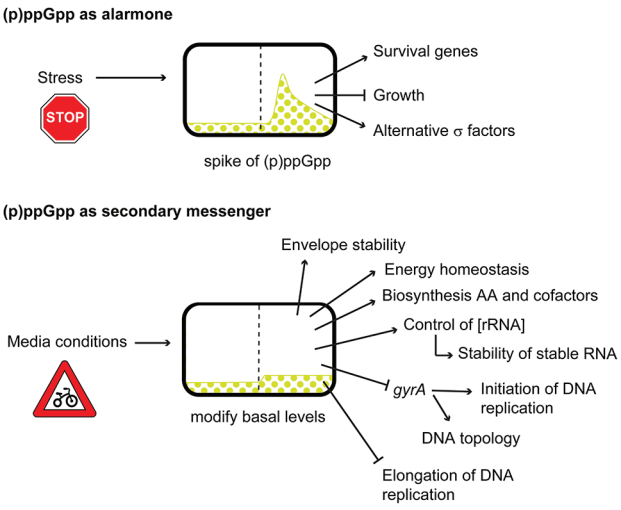

FIGURE 2 | Dual effects of (p)ppGpp acting as alarmone during burst or acting as a secondary messenger during changes in basal levels.

hibernation (not reviewed here). A major contribution comes from preventing RpoS sigma factor proteolysis, stabilized during stationary phase, or nutritional stress due to (p)ppGpp induction of the sRNA IraP (Bougdour and Gottesman, 2007; Gottesman, 2019). Other alternative sigma factors are also activated by (p)ppGpp (Österberg et al., 2011). AT rich and GC rich discriminator sequences at the promoter regions also determine whether (p)ppGpp stimulates or inhibits transcription, respectively (Travers, 1980; Winkelman et al., 2016; Sanchez-Vazquez et al., 2019).

Basal (p)ppGpp Levels and Cellular Component Homeostasis

Inhibition of key enzymes from a dozen of cellular processes has been assessed using CRISPRi in *E. coli* (Roghanian et al., 2019), in either a WT strain or in a *relA- spoT-* strain (referred as ppGpp^0). While WT cells stop growing after inhibition of the different processes with CRISPRi, the ppGpp^0 cells grow uncontrollably until they lyse, just like a car without breaks going downhill. It was found that CRISPRi inhibition of the biosynthesis of LPS (repressing *lptA* or *lpxA*) or ATP (repressing *adk*) increases the (p)ppGpp levels in wild type cells.

During exponential growth in LB and early stationary phase, the levels of ATP in wild type remain constant, in later stationary phase (more than 20 h) energy charge decreases (Chapman et al., 1971). In ppGpp^0, the levels of ATP are lower in exponential phase and early stationary phase compared to WT strains; this again suggests basal levels of (p)ppGpp are important for cellular energy homeostasis in *E. coli* by coordinating adenosine ribonucleotide synthesis with macromolecular production (Roghanian et al., 2019). That said, in wild type cells, the cellular levels of ATP do not seem to correlate with various exponential growth rates (Schneider and Gourse, 2004).

Basal levels of (p)ppGpp seem to be important for the stability of the cellular envelope. A mutant of the RNAP β' subunit (RpoC H419), that seems to have impaired binding of (p)ppGpp to site-1, shows an increase in the average lipid tail length, that results in changes in the cell membrane properties (Chen et al., 2020). A study on the effects of (p)ppGpp into T4 phage infection seems to reach, indirectly, similar conclusions. T4 phage plaques in *E. coli* show an increase on plaque size in absence of either (p)ppGpp or DksA (Patterson-West et al., 2018). Although DksA affected T4 gene expression, (p)ppGpp had almost no effect on the phage gene expression, suggesting that its effects on plaque size are related to effects in the host rather than the phage, which could be attributed to an increased membrane fragility in absence of (p)ppGpp (Patterson-West et al., 2018).

A useful phenotype of (p)ppGpp-deficiency is an inability to grow in minimal media without a set of eight amino acids (Xiao et al., 1991). These amino acids (DEILVFHST) are known as the Σ set (Potrykus et al., 2011). Interestingly, a few of the same amino acids are also required for ppGpp^0 in *Bacillus subtilis* (Kriel et al., 2014). Transcriptomic studies performed during amino acid starvation, show that (p)ppGpp is essential to activate several biosynthetic pathways to produce the amino acids of the Σ set (Traxler et al., 2008). At the same time, studies with ppGpp^0 synthetic lethal mutants reveal that (p)ppGpp activates several key components to produce D-erythrose-4-phosphate, the precursor of aromatic amino acids and vitamins (Harinarayanan et al., 2008). Apparently, basal levels of (p)ppGpp are important for uptake of iron (Vinella et al., 2005). This suggests that basal levels of (p)ppGpp are essential for biosynthesis of a growing list of metabolic intermediates, amino acids, and cofactors.

Incremental lowering of already low basal levels of (p)ppGpp by expression of the metazoan SAH Mesh1 in *E. coli* has been reported to slow growth and inferred to extend the inverse relation of ribosomal content and (p)ppGpp (Zhu and Dai, 2019). A direct relation of certain metabolic enzymes with (p)ppGpp, is found suggesting to the authors that (p)ppGpp basal levels are important to keep optimal allocation of resources during balanced exponential growth in *E. coli*. This conclusion rests on the assumption that Mesh1 activity is limited solely to (p)ppGpp hydrolysis. Traces of (p)ppApp have been detected by TLC in *E. coli* (Sobala et al., 2019), therefore, until the full range of Mesh1 substrates is known within *E. coli*, conclusions as to the mechanism of growth inhibition by Mesh1 are qualified.

Does Instability of tRNA and rRNA Depend on (p)ppGpp?

For more than a half century, with a few exceptions, it has been assumed that tRNA and rRNA are stable species, and regulation of their cellular abundance by starvation or by growth rate was exerted solely at the level of transcription. During the past 2 decades, studies with *E. coli* have focused on the mechanisms involving (p)ppGpp that could account for the many of the inhibitory and stimulatory regulatory effects on transcription.

The first systematic glimpses of rRNA turnover came from studies by Murray Deutscher's laboratory that were aimed at understanding the differences they found for ribonuclease sites for degradation of 30 and 50S ribosomal subunits during exponential growth *versus* more sites found for stationary phase and glucose-starved culture (Sulthana et al., 2016). A recent review of relevant enzymes in *E. coli* and *B. subtilis* has appeared (Bechhofer and Deutscher, 2019). For tRNA, a convincing demonstration of destabilizing effects on tRNA during abrupt starvation by filtration and resuspension for each of several individual amino acids appeared in a paper by (Svenningsen et al., 2016). Quantitating effects were normalized to a unique internal standard isolated from *Sulfolobus sulfutaricus*. Although the authors report general decay kinetics for a *relA* mutant to be similar to wild type, degradation attenuation can be observed in absence for *relA*. One example can be observed for HisR, that decreases down to a 30% after 60 min of histidine or leucine starvation in the wild type cells, but in a *relA* mutant up to a 50% remains after histidine starvation, and up to a 70% after leucine starvation. Despite of that, it was argued to indicate that degradation is independent of (p)ppGpp, since (p)ppGpp levels are reduced in an amino acid starved relaxed strain. Instead, a tRNA demand-based model has been proposed in which tRNA not engaged in protein synthesis is vulnerable to degradation; cells in slow exponential growth

are stated to have more tRNAs per ribosome than during fast growth with more active ribosomes. It is argued that increased EF-Tu content during slow growth binds the free tRNA to protect it from degradation (Sørensen et al., 2018).

Unstable rRNA has been also reported, using a similar normalization method than with tRNA studies. Fessler et al. (2020) looked at the kinetics of different filter-resuspend starvation regimens, showing that while glucose starvation produces minimal instability of rRNA, isoleucine and phosphate starvation reduced ribosome content in a similar manner than previosly observed by tRNA (Svenningsen et al., 2016). Again, the authors concluded that although (p)ppGpp may contribute, it is not essential for the degradation of rRNA, instead, inactive ribosomes are vulnerable to degradation. Therefore, it is possible that ppGpp affects rRNA stability indirectly by affecting translation. (p)ppGpp can bind to several GTPases involved in translation or ribosome biogenesis, including IF2, inhibiting their activity (Zhang et al., 2018).The end result would be a decrease on the number of active ribosomes, now susceptible of degradation. Interestingly, the inhibitory effects of (p)ppGpp over IF2 activity may depend on the mRNA being translated (Vinogradovaid et al., 2020).

As often noted here, growing *E. coli* in media with excess nutrients without starvation classically show a direct correlation between growth rates and RNA/DNA and RNA/protein ratios. This correlation is broken in the total absence of (p)ppGpp; instead, high ratios characteristic of fast growth persists even during slow growth (Potrykus et al., 2011). It can be shown that this aberrant behavior is due to (p)ppGpp and not to stress using constitutive elevated (p)ppGpp at different levels displayed by *spoT* hydrolase (*relA*$^-$) mutants that grow slowly in rich media as if it were poor (Sarubbi et al., 1988). The observed low ratios characteristic of slow growth for these mutants is consistent with the notion that (p)ppGpp is necessary and sufficient for slowing growth rates (Potrykus et al., 2011). Moreover, RNAP suppressor mutants isolated from ppGpp^0 strains that grow as prototrophs in minimal media lacking amino acids and grow slowly even rich media (Murphy and Cashel, 2003). This indicates that slow growth of RNAP mutants is a phenocopy of (p)ppGpp levels that can be exerted through transcriptional effects. Sucrose gradient comparisons of ribosomal content for slow and fast growing (p)ppGpp-deficient cells reveal normal ribosomal profiles that suggest they might be functional and more abundant than needed at slow growth rates, and yet the overall rate of translation is reduced compared to WT cells (Potrykus et al., 2011).

Differential effects on kinetics of *lacZ* transcripts have been observed on transcription and translation rates depending on overt starvation for carbon and nitrogen (Iyer et al., 2018) or steady-state starvation with chemostats for carbon, nitrogen, or phosphate source on the media (Li et al., 2018; see commentary by Potrykus and Cashel, 2018). There is a very good chance that RNA sequencing experiments just mentioned with slow growing ppGpp^0 cells will also result in high rates of tRNA and rRNA turnover. For completeness it seems worthwhile to verify this expectation by measuring the extent of instability for tRNA and rRNA in exponentially growing ppGpp^0 strains, because of unforeseen properties of *relA*$^-$ *spoT*$^-$ strains often not observed when using *relA*$^-$ *spoT*$^+$ strains.

Basal (p)ppGpp Levels and DNA

As previously described, during exponential growth, the amount of DNA and the number of replication origins per cell correlate with the growth rate (Churchward et al., 1981). During rapid growth in rich media, the time required to complete chromosomal replication is longer than the time for cell division, therefore, additional rounds of replication are necessarily initiated at the *ori* region before the previous round is completed (Cooper and Helmstetter, 1968). When determining the initiation of DNA replication by *ori*/*ter* ratios, cells growing in rich media show higher ratios of *ori*/*ter* than cells growing in poor media. However, in absence of (p)ppGpp, initiation of DNA replication becomes independent of the growth rate, showing high constant initiation rates (*ori*/*ter*) despite changing the growth rate by varying media composition and nutrient availability (Fernández-Coll et al., 2020). When the basal levels of (p)ppGpp are gradually increased without stress due to mutations on the SpoT hydrolase, as observed with RNA/DNA and RNA/protein (Potrykus et al., 2011), a proportional decrease on the growth rate and decrease on the *ori*/*ter* ratios were observed, suggesting that (p)ppGpp is also necessary and sufficient to control DNA replication initiation (Fernández-Coll et al., 2020).

The initial step of chromosomal DNA replication involves the ATP-dependent oligomerization of DnaA to *oriC*, followed by the unwinding of the DNA, loading of the replisome. While (p)ppGpp controls the expression of *dnaA* in *E. coli* (Chiaramello and Zyskind, 1990; Sanchez-Vazquez et al., 2019), the effect on DNA initiation seems to correlate with expression changes of DNA gyrase produced by (p)ppGpp that would change the local supercoiling surrounding the origin (Fernández-Coll et al., 2020). Also, these effects over DNA gyrase will promote changes on the global DNA topology (Travers and Muskhelishvili, 2015), and it will be interesting to determine which effects associated with (p)ppGpp require changes in the supercoiling state of the chromosome. As have been observed in *B. subtilis* and *S. aureus*, (p)ppGpp can also bind to the DNA primase DnaG and slow down elongation of DNA replication in *E. coli* (Wang et al., 2007; Maciag et al., 2010; Rymer et al., 2012; Maciąg-Dorszyńska et al., 2013).

EFFECTS OF GRADUAL ACCUMULATION OF (p)PPGPP Vs. SUDDEN BURSTS

The differential effects of basal levels of (p)ppGpp compared to high level bursts during stressful situations can be attributed to concentration and accumulation speed. Apart from tRNA and rRNA instability, other studies have revealed that differences between gradual accumulation of (p)ppGpp compared to a sudden burst during isoleucine starvation in *E. coli* K12 strains. In absence of isoleucine, the presence of valine will inhibit *E. coli* K12 strains growth (Leavitt and Umbarger, 1962) due to inhibition of isoleucine biosynthesis (Lawther et al., 1981). Addition of valine will abruptly increase the levels of (p)ppGpp that equal GTP within 5 min after induction (Cashel and Gallant, 1969; Fernández-Coll and Cashel, 2019).

This feature was used by Traxler et al. (2011) to progressively induce high levels of (p)ppGpp by growing *E. coli* K12 in media containing all amino acids in excess and almost limiting amounts of isoleucine that are exhausted during growth to the point where valine progressively induces starvation for isoleucine. As the levels of (p)ppGpp gradually increase, the first activation detected is a set of Lrp-dependent genes. Further, (p)ppGpp elevation is then followed by activation of RpoS and downstream by the set of genes under σS control. These results suggested that under a starvation stress situation, cells will first try to relocate resources to restore the normal growth, but as the amounts of (p)ppGpp keep rising, they will go into survival mode. Lrp-dependent regulon gene expression was not seen in the RNA sequencing studies during abrupt starvation of isoleucine by adding valine as noted by Gummesson et al. (2020). Moreover, abrupt starvation provokes unique gene regulation. such as *crp*, that increases at the 5 min peak of high (p)ppGpp levels during abrupt starvation, which is followed by lowering of gene expression to pre-induction levels or even lower (Gummesson et al., 2020).

Another study showing the effects of a (p)ppGpp on *E. coli* K12 strain expression pattern over time was recently published (Sanchez-Vazquez et al., 2019). In this study, the authors grow MG1655, together with several alleles that abolish the two binding sites of (p)ppGpp in RNAP. In MOPS with all the amino acids and IPTG induced RelA, a burst of (p)ppGpp occurs without starvation. When Gummesson et al. (2020) compared their results with those of Sanchez-Vazquez et al. (2019); they found big differences on the expression levels of genes involved in amino acid biosynthesis that they attributed to the media conditions. This suggests that, although in both experiments a burst of (p)ppGpp is being produced, the media conditions will affect the outcome.

It is important to note that the RNAP mutant strain lacking the both binding sites of (p)ppGpp (used in Sanchez-Vazquez et al., 2019), should behave as a (p)ppGpp-deficient strain and not be able to grow in minimal media (Xiao et al., 1991); it grows slowly on minimal medium (Ross et al., 2016). One possible explanation for the slow growth without amino acids is that while (p)ppGpp might not bind to the double site mutant RNAP, it still could have unappreciated functions at the metabolic level. Another possibility is that the RNAP mutant might confer similar conformational changes to those observed in $ppGpp^0$ spontaneous mutants that grow on minimal media without amino acids (Murphy and Cashel, 2003).

IS WHAT IS TRUE FOR *ESCHERICHIA COLI*, TRUE FOR ELEPHANTS AND OTHER BACTERIA?

The duality between basal levels of (p)ppGpp and stressful peaks has been observed in other organisms. When the genes affected by (p)ppGpp during exponential phase in *Rhizobium etli* were compared to those affected during stationary phase (Vercruysse et al., 2011), only 25% were found to be shared between both phases and of those, only half were similarly positive or negative controlled. This study clearly emphasizes the differential effects of basal levels of (p)ppGpp during exponential phase compared to a peak of (p)ppGpp during stationary phase.

In the Gram-negative bacteria *Caulobacter crescentus*, its complex cell cycle is controlled by (p)ppGpp, that affects gene expression and degradation of the main regulatory proteins DnaA and CtrA with antagonistic activities. DnaA activates initiation of DNA replication, and CtrA blocks it (Lesley and Shapiro, 2008; Boutte et al., 2012; Gonzalez and Collier, 2014; Stott et al., 2015).

As previously discussed, in Gram-positive bacteria (p)ppGpp will affect gene expression by changing the levels of GTP, sensed by CodY. Therefore, it is essential for Gram-positive to keep the homeostasis of GTP. In *B. subtilis*, increased levels of (p)ppGpp block the biosynthetic enzymes HprT and GmK that are essential for the production of GTP (Kriel et al., 2012; Anderson et al., 2019). The enzyme HprT, as a dimer, will synthesize GMP, but the binding of (p)ppGpp leads to formation of tetramers that are inactive (Anderson et al., 2019). Similar effects have been observed for GmK. Phylogenetical studies show that this is conserved among Gram-positive bacteria, but in Gram-negative bacteria, these enzymes are insensitive to (p)ppGpp (Anderson et al., 2019). In this work, the authors substituted *B. subtilis* HprT and GmK enzymes for the ones in *E. coli* (p)ppGpp insensitive enzymes that show an increase of GTP levels up to four times without stress. This is taken by the authors to underscore the conclusion that basal levels are essential in Gram-positive to maintain GTP homeostasis. Apart from its regulatory effects, maintaining low GTP levels is essential because high levels of GTP seem to be toxic for *B. subtilis* cells (Kriel et al., 2012). *Bacillus* contains a long bifunctional RSH enzyme (Rel) mediating the response to nutritional starvation (Wendrich and Marahiel, 1997; Pulschen et al., 2017; Takada et al., 2020), as well as two SASs (RelP and RelQ). It has been observed that while RelP is always active, RelQ requires pppGpp to be active, suggesting that RelQ will act as amplifier of the response of Rel during stress situation (Steinchen et al., 2018). Moreover, RelQ seems to be inhibited by the binding of certain single stranded RNA (Beljantseva et al., 2017). In contrast, RelP seems to be responsible for the basal levels of (p)ppGpp (Ababneh and Herman, 2015). In absence of Rel hydrolase activity there is an increase on the basal levels due to the SAS, producing a change from chained cells to unchained motile cells; thus, minor increases of (p)ppGpp basal levels will promote important cell changes (Ababneh and Herman, 2015). There is a report where the amount of uncharged tRNA was determined not by amino acid starvation, but by underproduction of aminoacyl tRNA synthetases (aaRS) in rich media conditions. It shows that (p)ppGpp enhances growth when there is insufficient aaRS activity in the absence of external starvation in *B. subtilis* (Parker et al., 2020). Interestingly, as they reduce the fitness by underproducing aaRS, the amount of ribosomal proteins

decreases in WT cells, but they keep constantly high in absence of (p)ppGpp, reminiscent of the observed behavior of ribosomes in *E. coli* (Potrykus et al., 2011). In Parker et al. (2020), the optimal growth happens when the amount of tRNA charging is not maximized and that (p)ppGpp is key to maintain the protein stoichiometry for the translation apparatus. Studies performed in tRNA maturation in *B. subtilis* (Trinquier et al., 2019) show that accumulation of immature tRNA triggers synthesis of (p)ppGpp that will interfere in the maturation of the 16S rRNA. Together with the data from Parker et al. (2020) seem to suggest that (p)ppGpp accommodates the number of ribosomes to the amount of functional tRNA. In contrast, a spike of (p)ppGpp during heat shock, seems to protect 16S rRNA from degradation (Schäfer et al., 2020), suggesting that the effects of basal levels of (p)ppGpp may have even opposite roles than spikes of (p)ppGpp suggesting that stress-dependent factors may be required.

A study made in the cyanobacterium *Synechococcus elongatus* has shown differential roles between basal levels of (p)ppGpp and spikes during stress (Puszynska and O'Shea, 2017). During growth with constant light (no stress), the basal levels of (p)ppGpp in *S. elongatus* are responsible for the control of protein levels and bacterial size. During the transition from light to dark, a spike of (p)ppGpp is produced inhibiting up to a 90% of the transcripts (Hood et al., 2016; Puszynska and O'Shea, 2017). This spike of (p)ppGpp increases the expression of *hfp*, a factor responsible for reducing the activity of ribosomes by promoting their dimerization, that will also decrease the levels of photosynthetic pigments and will stop growth (Hood et al., 2016).

BASAL LEVELS OF (p)ppGpp AND PATHOGENICITY

Levels of (p)ppGpp have been shown to be important for virulence or survival inside the host of different bacteria, like *Salmonella enterica* serovar Typhimurium that in absence of (p)ppGpp was found to be highly attenuated *in vivo* and non-invasive *in vitro* (Pizarro-Cerdá and Tedin, 2004). In this case, the levels of (p)ppGpp will spike after invasion due to the lack of nutrients or due to oxidative stress and acidic pH inside macrophages (Fitzsimmons et al., 2018, 2020). Even commensal *E. coli* expresses factors essential for biofilm and colonization of surfaces such as fimbria, flagella, or antigen 43, just after the peak of (p)ppGpp during stationary phase (Aberg et al., 2008, 2009; Cabrer-Panes et al., 2020).

However, a few examples exist where the basal levels of (p)ppGpp are also essential for virulence. *Enterococcus faecalis* is a Gram-positive bacterium responsible for approximately 30% of bacterial infectious endocarditis cases in the world (Chirouze et al., 2013). It contains a long bifunctional RSH enzyme (Rel) responsible for increasing the levels of (p)ppGpp in response to stress (nutritional and physical) and the SAS RelQ (Abranches et al., 2009). Basal levels of (p)ppGpp were found to be responsible for controlling energy production and for maintaining the GTP homeostasis (Gaca et al., 2013), but also are essential for heart valve colonization and endothelial cells invasion of human coronary arteries during infectious endocarditis (Colomer-Winter et al., 2018). Similar observations were made in *Mycobacterium tuberculosis*, where the basal levels of (p)ppGpp were modified using mutants in the long RSH enzyme Rel. Too low or too high levels of (p)ppGpp were proven to be lethal for *M. tuberculosis* during acute and chronic infections in mice, which seems to be a Goldilocks effect: not too little, not too much, and just right (Weiss and Stallings, 2013).

Considering the effects of (p)ppGpp on virulence factors and its absence in metazoan cells, several groups have pointed to the synthetases of (p)ppGpp as a target to develop new antibiotics. According to the CDC's Antibiotic Resistance Threats 2019 Report, each year in the United States, at least 2.8 million people are infected with antibiotic-resistant bacteria and more than 35,000 people die as a result. This number is estimated to escalate, someday rendering current antibiotic treatment completely obsolete.

Serious attention has been given to new antibiotic development based on microbial (p)ppGpp and its absence in eukaryotes. Exploitable possibilities are many, since so far, the $ppGpp^0$ state is generally associated with reduction of pathogenicity, basal levels with pathogenicity, and high levels with cessation of bacterial growth. At this point, there are no easy answers. Attempts have been made to produce (p)ppGpp analogs that interfere with the synthesis of (p)ppGpp (Wexselblatt et al., 2012; Beljantseva et al., 2017). A minor problem of that strategy is that the high polarity of (p)ppGpp and analogs interferes with their permeability, but this can be bypassed by chemically cloaking the nucleotide analogs with nonpolar tags, making them permeable. A troublesome problem is that strategies that block synthesis of (p)ppGpp even by inactivating multiple synthetases would be rendered impractical because of spontaneous RNAP suppressor mutants in (p)ppGpp-deficient strains, able to mimic the presence of (p)ppGpp (Murphy and Cashel, 2003; Kriel et al., 2012). Moreover, compounds that inhibit the long RSH enzymes are found, so far, to be inefficient inhibitors of SASs from *E. faecalis* (Gaca et al., 2015b; Beljantseva et al., 2017).

Perhaps, an alternative strategy would be to target the hydrolase domain of the RSH enzymes. As often mentioned above, (p)ppGpp inhibits bacterial growth. Analogs that give sufficient increases of intracellular of (p)ppGpp should severely slow growth, which could be interesting antibacterial target. Learning from different SpoT hydrolase mutants, such as SpoT 202 or 203 (Sarubbi et al., 1988), or the known binding of proteins to long RSH enzymes would help developing compounds able to tilt the balance through synthesis or blocking hydrolysis. This is also a slippery slope because increased (p)ppGpp often has been associated with antibiotic persistence (Svenningsen et al., 2019), although the mechanisms are still unclear. Development of drugs that give constitutive hydrolysis is another option. This would minimize interference by laterally transmitted synthetases as one mechanism of achieving drug resistance (Jimmy et al., 2020).

CONCLUDING REMARKS

In this review, we address effects of basal levels of (p)ppGpp on bacteria physiology with focus on *E. coli*, what we know best. However, when we try to expand it to organisms less familiar to us or when we try to generalize using model organisms, it is good to remember the variety of organisms and how they have adapted differently to synthesize (p)ppGpp and respond to its accumulation.

The duality of (p)ppGpp between "alarmone" during stress and secondary messenger during exponential growth seems to depend not only on the amount of (p)ppGpp, but also on the rate of its accumulation. Most studies use a burst of (p)ppGpp or excruciating starvation conditions to try to estimate physiological effects of (p)ppGpp. Some of those methods will highly increase the levels of (p)ppGpp even higher than direct starvation methods. For example, producing starvation with serine hydroxamate (SHX) or the overexpression of the catalytical region of a RSH enzyme, is useful tools to produce a burst of (p)ppGpp, but lack the feedback control mechanisms that starvation or stress may have. By pushing cells so far, one may end up making conclusions from close-to-death cells.

An alternative method is to use (p)ppGpp-deficient cells, it is far from perfect either. It will reveal a need for (p)ppGpp but not the specific mechanistic target. As previously discussed, these strains will not grow in minimal media without certain amino acids and will require a supplement of iron in the media, rendering some experiments impossible. The addition of the set of eight amino acids essential for *E. coli* provides a way to grow (p)ppGpp-deficient cells in poor media, but then we need to look for the appearance of suppressor mutants that may mask the results.

Most of basal levels of (p)ppGpp are described during balanced growth, where growth rate classically depends on the ability of bacteria to use certain nutrients, instead of their availability in the media. However, in several studies, they use chemostat cultures to achieve "balanced growth." We should say that from our perspective, chemostat steady state growth limits nutrients available and therefore systematically varies the intensity of starvation, which is likely to be very different from subtle cellular adjustments needed to optimize the efficiency of metabolizing otherwise poorly utilized nutrients.

Future work will try to navigate through these difficulties. It will probably involve designing strategies that will help distinguish between brute force and fine-tuning effects on bacterial physiology.

AUTHOR CONTRIBUTIONS

LF-C and MC conceived, drafted, and revised the manuscript. Both authors have read and approved the final version of this manuscript.

FUNDING

This research was supported the Intramural Research Program, and *Eunice Kennedy Shriver* National Institute of Child Health and Human Development, NIH.

ACKNOWLEDGMENTS

We would like to acknowledge our gratitude for the NIH Intramural allows research as full-time pursuit of our curiosity.

REFERENCES

Ababneh, Q. O., and Herman, J. K. (2015). RelA inhibits bacillus subtilis motility and chaining. *J. Bacteriol.* 197, 128–137. doi: 10.1128/JB.02063-14

Aberg, A., Fernández-Vázquez, J., Cabrer-Panes, J. D., Sánchez, A., and Balsalobre, C. (2009). Similar and divergent effects of ppGpp and DksA deficiencies on transcription in *Escherichia coli*. *J. Bacteriol.* 191, 3226–3236. doi: 10.1128/JB.01410-08

Aberg, A., Shingler, V., and Balsalobre, C. (2008). Regulation of the fimB promoter: a case of differential regulation by ppGpp and DksA in vivo. *Mol. Microbiol.* 67, 1223–1241. doi: 10.1111/j.1365-2958.2008.06115.x

Abranches, J., Martinez, A. R., Kajfasz, J. K., Chávez, V., Garsin, D. A., Lemos, J. A., et al. (2009). The molecular alarmone (p)ppGpp mediates stress responses, vancomycin tolerance, and virulence in *Enterococcus faecalis*. *J. Bacteriol.* 191, 2248–2256. doi: 10.1128/JB.01726-08

Anderson, B. W., Liu, K., Wolak, C., Dubiel, K., She, F., Satyshur, K. A., et al. (2019). Evolution of (P)ppGpp-HPRT regulation through diversification of an allosteric oligomeric interaction. *eLife* 8:e47534. doi: 10.7554/eLife.47534

Arenz, S., Abdelshahid, M., Sohmen, D., Payoe, R., Starosta, A. L., Berninghausen, O., et al. (2016). The stringent factor RelA adopts an open conformation on the ribosome to stimulate ppGpp synthesis. *Nucleic Acids Res.* 44, 6471–6481. doi: 10.1093/nar/gkw470

Atkinson, G. C., Tenson, T., and Hauryliuk, V. (2011). The RelA/SpoT homolog (RSH) superfamily: distribution and functional evolution of ppGpp synthetases and hydrolases across the tree of life. *PLoS One* 6:e23479. doi: 10.1371/journal.pone.0023479

Avilan, L., Puppo, C., Villain, A., Bouveret, E., Menand, B., Field, B., et al. (2019). RSH enzyme diversity for (p)ppGpp metabolism in *Phaeodactylum tricornutum* and other diatoms. *Sci. Rep.* 9:17682. doi: 10.1038/s41598-019-54207-w

Battesti, A., and Bouveret, E. (2006). Acyl carrier protein/SpoT interaction, the switch linking SpoT-dependent stress response to fatty acid metabolism. *Mol. Microbiol.* 62, 1048–1063. doi: 10.1111/j.1365-2958.2006.05442.x

Bechhofer, D. H., and Deutscher, M. P. (2019). Bacterial ribonucleases and their roles in RNA metabolism. *Crit. Rev. Biochem. Mol. Biol.* 54, 242–300. doi: 10.1080/10409238.2019.1651816

Beljantseva, J., Kudrin, P., Jimmy, S., Ehn, M., Pohl, R., Varik, V., et al. (2017). Molecular mutagenesis of ppGpp: turning a RelA activator into an inhibitor. *Sci. Rep.* 7:41839. doi: 10.1038/srep41839

Bougdour, A., and Gottesman, S. (2007). ppGpp regulation of RpoS degradation via anti-adaptor protein IraP. *Proc. Natl. Acad. Sci. U. S. A.* 104, 12896–12901. doi: 10.1073/pnas.0705561104

Boutte, C. C., Henry, J. T., and Crosson, S. (2012). ppGpp and polyphosphate modulate cell cycle progression in *Caulobacter crescentus*. *J. Bacteriol.* 194, 28–35. doi: 10.1128/JB.05932-11

Brown, A., Fernández, I. S., Gordiyenko, Y., and Ramakrishnan, V. (2016). Ribosome-dependent activation of stringent control. *Nature* 534, 277–280. doi: 10.1038/nature17675

Cabrer-Panes, J. D., Fernández-Coll, L., ernández-Vázquez, J., Gaviria-Cantin, T. C., El Mouali, Y., Åberg, A., et al. (2020). ppGpp mediates the growth phase-dependent regulation of *agn43*, a phase variable gene, by stimulating its promoter activity. Environ. *Environ. Microbiol. Rep.* 12, 444–453. doi: 10.1111/1758-2229.12860

Cashel, M., and Gallant, J. (1969). Two compounds implicated in the function of the RC gene of *Escherichia coli*. *Nature* 221, 838–841. doi: 10.1038/221838a0

Cashel, M., and Kalbacher, B. (1970). The control of ribonucleic acid synthesis in *Escherichia coli* V. characterization of a nucleotide associated with the stringent response. *J. Biol. Chem.* 245, 2309–2318.

Chapman, A. G., Fall, L., and Atkinson, D. E. (1971). Adenylate energy charge in *Escherichia coli* during growth and starvation. *J. Bacteriol.* 108, 1072–1086. doi: 10.1128/jb.108.3.1072-1086.1971

Chen, J., Bang, W. Y., Lee, Y., Kim, S., Lee, K. W., Kim, S. W., et al. (2014). AtObgC-AtRSH1 interaction may play a vital role in stress response signal transduction in Arabidopsis. *Plant Physiol. Biochem.* 74, 176–184. doi: 10.1016/j.plaphy.2013.10.022

Chen, Y., Boggess, E. E., Ocasio, E. R., Warner, A., Kerns, L., Drapal, V., et al. (2020). Reverse engineering of fatty acid-tolerant *Escherichia coli* identifies design strategies for robust microbial cell factories. *Metab. Eng.* 61, 120–130. doi: 10.1016/j.ymben.2020.05.001

Chiaramello, A. E., and Zyskind, J. W. (1990). Coupling of DNA replication to growth rate in *Escherichia coli*: a possible role for guanosine tetraphosphate. *J. Bacteriol.* 172, 2013–2019. doi: 10.1128/jb.172.4.2013-2019.1990

Chirouze, C., Athan, E., Alla, F., Chu, V. H., Ralph Corey, G., Selton-Suty, C., et al. (2013). Enterococcal endocarditis in the beginning of the 21st century: analysis from the international collaboration on endocarditis-prospective cohort study. *Clin. Microbiol. Infect.* 19, 1140–1147. doi: 10.1111/1469-0691.12166

Churchward, G., Estiva, E., and Bremer, H. (1981). Growth rate-dependent control of chromosome replication initiation in *Escherichia coli*. *J. Bacteriol.* 145, 1232–1238. doi: 10.1128/JB.145.3.1232-1238.1981

Colomer-Winter, C., Gaca, A. O., Chuang-Smith, O. N., Lemos, J. A., and Frank, K. L. (2018). Basal levels of (p)ppgpp differentially affect the pathogenesis of infective endocarditis in *Enterococcus faecalis*. *Microbiology* 164, 1254–1265. doi: 10.1099/mic.0.000703

Cooper, S., and Helmstetter, C. E. (1968). Chromosome replication and the division cycle of *Escherichia coli* B/r. *J. Mol. Biol.* 31, 519–540. doi: 10.1016/0022-2836(68)90425-7

Ding, C. K. C., Rose, J., Sun, T., Wu, J., Chen, P. H., Lin, C. C., et al. (2020). MESH1 is a cytosolic NADPH phosphatase that regulates ferroptosis. *Nat. Metab.* 2, 270–277. doi: 10.1038/s42255-020-0181-1

Fernández-Coll, L., and Cashel, M. (2018). Contributions of SpoT hydrolase, SpoT synthetase, and RelA synthetase to carbon source diauxic growth transitions in *Escherichia coli*. *Front. Microbiol.* 9:1802. doi: 10.3389/fmicb.2018.01802

Fernández-Coll, L., and Cashel, M. (2019). Using microtiter dish radiolabeling for multiple in vivo measurements of *Escherichia coli* (p)ppGpp followed by thin layer chromatography. *J. Vis. Exp.* 148:e59595. doi: 10.3791/59595

Fernández-Coll, L., Maciag-Dorszynska, M., Tailor, K., Vadia, S., Levin, P. A., Szalewska-Palasz, A., et al. (2020). The absence of (p)ppGpp renders initiation of *Escherichia coli* chromosomal DNA synthesis independent of growth rates. *mBio* 11, e03223–e03319. doi: 10.1128/mBio.03223-19

Fernández-Coll, L., Potrykus, K., and Cashel, M. (2018). Puzzling conformational changes affecting proteins binding to the RNA polymerase. *Proc. Natl. Acad. Sci. U. S. A.* 115, 12550–12552. doi: 10.1073/pnas.1818361115

Fessler, M., Gummesson, B., Charbon, G., Svenningsen, S. L., and Sørensen, M. A. (2020). Short-term kinetics of rRNA degradation in *Escherichia coli* upon starvation for carbon, amino acid or phosphate. *Mol. Microbiol.* 113, 951–963. doi: 10.1111/mmi.14462

Fitzsimmons, L. F., Liu, L., Kant, S., Kim, J. -S., Till, J. K., Jones-Carson, J., et al. (2020). SpoT induces intracellular salmonella virulence programs in the phagosome. *mBio* 11, e03397–e03419. doi: 10.1128/mBio.03397-19

Fitzsimmons, L. F., Liu, L., Kim, J. S., Jones-Carson, J., and Vázquez-Torres, A. (2018). Salmonella reprograms nucleotide metabolism in its adaptation to nitrosative stress. *mBio* 9, e00211–e00218. doi: 10.1128/mBio.00211-18

Gaca, A. O., Colomer-Winter, C., and Lemos, J. A. (2015a). Many means to a common end: the intricacies of (p)ppGpp metabolism and its control of bacterial homeostasis. *J. Bacteriol.* 197, 1146–1156. doi: 10.1128/JB.02577-14

Gaca, A. O., Kajfasz, J. K., Miller, J. H., Liu, K., Wang, J. D., Abranches, J., et al. (2013). Basal levels of (p)ppGpp in *Enterococcus faecalis*: the magic beyond the stringent response. *mBio* 4, e00646–e00713. doi: 10.1128/mBio.00646-13

Gaca, A. O., Kudrin, P., Colomer-Winter, C., Beljantseva, J., Liu, K., Anderson, B., et al. (2015b). From (p)ppGpp to (pp)pGpp: characterization of regulatory effects of pGpp synthesized by the small alarmone synthetase of *Enterococcus faecalis*. *J. Bacteriol.* 197, 2908–2919. doi: 10.1128/JB.00324-15

Germain, E., Guiraud, P., Byrne, D., Douzi, B., Djendli, M., and Maisonneuve, E. (2019). YtfK activates the stringent response by triggering the alarmone synthetase SpoT in *Escherichia coli*. *Nat. Commun.* 10:5763. doi: 10.1038/s41467-019-13764-4

Gonzalez, D., and Collier, J. (2014). Effects of (p)ppGpp on the progression of the cell cycle of caulobacter crescentus. *J. Bacteriol.* 196, 2514–2525. doi: 10.1128/JB.01575-14

Gottesman, S. (2019). Trouble is coming: signaling pathways that regulate general stress responses in bacteria. *J. Biol. Chem.* 294, 11685–11700. doi: 10.1074/jbc.REV119.005593

Gummesson, B., Shah, S. A., Borum, A. S., Fessler, M., Mitarai, N., Sørensen, M. A., et al. (2020). Valine-induced isoleucine starvation in *Escherichia coli* K-12 studied by spike-in normalized RNA sequencing. *Front. Genet.* 11:144. doi: 10.3389/fgene.2020.00144

Harinarayanan, R., Murphy, H., and Cashel, M. (2008). Synthetic growth phenotypes of *Escherichia coli* lacking ppGpp and transketolase a (tktA) are due to ppGpp-mediated transcriptional regulation of tktB. *Mol. Microbiol.* 69, 882–894. doi: 10.1111/j.1365-2958.2008.06317.x

Haseltine, W. A., and Block, R. (1973). Synthesis of guanosine tetra- and pentaphosphate requires the presence of a codon-specific, uncharged transfer ribonucleic acid in the acceptor site of ribosomes. *Proc. Natl. Acad. Sci. U. S. A.* 70, 1564–1568. doi: 10.1073/pnas.70.5.1564

Haseltine, W. A., Block, R., Gilbert, W., and Weber, K. (1972). MSI and MSII made on ribosome in idling step of protein synthesis. *Nature* 238, 381–384. doi: 10.1038/238381a0

Hogg, T., Mechold, U., Malke, H., Cashel, M., and Hilgenfeld, R. (2004). Conformational antagonism between opposing active sites in a bifunctional RelA/SpoT homolog modulates (p)ppGpp metabolism during the stringent response. *Cell* 117, 57–68. doi: 10.1016/S0092-8674(04)00260-0

Hood, R. D., Higgins, S. A., Flamholz, A., Nichols, R. J., and Savage, D. F. (2016). The stringent response regulates adaptation to darkness in the cyanobacterium *Synechococcus elongatus*. *Proc. Natl. Acad. Sci. U. S. A.* 113, E4867–E4876. doi: 10.1073/pnas.1524915113

Imholz, N., Noga, M., van den Broek, N., and Bokinsky, G. E. (2020). Calibrating the bacterial growth rate speedometer: a re-evaluation of the relationship between basal ppGpp, growth, and RNA synthesis in *Escherichia coli*. *Front. Microbiol.* 11:574872. doi: 10.3389/FMICB.2020.574872

Iyer, S., Le, D., Park, B. R., and Kim, M. (2018). Distinct mechanisms coordinate transcription and translation under carbon and nitrogen starvation in *Escherichia coli*. *Nat. Microbiol.* 3, 741–748. doi: 10.1038/s41564-018-0161-3

Jimmy, S., Saha, C. K., Kurata, T., Stavropoulos, C., Oliveira, S. R. A., Koh, A., et al. (2020). A widespread toxin–antitoxin system exploiting growth control via alarmone signaling. *Proc. Natl. Acad. Sci. U. S. A.* 117, 10500–10510. doi: 10.1073/pnas.1916617117

Kari, C., Török, I., and Travers, A. (1977). ppGpp cycle in *Escherichia coli*. *Mol. Gen. Genet.* 150, 249–255. doi: 10.1007/BF00268123

Kriel, A., Bittner, A. N., Kim, S. H., Liu, K., Tehranchi, A. K., Zou, W. Y., et al. (2012). Direct regulation of GTP homeostasis by (p)ppGpp: a critical component of viability and stress resistance. *Mol. Cell* 48, 231–241. doi: 10.1016/j.molcel.2012.08.009

Kriel, A., Brinsmade, S. R., Tse, J. L., Tehranchi, A. K., Bittner, A. N., Sonenshein, A. L., et al. (2014). GTP dysregulation in Bacillus subtilis cells lacking (p)ppGpp results in phenotypic amino acid auxotrophy and failure to adapt to nutrient downshift and regulate biosynthesis genes. *J. Bacteriol.* 196, 189–201. doi: 10.1128/JB.00918-13

Kudrin, P., Dzhygyr, I., Ishiguro, K., Beljantseva, J., Maksimova, E., Raquel, S., et al. (2018). The ribosomal A-site finger is crucial for binding and activation of the stringent factor RelA. *Nucleic Acids Res.* 46, 1973–1983. doi: 10.1093/nar/gky023

Lawther, R. P., Calhoun, D. H., Adams, C. W., Hauser, C. A., Gray, J., and Hatfield, G. W. (1981). Molecular basis of valine resistance in *Escherichia coli* K-12. *Proc. Natl. Acad. Sci. U. S. A.* 78, 922–925. doi: 10.1073/pnas.78.2.922

Leavitt, R. I., and Umbarger, H. E. (1962). Isoleucine and valine metabolism in *Escherichia coli*. XI. Valine inhibition of the growth of *Escherichia coli* strain K-12. *J. Bacteriol.* 83, 624–630. doi: 10.1128/JB.83.3.624-630.1962

Lee, J. -W., Park, Y. -H., and Seok, Y. -J. (2018). Rsd balances (p)ppGpp level by stimulating the hydrolase activity of SpoT during carbon source downshift in *Escherichia coli*. *Proc. Natl. Acad. Sci. U. S. A.* 115, E6845–E6854. doi: 10.1073/pnas.1722514115

Lesley, J. A., and Shapiro, L. (2008). SpoT regulates DnaA stability and initiation of DNA replication in carbon-starved *Caulobacter crescentus*. *J. Bacteriol.* 190, 6867–6880. doi: 10.1128/JB.00700-08

Li, S. H. -J. J., Li, Z., Park, J. O., King, C. G., Rabinowitz, J. D., Wingreen, N. S., et al. (2018). *Escherichia coli* translation strategies differ across carbon, nitrogen and phosphorus limitation conditions. *Nat. Microbiol.* 3, 939–947. doi: 10.1038/s41564-018-0199-2

Loveland, A. B., Bah, E., Madireddy, R., Zhang, Y., Brilot, A. F., Grigorieff, N., et al. (2016). Ribosome•RelA structures reveal the mechanism of stringent response activation. *eLife* 5:e17029. doi: 10.7554/eLife.17029

Maciag, M., Kochanowska, M., Lyzeń, R., Wegrzyn, G., and Szalewska-Pałasz, A. (2010). ppGpp inhibits the activity of *Escherichia coli* DnaG primase. *Plasmid* 63, 61–67. doi: 10.1016/j.plasmid.2009.11.002

Maciąg-Dorszyńska, M., Szalewska-Pałasz, A., and Węgrzyn, G. (2013). Different effects of ppGpp on *Escherichia coli* DNA replication in vivo and in vitro. *FEBS Open Bio.* 3, 161–164. doi: 10.1016/j.fob.2013.03.001

Magnusson, L. U., Gummesson, B., Joksimović, P., Farewell, A., Nyström, T., Joksimovic, P., et al. (2007). Identical, independent, and opposing roles of ppGpp and DksA in *Escherichia coli*. *J. Bacteriol.* 189, 5193–5202. doi: 10.1128/JB.00330-07

Mechold, U., Murphy, H., Brown, L., and Cashel, M. (2002). Intramolecular regulation of the opposing (p)ppGpp catalytic activities of RelSeq, the Rel/Spo enzyme from streptococcus equisimilis. *J. Bacteriol.* 184, 2878–2888. doi: 10.1128/JB.184.11.2878-2888.2002

Mechold, U., Potrykus, K., Murphy, H., Murakami, K. S., and Cashel, M. (2013). Differential regulation by ppGpp versus pppGpp in *Escherichia coli*. *Nucleic Acids Res.* 41, 6175–6189. doi: 10.1093/nar/gkt302

Molodtsov, V., Sineva, E., Zhang, L., Huang, X., Cashel, M., Ades, S. E., et al. (2018). Allosteric effector ppGpp potentiates the inhibition of transcript initiation by DksA. *Mol. Cell* 69, 828.e5–839.e5. doi: 10.1016/J.MOLCEL.2018.01.035

Murphy, H., and Cashel, M. (2003). Isolation of RNA polymerase suppressors of a (p)ppGpp deficiency. *Methods Enzymol.* 371, 596–601. doi: 10.1016/S0076-6879(03)71044-1

Neidhardt, F. C. (1999). Bacterial growth: constant obsession with dN/dt. *J. Bacteriol.* 181, 7405–7408. doi: 10.1128/JB.181.24.7405-7408.1999

Österberg, S., del Peso-Santos, T., and Shingler, V. (2011). Regulation of alternative sigma factor use. *Annu. Rev. Microbiol.* 65, 37–55. doi: 10.1146/annurev.micro.112408.134219

Parker, D. J., Lalanne, J. -B., Kimura, S., Johnson, G. E., Waldor, M. K., and Li, G. -W. (2020). Growth-optimized aminoacyl-tRNA synthetase levels prevent maximal tRNA charging. *Cell Syst.* 11, 121.e6–130.e6. doi: 10.1016/j.cels.2020.07.005

Patterson-West, J., James, T. D., Fernández-Coll, L., Iben, J. R., Moon, K., Knipling, L., et al. (2018). The *E. coli* global regulator DksA reduces transcription during T4 infection. *Viruses* 10:308. doi: 10.3390/v10060308

Petchiappan, A., Naik, S. Y., and Chatterji, D. (2020). RelZ-mediated stress response in mycobacterium smegmatis: PGPP synthesis and its regulation. *J. Bacteriol.* 202, e00444–e00519. doi: 10.1128/JB.00444-19

Peterson, B. N., Young, M. K. M., Luo, S., Wang, J., Whiteley, A. T., Woodward, J. J., et al. (2020). (p)ppGpp and c-di-AMP homeostasis is controlled by CbpB in *Listeria monocytogenes*. *mBio* 11, e01625–e01720. doi: 10.1128/mbio.01625-20

Pizarro-Cerdá, J., and Tedin, K. (2004). The bacterial signal molecule, ppGpp, regulates Salmonella virulence gene expression. *Mol. Microbiol.* 52, 1827–1844. doi: 10.1111/j.1365-2958.2004.04122.x

Potrykus, K., and Cashel, M. (2018). Growth at best and worst of times. *Nat. Microbiol.* 3, 862–863. doi: 10.1038/s41564-018-0207-6

Potrykus, K., Murphy, H., Philippe, N., and Cashel, M. (2011). ppGpp is the major source of growth rate control in *E. coli*. *Environ. Microbiol.* 13, 563–575. doi: 10.1111/j.1462-2920.2010.02357.x

Potrykus, K., Vinella, D., Murphy, H., Szalewska-Palasz, A., D'Ari, R., and Cashel, M. (2006). Antagonistic regulation of *Escherichia coli* ribosomal RNA rrnB P1 promoter activity by GreA and DksA. *J. Biol. Chem.* 281, 15238–15248. doi: 10.1074/jbc.M601531200

Pulschen, A. A., Sastre, D. E., Machinandiarena, F., Crotta Asis, A., Albanesi, D., de Mendoza, D., et al. (2017). The stringent response plays a key role in *Bacillus subtilis* survival of fatty acid starvation. *Mol. Microbiol.* 103, 698–712. doi: 10.1111/mmi.13582

Puszynska, A. M., and O'Shea, E. K. (2017). ppGpp controls global gene expression in light and in darkness in *S. elongatus*. *Cell Rep.* 21, 3155–3165. doi: 10.1016/j.celrep.2017.11.067

Que, L., Willie, G. R., Cashel, M., Bodley, J. W., and Gray, G. R. (1973). Guanosine 5' diphosphate, 3' diphosphate: assignment of structure by 13C nuclear magnetic resonance spectroscopy. *Proc. Natl. Acad. Sci. U. S. A.* 70, 2563–2566. doi: 10.1073/pnas.70.9.2563

Roghanian, M., Semsey, S., Løbner-Olesen, A., and Jalalvand, F. (2019). (p)ppGpp-mediated stress response induced by defects in outer membrane biogenesis and ATP production promotes survival in *Escherichia coli*. *Sci. Rep.* 9:2934. doi: 10.1038/s41598-019-39371-3

Ronneau, S., Caballero-Montes, J., Coppine, J., Mayard, A., Garcia-Pino, A., and Hallez, R. (2019). Regulation of (p)ppGpp hydrolysis by a conserved archetypal regulatory domain. *Nucleic Acids Res.* 47, 843–854. doi: 10.1093/nar/gky1201

Ronneau, S., and Hallez, R. (2019). Make and break the alarmone: regulation of (p)ppGpp synthetase/hydrolase enzymes in bacteria. *FEMS Microbiol. Rev.* 43, 389–400. doi: 10.1093/femsre/fuz009

Ross, W., Sanchez-Vazquez, P., Chen, A. Y. Y., Lee, J. -H. H., Burgos, H. L. L., and Gourse, R. L. L. (2016). ppGpp binding to a site at the RNAP-DksA interface accounts for its dramatic effects on transcription initiation during the stringent response. *Mol. Cell* 62, 811–823. doi: 10.1016/j.molcel.2016.04.029

Ruwe, M., Kalinowski, J., and Persicke, M. (2017). Identification and functional characterization of small alarmone synthetases in Corynebacterium glutamicum. *Front. Microbiol.* 8:1601. doi: 10.3389/fmicb.2017.01601

Rymer, R. U., Solorio, F. A., Tehranchi, A. K., Chu, C., Corn, J. E., Keck, J. L., et al. (2012). Binding mechanism of metal·NTP substrates and stringent-response alarmones to bacterial DnaG-type primases. *Structure* 20, 1478–1489. doi: 10.1016/j.str.2012.05.017

Sanchez-Vazquez, P., Dewey, C. N., Kitten, N., Ross, W., and Gourse, R. L. (2019). Genome-wide effects on *Escherichia coli* transcription from ppGpp binding to its two sites on RNA polymerase. *Proc. Natl. Acad. Sci. U. S. A.* 116, 8310–8319. doi: 10.1073/pnas.1819682116

Sarubbi, E., Rudd, K. E., and Cashel, M. (1988). Basal ppGpp level adjustment shown by new spoT mutants affect steady state growth rates and rrnA ribosomal promoter regulation in *Escherichia coli*. *Mol. Gen. Genet.* 213, 214–222. doi: 10.1007/BF00339584

Schäfer, H., Beckert, B., Frese, C. K., Steinchen, W., Nuss, A. M., Beckstette, M., et al. (2020). The alarmones (p)ppGpp are part of the heat shock response of Bacillus subtilis. *PLoS Genet.* 16:e1008275. doi: 10.1371/journal.pgen.1008275

Schneider, D. A., and Gourse, R. L. (2004). Relationship between growth rate and ATP concentration in *Escherichia coli*: a bioassay for available cellular ATP. *J. Biol. Chem.* 279, 8262–8268. doi: 10.1074/jbc.M311996200

Shyp, V., Tankov, S., Ermakov, A., Kudrin, P., English, B. P., Ehrenberg, M., et al. (2012). Positive allosteric feedback regulation of the stringent response enzyme RelA by its product. *EMBO Rep.* 13, 835–839. doi: 10.1038/embor.2012.106

Sinha, A. K., Winther, K. S., Roghanian, M., and Gerdes, K. (2019). Fatty acid starvation activates RelA by depleting lysine precursor pyruvate. *Mol. Microbiol.* 112, 1339–1349. doi: 10.1111/mmi.14366

Sobala, M., Bruhn-Olszewska, B., Cashel, M., and Potrykus, K. (2019). Methylobacterium extorquens RSH enzyme synthesizes (p)ppGpp and pppApp in vitro and in vivo, and leads to discovery of pppApp synthesis in *Escherichia coli*. *Front. Microbiol.* 10:859. doi: 10.3389/fmicb.2019.00859

Sørensen, M. A., Fehler, A. O., and Lo Svenningsen, S. (2018). Transfer RNA instability as a stress response in *Escherichia coli*: rapid dynamics of the tRNA pool as a function of demand. *RNA Biol.* 15, 586–593. doi: 10.1080/15476286.2017.1391440

Steinchen, W., Vogt, M. S., Altegoer, F., Giammarinaro, P. I., Horvatek, P., Wolz, C., et al. (2018). Structural and mechanistic divergence of the small (p)ppGpp synthetases RelP and RelQ. *Sci. Rep.* 8:2195. doi: 10.1038/s41598-018-20634-4

Stott, K. V., Wood, S. M., Blair, J. A., Nguyen, B. T., Herrera, A., Perez Mora, Y. G., et al. (2015). (p)ppGpp modulates cell size and the initiation of DNA replication in Caulobacter crescentus in response to a block in lipid biosynthesis. *Microbiology* 161, 553–564. doi: 10.1099/mic.0.000032

Sulthana, S., Basturea, G. N., and Deutscher, M. P. (2016). Elucidation of pathways of ribosomal RNA degradation: an essential role for RNase E. *RNA* 22, 1163–1171. doi: 10.1261/rna.056275.116

Sun, D., Lee, G., Lee, J. H., Kim, H. Y., Rhee, H. W., Park, S. Y., et al. (2010). A metazoan ortholog of SpoT hydrolyzes ppGpp and functions in starvation responses. *Nat. Struct. Mol. Biol.* 17, 1188–1194. doi: 10.1038/nsmb.1906

Svenningsen, S. L., Kongstad, M., Stenum, T. S., Muñoz-Gomez, A. J., and Sørensen, M. A. (2016). Transfer RNA is highly unstable during early amino acid starvation in *Escherichia coli*. *Nucleic Acids Res.* 45, 793–804. doi: 10.1093/nar/gkw1169

Svenningsen, M. S., Veress, A., Harms, A., Mitarai, N., and Semsey, S. (2019). Birth and resuscitation of (p)ppGpp induced antibiotic tolerant persister cells. *Sci. Rep.* 9:6056. doi: 10.1038/s41598-019-42403-7

Sy, J., and Lipmann, F. (1973). Identification of the synthesis of guanosine tetraphosphate (MS I) as insertion of a pyrophosphoryl group into the 3'-position in guanosine 5'-diphosphate. *Proc. Natl. Acad. Sci. U. S. A.* 70, 306–309. doi: 10.1073/pnas.70.2.306

Takada, H., Roghanian, M., Murina, V., Dzhygyr, I., Murayama, R., Akanuma, G., et al. (2020). The C-terminal RRM/ACT domain is crucial for fine-tuning the activation of 'long' RelA-SpoT homolog enzymes by ribosomal complexes. *Front. Microbiol.* 11:277. doi: 10.3389/fmicb.2020.00277

Tamman, H., Van Nerom, K., Takada, H., Vandenberk, N., Scholl, D., Polikanov, Y., et al. (2020). A nucleotide-switch mechanism mediates opposing catalytic activities of Rel enzymes. *Nat. Chem. Biol.* 16, 834–840. doi: 10.1038/s41589-020-0520-2

Travers, A. A. (1980). Promoter sequence for stringent control of bacterial ribonucleic acid synthesis. *J. Bacteriol.* 141, 973–976. doi: 10.1128/JB.141.2.973-976.1980

Travers, A., and Muskhelishvili, G. (2015). DNA structure and function. *FEBS J.* 282, 2279–2295. doi: 10.1111/febs.13307

Traxler, M. F., Summers, S. M., Nguyen, H. -T., Zacharia, V. M., Hightower, G. A., Smith, J. T., et al. (2008). The global, ppGpp-mediated stringent response to amino acid starvation in *Escherichia coli*. *Mol. Microbiol.* 68, 1128–1148. doi: 10.1111/j.1365-2958.2008.06229.x

Traxler, M. F., Zacharia, V. M., Marquardt, S., Summers, S. M., Nguyen, H. -T., Stark, S. E., et al. (2011). Discretely calibrated regulatory loops controlled by ppGpp partition gene induction across the "feast to famine" gradient in *Escherichia coli*. *Mol. Microbiol.* 79, 830–845. doi: 10.1111/j.1365-2958.2010.07498.x

Trinquier, A., Ulmer, J. E., Gilet, L., Figaro, S., Hammann, P., Kuhn, L., et al. (2019). tRNA maturation defects lead to inhibition of rRNA processing via synthesis of (p)ppGpp. *Mol. Cell* 74, 1227.e3–1238.e3. doi: 10.1016/j.molcel.2019.03.030

Vercruysse, M., Fauvart, M., Jans, A., Beullens, S., Braeken, K., Cloots, L., et al. (2011). Stress response regulators identified through genome-wide transcriptome analysis of the (p) ppGpp-dependent response in rhizobium etli. *Genome Biol.* 12:R17. doi: 10.1186/gb-2011-12-2-r17

Vinella, D., Albrecht, C., Cashel, M., and D'Ari, R. (2005). Iron limitation induces SpoT-dependent accumulation of ppGpp in *Escherichia coli*. *Mol. Microbiol.* 56, 958–970. doi: 10.1111/j.1365-2958.2005.04601.x

Vinella, D., Potrykus, K., Murphy, H., and Cashel, M. (2012). Effects on growth by changes of the balance between GreA, GreB, and DksA suggest mutual competition and functional redundancy in *Escherichia coli*. *J. Bacteriol.* 194, 261–273. doi: 10.1128/JB.06238-11

Vinogradovaid, D. S., Zegarraid, V., Maksimovaid, E., Nakamotoid, J. A., Kasatskyid, P., Paleskavaid, A., et al. (2020). How the initiating ribosome copes with ppGpp to translate mRNAs. *PLoS Biol.* 18:e3000593. doi: 10.1371/journal.pbio.3000593

Wang, B., Dai, P., Ding, D., Del Rosario, A., Grant, R. A., Pentelute, B. L., et al. (2019). Affinity-based capture and identification of protein effectors of the growth regulator ppGpp. *Nat. Chem. Biol.* 15, 141–150. doi: 10.1038/s41589-018-0183-4

Wang, B., Grant, R. A., and Laub, M. T. (2020). ppGpp coordinates nucleotide and amino-acid synthesis in *E. coli* during starvation. *Mol. Cell*, doi: 10.1016/j.molcel.2020.08.005 [Epub ahead of print]

Wang, J. D., Sanders, G. M., and Grossman, A. D. (2007). Nutritional control of elongation of DNA replication by (p)ppGpp. *Cell* 128, 865–875. doi: 10.1016/j.cell.2006.12.043

Weiss, L. A., and Stallings, C. L. (2013). Essential roles for *Mycobacterium tuberculosis* rel beyond the production of (p)ppGpp. *J. Bacteriol.* 195, 5629–5638. doi: 10.1128/JB.00759-13

Wendrich, T. M., Blaha, G., Wilson, D. N., Marahiel, M. A., and Nierhaus, K. H. (2002). Dissection of the mechanism for the stringent factor RelA. *Mol. Cell* 10, 779–788. doi: 10.1016/S1097-2765(02)00656-1

Wendrich, T. M., and Marahiel, M. A. (1997). Cloning and characterization of a relA/spoT homologue from *Bacillus subtilis*. *Mol. Microbiol.* 26, 65–79. doi: 10.1046/j.1365-2958.1997.5511919.x

Wexselblatt, E., Oppenheimer-Shaanan, Y., Kaspy, I., London, N., and Schueler-Furman, O. (2012). Relacin, a novel antibacterial agent targeting the stringent response. *PLoS Pathog.* 8:e1002925. doi: 10.1371/journal.ppat.1002925

Winkelman, J. T., Chandrangsu, P., Ross, W., and Gourse, R. L. (2016). Open complex scrunching before nucleotide addition accounts for the unusual transcription start site of *E. coli* ribosomal RNA promoters. *Proc. Natl. Acad. Sci. U. S. A.* 113, E1787–E1795. doi: 10.1073/pnas.1522159113

Winther, K. S., Roghanian, M., and Gerdes, K. (2018). Activation of the stringent response by loading of RelA-tRNA complexes at the ribosomal A-site. *Mol. Cell* 70, 95.e4–105.e4. doi: 10.1016/j.molcel.2018.02.033

Xiao, H., Kalman, M., Ikehara, K., Zemel, S., Glaser, G., and Cashel, M. (1991). Residual guanosine 3', 5'-bispyrophosphate synthetic activity of reZA null mutants can be eliminated by spoT null mutations. *J. Biol. Chem.* 266, 5980–5990.

Yang, N., Xie, S., Tang, N. Y., Choi, M. Y., Wang, Y., and Watt, R. M. (2019). The Ps and Qs of alarmone synthesis in *Staphylococcus aureus*. *PLoS One* 14:e0213630. doi: 10.1371/journal.pone.0213630

Yuzenkova, Y., Roghanian, M., and Zenkin, N. (2012). Multiple active centers of multi-subunit RNA polymerases. *Transcription* 3, 115–118. doi: 10.4161/trns.19887

Zenkin, N., and Yuzenkova, Y. (2015). New insights into the functions of transcription factors that bind the RNA polymerase secondary channel. *Biomol. Ther.* 5, 1195–1209. doi: 10.3390/biom5031195

Zhang, Y., Zborníková, E., Rejman, D., and Gerdes, K. (2018). Novel (p)ppGpp binding and metabolizing proteins of *Escherichia coli*. *mBio* 9, e02188–e02217. doi: 10.1128/mBio.02188-17

Zhu, M., and Dai, X. (2019). Growth suppression by altered (p)ppGpp levels results from non-optimal resource allocation in *Escherichia coli*. *Nucleic Acids Res.* 47, 4684–4693. doi: 10.1093/nar/gkz211

Conflict of Interest: The authors declare that the research was conducted in the absence of any commercial or financial relationships that could be construed as a potential conflict of interest.

frontiers in Microbiology

REVIEW
published: 09 October 2020
doi: 10.3389/fmicb.2020.563944

(p)ppGpp Metabolism and Antimicrobial Resistance in Bacterial Pathogens

Bhabatosh Das[1] and Rupak K. Bhadra[2]**

[1]*Infection and Immunology Division, Translational Health Science and Technology Institute (THSTI), Faridabad, India,* [2]*Infectious Diseases and Immunology Division, Council of Scientific and Industrial Research-Indian Institute of Chemical Biology (CSIR-IICB), Kolkata, India*

Single cell microorganisms including pathogens relentlessly face myriads of physicochemical stresses in their living environment. In order to survive and multiply under such unfavorable conditions, microbes have evolved with complex genetic networks, which allow them to sense and respond against these stresses. Stringent response is one such adaptive mechanism where bacteria can survive under nutrient starvation and other related stresses. The effector molecules for the stringent response are guanosine-5'-triphosphate 3'-diphosphate (pppGpp) and guanosine-3', 5'-bis(diphosphate) (ppGpp), together called (p)ppGpp. These effector molecules are now emerging as master regulators for several physiological processes of bacteria including virulence, persistence, and antimicrobial resistance. (p)ppGpp may work independently or along with its cofactor DksA to modulate the activities of its prime target RNA polymerase and other metabolic enzymes, which are involved in different biosynthetic pathways. Enzymes involved in (p)ppGpp metabolisms are ubiquitously present in bacteria and categorized them into three classes, i.e., canonical (p)ppGpp synthetase (RelA), (p)ppGpp hydrolase/synthetase (SpoT/Rel/RSH), and small alarmone synthetases (SAS). While RelA gets activated in response to amino acid starvation, enzymes belonging to SpoT/Rel/RSH and SAS family can synthesize (p)ppGpp in response to glucose starvation and several other stress conditions. In this review, we will discuss about the current status of the following aspects: (i) diversity of (p)ppGpp biosynthetic enzymes among different bacterial species including enteropathogens, (ii) signals that modulate the activity of (p)ppGpp synthetase and hydrolase, (iii) effect of (p)ppGpp in the production of antibiotics, and (iv) role of (p)ppGpp in the emergence of antibiotic resistant pathogens. Emphasis has been given to the cholera pathogen *Vibrio cholerae* due to its sophisticated and complex (p)ppGpp metabolic pathways, rapid mutational rate, and acquisition of antimicrobial resistance determinants through horizontal gene transfer. Finally, we discuss the prospect of (p)ppGpp metabolic enzymes as potential targets for developing antibiotic adjuvants and tackling persistence of infections.

Keywords: bacterial pathogen, antibiotic resistance, *spoT*, *relA*, stringent response, (p)ppGpp, alarmone

OPEN ACCESS

Edited by:
Michael Cashel, Eunice Kennedy Shriver National Institute of Child Health and Human Development (NICHD), United States

Reviewed by:
Agnieszka Szalewska-Pałasz, University of Gdansk, Poland
Rajendran Harinarayanan, Centre for DNA Fingerprinting and Diagnostics (CDFD), India

****Correspondence:***
Bhabatosh Das
bhabatosh@thsti.res.in
Rupak K. Bhadra
rupakbhadra@iicb.res.in

Specialty section:
This article was submitted to Microbial Physiology and Metabolism, a section of the journal Frontiers in Microbiology

Received: *20 May 2020*
Accepted: *09 September 2020*
Published: *09 October 2020*

Citation:
Das B and Bhadra RK (2020) (p)ppGpp Metabolism and Antimicrobial Resistance in Bacterial Pathogens. Front. Microbiol. 11:563944. doi: 10.3389/fmicb.2020.563944

INTRODUCTION

Living organisms from three domains of life (bacteria, archaea, and eukarya) use a number of purine derivatives like guanosine pentaphosphate (pppGpp), guanosine tetraphosphate (ppGpp), cyclic di-GMP (c-di-GMP), etc., as intracellular signaling molecules. Bacteria use these small molecules to monitor intra- and extracellular environmental conditions and modulate their growth and multiplications in response to the availability of nutrients and related local cues (Potrykus and Cashel, 2008; Tozawa and Nomura, 2011; Hauryliuk et al., 2015). Over 50 years ago, Cashel identified the small molecule alarmones, pppGpp, and ppGpp (**Figure 1**), collectively known as (p)ppGpp, as the key players for the bacterial stringent response under nutrient limitations and other stressful conditions (Cashel, 1969). Later several studies revealed that the effector molecules of stringent response (p)ppGpp modulates bacterial multiplication rate and survival during nutrient limitations, exposure to antimicrobial compounds, xenobiotics, and osmotic stress (Hauryliuk et al., 2015; Irving and Corrigan, 2018). The alarmone (p)ppGpp is the derivatives of guanosine nucleosides, where guanosine triphosphate (GTP) pyrophosphokinases (RelA/SpoT/RSH/RelV/RelP/RelQ) transfer a pyrophosphate moiety from ATP to the 3'-OH position of GTP/guanosine diphosphate (GDP; Cashel, 1969; Gaca et al., 2015; Ronneau and Hallez, 2019). It has been shown that the intracellular level of (p)ppGpp is critical for modulation of different bacterial physiological processes mainly by regulating the activities of RNA polymerase (RNAP), DNA primase (DnaG), growth rate, and several other metabolic enzymes in *Escherichia coli* (Potrykus and Cashel, 2008; Potrykus et al., 2011; Hauryliuk et al., 2015; Zhang et al., 2018; Wang et al., 2019). In addition, (p)ppGpp also modulates bacterial growth and viability indirectly through depletion of cellular level of guanosine and adenosine nucleotides or by repressing transcription of genes required for active growth (Kriel et al., 2012). In nutrient rich growth condition, the basal cellular level of (p)ppGpp in *E. coli* is less than 0.2 mM (Mechold et al., 2013). Upon induction of stress, the level of (p)ppGpp may increase from 10 to 100-fold depending upon the type of stress and the enzymes involved in the biosynthesis of different biomolecules (Kalia et al., 2013). Elevated level of (p)ppGpp may work independently or synergistically with the transcriptional factor DksA, an RNAP binding small transcriptional factor (Paul et al., 2004). It was discovered earlier that the *dksA* gene product suppresses temperature-sensitive growth and filamentation of a *dnaK* deletion mutant of *E. coli* (Kang and Craig, 1990). Later, it has been established that both DksA and (p)ppGpp biosynthetic enzymes are crucial for the stringent response in Gram-negative bacteria since, Δ*dksA* and Δ*relA*Δ*spoT* mutants exhibit similar phenotypes (Gourse et al., 2018). In addition, overexpression of DksA can compensate the loss of (p)ppGpp in regulating *uspA*, *livJ*, and *rrnBP1* (Magnusson et al., 2007). However, synergistic functions are not universal. DksA and (p)ppGpp can work independently or may have opposite effects on one another. For example, *E. coli* Δ*dksA* cells aggregate more efficiently compared to its isogenic wild-type strain. Similarly, overexpression of DksA decreases the adhesion of wild-type cells. In contrast, *E. coli* Δ*relA*Δ*spoT* mutant called (p)ppGpp^0 cells failed to sediment in a similar experimental condition and the adhesion phenotype is not affected upon overexpression of DksA (Magnusson et al., 2007). In addition, transcription of the *argX* operon containing *argX*, *hisR*, *leuT*, and *proM* genes is activated by DksA but inhibited in the presence of (p)ppGpp and DksA (Lyzen et al., 2016).

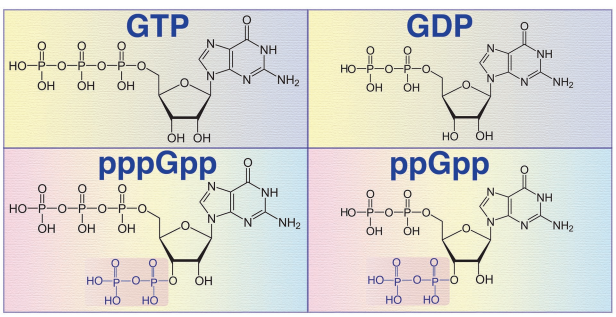

FIGURE 1 | Chemical structures of guanosine triphosphate (GTP), guanosine diphosphate (GDP), guanosine pentaphosphate (pppGpp), and guanosine tetraphosphate (ppGpp) molecules. The pyrophosphate group of pppGpp and ppGpp at the 3' hydroxyl (OH) position is transferred by the (p)ppGpp synthetase from another purine nucleotide ATP.

Other than the function in stringent response, (p)ppGpp also plays important roles in modulating bacterial virulence gene expression (Dalebroux et al., 2010; and the references therein), sporulation (Crawford and Shimkets, 2000), biofilm formation (He et al., 2012), antibiotic resistance (Wu et al., 2010; Strugeon et al., 2016), tolerance (Kim et al., 2018), and persistence (Hauryliuk et al., 2015; Harms et al., 2016). In order to access host cell nutrients, colonization on the cell surface and detachment from mucosal surface, pathogenic bacteria use (p)ppGpp signaling networks to modulate expression of genes those are part of secretion systems, flagellar components, adhesins, and serine/metallo proteases (Dalebroux et al., 2010; Pal et al., 2012; and reference therein). Regulation of spore formation in certain bacteria mediated by (p)ppGpp through complex array of regulatory circuits that sense the environmental signals through altered levels of intracellular (p)ppGpp leading to rapid change in the expression of relevant genes involved in spore formation (Crawford and Shimkets, 2000). It has been shown that the stringent response positively modulates biofilm formation in *E. coli*, *Vibrio cholerae*, and *Streptococcus mutans* (He et al., 2012; Teschler et al., 2015; Strugeon et al., 2016). In *Pseudomonas aeruginosa*, the antibiotic tolerance of nutrient-limited and biofilm dwelling cells is mediated by active responses to starvation where stringent response plays a crucial role (Nguyen et al., 2011). This starvation mediated protective mechanism in *P. aeruginosa* has been shown to be linked with tolerance under reduced level of oxidative stress in bacterial cells and, therefore, inactivating this protective mechanism sensitized biofilms by several orders of magnitude to different classes of antibiotics allowing enhanced efficacy of antibiotic treatment in experimental infection in an animal model (Nguyen et al., 2011).

From various studies, it appears that emergence of instant antibiotic resistant clones in a susceptible bacterial population solely depends on: (i) target modifications, (ii) reduced accessibility of antibiotics to the target, (iii) decreased effective concentration of antibiotic by reducing the membrane permeability or by increasing efflux activity, and (iv) acquisition of antibiotic resistance genes from other microbial species (Gaca et al., 2015; Verma et al., 2019; Das et al., 2020; Jung et al., 2020; Pant et al., 2020). A recent study has shown that the expression levels of ~300 and ~400 genes (total ~700 genes) are upregulated and downregulated, respectively, within 5 min upon induction of (p)ppGpp (Sanchez-Vazquez, 2018). In *Enterococcus faecalis* (p)ppGpp^0 cells, it has been found that the genes and pathways involved in pyruvate production and heterolactic fermentation are induced (Gaca et al., 2013). More importantly, (p)ppGpp induced RpoS expression, the stress response sigma factor, may lead to overproduction of error prone DNA polymerase IV (Pol IV; Storvik and Foster, 2010). In addition to antibiotic resistance, (p)ppGpp also reduces efficacy of antibiotics by inducing antibiotic tolerant persister cell formation in Gram-negative and Gram-positive bacterial populations (Korch et al., 2003; Kaspy et al., 2013).

As of 5th August 2020, more than 27,936 articles and reports are available in the National Center for Biotechnology Information[1] on the stringent response in bacteria. Considering this vast literature, however, the present review will focus on: (i) metabolisms, biosynthetic enzymes, signals, interaction partners, and targets of (p)ppGpp; (ii) effect of (p)ppGpp in antibiotic production; (iii) role of (p)ppGpp in antibiotic resistance in bacterial pathogens; and (iv) (p)ppGpp biosynthetic enzymes as potential targets for developing antibiotic adjuvants.

BODY

(p)ppGpp Metabolism in Bacteria

Principally, (p)ppGpp homeostasis in bacterial cells depends on the availability and activity of the four classes of enzymes: (i) multi-domain bifunctional (p)ppGpp synthetase-hydrolase, (ii) multi-domain monofunctional (p)ppGpp synthetase, (iii) short alarmone synthetase (SAS), and (iv) short alarmone hydrolase (SAH), also called RelH (**Figure 2**). Bifunctional (p)ppGpp synthetase-hydrolase enzymes (Rel/RSH/SpoT) can modulate their conformation depending on the environmental conditions with the help of their regulatory domains and stimulate their GTP/GDP pyrophosphokinase or pyrophosphohydrolase activities to synthesize or hydrolyze (p)ppGpp, respectively (Ronneau and Hallez, 2019). In the presence of (p)ppGpp synthetase, hydrolase activity of the bifunctional enzyme is essential for viability (Xiao et al., 1991; Das and Bhadra, 2008). However, bacterial cells can survive in the absence of (p)ppGpp synthetase activity in nutrient rich environments but it is essential for viability in nutrient limited medium (Xiao et al., 1991). Enzymes with (p)ppGpp synthetase-hydrolase activities are widely conserved across bacterial phyla (Atkinson et al., 2011).

[1]https://www.ncbi.nlm.nih.gov/

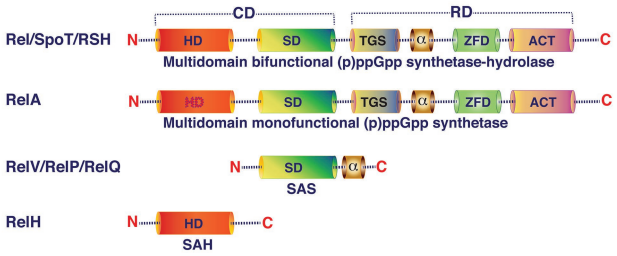

FIGURE 2 | Schematic representation of the domain organization of (p)ppGpp synthetase/hydrolase family of proteins. Bifunctional long multidomain (p)ppGpp synthetase-hydrolase and monofunctional long multidomain (p)ppGpp synthetase enzymes are composed of two regions: (i) N-terminal catalytic domain (CD) and (ii) C-terminal regulatory domain (RD). Both synthetase and hydrolase domains (SD and HD, respectively) are functional in bifunctional enzymes (Rel/RSH/SpoT). In monofunctional multidomain, (p)ppGpp synthetase enzyme (RelA) hydrolase activity is lost due to accumulation of spontaneous mutations in the catalytic residues. The C-terminal regulatory region of the multidomain protein contains TGS domain (ThrRS, GTPase, and SpoT), conserved α helical domain, ZFD domain (zinc-finger or conserved cysteine domain), and ACT (aspartate kinase, chorismate, and TyrA) RNA recognition motif. The small alarmone synthetase (SAS) enzyme (RelV/RelP/RelQ) contains SD and a small oligomeric α-domain. The RelH/small alarmone hydrolase (SAH) contains only the HD.

Nevertheless, presence of (p)ppGpp synthetase-hydrolase domain containing proteins has also been reported in eukarya including *Arabidopsis thaliana*, *Nicotiana tabacum*, and *Chlamydomonas reinhardtii* (Sun et al., 2010; Ito et al., 2012). In Firmicutes, (p)ppGpp synthetase-hydrolase domain containing enzymes are the major source of stringent response effector molecules during amino acid, glucose, and fatty acid starvations (Wolz et al., 2010). In contrast, several Proteobacteria use the bifunctional (p)ppGpp synthetase-hydrolase enzyme for alarmone synthesis during glucose and fatty acid starvations but not during amino acid starvation (Xiao et al., 1991; Cashel, 1969). Upon sensing nutrient depletions or other stress conditions, Rel/RSH/SpoT catalyze pyrophosphorylation of GDP or GTP at the 3' hydroxyl (OH) position using ATP as pyrophosphate donor (**Figure 3**). Once reprogramming of cellular functions from vegetative to survival mode is accomplished with the help of elevated intracellular levels of (p)ppGpp, the bifunctional Rel/RSH enzyme then may change its conformation from (p)ppGpp synthetase-ON/hydrolase-OFF to (p)ppGpp hydrolase-ON/synthetase-OFF state to reduce the (p)ppGpp level to restore again the gene expression and metabolic functions of enzymes associated with growth and multiplication under favorable conditions (Hogg et al., 2004). Although the exact molecular mechanism is unknown, but it has been proposed that the regulatory domains located at the carboxy terminal domain of Rel/RSH/SpoT play important roles in the modulation of synthetase and hydrolase functions of the bifunctional (p)ppGpp synthetase-hydrolase enzymes (Angelini et al., 2012).

Monofunctional (p)ppGpp synthetase, the enzyme that synthesizes (p)ppGpp only, further subdivided into two major sub-classes based on their size and domain organization: (i) long multi-domain monofunctional (p)ppGpp synthetase and (ii) short monodomain monofunctional (p)ppGpp synthetase

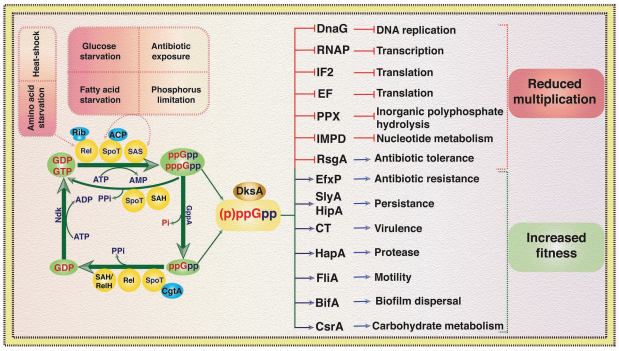

FIGURE 3 | An overview of signaling, metabolism, and effect of (p)ppGpp in virulence, antibiotic resistance, and other cellular processes in bacteria. GDP and GTP are converted to (p)ppGpp during stress conditions or upon exposure to xenobiotics due to transfer of a pyrophosphate moiety from ATP to the 3'-OH position of ribosugar of guanosine nucleotide. GTP pyrophospho kinase activity of Rel, SpoT, and SAS can mediate the transfer of pyrophosphate to GTP or GDP depending on the stress signaling and activity of other cellular proteins like acyl carrier protein (ACP) and functional state of protein synthesis machinery, i.e., ribosome (Rib). pppGpp can be converted to ppGpp due to phosphatase activity of GppA. SpoT, Rel, and SAH can hydrolyze the pyrophosphate moiety from 3'-OH position of pppGpp and ppGpp and generate GTP or GDP, respectively. Guanine nucleotide binding protein of the Obg/GTP1 subfamily CgtA induces (p)ppGpp hydrolase activity of SpoT. Nucleoside diphosphate kinase (Ndk) converts GDP to GTP using ATP as phosphate donor. Elevated intracellular level of (p)ppGpp independently or in conjunction with transcriptional factor DksA regulates several cellular processes including DNA replication, transcription, protein biosynthesis, carbohydrate metabolism, virulence, motility, antibiotic resistance, and biofilms formation. (p)ppGpp regulates several proteins involved in nucleotide metabolism, persistence, antibiotic resistance, etc., however, for simplicity, a representative protein for each case is depicted here and more details can be found in the references cited. SAS, small alarmone synthase; SAH, small alarmone hydrolase; GppA, guanosine-5'-triphosphate, 3'-diphosphate pyrophosphatase; DnaG, DNA primase; RNAP, RNA polymerase; IF2, initiation factor 2; EF, elongation factor; PPX, exopolyphosphatase; IMPD, inosine monophosphate dehydrogenase; RsgA, small ribosomal subunit biogenesis GTPase; EfxP, efflux pumps; SlyA, transcriptional regulator of *Salmonella enterica*; HipA, toxin component of *Escherichia coli* TA module; CT, cholera toxin; HapA, hemagglutinin protease; FliA, flagella regulatory sigma factor; BifA, biofilm formation protein; CsrA, carbon storage regulator (Dalebroux et al., 2010; Ronneau and Hallez, 2019; and the references therein).

also known as SAS (**Figure 2**). Presence of multi-domain monofunctional (p)ppGpp synthetase (for example, RelA) is common in Proteobacteria. RelA is a ribosome-associated protein, which recognizes stalled ribosomes due to presence of uncharged tRNA in the A-site of ribosome during amino acid starvation. It has been reported that the large subunit ribosomal protein L11 is crucial for the activation of (p)ppGpp synthetase activity of RelA (Parker et al., 1976; Cashel et al., 1996). Wendrich et al. (2002) initially proposed a "hopping model" for RelA mediated (p)ppGpp synthesis during amino acid starved condition. According to this model the RelA molecule hops from ribosome to ribosome to synthesize one (p)ppGpp molecule per dissociation event. Later, English et al. (2011) using single-molecule tracking methodology proposed an "extended hopping" model for RelA mediated (p)ppGpp synthesis during amino acid starvation. According to the extended hopping model several molecules of (p)ppGpp are synthesized by the free but enzymatically active RelA upon its dissociation from ribosomes. However, findings of Li et al. (2016) contradict the extended hopping model and they proposed a "short hopping time" model for RelA mediated (p)ppGpp synthesis during amino acid starvation. According to this model, RelA synthesizes (p)ppGpp while bound to the 70S ribosomes. Currently, however, the reasons behind these differences are not clear. Although amino acid starvation is the major cause of activation of (p)ppGpp synthetase function of RelA, heat shock can also induce its synthetase activity in *E. coli* (Gallant et al., 1977; English et al., 2011). Short monodomain monofunctional (p)ppGpp synthetases are widely distributed among Firmicutes (*Bacillus subtilis*, *S. mutans*, *E. faecalis*, etc.), Actinobacteria (*Mycobacterium smegmatis*), Proteobacteria (*V. cholerae*), Archaea (*Methanosarcina acetivorans*), and Eukarya (*Dictyostelium discoideum*) (Lemos et al., 2007; Nanamiya et al., 2008; Das et al., 2009; Atkinson et al., 2011; Murdeshwar and Chatterji, 2012; and the references therein). Unlike RelA, the SAS sub-class can recognize glucose, fatty acids, and other starvations and catalyze (p)ppGpp synthesis by transferring a pyrophosphate moiety from ATP to the 3'-OH position of GTP or GDP probably following same mechanistic pathways like RelA/RSH/Rel enzymes (**Figure 3**). Since SAS enzymes are devoid of any additional regulatory domain, their regulation for (p)ppGpp synthesis activity may primarily be dependent at the gene expression level (Dasgupta et al., 2014; Ronneau and Hallez, 2019) and needs further investigation.

The monodomain monofunctional (p)ppGpp hydrolase, also known as small alarmone hydrolase (SAH), was initially identified and functionally characterized in the metazoa as an ortholog of bacterial SpoT (Sun et al., 2010). Like multi-domain bacterial (p)ppGpp hydrolases, the metazoan ortholog, called Mesh1, contains an active site for (p)ppGpp hydrolysis and it carries the conserved His-Asp box motif for binding with Mn^{2+}. Later *in silico* analyses of more than 1,000 genome sequences identified seven subgroups of SAH (Atkinson et al., 2011). Recently, an SAH from *Corynebacterium glutamicum* has functionally been characterized and designated RelH (Ruwe et al., 2018). However, the regulatory signals, interaction partners, and importance of SAH in either kingdom are not clear. Thus, more intense research on these aspects of SAH is needed.

Mechanism of Actions of (p)ppGpp

Accumulation of (p)ppGpp in the cytosol due to nutrient limitations or other stress conditions leads to change in bacterial cellular physiology by: (i) reprogramming of transcription of rRNA operons, ribosomal protein encoding genes, and others by regulating RNAP activity, (ii) stalling DNA replication by inhibiting DnaG, and (iii) modulating metabolic pathways by regulating activity of the associated enzymes (**Figure 3**). Single or multiple molecules of (p)ppGpp binds to its targets and modulate their activity independently or synergistically with its functional partner DksA. In *E. coli*, (p)ppGpp binds to at least two sites of RNAP enzyme (Ross et al., 2013). Crystal structure of RNAP holoenzyme showed that (p)ppGpp binds to the cleft surrounded by the α, β', and ω subunits (site 1) and

also at an interface of RNAP and DksA (site 2). Binding of (p)ppGpp induces allosteric changes in RNAP, which either affects its catalytic activity by modulating the Mg^{+2} nucleotidyl transfer efficacy or by reducing stability of RNAP-promoter complex (Kanjee et al., 2012). DksA binds to the secondary channel of RNAP and can potentiate the effects (p)ppGpp by modulating RNAP-promoter complex stability (Perederina et al., 2004). In *B. subtilis*, (p)ppGpp regulates rRNA and ribosomal protein encoding genes transcription by interfering (p)ppGpp homeostasis. Elevated levels of (p)ppGpp inhibit hypoxanthine phosphoribosyl transferase (HprT) and GMP kinase (Gmk) activity in Firmicutes and reduce the intracellular GTP pool (**Figure 3**). HprT is essential for the conversion of hypoxanthine to IMP and guanine to GMP, while Gmk catalyzes synthesis of GDP from GMP. Both the enzymes are crucial for GTP biosynthesis in *B. subtilis* and other Firmicutes (Denapoli et al., 2013). It has been shown recently that in Gram-positive bacteria (p)ppGpp may bind with several ribosome-associated GTPases like RsgA, RbgA, Era, and HflX leading to strong inhibition of their activities (Corrigan et al., 2016). More recently, Zhang et al. (2018) have also reported similar target proteins, namely, RsgA, Era, HflX, etc., of (p)ppGpp in *E. coli*. However, the exact biochemical mechanism by which (p)ppGpp can inhibit GTPase activity is yet to be fully elucidated. Nonetheless, the findings clearly point toward the critical roles of (p)ppGpp in controlling ribosomal assembly/biogenesis in bacterial stress survival.

It is well established that (p)ppGpp drastically reduces bacterial multiplication by inhibiting initiation and elongation of DNA replication (Wang et al., 2007). It has been shown that (p)ppGpp binds to the RNA primer biosynthesis enzyme primase (DnaG) and directly inhibits its primer biosynthesis activity, which is essential for initiation of DNA replication (**Figure 3**). Initial finding hypothesized that the effect of (p)ppGpp in DNA replication is mostly restricted at the *oriC* region during initiation of DNA replication (Gourse and Keck, 2007). However, subsequent studies demonstrated that the arrest of DNA replication occurs throughout the chromosome during stringent response. Although elevated levels (>10–20-fold) of (p)ppGpp is detrimental to bacterial growth, complete lack of (p)ppGpp, called (p)ppGpp^0 phenotype, render several bacterial species auxotrophic to different amino acids, defective in cell division, deficient in protease production, and poor survival upon exposure to xenobiotics (Hauryliuk et al., 2015). More importantly, increasing numbers of reports suggest that elevated level of (p)ppGpp reduces efficacy of several clinically important antibiotics, while (p)ppGpp^0 strains are susceptible to numerous antibiotics with reduced minimum inhibitory concentration (MIC; Gaca et al., 2013; Kamarthapu et al., 2016; Hobbs and Boraston, 2019 and the references therein).

Effect of (p)ppGpp in the Production of Antibiotics

Production of antibiotics in Actinobacteria, one of the most diverse groups of Gram-positive bacteria that produce most of the clinically used antibiotics, is influenced by the availability of nutrients and external signals. Such factors work either by modulating the expression level of antibiotic biosynthetic gene clusters or through pleiotropic regulators, which play important roles in bacterial intracellular signaling (van der Heul et al., 2018). Role of (p)ppGpp in antibiotic production has been demonstrated both in environmental isolates as well as in clinically important bacterial pathogens (Ochi, 1987; Jin et al., 2004; Gomez-Escribano et al., 2008; van der Heul et al., 2018). Different soil living Gram-positive bacteria including *B. subtilis*, *Streptomyces clavuligerus*, produce a variety of antibiotics to inhibit the growth of other bacteria living in the same environment (van der Meij et al., 2017; and the references therein). Various reports suggest that (p)ppGpp may either positively or negatively regulate antibiotic production in Actinobacteria. For example, *Streptomyces coelicolor* synthesizes two well-known antibiotics, the polyketide actinorhodin, and the tripyrolle undecylprodigiosin and the production of each them was decreased in the Δ*relA* mutant of *S. coelicolor* under a continuous culture condition (Kang et al., 1998). On the other hand, it has been shown in *S. clavuligerus* that (p)ppGpp negatively regulates the production of clavulanic acid and cephamycin C antibiotics in the absence of (p)ppGpp biosynthetic gene *relA* (Gomez-Escribano et al., 2008). Role of (p)ppGpp in the antibiotic production has also been demonstrated in other species of *Streptomyces* including *Streptomyces antibioticus* and *Streptomyces griseus* (Sivapragasam and Grove, 2019). (p)ppGpp may promote antibiotic production in these bacteria by inducing transcription of antibiotic biosynthetic gene clusters. In fact, it has been shown that the elevated level of intracellular (p)ppGpp in *S. coelicolor* leads to reduction in the expression of vegetative sigma factor and induction of expression of alternative sigma factor, which play important role in the transcription of antibiotic biosynthesis gene cluster (Hesketh et al., 2007).

Bacterial Antibiotic Resistance and (p)ppGpp

Antibiotics, natural or synthetic chemical compounds that interfere with microbial growth or eliminate microbes from their niche, are one of the most important drugs in the medical history that has ever been discovered and deployed to prevent or cure microbial infections (Fischbach and Walsh, 2009). However, emergence of antibiotic resistance (AMR) and rapid dissemination of resistant traits in the clinically important bacterial species has drastically reduced the efficacy of several therapeutic agents commonly used to prevent or treat microbial infection (Das et al., 2017). AMR could be intrinsic or acquired and a wide range of metabolic pathways can confer resistance phenotype in bacteria (**Figure 4**; Das et al., 2020). Horizontal gene transfer (HGT), *de novo* mutation and changes in the expression profile of secreted proteins determine the rate of emergence of resistant variants (Davies and Davies, 2010). Alarmone molecule (p)ppGpp induces HGT while bacterial species are living in biofilms (Strugeon et al., 2016). Elevated level of (p)ppGpp derepressed the *intI1* promoter (P_{intI1}) by inducing autoproteolytic activity of SOS response master regulator LexA, possibly through reducing the activity of exopolyphosphatase enzyme PPX (Strugeon et al., 2016). In normal physiological conditions, LexA dimer reduces the

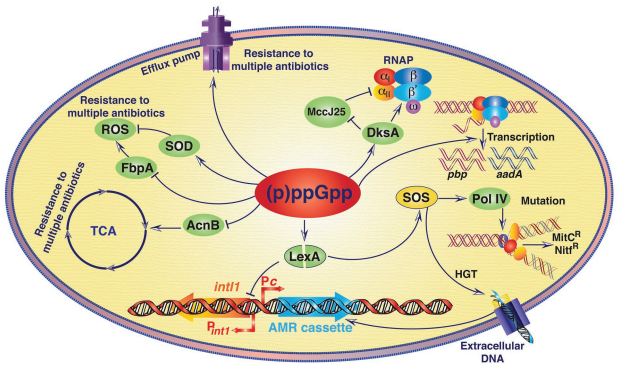

FIGURE 4 | A schematic representation showing the (p)ppGpp mediated antimicrobial resistance (AMR) in bacteria. Except AMR cassette acquisition at the integron integrase locus all other processes that are directly or indirectly associated with antibiotic resistance due to increased level of (p)ppGpp are non-inheritable. (p)ppGpp induces antibiotic resistance in bacteria *via* distinct mechanisms (see details in text), which are as follows. (i) (p)ppGpp increases the efficiency of horizontal gene transfer (HGT) and AMR cassette acquisition by derepressing the integron integrase 1 (*intI1*) gene promoter (P*intI1*). Elevated level of (p)ppGpp induces autoproteolytic activity of SOS response master regulator LexA, and thus increases expression of the *intI1* gene. In addition, SOS induction also derepressed the expression of error-prone DNA polymerase IV (Pol IV) and upturns accumulation of spontaneous point mutations *via* DNA replication, which in turn escalates development of resistant variants. (ii) (p)ppGpp upregulates the expression of the aminoglycoside adenylyl transferase gene (*aadA*), penicillin binding protein coding gene (*pbp*), and different components of the efflux pumps. (iii) (p)ppGpp helps DksA to compete with microcin J25 (MccJ25) peptide antibiotic for binding with RNA polymerase (RNAP) and confers resistance against this peptide antibiotic. (iv) (p)ppGpp represses the expression of aconitase B (AcnB) and suppresses tricarboxylic acid (TCA) cycle and increases non-inheritable resistance to antibiotics. (v) (p)ppGpp represses the expression of Fe(III) ABC transporter substrate-binding protein (FbpA) and activates superoxide dismutase (SOD) activity. Both the modulations reduce the level of reactive oxygen species (ROS) leading to increase in resistance against tetracycline and other antibiotics. Solid arrows indicate activating interactions and T-arrows indicate inhibiting interactions. Bent arrows at the integron locus indicate promoter for AMR cassette (Pc) and P*intI1*. MitC^R, Mitomycin C resistance; Nitf^R, Nitrofurantoin resistance.

expression of IntI1 integrase by inhibiting P_{intI1}. Increased expression of integrin integrase due to (p)ppGpp mediated moderate increase of SOS response in biofilm environment helps integron mediated acquisition/exchange of antibiotic resistance gene cassettes through HGT (**Figure 4**).

It has been observed that bacterial (p)ppGpp^0 strains are usually sensitive to diverse xenobiotics, antibiotics, and ultraviolet radiation (Hobbs and Boraston, 2019; and the references therein). Bacterial population that does not carry any specific antibiotic resistance trait or altered target, a small fraction of this population of cells may develop persistence to tolerate lethal doses of antibiotics, which seems to be mediated by the elevated level of intracellular (p)ppGpp. From several recent studies, it is gradually becoming clear that the increased intracellular levels of (p)ppGpp most likely activates the bacterial toxin-antitoxin module, also called TA module, through a complex regulatory mechanism, and the released toxin moiety then helps in maintaining the high intracellular levels of (p)ppGpp and thus, leading to the genesis of persister cells (Korch et al., 2003; Kaspy et al., 2013; Harms et al., 2016). It has been demonstrated recently that (p)ppGpp may play an important role in the nucleotide excision DNA repair process. Absence of (p)ppGpp or its functional partner DksA render bacterial cells highly sensitive to mitomycin C, 4-nitroquinoline 1-oxide and nitrofurantoin, the antibiotics that kill bacterial species by interfering DNA or RNA synthesis (Kamarthapu and Nudler, 2015). Bacterial cells with higher basal level of (p)ppGpp are more resistant to antibiotics that work through interfering nucleic acid biosynthesis or damage. (p)ppGpp directly modulates the activity of RNAP, therefore, it could support UvrD for the repair of damaged DNA through transcription coupled DNA repair pathway. In addition, induction of SOS during stress conditions including exposure to sub-lethal concentration of antibiotics also derepressed the expression of error-prone DNA polymerase IV and increases accumulation of spontaneous mutations, which in turn escalate development of resistant variants (Layton and Foster, 2005). When *Salmonella enterica* cells are treated with aminoglycoside antibiotics, they showed (p)ppGpp mediated upregulation of expression of the aminoglycoside adenylyl transferase gene (*aadA*) and thus, resulting in resistance to streptomycin and spectinomycin antibiotics (Koskiniemi et al., 2011).

Increased basal level of (p)ppGpp also contributes in the emergence of antibiotic resistant bacterial cells by directly modulating the expression profile of genes encoding penicillin binding proteins (PBPs) or components of the efflux pumps (Aedo and Tomasz, 2016). Rodionov and Ishiguro (1995) have reported about the importance of (p)ppGpp in inducing resistance against beta-lactam antibiotics namely penicillin. They showed that controlled expression of the *relA* gene resulted in inhibition of peptidoglycan and phospholipid biosynthesis subsequently resulting in penicillin tolerance. Oxacillin resistance in *Staphylococcus aureus* is directly associated with increased (p)ppGpp synthetase activity of RelQ or decreasing (p)ppGpp hydrolase activity of the Rel enzyme (Mwangi et al., 2013). Similarly, increase in intracellular (p)ppGpp concentration in *E. faecalis* has been found to be responsible for the development of non-inheritable resistance against the antibiotic vancomycin (Abranches et al., 2009). Very recently it has been shown that the *rel* gene deleted *Mycobacterium tuberculosis* cells become more susceptible to isoniazid killing under nutrient starved condition and also in the lungs of infected mice (Dutta et al., 2019). Thus, it appears that inhibition of Rel may be a useful approach to eliminate *M. tuberculosis* persister cells. On the other hand, a direct correlation has been found between intracellular (p)ppGpp accumulation and increase in resistance against the peptide antibiotic microcin in *E. coli* (Pomares et al., 2008). It was hypothesized that (p)ppGpp helps DksA to compete with microcin J25 peptide antibiotic for binding with RNAP (**Figure 4**). A very recent study showed that (p)ppGpp induces the expression of efflux pump related genes in *Acinetobacter baumannii* (Jung et al., 2020). MIC of several antibiotics drastically reduced in (p)ppGpp^0 *A. baumannii* strain compared to its wild-type ancestor, possibly due to reduction in expression of antibiotics expelling efflux pumps (Jung et al., 2020). In *E. coli*, homeostasis of purine nucleosides is regulated by the nucleosidase PpnN by cleaving

nucleoside monophosphates. (p)ppGpp binds to the PpnN and stimulates its catalytic activity, which helps cells to tolerate increased concentration of antibiotics (Zhang et al., 2019). The most common antibiotics for the treatment of cholera patients are tetracycline, erythromycin, and chloramphenicol. A recent study has shown that the increased level of intracellular (p)ppGpp helps *V. cholerae* cells to reduce the efficacy of all these antibiotics, at least under the laboratory testing conditions (Kim et al., 2018). (p)ppGpp metabolic cycle in *V. cholerae* is fairly unique in comparison to other Gram-negative bacteria (Das et al., 2009). The alarmone helps cholera pathogens for survival, disease development, and antibiotic resistance. Wild-type *V. cholerae* strain and its (p)ppGpp overproducing isogenic mutant Δ*relA*Δ*spoT* can survive better in the presence of different antibiotics compared to (p)ppGpp° Δ*relA*Δ*spoT*Δ*relV* strain. It was hypothesized that (p)ppGpp suppresses tricarboxylic acid cycle by repressing the aconitase B encoding gene *acnB* and increases non-inheritable resistance to antibiotics (Kim et al., 2018). In addition, (p)ppGpp also represses the expression of iron (III) ABC transporter substrate-binding protein in the wild-type *V. cholerae* strain, which is important for the generation of reactive oxygen species (ROS) and increased susceptibility to tetracycline (**Figure 4**). Nevertheless, it has also been reported that the Δ*dksA V. cholerae* mutants are also highly sensitive to different antibiotics compared to isogenic wild-type strain (Kim et al., 2018). In a murine infection model, substantial increase in the efficacy of several fluoroquinolones against the (p)ppGpp^0 *P. aeruginosa* mutant strain has been noticed compared to that of isogenic wild-type strain (Nguyen et al., 2011). In fact, it has been observed that increased intracellular concentration of (p)ppGpp may modulate non-inheritable resistance to different antibiotics possibly through regulation of bacterial ROS production. Several studies have demonstrated that the high intracellular levels of (p)ppGpp is associated with the antioxidant defense mechanisms in *P. aeruginosa* (Nguyen et al., 2011; Martins et al., 2018). Superoxide dismutase (SOD), an enzyme that catalyzes the dismutation of the superoxide (O_2^-) radical into ordinary molecular oxygen (O_2) and hydrogen peroxide (H_2O_2), is a key enzyme involved in stringent response mediated drug resistance in stationary phase cells of *P. aeruginosa* (Martins et al., 2018). It has been shown that deletions of (p)ppGpp biosynthetic genes reduce the SOD activity and diminish drug tolerance phenotypes in stationary phase cells of *P. aeruginosa*. Complementation of SOD activity in the (p)ppGpp^0 *P. aeruginosa* was able to restore the non-inheritable resistance against several antibiotics almost similar to that of isogenic wild-type strain. The authors have also found that in the absence of SOD activity, the membrane permeability of *P. aeruginosa* cells is high, which leads to increase in drug internalization and thus raising the efficacy of antibiotics.

Stringent Response Inhibitors Are Potential Antibiotic Adjuvant

The conserved distribution of stringent response across the bacterial phyla and its important roles in developing persistent bacterial infections made it a promising drug target. Subpopulation of bacteria can survive upon exposure to lethal concentration of antibiotic through growth arrest, while others are not (Balaban et al., 2004). Persister bacteria exhibit non-inheritable resistance to the bactericidal antibiotics (Dutta et al., 2019). It is well known that the stringent response effector molecules (p)ppGpp plays an important role in fine-tuning bacterial growth during nutritional stress and exposure to antibiotics. It helps bacterial pathogens to survive during growth-limiting conditions, to increase non-inheritable resistance and to develop persister cells for prolong infection (Abranches et al., 2009; Dutta et al., 2019). The major bacterial persistent infections are usually caused by *M. tuberculosis*, *Helicobacter pylori*, *Salmonella* Typhi, and several others, where the pathogens can overcome the antimicrobial effect of routinely used antimicrobials (Kester and Fortune, 2014). As discussed above, several studies have indicated that the stringent response plays a pivotal role in developing non-inheritable resistance and persister cell formation. Therefore, in recent years' attempts have been made to develop stringent response inhibitors to block long-term persistence, sporulation, and biofilm formation with a hope that blocking such important cellular functions may help in increasing the efficacy of antimicrobial drugs (Wexselblatt et al., 2012, 2013; Syal et al., 2017a,b). Thus, a number of potential stringent response inhibitory molecules, namely, 2'-deoxyguanosine-3'-5'-di(methylene bisphosphonate), relacin, relacin analog 2d, vitamin C, etc., have been developed and shown to be effective against *B. subtilis*, *Bacillus anthracis*, *M. smegmatis*, and *E. coli* both under *in vitro* and *in vivo* growth conditions (Wexselblatt et al., 2012, 2013; Syal et al., 2017a,b). Relacin, a well-studied ppGpp analog in which 3'-pyrophosphate moieties were substituted with glycyl-glycine dipeptide, inhibits (p)ppGpp synthetic activity of Rel/RelA proteins of both Gram-positive and Gram-negative bacteria under *in vitro* conditions. It has been demonstrated that relacin reduces bacterial viability by preventing the cells entering into stationary growth phase (Wexselblatt et al., 2012). Thus, it seems that inhibiting the (p)ppGpp synthesis activity in pathogens by stringent response inhibitor is a potential approach to reduce viability of persister and shortening the duration of antibiotic treatment of a patient. Development of such promising inhibitors against RelA/SpoT/RSH enzymes and its use as antibiotic adjuvants can potentially help in eradicating several chronic bacterial infections.

CONCLUSION

Although the (p)ppGpp metabolic pathway was originally discovered in bacteria about 50 years ago, continued research on this important molecule has made it clear that these alarmones are widely synthesized by the living organisms from all three domains of life. Enzymes involved in the (p)ppGpp metabolism and signals that activate or repress stringent response share substantial similarity between different organisms. Overwhelming evidences established that other than nutrient limitations, antibiotics, and non-antibiotic xenobiotics activate stringent response and help microbes to survive even in the absence of specific resistance genes. In addition to the regulation of DNA replication, RNA transcription and protein synthesis, (p)ppGpp molecules have a wide range of heterogeneous targets depending on the organisms and their habitats. It is becoming clear that the modulations of the activities of several such

targets/proteins are linked with the non-heritable resistance to antibiotics. The genetic program linked with the bacterial antibiotic resistance in the absence of specific resistance genes appears to have multiple components. Activity of several such molecules intricately depends on the alarmone (p)ppGpp and other small signaling molecules, which warrants further in depth research for effective management of infectious diseases.

AUTHOR CONTRIBUTIONS

BD and RKB designed the review, done literature search, and wrote the manuscript. All authors contributed to the article and approved the submitted version.

FUNDING

This study received financial support from the Dept. of Biotechnology (DBT), Govt. of India (no. BT/PR9983/MED/97/194/2013), Translational Health Science and Technology Institute core funds (2019-2020) and partial support from MLP118 laboratory project of CSIR-IICB.

ACKNOWLEDGMENTS

Authors acknowledge Prof. G. Balakrish Nair and Dr. Amit Ghosh for critical reading and valuable suggestions.

REFERENCES

Abranches, J., Martinez, A. R., Kajfasz, J. K., Chavez, V., Garsin, D. A., and Lemos, J. A. (2009). The molecular alarmone (p)ppGpp mediates stress responses, vancomycin tolerance, and virulence in *Enterococcus faecalis*. *J. Bacteriol.* 191, 2248–2256. doi: 10.1128/JB.01726-08

Aedo, S., and Tomasz, A. (2016). Role of the stringent stress response in the antibiotic resistance phenotype of methicillin-resistant *Staphylococcus aureus*. *Antimicrob. Agents Chemother.* 60, 2311–2317. doi: 10.1128/AAC.02697-15

Angelini, S., My, L., and Bouveret, E. (2012). Disrupting the acyl carrier protein/SpoT interaction *in vivo*: identification of ACP residues involved in the interaction and consequence on growth. *PLoS One* 7:e36111. doi: 10.1371/journal.pone.0036111

Atkinson, G. C., Tenson, T., and Hauryliuk, V. (2011). The RelA/SpoT homolog (RSH) superfamily: distribution and functional evolution of ppGpp synthetases and hydrolases across the tree of life. *PLoS One* 6:e23479. doi: 10.1371/journal.pone.0023479

Balaban, N. Q., Merrin, J., Chait, R., Kowalik, L., and Leibler, S. (2004). Bacterial persistence as a phenotypic switch. *Science* 305, 1622–1625. doi: 10.1126/science.1099390

Cashel, M. (1969). The control of ribonucleic acid synthesis in *Escherichia coli*. IV. Relevance of unusual phosphorylated compounds from amino acid-starved stringent strains. *J. Biol. Chem.* 244, 3133–3141.

Cashel, M., Gentry, D. R., Hernandez, V. J., and Vinella, D. (1996). "The stringent response" in *Escherichia coli* and *Salmonella: Cellular and molecular biology*. ed. F. C. Neidhardt (Washington, DC: ASM Press), 1458–1496.

Corrigan, R. M., Bellows, L. E., Wood, A., and Grundling, A. (2016). ppGpp negatively impacts ribosome assembly affecting growth and antimicrobial tolerance in Gram-positive bacteria. *Proc. Natl. Acad. Sci. U. S. A.* 113, E1710–E1719. doi: 10.1073/pnas.1522179113

Crawford, E. W. Jr., and Shimkets, L. J. (2000). The stringent response in *Myxococcus xanthus* is regulated by SocE and the CsgA C-signaling protein. *Genes Dev.* 14, 483–492.

Dalebroux, Z. D., Svensson, S. L., Gaynor, E. C., and Swanson, M. S. (2010). ppGpp conjures bacterial virulence. *Microbiol. Mol. Biol. Rev.* 74, 171–199. doi: 10.1128/MMBR.00046-09

Das, B., and Bhadra, R. K. (2008). Molecular characterization of *Vibrio cholerae* Δ*relA* Δ*spoT* double mutants. *Arch. Microbiol.* 189, 227–238. doi: 10.1007/s00203-007-0312-z

Das, B., Chaudhuri, S., Srivastava, R., Nair, G. B., and Ramamurthy, T. (2017). Fostering research into antimicrobial resistance in India. *BMJ* 358:j3535. doi: 10.1136/bmj.j3535

Das, B., Pal, R. R., Bag, S., and Bhadra, R. K. (2009). Stringent response in *Vibrio cholerae*: genetic analysis of *spoT* gene function and identification of a novel (p)ppGpp synthetase gene. *Mol. Microbiol.* 72, 380–398. doi: 10.1111/j.1365-2958.2009.06653.x

Das, B., Verma, J., Kumar, P., Ghosh, A., and Ramamurthy, T. (2020). Antibiotic resistance in *Vibrio cholerae*: understanding the ecology of resistance genes and mechanisms. *Vaccine* 38(Suppl. 1), A83–A92. doi: 10.1016/j.vaccine.2019.06.031

Dasgupta, S., Basu, P., Pal, R. R., Bag, S., and Bhadra, R. K. (2014). Genetic and mutational characterization of the small alarmone synthetase gene *relV* of *Vibrio cholerae*. *Microbiology* 160, 1855–1866. doi: 10.1099/mic.0.079319-0

Davies, J., and Davies, D. (2010). Origins and evolution of antibiotic resistance. *Microbiol. Mol. Biol. Rev.* 74, 417–433. doi: 10.1128/MMBR.00016-10

Denapoli, J., Tehranchi, A. K., and Wang, J. D. (2013). Dose-dependent reduction of replication elongation rate by (p)ppGpp in *Escherichia coli* and *Bacillus subtilis*. *Mol. Microbiol.* 88, 93–104. doi: 10.1111/mmi.12172

Dutta, N. K., Klinkenberg, L. G., Vazquez, M. J., Segura-Carro, D., Colmenarejo, G., Ramon, F., et al. (2019). Inhibiting the stringent response blocks *Mycobacterium tuberculosis* entry into quiescence and reduces persistence. *Sci. Adv.* 5:eaav2104. doi: 10.1126/sciadv.aav2104

English, B. P., Hauryliuk, V., Sanamrad, A., Tankov, S., Dekker, N. H., and Elf, J. (2011). Single-molecule investigations of the stringent response machinery in living bacterial cells. *Proc. Natl. Acad. Sci. U. S. A.* 108, E365–E373. doi: 10.1073/pnas.1102255108

Fischbach, M. A., and Walsh, C. T. (2009). Antibiotics for emerging pathogens. *Science* 325, 1089–1093. doi: 10.1126/science.1176667

Gaca, A. O., Colomer-Winter, C., and Lemos, J. A. (2015). Many means to a common end: the intricacies of (p)ppGpp metabolism and its control of bacterial homeostasis. *J. Bacteriol.* 197, 1146–1156. doi: 10.1128/JB.02577-14

Gaca, A. O., Kajfasz, J. K., Miller, J. H., Liu, K., Wang, J. D., Abranches, J., et al. (2013). Basal levels of (p)ppGpp in *Enterococcus faecalis*: the magic beyond the stringent response. *mBio* 4, e00646–e00713. doi: 10.1128/mBio.00646-13

Gallant, J., Palmer, L., and Pao, C. C. (1977). Anomalous synthesis of ppGpp in growing cells. *Cell* 11, 181–185. doi: 10.1016/0092-8674(77)90329-4

Gomez-Escribano, J. P., Martin, J. F., Hesketh, A., Bibb, M. J., and Liras, P. (2008). *Streptomyces clavuligerus relA*-null mutants overproduce clavulanic acid and cephamycin C: negative regulation of secondary metabolism by (p)ppGpp. *Microbiology* 154, 744–755. doi: 10.1099/mic.0.2007/011890-0

Gourse, R. L., Chen, A. Y., Gopalkrishnan, S., Sanchez-Vazquez, P., Myers, A., and Ross, W. (2018). Transcriptional responses to ppGpp and DksA. *Annu. Rev. Microbiol.* 72, 163–184. doi: 10.1146/annurev-micro-090817-062444

Gourse, R. L., and Keck, J. L. (2007). Magic spots cast a spell on DNA primase. *Cell* 128, 823–824. doi: 10.1016/j.cell.2007.02.020

Harms, A., Maisonneuve, E., and Gerdes, K. (2016). Mechanisms of bacterial persistence during stress and antibiotic exposure. *Science* 354:aaf4268. doi: 10.1126/science.aaf4268

Hauryliuk, V., Atkinson, G. C., Murakami, K. S., Tenson, T., and Gerdes, K. (2015). Recent functional insights into the role of (p)ppGpp in bacterial physiology. *Nat. Rev. Microbiol.* 13, 298–309. doi: 10.1038/nrmicro3448

He, H., Cooper, J. N., Mishra, A., and Raskin, D. M. (2012). Stringent response regulation of biofilm formation in *Vibrio cholerae*. *J. Bacteriol.* 194, 2962–2972. doi: 10.1128/JB.00014-12

Hesketh, A., Chen, W. J., Ryding, J., Chang, S., and Bibb, M. (2007). The global role of ppGpp synthesis in morphological differentiation and antibiotic production in *Streptomyces coelicolor* A3(2). *Genome Biol.* 8:R161. doi: 10.1186/gb-2007-8-8-r161

Hobbs, J. K., and Boraston, A. B. (2019). (p)ppGpp and the stringent response: an emerging threat to antibiotic therapy. *ACS Infect. Dis.* 5, 1505–1517. doi: 10.1021/acsinfecdis.9b00204

Hogg, T., Mechold, U., Malke, H., Cashel, M., and Hilgenfeld, R. (2004). Conformational antagonism between opposing active sites in a bifunctional RelA/SpoT homolog modulates (p)ppGpp metabolism during the stringent response. *Cell* 117, 57–68. doi: 10.1016/s0092-8674(04)00260-0

Irving, S. E., and Corrigan, R. M. (2018). Triggering the stringent response: signals responsible for activating (p)ppGpp synthesis in bacteria. *Microbiology* 164, 268–276. doi: 10.1099/mic.0.000621

Ito, D., Kato, T., Maruta, T., Tamoi, M., Yoshimura, K., and Shigeoka, S. (2012). Enzymatic and molecular characterization of arabidopsis ppGpp pyrophosphohydrolase, AtNUDX26. *Biosci. Biotechnol. Biochem.* 76, 2236–2241. doi: 10.1271/bbb.120523

Jin, W., Kim, H. K., Kim, J. Y., Kang, S. G., Lee, S. H., and Lee, K. J. (2004). Cephamycin C production is regulated by *relA* and *rsh* genes in *Streptomyces clavuligerus* ATCC27064. *J. Biotechnol.* 114, 81–87. doi: 10.1016/j.jbiotec.2004.06.010

Jung, H. W., Kim, K., Islam, M. M., Lee, J. C., and Shin, M. (2020). Role of ppGpp-regulated efflux genes in *Acinetobacter baumannii*. *J. Antimicrob. Chemother.* 75, 1130–1134. doi: 10.1093/jac/dkaa014

Kalia, D., Merey, G., Nakayama, S., Zheng, Y., Zhou, J., Luo, Y., et al. (2013). Nucleotide, c-di-GMP, c-di-AMP, cGMP, cAMP, (p)ppGpp signaling in bacteria and implications in pathogenesis. *Chem. Soc. Rev.* 42, 305–341. doi: 10.1039/c2cs35206k

Kamarthapu, V., Epshtein, V., Benjamin, B., Proshkin, S., Mironov, A., Cashel, M., et al. (2016). ppGpp couples transcription to DNA repair in *E. coli*. *Science* 352, 993–996. doi: 10.1126/science.aad6945

Kamarthapu, V., and Nudler, E. (2015). Rethinking transcription coupled DNA repair. *Curr. Opin. Microbiol.* 24, 15–20. doi: 10.1016/j.mib.2014.12.005

Kang, P. J., and Craig, E. A. (1990). Identification and characterization of a new *Escherichia coli* gene that is a dosage-dependent suppressor of a *dnaK* deletion mutation. *J. Bacteriol.* 172, 2055–2064. doi: 10.1128/jb.172.4.2055-2064.1990

Kang, S. G., Jin, W., Bibb, M., and Lee, K. J. (1998). Actinorhodin and undecylprodigiosin production in wild-type and *relA* mutant strains of *Streptomyces coelicolor* A3(2) grown in continuous culture. *FEMS Microbiol. Lett.* 168, 221–226. doi: 10.1111/j.1574-6968.1998.tb13277.x

Kanjee, U., Ogata, K., and Houry, W. A. (2012). Direct binding targets of the stringent response alarmone (p)ppGpp. *Mol. Microbiol.* 85, 1029–1043. doi: 10.1111/j.1365-2958.2012.08177.x

Kaspy, I., Rotem, E., Weiss, N., Ronin, I., Balaban, N. Q., and Glaser, G. (2013). HipA-mediated antibiotic persistence via phosphorylation of the glutamyl-tRNA-synthetase. *Nat. Commun.* 4:3001. doi: 10.1038/ncomms4001

Kester, J. C., and Fortune, S. M. (2014). Persisters and beyond: mechanisms of phenotypic drug resistance and drug tolerance in bacteria. *Crit. Rev. Biochem. Mol. Biol.* 49, 91–101. doi: 10.3109/10409238.2013.869543

Kim, H. Y., Go, J., Lee, K. M., Oh, Y. T., and Yoon, S. S. (2018). Guanosine tetra- and pentaphosphate increase antibiotic tolerance by reducing reactive oxygen species production in *Vibrio cholerae*. *J. Biol. Chem.* 293, 5679–5694. doi: 10.1074/jbc.RA117.000383

Korch, S. B., Henderson, T. A., and Hill, T. M. (2003). Characterization of the *hipA7* allele of *Escherichia coli* and evidence that high persistence is governed by (p)ppGpp synthesis. *Mol. Microbiol.* 50, 1199–1213. doi: 10.1046/j.1365-2958.2003.03779.x

Koskiniemi, S., Pränting, M., Gullberg, E., Näsvall, J., and Andersson, D. I. (2011). Activation of cryptic aminoglycoside resistance in *Salmonella enterica*. *Mol. Microbiol.* 80, 1464–1478. doi: 10.1111/j.1365-2958.2011.07657.x

Kriel, A., Bittner, A. N., Kim, S. H., Liu, K., Tehranchi, A. K., Zou, W. Y., et al. (2012). Direct regulation of GTP homeostasis by (p)ppGpp: a critical component of viability and stress resistance. *Mol. Cell* 48, 231–241. doi: 10.1016/j.molcel.2012.08.009

Layton, J. C., and Foster, P. L. (2005). Error-prone DNA polymerase IV is regulated by the heat shock chaperone GroE in *Escherichia coli*. *J. Bacteriol.* 187, 449–457. doi: 10.1128/JB.187.2.449-457.2005

Lemos, J. A., Lin, V. K., Nascimento, M. M., Abranches, J., and Burne, R. A. (2007). Three gene products govern (p)ppGpp production by *Streptococcus mutans*. *Mol. Microbiol.* 65, 1568–1581. doi: 10.1111/j.1365-2958.2007.05897.x

Li, W., Bouveret, E., Zhang, Y., Liu, K., Wang, J. D., and Weisshaar, J. C. (2016). Effects of amino acid starvation on RelA diffusive behavior in live *Escherichia coli*. *Mol. Microbiol.* 99, 571–585. doi: 10.1111/mmi.13252

Lyzen, R., Maitra, A., Milewska, K., Kochanowska-Lyzen, M., Hernandez, V. J., and Szalewska-Palasz, A. (2016). The dual role of DksA protein in the regulation of *Escherichia coli* pArgX promoter. *Nucleic Acids Res.* 44, 10316–10325. doi: 10.1093/nar/gkw912

Magnusson, L. U., Gummesson, B., Joksimovic, P., Farewell, A., and Nystrom, T. (2007). Identical, independent, and opposing roles of ppGpp and DksA in *Escherichia coli*. *J. Bacteriol.* 189, 5193–5202. doi: 10.1128/JB.00330-07

Martins, D., McKay, G., Sampathkumar, G., Khakimova, M., English, A. M., and Nguyen, D. (2018). Superoxide dismutase activity confers (p)ppGpp-mediated antibiotic tolerance to stationary-phase *Pseudomonas aeruginosa*. *Proc. Natl. Acad. Sci. U. S. A.* 115, 9797–9802. doi: 10.1073/pnas.1804525115

Mechold, U., Potrykus, K., Murphy, H., Murakami, K. S., and Cashel, M. (2013). Differential regulation by ppGpp versus pppGpp in *Escherichia coli*. *Nucleic Acids Res.* 41, 6175–6189. doi: 10.1093/nar/gkt302

Murdeshwar, M. S., and Chatterji, D. (2012). MS_RHII-RSD, a dual-function RNase HII-(p)ppGpp synthetase from *Mycobacterium smegmatis*. *J. Bacteriol.* 194, 4003–4014. doi: 10.1128/JB.00258-12

Mwangi, M. M., Kim, C., Chung, M., Tsai, J., Vijayadamodar, G., Benitez, M., et al. (2013). Whole-genome sequencing reveals a link between beta-lactam resistance and synthetases of the alarmone (p)ppGpp in *Staphylococcus aureus*. *Microb. Drug Resist.* 19, 153–159. doi: 10.1089/mdr.2013.0053

Nanamiya, H., Kasai, K., Nozawa, A., Yun, C. S., Narisawa, T., Murakami, K., et al. (2008). Identification and functional analysis of novel (p)ppGpp synthetase genes in *Bacillus subtilis*. *Mol. Microbiol.* 67, 291–304. doi: 10.1111/j.1365-2958.2007.06018.x

Nguyen, D., Joshi-Datar, A., Lepine, F., Bauerle, E., Olakanmi, O., Beer, K., et al. (2011). Active starvation responses mediate antibiotic tolerance in biofilms and nutrient-limited bacteria. *Science* 334, 982–986. doi: 10.1126/science.1211037

Ochi, K. (1987). A *rel* mutation abolishes the enzyme induction needed for actinomycin synthesis by *Streptomyces antibioticus*. *Agric. Biol. Chem.* 51, 829–835. doi: 10.1271/bbb1961.51.829

Pal, R. R., Bag, S., Dasgupta, S., Das, B., and Bhadra, R. K. (2012). Functional characterization of the stringent response regulatory gene *dksA* of *Vibrio cholerae* and its role in modulation of virulence phenotypes. *J. Bacteriol.* 194, 5638–5648. doi: 10.1128/JB.00518-12

Pant, A., Bag, S., Saha, B., Verma, J., Kumar, P., Banerjee, S., et al. (2020). Molecular insights into the genome dynamics and interactions between core and acquired genomes of *Vibrio cholerae*. *Proc. Natl. Acad. Sci. U. S. A.* doi: 10.1073/pnas.2006283117 [Epub ahead of print]

Parker, J., Watson, R. J., and Friesen, J. D. (1976). A relaxed mutant with an altered ribosomal protein L11. *Mol. Gen. Genet.* 144, 111–114. doi: 10.1007/BF00277313

Paul, B. J., Barker, M. M., Ross, W., Schneider, D. A., Webb, C., Foster, J. W., et al. (2004). DksA: a critical component of the transcription initiation machinery that potentiates the regulation of rRNA promoters by ppGpp and the initiating NTP. *Cell* 118, 311–322. doi: 10.1016/j.cell.2004.07.009

Perederina, A., Svetlov, V., Vassylyeva, M. N., Tahirov, T. H., Yokoyama, S., Artsimovitch, I., et al. (2004). Regulation through the secondary channel—structural framework for ppGpp-DksA synergism during transcription. *Cell* 118, 297–309. doi: 10.1016/j.cell.2004.06.030

Pomares, M. F., Vincent, P. A., Farias, R. N., and Salomon, R. A. (2008). Protective action of ppGpp in microcin J25-sensitive strains. *J. Bacteriol.* 190, 4328–4334. doi: 10.1128/JB.00183-08

Potrykus, K., and Cashel, M. (2008). (p)ppGpp: still magical? *Annu. Rev. Microbiol.* 62, 35–51. doi: 10.1146/annurev.micro.62.081307.162903

Potrykus, K., Murphy, H., Philippe, N., and Cashel, M. (2011). ppGpp is the major source of growth rate control in *E. coli*. *Environ. Microbiol.* 13, 563–575. doi: 10.1111/j.1462-2920.2010.02357.x

Rodionov, D. G., and Ishiguro, E. E. (1995). Direct correlation between overproduction of guanosine 3', 5'-bispyrophosphate (ppGpp) and penicillin tolerance in *Escherichia coli*. *J. Bacteriol.* 177, 4224–4229. doi: 10.1128/jb.177.15.4224-4229.1995

Ronneau, S., and Hallez, R. (2019). Make and break the alarmone: regulation of (p)ppGpp synthetase/hydrolase enzymes in bacteria. *FEMS Microbiol. Rev.* 43, 389–400. doi: 10.1093/femsre/fuz009

Ross, W., Vrentas, C. E., Sanchez-Vazquez, P., Gaal, T., and Gourse, R. L. (2013). The magic spot: a ppGpp binding site on *E. coli* RNA polymerase responsible for regulation of transcription initiation. *Mol. Cell* 50, 420–429. doi: 10.1016/j.molcel.2013.03.021

Ruwe, M., Ruckert, C., Kalinowski, J., and Persicke, M. (2018). Functional characterization of a small alarmone hydrolase in *Corynebacterium glutamicum*. *Front. Microbiol.* 9:916. doi: 10.3389/fmicb.2018.00916

Sanchez-Vazquez, P. (2018). Genome-wide effects of ppGpp binding to RNA polymerase on *E. coli* gene expression. [PhD Thesis]. USA: University of Wisconsin-Madison.

Sivapragasam, S., and Grove, A. (2019). The link between purine metabolism and production of antibiotics in *Streptomyces*. *Antibiotics* 8:76. doi: 10.3390/antibiotics8020076

Storvik, K. A., and Foster, P. L. (2010). RpoS, the stress response sigma factor, plays a dual role in the regulation of *Escherichia coli's* error-prone DNA polymerase IV. *J. Bacteriol.* 192, 3639–3644. doi: 10.1128/JB.00358-10

Strugeon, E., Tilloy, V., Ploy, M. C., and Da Re, S. (2016). The stringent response promotes antibiotic resistance dissemination by regulating integron integrase expression in biofilms. *mBio* 7, e00868–e00916. doi: 10.1128/mBio.00868-16

Sun, D., Lee, G., Lee, J. H., Kim, H. Y., Rhee, H. W., Park, S. Y., et al. (2010). A metazoan ortholog of SpoT hydrolyzes ppGpp and functions in starvation responses. *Nat. Struct. Mol. Biol.* 17, 1188–1194. doi: 10.1038/nsmb.1906

Syal, K., Bhardwaj, N., and Chatterji, D. (2017b). Vitamin C targets (p)ppGpp synthesis leading to stalling of long-term survival and biofilm formation in *Mycobacterium smegmatis*. *FEMS Microbiol. Lett.* 364:fnw282. doi: 10.1093/femsle/fnw282

Syal, K., Flentie, K., Bhardwaj, N., Maiti, K., Jayaraman, N., Stallings, C. L., et al. (2017a). Synthetic (p)ppGpp analogue is an inhibitor of stringent response in mycobacteria. *Antimicrob. Agents Chemother.* 61, e00443–e00517. doi: 10.1128/AAC.00443-17e00443-17

Teschler, J. K., Zamorano-Sanchez, D., Utada, A. S., Warner, C. J., Wong, G. C., Linington, R. G., et al. (2015). Living in the matrix: assembly and control of *Vibrio cholerae* biofilms. *Nat. Rev. Microbiol.* 13, 255–268. doi: 10.1038/nrmicro3433

Tozawa, Y., and Nomura, Y. (2011). Signalling by the global regulatory molecule ppGpp in bacteria and chloroplasts of land plants. *Plant Biol.* 13, 699–709. doi: 10.1111/j.1438-8677.2011.00484.x

van der Heul, H. U., Bilyk, B. L., McDowall, K. J., Seipke, R. F., and van Wezel, G. P. (2018). Regulation of antibiotic production in Actinobacteria: new perspectives from the post- genomic era. *Nat. Prod. Rep.* 35, 575–604. doi: 10.1039/c8np00012c

van der Meij, A., Worsley, S. F., Hutchings, M. I., and van Wezel, G. P. (2017). Chemical ecology of antibiotic production by actinomycetes. *FEMS Microbiol. Rev.* 41, 392–416. doi: 10.1093/femsre/fux005

Verma, J., Bag, S., Saha, B., Kumar, P., Ghosh, T. S., Dayal, M., et al. (2019). Genomic plasticity associated with antimicrobial resistance in *Vibrio cholerae*. *Proc. Natl. Acad. Sci. U. S. A.* 116, 6226–6231. doi: 10.1073/pnas.1900141116

Wang, B., Dai, P., Ding, D., Del Rosario, A., Grant, R. A., Pentelute, B. L., et al. (2019). Affinity-based capture and identification of protein effectors of the growth regulator ppGpp. *Nat. Chem. Biol.* 15:756. doi: 10.1038/s41589-019-0296-4

Wang, J. D., Sanders, G. M., and Grossman, A. D. (2007). Nutritional control of elongation of DNA replication by (p)ppGpp. *Cell* 128, 865–875. doi: 10.1016/j.cell.2006.12.043

Wendrich, T. M., Blaha, G., Wilson, D. N., Marahiel, M. A., and Nierhaus, K. H. (2002). Dissection of the mechanism for the stringent factor RelA. *Mol. Cell* 10, 779–788. doi: 10.1016/s1097-2765(02)00656-1

Wexselblatt, E., Kaspy, N., Glaser, G., Katzhendler, J., and Yavin, E. (2013). Design, synthesis and structure-activity relationship of novel Relacin analogs as inhibitors of Rel proteins. *Eur. J. Med. Chem.* 70, 497–504. doi: 10.1016/j.ejmech.2013.10.036

Wexselblatt, E., Oppenheimer-Shaanan, Y., Kaspy, I., London, N., Schueler-Furman, O., Yavin, E., et al. (2012). Relacin, a novel antibacterial agent targeting the stringent response. *PLoS Pathog.* 8:e1002925. doi: 10.1371/journal.ppat.1002925

Wolz, C., Geiger, T., and Goerke, C. (2010). The synthesis and function of the alarmone (p)ppGpp in firmicutes. *Int. J. Med. Microbiol.* 300, 142–147. doi: 10.1016/j.ijmm.2009.08.017

Wu, J., Long, Q., and Xie, J. (2010). (p)ppGpp and drug resistance. *J. Cell. Physiol.* 224, 300–304. doi: 10.1002/jcp.22158

Xiao, H., Kalman, M., Ikehara, K., Zemel, S., Glaser, G., and Cashel, M. (1991). Residual guanosine 3',5'-bispyrophosphate synthetic activity of *relA* null mutants can be eliminated by *spoT* null mutations. *J. Biol. Chem.* 266, 5980–5990.

Zhang, Y. E., Baerentsen, R. L., Fuhrer, T., Sauer, U., Gerdes, K., and Brodersen, D. E. (2019). (p)ppGpp regulates a bacterial nucleosidase by an allosteric two-domain switch. *Mol. Cell* 74, 1239–1249. doi: 10.1016/j.molcel.2019.03.035

Zhang, Y., Zborníková, E., Rejman, D., and Gerdes, K. (2018). Novel (p)ppGpp binding and metabolizing proteins of *Escherichia coli*. *mBio* 9, e02188–e02217. doi: 10.1128/mBio.02188-17

Conflict of Interest: The authors declare that the research was conducted in the absence of any commercial or financial relationships that could be construed as a potential conflict of interest.

frontiers in Microbiology

MINI REVIEW
published: 14 October 2020
doi: 10.3389/fmicb.2020.594024

Pleiotropic Effects of Bacterial Small Alarmone Synthetases: Underscoring the Dual-Domain Small Alarmone Synthetases in *Mycobacterium smegmatis*

*Sushma Krishnan and Dipankar Chatterji**

Molecular Biophysics Unit, Indian Institute of Science, Bangalore, India

The nucleotide alarmone (p)ppGpp, signaling the stringent response, is known for more than 5 decades. The cellular turnover of the alarmone is regulated by RelA/SpoT homolog (RSH) superfamily of enzymes. There are long RSHs (RelA, SpoT, and Rel) and short RSHs [small alarmone synthetases (SAS) and small alarmone hydrolases (SAH)]. Long RSHs are multidomain proteins with (p)ppGpp synthesis, hydrolysis, and regulatory functions. Short RSHs are single-domain proteins with a single (p)ppGpp synthesis/hydrolysis function with few exceptions having two domains. Mycobacterial RelZ is a dual-domain SAS with RNase HII and the (p)ppGpp synthetase activity. SAS is known to impact multiple cellular functions independently and in accordance with the long RSH. Few SAS in bacteria including RelZ synthesize pGpp, the third small alarmone, along with the conventional (p)ppGpp. SAS can act as an RNA-binding protein for the negative allosteric inhibition of (p)ppGpp synthesis. Here, we initially recap the important features and molecular functions of different SAS that are previously characterized to understand the obligation for the "alarmone pool" produced by the long and short RSHs. Then, we focus on the RelZ, especially the combined functions of RNase HII and (p)ppGpp synthesis from a single polypeptide to connect with the recent findings of SAS as an RNA-binding protein. Finally, we conclude with the possibilities of using single-stranded RNA (ssRNA) as an additional therapeutic strategy to combat the persistent infections by inhibiting the redundant (p)ppGpp synthetases.

Keywords: short alarmone, (p)ppGpp, pGpp, stress response, R-loop, replication stress, ssRNA, RNase HII

OPEN ACCESS

Edited by:
Gert Bange,
University of Marburg, Germany

Reviewed by:
Mohammad Roghanian,
Umeå University, Sweden
Christiane Wolz,
University of Tübingen, Germany

***Correspondence:**
Dipankar Chatterji
dipankar@iisc.ac.in

Specialty section:
This article was submitted to Microbial Physiology and Metabolism, a section of the journal Frontiers in Microbiology

Received: *12 August 2020*
Accepted: *17 September 2020*
Published: *14 October 2020*

Citation:
Krishnan S and Chatterji D (2020) Pleiotropic Effects of Bacterial Small Alarmone Synthetases: Underscoring the Dual-Domain Small Alarmone Synthetases in Mycobacterium smegmatis. Front. Microbiol. 11:594024. doi: 10.3389/fmicb.2020.594024

INTRODUCTION

In 1969, Cashel and Gallant first identified the nucleotide alarmone molecules, guanosine-5', 3'-pentaphosphate (pppGpp) and guanosine-5', 3' -tetraphosphate (ppGpp), from amino acid-starved *Escherichia coli* (Cashel and Gallant, 1969). Intracellular levels of (p)ppGpp are controlled by RelA/SpoT homolog (RSH) proteins as a response to various external and internal stresses encountered by the organisms (Chatterji and Ojha, 2001; Potrykus and Cashel, 2008; Srivatsan

and Wang, 2008; Wu and Xie, 2009; Roghanian et al., 2019). This is a direct pathway of stringent response in which the (p)ppGpp signals the massive switch from energy-consuming to energy-conserving process (Potrykus and Cashel, 2008; Abranches et al., 2009; Kriel et al., 2012; Gaca et al., 2013; Hauryliuk et al., 2015; Liu et al., 2015; Steinchen and Bange, 2016). In Gram-negative organisms, beta and gamma subgroups of proteobacteria carry two such enzymes where the main role of RelA is (p)ppGpp synthesis and SpoT in hydrolysis. SpoT can also synthesize (p)ppGpp and is therefore bifunctional (Xiao et al., 1991; Gentry and Cashel, 1996). In Gram-positive organisms, there is a single bifunctional Rel enzyme which synthesizes and degrades (p)ppGpp (Mittenhuber, 2001; Jain et al., 2006; Srivatsan and Wang 2008; Takada et al., 2020).

Apart from these classical, long, multidomain RSHs, few small RSH homologs were identified in organisms ranging from bacteria to plants. They are mostly monodomain, monofunctional proteins either with short alarmone synthetase (SAS) or short alarmone hydrolase (SAH) activity (Sun et al., 2010; Atkinson et al., 2011; Jimmy et al., 2020). The discovery of SAS and SAH opened a new line of research, to understand the indirect pathways of stress response induced by cues such as cell wall antibiotics, acid, alkali, hydrogen peroxide, ethanol, etc. (Horsburgh and Moir, 1999; Cao et al., 2002; Mascher et al., 2003; Thackray and Moir, 2003; Weinrick et al., 2004; D'Elia et al., 2009; Kim et al., 2012; Geiger et al., 2014; Pando et al., 2017). We have identified a dual-domain SAS in *Mycobacterium smegmatis* with RNase HII and (p)ppGpp synthesis activity (Murdeshwar and Chatterji, 2012).

Small alarmone synthetases play an important role to maintain the basal level of (p)ppGpp, which in turn induces the virulence of the pathogenic bacteria. The "(p)ppGpp pool" produced by the long and short RSH enzymes (Ronneau and Hallez, 2019) and the consecutive guanosine triphosphate (GTP) depletion are the key factors determining the formation of bacterial persister cells (Fung et al., 2020). Therefore, understanding the SAS-mediated synthesis and regulation of (p)ppGpp is the need of the hour to modify the current antibacterial therapy.

SALIENT FEATURES OF SMALL ALARMONE SYNTHETASES

Small alarmone synthetases were identified in bacteria, such as *Streptococcus mutans*, *Bacillus subtilis*, *Enterococcus faecalis*, *Streptococcus pneumoniae*, *Mycobacterium smegmatis*, *Staphylococcus aureus*, *Corynebacterium glutamicum*, *Clostridium difficile*, *Vibrio cholerae*, and *Pseudomonas aeruginosa*. There are two highly homologous SAS proteins in bacteria and are named as RelP (SAS2, YwaC) and RelQ (SAS1, YjbM). Jimmy et al. (2020) reported the recent classification of SAS and identified 30 subfamilies. The functions of five of these subgroup enzymes were experimentally validated (**Table 1**) and found to be present in toxin–antitoxin (TA) system (Jimmy et al., 2020). The list of previously characterized bacterial SAS is given in **Table 1**. Their domain structures are given in **Figure 1**.

MOLECULAR FUNCTIONS OF SMALL ALARMONE SYNTHETASES

Different SAS have different roles because they are induced by different signals (**Figure 2**). RSH is activated mostly under starvation and to the intracellular imbalances involving LPS biosynthesis and ADP metabolism (Roghanian et al., 2019), whereas SAS may respond to various types of environmental stimuli (**Figure 2**). Maintaining the basal level of (p)ppGpp is important for protection against different kinds of stresses, especially antibiotics stress. Most of the SAS proteins prefer guanosine diphosphate (GDP) to GTP as a substrate (Murdeshwar and Chatterji, 2012; Geiger et al., 2014; Gaca et al., 2015b). Rel and SAS are involved in the allosteric regulation of guanosine and GTP biosynthesis (Gaca et al., 2013; Bittner et al., 2014; Kriel et al., 2014).

RelP AND RelQ

RelP and RelQ share nearly 50% sequence similarity at the amino acid level. *relP/relQ* genes are upregulated due to various stress cues, such as cell envelope (Cao et al., 2002; D'Elia et al., 2009; Geiger et al., 2014), alkali (Nanamiya et al., 2008), ethanol (Pando et al., 2017), high salt, acidic, heat, and hydrogen peroxide (Thackray and Moir, 2003; Weinrick et al., 2004; Kim et al., 2012; Zweers et al., 2012). The first SAS proteins (RelP and RelQ) were identified in *S. mutans* (Lemos et al., 2004, 2007). During oxidative and acidic stress, RelP helped to slow the growth of the bacteria (Kim et al., 2012). Rel inactivation did not yield a lethal phenotype of *S. mutans*, and the basal level of (p)ppGpp was not increased through RelP and RelQ-dependent (p)ppGpp synthesis (Lemos et al., 2007). This could be due to the existence of an alternative mechanism for (p)ppGpp degradation in Streptococci (Lemos et al., 2007). In *B. subtilis*, RelP and RelQ have growth phase-dependent regulation. *relQ* is mainly transcribed in mid-exponential phase and it slows down its expression in the late-exponential phase; in addition, the *relP* is highly induced at this phase (Nanamiya et al., 2008). The (p)ppGpp synthesis of *B. subtilis* RelP is induced by alkaline stress (Nanamiya et al., 2008). In *E. faecalis*, only RelQ synthesizes (p)ppGpp apart from Rel (Abranches et al., 2009). The Δ*relAQ* strain showed significant sensitivity to vancomycin, ampicillin, and norfloxacin (Abranches et al., 2009; Gaca et al., 2013). In *E. faecalis*, (p)ppGpp-mediated antibiotic resistance happens at a concentration below the required value to mount stringent response. *Staphylococcus aureus* contains RelP and RelQ homologs. The expression of these two SAS is induced upon cell wall stress with vancomycin and ampicillin. The presence of three (p)ppGpp synthetases plays a significant role in the development of methicillin-resistant *S. aureus* (MRSA). Like the RelP of *S. mutans*, the RelP of *S. aureus* is also a more potent (p)ppGpp synthetase (Geiger et al., 2014). *Clostridium difficile* has a RelQ that is induced by antibiotic stress. There is a 2-fold upregulation of *relQ* after exposure to ampicillin and clindamycin, which explains the role of RelQ in antibiotic survival (Pokhrel et al., 2020).

Crystal structures of RelP and RelQ from *B. subtilis* and *S. aureus* revealed the homotetramer structures with highly

TABLE 1 | Short alarmone synthetases in bacteria.

Name of the bacteria	SAS type	Function	References
Gram-positive bacteria			
Streptococcus mutans	RelP	- Stronger (p)ppGpp synthetic activity than RelQ - Induced by H_2O_2 stress	Lemos et al., 2004, 2007, 2008; Seaton et al., 2011; Kim et al., 2012
	RelQ	- Involved in acid and oxidative stresses	
Bacillus subtilis	RelP	- Induced by alkaline stress - Dimerization of 70S ribosome	Nanamiya et al., 2008; Natori et al., 2009; Tagami et al., 2012; Schafer et al., 2020
	RelQ	- Synthesize pGpp - Contribute to thermoresistant phenotype	
Enterococcus faecalis	RelQ	- Vancomycin tolerance - Virulence - Synthesize pGpp - Negative allosteric regulation by ssRNA	Abranches et al., 2009; Gaca et al., 2013, 2015a,b; Beljantseva et al., 2017; Colomer-Winter et al., 2018
Streptococcus pneumoniae	RelP RelQ	- Both are low active (p)ppGpp synthetase	Battesti and Bouveret, 2009; Kazmierczak et al., 2009
Mycobacterium smegmatis	RelZ	- Bifunctional protein with (p)ppGpp synthetase and RNase HII activity - Induced under replication stress - Synthesize pGpp - Regulation by ssRNA	Murdeshwar and Chatterji, 2012; Krishnan et al., 2016; Petchiappan et al., 2020
Staphylococcus aureus	RelP	- Cell envelope stress - Synthesize pGpp	Geiger et al., 2014; Gratani et al., 2018; Manav et al., 2018; Bhawini et al., 2019; Yang et al., 2019; Li et al., 2020
	RelQ	- Mediates β-lactum resistance in methicillin-resistant strains - Synthesize pGpp	
Corynebacterium glutamicum	$RelP_{Cg}$	- Role in primary nucleotide metabolism - Respond to low temperatures	Ruwe et al., 2017
	$RelS_{Cg}$	- Synthesize pGpp	
Clostridium difficile	RelQ	- Antibiotic resistance	Pokhrel et al., 2020
Bacillus subtilis	PhRel2	- All of these are grouped as toxSASs since they are toxic component of TA system	Jimmy et al., 2020; Dedrick et al., 2017
Coprobacillus sp.,	FaRel2		
Mycobacterium phage Phrann	PhRel	- PhRel helps in preventing the superinfection by other bacteriophages	
Cellulomonas marina	FaRel		
Mycobacterium tuberculosis	CapRel		
Gram-negative bacteria			
Vibrio cholerae	RelV	- Regulate basal level of (p)ppGpp - Induced upon glucose or fatty acid starvation	Das and Bhadra, 2008; Das et al., 2009; Dasgupta et al., 2014
Pseudomonas aeruginosa	Tas1 (RelV)	- Important role in interbacterial antagonism	Ahmad et al., 2019

similar monomers and homologs of (p)ppGpp synthetase domains. RelQ activity is inhibited by ssRNA (Beljantseva et al., 2017) and positively regulated by pppGpp (not ppGpp), whereas RelP is not allosterically regulated by (p)ppGpp. This is because of the difference in the conformation of the substrate binding site of these proteins. The RelQ, homotetramer of *B. subtilis*, has a distinct cleft in its center for the binding of two allosteric (p)ppGpp molecules (Steinchen et al., 2015, 2018; Steinchen and Bange, 2016). RelP has been shown to influence the formation of ribosome dimers to inactivate the translation of metabolic pathway (Tagami et al., 2012).

RelS

Corynebacterium glutamicum has two SAS proteins (**Figure 2**), represented as $RelP_{Cg}$ and $RelS_{Cg}$ (actRel subgroup). The SAS

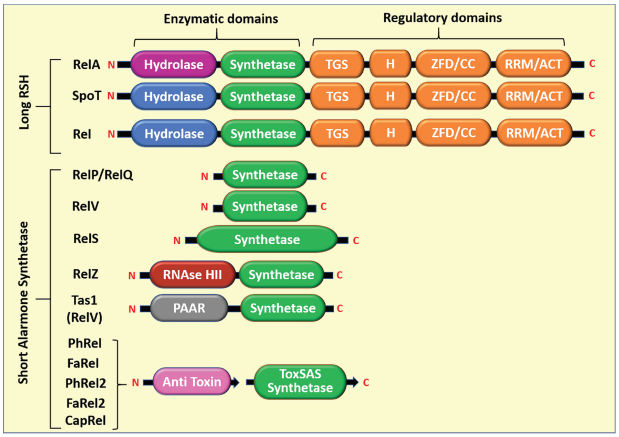

FIGURE 1 | Domain structure of long RelA/SpoT homolog (RSH) and short alarmone synthetase (SAS). SAS proteins have only (p)ppGpp synthetic domain (~25–29 kDa), the hydrolysis and regulatory domains are absent. RelS is a 39.8-kDa protein with extended synthetase domain than other SAS. RelZ is a 64.5-kDa protein with RNase HII domain. The hydrolysis and regulatory domains are TGS, ThrRs, GTPase, and SpoT; H, helical domain; ZFD, zinc finger domain; CC, conserved cysteine; RRM, ribosome recognition motif; ACT, aspartokinase, chorismate mutase, and TyrA. Tas1 synthetase is a toxin effector domain, and proline-alanine-alanine-arginine (PAAR) is a toxin delivery domain; PhRel, FaRel, PhRel2, FaRel2, and CapRel are known as ToxSAS because of their presence in toxin–antitoxin (TA) module.

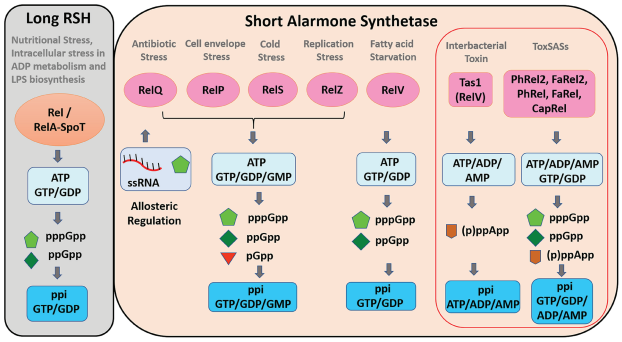

FIGURE 2 | Functions of long RSH and short alarmone synthetase. Long RSH, Rel/RelA-SpoT, synthesize pppGpp and ppGpp using GTP/GDP as substrates during nutritional stress. SAS protein expression is induced by various stress signals. SAS Rels synthesize pGpp in addition to pppGpp and ppGpp using GTP/GDP/GMP as substrates. pppGpp and ssRNA bind to RelQ and mediate the allosteric regulation. The pppGpp synthesis activity of RelZ is also inhibited by RNA and pppGpp. Tas1 synthesize (p)ppApp using ATP/ADP/AMP as substrates. ToxSASs (not Tas1) synthesize both (p)ppGpp and (p)ppApp. ToxSASs are represented within red outlined box.

protein encoded by cg2324 is named as RelS and shares sequence similarity with the (p)ppGpp synthetase domain of RelQ. (p)ppGpp synthesis activity is not found for $RelP_{Cg}$. The maximum activity of the $RelS_{Cg}$ is obtained at a temperature below optimum; therefore, it is assumed that (p)ppGpp is synthesized in response to low temperatures (Ruwe et al., 2017).

ToxSASs

Many SAS subfamilies were identified in conserved bicistronic operon of TA system from *actinobacteria*, firmicutes, and *proteobacteria*. Five of these SAS were demonstrated to be the toxic component of the TA system and hence named as toxSASs (Jimmy et al., 2020). They are *B. subtilis* PhRel2, *Coprobacillus* sp., FaRel2, *Mycobacterium* phage Phrann PhRel, *Cellulomonas marina* FaRel, and *Mycobacterium tuberculosis* CapRel (**Figures 1, 2**). The toxicity of the toxSASs was neutralized by the six adjacent antitoxin proteins, among which five are specific to corresponding toxSASs and *C. marina* FaRel2 can neutralize all the five toxSASs. The specific function of the toxSASs is not identified, except of PhRel (also known as Gp29), which plays a role in preventing the superinfection by other bacteriophages (Dedrick et al., 2017).

RelV

RelV (relA-like (p)ppGpp synthetase domain coding gene in vibrios) shared poor homology with RelP and RelQ, because the bacteria itself are phylogenetically different from firmicutes, but there is a high conservation of amino acid residues in the synthetase domains of RelV, RelP, and RelQ. In *V. cholerae*, RelV can produce (p)ppGpp upon glucose or fatty acid starvation (Das and Bhadra, 2008; Das et al., 2009; Dasgupta et al., 2014). Another RelV subfamily homolog Tas1 was identified in *P. aeruginosa*. Tas1 RSH domain is encoded within a large conserved T6SS cluster (type 6 secretion system) and fused to a toxin delivery domain (**Figure 2**), which exhibits its toxic effect on another competitor cell, thus playing an important function in interbacterial antagonism (Ahmad et al., 2019).

RelZ (MS_RHII-RSD)

In *M. smegmatis*, MSMEG_5849 codes for a bifunctional protein MS_RHII-RSD (renamed as RelZ), which has a C-terminal RSD domain similar to the other SAS but is different from them due to the presence of N-terminal RNase HII domain in the same polypeptide chain (**Figure 3**). RelZ efficiently hydrolyze RNA–DNA hybrids (Murdeshwar and Chatterji, 2012) and R-loops (Krishnan et al., 2016). R-loops have a major role in replication–transcription conflicts and lead to stalled arrays of RNA polymerase to block the replication fork movement, thereby promoting replication stress (Drolet, 2006; Poveda et al., 2010; Stirling et al., 2012). This stress can be efficiently managed by two mechanisms: R-loop removal by RNase HII (Aguilera and García-Muse, 2012) and destabilization of stalled RNA polymerase by (p)ppGpp synthesis (Cashel et al., 1996; Ross et al., 2013). RelZ possesses both these important activities (RNase HII and (p)ppGpp synthetase) in a single polypeptide. Our previous study (Krishnan et al., 2016) showed that under UV stress, RelZ removes the accumulated R-loops in RNase H-deficient *E. coli*, and *relZ* expression is upregulated in *M. smegmatis* to remove the R-loops generated due to UV

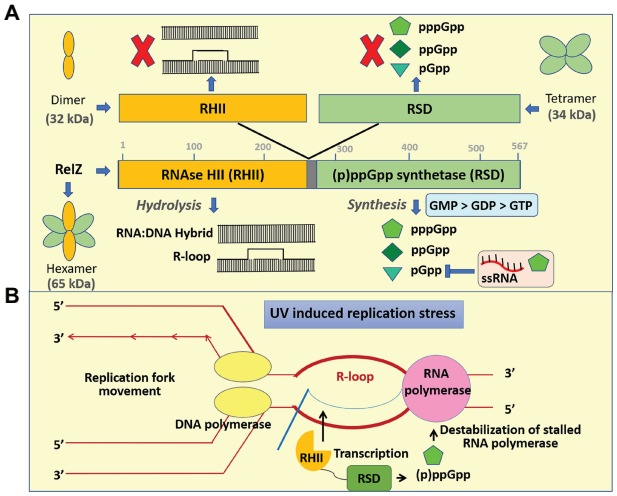

FIGURE 3 | Mechanism of regulation and functions of RelZ. **(A)** RelZ contains an RNAse HII (RHII) domain in tandem with the (p)ppGpp synthetase domain (RSD, RelA SpoT nucleotidyl transferase domain). Full-length protein in *cis* has both RNAse HII activity and (p)ppGpp synthetase activity whereas neither the purified domain variants in isolation nor on *trans* complementation can function independently. RelZ can hydrolyze RNA:DNA hybrid as well as R-loop. It can synthesize pGpp, ppGpp, and pppGpp having the substrate preferences as GMP > GDP > GTP. pGpp synthesis is negatively regulated by ssRNA and high concentrations of pppGpp. From our earlier studies on active site mutational analysis, gel filtration chromatography followed by native PAGE revealed that the N-terminal RHII domain is monomeric and C-terminal RSD domain is tetrameric upon isolation. The full-length active protein is, however, hexamer in solution. We also found that RelZ and all the mutant variants of the full-length RelZ remain as hexameric form in solution. **(B)** In our previous study, we demonstrated that RelZ can hydrolyze R-loops in *Escherichia coli* exposed to UV stress. RelZ gene expression was upregulated under UV stress, and this gene-deleted strain showed increased R-loop accumulation as compared to the wild type. Based on these results, we proposed a model for the physiological function of RelZ. UV stress leads to increased R-loop formation and replication–transcription conflicts. Under UV stress, RelZ expression is upregulated than the conventional RNase HI and HII. Its RHII activity removes the R-loops and the stalled RNA polymerase is destabilized indirectly by (p)ppGpp. Thus, RelZ plays an important role during R-loop-induced replication stress response in *Mycobacterium smegmatis*. **(B)** is adapted and redrawn from Krishnan et al. (2016).

stress. Based on these results, we proposed a model to explain the function of RelZ. Upon UV stress, the levels of RelZ increase within the cell. Any R-loops formed are removed by the RNase HII and (p)ppGpp helps to destabilize the stalled RNA polymerase *via* an unknown mechanism to rescue the cells from replication stress (Krishnan et al., 2016). In addition, RelZ mediates antibiotic tolerance in *M. smegmatis* but does not impact biofilm formation significantly (Petchiappan et al., 2020).

Active site mutational studies of RelZ revealed that inactivation of one domain does not affect the activity of the other domain. However, the purified subdomains are nonfunctional when separated and expressed independently (**Figure 3**). This kind of domain interdependence was extensively characterized, and the results showed that the full-length RelZ is essential for its function and it is a hexamer (Krishnan et al., 2016). The synthetic subdomain of RelZ is a tetramer in solution like the other solved structures of RelP and RelQ (Steinchen et al., 2015, 2018, 2020; Steinchen and Bange, 2016). Petchiappan et al. (2020) showed that RelZ prefers guanosine monophosphate (GMP) as a substrate and synthesizes pGpp. To understand the difference between pGpp and ppGp, the reaction mixture was treated with NaOH that hydrolyzes only pGpp. From thin layer chromatography, it was shown that Rel hydrolyzes pGpp to GMP and pyrophosphate as evidenced by the comigration of the radiolabeled product with the purified pyrophosphate whereas RelZ showed weak hydrolysis. We found that ssRNA inhibits RelZ-mediated pGpp synthesis, but R-loop did not show any effect (Petchiappan et al., 2020). The pGpp synthesis activity of the RelZ is inhibited by pppGpp whereas ppGpp and pGpp did not have significant effect. Therefore, we infer that the cellular pppGpp levels determine the RelZ-mediated synthesis, whereas ssRNA and pppGpp carefully regulate it. The altered cell surface properties of Δ*relZ* strain indicated that RelZ plays a role in cell wall metabolism (Petchiappan et al., 2020).

Mycobacterium tuberculosis has a SAS encoding (p)ppGpp synthetase, Rv1366. But it has no RNase H domain and it is incapable of synthesizing (p)ppGpp (Nanamiya et al., 2008; Weiss and Stallings, 2013; Bag et al., 2014). Few RHII-RSD dual-domain orthologs were identified from Mycobacteria; *Mycobacterium vanbaalenii* (YP_995923.1), *Mycobacterium tusciae* (ZP_09680741.1), and *Mycobacterium gilvum* (YP_001132882.1). However, RelZ is the only dual-domain mycobacterial SAS characterized so far. RelZ type of SAS with RNase H and (p)ppGpp synthetase domains are found only in the environmental species and they are absent in the pathogenic species of mycobacteria.

SAS SYNTHESIZE pGpp

Recently, SAS proteins but not Rel are found to use GMP as a substrate and synthesize pGpp, a third alarmone which makes the alarmone group representation from (p)ppGpp to (pp)pGpp (Gaca et al., 2015b). pGpp can function like (p)ppGpp as well and may have different functions which is not regulated by (p)ppGpp (Gaca et al., 2015a). The pGpp can be hydrolyzed by Rel, like the hydrolysis of (p)ppGpp (Gaca et al., 2015b; Yang et al., 2019). In *B. subtilis*, RelP and RelQ are shown to synthesize ppGp or pGpp. (Tagami et al., 2012). RelQ from *E. faecalis* is an efficient producer of pGpp (Gaca et al., 2015a). RelQ and RelP of *S. mutans* showed much weaker pGpp synthesis activity upon comparison with $RelQ_{Ef}$. RelP and RelQ of *S. aureus* and $RelS_{Cg}$ of *C. glutamicum* synthesize pGpp along with (p)ppGpp. ppGpp/pGpp effectively reduce the intracellular levels of GTP and these guanine nucleotides are synthesized only when RelA is inactive in the cells (Ruwe et al., 2017). The synthesis of pGpp will become relevant only when the GMP levels in the cells are increased like GTP level. Such kind of GMP accumulation has been reported in *B. subtilis* (Liu et al., 2015). It was also speculated that pGpp may be involved in stretching the stress response after the depletion of GTP and GDP in the cell (Gaca et al., 2015b; Ruwe et al., 2017). However, pGpp regulates the purine synthesis but does not involve in ribosome biogenesis (Tagami et al., 2012; Yang et al., 2020).

SAS SYNTHESIZE (p)ppApp

Recent studies by Ahmad et al. (2019) and Jimmy et al. (2020) revealed that SAS not only synthesize ppGpp but also synthesize ppApp. In *P. aeruginosa*, a secreted toxic effector of T6SS was identified as Tas1. Though the crystal structure of Tas1 is similar to the other (p)ppGpp synthetases, it does not synthesize (p)ppGpp but produces (p)ppApp (Ahmad et al., 2019). Another SAS that produces (p)ppApp was identified in *C. marina* FaRel. The toxicity of this toxSAS is mediated by ppGpp and ppApp followed by the depletion of intracellular GTP and ATP pools (Jimmy et al., 2020).

SAS BIND TO ssRNA

Hauryliuk and Atkinson (2017) reviewed the RNA-binding properties of SAS. Beljantseva et al. (2017) discovered that $RelQ_{Ef}$ activity is inhibited when it binds to ssRNA. RNA binds to RelQ in a sequence-specific manner with GGNGG, a putative Shine–Dalgarno-like consensus sequence. pppGpp strongly counteracts the inhibition by RNA and destabilizes the RNA:RelQ complex. In this way, RelQ has both enzyme activity and RNA-binding property. In a RelQ:RNA complex, (p)ppGpp synthesis and pppGpp binding are mutually incompatible. Hence, there is a possibility that the RelQ:RNA complex acts a regulatory switch between inactive and active forms of the enzyme. ssRNA and pppGpp compete with each other to bind into the central cleft of the homotetramer, but this property is not conserved in RelP of *S. aureus*, because pppGpp is not an allosteric regulator of RelP. The central cleft in the RelP tetramer could be an allosteric site bound by other small molecules (Manav et al., 2018; Steinchen et al., 2018).

The RNA-binding property of RelQ can be compared with that of RelZ since the ssRNA inhibits the activity of RelZ (Petchiappan et al., 2020). Since RelZ is involved in R-loop-mediated replication stress (Krishnan et al., 2016), (p)ppGpp synthesis can occur by sensing the R-loops. Once the RNase H cleaves the R-loop into dsDNA and ssRNA (Dutta et al., 2011), the replication stress is relieved and hence the (p)ppGpp synthesis stops. This could be the reason for ssRNA showing inhibitory effect on RelZ-mediated alarmone synthesis. Structural analysis of RelZ is in progress to understand the RelZ:ssRNA complex.

Arresting the (p)ppGpp synthetase activity using (p)ppGpp analogues is emerging as a clinically important method in eradicating persistent infections (de la Fuente-Núñez et al., 2014; Andresen et al., 2016; Petchiappan and Chatterji, 2017; Syal et al., 2017; Dutta et al., 2019). Similarly, the ssRNA-binding property of the SAS can be explored to regulate the SAS-mediated (p)ppGpp synthesis. Mutant huntingtin protein that causes Huntington's disease was selectively and effectively inhibited by ss siRNA approach (Yu et al., 2012). According to Lima et al. (2012), the identification of potent ssRNA would provide an easy route to therapeutics than dsRNA. ssRNA do not require special formulations for tissue penetration (Bennett and Swayze, 2010), whereas the ds siRNAs need to undergo complex and expensive lipid formulations (Tao et al., 2011). Nucleic acids not only recognize specific target sequences by complementary base pairing but they can interact with proteins and this property is currently being explored in therapeutics (Roberts et al., 2020).

CONCLUSION

The co-evolution of SAS along with Rel, redundant (p)ppGpp synthetases, and multiple types of closely related alarmones in bacteria is intriguing. (p)ppGpp is a key factor for biofilm formation, antibiotic tolerance, virulence, and persistence in many pathogenic bacteria. Therefore, inhibition of (p)ppGpp synthesis will inhibit the long-term survival of the pathogen. Therefore, finding an inhibitor to prevent (p)ppGpp synthesis is of high therapeutic interest. In addition to that, ssRNA with specific binding sequence could be a supplementary therapeutic element to inhibit the SAS-dependent (p)ppGpp synthesis because SAS is an RNA-binding protein. The discovery of SAS has not only augmented the prospects of stringent response but also adds value to the upcoming field of RNA therapies.

AUTHOR CONTRIBUTIONS

DC and SK conceptualized and wrote the manuscript. All authors contributed to the article and approved the submitted version.

FUNDING

The work was partially supported by JC Bose fellowship, Department of Science and Technology, Government of India.

ACKNOWLEDGMENTS

SK thanks the Department of Biotechnology for the fellowship.

REFERENCES

Abranches, J., Martinez, A. R., Kajfasz, J. K., Chávez, V., Garsin, D. A., and Lemos, J. A. (2009). The molecular alarmone (p)ppGpp mediates stress responses, vancomycin tolerance, and virulence in *Enterococcus faecalis*. *J. Bacteriol.* 191, 2248–2256. doi: 10.1128/JB.01726-08

Aguilera, A., and García-Muse, T. (2012). R loops: from transcription by products to threats to genome stability. *Mol. Cell* 46, 115–124. doi: 10.1016/j.molcel.2012.04.009

Ahmad, S., Wang, B., Walker, M. D., Tan, H. R., Sogios, P. J., Savchenko, A., et al. (2019). An interbacterial toxin inhibits target cell growth by synthesizing (p)ppApp. *Nature* 575, 674–678. doi: 10.1038/s41586-019-1735-9

Andresen, L., Varik, V., Tozawa, Y., Jimmy, S., Lindberg, S., Tenson, T., et al. (2016). Auxotrophy-based high throughput screening assay for the identification of *Bacillus subtilis* stringent response inhibitors. *Sci. Rep.* 6:35824. doi: 10.1038/srep35824

Atkinson, G. C., Tenson, T., and Hauryliuk, V. (2011). The RelA/SpoT homolog (RSH) superfamily: distribution and functional evolution of ppGpp synthetases

and hydrolases across the tree of life. *PLoS One* 6:e23479. doi: 10.1371/journal.pone.0023479

Bag, S., Das, B., Dasgupta, S., and Bhadra, R. K. (2014). Mutational analysis of the (p)ppGpp synthetase activity of the Rel enzyme of *Mycobacterium tuberculosis*. *Arch. Microbiol.* 196, 575–588. doi: 10.1007/s00203-014-0996-9

Battesti, A., and Bouveret, E. (2009). Bacteria possessing two RelA/SpoT-like proteins have evolved a specific stringent response involving the acyl carrier protein-SpoT interaction. *J. Bacteriol.* 191, 616–624. doi: 10.1128/JB.01195-08

Beljantseva, J., Kudrin, P., Andresen, L., Shingler, V., Atkinson, G. C., Tenson, T., et al. (2017). Negative allosteric regulation of *Enterococcus faecalis* small Alarmone Synthetase RelQ by single stranded RNA. *Proc. Natl. Acad. Sci. U. S. A.* 114, 3726–3731. doi: 10.1073/pnas.1617868114

Bennett, C. F., and Swayze, E. E. (2010). RNA targeting therapeutics: molecular mechanisms of antisense oligonucleotides as a therapeutic platform. *Annu. Rev. Pharmacol. Toxicol.* 50, 259–293. doi: 10.1146/annurev.pharmtox.010909.105654

Bhawini, A., Pandey, P., Dubey, A. P., Zehra, A., Gopal, N., and Mishra, M. N. (2019). RelQ mediates the expression of β-lactam resistance in methicillin-resistant *Staphylococcus aureus*. *Front. Microbiol.* 10:339. doi: 10.3389/fmicb.2019.00339

Bittner, A. N., Kriel, A., and Wang, J. D. (2014). Lowering GTP level increases survival of amino acid starvation but slows growth rate for *Bacillus subtilis* cells lacking (p)ppGpp. *J. Bacteriol.* 196, 2067–2076. doi: 10.1128/JB.01471-14

Cao, M., Kobel, P. A., Morshedi, M. M., Wu, M. F., Paddon, C., and Helmann, J. D. (2002). Defining the *Bacillus subtilis* sigma (W) regulon: a comparative analysis of promoter consensus search, run-off transcription/macroarray analysis (ROMA), and transcriptional profiling approaches. *J. Mol. Biol.* 316, 443–457. doi: 10.1006/jmbi.2001.5372

Cashel, M., and Gallant, J. (1969). Two compounds implicated in the function of the RC gene of *Escherichia coli*. *Nature* 221, 838–841. doi: 10.1038/221838a0

Cashel, M., Gentry, D. M., Hernandez, V. J., and Vinella, D. (1996). "The stringent response" in *Escherichia coli and Salmonella typhimurium: Cellular and molecular biology*. ed. F. C. Neidhardt (Washington, DC: ASM Press), 1458–1496.

Chatterji, D., and Ojha, A. K. (2001). Revisiting the stringent response, ppGpp and starvation signaling. *Curr. Opin. Microbiol.* 4, 160–165. doi: 10.1016/s1369-5274(00)00182-x

Colomer-Winter, C., Gaca, O. A., Chuang-Smith, O., Lemos, A. J., and Frank, K. L. (2018). Basal levels of (p)ppGpp differentially affect the pathogenesis of infective endocarditis in *Enterococcus faecalis*. *Microbiology* 164, 1254–1265. doi: 10.1099/mic.0.000703

D'Elia, M. A., Millar, K. E., Bhavsar, A. P., Tomljenovic, A. M., Hutter, B., Schaab, C., et al. (2009). Probing teichoic acid genetics with bioactive molecules reveals new interactions among diverse processes in bacterial cell wall biogenesis. *Chem. Biol.* 16, 548–556. doi: 10.1016/j.chembiol.2009.04.009

Das, B., and Bhadra, R. K. (2008). Molecular characterization of Vibrio cholerae DrelA DspoT double mutants. *Arch. Microbiol.* 189, 227–238. doi: 10.1007/s00203-007-0312-z

Das, B., Pal, R. R., Bag, S., and Bhadra, R. K. (2009). Stringent response in Vibrio cholerae: genetic analysis of spoT gene function and identification of a novel (p)ppGpp synthetase gene. *Mol. Microbiol.* 72, 380–398. doi: 10.1111/j.1365-2958.2009.06653.x

Dasgupta, S., Basu, P., Pal, R. R., Bag, S., and Bhadra, R. K. (2014). Genetic and mutational characterization of the small alarmone synthetase gene relV of Vibrio cholerae. *Microbiology* 160, 1855–1866. doi: 10.1099/mic.0.079319-0

de la Fuente-Núñez, C., Reffuveille, F., Haney, E. F., Straus, S. K., and Hancock, R. E. W. (2014). Broad-Spectrum anti-biofilm peptide that targets a cellular stress response. *PLoS Pathol.* 10:e1004152. doi: 10.1371/journal.ppat.1004152

Dedrick, R. M., Jacobs-Sera, D., Bustamante, C. A., Garlena, R. A., Mavrich, T. N., Pope, W. H., et al. (2017). Prophage-mediated defence against viral attack and viral counter-defence. *Nat. Microbiol.* 2:16251. doi: 10.1038/nmicrobiol.2016.251

Drolet, M. (2006). Growth inhibition mediated by excess negative supercoiling: the interplay between transcription elongation, R-loop formation, and DNA topology. *Mol. Microbiol.* 59, 723–730. doi: 10.1111/j.1365-2958.2005.05006.x

Dutta, N. K., Klinkenberg, L. G., Vazquez, M. J., Segura-Carro, D., Colmenarejo, G., Ramon, F., et al. (2019). Inhibiting the stringent response blocks *Mycobacterium tuberculosis* entry into quiescence and reduces persistence. *Sci. Adv.* 5:eaav2104. doi: 10.1126/sciadv.aav2104

Dutta, D., Shatalin, K., Epshtein, V., Gottesman, M. E., and Nudler, E. (2011). Linking RNA polymerase backtracking to genome instability in *E. coli*. *Cell* 146, 533–543. doi: 10.1016/j.cell.2011.07.034

Fung, D. K., Barra, J. T., Schroeder, J. W., Ying, D., and Wang, J. D. (2020). A shared alarmone-GTP switch underlies triggered and spontaneous persistence. *bioRxiv* [Preprint] doi: 10.1101/2020.03.22.002139

Gaca, A. O., Colomer-Winter, C., and Lemos, J. A. (2015a). Many means to a common end: the intricacies of (p)ppGpp metabolism and its control of bacterial homeostasis. *J. Bacteriol.* 197, 1146–1156. doi: 10.1128/JB.02577-14

Gaca, A. O., Kajfasz, J. K., Miller, J. H., Liu, K., Wang, J. D., Abranches, J., et al. (2013). Basal levels of (p)ppGpp in *Enterococcus faecalis*: the magic beyond the stringent response. *MBio* 4:e00646–13. doi: 10.1128/mBio.00646-13

Gaca, A. O., Kudrin, P., Colomer-Winter, C., Beljantseva, J., Liu, K., Anderson, B., et al. (2015b). From (p)ppGpp to (pp)pGpp: characterization of regulatory effects of pGpp synthesized by the small Alarmone Synthetase of *Enterococcus faecalis*. *J. Bacteriol.* 197, 2908–2919. doi: 10.1128/JB.00324-15

Geiger, T., Kastle, B., Gratani, F. L., Goerke, C., and Wolz, C. (2014). Two small (p)ppGpp synthases in *Staphylococcus aureus* mediate tolerance against cell envelope stress conditions. *J. Bacteriol.* 196, 894–902. doi: 10.1128/JB.01201-13

Gentry, R. D., and Cashel, M. (1996). Mutational analysis of the *Escherichia coli* spoT gene identifies distinct but overlapping regions involved in ppGpp synthesis and degradation. *Mol. Microbiol.* 19, 1373–1384. doi: 10.1111/j.1365-2958.1996.tb02480.x

Gratani, F. L., Horvatek, P., Geiger, T., Borisova, M., Mayer, C., Grin, I., et al. (2018). Regulation of the opposing (p)ppGpp synthetase and hydrolase activities in a bifunctional RelA/SpoT homologue from *Staphylococcus aureus*. *PLoS Genet.* 14:e1007514. doi: 10.1371/journal.pgen.1007514

Hauryliuk, V., and Atkinson, G. C. (2017). Small Alarmone Synthetases as novel bacterial RNA-binding proteins. *RNA Biol.* 14, 1695–1699. doi: 10.1080/15476286.2017.1367889

Hauryliuk, V., Atkinson, G. C., Murakami, K. S., Tenson, T., and Gerdes, K. (2015). Recent functional insights into the role of (p)ppGpp in bacterial physiology. *Nat. Rev. Microbiol.* 13, 298–309. doi: 10.1038/nrmicro3448

Horsburgh, M. J., and Moir, A. (1999). sM, an ECF RNA polymerase sigma factor of Bacillus subtilis, is essential for growth and survival in high concentrations of salt. *Mol. Microbiol.* 32, 41–50. doi: 10.1046/j.1365-2958.1999.01323.x

Jain, V., Saleem-Batcha, R., China, A., and Chatterji, D. (2006). Molecular dissection of the mycobacterial stringent response protein Rel. *Protein Sci.* 15, 1449–1464. doi: 10.1110/ps.062117006

Jimmy, S., Saha, C. K., Kurata, T., Stavropoulos, C., Oliveira, S., Koh, A., et al. (2020). A widespread toxin-antitoxin system exploiting growth control via alarmone signalling. *Proc. Natl. Acad. Sci. U. S. A.* 117, 10500–10510. doi: 10.1073/pnas.1916617117

Kazmierczak, K. M., Wayne, K. J., Rechtsteiner, A., and Winkler, M. E. (2009). Roles of rel in stringent response, global regulation and virulence of serotype 2 *Streptococcus pneumoniae* D39. *Mol. Microbiol.* 72, 590–611. doi: 10.1111/j.1365-2958.2009.06669.x

Kim, J. N., Ahn, S.-J., Seaton, K., Garrett, S., and Burne, A. R. (2012). Transcriptional organization and physiological contributions of the relQ operon of *Streptococcus mutans*. *J. Bacteriol.* 194, 1968–1978. doi: 10.1128/JB.00037-12

Kriel, A., Bittner, A. N., Kim, S. H., Liu, K., Tehranchi, A. K., Zou, W. Y., et al. (2012). Direct regulation of GTP homeostasis by (p) ppGpp: a critical component of viability and stress resistance. *Mol. Cell* 48, 231–241. doi: 10.1016/j.molcel.2012.08.009

Kriel, A., Brinsmade, S. R., Tse, J. L., Tehranchi, A. K., Bittner, A. N., Sonenshein, A. L., et al. (2014). GTP Dysregulation in Bacillus subtilis cells lacking (p)ppGpp results in phenotypic amino acid Auxotrophy and failure to adapt to nutrient downshift and regulate biosynthesis genes. *J. Bacteriol.* 196, 189–201. doi: 10.1128/JB.00918-13

Krishnan, S., Petchiappan, A., Singh, A., Bhatt, A., and Chatterji, D. (2016). R-loop induced stress response by second (p)ppGpp synthetase in Mycobacterium smegmatis: functional and domain interdependence. *Mol. Microbiol.* 102, 168–182. doi: 10.1111/mmi.13453

Lemos, J. A., Brown, T. A., and Burne, R. A. (2004). Effects of RelA on key virulence properties of planktonic and biofilm populations of *Streptococcus mutans*. *Infect. Immun.* 72, 1431–1440. doi: 10.1128/IAI.72.3.1431-1440.2004

Lemos, J. A., Lin, V. K., Nascimento, M. M., Abranches, J., and Burne, R. A. (2007). Three gene products govern (p)ppGpp production by *Streptococcus mutans*. *Mol. Microbiol.* 65, 1568–1581. doi: 10.1111/j.1365-2958.2007.05897.x

Lemos, J. A., Nascimento, M. M., Lin, V. K., Abranches, J., and Burne, R. A. (2008). Global regulation by (p)ppGpp and CodY in *Streptococcus mutans*. *J. Bacteriol.* 190, 5291–5299. doi: 10.1128/JB.00288-08

Li, L., Bayer, A. S., Cheung, A., Lu, L., Abdelhady, W., Donegan, N. P., et al. (2020). The stringent response contributes to persistent methicillin-resistant *Staphylococcus aureus* endovascular infection through the purine biosynthetic pathway. *J. Infect. Dis.* 222, 1188–1198. doi: 10.1093/infdis/jiaa202

Lima, W. F., Prakash, T. P., Murray, H. M., Kinberger, G. A., Li, W., Chappell, A. E., et al. (2012). Single-stranded siRNAs activate RNAi in animals. *Cell* 150, 883–894. doi: 10.1016/j.cell.2012.08.014

Liu, K., Bittner, A. N., and Wang, J. D. (2015). Diversity in (p)ppGpp metabolism and effectors. *Curr. Opin. Microbiol.* 24, 72–79. doi: 10.1016/j.mib.2015.01.012

Manav, M. C., Beljantseva, J., Bojer, M. S., Tenson, T., Ingmer, H., Hauryliuk, V., et al. (2018). Structural basis for (p)ppGpp synthesis by the *Staphylococcus aureus* small alarmone synthetase RelP. *J. Biol. Chem.* 293, 3254–3264. doi: 10.1074/jbc.RA117.001374

Mascher, T., Margulis, N. G., Wang, T., Ye, R. W., and Helmann, J. D. (2003). Cell wall stress responses in *Bacillus subtilis*: the regulatory network of the bacitracin stimulon. *Mol.Microbiol.* 50, 1591–1604. doi: 10.1046/j.1365-2958.2003.03786.x

Mittenhuber, G. J. (2001). Comparative genomics and evolution of genes encoding bacterial (p)ppGpp synthetases/hydrolases (the Rel, RelA and SpoT proteins). *J. Mol. Microbiol. Biotechnol.* 3, 585–600.

Murdeshwar, M. S., and Chatterji, D. (2012). MS_RHII-RSD, a dual-function RNase HII-(p)ppGpp synthetase from *Mycobacterium smegmatis*. *J. Bacteriol.* 194, 4003–4014. doi: 10.1128/JB.00258-12

Nanamiya, H., Kasai, K., Nozawa, A., Yun, C. S., Narisawa, T., Murakami, K., et al. (2008). Identification and functional analysis of novel (p)ppGpp synthetase genes in Bacillus subtilis. *Mol. Microbiol.* 67, 291–304. doi: 10.1111/j.1365-2958.2007.06018.x

Natori, Y., Tagami, K., Murakami, K., Yoshida, S., Tanigawa, O., Moh, Y., et al. (2009). Transcription activity of individual rrn operons in Bacillus subtilis mutants deficient of (p)ppGpp synthetase genes relA, yjbM, and ywaC. *J. Bacteriol.* 191, 4555–4561. doi: 10.1128/JB.00263-09

Pando, J. M., Pfeltz, R. F., Cuaron, J. A., Nagarajan, V., Mishra, M. N., Torres, N. J., et al. (2017). Ethanol-induced stress response of *Staphylococcus aureus*. *Can. J. Microbiol.* 63, 745–757. doi: 10.1139/cjm-2017-0221

Petchiappan, A., and Chatterji, D. (2017). Antibiotic resistance: current perspectives. *ACS Omega* 2, 7400–7409. doi: 10.1021/acsomega.7b01368

Petchiappan, A., Naik, S. Y., and Chatterji, D. (2020). RelZ-mediated stress response in *Mycobacterium smegmatis*: pGpp synthesis and its regulation. *J. Bacteriol.* 202:e00444–19. doi: 10.1128/JB.00444-19

Pokhrel, A., Poudel, A., Kory, B., Castro, K. B., Celestine, M. J., Oludiran, A., et al. (2020). The (p)ppGpp synthetase RSH mediates stationary phase onset and antibiotic stress survival in Clostridioides difficile. *J. Bacteriol.* 202:e00377–20. doi: 10.1128/JB.00377-20

Potrykus, K., and Cashel, M. (2008). (p)ppGpp: still magical? *Annu. Rev. Microbiol.* 62, 35–51. doi: 10.1146/annurev.micro.62.081307.162903

Poveda, A. M., Le Clech, M., and Pasero, P. (2010). Transcription and replication: breaking the rules of the road causes genomic instability. *Transcription* 1, 99–102. doi: 10.4161/trns.1.2.12665

Roberts, T. C., Langer, R., and Wood, M. J. A. (2020). Advances in oligonucleotide drug delivery. *Nat. Rev. Drug Discov.*, 9, 673–694. doi: 10.1038/s41573-020-0075-7

Roghanian, M., Semsey, S., Løbner-Olesen, A., and Jalalvand, F. (2019). (p)ppGpp-mediated stress response induced by defects in outer membrane biogenesis and ATP production promotes survival in *Escherichia coli*. *Sci. Rep.* 9:2934. doi: 10.1038/s41598-019-39371-3

Ronneau, S., and Hallez, R. (2019). Make and break the alarmone: regulation of (p)ppGpp synthetase/hydrolase enzymes in bacteria. *FEMS Microbiol. Rev.* 43, 389–400. doi: 10.1093/femsre/fuz009

Ross, W., Vrentas, C. E., Sanchez-Vazquez, P., Gaal, T., and Gourse, R. L. (2013). The magic spot: a ppGpp binding site on *E. coli* RNA polymerase responsible for regulation of transcription initiation. *Mol. Cell* 50, 420–429. doi: 10.1016/j.molcel.2013.03.021

Ruwe, M., Kalinowski, J., and Persicke, M. (2017). Identification and functional characterization of small Alarmone Synthetases in *Corynebacterium glutamicum*. *Front. Microbiol.* 8:1601. doi: 10.3389/fmicb.2017.01601

Schafer, H., Beckert, B., Frese, C. K., Shields, R. C., Kim, J. N., Ahn, S.-J., et al. (2020). Peptides encoded in the Streptococcus mutans RcrRPQ operon are essential for thermotolerance. *Microbiology* 166, 306–317. doi: 10.1099/mic.0.000887

Seaton, K., Ahn, S. J., Sagstetter, A. M., and Burne, R. A. (2011). A transcriptional regulator and ABC transporters link stress tolerance, (p)ppGpp, and genetic competence in *Streptococcus mutans*. *J. Bacterial.* 193, 862–874. doi: 10.1128/JB.01257-10

Srivatsan, A., and Wang, J. D. (2008). Control of bacterial transcription, translation and replication by (p)ppGpp. *Curr. Opin. Microbiol.* 11, 100–105. doi: 10.1016/j.mib.2008.02.001

Steinchen, W., and Bange, G. (2016). The magic dance of the alarmones (p)ppGpp. *Mol. Microbiol.* 101, 531–544. doi: 10.1111/mmi.13412

Steinchen, W., Nuss, A. M., Beckstette, M., Hantke, I., Driller, K., Sudzinova, P., et al. (2020). The alarmones (p)ppGpp are part of the heat shock response of Bacillus subtilis. *PLoS Genet.* 16:e1008275. doi: 10.1371/journal.pgen.1008275

Steinchen, W., Vogt, M. S., Altegoer, F., Giammarinaro, P. I., Horvatek, P., Wolz, C., et al. (2018). Structural and mechanistic divergence of the small (p)ppGpp synthetases RelP and RelQ. *Sci. Rep.* 8:2195. doi: 10.1038/s41598-018-206344

Steinchen, W., Schuhmacher, J. S., Altegoer, F., Fage, C. D., Srinivasan, V., Linne, U., et al. (2015). Catalytic mechanism and allosteric regulation of an oligomeric (p)ppGpp synthetase by an alarmone. *Proc. Natl. Acad. Sci. U. S. A.* 112, 13348–13353. doi: 10.1073/pnas.1505271112

Stirling, P. C., Chan, Y. A., Minaker, S. W., Aristizabal, M. J., Barrett, I., Sipahimalani, P., et al. (2012). R-loop-mediated genome instability in mRNA cleavage and polyadenylation mutants. *Genes Dev.* 26, 163–175. doi: 10.1101/gad.179721.111

Sun, D., Lee, G., Lee, J. H., Kim, H. Y., Rhee, H. W., Park, S. Y., et al. (2010). A metazoan ortholog of SpoT hydrolyzes ppGpp and functions in starvation responses. *Nat. Struct. Mol. Biol.* 17, 1188–1194. doi: 10.1038/nsmb.1906

Syal, K., Flentie, K., Bhardwaj, N., Maiti, K., Jayaraman, N., Stallings, C. L., et al. (2017). Synthetic (p) ppGpp analogue is an inhibitor of stringent response in mycobacteria. *Antimicrob. Agents Chemother.* 61:e00443–17. doi: 10.1128/AAC.00443-17

Tagami, K., Nanamiya, H., Kazo, Y., Maehashi, M., Suzuki, S., Namba, E., et al. (2012). Expression of a small (p)ppGpp synthetase, YwaC, in the (p)ppGpp0 mutant of Bacillus subtilis triggers YvyD-dependent dimerization of ribosome. *MicrobiologyOpen* 1, 115–134. doi: 10.1002/mbo3.16

Takada, H., Roghanian, M., Murina, V., Dzhygyr, I., Murayama, R., Akanuma, G., et al. (2020). The C-terminal RRM/ACT domain is crucial for fine-tuning the activation of 'Long' RelA-SpoT homolog enzymes by ribosomal complexes. *Front. Microbiol.* 11:277. doi: 10.3389/fmicb.2020.00277

Tao, W., Mao, X., Davide, J. P., Ng, B., Cai, M., Burke, P. A., et al. (2011). Mechanistically probing lipid-siRNA nanoparticle associated toxicities identifies Jak inhibitors effective in mitigating multifaceted toxic responses. *Mol. Ther.* 19, 567–575. doi: 10.1038/mt.2010.282

Thackray, P. D., and Moir, A. (2003). SigM, an extra cytoplasmic function sigma factor of Bacillus subtilis, is activated in response to cell wall antibiotics, ethanol, heat, acid, and superoxide stress. *J. Bacteriol.* 185, 3491–3498. doi: 10.1128/JB.185.12.3491-3498.2003

Weinrick, B., Dunman, P. M., McAleese, F., Murphy, E., Projan, S. J., Fang, Y., et al. (2004). Effect of mild acid on gene expression in *Staphylococcus aureus*. *J. Bacteriol.* 186, 8407–8423. doi: 10.1128/JB.186.24.8407-8423.2004

Weiss, L. A., and Stallings, C. L. (2013). Essential roles for Mycobacterium Rel beyond the production of (p)ppGpp. *J. Bacteriol.* 95, 5629–5638. doi: 10.1128/JB.00759-13

Wu, J., and Xie, J. (2009). Magic spot: (p)ppGpp. *J. Cell. Physiol.* 220, 297–302. doi: 10.1002/jcp.21797

Xiao, H., Kalman, M., Ikehara, K., Zemel, S., Glaser, G., and Cashel, M. (1991). Residual guanosine bispyrophosphate synthetic activity of relA null mutants can be eliminated by spoT null mutations. *J. Biol. Chem.* 266, 5980–5990.

Yang, J., Anderson, B. W., Turdiev, A., Turdiev, H., Stevenson, D. M., Amador-Noguez, D., et al. (2020). Systemic characterization of pppGpp, ppGpp and pGpp targets in Bacillus reveals NahA converts (p)ppGpp to pGpp to regulate alarmone composition and signalling. *bioRxiv* [Preprint] doi: 10.1101/2020.03.23.003749

Yang, N., Xie, S., Tang, N.-Y., Choi, M. Y., Wang, Y., and Wat, R. M. (2019). The Ps and Qs of alarmone synthesis in *Staphylococcus aureus*. *PLoS One* 14:e0213630. doi: 10.1371/journal.pone.0213630

Yu, D., Pendergraff, H., Liu, J., Kordasiewicz, H. B., Cleveland, D. W., Swayze, E. E., et al. (2012). Single-stranded RNAs use RNAi to potently and allele-selectively inhibit mutant huntingtin expression. *Cell* 150, 895–908. doi: 10.1016/j.cell.2012.08.002

Zweers, J. C., Nicolas, P., Wiegert, T., van Dijl, J. M., and Denham, E. L. (2012). Definition of the sigma(W) regulon of Bacillus subtilis in the absence of stress. *PLoS One* 7:e48471. doi: 10.1371/journal.pone.0048471

Conflict of Interest: The authors declare that the research was conducted in the absence of any commercial or financial relationships that could be construed as a potential conflict of interest.

frontiers in Microbiology

ORIGINAL RESEARCH
published: 15 October 2020
doi: 10.3389/fmicb.2020.562804

Studies on the Regulation of (p)ppGpp Metabolism and Its Perturbation Through the Over-Expression of Nudix Hydrolases in *Escherichia coli*

*Rajeshree Sanyal, Allada Vimala and Rajendran Harinarayanan**

Laboratory of Bacterial Genetics, Centre for DNA Fingerprinting and Diagnostics, Hyderabad, India

Stringent response mediated by modified guanosine nucleotides is conserved across bacteria and is regulated through the Rel/Spo functions. In *Escherichia coli*, RelA and SpoT proteins synthesize the modified nucleotides ppGpp and pppGpp, together referred to as (p)ppGpp. SpoT is also the primary (p)ppGpp hydrolase. In this study, using hypomorphic *relA* alleles, we provide experimental evidence for SpoT-mediated negative regulation of the amplification of RelA-dependent stringent response. We investigated the kinetics of ppGpp degradation in cells recovering from stringent response in the complete absence of SpoT function. We found that, although greatly diminished, there was slow ppGpp degradation and growth resumption after a lag period, concomitant with decrease in ppGpp pool. We present evidence for reduction in the ppGpp degradation rate following an increase in pppGpp pool, during recovery from stringent response. From a genetic screen, the nudix hydrolases MutT and NudG were identified as over-expression suppressors of the growth defect of Δ*spoT* and Δ*spoT* Δ*gppA* strains. The effect of over-expression of these hydrolases on the stringent response to amino acid starvation and basal (p)ppGpp pool was studied. Over-expression of each hydrolase reduced the strength of the stringent response to amino acid starvation, and additionally, perturbed the ratio of ppGpp to pppGpp in strains with reduced SpoT hydrolase activity. In these strains that do not accumulate pppGpp during amino acid starvation, the expression of NudG or MutT supported pppGpp accumulation. This lends support to the idea that a reduction in the SpoT hydrolase activity is sufficient to cause the loss of pppGpp accumulation and therefore the phenomenon is independent of hydrolases that target pppGpp, such as GppA.

Keywords: (p)ppGpp, stringent response, SpoT, RelA, nudix hydrolases

OPEN ACCESS

Edited by:
Katarzyna Potrykus,
University of Gdańsk, Poland

Reviewed by:
Gad Glaser,
Hebrew University of Jerusalem, Israel
Michael Cashel,
Eunice Kennedy Shriver National Institute of Child Health and Human Development (NICHD), United States

****Correspondence:***
Rajendran Harinarayanan
hari@cdfd.org.in

Specialty section:
This article was submitted to Microbial Physiology and Metabolism, a section of the journal Frontiers in Microbiology

Received: *16 May 2020*
Accepted: *23 September 2020*
Published: *15 October 2020*

Citation:
Sanyal R, Vimala A and Harinarayanan R (2020) Studies on the Regulation of (p)ppGpp Metabolism and Its Perturbation Through the Over-Expression of Nudix Hydrolases in Escherichia coli. Front. Microbiol. 11:562804. doi: 10.3389/fmicb.2020.562804

INTRODUCTION

Stringent response is a stress response ubiquitously found in microorganisms. It is characterized by the accumulation of the signaling molecules ppGpp and pppGpp that are synthesized by the transfer of a pyrophosphate moiety from ATP to GDP or GTP, respectively, and collectively referred to as (p)ppGpp (Cashel et al., 1996). Accumulation of (p)ppGpp modifies

the cellular physiology globally resulting in the cell switching from a growth and proliferation mode to a survival mode (Chatterji and Kumar Ojha, 2001; Braeken et al., 2006; Potrykus and Cashel, 2008; Hauryliuk et al., 2015). In the gram-negative model organism *Escherichia coli*, nutritional starvation signals activate the stringent response leading to the accumulation of (p)ppGpp and reprogramming of transcription (Durfee et al., 2008; Traxler et al., 2011). This is brought about by the binding of (p)ppGpp to RNA polymerase that is facilitated by DksA, an RNA polymerase binding protein (Ross et al., 2013, 2016; Zuo et al., 2013). Additionally, (p)ppGpp binds several proteins and alters their activity (Wang et al., 2019). (p)ppGpp is required for bacterial virulence, and in many pathogens, the expression and activity of virulence regulators are integrated into a global response mediated by ppGpp, thereby coupling pathogenesis to metabolic status (Dalebroux et al., 2010).

In β- and γ-proteobacteria, including *E. coli*, (p)ppGpp metabolism is primarily driven by the paralogs, RelA and SpoT, which are members of the multi-domain Rel/Spo homolog (RSH) family of proteins (Mittenhuber, 2001; Atkinson et al., 2011). The arrangement of domains within the RSH proteins are conserved. The domains responsible for (p)ppGpp synthesis and hydrolysis are carried within the N-terminal half of the protein, while domains implicated in regulatory functions reside within the C-terminal half of the protein. The (p)ppGpp synthetase and hydrolase domains are functional in SpoT, while the latter domain is non-functional in RelA due to the presence of mutations. The data available in the literature suggest that the stress signals are sensed by the regulatory domains of the RSH proteins, leading to conformation changes that modulate the synthase or hydrolase activity. RelA is a ribosome-bound protein activated by the "hungry" codons that appear following amino acid starvation and the consequent increase in the concentration of uncharged tRNA (Cashel et al., 1996). Cryo-electron microscopy studies have provided insights on the structural basis for RelA activation by the entry of uncharged tRNA into the A-site of a translating ribosome and as well as the role of C-terminal domains in ribosome interaction (Arenz et al., 2016; Brown et al., 2016; Loveland et al., 2016). A recent report has presented evidence for accumulation of uncharged $tRNA^{Lys}$ in response to fatty acid starvation and consequent activation of RelA-dependent (p)ppGpp synthesis (Sinha et al., 2019).

In the absence of stress, SpoT is associated with a weak synthase and a strong (p)ppGpp hydrolase activity, and the hydrolase function is essential for the growth of *E. coli* (An et al., 1979; Xiao et al., 1991). The basal (p)ppGpp pool in *E. coli* is regulated through SpoT activity (Sarubbi et al., 1988) and it can elicit stringent response following carbon (Xiao et al., 1991), fatty acid (Seyfzadeh et al., 1993), and iron (Vinella et al., 2005) limitation. The SpoT hydrolase activity was inhibited by uncharged tRNA and the inhibition was more severe in the presence of ribosomes (Richter, 1980), conditions that mimic amino acid starvation. Interaction of SpoT with other factors regulate the balance between its synthase and hydrolase functions. It has been reported that the acyl carrier protein interacts with the TGS domain of SpoT and increases the synthase activity during fatty acid starvation (Battesti and Bouveret, 2006). During exponential growth the interaction of SpoT with the GTPase, CgtA/ObgE can modulate the hydrolase activity during exponential growth (Jiang et al., 2007). In a recent report, a small protein called YtfK was proposed to activate stringent response by tilting the catalytic balance of SpoT toward (p)ppGpp synthesis (Germain et al., 2019). In addition to SpoT, pppGpp is hydrolyzed into ppGpp by the guanosine pentaphosphate phosphohydrolase GppA in *E. coli* (Somerville and Ahmed, 1979; Harat and Sy, 1983; Keasling et al., 1993). The physiological significance of the conversion of pppGpp to ppGpp is not apparent. However, pppGpp was found to be less potent than ppGpp with respect to regulation of growth rate, RNA/DNA ratios, ribosomal RNA P1 promoter transcription inhibition, threonine operon promoter activation and RpoS induction in *E. coli* (Mechold et al., 2013). When pppGpp hydrolysis was prevented by the elimination of SpoT and GppA functions, RelA mediated (p)ppGpp synthesis was activated in the absence of starvation (Sanyal and Harinarayanan, 2020). Many (p)ppGpp binding and metabolizing proteins were identified from a DRaCALA (differential radial capillary action of ligand assay) based screen, but interestingly, both SpoT and GppA were not identified in this screen (Zhang et al., 2018). One way to examine the role of hydrolases other than SpoT in the turn-over of (p)ppGpp can be through studying a Δ*spoT* strain. Although SpoT hydrolase activity is essential for the growth of wild type *E. coli*, non-inactivating suppressor mutations in the *relA* locus have been found to rescue the growth defect of Δ*spoT* strain (Montero et al., 2014; Sanyal and Harinarayanan, 2020). These *relA* hypomorphs can be used to address (p)ppGpp turnover in the absence SpoT function.

In this study, using hypomorphic *relA* alleles or the over-expression of nudix hydrolases – conditions that support *E. coli* growth in the absence of SpoT function, we have examined the role of SpoT hydrolase function in (p)ppGpp metabolism during RelA mediated stringent response to amino acid starvation. Specifically, we have studied, (i) the role of SpoT hydrolase activity in the regulation of the amplification of the *relA*-mediated stringent response after amino acid starvation; (ii) the degradation of stringent nucleotide ppGpp in the absence of SpoT activity; (iii) the effect of increase in pppGpp pool on the SpoT mediated turnover of (p)ppGpp, and (iv) the effect of over-expression of nudix hydrolases, NudG and MutT, on the (p)ppGpp pool during stringent response in wild type strain and strains with lowered SpoT hydrolase activity. Our results indicate, the SpoT hydrolase activity modulates the quorum of deacylated tRNA required for RelA dependent increase in (p)ppGpp. Our results also show that the cellular pppGpp pool responds to the overall (p)ppGpp hydrolase activity of the cell in a counterintuitive manner, that is, when the cellular hydrolase activity was lowered its pool size decreased and when the hydrolase activity was increased using nudix hydrolases, its pool size increased.

RESULTS

Growth Phenotype of Strains Carrying Hypomorphic *relA* Alleles in SMG

We had reported the isolation of two hypomorphic *relA* alleles, namely *relA*:Tn*10*dTet and *rlmD*:Tn*10*dKan through transposon mutagenesis that suppressed the growth defect of the Δ*spoT* strain (Sanyal and Harinarayanan, 2020). We expected the *relA*:Tn*10*dTet transposon insertion after the 496th codon in the *relA* ORF to lead to synthesis of truncated RelA polypeptide (full length RelA is 744 amino acids), therefore, early stop codons were introduced in the *relA* ORF (see methods) to allow synthesis of truncated RelA polypeptides with the N-terminal 455 amino acids (*relA455*Δ:Kan) or 496 amino acids (*relA496*Δ:Kan). *relA* allele encoding the N-terminal 455 aa of RelA polypeptide has been expressed from plasmid, the truncated protein synthesized (p)ppGpp constitutively and did not respond to amino acid starvation (Schreiber et al., 1991; Svitil et al., 1993). The phenotype of these alleles was qualitatively compared with the *relA*:Tn*10*dTet transposon insertion by studying growth on medium containing the amino acids serine, methionine, and glycine (SMG), which is known to induce isoleucine starvation (Uzan and Danchin, 1976). The *relA* null mutant or an allele with very low activity such as *relA1* (Metzger et al., 1989) does not grow in this medium (**Figure 1**, rows 1 and 2). Strains carrying the *relA*:Tn*10*dTet, *relA455*Δ:Kan, or *relA496*Δ:Kan allele exhibited a similar SMG-sensitive phenotype (**Figure 1**, rows 3, 5, and 7). However, the growth sensitivity was overcome after the elimination of SpoT function (**Figure 2**, rows 4, 6, and 8). These results suggest, after isoleucine starvation, the truncated RelA polypeptides, unlike full length RelA, are unable to increase the (p)ppGpp pool due to the presence of SpoT hydrolase activity. Notably, over-expression of truncated RelA polypeptide from plasmid confers SMG resistance (data not shown) and causes gratuitous stringent response. As expected for a RelA polypeptide lacking the C-terminal domain necessary for interaction with the ribosome, the *relA*:Tn*10*dTet allele did not respond to amino acid starvation (**Figure 2A**). Stringent response elicited in the presence of SMG or after amino acid starvation by the *relA* alleles studied here has been tabulated (**Table 1**). The above results highlight the importance of SpoT hydrolase activity in regulating stringent response from RelA variants incapable of ribosome interaction. This may be useful to understand the stringent response elicited through small alarmone synthases.

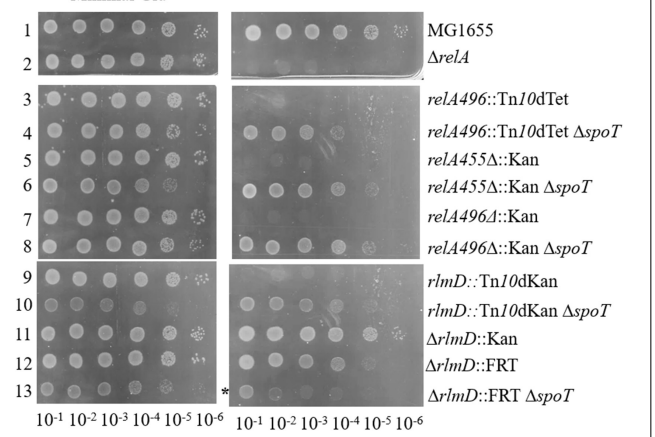

FIGURE 1 | SMG resistance phenotype of hypomorphic RelA alleles was modulated by SpoT function. Cultures grown to saturation were washed, serially diluted, and spotted on minimal medium containing glucose with or without SMG (serine, methionine, and glycine) and photographed after 20 h incubation at 37°C. The relevant strain genotypes are indicated. *Growth in the presence of SMG was significantly retarded but not abolished. The strains from rows 1 to 13 are – RS1, RS8, RS9, RS17 white colony, RS53, RS92 white colony, RS54, RS420 white colony, RS11, RS18 white colony, RS303, RS316, RS361 white colony. Strains and their genotype are listed in **Supplementary Table 1**. The white colony of a strain refers to the derivative cured of plasmid P_{lac}-spoT^{+}.

The *rlmD*:Tn*10*dKan transposon insertion was very close to the 3′-end of *rlmD*, the gene immediately upstream of RelA (Sanyal and Harinarayanan, 2020). Therefore, it was expected that the *relA* expression could be lowered in this strain due to premature termination of transcripts initiating from the promoters upstream of the insertion. To test the role of the promoters within the *rlmD* ORF (Metzger et al., 1988; Nakagawa et al., 2006; Brown et al., 2014) in the SMG resistance phenotype, the Δ*rlmD*:kan allele from Keio collection (Baba et al., 2006) and Δ*rlmD*:FRT derivative obtained by FLP mediated excision of the Kan^{R} determinant (Datsenko and Wanner, 2000) were tested for stringent response using the SMG test. While the *rlmD*:Tn*10*dKan strain did not grow in the SMG plate in the presence of SpoT function (**Figure 1**, rows 9 and 10), this was not the case for strains carrying the Δ*rlmD*:kan or Δ*rlmD*:FRT alleles. Growth of the Δ*rlmD*:FRT strain was significantly slower in the presence of Δ*spoT* allele, irrespective of the presence or absence of SMG. This may be due to increase in the basal (p)ppGpp pool, which is known to reduce the growth rate (Sarubbi et al., 1988, 1989). The Δ*rlmD*:kan Δ*spoT* strain was lethal (data not shown). Isoleucine starvation did not elicit stringent response in the *rlmD*:Tn*10*dKan, Δ*rlmD*:FRT, and *rlmD*:Tn*10*dKan Δ*spoT* strains (**Figures 2B,C**), but importantly, stringent response was elicited in the Δ*rlmD*:FRT Δ*spoT* strain (**Figure 3A**, lanes 1–4). This indicated, the hydrolase activity of SpoT prevented the accumulation of (p)ppGpp following amino acid starvation in the case of Δ*rlmD*:FRT allele. The *rlmD*:Tn*10*dKan allele failed to accumulate (p)ppGpp even in the absence of SpoT hydrolase activity, however, the removal of SpoT function conferred SMG-resistance in this strain (**Figure 1** row 10) and suggested that there was an increase in the basal (p)ppGpp concentration.

The above data is consistent with an idea that there can be at least two levels of negative regulation of (p)ppGpp accumulation during RelA-mediated stringent response. One is the SpoT mediated degradation of (p)ppGpp, which is illustrated by the accumulation of (p)ppGpp in the Δ*rlmD*:FRT strain only after the loss of SpoT function (compare **Figures 2C**, **3A**). A second SpoT-independent regulation may explain the absence of (p)ppGpp accumulation in the *rlmD*:Tn*10*dKan Δ*spoT* strain, wherein, hydrolases other than SpoT may be involved in the turnover of the small amounts of (p)ppGpp synthesized. The

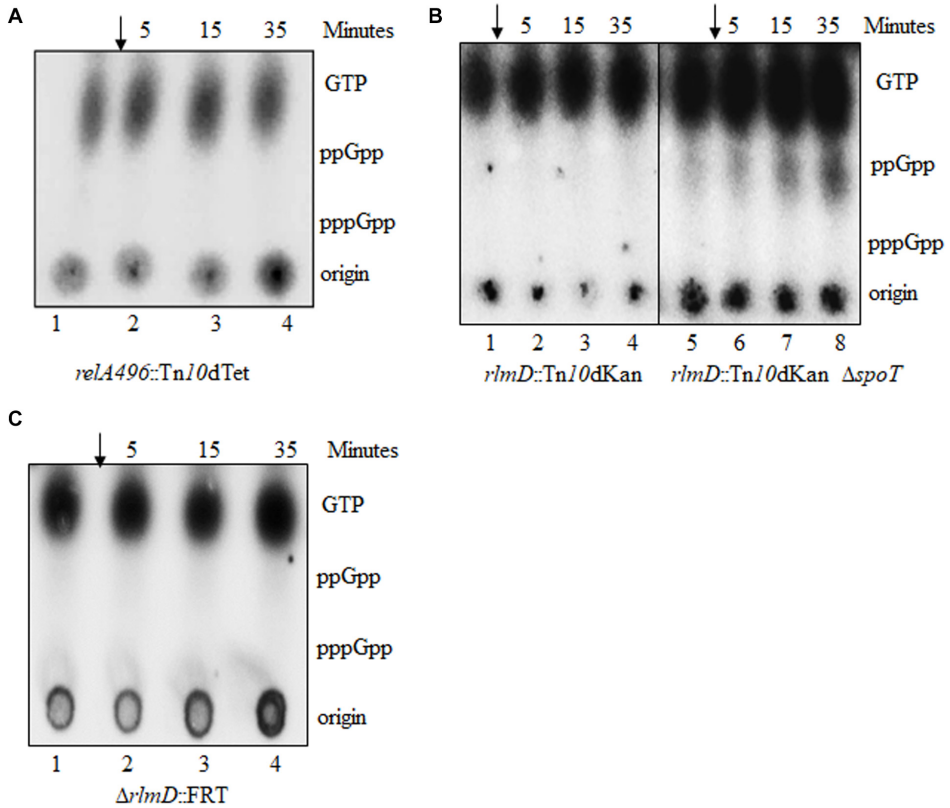

FIGURE 2 | Hypomorphic *relA* alleles do not accumulate (p)ppGpp in response to isoleucine starvation. (p)ppGpp accumulation in response to isoleucine starvation was monitored in strains carrying the following *relA* alleles *relA496*:Tn*10*dTet **(A)**, *rlmD*:Tn*10*dKan and *rlmD*:Tn*10*dKan Δ*spoT* **(B)**, and Δ*rlmD*:FRT **(C)**. Strains were cultured in MOPS glucose medium, labeled with P^{32}, isoleucine starvation was induced with valine (arrow), and samples were collected immediately before valine addition and subsequently at the times indicated above the lanes and subjected to PEI-TLC (see section "Materials and Methods" for details). Data presented is a representative of experiments done at least 3 times. Strains used are RS9 **(A)**, RS11 and RS18 white colony **(B)**, and RS316 **(C)**. The white colony of a strain refers to the derivative cured of plasmid P_{lac}-spoT$^+$.

small amount of ppGpp observed in the *rlmD*:Tn10dKan Δ*spoT* strain (as compared to the isogenic *rlmD*:Tn10dKan strain) can be attributed to over-loading of TLC as seen from the higher intensity of the GTP spots.

ppGpp Degradation and Growth Recovery From Stringent Response in the Absence of SpoT Function

When subjected to isoleucine starvation, the Δ*rlmD*:FRT Δ*spoT* strain accumulated ppGpp (**Figure 3A**). Strikingly, there was no accumulation of pppGpp unlike in a wild type strain. This has been reported for the hydrolase deficient *spoT1* allele and was called the "spotless" phenotype (Laffler and Gallant, 1974). The *spoT1* encoded protein has three changes, a substitution (H255Y) and a two amino acid insertion between residues 82 and 83 (+QD) as compared to the *spoT*$^+$ encoded protein (Spira et al., 2008). We studied the synthesis and turnover rate of ppGpp in the complete absence of SpoT function using this strain. Following valine induced isoleucine starvation, the rate of ppGpp accumulation was diminished, with the ppGpp level continuing to increase beyond 5 min unlike in the wild type strain (**Figures 3A,B**, **4A**). This may be attributed to lowered *relA* expression in the Δ*rlmD*:FRT genetic background. After

TABLE 1 | SMG and amino acid starvation phenotypes of *relA* alleles.

Genotype	SMG phenotype[a]	Amino acid starvation[b]
Wild type	R	ppGpp and pppGpp
Δ*relA*	S	None
relA496:Tn10dTet	S	None
relA496:Tn10dTet Δ*spoT*	R	None
*relA455*Δ:Kan	S	None
*relA455*Δ:Kan Δ*spoT*	R	None
*relA496*Δ:Kan	S	None
*relA496*Δ:Kan Δ*spoT*	R	None
rlmD:Tn10dKan	S	None
rlmD:Tn10dKan Δ*spoT*	R	None
Δ*rlmD*:Kan	R	ND[c]
Δ*rlmD*:FRT	R	None
Δ*rlmD:FRT* Δ*spoT*	R	ppGpp

[a]*Growth in the presence of serine, methionine, and glycine; R- resistant, S- sensitive;* [b]*stringent nucleotides in response to amino acid starvation;* [c]*not determined.*

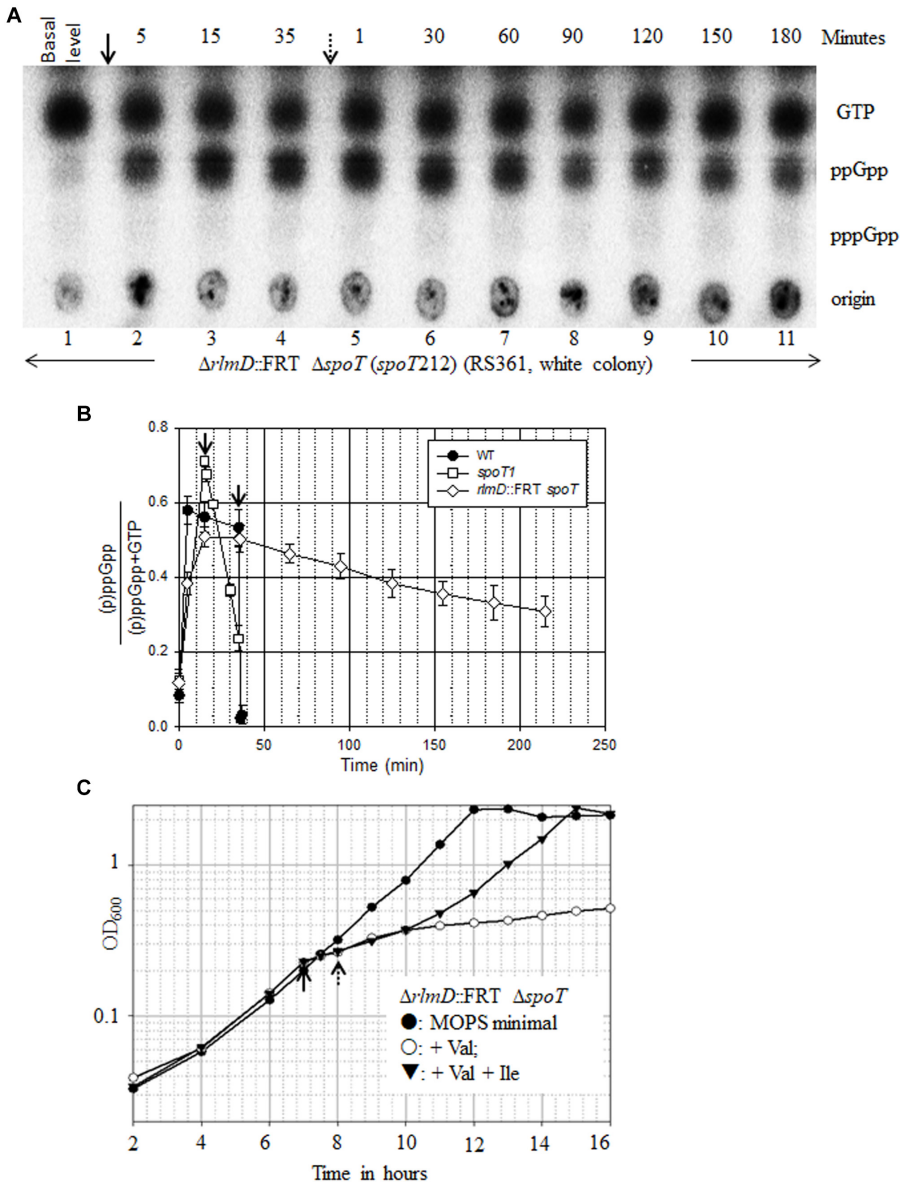

FIGURE 3 | ppGpp turnover in the absence of SpoT function and its effect on growth. **(A)** The Δ*rlmD*:FRT Δ*spoT* strain (RS361, white colony) was cultured in MOPS minimal medium containing glucose, labeled with P^{32} and subjected to PEI-TLC. Isoleucine starvation was induced with valine (arrow), and samples were collected immediately before valine addition and subsequently at time points indicated above the lanes. Starvation was reversed by the addition of isoleucine (dotted arrow), and samples were collected at the time points indicated. The white colony of a strain refers to the derivative cured of plasmid P_{lac}-spoT^{+}. Data presented is representative of experiments done 3 times. **(B)** The amount of (p)ppGpp over total [(p)ppGpp + GTP] at different time points after isoleucine starvation and after the reversal of starvation was plotted for the strains indicated using the data in **Supplementary Tables 2, 3, 5**. **(C)** Δ*rlmD*:FRT Δ*spoT* strain was grown in MOPS minimal medium containing glucose and subjected to isoleucine starvation by the addition of valine (solid arrow) and subsequently reversed by the addition of isoleucine (dotted arrow). Data from a representative experiment was plotted.

the reversal of amino acid starvation by isoleucine addition, the rate of ppGpp degradation was greatly diminished (**Figure 3A**). There was 38% decrease in ppGpp pool 180 min after the reversal of starvation (**Figure 3B** and **Supplementary Table 2**). The degradation rates are lower than that seen in the hydrolase defective *spoT1* strain, where there was 67% decrease in ppGpp pool 20 min after the reversal of starvation (**Figures 3B**, **4D** and **Supplementary Table 3**). These results indicate SpoT as the primary ppGpp hydrolase during stringent response. However, the very slow turnover of (p)ppGpp in the Δ*spoT* background suggest to the possible existence of alternative hydrolases (see below).

Since an increase in (p)ppGpp pool inhibits growth rate (Sarubbi et al., 1988; Sanyal and Harinarayanan, 2020), we studied how the slower ppGpp accumulation and reduced ppGpp degradation in the Δ*rlmD*:FRT Δ*spoT* strain affected

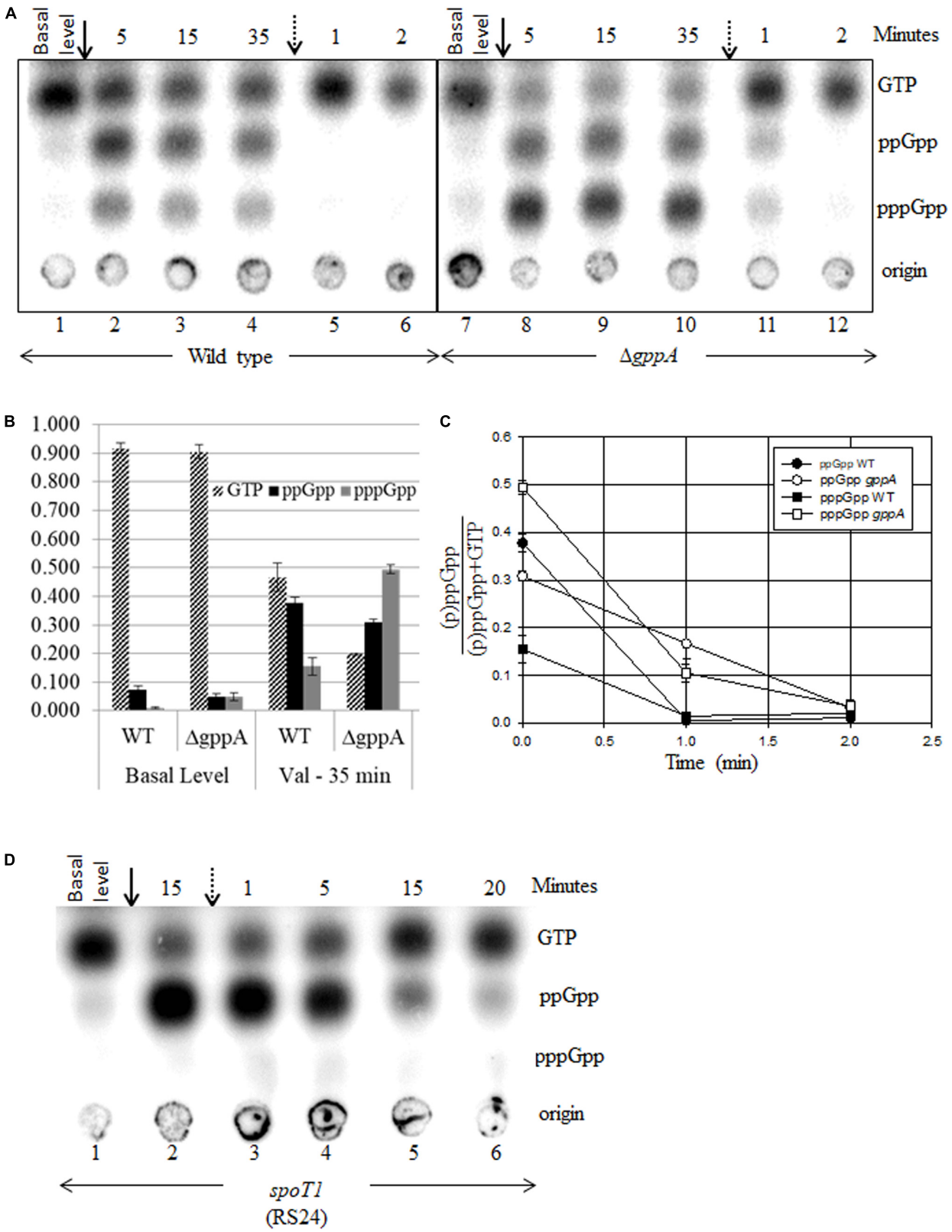

FIGURE 4 | Continued

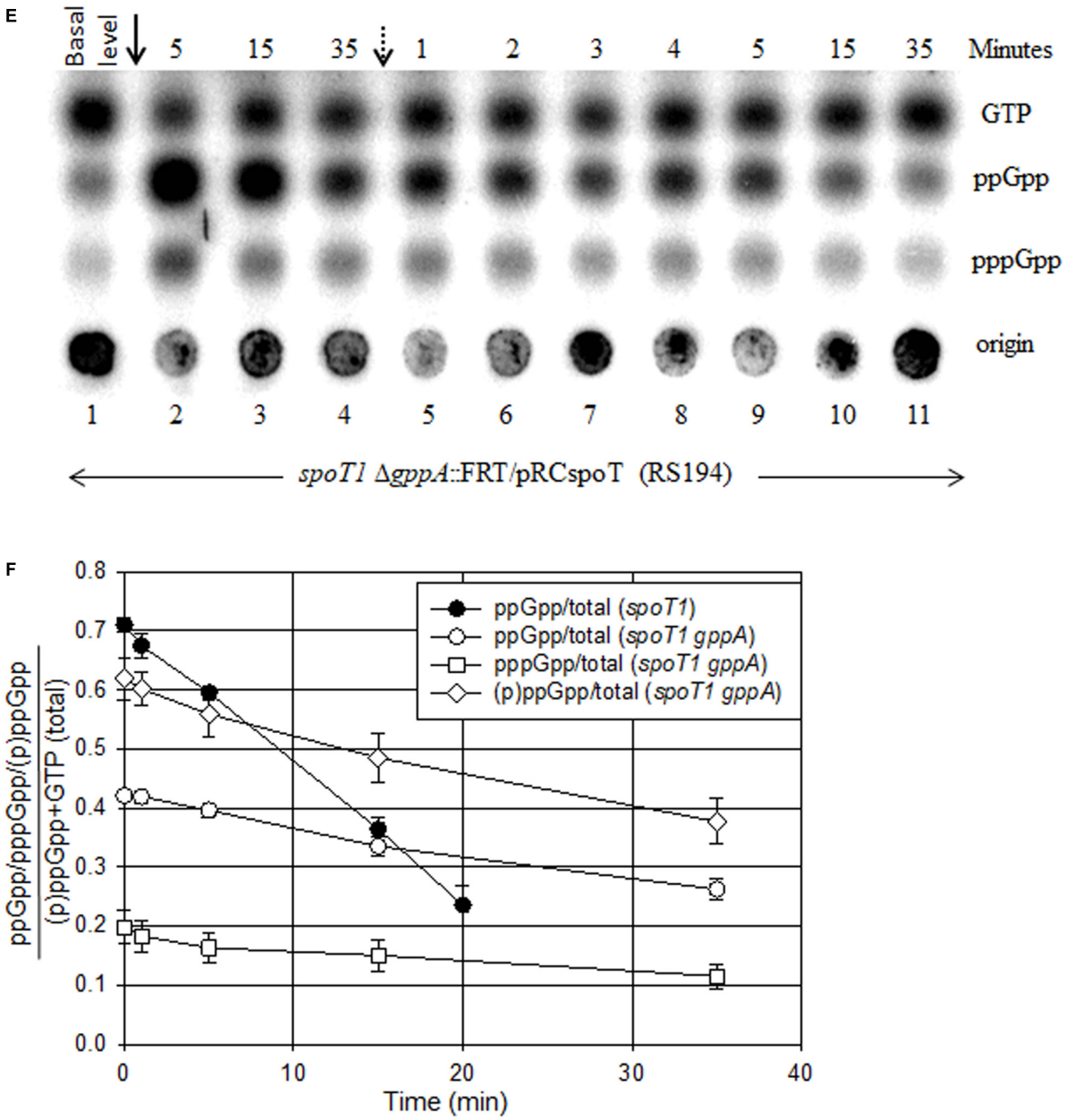

FIGURE 4 | Effect of SpoT and/or GppA hydrolase activity on the synthesis and turnover of stringent nucleotides during amino acid starvation and recovery. Isoleucine starvation was induced by the addition of valine (solid arrow) and reversed by the addition of isoleucine (dotted arrow) in the wild type and Δ*gppA* **(A)**, *spoT1* **(D)**, and *spoT1* Δ*gppA*/P_{lac}-spoT^{+} strain after reducing the *spoT* expression by allowing growth in the absence of IPTG **(E)**. A representative TLC is shown for each strain. **(B)** The concentration of ppGpp, pppGpp, or GTP over total [(p)ppGpp + GTP] at the time points indicated was plotted as bar graph using data from two independent experiments (**Supplementary Table 5**). Fraction of ppGpp or pppGpp or (p)ppGpp over total [(p)ppGpp + GTP] after the reversal of starvation was plotted for the wild type and *gppA* mutant with data from two independent experiments **(C)** the *spoT1* and *spoT1* Δ*gppA*/P_{lac}-spoT^{+} strains **(F)** with data from three independent experiments (**Supplementary Tables 3**, **4**). The strains are wild type (RS1), Δ*gppA* (RS307 white colony), *spoT1* (RS24), and *spoT1* Δ*gppA*:FRT/P_{lac}-spoT^{+} (RS194). The white colony of a strain refers to the derivative cured of plasmid P_{lac}-spoT^{+}.

growth during onset and reversal of isoleucine starvation. For comparison, we also studied the kinetics of growth arrest and recovery in the wild type, *spoT1*, and Δ*rlmD*:FRT strains. As expected, growth ceased following the addition of valine and resumed after the addition of isoleucine in the wild type strain (**Supplementary Figure 1A**). In the *spoT1* strain, the kinetics of isoleucine starvation-induced growth arrest was similar to that observed the wild type, but there was a lag of ∼30 min before growth resumed after the reversal of starvation (**Supplementary Figure 1B**). This is consistent with the reduced rate of ppGpp

degradation in the *spoT1* strain (**Figure 4D** and **Supplementary Table 3**). Growth arrest after isoleucine starvation in the Δ*rlmD*:FRT Δ*spoT* strain was similar to that in the wild type and *spoT1* strains, but following the reversal of starvation, growth resumed after a lag of 120 min, when the ppGpp pool was 54% of GTP (**Figure 3C** and **Supplementary Table 2**). One hour after growth resumed, that is, 180 min after isoleucine addition, the ppGpp pool was 45% of GTP. Our data indicates, ppGpp > 54% of GTP conferred growth inhibition as strong as that observed during amino acid starvation. There was gradual growth recovery as the ppGpp pool dropped, with the growth rate inversely proportional to ppGpp concentration as reported (Sarubbi et al., 1988). Unlike the Δ*rlmD*:FRT Δ*spoT* strain, growth resumed immediately after the reversal of isoleucine starvation in the isogenic Δ*rlmD*:FRT strain, which did not accumulate ppGpp (**Supplementary Figure 1C** and **Figure 2C**). This indicated, the reduced turnover of ppGpp was the sole cause of growth lag in the former strain.

Previously, we had reported RelA-dependent synthetic lethality in the *spoT1* Δ*gppA* strain with an associated accumulation of (p)ppGpp (Sanyal and Harinarayanan, 2020). Consistent with this, we observed growth inhibition in the *spoT1* Δ*gppA*/P_{lac}-spoT^{+} strain after lowering *spoT* gene expression by IPTG withdrawal (**Supplementary Figure 2**). We compared the level of (p)ppGpp or ppGpp as a ratio of GTP in the *spoT1* Δ*gppA*/P_{lac}-spoT^{+} and Δ*rlmD*:FRT Δ*spoT* strains, respectively, to the extent of growth inhibition. Accumulation of ppGpp to 45% of GTP in the Δ*rlmD*:FRT Δ*spoT* strain, 180 min after addition of isoleucine (**Supplementary Table 2**) increased the doubling time 1.7-fold from 90 to 156 min (**Figure 3C**). On the other hand, accumulation of ppGpp and pppGpp to 38 and 14% of GTP, respectively, in the *spoT1* Δ*gppA*/P_{lac}-spoT^{+} strain after IPTG withdrawal (**Figure 4E** lane 1 and **Supplementary Table 4**) conferred a significantly stronger growth inhibition – 4.9-fold increase in doubling time from 78 to 384 min (**Supplementary Figure 2**). Assuming, the growth properties of the strains were primarily determined by the intracellular pool of stringent nucleotides, we attribute the stronger growth inhibition in the latter strain to the presence of pppGpp.

Increase in pppGpp Reduced the Degradation Rate of ppGpp

As reported, only ppGpp accumulation was observed after amino acid starvation in the hydrolase deficient *spoT1* mutant, and the degradation rate of ppGpp was significantly reduced during recovery from stringent response (**Figure 4D**; Laffler and Gallant, 1974). We wanted to test if the SpoT hydrolase defect would also affect the degradation of pppGpp and if the presence of pppGpp would perturb ppGpp degradation. In the *spoT1* Δ*gppA*/P_{lac}-spoT^{+} strain, isoleucine starvation after lowering *spoT* gene expression caused further accumulation of ppGpp and pppGpp (**Figure 4E**). We studied the degradation rate of the stringent nucleotides during recovery from isoleucine starvation in this strain and compared it with that seen in the g*ppA* and *spoT1* strains.

Consistent with GppA being a pppGpp hydrolase, the pppGpp pool increased relative to ppGpp in the Δ*gppA* strain (**Figure 4A**). However, in the SpoT hydrolase deficient background, the pppGpp pool was significantly lower than ppGpp, despite the absence of GppA activity (**Figure 4E**). In the *gppA* mutant, the GTP and pppGpp pools were, respectively, 2.5-fold lower and 3.8-fold higher as compared to the wild type strain, while the ppGpp pool did not change significantly (**Figures 4A,B** and **Supplementary Table 5**). While a relative increase in the pppGpp pool was expected in the *gppA* mutant, the decrease in GTP pool is not consistent with current knowledge. Degradation of pppGpp to GTP is primarily SpoT hydrolase mediated and there is no evidence to our knowledge this can be inhibited in a *gppA* mutant. As compared to the wild type, in the Δ*gppA* strain, after the inhibition of RelA activity by isoleucine addition, a significant decrease in the degradation rate of ppGpp was observed (**Figures 4A,C** and **Supplementary Table 5**). In the *spoT1* Δ*gppA*:FRT/P_{lac}-spoT^{+} strain recovering from isoleucine starvation, there was 22 and 19% degradation of ppGpp and pppGpp, respectively, 15 min after the reversal of isoleucine starvation (**Figures 4E,F** and **Supplementary Table 4**). The degradation rate of ppGpp was more than two-fold lower than in the *spoT1* strain, where 54% of ppGpp was degraded 15 min after reversal of starvation (**Figure 4F** and **Supplementary Table 3**). The results show that, increasing the concentration of pppGpp slows down the SpoT-mediated degradation of ppGpp. From the data we have calculated the half-lives of (p)ppGpp using the formula $t_{1/2} = A_0/2K$ for a zero-order reaction, where A_0 is the initial concentration and K the slope. From less than a minute in the wild-type strain the half-life of ppGpp increases to 15 min in the *spoT1* strain and to 229 min in the Δ*rlmD*:FRT Δ*spoT* strain. In the presence of pppGpp the half-lives of ppGpp and pppGpp in the *spoT1* strain was 47 and 41 min, respectively.

To explain the above results, we would like to propose a model based on differential substrate specificity of the SpoT protein. In an earlier study, by comparing the SpoT mediated hydrolysis of ppGpp and pppGpp separately and when presented together at equimolar concentration *in vitro*, it was shown that SpoT did not exhibit substrate preference (Mechold et al., 1996). To explain our observation, we would like to propose that when pppGpp is present at a higher concentration than ppGpp, it competitively inhibits the hydrolysis of ppGpp by SpoT *in vivo*. However, the hydrolase deficient protein encoded by the *spoT1* allele is more sensitive to the inhibition of ppGpp hydrolysis by pppGpp. Reduced ppGpp hydrolysis can slow down GTP regeneration if the hydrolysis of ppGpp to GDP by SpoT and subsequent conversion of GDP to GTP by nucleotide diphosphate kinase (NDK) is the predominant GTP regeneration pathway during the stringent response.

Genetic Evidence for Compensation of SpoT Requirement by Over-Expression of MutT or NudG

Previously, we reported that the growth of Δ*rlmD* Δ*spoT* strain was dependent on GppA function (Sanyal and Harinarayanan,

2020). Using a multi-copy plasmid library of *E. coli* genes, we identified and sequenced plasmid clones that suppressed the growth defect of the Δ*rlmD* Δ*spoT* Δ*gppA* strain (details under section "Materials and Methods"). Among the plasmid clones conferring suppression, many carried the *spoT* or the *gppA* gene (which was expected). Additionally, the *nudG* gene was identified in three independent clones, and it was the only full-length gene in one of the three clones. This suggested, over-expression of *nudG* gene function could be responsible for suppression of growth defect. NudG is a member of the Nudix hydrolase superfamily of proteins and reported to be primarily a 5-hydroxy-CTP diphosphatase (Fujikawa and Kasai, 2002). We also identified a plasmid clone having the *coaE'-zapD-yacZ-mutT-secA'* genomic fragment that suppressed growth defect. Since this fragment included the *mutT* gene, which, like *nudG*, is a nudix hydrolase, an 8-oxo-dGTP diphosphatase (Akiyama et al., 1987; Bhatnagar and Bessman, 1988), we considered it a candidate gene responsible for suppression. We used the unstable plasmid based segregation assay (described under section "Materials and Methods") to show that plasmids with chromosomal DNA fragment having *nudG* or the *mutT* gene suppressed the Δ*rlmD*:FRT Δ*spoT* Δ*gppA* synthetic lethality in LB as well as defined media (**Supplementary Figure 3**). Suppression of Δ*rlmD*:FRT Δ*spoT* Δ*gppA* synthetic lethality by a subset of multi-copy clones and their effect on the growth defect of the Δ*relA* Δ*spoT* strain on minimal medium was studied (**Supplementary Table 6**). As expected, all clones suppressed the synthetic lethality and only the clone with *spoT* gene supported growth of Δ*relA* Δ*spoT* strain on minimal medium. We used corresponding plasmid clones from the ASKA plasmid collection to ask if the *nudG* or *mutT* gene functions were sufficient to suppress the growth defect arising from the loss of SpoT function and both SpoT and GppA functions. Plasmids pCA24N (vector), pCAmutT, and pCAnudG were individually introduced into the Δ*spoT*/P_{lac}-spoT$^+$ and Δ*spoT* Δ*gppA*/P_{lac}-spoT$^+$ strains to ask if the over-expression of each nudix hydrolase could compensate for the loss of SpoT and as well as the loss of both SpoT and GppA [which accentuates the growth defect from reduction in SpoT hydrolase function (Sanyal and Harinarayanan, 2020)]. Plasmid segregation assay showed that, SpoT function or both SpoT and GppA functions were dispensable in the presence of pCAnudG or pCAmutT plasmid, but not the vector pCA24N (**Figure 5**). The simplest explanation for these results will be that NudG or MutT over-expression prevents the accumulation of (p)ppGpp. Indeed, it has been shown that NudG and MutT proteins bind and metabolize (p)ppGpp (Zhang et al., 2018). It is interesting that MutT and NudG were identified from two completely different screens. In the study by Zhang et al. (2018), where systematic screening was carried out using DRaCALA (differential radial capillary action of ligand assay) for (p)ppGpp binding proteins, NudG and MutT were identified amongst other proteins. It was shown that these proteins hydrolyzed ppGpp to pGp and this was competed out by the natural nucleotide substrates of the proteins, namely, 8-oxo-(d)GTP (MutT) and 2-OH-(d)ATP (NudG). The ability to delete *spoT* under conditions of MutT or NusG over-expression suggested that they constitute alternative (p)ppGpp degradation pathways.

The hydrolase deficient *spoT202* and *spoT203* alleles elevate the basal ppGpp pool (Sarubbi et al., 1988) and supported the growth of Δ*relA* strain after SMG induced isoleucine starvation (**Supplementary Table 7**). Introduction of ASKA plasmid carrying the *nudG* or *mutT* gene into the Δ*relA spoT202* and Δ*relA spoT203* strains inhibited the growth of these strains in the presence of SMG, and also improved their growth in the absence of SMG (**Supplementary Table 7**). This growth pattern is consistent with the lowering of basal (p)ppGpp pool by over-expression of nudix hydrolases.

Over-Expression of NudG or MutT Alleviates Stringent Response and Restores pppGpp Accumulation in Strains With Reduced SpoT Hydrolase Activity

Isoleucine starvation in the Δ*rlmD*:FRT strain showed that when the *relA* expression was reduced, physiological levels of SpoT hydrolase activity was sufficient to inhibit stringent response (**Figures 2C**, **3A**). It is therefore possible, with increased expression of SpoT, there could be a proportionate increase in the hydrolase activity so that the stringent response elicited through amino acid starvation could be alleviated in an otherwise wild type strain. To test this, *spoT* expression was induced from plasmid pCAspoT (ASKA collection) (Kitagawa et al., 2005) in the wild type strain and then subjected to isoleucine

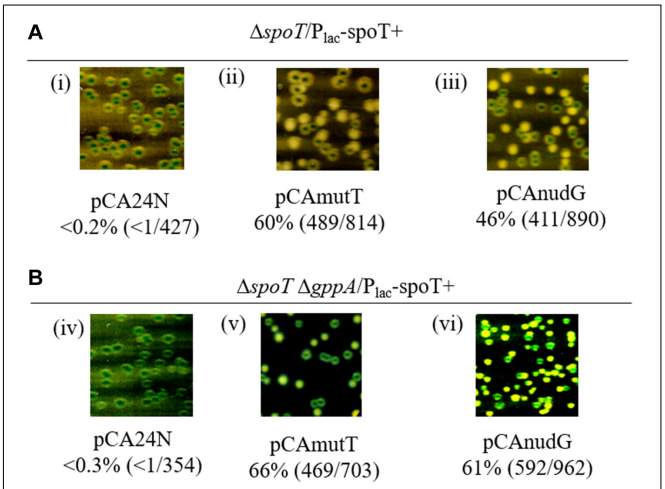

FIGURE 5 | Suppression of SpoT requirement by over-expression of *mutT* or *nudG*. Plasmid segregation assay was used to study the role of *mutT* and *nudG* genes in suppression of the growth defect of Δ*spoT* and Δ*spoT* Δ*gppA* strains in LB medium containing IPTG and Cm. A representative section from the plate has been included for each strain to show the color of the colonies after non-selective growth. The percentage of white colonies and the number of white colonies over the total number of colonies scored (white + blue) are provided for each panel. The ASKA plasmids carrying the *mutT* or *nudG* gene was used and the plasmid vector served as control. The Δ*spoT*/P_{lac}-spoT$^+$ strain was grown in the presence of 0.1 mM IPTG **(A)** and the Δ*spoT* Δ*gppA*/P_{lac}-spoT$^+$ strain was grown in the presence of 1 mM IPTG **(B)**. The strains in panels (i–vi) are RS444, RS680, RS681, RS684, RS685, and RS686, respectively.

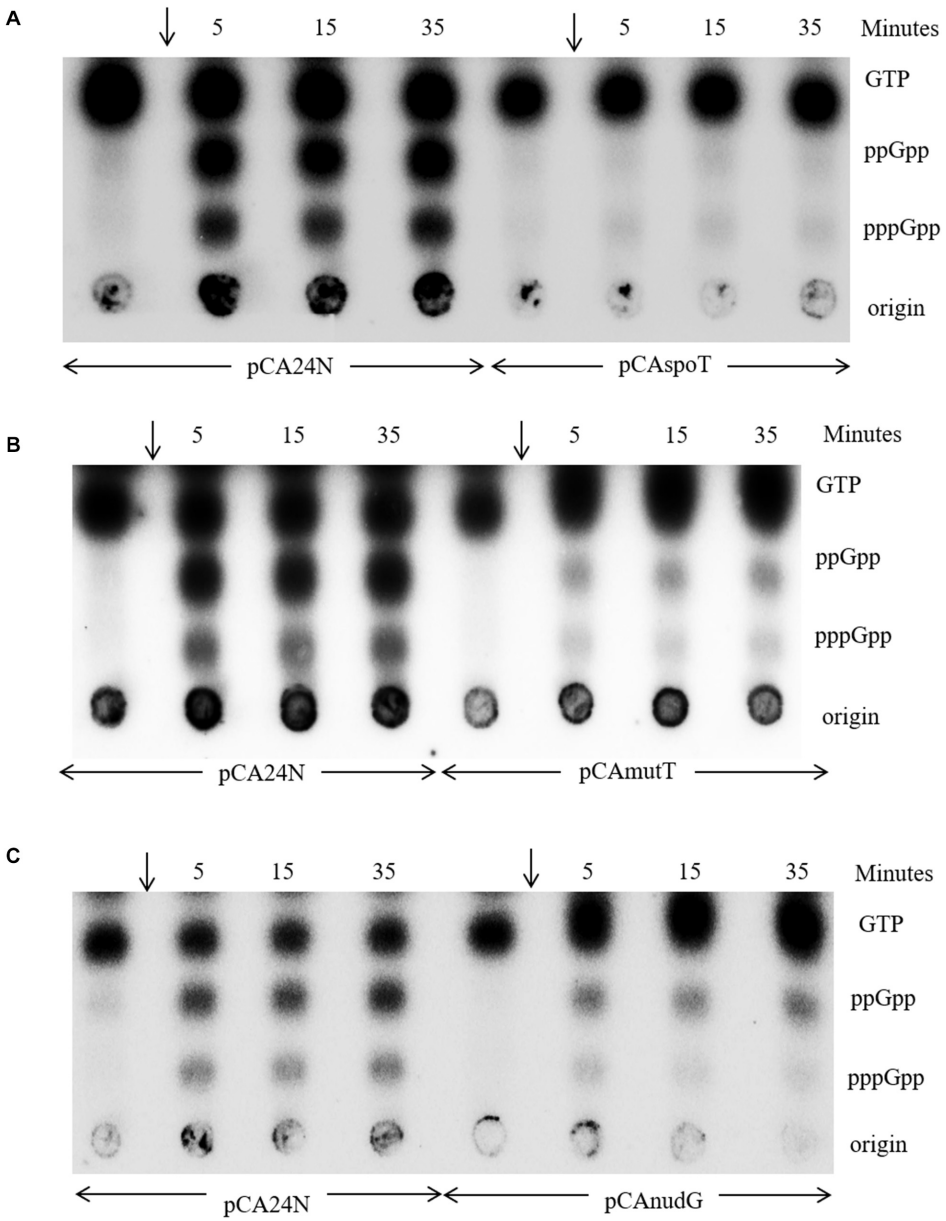

FIGURE 6 | Increased expression of *spoT* or *mutT* or *nudG* alleviates the stringent response to isoleucine starvation. A representative TLC of MG1655 Δ*lacZYAI*:FRT strain carrying the ASKA plasmids indicated below each panel was cultured in MOPS minimal medium containing glucose Cm and 0.1 mM IPTG. The culture was labeled with P^{32} to follow the accumulation of stringent nucleotides after isoleucine starvation by the addition of valine (arrow). Samples were collected immediately before the addition of valine or at the time points indicated and subjected to PEI-TLC. The strains in panels **(A–C)** are RS688, RS760, RS689, and RS690.

starvation. While a wild type like stringent response was observed in the presence of plasmid vector, (p)ppGpp accumulation was almost completely abolished after SpoT expression (**Figure 6A**). This indicated the (p)ppGpp synthesized could be completely hydrolyzed due to net increase in hydrolase activity following over-expression of SpoT. Stringent response to isoleucine starvation was also alleviated during the over-expression of nudix hydrolases NudG or MutT (**Figures 6B,C**). However, unlike SpoT over-expression, some residual (p)ppGpp accumulation was observed. Although this seems to suggest (p)ppGpp is less efficiently hydrolyzed by the nudix hydrolases than by SpoT, since the expression level of the proteins have not been determined, definitive conclusions cannot be drawn.

When amino acid starvation was induced in a Δ*spoT*/P_{lac}-spoT^{+} strain after IPTG withdrawal to lower *spoT* expression, only ppGpp accumulation was observed (Figure 4C in Sanyal and Harinarayanan, 2020). As mentioned earlier, absence of pppGpp accumulation after amino acid starvation was also a feature of the *spoT1* strain, which has reduced SpoT hydrolase activity (Laffler and Gallant, 1974). While many strains of *E. coli* accumulate both

pppGpp and ppGpp during amino acid starvation. It was noted that strains of the 58–161 lineage (Alfoldi et al., 1962) accumulate ppGpp but not pppGpp during stringent response. This was called the "spotless" phenotype. The genetic locus responsible for the phenotype was called as *spoT* and was defined by a mutant allele that had arisen spontaneously (Laffler and Gallant, 1974). Commonly studied laboratory strains of *E. coli* such as MC4100 also carry the mutant allele of *spoT* (Spira et al., 2008). Based on our results, we believe, the decrease in SpoT hydrolase activity can explain the absence of pppGpp in both instances. However, the molecular basis for the phenotype has not been addressed. Since *mutT* or *nudG* over-expression was able to hydrolyze (p)ppGpp like SpoT (**Figure 6**), we asked, if the decrease in pppGpp pool associated with reduced SpoT hydrolase activity could be rescued by the expression of the nudix hydrolases.

In the *spoT1* strain carrying the plasmid vector pCA24N, when stringent response was induced by isoleucine starvation, as expected, there was accumulation of ppGpp but not pppGpp (**Figure 7A**, lanes 1–4). In the *spoT1* strain carrying either pCAnudG or pCAmutT and grown in the presence of IPTG to induce expression of the nudix hydrolases, isoleucine starvation resulted in the accumulation of ppGpp and pppGpp (**Figure 7A**, lanes 5–12). As compared to the *spoT1*/pCA24N strain, the concentration of ppGpp relative to GTP decreased in the strains induced for *nudG* or *mutT* expression, and this would be expected due to enhanced hydrolysis of ppGpp. The decrease in ppGpp was more pronounced with MutT over-expression than with NudG. This may be attributed to differences in the expression/activity of the two proteins under our experimental conditions or possibly more efficient hydrolysis of ppGpp by MutT than by NudG. Given that pppGpp was not detected during stringent response in the *spoT1*/pCA24N strain, accumulation of this nucleotide in the *spoT1* strain over-expressing a nudix hydrolase indicated a positive correlation between pppGpp level and cellular (p)ppGpp hydrolase activity. Since an increase in hydrolase activity is associated with an increase in pppGpp pool, it would be reasonable to conclude that the absence of pppGpp accumulation in the *spoT1* is not due to hydrolases such as GppA, which specifically target pppGpp.

Since *nudG* or *mutT* over-expression rescued the growth defect of Δ*spoT* strain, we studied the stringent response in Δ*spoT*/pCAnudG and Δ*spoT*/pCAmutT strains and compared it to that seen in the Δ*spoT*/P_{lac}-spoT^{+}/pCA24N strain after *spoT* expression was reduced by IPTG withdrawal. Amino acid starvation after lowering *spoT* expression and without the over-expression of nudix hydrolases resulted in the accumulation of ppGpp but not pppGpp (**Figure 7B**, lanes 1–4). Amino acid starvation with the over-expression of NudG or MutT lowered the ppGpp pool relative to GTP (**Figure 7B**, lanes 5–12). This effect of NudG or MutT over-expression was similar to that observed in the wild type or *spoT1* background (**Figures 6B,C**, 7A) and can be expected from the constitutive degradation of ppGpp to pGp. On the other hand, there was an increase in pppGpp level relative to ppGpp following the expression of nudix hydrolases, once again revealing a positive correlation between pppGpp level and (p)ppGpp hydrolase activity. Since SpoT is also a (p)ppGpp synthase, it may be argued that, reducing the *spoT* expression in Δ*spoT*/P_{lac}-spoT^{+} strain lowered the pppGpp pool due to reduction in the synthase activity. The recovery of pppGpp pool following the expression of nudix hydrolase would rule out this possibility.

DISCUSSION

Physiological Significance of Negative Regulation of RelA-Mediated Stringent Response by SpoT Hydrolase Activity

Because SpoT has a (p)ppGpp hydrolase activity, it could, in theory, negatively regulate the increase in (p)ppGpp pool during RelA mediated stringent response, but verifying this experimentally is important. Firstly, SpoT is a dual function protein with (p)ppGpp synthase (S) and hydrolase activities (H) that are reported to be reciprocally regulated (H^{+} S^{-} or $H^{-}S^{+}$) (Hogg et al., 2004) – only the H^{+} S^{-} conformation of the SpoT protein would confer negative regulation. Secondly, it was reported that uncharged tRNA's inhibit the SpoT hydrolase activity (Richter, 1980), suggesting that an $H^{-}S^{+}$ state of SpoT may be possible during amino acid starvation. Thirdly, there are reports with evidence for ppGpp (Shyp et al., 2012) or pppGpp (Kudrin et al., 2018) mediated positive allosteric feedback regulation of RelA *in vitro*, and our earlier study had suggested that an increase in the basal pppGpp pool could activate RelA (Sanyal and Harinarayanan, 2020). Therefore, by regulating the cellular concentration of (p)ppGpp, the SpoT hydrolase activity can modulate the amplification of stringent response. Due to the essential nature of SpoT hydrolase function, experimentally verifying its role in counteracting the RelA-dependent increase in (p)ppGpp is not straightforward. Our experimental evidence for negative regulation by SpoT comes from comparing stringent response in isogenic strains with lowered *relA* expression (Δ*rlmD*:FRT and Δ*rlmD*:FRT Δ*spoT* strains, **Figures 2C**, **3A**). The *rlmD* gene is located immediately upstream of *relA*. Three promoters of *relA* are located within and one at the end of the *rlmD* ORF. Two of these promoters are sigma-54 regulated (Brown et al., 2014) and two by the sigma-70 transcription factor (Metzger et al., 1988; Maciąg et al., 2011). Therefore, a non-polar deletion of the *rlmD* gene (Δ*rlmD*:FRT) can be expected to reduce the expression of *relA*. The residual expression of *relA* may be supported from the promoter upstream of *rlmD* (Mendoza-Vargas et al., 2009). As there is no evidence in literature to suggest a change in *relA* expression can influence the hydrolase activity of SpoT, the SpoT mediated degradation of ppGpp observed during the stringent response in Δ*rlmD*:FRT strain may be expected in the wild type strain as well. It was reported, uncharged t-RNA's inhibit the SpoT hydrolase activity (Richter, 1980). This suggests, the SpoT hydrolase activity could be inhibited during amino acid starvation. Further studies are needed to address the biological significance of this finding.

A molecular complex comprising of 70S ribosome with an A-site deacylated tRNA and RelA in a stoichiometry of 1:1:1 initiates stringent response (Cashel et al., 1996). It

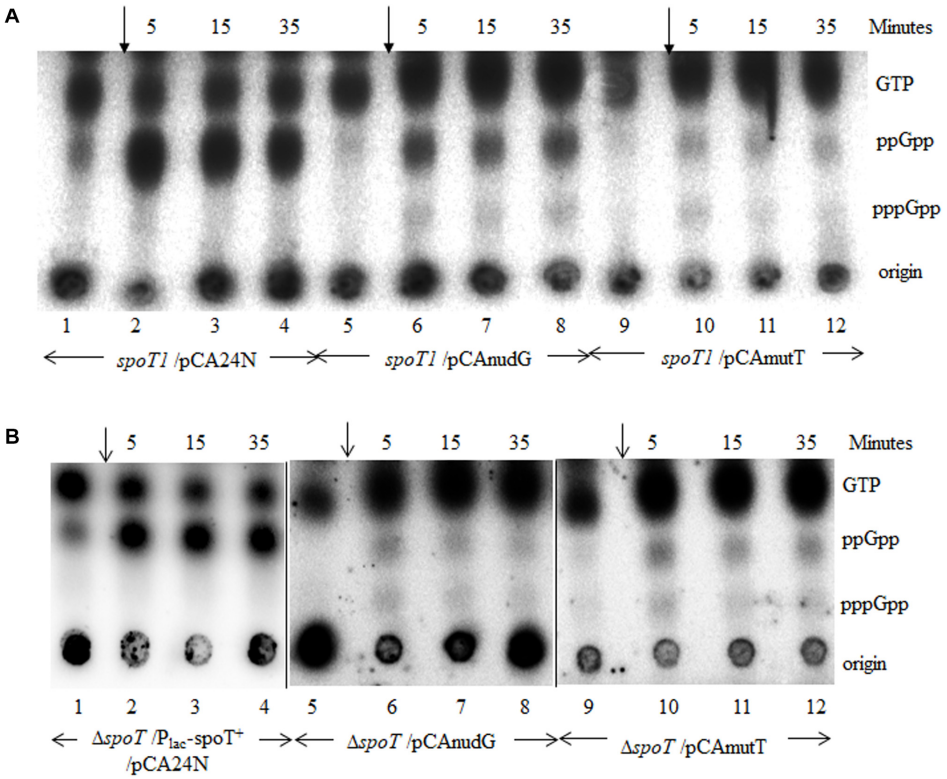

FIGURE 7 | Increased expression of *mutT* or *nudG* lowers the ppGpp pool and elevates pppGpp pool during stringent response in strains with reduced SpoT hydrolase activity. **(A)** Isoleucine starvation was induced by the addition of valine (arrow) to cultures of the *spoT1* strain carrying the vector pCA24N (lanes 1–4), the vector with *nudG* (lanes 5–8), or *mutT* (lanes 9–12). **(B)** Isoleucine starvation was induced in the Δ*spoT*/P_{lac}-spoT^{+}/pCA24N strain after reducing *spoT* + expression by growth in the absence of IPTG (lanes 1–4), in the Δ*spoT*/pCAnudG (lanes 5–8), and Δ*spoT*/pCAmutT (lanes 9–12) strains cultured in the presence of 0.1 mM IPTG. The accumulation of stringent nucleotides was followed with P^{32} labeled cultures as described in the methods. The strains used are, panel **A**, HR1348 (lanes 1–4), HR1350 (lanes 5–8), and HR1349 (lanes 9–12); Panel **B**, RS444 (lanes 1–4), RS460 (lanes 5–8), and RS459 (lanes 9–12).

would be expected that changes in the concentration of RelA or deacylated tRNA will identically affect the concentration of this stringent response ribosomal complex (SRC). After lowering RelA expression, the accumulation of deacylated tRNA elicited stringent response only in the absence of SpoT activity (**Figures 2C**, **3A**). This suggested, a lower concentration of SRC could support (p)ppGpp accumulation in the absence of SpoT hydrolase activity than in a wild type strain. Since SRC concentration would be altered identically from lowering RelA expression or decreasing deacylated tRNA pool, it is plausible that a smaller pool of deacylated tRNA can elicit stringent response in the absence of SpoT hydrolase activity than in the wild type strain. A constitutive SpoT mediated hydrolysis of (p)ppGpp would dampen the amplification of RelA-dependent stringent response, until a quorum of A-site deacylated tRNA molecules are present to cause an aggregate increase in (p)ppGpp pool. It can be argued that SpoT hydrolase activity causes a futile cycling of GTP/GDP to (p)ppGpp to GTP/GDP together with draining of ATP before an increase in (p)ppGpp concentration is apparent. We propose, SpoT hydrolase activity could counteract the onset of stringent response from small contractions in the size of amino acid pool.

In experiments reconstituting RelA-dependent stringent response *in vitro*, it was observed that ppGpp enhanced the rate of RelA-mediated ppGpp synthesis 10-fold in the presence of 70S ribosomes (without starvation signals), leading to the proposal that ppGpp conferred positive allosteric regulation of RelA (**Figure 1**; Shyp et al., 2012). If such a regulation were to operate *in vivo*, we believe this could be revealed in the Δ*rlmD*:FRT Δ*spoT* strain, where it was possible to maintain substantially high levels of ppGpp without amino acid starvation over prolonged time periods due to the absence of SpoT hydrolase activity (**Figure 3A**, lanes 5–11). The gradual decrease in ppGpp pool observed here would suggest, if there was any allosteric activation of RelA by ppGpp, it has to be a very weak phenomenon as no increase in ppGpp was detected even in the absence of the primary hydrolase SpoT (which arguably could mask any increase in ppGpp pool from allosteric activation). However, it is possible, the allosteric regulation was not apparent due to reduced expression of *relA* in the strain.

The Relationship Between pppGpp and SpoT Hydrolase Activity

The over-expression of MutT or NudG lowered the concentration of (p)ppGpp relative to GTP in the wild type strain (**Figures 6B,C**). This is consistent with the study by Zhang

et al. (2018) which showed the over-expression of the proteins lowered the cellular (p)ppGpp pool and hydrolyzed ppGpp to pGp. Although not verified experimentally, pppGpp may also be degraded to pGp. The pGp spot could not be detected under our experimental conditions probably because it co-migrated with GTP. If ppGpp and pppGpp are hydrolyzed with equal efficiency to pGp, then it may be expected that the total amount of this molecule would be similar in the Δ*rlmD*:FRT Δ*spoT* and *spoT1* Δ*gppA*:FRT/P_{lac}-spoT$^+$ strains. This is because, relative to GTP, the ppGpp or (p)ppGpp pool size is similar in the two strains in the absence of amino acid starvation (**Supplementary Tables 2, 4**). We therefore favor the idea that it was the presence of pppGpp, but not pGp that enhanced the growth inhibition in the latter strain. Reduction in hydrolase activity, as in the *spoT1* strain or the reduced expression of *spoT*, lowers the pppGpp pool relative to ppGpp and GTP during amino acid starvation (Laffler and Gallant, 1974; Sanyal and Harinarayanan, 2020). To our knowledge, the molecular basis for this phenotype has not been addressed. Results from an earlier study suggested the phenotype was not dependent on the pppGpp hydrolase, GppA (Sanyal and Harinarayanan, 2020), but did not definitively rule it out. In the strains deficient for *spoT* hydrolase activity, following the over-expression of nudix hydrolase, the ppGpp concentration dropped relative to GTP as seen in the wild type strain, but interestingly, there was an increase in the pppGpp pool relative to ppGpp (**Figure 7**). These results suggest, the unexpected decline in pppGpp pool in strains deficient for SpoT hydrolase activity is caused by the decrease in (p)ppGpp hydrolase activity and not the presence of pppGpp hydrolase such as GppA. Further studies are needed to address the molecular basis of the "spotless" phenotype.

MATERIALS AND METHODS

Media and Growth Conditions

LB medium had the final composition of 1% tryptone, 0.5% yeast extract, and 1% NaCl. MOPS buffered minimal medium (Neidhardt et al., 1974), and minimal A medium (Miller, 1992) were prepared as reported. The minimal medium was supplemented with 0.5% glucose, unless mentioned otherwise. In plates, glucose and casamino acids were each supplemented at 0.2% final concentration. serine, methionine, and glycine were supplemented to final concentration of 100 μg ml^{-1} in plates. Antibiotics and their final concentration in the growth medium are ampicillin (Amp) 50 μg ml^{-1}, kanamycin (Kan) 25 μg ml^{-1}, tetracycline (Tet) 10 μg ml^{-1}, and chloramphenicol (Cm) 15 μg ml^{-1}. Isopropyl β-D-thiogalactopyranoside (IPTG) was supplemented to final concentration of 1 or 0.1 mM as indicated and 5-Bromo-4-chloro 3-indolyl-β-D-thiogalactoside (X-gal) was used at a final concentration of 50 μg ml^{-1}.

Construction of Strains and Plasmids

All strains were derived from the *E. coli* K-12 strain MG1655. Strains, plasmids, and primers used in this study are tabulated in **Supplementary Table 1**. Phage P1 mediated transduction was used to introduce mutations into the chromosome following standard protocol (Miller, 1992). Gene deletions were sourced from the Keio collection (Baba et al., 2006), and if necessary, the kanamycin resistance cassette was removed using the FLP recombinase expressed from the pCP20 plasmid (Cherepanov and Wackernagel, 1995). For the construction of *relA496*Δ:Kan and *relA455*Δ:Kan alleles, all codons after 496 or 455 were deleted and replaced with a TAG stop codon and the kanamycin cassette from pKD13 (Datsenko and Wanner, 2000) by recombineering (Yu et al., 2000) using the primers JGOrelA496aaPS4 or JGOrelA455aaPS4 with JGOrelAPS1, respectively. The sequence of the constructs were verified using primers JGOrelA + 882 and K1. The plasmid P_{lac}-spoT$^+$ was constructed using the vector pRC7 (Bernhardt and De Boer, 2004) and has been referred to as pRCspoT previously (Nazir and Harinarayanan, 2016). The *spoT* gene in P_{lac}-spoT$^+$ is under the lac promoter and has the native RBS and the TTG start codon. The plasmids pCA24N, pCAspoT, pCAmutT, and pCAnudG were obtained from the ASKA collection (Kitagawa et al., 2005).

Depletion of SpoT Using the Plasmid P_{lac}-spoT$^+$

The chromosomal *spoT* gene was either deleted or replaced with *spoT1* in the presence of the single-copy plasmid P_{lac}-spoT$^+$. In this plasmid spoT expression was driven from the *lac* promoter. A tight regulation of expression was expected due to the very low copy number of the plasmid and the plasmid encoding for the LacI repressor protein. Further, there is an elevated expression of *lacI* due to the presence of the *lacI*^{q} mutation. Expression of spoT was lowered by the withdrawal of IPTG from the growth medium. Cultures grown in the presence of ampicillin and IPTG (1 mM), were washed with minimal medium to remove IPTG and diluted 100-fold into medium lacking IPTG.

Plasmid Segregation Assay

The assay works on the principle that an essential gene function provided from an unstable plasmid, would stabilize the plasmid. Since the plasmid carries the *lacZ* gene, blue and white colonies indicate the retention and loss of the plasmid, respectively, in plates containing the inducer IPTG and the indicator X-gal. The assay referred to as the 'blue–white assay' and was carried out in strains having the Δ*lacZYAI*:FRT mutation. The absence of white colonies after growth without selection for the plasmid would indicate that the plasmid encoded function was essential under the conditions. Strains carrying P_{lac}-spoT$^+$ were grown in LB broth containing ampicillin and IPTG. Cultures were washed with minimal medium to remove IPTG. For the 'blue-white' assay appropriate dilutions of the culture were spread on plates containing IPTG and X-gal so as to obtain ∼300 colonies per plate. Plates were incubated at 37°C for 24 h in the case of LB or minimal A medium containing glucose and casaminoacids and 48 h in the case of minimal A medium with glucose. Incubation was extended to 72 h when white colonies were not evident after 24 or 48 h of incubation. The percentage of white colonies was calculated from the ratio of white colonies over the total number of colonies scored (white + blue).

(p)ppGpp Estimation by Thin Layer Chromatography

Cultures were grown to saturation in MOPS minimal medium containing 0.5% glucose. These cultures were diluted 100-fold and allowed to grow till an A_{600} of ∼ 0.4 to 0.5, and then diluted 10-fold into a pre-warmed low-phosphate medium with 0.4 mM K_2HPO_4 and 100–200 μCi ml^{-1} of ^{32}P-H_3PO_4. After at least two doublings in this medium, isoleucine starvation was induced by the addition of valine. An unlabeled culture was used to monitor A_{600}. Samples were collected in tubes containing an equal volume of 2 N HCOOH kept chilled on ice, subjected to 3 cycles of freeze-thaw and centrifuged at 10000 rpm for 5 min at 4°C. The supernatant was spotted on PEI cellulose sheets and resolved using 1.5 M KH_2PO_4, pH 3.4. The nucleotide spots were imaged using phosphorimager (Typhoon FLA 9500). Quantification of the spots was carried out by densitometry after subtracting background, using the multi-gage V3.0 software (Fujifilm).

Isolation of Multi-Copy Suppressors

The Δ*rlmD*:FRT Δ*spoT* Δ*gppA*/P_{lac}-spoT$^+$ strain was transformed with an *E. coli* genomic library made in plasmid pACYC184 (Saxena and Gowrishankar, 2011) and chloramphenicol resistant transformants were selected on media without ampicillin and IPTG which is non-permissive for the parental strain. Minimal A glucose medium with or without casaminoacids was used to select the plasmid clones that rescued the growth defect of the parental strain (from approximately 80,000 transformants obtained in each medium). A total of 72 ampicillin sensitive white colonies were identified, which indicated that the growth of these clones were independent of SpoT function. When plasmid isolated from 25 out of the 72 colonies was individually transformed into the Δ*rlmD*:FRT Δ*spoT* Δ*gppA*/P_{lac}-spoT$^+$ strain, 22 were found to support growth of Δ*rlmD*:FRT Δ*spoT* Δ*gppA* strain. Four out of the 22 plasmids also rescued the growth defect of the Δ*relA* Δ*spoT* ($ppGpp^0$) strain in minimal A glucose medium, and therefore, thought to carry the *spoT* gene and sequencing one of the 4 clones showed this was indeed the case. After sequencing the other 18 clones, unique DNA fragments were identified in five clones.

Isoleucine Starvation and Reversal of Starvation

The addition of valine inhibits isoleucine biosynthesis in *E. coli* K-12 strains causing isoleucine starvation. This is because, enzymes catalyzing the first common step in the biosynthesis of the branched chain amino acids isoleucine and valine are feedback inhibited by valine and the feedback resistant enzyme encoded by the *ilvG* gene is inactive in this strain due to a chain terminating mutation (Umbarger and Brown, 1957). Valine was added to a final concentration of 100 μg ml^{-1} to induce isoleucine starvation, and this was reversed by the addition of 100 μg ml^{-1} of isoleucine.

DATA AVAILABILITY STATEMENT

All datasets presented in this study are included in the article/**Supplementary Material**.

AUTHOR CONTRIBUTIONS

RH conceived the study. RS and RH designed the experiments. RS and AV performed the experiments. All authors contributed to the article and approved the submitted version.

FUNDING

The study was funded by the Centre of Excellence in Microbial Biology – Phase 2 research grant of the Department of Biotechnology, Government of India and research fund provided by the Centre for DNA Fingerprinting and Diagnostics. RS is a recipient of DBT-SRF fellowship.

ACKNOWLEDGMENTS

We acknowledge the use of strains from the Keio and ASKA collections (NBRP, Japan). We thank the reviewers for their comments that helped improve the data presentation. We would like to thank Bhagyashree Koyalada for the construction of strains HR1348, HR1349, and HR1350.

SUPPLEMENTARY MATERIAL

The Supplementary Material for this article can be found online at: https://www.frontiersin.org/articles/10.3389/fmicb.2020.562804/full#supplementary-material

REFERENCES

Akiyama, M., Horiuchi, T., and Sekiguchi, M. (1987). Molecular cloning and nucleotide sequence of the *mutT* mutator of *Escherichia coli* that causes A:T to C: G transversion. *Mol. Gen. Genet.* 206, 9–16. doi: 10.1007/BF00326530

Alfoldi, L., Stent, G. S., and Clowes, R. C. (1962). The chromosomal site of the RNA control (RC) locus in *Escherichia coli*. *J. Mol. Biol.* 5, 348–355. doi: 10.1016/S0022-2836(62)80077-1

An, G., Justesen, J., Watson, R. J., and Friesen, J. D. (1979). Cloning the *spoT* gene of *Escherichia coli*: identification of the *spoT* gene product. *J. Bacteriol.* 137, 1100–1110. doi: 10.1128/JB.137.3.1100-1110.1979

Arenz, S., Abdelshahid, M., Sohmen, D., Payoe, R., Starosta, A. L., Berninghausen, O., et al. (2016). The stringent factor RelA adopts an open conformation on the ribosome to stimulate ppGpp synthesis. *Nucleic Acids Res.* 44, 6471–6481. doi: 10.1093/nar/gkw470

Atkinson, G. C., Tenson, T., and Hauryliuk, V. (2011). The RelA/SpoT homolog (RSH) superfamily: distribution and functional evolution of ppGpp synthetases and hydrolases across the tree of life. *PLoS One* 6:e23479. doi: 10.1371/journal.pone.0023479

Baba, T., Ara, T., Hasegawa, M., Takai, Y., Okumura, Y., Baba, M., et al. (2006). Construction of *Escherichia coli* K-12 in-frame, single-gene knockout

mutants: the Keio collection. *Mol. Syst. Biol.* 2:2006.0008. doi: 10.1038/msb4100050

Battesti, A., and Bouveret, E. (2006). Acyl carrier protein/SpoT interaction, the switch linking SpoT-dependent stress response to fatty acid metabolism. *Mol. Microbiol.* 62, 1048–1063. doi: 10.1111/j.1365-2958.2006.05442.x

Bernhardt, T. G., and De Boer, P. A. J. (2004). Screening for synthetic lethal mutants in *Escherichia coli* and identification of EnvC (YibP) as a periplasmic septal ring factor with murein hydrolase activity. *Mol. Microbiol.* 52, 1255–1269. doi: 10.1111/j.1365-2958.2004.04063.x

Bhatnagar, S., and Bessman, M. (1988). Studies on the Mutator Gene, *mutT* of *Escherichia coli*. *J. Biol. Chem.* 263, 8953–8957.

Braeken, K., Moris, M., Daniels, R., Vanderleyden, J., and Michiels, J. (2006). New horizons for (p)ppGpp in bacterial and plant physiology. *Trends Microbiol.* 14, 45–54. doi: 10.1016/j.tim.2005.11.006

Brown, A., Fernández, I. S., Gordiyenko, Y., and Ramakrishnan, V. (2016). Ribosome-dependent activation of stringent control. *Nature* 534, 277–280. doi: 10.1038/nature17675

Brown, D. R., Barton, G., Pan, Z., Buck, M., and Wigneshweraraj, S. (2014). Nitrogen stress response and stringent response are coupled in *Escherichia coli*. *Nat. Commun.* 5, 1–8. doi: 10.1038/ncomms5115

Cashel, M., Gentry, D. R., Hernandez, V. J., and Vinella, D. (1996). "The stringent response," in *Escherichia coli and Salmonella: Cellular and Molecular Biology*, eds F. C. Neidhardt, R. Curtiss III, J. L. Ingraham, E. C. C. Lin, K. B. Low, B. Magasanik, et al. (Cham: Springer), 1458–1496.

Chatterji, D., and Kumar Ojha, A. (2001). Revisiting the stringent response, ppGpp and starvation signaling. *Curr. Opin. Microbiol.* 4, 160–165. doi: 10.1016/S1369-5274(00)00182-X

Cherepanov, P. P., and Wackernagel, W. (1995). Gene disruption in *Escherichia coli*: TcR and KmR cassettes with the option of Flp-catalyzed excision of the antibiotic-resistance determinant. *Gene* 158, 9–14. doi: 10.1016/0378-1119(95)00193-A

Dalebroux, Z. D., Svensson, S. L., Gaynor, E. C., and Swanson, M. S. (2010). ppGpp conjures bacterial virulence. *Microbiol. Mol. Biol. Rev.* 74, 171–199. doi: 10.1128/MMBR.00046-09

Datsenko, K., and Wanner, B. L. (2000). One-step inactivation of chromosomal genes in *Escherichia coli* K-12 using PCR products. *Proc. Natl. Acad. Sci. U.S.A.* 97, 6640–6645. doi: 10.1073/pnas.120163297

Durfee, T., Hansen, A. M., Zhi, H., Blattner, F. R., and Ding, J. J. (2008). Transcription profiling of the stringent response in *Escherichia coli*. *J. Bacteriol.* 190, 1084–1096. doi: 10.1128/JB.01092-07

Fujikawa, K., and Kasai, H. (2002). The oxidized pyrimidine ribonucleotide, 5-hydroxy-CTP, is hydrolyzed efficiently by the *Escherichia coli* recombinant Orf135 protein. *DNA Repair* 1, 571–576. doi: 10.1016/S1568-7864(02)00057-5

Germain, E., Guiraud, P., Byrne, D., Douzi, B., Djendli, M., and Maisonneuve, E. (2019). YtfK activates the stringent response by triggering the alarmone synthetase SpoT in *Escherichia coli*. *Nat. Commun.* 10:5763. doi: 10.1038/s41467-019-13764-4

Harat, A., and Sy, J. (1983). Guanosine 5'-triphosphate, 3'-diphosphate 5'-phosphohydrolase: purification and substrate specificity. *J. Biol. Chem.* 258, 1678–1683.

Hauryliuk, V., Atkinson, G. C., Murakami, K. S., Tenson, T., and Gerdes, K. (2015). Recent functional insights into the role of (p)ppGpp in bacterial physiology. *Nat. Rev. Microbiol.* 13, 298–309. doi: 10.1038/nrmicro3448

Hogg, T., Mechold, U., Malke, H., Cashel, M., and Hilgenfeld, R. (2004). Conformational antagonism between opposing active sites in a bifunctional RelA/SpoT homolog modulates (p)ppGpp metabolism during the stringent response. *Cell* 117, 57–68. doi: 10.1016/S0092-8674(04)00260-0

Jiang, M., Sullivan, S. M., Wout, P. K., and Maddock, J. R. (2007). G-protein control of the ribosome-associated stress response protein SpoT. *J. Bacteriol.* 189, 6140–6147. doi: 10.1128/JB.00315-07

Keasling, J. D., Bertsch, L., and Kornberg, A. (1993). Guanosine pentaphosphate phosphohydrolase of *Escherichia coli* is a long-chain exopolyphosphatase. *Proc. Natl. Acad. Sci. U.S.A.* 90, 7029–7033. doi: 10.1073/pnas.90.15.7029

Kitagawa, M., Ara, T., Arifuzzaman, M., Ioka-Nakamichi, T., Inamoto, E., Toyonaga, H., et al. (2005). Complete set of ORF clones of *Escherichia coli* ASKA library (A complete set of *E. coli* K-12 ORF archive): unique resources for biological research. *DNA Res.* 12, 291–299. doi: 10.1093/dnares/dsi012

Kudrin, P., Dzhygyr, I., Ishiguro, K., Beljantseva, J., Maksimova, E., Oliveira, S. R. A., et al. (2018). The ribosomal A-site finger is crucial for binding and activation of the stringent factor RelA. *Nucleic Acids Res.* 46, 1973–1983. doi: 10.1093/nar/gky023

Laffler, T., and Gallant, J. (1974). spoT, a new genetic locus involved in the stringent response in *E. coli*. *Cell* 1, 27–30. doi: 10.1016/0092-8674(74)90151-2

Loveland, A. B., Bah, E., Madireddy, R., Zhang, Y., Brilot, A. F., Grigorieff, N., et al. (2016). Ribosome RelA structures reveal the mechanism of stringent response activation. *eLife* 5:e17029. doi: 10.7554/eLife.17029.043

Maciąg, A., Peano, C., Pietrelli, A., Egli, T., De Bellis, G., and Landini, P. (2011). *In vitro* transcription profiling of the σS subunit of bacterial RNA polymerase: re-definition of the σS regulon and identification of σS-specific promoter sequence elements. *Nucleic Acids Res.* 39, 5338–5355. doi: 10.1093/nar/gkr129

Mechold, U., Cashel, M., Steiner, K., Gentry, D., and Malke, H. (1996). Functional analysis of a relA/spoT gene homolog from Streptococcus equisimilis. *J. Bacteriol.* 178, 1401–1411. doi: 10.1128/JB.178.5.1401-1411.1996

Mechold, U., Potrykus, K., Murphy, H., Murakami, K. S., and Cashel, M. (2013). Differential regulation by ppGpp versus pppGpp in *Escherichia coli*. *Nucleic Acids Res.* 41, 6175–6189. doi: 10.1093/nar/gkt302

Mendoza-Vargas, A., Olvera, L., Olvera, M., Grande, R., Vega-Alvarado, L., Taboada, B., et al. (2009). Genome-wide identification of transcription start sites, promoters and transcription factor binding sites in *E. coli*. *PLoS One* 4:e7526. doi: 10.1371/journal.pone.0007526

Metzger, S., Dror, I. B., Aizenman, E., Schreiber, G., Toone, M., Friesen, J. D., et al. (1988). The nucleotide sequence and characterization of the *relA* gene of *Escherichia coli*. *J. Biol. Chem.* 263, 15699–15704.

Metzger, S., Schreiber, G., Aizenman, E., Cashel, M., and Glaser, G. (1989). Characterization of the relA1 mutation and a comparison of relA1 with new *relA* null alleles in *Escherichia coli*. *J. Biol. Chem.* 264, 21146–21152.

Miller, J. H. (1992). *A Short Course in Bacterial Genetics: A Laboratory Manual and Handbook for and Related Bacteria*. Cold Spring Harbor, NY: Cold Spring Harbor Laboratory Press.

Mittenhuber, G. (2001). Comparative genomics and evolution of genes encoding bacterial (p)ppGpp synthetases/hydrolases (the Rel, RelA and SpoT proteins). *J. Mol. Microbiol. Biotechnol.* 3, 585–600.

Montero, M., Rahimpour, M., Viale, A. M., Almagro, G., Eydallin, G., Sevilla, A., et al. (2014). Systematic production of inactivating and non-inactivating suppressor mutations at the *relA* locus that compensate the detrimental effects of complete *spoT* loss and affect glycogen content in *Escherichia coli*. *PLoS One* 9:e106938. doi: 10.1371/journal.pone.0106938

Nakagawa, A., Oshima, T., and Mori, H. (2006). Identification and characterization of a second, inducible promoter of *relA* in *Escherichia coli*. *Genes Genet. Syst.* 81, 299–310. doi: 10.1266/ggs.81.299

Nazir, A., and Harinarayanan, R. (2016). Inactivation of cell division protein FtsZ by SulA makes Lon indispensable for the viability of a ppGpp0 strain of *Escherichia coli*. *J. Bacteriol.* 198, 688–700. doi: 10.1128/JB.00693-15

Neidhardt, F. C., Bloch, P. L., and Smith, D. F. (1974). Culture medium for enterobacteria. *J. Bacteriol.* 119, 736–747. doi: 10.1128/JB.119.3.736-747.1974

Potrykus, K., and Cashel, M. (2008). (p)ppGpp: still magical? *Annu. Rev. Microbiol.* 62, 35–51. doi: 10.1146/annurev.micro.62.081307.162903

Richter, D. (1980). Uncharged tRNA inhibits guanosine 3',5'-bis (diphosphate) 3'-pyrophosphohydrolase [ppGppase], the *spoT* gene product, from *Escherichia coli*. *Mol. Gen. Genet.* 178, 325–327. doi: 10.1007/BF00270479

Ross, W., Sanchez-Vazquez, P., Chen, A. Y., Lee, J. H., Burgos, H. L., and Gourse, R. L. (2016). ppGpp binding to a site at the RNAP-DksA interface accounts for its dramatic effects on transcription initiation during the stringent response. *Mol. Cell.* 62, 811–823. doi: 10.1016/j.molcel.2016.04.029

Ross, W., Vrentas, C. E., Sanchez-Vazquez, P., Gaal, T., and Gourse, R. L. (2013). The magic spot: A ppGpp binding site on *E. coli* RNA polymerase responsible for regulation of transcription initiation. *Mol. Cell.* 50, 420–429. doi: 10.1016/j.molcel.2013.03.021

Sanyal, R., and Harinarayanan, R. (2020). Activation of RelA by pppGpp as the basis for its differential toxicity over ppGpp in *Escherichia coli*. *J. Biosci.* 45:28. doi: 10.1007/s12038-020-9991-2

Sarubbi, E., Rudd, E., Xiao, H., Ikeharat, K., Kalman, M., and Cashell, M. (1989). Characterization of the *spoT* gene of *Escherichia coli*. *J. Biol. Chem.* 264, 15074–15082.

Sarubbi, E., Rudd, K. E., and Cashel, M. (1988). Basal ppGpp level adjustment shown by new *spoT* mutants affect steady state growth rates and *rrnA* ribosomal promoter regulation in *Escherichia coli*. *Mol. Gen. Genet.* 213, 214–222. doi: 10.1007/BF00339584

Saxena, S., and Gowrishankar, J. (2011). Modulation of Rho-dependent transcription termination in *Escherichia coli* by the H-NS family of proteins. *J. Bacteriol.* 193, 3832–3841. doi: 10.1128/JB.00220-11

Schreiber, G., Metzger, S., Aizenman, E., Roza, S., Cashel, M., and Glaser, G. (1991). Overexpression of the *relA* gene in *Escherichia coli*. *J. Biol. Chem.* 266, 3760–3767.

Seyfzadeh, M., Keener, J., and Nomura, M. (1993). spoT-dependent accumulation of guanosine tetraphosphate in response to fatty acid starvation in *Escherichia coli*. *Proc. Natl. Acad. Sci. U.S.A.* 90, 11004–11008. doi: 10.1073/pnas.90.23.11004

Shyp, V., Tankov, S., Ermakov, A., Kudrin, P., English, B. P., Ehrenberg, M., et al. (2012). Positive allosteric feedback regulation of the stringent response enzyme RelA by its product. *EMBO Rep.* 13, 835–839. doi: 10.1038/embor.2012.106

Sinha, A. K., Winther, K. S., Roghanian, M., and Gerdes, K. (2019). Fatty acid starvation activates RelA by depleting lysine precursor pyruvate. *Mol. Microbiol.* 112, 1339–1349. doi: 10.1111/mmi.14366

Somerville, C. R., and Ahmed, A. (1979). Mutants of *Escherichia coli* defective in the degradation of guanosine 5'-triphosphate, 3'-diphosphate (pppGpp). *Mol. Gen. Genet.* 169, 315–323. doi: 10.1007/BF00382277

Spira, B., Hu, X., and Ferenci, T. (2008). Strain variation in ppGpp concentration and RpoS levels in laboratory strains of *Escherichia coli* K-12. *Microbiology* 154, 2887–2895. doi: 10.1099/mic.0.2008/018457-0

Svitil, A. L., Cashel, M., and Zyskind, J. W. (1993). Guanosine tetraphosphate inhibits protein synthesis *in vivo*. *J. Biol. Chem.* 268, 2307–2311.

Traxler, M. F., Zacharia, V. M., Marquardt, S., Summers, S. M., Nguyen, T., Stark, S. E., et al. (2011). Discretely calibrated regulatory loops controlled by ppGpp partition gene induction across the 'feast to famine' gradient in *Escherichia coli*. *Mol. Microbiol.* 79, 830–845. doi: 10.1111/j.1365-2958.2010.07498.x

Umbarger, H. E., and Brown, B. (1957). A negative feedback mechanism controlling isoleucine biosynthesis. *J. Biol. Chem.* 233, 415–420.

Uzan, M., and Danchin, A. (1976). A rapid test for the RelA mutation in *E. coli*. *Biochem. Biophys. Res. Commun.* 69, 751–758. doi: 10.1016/0006-291X(76)90939-6

Vinella, D., Albrecht, C., Cashel, M., and D'Ari, R. (2005). Iron limitation induces SpoT-dependent accumulation of ppGpp in *Escherichia coli*. *Mol. Microbiol.* 56, 958–970. doi: 10.1111/j.1365-2958.2005.04601.x

Wang, B., Dai, P., Ding, D., Del Rosario, A., Grant, R. A., Pentelute, B. L., et al. (2019). Affinity-based capture and identification of protein effectors of the growth regulator ppGpp. *Nat. Chem. Biol.* 15, 141–150. doi: 10.1038/s41589-019-0296-4

Xiao, H., Kalman, M., Ikehara, K., Zemel, S., Glaser, G., and Cashel, M. (1991). Residual guanosine 3',5'-bispyrophosphate synthetic activity of *relA* null mutants can be eliminated by *spoT* null mutations. *J. Biol. Chem.* 266, 5980–5990.

Yu, D., Ellis, H. M., Lee, E., Jenkins, N. A., Copeland, N. G., and Court, D. L. (2000). An efficient recombination system for chromosome engineering in *Escherichia coli*. *Proc. Natl. Acad. Sci. U.S.A.* 97, 5978–5983. doi: 10.1073/pnas.100127597

Zhang, Y., Eva, Z., Rejman, D., and Gerdes, K. (2018). Novel (p)ppGpp binding and metabolizing proteins of *Escherichia coli*. *mBio* 9:e02188-17. doi: 10.1128/mBio.02188-17

Zuo, Y., Wang, Y., and Steitz, T. A. (2013). The mechanism of *E. coli* RNA polymerase regulation by ppGpp is suggested by the structure of their complex. *Mol. Cell* 50, 430–436. doi: 10.1016/j.molcel.2013.03.020

Conflict of Interest: The authors declare that the research was conducted in the absence of any commercial or financial relationships that could be construed as a potential conflict of interest.

frontiers in Microbiology

ORIGINAL RESEARCH
published: 23 October 2020
doi: 10.3389/fmicb.2020.581271

Estimates of Rel_{Seq}, Mesh1, and SAH_{Mex} Hydrolysis of (p)ppGpp and (p)ppApp by Thin Layer Chromatography and NADP/NADH Coupled Assays

Katarzyna Potrykus[1], Nathan E. Thomas[2†], Bożena Bruhn-Olszewska[1], Michał Sobala[1], Maciej Dylewski[1], Tamara James[2] and Michael Cashel[2]**

[1] Department of Bacterial Molecular Genetics, Faculty of Biology, University of Gdańsk, Gdańsk, Poland, [2] Intramural Program, Eunice Kennedy Shriver National Institute of Child Health and Human Development, National Institutes of Health, Bethesda, MD, United States

OPEN ACCESS

Edited by:
Kenneth C. Keiler,
The Pennsylvania State University (PSU), United States

Reviewed by:
Jen-Tsan Ashley Chi,
Duke University, United States
Gemma Atkinson,
Umeå University, Sweden

***Correspondence:**
Michael Cashel
cashelm@mail.nih.gov
Katarzyna Potrykus
katarzyna.potrykus@ug.edu.pl

†Present address:
Nathan E. Thomas,
Department of Biochemistry, University of Wisconsin-Madison, Madison, WI, United States

Specialty section:
This article was submitted to Microbial Physiology and Metabolism, a section of the journal Frontiers in Microbiology

Received: 08 July 2020
Accepted: 06 October 2020
Published: 23 October 2020

Citation:
Potrykus K, Thomas NE, Bruhn-Olszewska B, Sobala M, Dylewski M, James T and Cashel M (2020) Estimates of Rel_{Seq}, Mesh1, and SAH_{Mex} Hydrolysis of (p)ppGpp and (p)ppApp by Thin Layer Chromatography and NADP/NADH Coupled Assays. Front. Microbiol. 11:581271. doi: 10.3389/fmicb.2020.581271

The Mesh1 class of hydrolases found in bacteria, metazoans and humans was discovered as able to cleave an intact pyrophosphate residue esterified on the 3′hydroxyl of (p)ppGpp in a Mn^{2+} dependent reaction. Here, thin layer chromatography (TLC) qualitative evidence is presented indicating the substrate specificity of Mesh1 from *Drosophila melanogaster* and human MESH1 also extends to the (p)ppApp purine analogs. More importantly, we developed real time enzymatic assays, coupling ppNpp hydrolysis to NADH oxidation and pppNpp hydrolysis to $NADP^+$ reduction, which facilitate estimation of kinetic constants. Furthermore, by using this assay technique we confirmed TLC observations and also revealed that purified small alarmone hydrolase (SAH_{Mex}) from *Methylobacterium extorquens* displays a strong hydrolase activity toward (p)ppApp but only negligible activity toward (p)ppGpp. In contrast, the substrate specificity of the hydrolase present in catalytically active N-terminal domain of the RSH protein from *Streptococcus equisimilis* (Rel_{Seq}) includes (p)ppGpp but not (p)ppApp. It is noteworthy that the RSH protein from *M. extorquens* (RSH_{Mex}) has been recently shown to synthesize both (p)ppApp and (p)ppGpp.

Keywords: (p)ppGpp, (p)ppApp, RSH, Mesh1, SAH, stringent response, *Methylobacterium extorquens*, *Escherichia coli*

INTRODUCTION

Bacterial global regulatory stress responses play a major role in their adaptation to constantly changing environmental conditions. One of the best studied responses is the stringent response, characterized by a swift synthesis of large amounts of guanosine tetra- and penta-phosphates, collectively referred to as (p)ppGpp (Potrykus and Cashel, 2008). These second messengers may act through several different modes of action. For example in *Escherichia coli* they directly interact with the RNA polymerase (RNAP) by binding at two distinct sites (Mechold et al., 2013; Ross et al., 2016; Molodtsov et al., 2018), which leads to transcriptional reprogramming allowing for

cell survival under harsh conditions. On the other hand, in *Bacillus subtilis* (p)ppGpp accumulation leads to depletion of GTP levels [by using up GTP as a substrate for (p)ppGpp synthesis and by direct inhibition of GTP synthesizing enzymes (Kriel et al., 2012)] that in turn also leads to alterations in gene expression at the transcription initiation level (Krásný and Gourse, 2004; Kriel et al., 2012). Other putative ppGpp targets have been also recently identified in *E. coli* (Wang et al., 2019).

The mode of (p)ppGpp synthesis may differ, depending on the stress condition that triggers its synthesis. For example, two (p)ppGpp synthetases exist in *E. coli* and in other γ- and β-proteobacteria: RelA (active under amino acid deprivation), and SpoT (active under other stresses) (Potrykus and Cashel, 2008). In Firmicutes, as well as in α-, δ- and ε-proteobacteria, (p)ppGpp is synthesized by what we call here RSH proteins (Potrykus and Cashel, 2008) also referred to as Rel (Mittenhuber, 2001; Atkinson et al., 2011), and small synthetases (called SAS, for small alarmone synthetase) seemingly devoid of large regulatory domains (Lemos et al., 2007; Nanamiya et al., 2008; Atkinson et al., 2011; Steinchen et al., 2018).

Still, no matter what the mode of (p)ppGpp synthesis is, regulation of (p)ppGpp hydrolysis is equally crucial for the cell, so that it can quickly respond once the environmental conditions improve. In *E. coli* (and other γ- and β- proteobacteria) that function is carried out by SpoT, while in Firmicutes, α-, δ- and ε-proteobacteria it is carried out by long bifunctional RSH enzymes. Interestingly, in the latter case, stand-alone (p)ppGpp hydrolases called SAH (for small alarmone hydrolases) have been also identified by bioinformatics methods (Atkinson et al., 2011). These enzymes are related to Mesh1 enzymes found in the metazoan species, such as *Drosophila melanogaster*, worms, mice, and humans (Sun et al., 2010). There, it was demonstrated that the *D. melanogaster* Mesh1 and human MESH1 enzymes (for Metazoan SpoT Homolog-1) are structurally similar to the hydrolysis domain of an RSH enzyme from *Streptococcus equisimilis* (Rel_{Seq}) and are capable of ppGpp hydrolysis, although no source of ppGpp synthesis in metazoa has been discovered. The authors had noted that the Mesh1 enzyme requires Mn^{2+} and reverses the toxicity of RelA induction due to ppGpp synthesis when expressed in *E. coli*, as well as in *D. melanogaster* tissue culture cells (Sun et al., 2010). Yet, bacterial SAH enzymes have been neglected for several years, with only one recent report characterizing SAH from *Corynebacterium glutamicum* (Ruwe et al., 2018).

In this study, we report findings accumulated over the past several years in the Cashel and the Potrykus labs. Our interest arose from several leads. First, as mentioned above, (p)ppGpp hydrolysis regulation is as important as its synthesis. For many years the Cashel lab has been investigating the SpoT and Rel_{Seq} hydrolysis regulation (e.g., Gentry and Cashel, 1995; Mechold et al., 2002). Second, the discovery of Mesh1 with concomitant inability to demonstrate (p)ppGpp synthesis in metazoa, has led both labs to search for a different substrate for these enzymes. An obvious candidate was ppApp, a structural analog of ppGpp. This nucleotide has been observed long ago in *B. subtilis*, and its synthesis was thought to be carried out by factors associated with ribosomes under starvation conditions inducing sporulation (Rhaese et al., 1977; Nishino et al., 1979). Later, the role of (p)ppGpp in sporulation was shown as due to indirect effects on GTP pool depletion (Ochi et al., 1982), while the (p)ppApp occurrence was deemed as an experimental artifact, and thus this nucleotide has been neglected for many years.

As we discuss later, we confirm that Mesh1 and MESH1 hydrolyze ppGpp (as reported by Sun et al. (2010), but also find that pppGpp and (p)ppApp can serve as substrates. These findings have led the Potrykus lab to wonder if the same would be true for bacterial SAH enzymes, and whether (p)ppApp might serve as a second messenger, in parallel to (p)ppGpp. *Methylobacterium extorquens* (a SAH- bearing bacterium) and *E. coli* have been chosen as the model organisms. As we reported elsewhere, we found pppApp to be synthesized by *M. extorquens* and *E. coli* cells *in vivo*, and RSH_{Mex} enzyme (a long bifunctional RSH protein) is the source of both, (p)ppGpp and pppApp in *M. extorquens* (Sobala et al., 2019). At the same time, we confirmed and dissected the role of (p)ppApp in regulating *E. coli* RNAP activity at the ribosomal *rrnB* P1 promoter (Bruhn-Olszewska et al., 2018).

Here, we report our initial findings on the Mesh1 and MESH1 degradation of pppGpp and (p)ppApp, supplemented by later findings for the SAH enzyme from *M. extorquens* AM1 strain (SAH_{Mex}). Interestingly, the *M. extorquens* SAH enzyme is active toward (p)ppApp but not (p)ppGpp. Moreover, our joint investigation has led the Cashel lab to develop a real time kinetic optical assay by coupling NADH oxidation or NADP+ reduction to monitor hydrolysis of nucleotide tetraphosphates or pentaphosphates, respectively. Compared to thin layer chromatography (TLC) or HPLC methods where the reaction needs to be terminated to make a reading, these coupled assays generate real time data that greatly facilitates estimating kinetic constants for (p)ppGpp and (p)ppApp hydrolysis. Here, this method is used to document all three possible classes of hydrolase substrate specificities: Rel_{Seq} is active toward (p)ppGpp but not (p)ppApp; SAH_{Mex} is active toward (p)ppApp but not (p)ppGpp; and the Mesh1 enzyme from *D. melanogaster* hydrolyzes both.

MATERIALS AND METHODS

Strains and Plasmids

Plasmid pUM77, a pET21 derivative, was used as source of $Rel_{Seq1-385}$ (catalytically active N-terminal fragment containing a C-terminal his-tag) (Mechold et al., 2002). Mesh1 (*D. melanogaster*) and MESH1 (human) were overexpressed from pET28 derivatives (Sun et al., 2010). For SAH_{Mex} overexpression, sequences of the SAH encoding gene from *M. extorquens* AM1 strain (GenBank locus tag: MexAM1_META1p3226) was optimized for GC content and codon usage for *E. coli* (GeneArt Strings service, Thermo Scientific) the synthetic DNA fragment was cloned into pCIOX (pET28 derivative; a gift from Dr. Andrea Mattevi, Addgene plasmid #51300), yielding plasmid pKP2117.

In all cases, BL21 (λDE3) was used for protein overexpression. *Streptomyces morookaensis* (ATCC#19166) was used as the source of the promiscuous pyrophosphotransferase capable of the

βγ-pyrophosphate transfer from ATP or GTP onto the ribosyl-3′ hydroxyl group of any purine nucleotide (Oki et al., 1975). Plasmid and strain requests should be sent to K. Potrykus.

Protein Purification

Rel_{Seq}1-385 was purified as described in Mechold et al. (2002). Mesh1 and MESH1 were purified according to Sun et al. (2010), with slight modifications. Briefly, BL21(λDE3) cells transformed with appropriate pET28a-derived plasmids, were grown in LB and when the culture reached OD_{600}∼0.5, protein overproduction was induced with 1 mM IPTG for 1 h. The cells were spun, resuspended in the lysis buffer (20 mM β-ME, 50 mM $NaPO_4$ pH 8.0, 0.5 M NaCl, 10% glycerol, 20 mM imidazole), supplemented by lysozyme and a tablet of Complete Protease Inhibitor Cocktail (Roche), incubated on ice for 30 min, and then disrupted by sonication. After clearing by centrifugation, the supernatants were batch-adsorbed onto Ni^{2+}-NTA agarose (Qiagen) or TALON-agarose (Clontech). Next, the resins were washed with the wash buffer (the same as lysis buffer, but containing 40 mM imidazole), and the proteins were eluted with the same buffer but containing 300 mM imidazole. All fractions were checked by SDS-PAGE, appropriate fractions were pooled and dialyzed against thrombin-cleavage buffer (20 mM Tris–Cl pH 8.0, 150 mM NaCl, 5 mM $CaCl_2$, 5% glycerol, 0.5 mM β-ME). His-tags were removed with the Thrombin Capture Kit, Novagen. The fractions were then dialyzed against 2× storage buffer (100 mM Tris–Cl pH 8.0, 500 mM NaCl), and then glycerol and DTT were added to 50% and 2 mM, respectively.

SAH_{Mex} was purified under similar conditions, except that the His8-SUMO tags were cleaved with in-house purified his-tagged-Ulp1 SUMO protease. To this end, after initial fractionation and purification, the pooled fractions were dialyzed against the following buffer: 20 mM Tris–HCl pH 8.0, 250 mM NaCl, 10% glycerol, and processed as described for the His8-SUMO tagged proteins in Sobala et al. (2019). The storage buffer was the same as for the Mesh1 and MESH1 proteins mentioned above.

(p)ppNpp Preparation

The (p)ppNpp standards were prepared and purified generally as described in Bruhn-Olszewska et al. (2018). In detail, the *S. morookaensis* extract was prepared by inoculating 500 ml of LB in flasks containing glass beads (∼2–3 mm in diameter) to disperse the culture. After overnight cultivation, the cultures were centrifuged, and Tris–Cl (pH 8.0) was added to the collected supernatants to 50 mM. Next, the pyrophosphotransferase fraction was precipitated with ammonium sulfate in the cold room (200 g NH_2SO_4/500 ml extract) with stirring for 30 min. After centrifugation, the pellet was resuspended in 11 ml of 10 mM Tris–Cl pH 8.0, 0.1 mM EDTA, 10% glycerol, followed by overnight dialysis against 800 ml of the same buffer, in the cold, using Slide-a-lyzer Cassettes (Pierce, cut-off 10 kDa). After dialysis, the extract can be either used directly or stored at 4°C (stable for at least 6 months).

The (p)ppNpp synthesis reactions were prepared in the following buffer: 50 mM Tris–Cl pH 8.0, 0.5 mM EDTA, 20 mM $MgCl_2$, 9 mM donor NTP (ATP), and 9 mM acceptor (ATP, ADP, GTP or GDP). Depending on the *S. morookaensis* extract activity, the extract was added to 1/8–1/2 of the final volume. Reactions were carried out at 30–37°C for 15–60 min, and stopped by adding 1/4 volume of phenol and 1/10 volume of chloroform. After vortexing and centrifugation, the supernatant was collected and LiCl was added to 2 M. Nucleotides were precipitated by adding five volumes of 96% EtOH, stored overnight at −20°C, and centrifuged. The pellets were air-dried, resuspended in 25 mM Tris–Cl pH 8.0, 0.5 mM EDTA, 0.1 M LiCl, and applied on a QAE A25 Sephadex column. The column was washed first with the same buffer, and then nucleotide fractions were eluted with a linear gradient of 0.1–0.5 M LiCl in the same buffer. Each fraction was monitored by UV_{260} and checked for purity by TLC. The final purified fractions were pooled, adjusted to 3 M LiCl, and 5 volumes of 96% EtOH were added, followed by aliquoting, precipitation at −20°C and centrifugation. The resulting nucleotide pellets were washed at least twice with 80% EtOH, air dried and stored at −20°C until use (stable for at least a year). To use, pellets were resuspended in 25 mM Tris–Cl pH 8.0, 0.05 mM EDTA. Nucleotide concentrations are estimated by absorbance at 260 nm for (p)ppApp ($\varepsilon = 15\ mM^{-1}\ cm^{-1}$), and at 254 nm for (p)ppGpp ($\varepsilon = 13.7\ mM^{-1}\ cm^{-1}$).

(p)ppNpp Hydrolysis Tests by Thin Layer Chromatography (TLC)

These reactions were carried out in the following buffer: 5 mM (p)ppNpp, 50 mM Tris–Cl (pH 8.0), 250 mM NaCl, 14 mM $MgCl_2$ and 6.5 mM $MnCl_2$. Mesh1, MESH1 and SAH_{Mex} were added to 0.025 μg/μl, and Rel_{Seq}1-385 was used at 1 μg/μl (final concentration). The reactions were carried out at 37°C and were stopped at indicated times by addition of an equal volume of 2 M formic acid. TLC was performed by spotting samples on PEI- cellulose plates (Merck). To resolve the samples, 1.5 M KH_2PO_4 buffer (pH 3.4) was used. The plates were viewed under UV_{254} light.

NADP$^+$/NADH Coupled Assay

For the ppApp and ppGpp hydrolysis assays, the reactions contained: 50 mM Tris–HCl (pH 8.0), 200 mM NaCl, 50 mM KCl, 5 mM $MgCl_2$, 1 mM $MnCl_2$, 60 μM EDTA, 300 μM NADH, 5 mM phosphoenolpyruvate (PEP), 6 U/ml pyruvate kinase (PK), and 6 U/ml lactate dehydrogenase (LDH). For pppGpp assays, the reactions contained: 50 mM Tris–HCl (pH 8.0), 200 mM NaCl, 50 mM KCl, 5 mM MgCl2, 1 mM $MnCl_2$, 60 μM EDTA, 300 μM $NADP^+$, 1.1 mM glucose, 5 U/ml hexokinase (HK) and 4 U/ml G6P dehydrogenase (G6PD). In case of pppApp hydrolysis, the reaction buffer was the same as for pppGpp, except that 500 μM ADP and 15 U/ml nucleoside diphosphate kinase (NDK) were also added. All of the above reagents and enzymes were purchased from Sigma-Aldrich. The initial reaction volume was 180 μl and the concentrations given above were calculated for that volume. In all cases, Mesh1 and SAH_{Mex} were added to 75 ng/reaction (18 nM), and $Rel_{Seq1-385}$ was used at 1.6 μg/reaction (0.176 μM).

The reaction work-up was as follows: 180 μl of the reaction buffers, already containing enzymes to be tested for hydrolysis, were aliquoted into 96 well-plates and pre-warmed to 37°C for 15 min. Next, 20 μl of (p)ppNpp solutions at appropriate

(10×) concentrations were dispensed, so that the final tested concentrations were: 0, 62.5 μM, 125 μM, 250 μM, 500 μM, and 1 mM. Reaction progress was monitored by measuring absorbance at 352 nm, an approximation of the ideal 340 nM necessitated by available filters. For a 200 μl well, the extinction coefficient of NAD(P)H is 3100 M^{-1}. Readings were taken automatically at close intervals (every 15–30 s) for 30 to 40 min. Synergy HT (BioTek) or EnSpire (Perkin Elmer) plate readers were used. All reactions were always carried out at least in triplicate.

NADPH Hydrolysis Tests

In these assays, scheme for (p)ppNpp hydrolysis was followed in order to produce NADPH, except that ATP was added directly to the assay and (p)ppNpp's were omitted. All enzyme concentrations (if employed) and buffer conditions were the same as for the standard coupled enzymatic assay except where noted otherwise. First, glucose-6-P was produced by using HK and glucose in the presence of 0.5 mM ATP. The reaction was incubated at 37°C for 20 min. Full conversion of ATP into ADP was monitored by TLC. Next, $NADP^+$ (0.5 mM, final concentration) was added to initiate NADPH production by G6PDH. The reaction was carried out at 37°C for 20 min, and full conversion of NADP+ into NADPH was also monitored by TLC. Then, Mesh1, MESH1 or SAH_{Mex} were added at 4 ng/μl (0.2 μM final) and the reactions were allowed to proceed for 30 min at 37°C, and then stopped by addition of formic acid to 1 M. Samples were spotted on PEI-cellulose TLC plates and resolved in a LiCl step gradient (0.2 M LiCl for the first 2 cm; 1 M LiCl for the next 4 cm; 1.6 M LiCl for the final 6.5 cm).

For the malachite green assay, the same conditions were used, except that the tested proteins were used either at 18 nM or 0.2 μM concentrations, and ATP and NADP+ were added to 0.3 mM. Samples were withdrawn at 5, 10, and 30 min after Mesh1, MESH1 or SAH_{Mex} addition, and the reactions were stopped by adding formic acid to 1 M. 20 μl of each reaction were diluted to 400 μl with water, and then 100 μl of the malachite green reagent were added, freshly prepared according to Baykov et al. (1988); the assay was carried out as described in that report. Standard curve was prepared in the same reaction buffer as the assays, and known concentrations of NaH_2PO_4 were used. Under these conditions, detection limit was established as 5 μM free phosphate.

Data Analysis

Initial reaction rates for the kinetic assays were determined by linear regression with the use of Microsoft Excel software. Kinetic constants were estimated with the KaleidaGraph software by plotting initial reaction rates against substrate concentration, and using non-linear regression to fit the Michaelis-Menten equation. Prior to plotting in KaleidaGraph, the initial reaction rate data were corrected for the expected basal assay activity. This basal activity was established by estimating NADH oxidation or NADP+ reduction in the absence of the (p)ppNpp hydrolase, but in the presence of a given pppNpp or ppNpp, respectively (discussed below and **Supplementary Figure S1**).

RESULTS AND DISCUSSION

Qualitative Estimates of (p)ppNpp Hydrolysis by Thin Layer Chromatography

Figure 1 documents TLC assays of (p)ppApp and (p)ppGpp hydrolysis by the *Drosophila* Mesh1 protein, human MESH1,

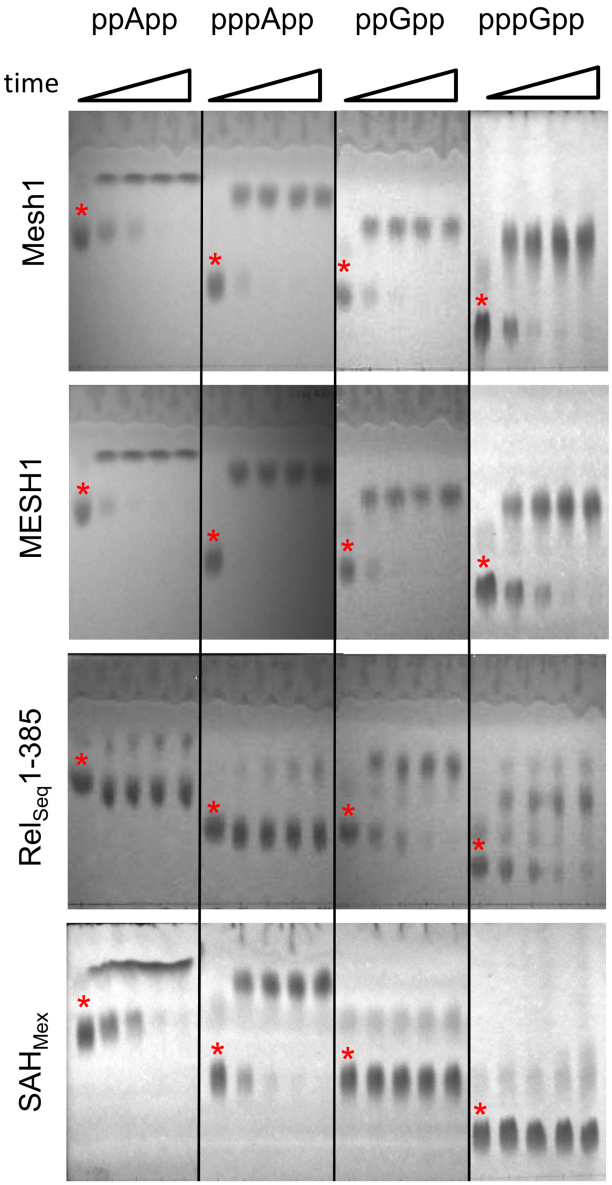

FIGURE 1 | Thin layer chromatography analysis of hydrolytic activities of Mesh1 (*D. melanogaster*), MESH1 (*Homo sapiens*), Rel_{Seq}1-385, and SAH_{Mex}. Hydrolysis of (p)ppApp and (p)ppGpp was monitored over time (0, 5, 10, 20, and 30 min). Samples were spotted on PEI-cellulose plates, resolved in the 1.5 M KH_2PO_4 buffer (pH 3.4) and visualized under UV light. Asterisks are placed just above spots corresponding to the given (p)ppNpp time 0 controls. Products of ppApp, pppApp, ppGpp, and pppGpp hydrolysis are ADP, ATP, GDP, and GTP, respectively.

SAH_{Mex} and Rel_{Seq}1-385. Standard development conditions for PEI cellulose TLC were used with 1.5 M KH_2PO_4 (pH 3.4) buffer, followed by visualization under UV_{254} light. The chromatograms indicate that Mesh1 is able to hydrolyze all four substrates tested, i.e., ppApp, pppApp, ppGpp, and pppGpp. It seems that pppApp is the most efficiently hydrolyzed substrate. The human MESH1 hydrolase displays similar activities as shown for *Drosophila* Mesh1. Surprisingly, the SAH_{Mex} protein is able to hydrolyze (p)ppApp but not (p)ppGpp. For SAH_{Mex}, pppApp seems to be hydrolyzed faster than ppApp, as was observed for Mesh1. The Rel_{Seq}1-385 protein hydrolytic activity toward guanosine derivatives is confirmed as expected (Mechold et al., 2002), but it is exceptional in that this enzyme displays only negligible activity toward (p)ppApp. Quantitative activity comparisons of the different enzymes require determining their kinetic constants.

It is noteworthy that the standard TLC resolution of (p)ppGpp and (p)ppApp using PEI cellulose and 1.5 M KPi (pH 3.4) is found to be inadequate for clearly distinguishing between co-migrating pairs: ppApp and GTP; pppApp and ppGpp; and possibly pApp and GDP (Sobala et al., 2019). A more rigorous comparison comes from using 2-dimensional TLC (Sobala et al., 2019), however, when using known substrates, a 1-D TLC is still sufficient.

Similarly, currently, a rigorous analysis of complex nucleotide mixtures in cell extracts appears to require HPLC coupled to mass spectrometry or recently reported capillary electrophoresis, capable of detecting all four (p)ppNpp's in one run (Haas et al., 2020). Still, determining kinetic constants with these methods would be very time consuming, as each reaction for a given nucleotide concentration would have to be stopped at several time points, and then each would have to be processed separately. Thus, for purified enzymes and known substrates, a coupled enzymatic assay is more useful, where the reaction rate can be followed in real-time.

Coupled Enzymatic Assay Rationale

In order to devise a real-time enzymatic assay to monitor (p)ppNpp hydrolysis, we adapted classical NADH oxidation and NADP+ reduction assays for near UV optical measurements. Schemes illustrating the reaction pathways of our enzyme coupled assays are shown in **Figure 2**.

Since, the products of ppGpp and ppApp hydrolysis are GDP and ADP, respectively, we coupled these enzymatic reactions with the NADH oxidation assay. In our set-up, NADH is oxidized to NAD^+ by LDH *via* production of pyruvate by PK from PEP and ADP or GDP. This approach was possible because of the broad specificity of PK, which phosphorylates GDP about 70% as efficiently as ADP (Plowman and Krall, 1965). Thus, the same set of buffer and enzyme conditions can be used to follow both, the ppApp and ppGpp hydrolysis.

On the other hand, products of pppApp and pppGpp hydrolysis are ATP and GTP, respectively. Accordingly, we coupled hydrolysis of pppApp to NADP+ reduction by glucose-6-phosphate dehydrogenase (G6PD) *via* production of glucose-6-phosphate (G6P) by hexokinase (HK) from ATP and glucose. Unlike PK, HK is very specific for ATP, and GTP cannot serve as a substrate. Thus, to follow pppGpp hydrolysis, it was necessary to add nucleoside diphosphate kinase (NDK) and ADP, which catalyzes the reactions of forming ATP and GDP from ADP

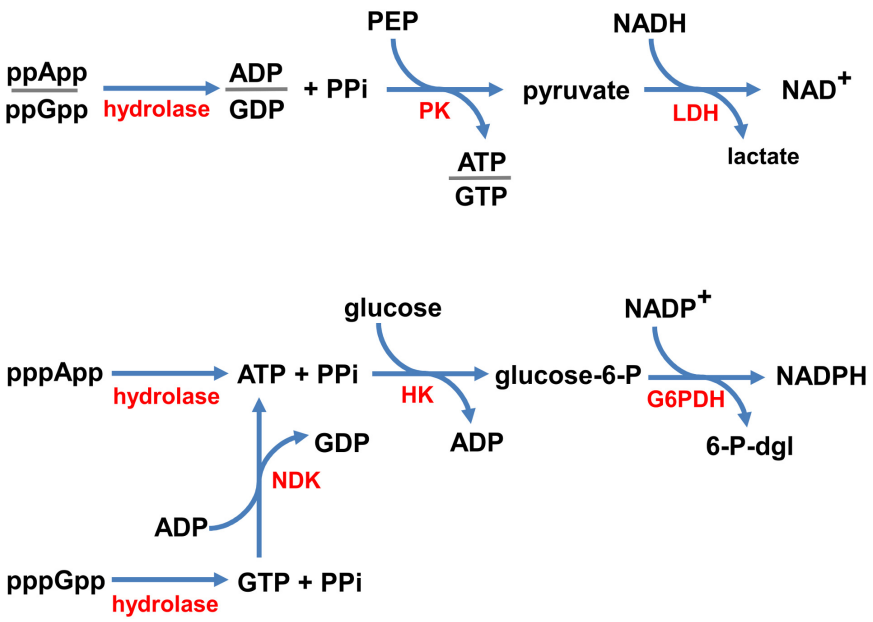

FIGURE 2 | Coupled enzymatic reaction schemes. ppNpp hydrolysis is coupled to the disappearance of NADH (top), and pppNpp hydrolysis is coupled to the appearance of NADPH (bottom), monitored in real time as changes in absorbance at 340 nm. Enzymes are denoted in red (hydrolase – the investigated enzyme; PK, pyruvate kinase; LDH, lactate dehydrogenase; NDK, nucleotide kinase; HK, hexokinase; G6PDH, glucose-6-phosphate dehydrogenase) and substrates/products are in black (PPi, pyrophosphate; PEP, phosphoenolpyruvate; glucose-6-P, glucose-6-phosphate; 6-P-dgl, 6-phospho-D-glucono-1,5-lactone).

and GTP, respectively. Since ATP is then recycled back into ADP by the hexokinase reaction, it is only necessary to add catalytic amounts of ADP.

In summary, ppNpp hydrolysis ultimately leads to depletion in NADH levels, which we monitored by measuring a drop in absorbance at UV_{352}, while pppNpp hydrolysis is followed by monitoring accumulation of NADPH, which is monitored by an increase in absorbance at the same wavelength. Examples of raw data obtained with these assays are shown in **Supplementary Figure S2**.

Coupled Enzymatic Assay Reaction Controls

Several potential side reactions could invalidate the coupled reactions shown in **Figure 2**. One class of errors arises from structural similarities between ppApp and ADP, and another from similarities between pppApp and ATP. For example, PK might use ppApp instead of ADP, or ppGpp instead of GDP. A similar scenario is that pppApp or pppGpp might substitute for ATP in the hexokinase catalyzed reaction. Either of these side reactions could break the coupled assay, if substantial. If modest, the extent of the reaction could be used as a correction factor.

Control reactions for ppNpp hydrolysis assay led to the finding that indeed PK may remove phosphate group from PEP to phosphorylate either ppApp to pppApp or ppGpp to pppGpp, yielding pyruvate that can be used in the downstream reaction. Calculated Vmax values are almost identical for both ppNpp's: 0.38 ± 0.06 μM/min for ppApp, and 0.38 ± 0.01 μM/min for ppGpp (**Supplementary Figure S1**).

In case of the pppNpp hydrolysis assay, we found that HK can catalyze a transfer of a phosphate to glucose from pppApp with a very slow rate (Vmax = 0.066 ± 0.009 μM/min; **Supplementary Figure S1**). Similarly, pppGpp may be used

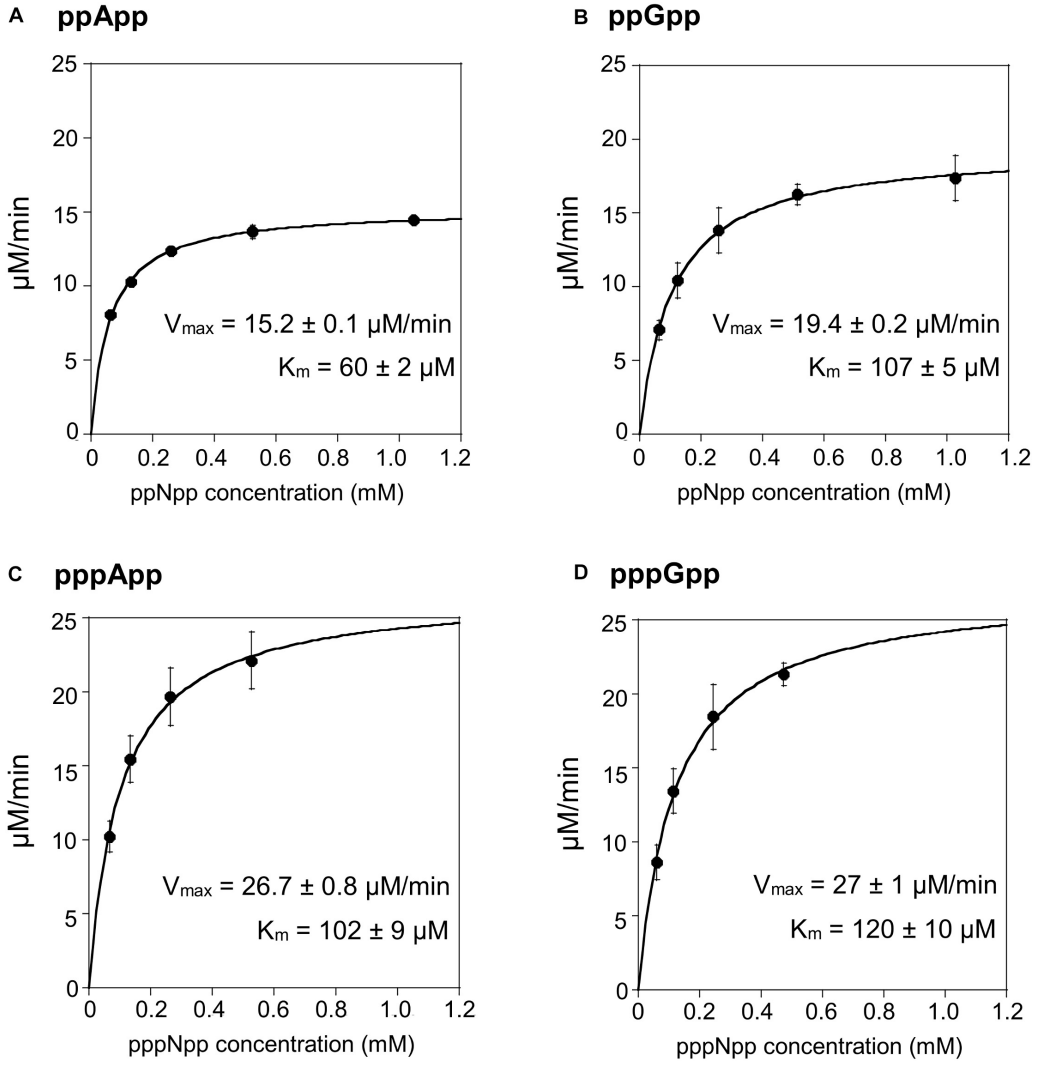

FIGURE 3 | (p)ppApp and (p)ppGpp hydrolysis by Mesh1. Non-linear regression of rate vs. (p)ppNpp concentration. **(A)** ppApp, **(B)** ppGpp, **(C)** pppApp, and **(D)** pppGpp. The kinetic constant calculations are corrected for hydrolysis-independent activity.

by either HK or NDK as a phosphate group donor to yield G6P or ATP, respectively, although this is also a slow reaction (Vmax = 0.075 ± 0.008 μM/min; **Supplementary Figure S1**). Correction for this side reaction involves subtracting individual data points obtained without added hydrolase from data with hydrolase and recalculating kinetic constants.

An additional control is needed to be sure that the capacity of the coupled assay component concentrations is not exceeded by excessive hydrolytic activity of added enzymes. To achieve this, small titrated amounts (50–60 μM) of immediate hydrolysis products, ADP, GDP, or ATP, were added to the coupled reactions but without hydrolase and the activities were measured. If the total assay capacity is not exceeded then coupled activities with even the small levels of these products should sustain substantially greater activities than those measured with hydrolase at higher substrate levels. **Supplementary Figure S3** indicates initial rates for ATP (36 μM/min), ADP (81 μM/min), and GDP (60 μM/min); as demonstrated in the following sections, rates achieved with the tested (p)ppNpp hydrolases were much slower (Vmax values ranged from 1.1 to 26 μM/min for hydrolysis of (p)ppApp and (p)ppGpp by all enzymes). This means that the activities of enzymes used in the coupled assay itself are not limiting to determine accurate rates of (p)ppNpp hydrolysis by the enzymes investigated here.

Mesh1 Hydrolyzes ppApp and pppApp Equally Well, While ppGpp Is the Least Efficiently Used Substrate

In order to test the enzymatic coupled assay, we first decided to employ the *Drosophila* Mesh-1 enzyme which in our initial hydrolysis tests visualized by TLC was shown to be active toward both, (p)ppGpp and (p)ppApp. Examples of raw data obtained for this enzyme are shown in **Supplementary Figure S2**, while the processed data is presented in **Figure 3** and **Table 1**.

The Mesh1 hydrolysis rates measured for both ppApp and ppGpp fit well to Michaelis-Menten kinetics over the entire range of substrate concentrations tested. This was also true for pppApp and pppGpp but only for substrate concentrations ranging from approximately 50 to 500 μM. The highest substrate concentration (1000 μM) gave consistently lower rates in the pppNpp assay. Therefore, in **Figure 3** the data from the highest pppNpp substrate concentration was excluded and this value is not used for calculating V_{max} and K_m. The reason for this anomaly is unclear.

The comparative results shown in **Table 1** indicate that V_{max} and K_m values for Mesh-1 hydrolysis for both adenosine or guanosine pentaphosphate derivatives are not very different (26.7 vs. 27.0 μM/min [V_{max}], and 102 vs. 120 μM [K_m]). For the tetraphosphate substrates, the V_{max} for ppGpp (19.4 μM/min) is 1.27-fold higher than for ppApp (15.2 μM/min), while the Michaelis constant for ppApp (60 μM) is 1.78-fold lower than for ppGpp (107 μM). Still, k_{cat} seems to compensate for these differences, and when comparing the overall catalytic efficiency of the enzyme (k_{cat}/K_m [$s^{-1}M^{-1}$]) it is evident, that the enzyme is hydrolyzing ppApp and pppApp equally well, while ppGpp is the least efficiently used substrate.

TABLE 1 | Summary of kinetic constants for (p)ppNpp hydrolases, estimated by the coupled enzymatic assay.

Enzyme	Substrate	Vmax (μM/min)	Km (μM)	kcat (s^{-1})	kcat/Km ($s^{-1}M^{-1}$)
Mesh1	ppApp	15.2 ± 0.1	60 ± 2	13.6 ± 0.01	2.3 ± 0.1 × 10^5
	pppApp	26.7 ± 0.8	102 ± 9	23.9 ± 0.64	2.4 ± 0.2 × 10^5
	ppGpp	19.4 ± 0.2	107 ± 5	17.4 ± 0.17	1.6 ± 0.1 × 10^5
	pppGpp	27.0 ± 1	120 ± 10	24.0 ± 0.89	2.0 ± 0.2 × 10^5
Rel_{Seq} 1-385	ppApp	*no activity*	*no activity*	*no activity*	*no activity*
	ppGpp	1.7 ± 0.1	60 ± 10	0.16 ± 1.7	3.0 ± 1.0 × 10^3
SAH_{Mex}	ppApp	1.3 ± 0.1	114 ± 26	1.19 ± 0.1	1.05 ± 0.1 × 10^4
	pppApp	6.1 ± 0.4	222 ± 37	5.49 ± 0.3	2.47 ± 0.2 × 10^4
	ppGpp	*no activity*	*no activity*	*no activity*	*no activity*
	pppGpp	*no activity*	*no activity*	*no activity*	*no activity*

*Calculations for Mesh1, Rel_{Seq}1-385, and SAH_{Mex} are based on data presented in **Figures 3–5**. Error estimates are rounded off from values presented in these figures. V_{max} and K_m were calculated using the KaleidaGraph software.*

SAH_{Mex} Hydrolyzes pppApp More Efficiently Than ppApp, and Displays Only Negligible Activity Toward (p)ppGpp

We then tested the hydrolysis activity of SAH_{Mex}, which based on the TLC assays (**Figure 1**) was expected to hydrolyze (p)ppApp nucleotides but not (p)ppGpp. Indeed, these results were confirmed with the coupled enzymatic assay (**Figure 4** and **Table 1**). Also, in both cases, SAH_{Mex} is more efficient at hydrolyzing pppApp than ppApp, even though this enzyme's Km for pppApp is 1.9-fold higher than for ppApp (222 vs. 122 μM). Apparently, the enzyme compensates for this by having a 4.6-fold higher V_{max} in case of pppApp than ppApp (6.1 vs. 1.3 μM/min), which ultimately leads to 3.7 higher catalytic efficiency toward the pentaphosphate derivative than the tetraphosphate when calculating kcat/Km (2.47 ± 0.2 × 10^4 $s^{-1}M^{-1}$ vs. 1.05 ± 0.1 × 10^4 $s^{-1}M^{-1}$).

The fact that SAH_{Mex} is more efficient at hydrolyzing pppApp than ppApp is very interesting in the light of a recent discovery that the RSH enzyme from *M. extorquens* (RSH_{Mex}) synthesizes pppApp but not ppApp *in vitro*; this was also true for *in vivo* assessment of *M. extorquens* produced (p)ppNpps–only pppApp, ppGpp, and pppGpp were detected (Sobala et al., 2019). This highlights the complexity of the evolved systems regulating (p)ppNpp synthesis and degradation. However, it cannot be excluded that under certain conditions, ppApp might be still produced.

(p)ppNpp Hydrolysis by Rel_{Seq}1-385

The TLC assays presented in **Figure 1**, led to the expectation that the coupled ppGpp hydrolysis activities displayed by the Rel_{Seq}1-385 hydrolase would be higher than for ppApp because the ADP hydrolysis product was barely evident even after prolonged incubation. The results of the enzymatic coupled assay shown in **Figure 5** quantitatively validate the TLC assay. After correction for the basal assay activity there is no evident hydrolysis activity toward ppApp while appreciable ppGpp hydrolysis persists. We estimate that this

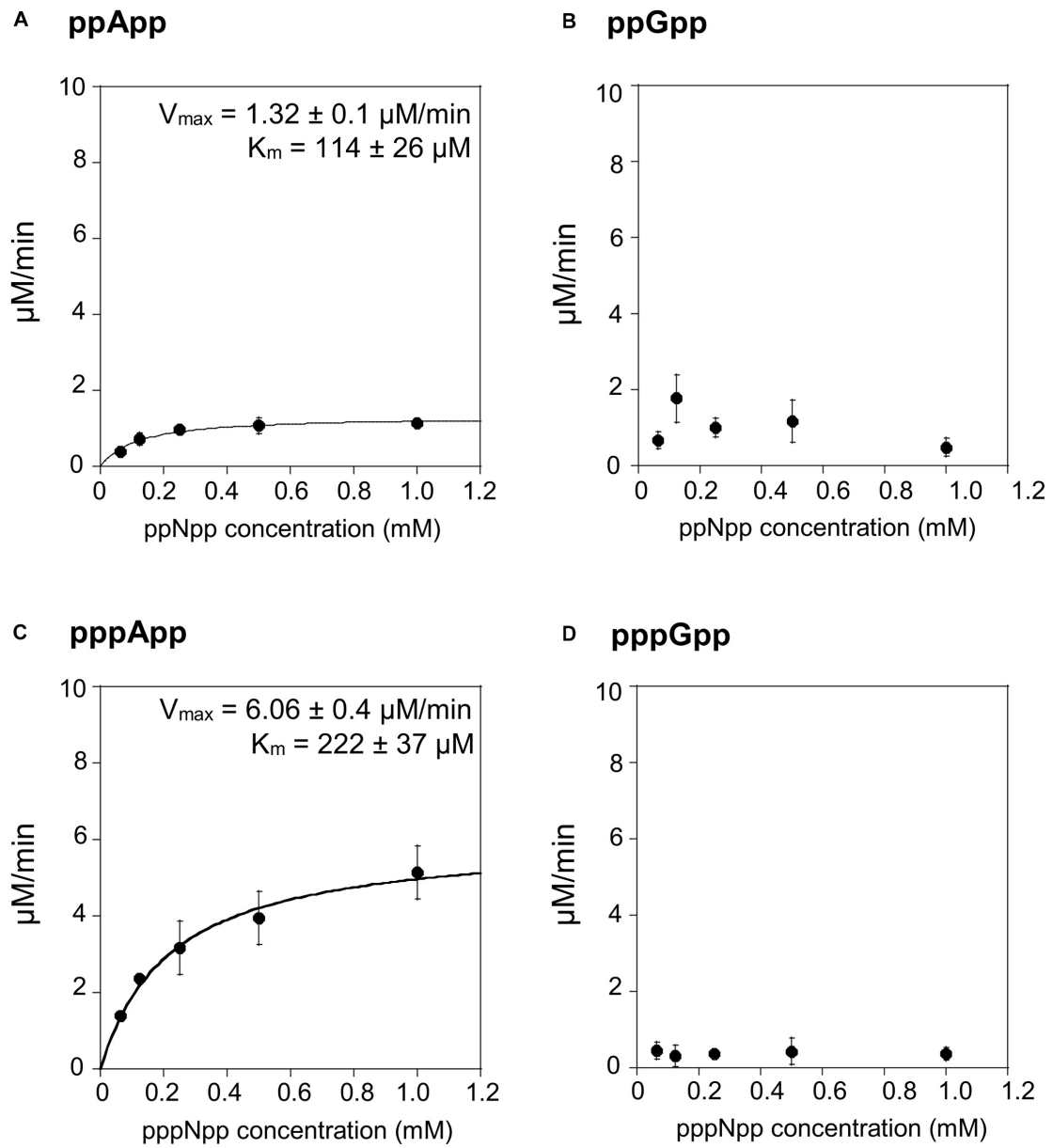

FIGURE 4 | (p)ppApp and (p)ppGpp hydrolysis by SAH_{Mex}. Non-linear regression of rate vs. (p)ppNpp concentration. **(A)** ppApp, **(B)** ppGpp, **(C)** pppApp, and **(D)** pppGpp. The kinetic constant calculations are corrected for hydrolysis-independent activity.

enzyme's kinetic constants are as follows: Km for ppGpp is 60 ± 10 μM, while V_{max} is 1.7 μM/min. The overall Rel_{Seq}1-385 fragment hydrolytic activity is rather low when calculating kcat/Km ($3 \pm 1 \times 10^3$ $s^{-1}M^{-1}$), although this is not entirely unexpected since it was reported previously that this protein has a lower hydrolase activity than full-length RelSeq (Mechold et al., 2002).

It is intriguing that the tested enzymes display such diverse activities toward (p)ppNpp's. **Supplementary Figure S4** shows amino acid sequence comparison between these enzymes. It is not evident which residues might be responsible for the base specificity (A, G or both). However, in close proximity to the key conserved residues, there are several examples of residues that are not present in enzymes unable to hydrolyze (p)ppApp and those unable to hydrolyze (p)ppGpp. Taking RelSeq sequence as the reference, examples of the former are: T36A, V54N, C77A, R149K, and M153L; and of the latter: I57A, V84L, D80Q, and L150T. It may be that they affect orientation of the key residues and thus affect the enzyme's specificity. On the other hand, another set of possible candidates concerns those residues that are only present in Mesh1 and MESH1 (able to hydrolyze both, (p)ppApp and (p)ppGpp) but differ in SAH_{Mex} and Rel_{Seq}. Clearly, further investigations are needed to resolve this problem.

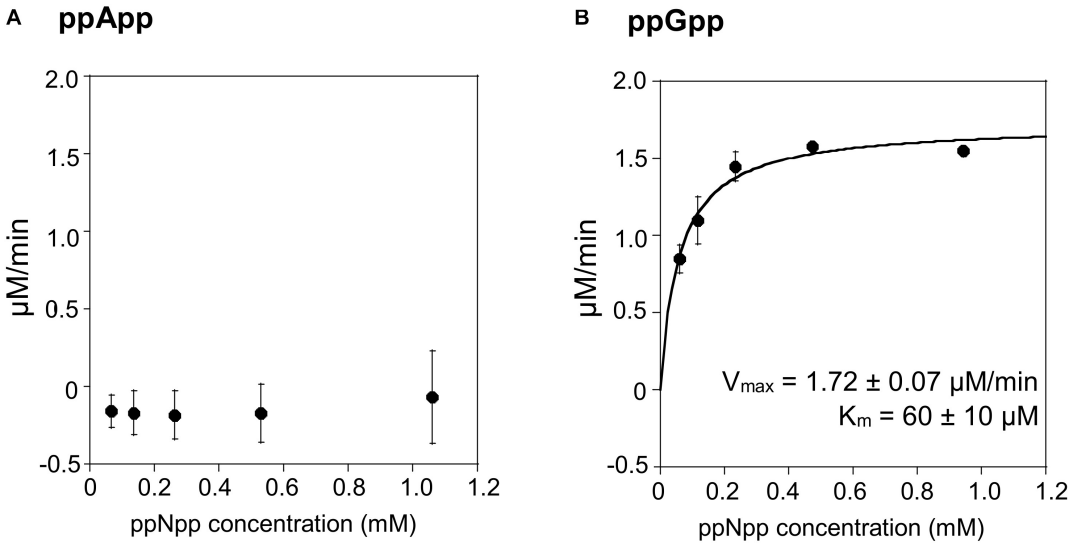

FIGURE 5 | ppApp and ppGpp hydrolysis by Rel_{Seq}. Non-linear regression of rate vs. (p)ppNpp concentration. **(A)** ppApp, **(B)** ppGpp. The kinetic constant calculations are corrected for hydrolysis-independent activity.

NADPH Does Not Seem to Be Hydrolyzed by Mesh1, MESH1, or SAH_{Mex} Under Coupled Assay Conditions

Recently, is has been suggested that that the human MESH1 enzyme is an NADPH phosphatase that degrades NADPH to NADH (Ding et al., 2020). Since in the coupled assay for pppNpp hydrolysis NADPH accumulation is being followed (see **Figure 2**), this could have a potential impact on the obtained results. Even though we would not observe a change in A_{352} because NADH and NADPH display the same absorption profile, there could be an impact on the kinetic values observed due to substrate competition between NADPH and pppNpp for Meshl/SAH binding.

In order to resolve this question, we tested NADPH hydrolysis under our coupled assay conditions. First, we used ATP (0.5 mM), glucose (1.1 mM), and HK to produce glucose-6-phosphate, which was then used by G6PD to produce NADPH from NADH (supplied at 0.5 mM). The reactions were carried out at 37°C, each for 20 min. Upon the second reaction's completion, Mesh1, MESH1 or SAH_{Mex} enzymes were added and the reaction was incubated for another 30 min. In this case, 200 ng of each enzyme were added to a 50 µl reaction, which gives an over 11-fold enzyme excess in respect to concentrations used for our standard coupled assay conditions (0.2 µM vs. 18 nM). TLC was used to visualize nucleotides and their derivatives. As demonstrated in **Figure 6**, we did not detect any NADPH hydrolysis, neither by the human MESH1 enzyme, nor *D. melanogaster* Mesh1 and SAH_{Mex}. These results are consistent with observations made by Zhu and Dai (2019) who did not note a disruption in NADP(H)/NAD(H) pools in *E. coli* cells upon Mesh1 overproduction.

Since the TLC assay might be less sensitive than the malachite green assay to detected free phosphate used by Ding et al. (2020), we employed this type of assay under our kinetics assay conditions as well (**Table 2**). We found no detectable phosphate release when using the same protein concentrations as in the coupled kinetics assay (18 nM) for Mesh1 (*D. melanogaster*) and SAH_{Mex}. We observed only negligible phosphate release for MESH1 (human) at the 30 min time point. The procedure was set up to synthesize 300 µM NADPH, followed by addition of either hydrolase. We estimate the detection limit to be at 5 µM phosphate (1.66%). However, when increasing the tested protein concentrations to those that were used in the NADPH-hydrolysis TLC assay (0.2 µM), we did detect phosphate release for MESH1 at other time points (seemingly corresponding to 6.5, 12.1, and 33.3% for the 5, 10, and 30 min, respectively; **Table 2**) and Mesh1 (6.3 and 14.8% for the 10 and 30 min time points, respectively; **Table 2**). SAH_{Mex} did not lead to phosphate release in the presence of NADPH under any tested protein concentration.

Still, it should be noted that the reported human MESH1 affinity for NADPH (Km) is 120 ± 10 µM, while calculated catalytic efficiency (kcat/Km) is 14.4 ± 1 × 10^3 $s^{-1}M^{-1}$ (Ding et al., 2020). This activity seems rather low in comparison to the catalytic efficiency we found for (p)ppNpp's and *D. melanogaster* Mesh1, which is about 10-fold higher (see **Table 1**). Judging by TLC analysis, both enzymes (Mesh1 and MESH1) display similar activities toward (p)ppNpp's (**Figure 1**). In this analysis (p)ppNpp's seem to be better substrates than NADPH. In the (Ding et al., 2020) report, 50 nM MESH1 was used, but the Mn^{2+} concentration which is crucial for most (p)ppNpp hydrolases was the same in both cases (1 mM). However, Mg^{2+} was also included in our assays at 5 mM. In addition, it cannot be excluded that other buffer components had negatively influenced activity of the tested hydrolases toward NADPH. Still, the 30% NADPH hydrolysis by MESH1 inferred from the malachite green assay should have been also observed with the

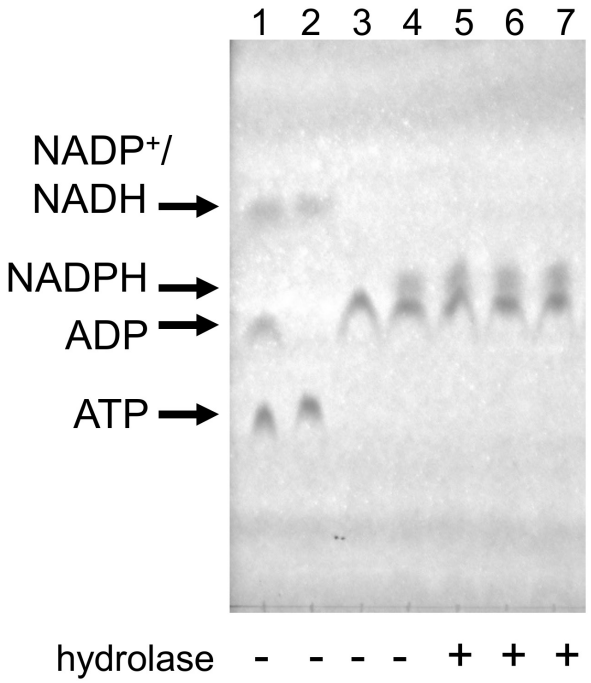

FIGURE 6 | NADPH does not seem to be hydrolyzed by Mesh1, MESH1, and SAH_{Mex} under the coupled assay conditions when visualized by TLC assay. Reactions were carried under conditions described for the coupled assay, except that first NADPH was allowed to be produced and then individual hydrolases were added. In the first step, ATP and glucose were employed to yield glucose-6-P and ADP; only then $NADP^+$ was added to yield NADPH. To resolve samples, LiCl step gradient was used (see section "Materials and Methods" for details). Lane 1: mock reaction to visualize migration of ATP, ADP, $NADP^+$, and NADH ($NADP^+$ co-migrates with NADH under these conditions); Lane 2: mock reaction with only ATP and $NADP^+$; Lane 3: control reaction for the first step (all ATP is converted to ADP); Lane 4: control reaction for the second step (all $NADP^+$ is converted to NADPH); Lane 5–7, MESH-1, Mesh1, and SAH_{Mex} were added.

TABLE 2 | Release of free phosphate assessed by the malachite green assay and expressed as percentage of NADPH present in the coupled enzymatic assay.

Enzyme	Concentration	Phosphate released (%)		
		5 min	10 min	30 min
Mesh1	18 nM	*no activity*	*no activity*	*no activity*
	0.2 μM	*no activity*	6.3 ± 1.2	14.8 ± 2.2
MESH1	18 nM	*no activity*	*no activity*	1.66 ± 1.4
	0.2 μM	6.5 ± 0.24	12.1 ± 0.19	33.3 ± 2
SAH_{Mex}	18 nM	*no activity*	*no activity*	*no activity*
	0.2 μM	*no activity*	*no activity*	*no activity*

The reactions were set up so that 300 μM NADPH was synthesized, and then Mesh1, MESH1, or SAH_{Mex} were added at two different concentrations (18 nM – the same as used in the coupled enzymatic assays; 0.2 μM – the same as in the TLC NADPH hydrolysis assay presented in ***Figure 6****). Samples were removed at 5, 10, and 30 min after hydrolase addition. All reactions were carried out in triplicate. No activity – below detection limit, estimated to be 5 μM (1.66%).*

TLC assay (it is a prominent change) and it wasn't. Thus, it cannot be said with certainty that the observed free phosphate is really released due to NADPH hydrolysis, or is possibly due to hydrolysis of a different substrate, such as e.g., 6-P-dgi which is also produced in our assay. On the other hand, (Ding et al., 2020) worked with pure NADPH substrate. Clearly, while our enzymatic coupled assay is not affected by possible NADPH hydrolysis as the initial reaction rates were not estimated at time points beyond 5 min, further studies are needed to resolve this issue.

CONCLUDING REMARKS

Historically, an abundance of second messenger global regulators is found among incredibly diverse microorganisms; this has led to a fascinating path of constantly increasing complexity of compounds and their functions. First came cAMP and regulation of preferential carbon source utilization. Then (p)ppGpp was associated with arrays of global regulatory responses to multiple nutritional and physical sources of physiological stress. This was followed by multiple sources of cyclic and homo- and hetero-dicyclic purine nucleotides within the same cell interacting to perform specific tasks. The (p)ppApp class of possible nucleotide regulators is now making a debut.

Recently, (p)ppApp was found to be produced by a *Pseudomonas aeruginosa* excreted toxin, which is a part of this organism's T6SS system (Ahmad et al., 2019). There, cellular toxicity of (p)ppApp has been proposed as due to massive overproduction of (p)ppApp that reaches levels that inhibit PurF, an enzyme which catalyzes the first step in purine nucleotide synthesis, and argued to deplete ATP levels, although GTP depletion is also predicted (Ahmad et al., 2019). The metabolic stress caused by depletion of ATP levels and resulting simply from using it up for overly abundant (p)ppApp synthesis might play an important part here. Also, very recently (Jimmy et al., 2020) used a bioinformatics search to identify numerous presumed toxin-antitoxin clusters, where SAS is the toxin that usually produces ppGpp (toxSAS). Some of these proteins, such as *Cellulomonas marina* toxSAS FaRel can also synthesize ppApp. The authors have demonstrated under *in vivo* conditions, that when this protein is overproduced in the wild type *E. coli* background, it is lethal to the cells. This effect was alleviated by overproduction of three antitoxins–*C. marina* ATfaRel SAH, *Salmonella* phage PVP-SE1 SAH and SSU5 SAH (Jimmy et al., 2020). The authors also showed similar effect for human MESH1 (Jimmy et al., 2020), which was a first reported *in vivo* indication that MESH1 presumably hydrolyzes both, ppGpp and ppApp. Our *in vitro* findings that we present in detail here (first mentioned in Sobala et al., 2019), directly confirm this observation for MESH1.

Still, we would like to stress that since low levels of (p)ppApp are found in growing cells of *E. coli*, *B. subtilis*, and *M. extorquens*, and there is evidence of its transcriptional regulatory activities along with structural data pointing to its unique binding site on *E. coli* RNA polymerase, it is evident that (p)ppApp is not necessarily lethal, but instead might take its place among the second messenger regulators (Bruhn-Olszewska et al., 2018; Sobala et al., 2019).

Nevertheless, assigning regulatory roles for (p)ppApp will require determining its sources of synthesis and hydrolysis

among RSH, SAS, and SAH enzymes and whether catalysis is nucleobase specific or mixed. The results obtained here with basically only four hydrolases suggest that a high degree of complexity can be anticipated, since each one of them has different specificity toward the four (p)ppNpp's. It seems likely that a similar high degree of complexity for fundamental synthetase substrate specificities also exists, let alone diverse regulatory considerations governing their effector properties.

Again, questions arise as to accurate assays needed to assess cellular abundance, physiological functions and enzymatic sources of synthesis and degradation of (p)ppNpp's. The early TLC assay worked out for (p)ppGpp led to a simple one-dimensional PEI cellulose TLC resolution but this turns out to be inadequate 50 years later. A real advantage of HPLC and MS is that they provide vitally important product purity information. However, these assays are time consuming and are not easily accessible to all. This work describes real time optical coupled assays to monitor the ability of purified proteins to hydrolyze pure, synthesized ppGpp, ppApp, pppGpp, or pppApp for estimating kinetic constants of catalysis. Automated data collection using 96 well microtiter plates greatly facilitates accurate estimates which is crucial for unraveling the complex physiological roles of (p)ppNpp's.

DATA AVAILABILITY STATEMENT

The original contributions presented in the study are included in the article/**Supplementary Material**, further inquiries can be directed to the corresponding author/s.

AUTHOR CONTRIBUTIONS

KP and MC conceived this study and wrote the main text. KP, MC, and NET designed the experiments. NET and MC developed the method. KP, NET, BB-O, and TJ performed the experiments. KP, NET, BB-O, MS, and TJ purified the proteins used in this study. KP, BB-O, MC, and NET purified the (p)ppNpp. KP, NET, BB-O, MD, and MC analyzed the data. All authors commented on the manuscript and approved its final version.

FUNDING

This work has been funded by the National Science Centre (Poland) (UMO-2013/10/E/NZ1/00657 awarded to KP), and by the Intramural Program of the Eunice Kennedy Shriver National Institute of Child Health and Human Development (MC).

ACKNOWLEDGMENTS

We want to thank the Friday Seminar for helpful suggestions and discussions. We gratefully acknowledge Dr. Dawei Sun for providing the Mesh1 and MESH1 overproducing plasmids. Malgorzata Bohdanowicz assisted in preliminary analyses.

SUPPLEMENTARY MATERIAL

The Supplementary Material for this article can be found online at: https://www.frontiersin.org/articles/10.3389/fmicb.2020.581271/full#supplementary-material

REFERENCES

Ahmad, S., Wang, B., Walker, M. D., Tran, H. R., Stogios, P. J., Savchenko, A., et al. (2019). An interbacterial toxin inhibits target cell growth by synthesizing (p)ppApp. *Nature* 575, 674–678. doi: 10.1038/s41586-019-1735-9

Atkinson, G. C., Tenson, T., and Hauryliuk, V. (2011). The RelA/SpoT homolog (RSH) superfamily: distribution and functional evolution of ppGpp synthetases and hydrolases across the tree of life. *PLoS One* 6:e23479. doi: 10.1371/journal.pone.0023479

Baykov, A. A., Evtushenko, O. A., and Avaeva, S. M. (1988). A malachite green procedure for orthophosphate determination and its use in alkaline phosphatase-based enzyme immunoassay. *Anal. Biochem.* 171, 266–270. doi: 10.1016/0003-2697(88)90484-8

Bruhn-Olszewska, B., Molodtsov, V., Sobala, M., Dylewski, M., Murakami, K. S., Cashel, M., et al. (2018). Structure-function comparisons of (p)ppApp vs (p)ppGpp for *Escherichia coli* RNA polymerase binding sites and for rrnB P1 promoter regulatory responses in vitro. *Biochim. Biophys. Acta Gene Regul. Mech.* 1861, 731–742. doi: 10.1016/j.bbagrm.2018.07.005

Ding, C. C., Rose, J., Sun, T., Wu, J., Chen, P. H., Lin, C. C., et al. (2020). MESH1 is a cytosolic NADPH phosphatase that regulates ferroptosis. *Nature metab.* 2, 270–277. doi: 10.1038/s42255-020-0181-1

Gentry, D. R., and Cashel, M. (1995). Cellular localization of the Escherichia coli SpoT protein. *J. Bacter*. 177, 3890–3893. doi: 10.1128/jb.177.13.3890-3893.1995

Haas, T. M., Qiu, D., Häner, M., Angebauer, L., Ripp, A., Singh, J., et al. (2020). Four phosphates at one blow: Access to pentaphosphorylated magic spot nucleotides and their analysis by capillary electrophoresis. *J. Org. Chem.* doi: 10.1021/acs.joc.0c00841 [Epub ahead of print].

Jimmy, S., Saha, C. K., Kurata, T., Stavropoulos, C., Oliveira, S. R. A., Koh, A., et al. (2020). A widespread toxin-antitoxin system exploiting growth control via alarmone signaling. *Proc Natl Acad Sci U S A.* 117, 10500–10510. doi: 10.1073/pnas.1916617117

Krásný, L., and Gourse, R. L. (2004). An alternative strategy for bacterial ribosome synthesis: *Bacillus subtilis* rRNA transcription regulation. *EMBO J.* 23, 4473–4483. doi: 10.1038/sj.emboj.7600423

Kriel, A., Bittner, A. N., Kim, S. H., Liu, K., Tehranchi, A. K., Zou, W. Y., et al. (2012). Direct regulation of GTP homeostasis by (p)ppGpp: a critical component of viability and stress resistance. *Mol. Cell* 48, 231–241. doi: 10.1016/j.molcel.2012.08.009

Lemos, J. A., Nascimento, M. M., Abranches, J., and Burne, R. A. (2007). Three gene products govern (p)ppGpp production in *Streptococcus mutans*. *Mol. Microbiol.* 65, 1568–1581. doi: 10.1111/j.1365-2958.2007.05897.x

Mechold, U., Murphy, H., Brown, L., and Cashel, M. (2002). Intramolecular regulation of the opposing (p)ppGpp catalytic activities of Rel(Seq), the Rel/Spo enzyme from *Streptococcus equisimilis*. *J. Bacteriol.* 184, 2878–2888. doi: 10.1128/JB.184.11.2878-2888.2002

Mechold, U., Potrykus, K., Murphy, H., Murakami, K. S., and Cashel, M. (2013). Differential regulation by ppGpp versus pppGpp in *Escherichia coli*. *Nucleic Acids Res.* 41, 6175–6189. doi: 10.1093/nar/gkt302

Mittenhuber, G. (2001). Comparative genomics and evolution of genes encod-ing bacterial (p)ppGpp synthetases/hydrolases (the Rel, RelA and SpoT proteins). *J. Mol. Microbiol. Biotechnol.* 3, 585–600.

Molodtsov, V., Sineva, E., Zhang, L., Huang, X., Cashel, M., Ades, S. E., et al. (2018). Allosteric effector ppGpp potentiates the inhibition of transcript initiation by DksA. *Mol. Cell.* 69, 828.e5–839.e5. doi: 10.1016/j.molcel.2018.01.035

Nanamiya, H., Kasai, K., Nosawa, H., Yun, C.-S., Narisawa, T., Murakami, K., et al. (2008). Identification and functional analysis of novel (p)ppGpp synthetase genes in *Bacillus subtilis*. *Mol. Microbiol.* 67, 291–304. doi: 10.1111/j.1365-2958.2007.06018.x

Nishino, T., Gallant, J., Shalit, P., Palmer, L., and Wehr, T. (1979). Regulatory nucleotides involved in the Rel function of *Bacillus subtilis*. *J. Bacteriol.* 140, 671–679. doi: 10.1128/JB.140.2.671-679.1979

Ochi, K., Kandala, J., and Freese, E. (1982). Evidence that Bacillus subtilis sporulation induced by the stringent response is caused by the decrease in GTP or GDP. *J. Bacteriol.* 151 : 1062-1065. doi: 10.1128/JB.151.2.1062-1065.1982

Oki, T., Yoshimoto, A., Sato, S., and Takamatsu, A. (1975). Purine nucleotide pyrophosphotransferase from *Streptomyces morookaensis*, capable of synthesizing pppApp and pppGpp. *Biochim. Biophys. Acta* 410, 262–272. doi: 10.1016/0005-2744(75)90228-4

Plowman, K. M., and Krall, A. R. (1965). A kinetic study of nucleotide interactions with pyruvate kinase. *Biochemistry* 4, 2809–2814. doi: 10.1021/bi00888a035

Potrykus, K., and Cashel, M. (2008). (p)ppGpp: still magical? *Annu. Rev. Microbiol.* 62, 35–51. doi: 10.1146/annurev.micro.62.081307.162903

Rhaese, H. J., Hoch, J. A., and Groscurth, R. (1977). Studies on the control of development: isolation of Bacillus subtilis mutants blocked early in sporulation and defective in synthesis of highly phosphorylated nucleotides. *Proc. Natl. Acad. Sci. U. S. A.* 74, 1125–1129. doi: 10.1073/pnas.74.3.1125

Ross, W., Sanchez-Vazquez, P., Chen, A. Y., Lee, J. H., Burgos, H. L., and Gourse, R. L. (2016). ppGpp binding to a site at the RNAP-DksA interface accounts for its dramatic effects on transcription initiation during the stringent response. *Mol. Cell.* 62, 811–823. doi: 10.1016/j.molcel.2016.04.029

Ruwe, M., Rückert, C., Kalinowski, J., and Persicke, M. (2018). Functional characterization of a small alarmone hydrolase in *Corynebacterium glutamicum*. *Front. Microbiol.* 9:916. doi: 10.3389/fmicb.2018.00916

Sobala, M., Bruhn-Olszewska, B., Cashel, M., and Potrykus, K. (2019). Methylobacterium extorquens RSH enzyme synthesizes (p)ppGpp and pppApp in vitro and in vivo, and leads to discovery of pppApp synthesis in *Escherichia coli*. *Front. Microbiol.* 10:859. doi: 10.3389/fmicb.2019.00859

Steinchen, W., Vogt, M. S., Altegoer, F., Giammarinaro, P. I., Horvatek, P., Wolz, C., et al. (2018). Structural and mechanistic divergence of the small (p)ppGpp synthetases RelP and RelQ. *Sci. Rep.* 8:2195. doi: 10.1038/s41598-018-20634-4

Sun, D., Lee, G., Lee, J. H., Kim, H. Y., Rhee, H. W., Park, S. Y., et al. (2010). A metazoan ortholog of SpoT hydrolyzes ppGpp and functions in starvation responses. *Nat. Struct. Mol. Biol.* 17, 1188–1194. doi: 10.1038/nsmb.1906

Wang, B., Dai, P., Ding, D., Del Rosario, A., Grant, R. A., Pentelute, B. L., et al. (2019). Affinity-based capture and identification of protein effectors of the growth regulator ppGpp. *Nat. Chem. Biol.* 15, 141–150. doi: 10.1038/s41589-018-0183-4

Zhu, M., and Dai, X. (2019). Growth suppression by altered (p)ppGpp levels results from non-optimal resource allocation in *Escherichia coli*. *Nucleic Acids Res.* 47, 4684–4693. doi: 10.1093/nar/gkz211

Conflict of Interest: The authors declare that the research was conducted in the absence of any commercial or financial relationships that could be construed as a potential conflict of interest.

frontiers in Microbiology

ORIGINAL RESEARCH
published: 03 November 2020
doi: 10.3389/fmicb.2020.572419

Escherichia coli RelA Regulation *via* Its C-Terminal Domain

*Ilana Kaspy and Gad Glaser**

Department of Developmental Biology and Cancer Research, Institute for Medical Research Israel-Canada, Hebrew University of Jerusalem, Jerusalem, Israel

One of the most important stress responses in bacteria is the stringent response. The main player in this response is the signal molecule (p)ppGpp, which is synthesized by a Rel family protein. In *Escherichia coli*, RelA is the main synthetase of (p)ppGpp in response to amino acid starvation. Although the synthetic activity of RelA is well-understood, its regulation is not yet fully characterized. The C-terminus domain (CTD) of the *E. coli* RelA is responsible for the regulation of the protein and for its complete dependency on wild-type (WT) ribosome. The CTD contains three Cysteine residues, positioned in a very conserved order. Together with our previous results, we show *in vitro* the negative dominant effect of a part of the WT CTD (AA 564–744) named YG4 on RelA synthetic activity. This effect is abolished using mutated YG4 (YG4-638). *In vitro* and mass spectrometry (MS)-MS analysis of the native RelA and the mutated RelA in Cys-638 (Rel638) in the presence of the native and mutated YG4 (YG4-638) reveals that RelA forms a homodimer *via* its CTD by the formation of a disulfide bond between the two Cys-638 residues. This supports our previous data which showed, using a two-hybrid system, interactions between RelA proteins *via* the CTD. Finally, we show *in vitro* that excess of the native YG4 inhibited RelA synthetic activity but did not affect the amount of RelA bound to the ribosome. Our results suggest that the regulatory mechanism of RelA is by the dimerization of the protein *via* disulfide bonds in the CTD. Upon amino-acid starvation, the dimer changes its conformation, thus activating the stringent response in the cell.

Keywords: RelA-C-terminus domain, stringent response, *Escherichia coli*, *relA*, (p)ppGpp

OPEN ACCESS

Edited by:
Katarzyna Potrykus, University of Gdansk, Poland

Reviewed by:
Gert Bange, University of Marburg, Germany
Emmanuellle Bouveret, Institut Pasteur, France

***Correspondence:**
Gad Glaser
glaser@cc.huji.ac.il;
glaser@mail.huji.ac.il

Specialty section:
This article was submitted to Microbial Physiology and Metabolism, a section of the journal Frontiers in Microbiology

Received: *14 June 2020*
Accepted: *09 October 2020*
Published: *03 November 2020*

Citation:
Kaspy I and Glaser G (2020) Escherichia coli RelA Regulation via Its C-Terminal Domain. Front. Microbiol. 11:572419. doi: 10.3389/fmicb.2020.572419

INTRODUCTION

To survive, bacteria must be able to respond to changes in their environment. Depriving *Escherichia coli* of one or more amino acids (AAs) triggers the stringent response (Stent and Brenner, 1961; Cashel, 1969; Cashel and Gallant, 1969; Kaspy et al., 2013). Within a few seconds after the onset of amino-acid starvation, one can observe the accumulation of phosphorylated derivatives of GTP and GDP, collectively called (p)ppGpp (Cashel, 1969; Cashel and Gallant, 1969; Fiil et al., 1972; Lund and Kjeldgaard, 1972). The transcription factor DksA and (p)ppGpp bind together to RNA polymerase (RNAP; Metzger et al., 1988; Gentry et al., 1993; Gourse et al., 1996; Paul et al., 2004) affecting a large number of physiological activities, most particularly transcription (Pedersen and Kjeldgaard, 1977; Gentry et al., 1993; Magnusson et al., 2005). (p)ppGpp is important not only in overcoming nutritional deprivation but has a role also in virulence, survival during host infection, antibiotic resistance,

and formation of persister cells (Dalebroux et al., 2010; Dalebroux and Swanson, 2012; Kaspy et al., 2013).

In *E. coli* and other proteobacteria, (p)ppGpp synthesis is driven by RelA, a 84 kDa ribosome-associated enzyme (Alfoldi et al., 1962; Metzger et al., 1988). RelA is activated in response to amino-acid starvation (Cashel and Gallant, 1969; Fiil et al., 1972; Lipmann and Sy, 1976). Uncharged tRNAs bind to the ribosomal "A" site, stalling protein synthesis (Haseltine et al., 1972; Haseltine and Block, 1973) and stimulating a reaction in which, within seconds, RelA synthesizes (p)ppGpp (Fiil et al., 1972). In extracts of normally growing cells, RelA is associated with a small fraction (about 1%) of the ribosomes (Pedersen and Kjeldgaard, 1977). Both physically and functionally, *E.coli* RelA includes two distinct domains: the N-terminal domain [NTD; amino acids (AAs) 1-455], which is responsible for (p)ppGpp synthesis and the C-terminal domain (CTD; AAs 405–744), which is responsible for regulating RelA activity (Metzger et al., 1989; Schreiber et al., 1991; Gropp et al., 2001). When RelA bears a mutation in amino acid Gly-251, it lacks synthetic activity both *in vivo* and *in vitro* (Wendrich and Marahiel, 1997; Gropp et al., 2001). The open reading frame (ORF) of RelA is known to end with an amber codon which, when suppressed, yields a longer protein containing 771 AA that is no longer regulated (Metzger et al., 1988). Although the stringent response has been investigated for over 50 years, the regulatory mechanism of RelA responsible for the synthesis of the key regulator of this response is still not fully understood. Much work has been devoted to trying to decipher the regulatory mechanism of the Rel protein family (Wendrich et al., 2002; Agirrezabala et al., 2013; Turnbull et al., 2019; Takada et al., 2020).

Here, we shed more light on the regulatory mechanism of *E. coli* RelA. The CTD of *E. coli* RelA can be divided into four domains that were shown to interact with ribosome at different sites, and are responsible for RelA binding to the ribosome (Agirrezabala et al., 2013; Arenz et al., 2016; Brown et al., 2016; Loveland et al., 2016). It was shown previously that overexpression of the RelA CTD in wild-type (WT) cells starved for AAs causes a reduction in the accumulation of (p)ppGpp (Gropp et al., 2001). A mutation in the conserved sequence AA 612–638, in which Cys-638 is replaced by phenylalanine (RelA-C638F) leads to the constitutive ribosome-independent synthesis of (p)ppGpp. Thus, the RelA CTD cannot regulate the production of (p)ppGpp without AA Cys-638 (Gropp et al., 2001). Moreover, in earlier bacterial two-hybrid system experiments, we found that a fragment of the CTD, YG4 (AA 564–744, MW 21 kDa; **Figure 1A**), is involved in RelA-RelA interactions (Gropp et al., 2001). The YG4 fragment, which inhibited RelA synthetic activity, contains two of the four domains; the ribosome inter-subunit (RIS; AA 585–660) and the ACT domain (AA 665–744), as described previously (Loveland et al., 2016). Both of these domains bind near the A and P sites of the ribosome. According to Cryo-EM data, Cys-638 is part of an α-helix structure in the RIS domain that docks into the A-site finger. The other two domains (TGS and AH AA 405–580) are also found inside the ribosome and connect the YG4 part to the synthetase domain (Loveland et al., 2016; **Figure 1A**). The NTD does not form a clear structure under

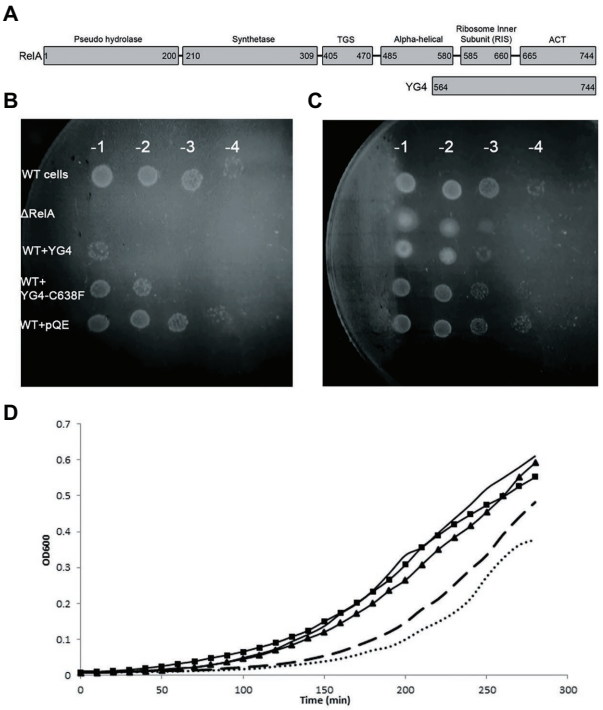

FIGURE 1 | Over expression of RelA-C-terminus domain (CTD) on cell growth. **(A)** RelA domains as described in Loveland et al. (2016) and YG4 fragment. **(B,C)** W3110 [wild type (WT)] cells bearing a plasmid overexpressing YG4 or YG4-C638F were grown in Luria-Bertani (LB) medium for 2 h, after which overexpression was induced by the addition of 1 mg/ml of IPTG for 1 h. Cells were collected and washed, diluted in serial dilutions, and plated on M9 medium. ΔRelA and WT + pQE (an empty plasmid) were used as controls. **(B)** containing AT; **(C)** without AT. All plates were incubated at 37°C overnight. WT cells with an "empty" plasmid (WT) and cells deleted for RelA (ΔRelA) were used as controls. **(D)** All cell types were grown in duplicates in a 24-well plate in LB medium supplemented with 100 μg/ml of ampicillin. After 2 h of growth, all cells were supplemented with 1 mg/ml of IPTG and were grown for an additional 2.5 h at 37°C with shaking. Cell growth was monitored by optical density (OD) measuring OD_{600}. No bullets – WT cells with an empty plasmid; square (■) – WT cells overexpressing YG4; triangle (▲) – WT cells overexpressing Rel251; dashed – WT cells overexpressing Rel-C638F; dots – WT cells overexpressing RelA.

normal translation, but upon binding of an uncharged tRNA to the A-site, RelA undergoes conformational change, stabilizing the NTD in order for it to synthesize (p)ppGpp (Agirrezabala et al., 2013; Loveland et al., 2016). Recent work suggests that RelA is incapable of self-oligomerization and that the regulatory mechanism is likely in *cis* by intramolecular interactions, rather than in *trans* (Turnbull et al., 2019). In that report, the authors used the "full length" CTD (containing all four domains; Turnbull et al., 2019). In contrast, in our and other's previous results, no interaction was observed between the NTD and the full length RelA or between the NTD and the YG4 (Gropp et al., 2001; Yang and Ishiguro, 2001; Jain et al., 2006). Together with our present *in vitro* study, we show that YG4 inhibits (p)ppGpp synthesis without competing for ribosome binding of the full length RelA. Furthermore, we found that Cysteine

residues in the CTD, especially Cys-638, are essential for RelA regulation and the formation of disulfide bonds between CTDs.

MATERIALS AND METHODS

Strains and Plasmids

As we have described previously (Gross et al., 2006), all of our vectors contain a 6-his tag coding sequence between the start codon and the multi-linker for the desired gene cloning. Cloning the proteins, especially RelA, after the addition of a His tag does not affect the regulation of the proteins (Schreiber et al., 1991).

Media

Luria-Bertani (LB), LB-agar (from BIO101) or M9 minimal media were used for growth media. When required, these media were supplemented with either 100 μg/ml ampicillin or 50 μg/ml kanamycin. To induce nutritional stress in liquid culture, 1 mM serine hydroxamate (SHX; Tosa and Pizer, 1971) was added. Selection for resistance to 3-amino-1,2,4-triazole (AT) was performed on minimal M9 AT plates containing 15 mM AT and all amino acids except histidine, as described previously (Gross et al., 2006).

Growth Curves

W3110 or CF9467 cells bearing different plasmids as indicated in the results section were grown in LB medium at 37°C with shaking (**Table 1**). The optical density was measured using TECAN device every 10 min. At OD_{600} of 0.2, 1 mg/ml of isopropyl-β-D-1-thiogalactoside (IPTG) was added to induce the overexpression of the proteins, and growth was monitored for the indicated time period. For the colony forming assay, 1 h after protein induction by IPTG, cells were collected and washed in saline three times, diluted in serial dilutions, and plated on M9-agar plates in the presence or absence of 3-amino-1,2,4-Triazole (AT). All plates were incubated at 37°C overnight, and colony formation was monitored.

Protein Purification

Escherichia coli CF9467 cells were transformed with pQE_{30}-*relA*, pYG4, or pYG4-C638F (**Table 2**) and were grown to mid-exponential phase at 37°C with shaking in LB medium supplemented with 100 μg/ml ampicillin. The expression of his-tagged RelA, YG4, or YG4-C638F was induced by the addition of 1 mM IPTG. After 2 h of growth at 37°C, the cells were harvested by centrifugation, resuspended in buffer A (20 mM Naphosphate buffer pH 7.4, 0.5 M NaCl, 10 mM imidazole), supplemented with protease inhibitor cocktail Complete EDTA free (Roche Diagnostics), and then sonicated. To remove cell debris and unbroken cells, lysates were centrifuged at 10,000 *g* for 15 min. Supernatants were loaded onto Ni-NTA agarose columns (Qiagen). The columns were washed with buffer A containing 20 mM imidazole, and his-tagged protein was eluted with 250 mM imidazole in buffer A. The protein-containing fractions were analyzed by SDS page, and then pooled and dialyzed against buffer B (100 mM Tris-HCl pH 8.5, 10 mM EDTA, 1 mM DTT and 25% glycerol). Final protein concentrations were measured using the Bio-Rad Protein Assay dye reagent.

TABLE 1 | Bacterial strains.

Strain name	Genotype	Source
W3110	WT $lacI^q$::Kan^R	Laboratory collection
CF9467	W3110Δ*relA*$lacI^q$::Kan^R	Schreiber et al., 1991

Lowsalt Crude Ribosome Preparation

Crude ribosomes are ribosomes associated with both mRNA and tRNA. These were prepared as described by Block and Haseltine (1975) with the following modifications: Δ*rel*A cells were grown in LB medium with shaking at 37°C. At OD_{600} = 1.5, the cell culture was centrifuged at 4,000 *g* at 4°C for 20 min and frozen overnight at −70°C. The pellet was resuspended in cold buffer R [consisting of 100 mM Tris-acetate pH 8, 10 mM $Mg(AcO)_2$ and 1 mM DTT]. Lysozyme, supplemented with protease inhibitor cocktail Complete EDTA free (Roche Diagnostics), was added to a final concentration of 3 mg/ml, and cells were sonicated. Cell lysates were centrifuged at 12,000 *g* for 40 min to remove cell debris and unbroken cells. The supernatants were centrifuged in a Beckman Ti-65 rotor at 28,000 g at 4°C for 4 h. The pellets were resuspended in buffer R and were incubated at 4°C overnight. To remove excess of membrane residues, all of the suspended pellets were combined together and centrifuged at 8,000 *g* at 4°C for 15 min. The supernatant from this centrifugation was then centrifuged again, using a sucrose cushion, at 4°C for 4 h in a Beckman Ti-65 rotor at 30,000 g. The final pellet, containing the purified ribosomes was then resuspended in buffer R, and the ribosomal concentration was determined based on RNA measurements in an ND-1000 Spectrophotometer (Nano-Drop). The ribosomes were frozen and stored at −70°C.

In vitro RelA Activity Assay

For the *in vitro* RelA activity assay, reaction buffer (RM) was used containing 0.5 mM GTP, 4 mM ATP, 50 mM Tris-HCl (pH 7.4), 1 mM DTT, 10 mM $MgCl_2$, 10 mM KCl, and 27 mM $(NH_4)_2SO_4$. For each reaction, 10 μCi of (α-^{32}P)GTP was added. In a total volume of 20 μl, 1 μg of purified RelA or purified RelA-C638F was mixed together with RM, 30 μg of ribosomes and varying amounts of YG4, YG4-C638F, or RelA-G251E proteins. After 1 h of incubation at room temperature, the reactions were stopped by the addition of 5 μl of formic acid reaching a final concentration of 20%. 5 μl aliquots of each reaction were loaded and separated on Cellulose PEI TLC plates (Merck) using 1.5 M KH_2PO_4 as mobile phase. The plates were autoradiographed using the Fijix Bas100 PhosphorImager (Japan); the (p)ppGpp content was determined based on relative intensities calculated using TINA 2.0 software (Raytest).

Ribosome Binding Assay

In vitro reactions containing increasing concentrations of either YG4 or YG4-C638F were carried out as described above for the RelA activity assay but without the addition of radio-labeled GTP.

The reaction mixtures were centrifuged at 30,000 *g* at 4°C for 4 h. The soluble fractions were removed, and ribosomal samples from the pellets were separated by 12% SDS-polyacrylamide gel electrophoresis, transferred to PVDF membrane (Millipore), and processed for immunoreaction using mouse-anti-His monoclonal antibody (GE Healthcare). Immuno-reactive proteins were detected using a chemi-luminescence kit (Biological Industries) according to the protocol of the manufacturer.

In vitro Cross-Linking

Protein cross-linking was carried out in a 10 µl reaction mixture containing 12.5 mM Naphosphate pH 7.2, 12.5 mM NaCl, 2.5% glycerol, 1×10^{-3}% glutaraldehyde, and 4 µg of protein. After 15 min of incubation in ice, each sample was loaded onto SDS polyacrylamide gel and electrophoresed for further Western Blot Analysis, as described above.

Mass Spectrometric Analysis (MS-MS)

A sample of YG4 dimers after cross-linking with glutaraldehyde as mentioned earlier was divided into two. To cleave possible disulfide bonds, dithiothreitol (DTT) was added to one of the samples; the second sample was left untreated. Both samples were digested with Trypsin. The peptide mixtures were solid phase extracted using C18 resin filled tips (ZipTip Milipore) and subsequently nanosprayed into the Orbi-trap MS system in 50% acetonitrile containing 1% formic acid.

Mass spectrometry (MS) was carried out with Orbi-trap (Thermo Finnigen) using a nanospray attachment. Data analysis was done using bioworks 3.3 package, and database searches were performed against the NCBInr database with Mascot package (Matrix Science).

RESULTS

Dominant Negative Effect of RelA-CTD on the Stringent Response

Our previous data showed a dominant negative effect of RelA-CTD fragment (YG4) on RelA activity in *E. coli* (Gropp et al., 2001). Following this, we overexpressed YG4 and YG4-C638F in WT *E. coli* cells and plated them on M9 medium together with 3-amino-1,2,4-Triazole (AT; **Figure 1B**), thereby creating histidine starvation conditions. It was clear that under these conditions, cells overexpressing YG4 exhibited difficulties in overcoming the AA starvation (by three orders of magnitude) unlike cells overexpressing YG4-C638F (by two orders of magnitude; **Figure 1B**). Under the same conditions without AT a less negative effect on cell growth was observed (one order of magnitude in presence of YG4 or YG4-C638F; **Figure 1C**). This phenomenon can have two possible explanations: (i) YG4 binds to RelA, thus inhibiting its activity on the ribosome and (ii) YG4 competes with RelA for ribosome binding. Both theories are valid for explaining poor RelA activity. Additionally, in order to overexpress the proteins, all genes were cloned under a *lac* promoter, and IPTG was used to induce their overexpression. Massive overexpression following the use of a *lac* promoter and IPTG can interrupt normal cell activity, regardless of the target itself and cause different effects on cell function. In order to rule out this theory, we plated the same cells on M9 medium without AT. Cells overexpressing YG4 or YG4-C638F showed the same growth rate (**Figure 1C**), indicating that the overexpression itself probably did not affect the cell growth, although a slight growth arrest was seen on M9 medium without AT (**Figure 1C**) We next examined the effect of overexpression of alternate Rel proteins on *E. coli* growth in rich medium. As previously shown (Schreiber et al., 1991), overexpression of an active full-length RelA, such as the WT RelA (**Figure 1D** dots) or Rel-C638F (**Figure 1D** dashed) displayed delayed growth as compared to the WT cells that showed no overexpression at all (**Figure 1** solid line, no bullets). This can be explained by the production of (p)ppGpp in those cells, which is known to inhibit cell growth. However, when RelA bearing a mutation in position 251(Gropp et al., 2001; **Figure 1D** triangles) that renders the protein incapable of synthetic activity, or YG4 was overexpressed (**Figure 1D** squares), no effect on growth rate was observed. Meaning that an excess of a protein lacking synthetic activity, in this case, did not inhibit cell growth in rich medium. The lac-IPTG system is known to produce large amounts of proteins in bacterial cells which, in some cases, can inhibit cell growth, especially in poor medium, such as M9. Our results indicate that while overexpression itself of these proteins does not affect cell growth, cell growth is inhibited by (p)ppGpp synthesis.

TABLE 2 | Plasmids.

Plasmid name	Relevant characteristics	Source
pQE_{30}	::amp	Qiagen
pYG4	pQE_{30} carrying His-tagged YG4 under tac promoter::amp	Gropp et al., 2001
pYG4-C638F	pQE_{30} carrying His-tagged YG4-C638F under tac promoter::amp	Gropp et al., 2001
pRelA	pQE_{30} carrying His-tagged RelA under tac promoter::amp	Gropp et al., 2001
pRelA-C638F	pQE_{30} carrying His-tagged RelA-C638F under tac promoter::amp	Gropp et al., 2001
pRel251	pQE_{30} carrying His-tagged RelA-G251E under tac promoter::amp	Gropp et al., 2001

Cys-638 in *E. coli*-RelA-CTD Is Essential for Protein Regulation

We next examined what the effect of an excess of RelA variants or fragments was on *E. coli* RelA activity *in vitro*. In order to synthesize (p)ppGpp, the *E. coli* RelA must be activated by a stalled ribosome. Protein binding to the ribosome is *via* its CTD (Wendrich and Marahiel, 1997) and as described more recently *via* the RIS and the ACT domain (Loveland et al., 2016). Three Cys residues are present in the CTD and extremely conserved throughout the Rel protein family (Atkinson et al., 2011). The importance of all three Cys residues in the CTD was shown in previous publications (Gropp et al., 2001; Atkinson et al., 2011), but the strongest effect on RelA activity and the RelA-RelA interaction was observed by a single mutation in Cys-638 (Gropp et al., 2001). Thus, in the present study,

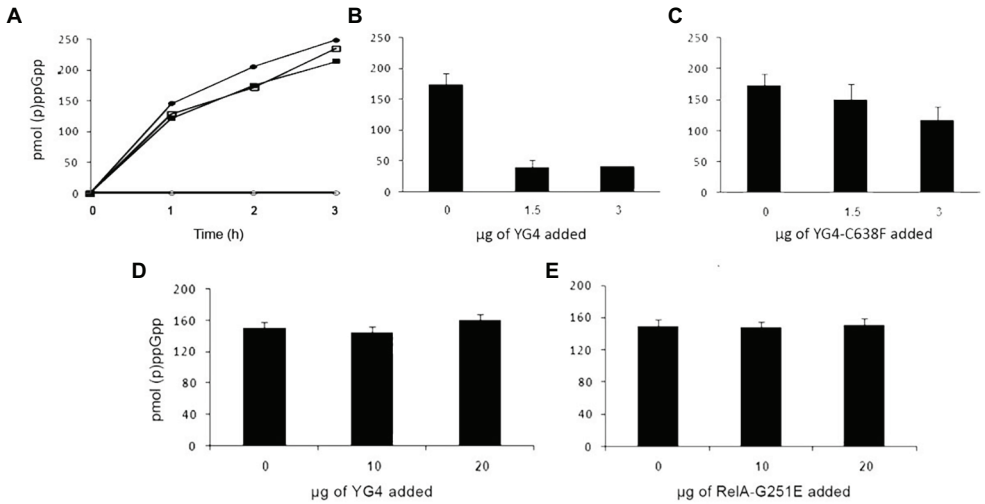

FIGURE 2 | Dominant negative effect of CTD on RelA synthetic activity *in vitro*. (p)ppGpp production by RelA *in vitro*. **(A)** Solid circles (●) WT-RelA in the presence of ribosomes; empty circles (o) – WT-RelA in the absence of ribosomes; solid squares (■) – Rel-C638F in the presence of ribosomes; empty squares (□) – Rel-C638F in the absence of ribosomes. **(B,C)** (p)ppGpp production by 1 µg of RelA with the addition of increasing amounts of **(B)** YG4 and **(C)** YG4-C638F. **(D,E)** (p)ppGpp production by 1 µg of Rel-C638F with the addition of increasing amounts of **(D)** YG4 and **(E)** Rel251.

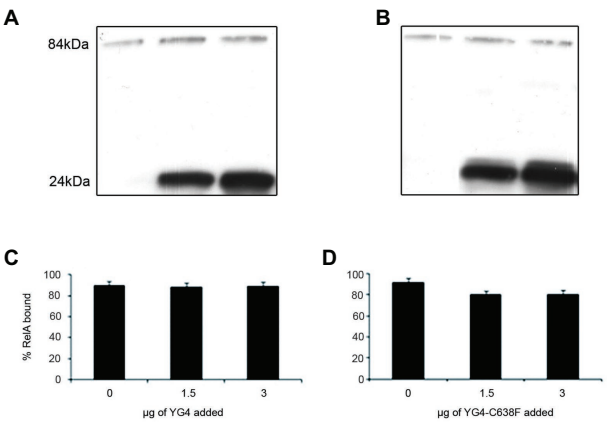

FIGURE 3 | RelA binding to the ribosomes. Western blot analysis of the ribosomal fraction from an *in vitro* reaction of (p)ppGpp synthesis by 1 µg of RelA, with the addition of increasing amounts of **(A)**. YG4 and **(B)** YG4-C638F as indicated in **(C)** and **(D)**, respectively. **(C,D)** Quantification of RelA bound to the ribosome from **(A)** and **(B)**, respectively.

we chose to focus on the C638F mutation. We first tested the synthetic activity of both WT RelA and Rel-C638F *in vitro*, focusing on the regulatory effect of the YG4, especially on the role of Cys-638. When examining the synthetic activity of the mutated Rel-C638F *in vitro*, the protein lacked regulatory activity, producing (p)ppGpp in a ribosome-independent manner as compared to the WT RelA (**Figure 2A**; Gropp et al., 2001). The replacement of a single amino acid was sufficient in rendering the protein ribosome-independent, showing that Cys-638 is essential for the regulation of RelA activity. We next examined the synthetic activity of both proteins following the addition of YG4. The results correlated with our previous data showing that, where (p)ppGpp production by RelA in the presence of YG4 (**Figure 2B**) was poor, there was almost no effect on its synthetic activity in the presence of YG4-C638F (**Figure 2C**). The synthetic activity of Rel-C638F was not affected by either the presence of YG4 or Rel251 that supplies WT CTD (**Figures 2D,E**), which may be a hint to the lack of ability of Rel-C638F to form RelA-RelA interactions. In all cases, the additional protein was in a greater excess (at least 1:6 molar ratio) than the synthetase in the reaction. These results indicate that a change in Cys-638 causes the reversal of the protein YG4's dominant negative effect on the synthetic ability of a ribosome-dependent protein.

Excess of CTD During (p)ppGpp Production Does Not Affect the Amount of RelA on the Ribosomes

When performing *in vitro* (or *in vivo* in previous publications; Gropp et al., 2001) activity tests, we usually employ a substantial excess of the YG4. This could possibly explain the inhibition of RelA activity as being the result of this excess YG4 competing with RelA for ribosomal binding. This contradicts the theory that this inhibition is the result of the YG4 forming an "incorrect" dimer with RelA. In order to test these two theories, we performed a ribosome binding assay with RelA in the presence of the native or the mutated YG4. The reaction included all components of an *in vitro* activity assay. After 45 min of incubation, the ribosomal fraction was separated by centrifugation, and the amount of RelA in each sample was tested by Western blot analysis (**Figure 3**). Interestingly, neither the excess of the native (**Figure 3C**) nor the mutated YG4 (**Figure 3D**) affected RelA's ability to bind to the ribosome. Another interesting observation is that most of the YG4 or YG4-C638F that was present in the reaction tube was also

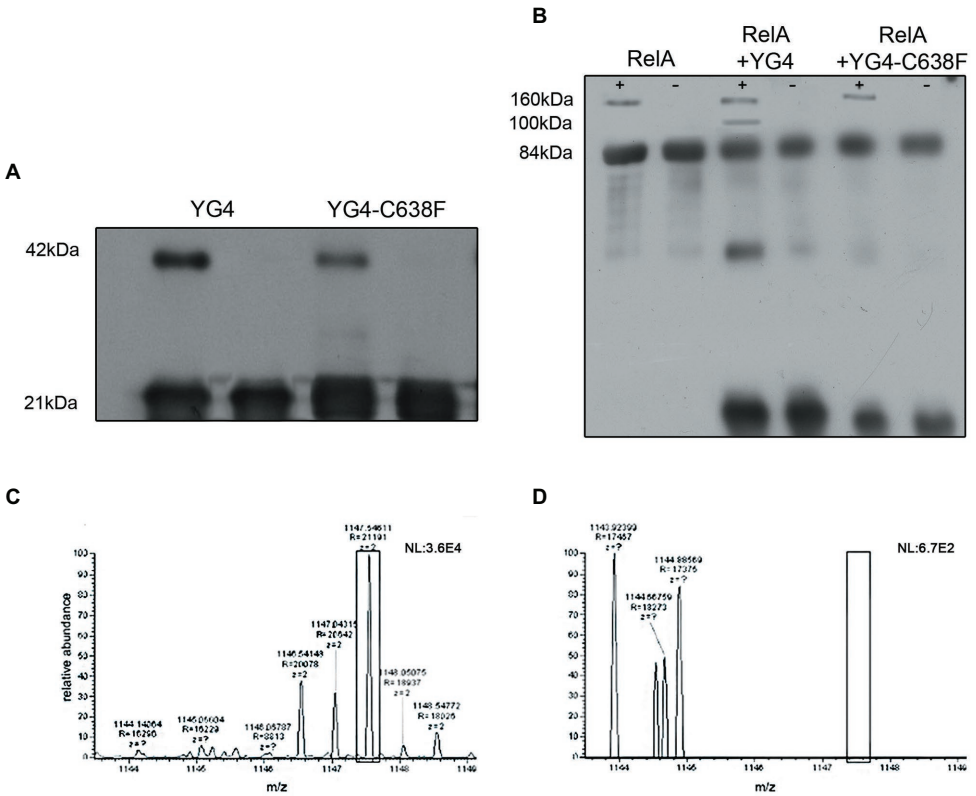

FIGURE 4 | Dimerization of YG4 and RelA. *In vitro* cross-linking reactions were performed by incubating the proteins and analyzing them by Western Blot. (+): with glutaraldehyde; (–): without glutaraldehyde. **(A)** Cross-linking of YG4 (left) and YG4-C638F (right). **(B)** From left to right: cross-linking of RelA, RelA and YG4, RelA, and YG4-C638F. **(C,D)** Mass spectrometry (MS)-MS analysis of digested YG4 peptides. **(C)** MS-MS analysis of YG4 dimers, digested without DTT reducing treatment, showing a fragment including an inter-chain S-S bond corresponding to Cys638-Cys638 (box); m/z = 1,147; **(D)** MS-MS analysis of reduced and digested YG4 dimers; note the absence of the fragment seen in (**C**; see box).

bound to the ribosomes (**Figures 3A,B**). These results stand together with the results of RelA activity test in the presence of YG4 and YG4-C638F (**Figure 2**), thus indicating that the inhibitory effect of YG4 on RelA is by its binding to the protein itself. These results also emphasize YG4's ability to bind to the ribosome.

The CTD Forms Dimers *in vitro*

We further wanted to explore whether RelA and YG4 are capable of forming dimers *in vitro*. Cross-linking experiments revealed the formation of dimers for both these proteins (**Figures 4A,B**). It can be seen that YG4-C638F forms fewer dimers than the native YG4 (**Figure 4A**). Full-length RelA was also capable of forming homo-dimers, and also hetero-dimers with YG4, which was seen at 100 kDa. This is probably due to the fact that both proteins have a Cys residue at position 638 (**Figure 4B**). But no dimers with YG4-C638F were observed due to the lack of a Cys residue at position 638 in the mutant YG4 (**Figure 4B**). These results reinforce the importance of Cys638 for RelA-RelA interactions. The fact that YG4-C638F forms homodimers and that no RelA-YG4-C638F dimers were seen indicates that only WT-YG4 is capable of inhibiting RelA activity, similar to the results of RelA synthetic activity (**Figure 2**). This probably happens due to the formation of an incorrect dimer between RelA and YG4. It should be noted that we used glutaraldehyde when performing the cross-linking, which is an unspecific cross-linker that covalently links molecules that are present close enough to each other. In both cross-linking experiments (**Figures 4A,B**), only a small portion, out of the large amounts of protein that were used, formed dimers. It should be noted that the amplified amounts of protein that were used in these experiments are not proportional to the actual protein concentrations in the cell. Our main purpose was to examine the ability of these proteins to interact with each other *in vitro*, based on our previous results (Gropp et al., 2001) and to further investigate the basis for the dimer formation. Thus, we were able to examine whether the dimers were formed specifically due to S-S bonds between two Cys-638. Employing MS-MS analysis, we examined a YG4 dimer that showed the existence of a di-sulfide bond at C-638 only when YG4 dimer was not treated with DTT, which breaks S-S bonds (**Figure 4C**). But when YG4 dimer was treated with DTT no S-S bond was found (**Figure 4D**). Based on these findings, it seems that the interactions between YG4-C638F with itself or other proteins are not specific and not strong enough to inhibit RelA synthetic activity.

DISCUSSION

The stringent response is most likely one of the most important stress responses in bacteria, and, as such, is persistently studied. Due to the fast, synthetic activity of RelA in response to a lack of amino acids, the cell is able to respond very quickly by entering cell-growth arrest, indispensable for its survival. While small amounts of RelA are present in the cell throughout its entire lifetime, it is mostly in a low activity mode. Binding of an uncharged tRNA to the ribosome activates RelA and enables its catalytic activity. Although the stringent response has been studied for over 5 decades, the regulatory mechanism of RelA is poorly understood. The CTD domain is responsible for the regulation and ribosome binding, and is composed of four sub-domains (Atkinson et al., 2011; Loveland et al., 2016). Our previous results (Gropp et al., 2001) showed the importance of the last two domains (AA 564–744), and the importance of the three Cys residues present in the RIS domain (Loveland et al., 2016; **Figure 1A**), especially in protein-protein interactions. This was also reinforced with recent reports about the involvement of the CTD in the oligomerization of Rel protein in *Mycobacterium* (Singal et al., 2017) and also in the regulation of *Bacillus Subtilis* Rel synthetic activity (Pausch et al., 2020). Here, we closely examined RelA-RelA *via* its CTD interactions *in vitro* by using purified ribosomes (70S) where lack of charged tRNA in the tube mimic amino acid stress conditions. Our results show that *in vitro*, excess of YG4 inhibits synthetic activity of RelA under stress conditions. On the other hand, YG4 did not inhibit cell growth under normal growth conditions *in vivo*, showing that while the excess of protein itself does not affect cell growth, it has a direct effect on RelA synthetic activity. When Cys-638 was replaced by Phenylalanine, this effect was abolished. Moreover, cross-linking experiments and MS-MS analysis revealed the ability of the native RelA and YG4 to form dimers *via* the formation of S-S bonds between Cys-638 both between the full length proteins and between YG4 fragments (**Figure 4**), which we believe also exist *in vivo*. These observations suggest that a direct interaction between YG4 and RelA causes inhibition of RelA synthetic activity. Finally, a ribosome binding assay showed that the amount of RelA on the ribosome did not change in spite of increasing amounts of YG4 in the reaction tube. These results indicate that the inhibitory effect of the YG4 on RelA is not *via* competitive binding, but rather a direct interaction between RelA and YG4. Taking together our present and previous results, we believe that the regulation of *E. coli* RelA activity is controlled by its CTD, especially by the RIS and ACT domain, which are part of YG4. In all Cryo-EM studies (Agirrezabala et al., 2013; Arenz et al., 2016; Brown et al., 2016; Loveland et al., 2016), RelA was found as a monomer on the ribosome. Together with our results, it appears that the CTD is responsible not only for ribosomal binding of the protein, but also for the oligomerization of the protein, which prevents RelA synthetic activity in the cytosol. Under stress conditions and a binding of an uncharged tRNA to the ribosome, RelA is stabilized, thus enabling its ability to synthesize (p)ppGpp (Loveland et al., 2016). This was also recently shown in Rel protein from *B. subtilis*, where Rel is in an oligomeric state in the cytosol during normal growth conditions, but upon accumulation of uncharged tRNA the dimer dissociates by interaction with the CTD and together binds to a cognate ribosome (Pausch et al., 2020). Here, based on all of our present data together with our previous results (Gropp et al., 2001) and recent studies (Loveland et al., 2016; Pausch et al., 2020), we present a partial model for RelA regulation, which uncovers additional part in the complex "RelA regulation puzzle". It is likely that RelA forms the dimer only in the cytosol *via* the formation of a disulfide bond with Cys-638 residues. Based on Pausch study (Pausch et al., 2020), dimer is probably separated when RelA-CTD binds an uncharged tRNA in the cytosol, which enables the dissociation of the dimer to monomer which then binds to the ribosome. The dominant negative effect of YG4 on RelA synthetic activity is probably by inhibiting this interaction with an uncharged tRNA, thus interrupting the dissociation of the dimer. The importance of Cys-638 is probably not only in the formation of the disulfide bonds but also in stabilizing RelA structure in order for it to be activated, as exhibited by the ability of Rel-C638F to synthesize (p)ppGpp also in absence of ribosomes (**Figure 2A**). This is probably due to the fact that Rel-C638F folds in the cytosol as the native RelA does, when bound to a stalled ribosome. A possible explanation of our results in which YG4 inhibits RelA synthetic activity could be due to the fact that the addition of a native YG4 *in vivo* or *in vitro*, creates an "incorrect" dimer which either disables RelA to form a monomer, or disables the conformational change of RelA allowing its synthetic activity on the ribosome. It is possible that the full length CTD is unable to form such interactions with the full length RelA resulting in its inability to inhibit RelA synthetic activity. Taken together all results, it seems that parts in the CTD are responsible for RelA-RelA interactions, which are responsible and important for RelA regulation.

DATA AVAILABILITY STATEMENT

The raw data supporting the conclusions of this article will be made available by the authors, without undue reservation.

AUTHOR CONTRIBUTIONS

GG and IK conceived the study. IK performed all experiments. Both the authors contributed to the article and approved the submitted version.

FUNDING

This work was supported by the Israeli Science Foundation (GG grant #242/15).

ACKNOWLEDGMENTS

We thank Ofra Moshel and Alex Eliassaf Feldstein for performing the MS-MS analysis.

REFERENCES

Agirrezabala, X., Fernandez, I. S., Kelley, A. C., Carton, D. G., Ramakrishnan, V., and Valle, M. (2013). The ribosome triggers the stringent response by RelA via a highly distorted tRNA. *EMBO Rep.* 14, 811–816. doi: 10.1038/embor.2013

Alfoldi, L., Stent, G. S., and Clowes, R. C. (1962). The chromosomal site of the RNA control (RC) locus in *Escherichia coli*. *J. Mol. Biol.* 5, 348–355. doi: 10.1016/s0022-2836(62)80077-1

Arenz, S., Abdelshahid, M., Sohmen, D., Payoe, R., Starosta, A. L., Berninghausen, O., et al. (2016). The stringent factor RelA adopts an open conformation on the ribosome to stimulate ppGpp synthesis. *Nucleic Acids Res.* 44, 6471–6481. doi: 10.1093/nar/gkw470

Atkinson, G. C., Tenson, T., and Hauryliuk, V. (2011). The RelA/SpoT homolog (RSH) superfamily: distribution and functional evolution of ppGpp synthetases and hydrolases across the tree of life. *PLoS One* 6:e23479. doi: 10.1371/journal.pone.0023479

Block, R., and Haseltine, A. W. (1975). Purification and properties of stringent factor. *J. Biol. Chem.* 250, 1212–1217.

Brown, A., Fernandez, I. S., Gordiyenko, Y., and Ramakrishnan, V. (2016). Ribosome-dependent activation of stringent control. *Nature* 534, 277–280. doi: 10.1038/nature17675

Cashel, M. (1969). The control of ribonucleic acid synthesis in *Escherichia coli*. IV. Relevance of unusual phosphorylated compounds from amino acid-starved stringent strains. *J. Biol. Chem.* 244, 3133–3141.

Cashel, M., and Gallant, J. (1969). Two compounds implicated in the function of the RC gene of *Escherichia coli*. *Nature* 221, 838–841. doi: 10.1038/221838a0

Dalebroux, Z. D., Svensson, S. L., Gaynor, E. C., and Swanson, M. S. (2010). ppGpp conjures bacterial virulence. *Microbiol. Mol. Biol. Rev.* 74, 171–199. doi: 10.1128/MMBR.00046-09

Dalebroux, Z. D., and Swanson, M. S. (2012). ppGpp: magic beyond RNA polymerase. *Nat. Rev. Microbiol.* 10, 203–212. doi: 10.1038/nrmicro2720

Fiil, N. P., von Meyenburg, K., and Friesen, J. D. (1972). Accumulation and turnover of guanosine tetraphosphate in *Escherichia coli*. *J. Mol. Biol.* 71, 769–783. doi: 10.1016/s0022-2836(72)80037-8

Gentry, D. R., Hernandez, V. J., Nguyen, L. H., Jensen, D. B., and Cashel, M. (1993). Synthesis of the stationary-phase sigma factor sigma s is positively regulated by ppGpp. *J. Bacteriol.* 175, 7982–7989. doi: 10.1128/jb.175.24.7982-7989.1993

Gourse, R. L., Gaal, T., Bartlett, M. S., Appleman, J. A., and Ross, W. (1996). rRNA transcription and growth rate-dependent regulation of ribosome synthesis in *Escherichia coli*. *Annu. Rev. Microbiol.* 50, 645–677. doi: 10.1146/annurev.micro.50.1.645

Gropp, M., Strausz, Y., Gross, M., and Glaser, G. (2001). Regulation of *Escherichia coli* RelA requires oligomerization of the C-terminal domain. *J. Bacteriol.* 183, 570–579. doi: 10.1128/JB.183.2.570-579.2001

Gross, M., Marianovsky, I., and Glaser, G. (2006). MazG--a regulator of programmed cell death in *Escherichia coli*. *Mol. Microbiol.* 59, 590–601. doi: 10.1111/j.1365-2958.2005.04956.x

Haseltine, W. A., and Block, R. (1973). Synthesis of guanosine tetra- and pentaphosphate requires the presence of a codon-specific, uncharged transfer ribonucleic acid in the acceptor site of ribosomes. *Proc. Natl. Acad. Sci. U. S. A.* 70, 1564–1568. doi: 10.1073/pnas.70.5.1564

Haseltine, W. A., Block, R., Gilbert, W., and Weber, K. (1972). MSI and MSII made on ribosome in idling step of protein synthesis. *Nature* 238, 381–384. doi: 10.1038/238381a0

Jain, V., Saleem-Batcha, R., China, A., and Chatterji, D. (2006). Molecular dissection of the mycobacterial stringent response protein Rel. *Protein Sci.* 15, 1449–1464. doi: 10.1110/ps.062117006

Kaspy, I., Rotem, E., Weiss, N., Ronin, I., Balaban, N. Q., and Glaser, G. (2013). HipA-mediated antibiotic persistence via phosphorylation of the glutamyl-tRNA-synthetase. *Nat. Commun.* 4:3001. doi: 10.1038/ncomms4001

Lipmann, F., and Sy, J. (1976). The enzymic mechanism of guanosine 5',3'-polyphosphate synthesis. *Prog. Nucleic Acid Res. Mol. Biol.* 17, 1–14. doi: 10.1016/s0079-6603(08)60063-x

Loveland, A. B., Bah, E., Madireddy, R., Zhang, Y., Brilot, A. F., Grigorieff, N., et al. (2016). Ribosome•RelA structures reveal the mechanism of stringent response activation. *elife* 5:e17029. doi: 10.7554/eLife.17029

Lund, E., and Kjeldgaard, N. O. (1972). Metabolism of guanosine tetraphosphate in *Escherichia coli*. *Eur. J. Biochem.* 28, 316–326. doi: 10.1111/j.1432-1033.1972.tb01916.x

Magnusson, L. U., Farewell, A., and Nystrom, T. (2005). ppGpp: a global regulator in *Escherichia coli*. *Trends Microbiol.* 13, 236–242. doi: 10.1016/j.tim.2005.03.008

Metzger, S., Dror, I. B., Aizenman, E., Schreiber, G., Toone, M., Friesen, J. D., et al. (1988). The nucleotide sequence and characterization of the relA gene of *Escherichia coli*. *J. Biol. Chem.* 263, 15699–15704.

Metzger, S., Sarubbi, E., Glaser, G., and Cashel, M. (1989). Protein sequences encoded by the relA and the spoT genes of *Escherichia coli* are interrelated. *J. Biol. Chem.* 264, 9122–9125.

Paul, B. J., Barker, M. M., Ross, W., Schneider, D. A., Webb, C., Foster, J. W., et al. (2004). DksA: a critical component of the transcription initiation machinery that potentiates the regulation of rRNA promoters by ppGpp and the initiating NTP. *Cell* 118, 311–322. doi: 10.1016/j.cell.2004.07.009

Pausch, P., Abdelshahid, M., Steinchen, W., Schafer, H., Gratan, F. L., Freibert, S. A., et al. (2020). Structural basis for regulation of the opposing (p)ppGpp synthetase and hydrolase within the stringent response orchestrator Rel. *Cell Rep.* 32:108157. doi: 10.1016/j.celrep.2020.108157

Pedersen, F. S., and Kjeldgaard, N. O. (1977). Analysis of the relA gene product of *Escherichia coli*. *Eur. J. Biochem.* 76, 91–97. doi: 10.1111/j.1432-1033.1977.tb11573.x

Schreiber, G., Metzger, S., Aizenman, E., Roza, S., Cashel, M., and Glaser, G. (1991). Overexpression of the relA gene in *Escherichia coli*. *J. Biol. Chem.* 266, 3760–3767.

Singal, B., Balakrishna, A. M., Nartey, W., Manimekalai, M. S. S., Jeyakanthan, J., and Gruber, G. (2017). Crystallographic and solution structure of the N-terminal domain of the Rel protein from *Mycobacterium tuberculosis*. *FEBS Lett.* 591, 2323–2337. doi: 10.1002/1873-3468.12739

Stent, G. S., and Brenner, S. (1961). A genetic locus for the regulation of ribonucleic acid synthesis. *Proc. Natl. Acad. Sci. U. S. A.* 47, 2005–2014. doi: 10.1002/1873-3468.12739

Takada, H., Roghanian, M., Murina, V., Dzhygyr, I., Murayama, R., Akanuma, G., et al. (2020). The C-terminal RRM/ACT domain is crucial for fine-tuning the activation of 'long' RelA-SpoT homolog enzymes by ribosomal complexes. *Front. Microbiol.* 11:277. doi: 10.3389/fmicb.2020.00277

Tosa, T., and Pizer, L. I. (1971). Biochemical bases for the antimetabolite action of L-serine hydroxamate. *J. Bacteriol.* 106, 972–982. doi: 10.1128/JB.106.3.972-982.1971

Turnbull, K. J., Dzhygyr, I., Lindemose, S., Hauryliuk, V., and Roghanian, M. (2019). Intramolecular interactions dominate the autoregulation of *Escherichia coli* stringent factor RelA. *Front. Microbiol.* 10:1966. doi: 10.3389/fmicb.2019.01966

Wendrich, T. M., Blaha, G., Wilson, D. N., Marahiel, M. A., and Nierhaus, K. H. (2002). Dissection of the mechanism for the stringent factor RelA. *Mol. Cell* 10, 779–788. doi: 10.1016/s1097-2765(02)00656-1

Wendrich, T. M., and Marahiel, M. A. (1997). Cloning and characterization of a relA/spoT homologue from *Bacillus subtilis*. *Mol. Microbiol.* 26, 65–79. doi: 10.1046/j.1365-2958.1997.5511919.x

Yang, X., and Ishiguro, E. E. (2001). Involvement of the N terminus of ribosomal protein L11 in regulation of the RelA protein of *Escherichia coli*. *J. Bacteriol.* 183, 6532–6537. doi: 10.1128/JB.183.22.6532-6537.2001

Conflict of Interest: The authors declare that the research was conducted in the absence of any commercial or financial relationships that could be construed as a potential conflict of interest.

frontiers in Microbiology

ORIGINAL RESEARCH
published: 05 November 2020
doi: 10.3389/fmicb.2020.575041

Structural Analysis of (p)ppGpp Reveals Its Versatile Binding Pattern for Diverse Types of Target Proteins

Gajraj Singh Kushwaha[1,2], Anupam Patra[1] and Neel Sarovar Bhavesh[1]**

[1] *Transcription Regulation Group, International Centre for Genetic Engineering and Biotechnology (ICGEB), New Delhi, India,* [2] *KIIT Technology Business Incubator (KIIT-TBI), Kalinga Institute of Industrial Technology (KIIT) (Deemed to be University), Bhubaneswar, India*

OPEN ACCESS

Edited by:
Katarzyna Potrykus, University of Gdańsk, Poland

Reviewed by:
Kenneth A. Satyshur, University of Wisconsin–Madison, United States
Punit Kaur, All India Institute of Medical Sciences, India

***Correspondence:**
Gajraj Singh Kushwaha
gajrajsk@gmail.com
Neel Sarovar Bhavesh
neelsb@icgeb.res.in

Specialty section:
This article was submitted to Microbial Physiology and Metabolism, a section of the journal Frontiers in Microbiology

Received: *22 June 2020*
Accepted: *06 October 2020*
Published: *05 November 2020*

Citation:
Kushwaha GS, Patra A and Bhavesh NS (2020) Structural Analysis of (p)ppGpp Reveals Its Versatile Binding Pattern for Diverse Types of Target Proteins. Front. Microbiol. 11:575041. doi: 10.3389/fmicb.2020.575041

(p)ppGpp, highly phosphorylated guanosine, are global regulatory nucleotides that modulate several biochemical events in bacterial physiology ranging from core central dogma to various metabolic pathways. Conventionally, (p)ppGpp collectively refers to two nucleotides, ppGpp, and pppGpp in the literature. Initially, (p)ppGpp has been discovered as a transcription regulatory molecule as it binds to RNA polymerase and regulates transcriptional gene regulation. During the past decade, several other target proteins of (p)ppGpp have been discovered and as of now, more than 30 proteins have been reported to be regulated by the binding of these two signaling nucleotides. The regulation of diverse biochemical activities by (p)ppGpp requires fine-tuned molecular interactions with various classes of proteins so that it can moderate varied functions. Here we report a structural dynamics of (p)ppGpp in the unbound state using well-defined computational tools and its interactions with target proteins to understand the differential regulation by (p)ppGpp at the molecular level. We carried out replica exchange molecular dynamics simulation studies to enhance sampling of conformations during (p)ppGpp simulation. The detailed comparative analysis of torsion angle conformation of ribose sugar of unbound (p)ppGpp and bound states of (p)ppGpp was carried out. The structural dynamics shows that two linear phosphate chains provide plasticity to (p)ppGpp nucleotides for the binding to diverse proteins. Moreover, the intermolecular interactions between (p)ppGpp and target proteins were characterized through various physicochemical parameters including, hydrogen bonds, van der Waal's interactions, aromatic stacking, and side chains of interacting residues of proteins. Surprisingly, we observed that interactions of (p)ppGpp to target protein have a consensus binding pattern for a particular functional class of enzymes. For example, the binding of (p)ppGpp to RNA polymerase is significantly different from the binding of (p)ppGpp to the proteins involved in the ribosome biogenesis pathway. Whereas, (p)ppGpp binding to enzymes involved in nucleotide metabolism facilitates the functional regulation through oligomerization. Analysis of these datasets revealed

that guanine base-specific contacts are key determinants to discriminate functional class of protein. Altogether, our studies provide significant information to understand the differential interaction pattern of (p)ppGpp to its target and this information may be useful to design antibacterial compounds based on (p)ppGpp analogs.

Keywords: stringent response, (p)ppGpp, secondary messenger nucleotide, interaction analysis, structural dynamics, (p)ppGpp synthetase

INTRODUCTION

Bacterial physiology is regulated by various types of secondary messenger nucleotides and these nucleotides regulate almost all major biochemical events (Hengge et al., 2019). These nucleotides are key players of the signaling network intended to responsive cellular behavior to various environmental conditions. The stringent response is such a pleiotropic and global regulatory process which modulates at least one-third of bacterial physiological processes (Cashel and Gallant, 1969; Cashel et al., 1996; Hauryliuk et al., 2015). It is meticulously regulated by the synthesis of two signaling nucleotides namely, pppGpp and ppGpp (together called (p)ppGpp) (Potrykus and Cashel, 2008; Hauryliuk et al., 2015; Steinchen and Bange, 2016). (p)ppGpp messenger nucleotides are highly phosphorylated and bind to several protein targets to regulate biochemical events (Dalebroux and Swanson, 2012; Kanjee et al., 2012; Zhang et al., 2018). Historically, these nucleotides were discovered by two-dimensional thin-layer chromatography of samples from amino acid starved *Escherichia coli* culture. The concentration of these nucleotides was enhanced drastically in *E coli* cells during amino acid starvation and these nucleotides were inhibiting rRNA synthesis (Cashel and Gallant, 1969). Initially, the functional role of (p)ppGpp was discovered as transcriptional regulatory as it binds to bacterial RNA polymerase to down-regulate rRNA gene expression (Cashel and Gallant, 1969; Ross et al., 2013; Zuo et al., 2013). Later on, several enzymes from various pathways were identified which are regulated by binding of (p)ppGpp nucleotides. Most of those proteins are part of the core process of molecular machinery such as replication, transcription, translation, and cellular metabolism (Rojas et al., 1984; Wang et al., 2007, 2019; Srivatsan and Wang, 2008; Kriel et al., 2012; Bærentsen et al., 2019; Kushwaha et al., 2019b). The resultant effects of (p)ppGpp mediated regulation has been shown in virulence, host invasion, biofilm formation, persistence, long term survival, pathogenesis, antibiotic resistance, and antibiotic tolerance (Primm et al., 2000; Abranches et al., 2009; Dalebroux et al., 2010; Kudrin et al., 2017; Prusa et al., 2018). Therefore, being a modulator of several processes, (p)ppGpp has been considered as a master regulator for the survival of bacteria during unfavorable conditions.

Conventionally, term (p)ppGpp is used for two nucleotides, guanosine 5′-diphosphate-3′-diphosphate (ppGpp) and guanosine 5′-triphosphate-3′-diphosphate (pppGpp). These nucleotides are synthesized by (p)ppGpp synthetase by transferring pyrophosphate groups from ATP to GDP/GTP to form ppGpp and pppGpp, respectively (Mechold et al., 2002; Hogg et al., 2004; Tamman et al., 2020). There are primarily two types of (p)ppGpp synthetases that have been identified, multi-domain long RelA type and small alarmone synthetases. The long-form (p)ppGpp synthetases are found in two forms; mono functional comprises active synthetase and inactive hydrolase domain while bifunctional (p)ppGpp synthetases have both synthetase and hydrolase active domain. These are classified and named as RelA/SpoT Homolog (RSH) proteins (Atkinson et al., 2011; Hauryliuk et al., 2015). Several regulatory mechanisms have been proposed to explain the activation of (p)ppGpp synthetase enzymes (Hogg et al., 2004; Shyp et al., 2012; Steinchen et al., 2015; Beljantseva et al., 2017; Hauryliuk and Atkinson, 2017; Winther et al., 2018; Kushwaha et al., 2019a; Ronneau and Hallez, 2019). Subsequently, these nucleotide binds to various proteins to modulate the functional activity of respective biochemical reactions, hence, the structural information at the molecular level is essential to understand the fundamental differences associated with these biomolecular interactions. Although the structural studies on (p)ppGpp have been carried out in the bound form as complexes with its binding protein, the structural conformation and dynamics on (p)ppGpp in unbound states have not been reported so far. The computational methods have been an efficient choice to understand the structural dynamics of secondary messenger nucleotides (Stern et al., 2010; Wang et al., 2017). Here, we report a detailed structural analysis on (p)ppGpp in the unbound state using extensive conformation sampling molecular dynamics simulation along with their comparison with structural conformation in bound states. Additionally, a systematic analysis of the interactions between (p)ppGpp and binding proteins has been carried out to probe the particular binding pattern of these interactions for various types of proteins.

MATERIALS AND METHODS

Replica Exchange Molecular Dynamics (REMD) Simulation on Unbound (p)ppGpp

The molecular dynamics simulation studies provide structural dynamic information in the solution state of a molecule. Although, glycosidic bond and ribose sugar in the nucleotide structure exhibit conformational flexibility and classical molecular dynamics simulation on nucleotides is challenging because of energy barriers and sampling of conformations are limited. Therefore, Replica Exchange Molecular Dynamics (REMD) simulation was carried out on ppGpp and pppGpp nucleotides in solution states. In REMD, several identical

replicas run in parallel at different temperatures and these allow enhanced sampling of high energy conformations. Moreover, these replicas are allowed to swap their states based on Boltzmann-weighted probability at neighboring temperature state. This process is repeated iteratively during the simulation and subsequently enhanced sampling of conformations is achieved at various temperatures.

The structural coordinates of ppGpp and pppGpp were extracted from Protein Data Bank (Berman et al., 2000) and were prepared for simulation using the Maestro program from Schrodinger suite (**Figures 1A–D**). LigPrep tool was used to retain original chirality and biological pH 7.0 ± 2.0 of the (p)ppGpp nucleotides. For each nucleotide, the lowest energy conformer was used for the simulation process. The simulation system was built using the system builder tool in Maestro. The explicit solvent model TIP3P (Jorgensen et al., 1983)was included in an orthorhombic periodic boundary condition (PBC) computational box. The initial absolute box volume was 1000 $Å^3$ for both molecules and upon addition of buffer, the box volume was expanded to 145262 and 150766 $Å^3$ for ppGpp and pppGpp, respectively. Negative charges, due to phosphates groups of (p)ppGpp molecule, were neutralized by the addition of 20 mM Mg^{2+} in the simulation system. The Optimized Potential for Liquid Simulations 3 enhanced (OPLS3e) force field was selected for the simulation (Roos et al., 2019). Next, the prepared systems of ppGpp and pppGpp were loaded to Desmond workspace for energy minimization and replica-exchange simulation. The system was energy minimized before running the simulations. The replica-exchange parameters were set in a replica-exchange panel in Desmond. A tempering method was selected with nine replicas covering of temperature range from 273 to 373 K. The simulation time was fixed as 200 ns with a recording interval of 200 ps trajectory with energy of 1.2. The ensemble was selected as NPT for replica exchange. Finally, both REMD simulations were carried out for 200 ns. The REMD simulation result statistics were analyzed using the Desmond simulation interaction diagram report. The molecular properties of simulation trajectory were plotted using root-mean-square fluctuation (RMSF), root-mean-square deviation (RMSD), radius of gyration (rGyr), intramolecular hydrogen bonds (intraHB), molecular surface area (MolSA), solvent-accessible surface area (SASA), and polar surface area (PSA) parameters.

Structural Comparison of (p)ppGpp in Unbound and Bound State

The energy minimized three-dimensional structural coordinates of ppGpp and pppGpp were compared with coordinates extracted from crystal structures of (p)ppGpp-protein complexes. The structural alignment was carried out in PyMol using an atom alignment algorithm. The distribution frequency of glycosidic bonds in unbound states of ppGpp and pppGpp were plotted at 300 K simulation pose in Schrodinger. The torsion angle and phase angle values were calculated from Pseudo-Rotational Online Service and Interactive Tool (PROSIT) (Sun et al., 2004, 2005).

Interactions Analysis of (p)ppGpp and Proteins

The structures of (p)ppGpp-protein complexes were downloaded from Protein Data Bank (PDB). The PDB ligand code G4P for ppGpp, 0o2, and C1Z for pppGpp was used as a search term to obtain structures of ppGpp-protein and pppGpp-protein complexes, respectively. As shown in **Table 1**, there were 26 structures of ppGpp-protein while eight structures of pppGpp-protein complexes were found in the database. Four crystal structures of ppGpp-riboswitch complex were also found. The protein structures in complex with ppGpp and pppGpp were uploaded to the Arpeggio server (Jubb et al., 2017). Arpeggio server, based on Python, extract the interaction data between atoms located within 5 Å radial cutoff. The interaction results of each structures were downloaded from the server and converted to tabular form. The columns containing interactions involving proximal, clashes, covalent bond, halogen bonds, hydrophobic, carbonyl were removed before calculations. The nine interaction parameters were included in the interaction calculations including, van der Waal's clashes, van der Waal's interactions, hydrogen bonds, weak hydrogen bonds, ionic, metal complex, aromatic, polar, and weak polar interactions. The stereochemical parameters for the definition of interatomic interactions in the Arpeggio program are employed from the CREDO database (Marcou and Rognan, 2007; Schreyer and Blundell, 2009). The hydrogen bonds were considered as the distance at 2.8 to 3.5 Å and the angle between 120 and 180° while weak hydrogen bonds were shorter than 2.8 Å and having an angle less than 120°(Marcou and Rognan, 2007). The van der Waal's interactions are defined as interactions between two non-hydrogen bonding atoms which are present in their van der Waal's radii of corresponding atoms. The distance parameters for van der Waal's interactions and clashes in the Arpeggio program are taken from Open Babel. All these interactions for 33 complexes of (p)ppGpp-protein are provided in the table (**Supplementary Table S1**). The occurrence of these non-covalent interactions between (p)ppGpp and functional class of protein was plotted to identify the binding pattern of (p)ppGpp to respective class. For the sake of clarity, the two-dimensional interaction diagrams of each representative (p)ppGpp-protein complex were also plotted using the PoseView tool from the Protein Plus server (Stierand et al., 2006; Fährrolfes et al., 2017).

RESULTS AND DISCUSSION

Structural Dynamics of Unbound (p)ppGpp

Molecular dynamics simulation is one of the most commonly used approaches to understand structural dynamics of biomolecules in solution state (Karplus and Petsko, 1990; Karplus and McCammon, 2002; Hollingsworth and Dror, 2018). It has been an efficient choice for the characterization of structural dynamics of free nucleotides and nucleic acid (Stern et al., 2010; Kobayashi et al., 2013; Šponer et al., 2014; Wang et al., 2017; Mlýnský and Bussi, 2018; Cassone et al., 2019). However,

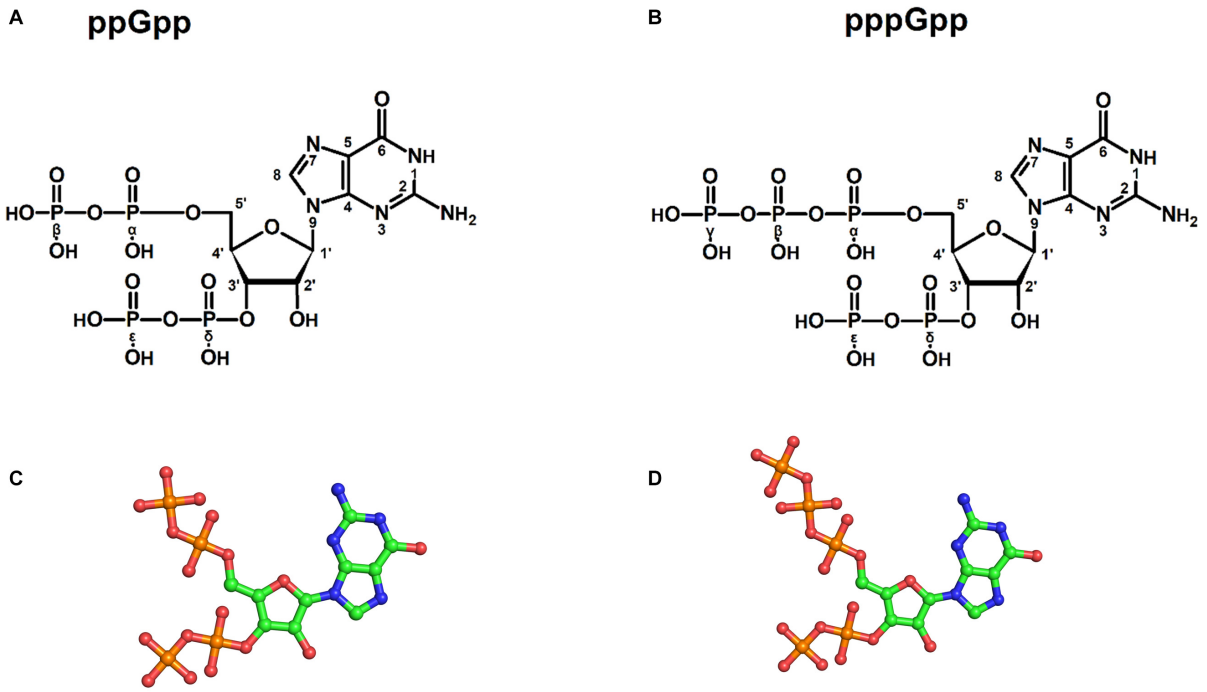

FIGURE 1 | Structures of (p)ppGpp signaling nucleotides: a two-dimensional chemical sketch of ppGpp **(A)**, and pppGpp **(B)**. Ball and stick model of ppGpp **(C)**, and pppGpp **(D)**. The color coding for atoms in ball stick model is displayed as follows; green-carbon, blue-nitrogen, red-oxygen, and orange-phosphorous atoms.

classical MD simulations studies on small molecules such as free nucleotides are challenging due to the presence of high energy barriers of the glycosidic bond between nucleotide base and ribose sugar as well as conformational flexibility of ribose moiety (Wang et al., 2017; Wang and Berne, 2018; Yang et al., 2019). To overcome the sampling issue, the replica-exchange method has been explored previously on small biomolecules to enhance sampling to cover more conformation space (Smith et al., 2016; Wang and Berne, 2018). Recently, cyclic nucleotides and small nucleic acid have been characterized for structural dynamics using REMD enhanced sampling methods (Šponer et al., 2014; Wang et al., 2017; Mlýnský and Bussi, 2018).

We used a well-defined protocol for REMD simulation to obtain the structural dynamics information of unbound ppGpp and pppGpp nucleotides in the solution state. A total of eight replicas simulation were exchanged at the 273, 285, 298, 310, 323, 335, 348, 360, 373 K during simulation covering temperature range from 273 to 373 K (**Supplementary Figure S1**). As shown in the graph, the RMSF, a parameter for displacement measurement of an atom in a molecular simulation trajectory in comparison with reference position, indicates that the major structural changes in (p)ppGpp molecules are observed (**Figures 2A,B**). There are 18 torsion bonds in pppGpp and 15 torsion bonds in ppGpp which can rotate therefore higher RMSF values are observed in these corresponding atoms. Although the negatively charged phosphate groups were neutralized by two Mg^{2+} ions during the simulation, yet higher flexibility of phosphate atoms was observed in the RMSF plot. In contrast to (p)ppGpp, the phosphate groups in cyclic messenger nucleotides show lesser flexibility due to the unavailability of free phosphate chains (Stern et al., 2010; Wang et al., 2017; Cassone et al., 2019). Based on our results, we propose that the dynamics in two free phosphate chains may provide greater flexibility to (p)ppGpp nucleotides for binding to diverse proteins. Surprisingly, the higher value of RMSF was observed in the NH_2 group of guanine ring of (p)ppGpp in REMD simulation. The detailed analysis of molecular properties shows the overall quality and conformational dynamics of (p)ppGpp during the simulation (**Figures 3A,B**). These graphs show that molecular properties in ppGpp and pppGpp are similar, however, there are minor differences in these values that may be because of additional phosphate group present in pppGpp. The higher RMSD and rGyr show the conformational flexibility which indicates that (p)ppGpp nucleotides show dynamics in the unbound states which is necessary to accommodate in the various types of the binding site. The other important parameter of (p)ppGpp nucleotides is the SASA which depicts the surface area of molecules accessible by the water molecules. The higher SASA values of (p)ppGpp contribute water-mediated interactions to the proteins and it is consistent with structures of (p)ppGpp-protein-complexes. The molecular parameters including rGyr, intraHB, MolSA, SASA, and PSA exhibit slightly higher value for pppGpp as compare to ppGpp because of an additional γ phosphate group present in pppGpp. In addition to inter-molecular non-covalent interactions, water-mediated hydrogen bonds play a significant role in stabilizing small molecules in the binding site of the protein.

TABLE 1 | List of available structures in complex with (p)ppGpp (ligand code G4P C1Z, and 0o2) in Protein Data Bank. The references are provided within the main text.

S.No	Macromolecule Name	Resolution (Å)	PDB ID
1	SAS1 (RelQ)	2.94	5DED
2	SAS2 (RelP)	2.78	6EX0
3	Rel_{Tt}	2.75	6S2T
4	SPO0B-associated GTP-binding protein	2.60	1LNZ
5	GTP-binding protein TypA/BipA	3.31	4ZCM
6	GTPase RbgA	1.80	6G14
7	GTPase RbgA	1.65	6G15
8	GTP-binding protein	4.00	5A9Y
9	Amidophosphoribosyltransferase PurF	1.95	6CZF
10	Hypoxanthine phosphoribosyltransferase	2.10	6D9S
11	Xanthine phosphoribosyltransferase	1.80	6W1I
12	Guanylate kinase	1.65	4QRH
13	Nucleosidase PpnN	2.77	6GFM
14	Putative phosphoribosyltransferase	1.50	5VOG
15	RNA polymerase	2.70	1SMY
16	RNA polymerase	3.90	4JK1
17	RNA polymerase	4.20	4JKR
18	RNA polymerase	2.71	5TMC
19	RNA polymerase	4.20	4JK2
20	RNA polymerase	4.29	5VSW
21	RNA polymerase	3.58	6WRG
22	RNA polymerase	3.62	6WRD
23	Exopolyphosphatase	2.71	2J4R
24	Guanosine pentaphosphate phosphohydrolase	2.76	6PC1
25	Peptide chain release factor 3	3.00	3VR1
26	Acetyltransferase A	2.34	4HNX
27	Acetyltransferase A	2.81	4XPD
28	Acetyltransferase A	3.95	4Y49
29	PRPP riboswitch	3.10	6CK4
30	ppGpp Riboswitch	2.20	6DMC
31	ppGpp Riboswitch	2.65	6DMD
32	ppGpp Riboswitch	2.70	6DME
33	DNA primase	2.01	4EDV
34	DNA primase	2.00	4EDT
35	Lysine decarboxylase, inducible	2.00	3N75
36	Aldo-keto reductase family protein	3.62	6GTM
37	Stringent starvation protein A	2.80	5U51
38	RNA pyrophosphohydrolase	2.06	6VCL

Structural Comparison of (p)ppGpp in Unbound and Bound State

The three-dimensional structures of unbound (p)ppGpp were obtained by energy minimization in Maestro. The structural coordinates of bound (p)ppGpp were extracted from structures of (p)ppGpp-protein complexes. The structural alignment of unbound state and bound state of (p)ppGpp shows substantial similarity in the guanine ring region with RMSD of atoms less than one. However, the phosphate chain shows divergence upon structural alignment which is in agreement with our simulation RMSF plot.

(p)ppGpp nucleotides exhibit a substantial extent of conformational flexibility because of various rotatable torsion angles present in the structure particularly a ribose ring (**Figure 4**). Therefore, we analyzed the glycosidic bond conformation of (p)ppGpp in unbound and bound states. The glycosidic conformation signifies the orientation of base and sugar in nucleotides and is measured as a torsion angle (χ) between O4'-C1'-N9-C4 of guanine. As shown in **Figure 5**, the distribution frequency of glycosidic bond conformation in both nucleotides observed during REMD was mostly in *syn* conformation, however, some occurrences were observed in *anti* conformation. Our results on the frequency distribution of glycosidic conformation in unbound states are similar to those observed in the bound states in the crystal structure. As most of the structures of (p)ppGpp-protein complexes have *anti* conformation of glycosidic bond except in few cases it was found in *syn* conformation such as nucleosidase (6GFM) (Zhang et al., 2019), lysine decarboxylase (3N75) (Kanjee et al., 2011). The sugar pucker in (p)ppGpp nucleotides in the bound state is observed majorly in *endo* conformation (**Table 2**). Whereas, the sugar pucker conformation energy minimized unbound states are found as *exo* for ppGpp and pppGpp (**Table 2**). The five endocyclic torsion angles, ν_0, ν_1, ν_2, ν_3, and ν_4, of backbone atoms, define the conformation description of the ribose sugar (**Figure 4**). The ribose sugar of (p)ppGpp nucleotides shows substantial conformational flexibility in unbound and bound states (**Table 2**). Additional parameters to characterize ribose sugar conformation are pseudorotational phase angle (P) and maximum puckering amplitude (ν_{max}) which show that ribose sugar adopts north conformation in both states (Sun et al., 2004). The comparative description of these torsion angles is given in the **Table 2** for unbound states and few bound states of (p)ppGpp. All these parameters indicate that ribose moiety in (p)ppGpp behave dynamically in both unbound and bound states.

Interactions Between (p)ppGpp and Proteins

The structural diversity of secondary messenger nucleotides deliver generous adaptability for the binding to the cognate proteins. Based on their structural architecture, these nucleotides may be divided into two classes; linear and cyclic secondary nucleotides. The interaction analysis of cyclic secondary nucleotides with their binding protein complexes have been characterized extensively (Moodie and Thornton, 1993; Wang et al., 2017; Cassone et al., 2019; He et al., 2020). These studies provide significant information about the binding mode and interaction pattern of cyclic nucleotides and their protein complexes (He et al., 2020). Similarly, linear secondary messenger nucleotides, (p)ppGpp binds to a diverse class of proteins and should exhibit a particular binding mode for each functional class of protein. We have examined these interaction patterns using various computational tools to assess the binding stereochemistry between (p)ppGpp and respective protein. A detailed survey has been carried out on available structures of (p)ppGpp-protein complexes and the non-covalent interactions were

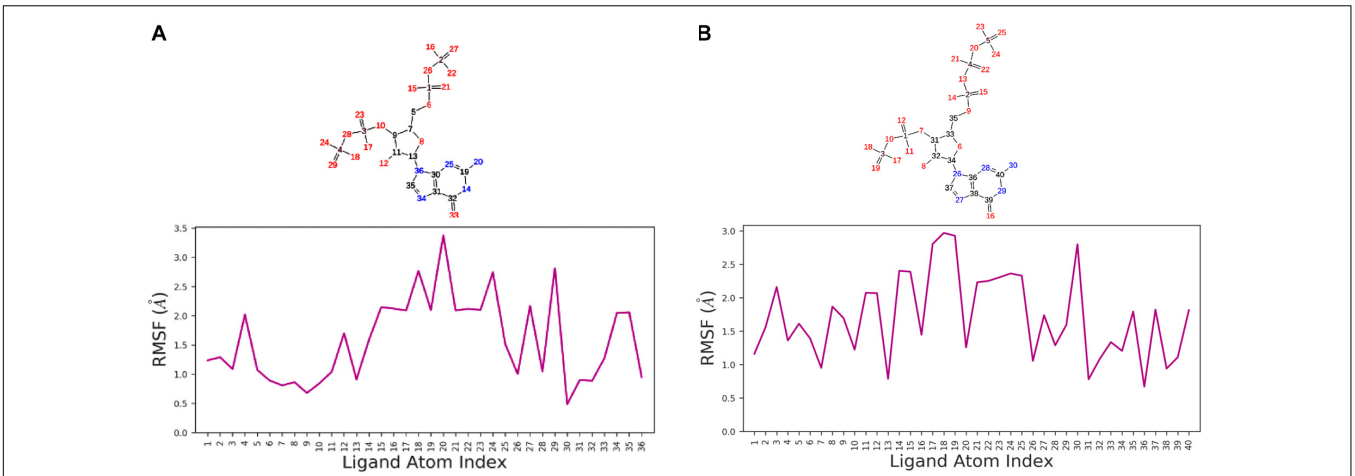

FIGURE 2 | Replica exchange molecular dynamics simulation analysis. Atom numbering at top panel and root-mean-square fluctuation (RMSF) plot for ppGpp **(A)** and pppGpp **(B)** displays the fluctuation in individual atoms with reference to an initial state.

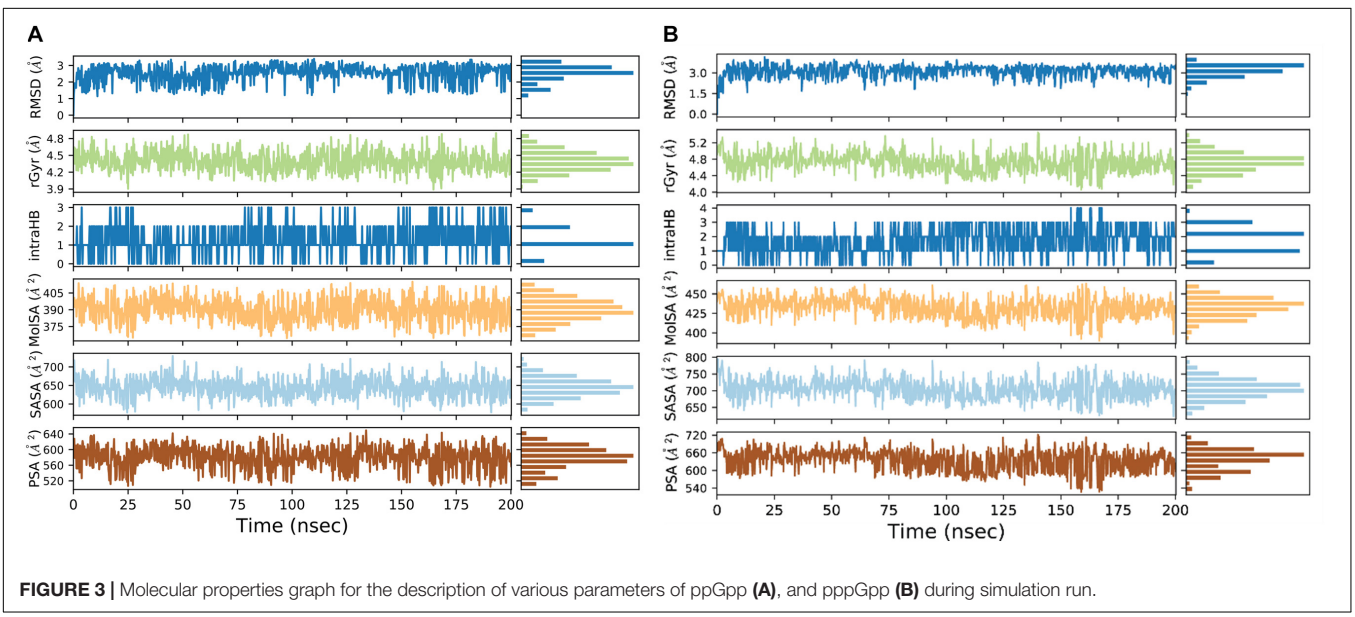

FIGURE 3 | Molecular properties graph for the description of various parameters of ppGpp **(A)**, and pppGpp **(B)** during simulation run.

quantified (**Figure 6A**). In addition to conventional interatomic interactions, various other types of molecular interaction fingerprints were included in the study which provides additional information for binding stability of ligand (Marcou and Rognan, 2007). Other types of non-conventional interactions that were included in the analysis are weak polar and weak hydrogen bonds that denote the hydrogen bonds without considering angles. A total of five major types of bonding parameters were included in the analysis interactions between (p)ppGpp and proteins. Among these interactions, hydrogen bonds contribute most as five nitrogen and 17 oxygen atoms in the (p)ppGpp have properties to make hydrogen bonds (**Figure 6B**). In the structures of many complexes, the phosphate group of (p)ppGpp nucleotide is observed as making interaction to protein through Mg^{2+} ions. As seen by the hydrogen bonds histogram, the major interatomic polar interactions were observed in guanine ring and phosphate group atoms. The aromatic ring of guanine had π-π base stacking interactions with the side chain of tyrosine in the structures of (p)ppGpp synthetases and nucleotide metabolic enzymes. The ribose moiety of (p)ppGpp makes comparatively fewer interactions with protein atoms which may be the consequence of the structural restrain of the ribose ring. Similarly, van der Waal's interactions were found majorly in the region of the guanine ring of (p)ppGpp (**Figure 6C**). The available structures of the complexes between (p)ppGpp and protein span several functional classes. Here the characterization of (p)ppGpp-protein interactions focuses only on four major functional classes.

(p)ppGpp Synthetase

The (p)ppGpp synthetases are apparent (p)ppGpp binding proteins as these enzymes synthesize ppGpp and pppGpp from

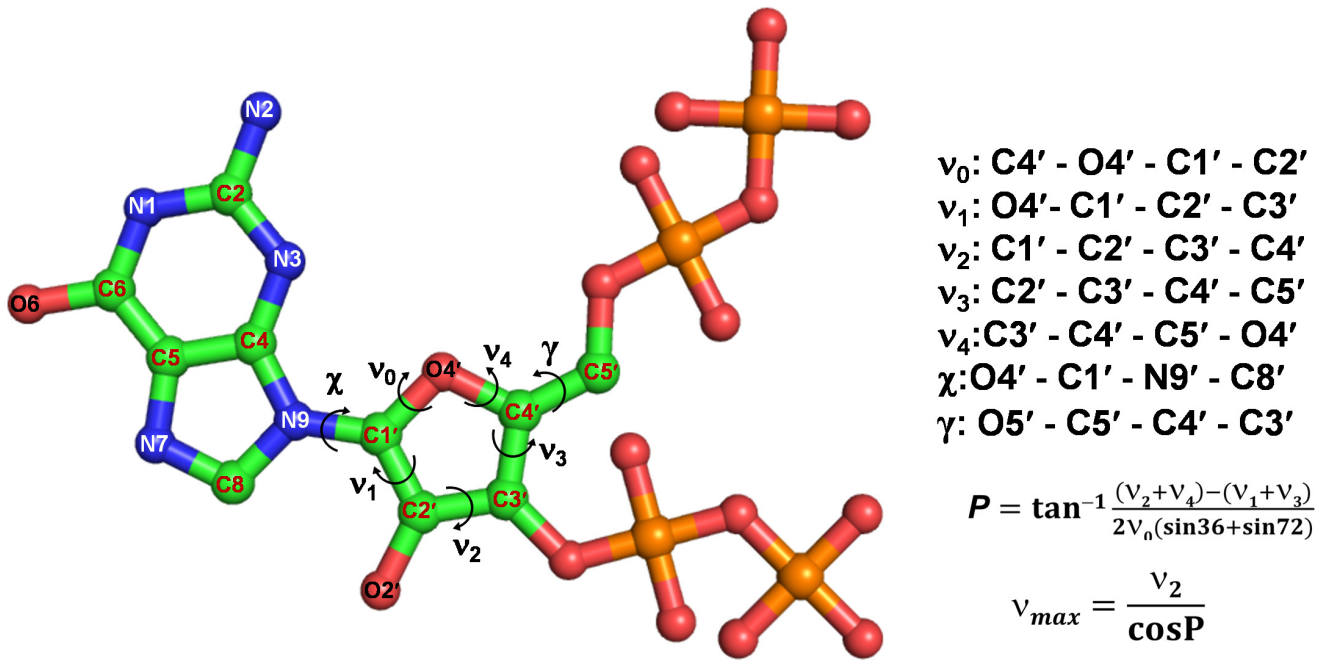

FIGURE 4 | Different torsion angles in the structure of (p)ppGpp. The glycosidic torsion angle (χ) depicts the rotation between guanine and ribose ring, the angle γ denotes rotation between ribose ring and C4 branch of ribose sugar. The torsion angles of ribose rings are denoted from ν_0 to ν_4.

ATP and GDP/GTP, respectively. However, most of the structures determined so far are in complexes with substrate analogs as these complexes explain the catalytic mechanism. A brief structural review on (p)ppGpp synthetase proteins has been described previously (Kushwaha et al., 2019b) hence current study focus only on (p)ppGpp and (p)ppGpp synthetase complexes. There are three structures of (p)ppGpp synthetases available in the Protein Data Bank in complex with (p)ppGpp. It includes two single domain (p)ppGpp synthetases, small alarmone synthetase-1 (SAS1) from *Bacillus subtilis* (Steinchen et al., 2015); small alarmone synthetase-2 (SAS2) from *Staphylococcus aureus* (Manav et al., 2018) and one long (p)ppGpp synthetase Rel_{Tt} from *Thermus thermophiles* (Tamman et al., 2020). The (p)ppGpp binding site is primarily comprised of polar residues which hold the (p)ppGpp strongly by making several hydrogen bonds. The most distinguishing feature of these complexes is aromatic stacking with the guanine ring which is stacked by the side chain-ring of tyrosine. The negatively charged phosphate groups are stabilized by ionic interactions with the guanidinium group of several arginine residues. The Mg^{2+} ions also contribute to stabilizing these phosphate groups. As shown the **Figure 7A**, the nitrogen and oxygen atoms of the guanine ring significantly contribute to the hydrogen bond interactions with (p)ppGpp synthetase proteins. This type of binding pattern of (p)ppGpp may be considered as an optimum binding pattern for (p)ppGpp interactions with proteins.

Nucleotide Metabolic Enzymes

There are six crystal structures of (p)ppGpp and nucleotide metabolic enzymes complexes available in the Protein Data Bank which includes Xanthine phosphoribosyltransferase (XPRT) (Anderson et al., 2020), Pyrimidine/purine nucleotide 5′-monophosphate nucleosidase (nucleosidase, PpnN) (Zhang et al., 2019), Hypoxanthine phosphoribosyltransferase (HPRT) (Anderson et al., 2019), Amidophosphoribosyltransferase (PurF) (Wang et al., 2019), Guanylate kinase (Liu et al., 2015; **Table 1**). A most striking feature of the structures of these enzyme-(p)ppGpp complexes are oligomeric stoichiometry in these complexes. The (p)ppGpp nucleotides facilitates the oligomeric cooperation through binding at an oligomeric interface. Similar to (p)ppGpp synthetases, (p)ppGpp binding site in these enzymes is primarily comprised of residues containing side chains with the polar groups for hydrogen bonding and aromatic ring for stacking interactions. The characteristic feature of (p)ppGpp binding to enzymes involved in nucleotide metabolism is aromatic stacking interaction between guanine base of (p)ppGpp and the aromatic ring-containing side chain of residues of corresponding binding proteins (**Figure 7B**). For example, Phe126 in XPRT, Trp153 in XGPRT, Tyr346 in PpnN, Phe152 in HPRT, Tyr83 in guanylate kinase makes stacking interactions. However, the aromatic stacking was not observed in the structure of PurF-ppGpp complex. The ribose ring generally interacted with protein though water-mediated hydrogen bonds interactions. The negatively charged phosphate groups of (p)ppGpp nucleotides are stabilized by mostly guanidine moiety of arginine side chains and Mg^{2+} ions. Therefore, these interactions are considered as ionic interactions. The observed binding mode of (p)ppGpp to the nucleotide enzymes is similar due to an analogy of substrate nucleotide structure to the (p)ppGpp. As shown in the graph, the N1, N2, N7, and O6 atoms

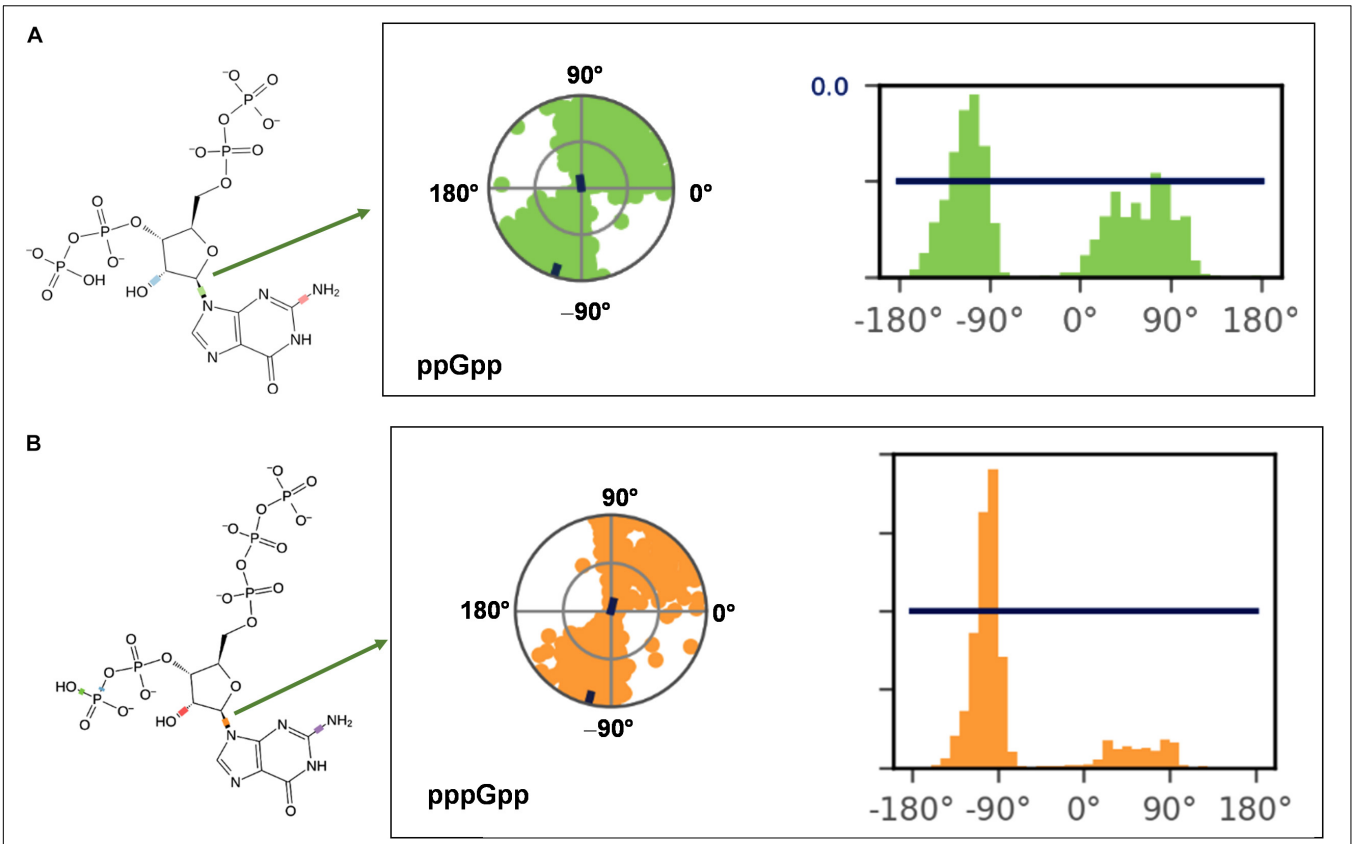

FIGURE 5 | Probable frequency distribution of glycosidic torsion angle (χ) conformation in ppGpp **(A)** and pppGpp **(B)** during REMD simulation. The radial plot denotes the conformation of glycosidic bond throughout the simulation time course. The beginning of the simulation started at the center of a circle and radially outward portrays time evolution during the simulation run. The bar diagram representation of the distribution data of torsion angle. *X*-axis denotes the angle of glycosidic bond and *Y*-axis shows the number of times the bond was observed at this angle i.e., percentage frequency distribution. The value of χ falls into ranges of +90 to +180° (or 180 to 270°) corresponds to *anti* conformation while the value χ founds in the ranges of –90 to +90° refers to *syn* conformation of glycosidic bond.

TABLE 2 | Pseudorotational phase angle and puckering amplitude for (p)ppGpp nucleotides.

(p)ppGpp state	PDB	ν_0	ν_1	ν_2	ν_3	ν_4	*P*	ν_{max}	χ	γ	Sugar pucker
Unbound	ppGpp	−6.88	26.92	−35.87	33.24	−16.53	188.23	36.24	−99.58	−172.55	C3′-exo
Unbound	pppGpp	−7.88	26.79	−34.64	31.48	−14.82	186.23	34.85	84.22	−177.41	C3′-exo
(p)ppGpp synthetase	6EX0	−8.46	−13.71	31.52	−37.17	27.46	31.47	36.96	171.65	61.18	C3′-endo
RNA polymerase	5VSW	−13.05	25.53	−27.83	19.75	−4.28	170.36	28.23	−116.08	−177.02	C2′-endo
GTPase RbgA	6G14	−22.30	33.40	−32.51	18.75	2.27	158.59	34.92	−112.79	53.43	C2′-endo
Nucleosidase	6GFM	−32.38	44.35	−38.72	19.11	8.42	151.01	44.27	65.89	−143.14	C2′-endo

of the aromatic guanine ring of (p)ppGpp is a major contributor to hydrogen bond interaction with protein residues.

GTP Binding GTPase Proteins

There are five crystal structures of GTP binding GTPase proteins in complex with (p)ppGpp available till now. These include Obg GTP binding protein (Buglino et al., 2002), GTPase BipA/TypA (Fan et al., 2015), GTPase BipA (Kumar et al., 2015), and GTPase RbgA (Pausch et al., 2018). The (p)ppGpp binding site in GTPases proteins are shallower in comparison to (p)ppGpp synthetases and nucleotide metabolic enzymes. In contrast to (p)ppGpp synthetases, and nucleotide metabolic enzymes, aromatic stacking and guanidinium moiety was not observed in the structures of GTPases in complexes with (p)ppGpp. Interestingly, the major interaction of (p)ppGpp guanine ring was contributed by the O6 atom of (p)ppGpp (**Figure 7C**). The metal ions were also not observed to neutralize the negatively charged phosphate group of (p)ppGpp. Therefore, the major forces for the stabilization of (p)ppGpp are hydrogen bonds and van der Waal's interactions.

RNA Polymerase

RNA polymerase was the first protein complex reported to regulate its activity by binding of (p)ppGpp

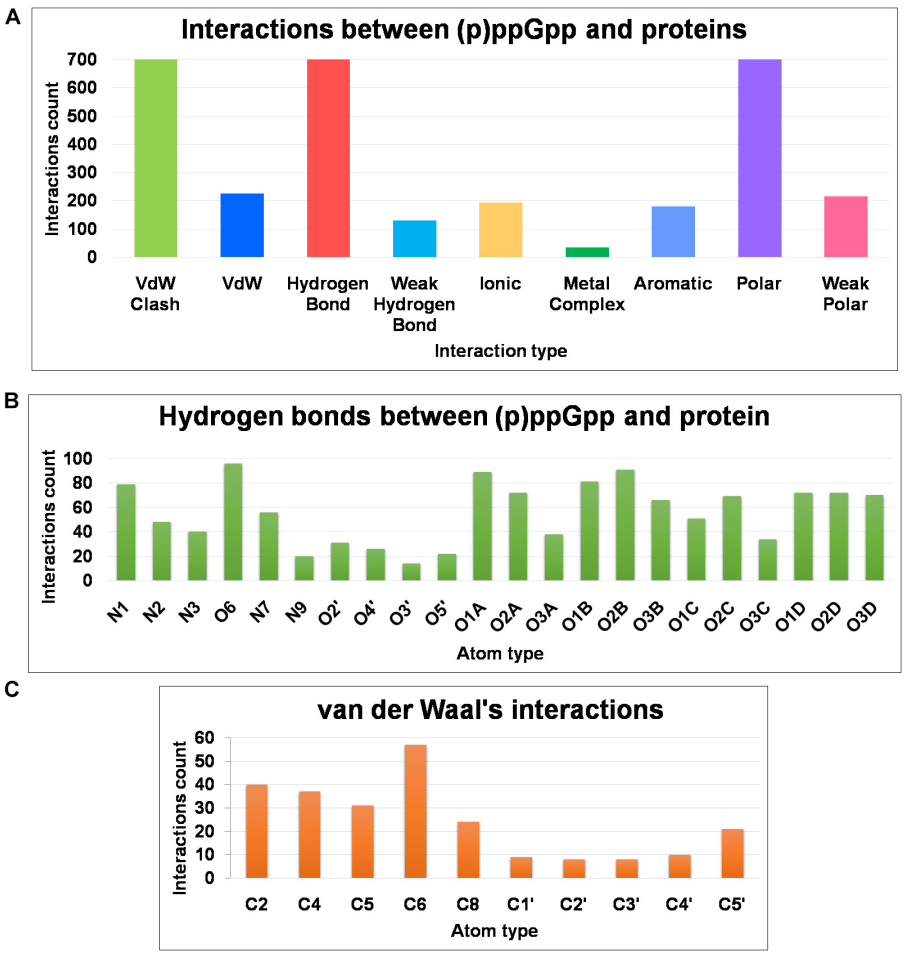

FIGURE 6 | Frequency distribution of non-covalent interactions, between (p)ppGpp and protein, extracted from available crystal structures of (p)ppGpp-protein complexes. **(A)** Various types of inter-molecular interactions and their occurrences. **(B)** Atom-level distribution frequency of hydrogen bonds found in the (p)ppGpp-protein complexes. **(C)** Atom-level distribution frequency of van der Waal's interactions found between (p)ppGpp and protein.

(Potrykus and Cashel, 2008). There are two (p)ppGpp binding sites that have been reported in the RNA polymerase which modulates allosteric transcription regulation (Molodtsov et al., 2018). Site 1 is located at the interface formed by β′ and ω subunits of RNA polymerase. This site is comparatively shallower and the guanine ring of (p)ppGpp interacts with the side chain of arginine, isoleucine, histidine, and aspartic acid residues. The second (p)ppGpp binding site is found at the secondary channel and it acts synergistically by the binding of a transcription regulator protein, DksA. Therefore, complete binding of (p)ppGpp to site 2 is accomplished by the interactions between (p)ppGpp and residues of β′ rim and DksA. In the site 2, the guanine ring of (p)ppGpp is stabilized by interactions between (p)ppGpp and side chains of aspartic acid, tyrosine, asparagine, and isoleucine while negatively charged phosphate group is neutralized by basic residues such as lysine and arginine (**Figure 7D**). The binding of (p)ppGpp to site 2, exhibit a allosteric change in the corresponding areas of RNAP and DksA to facilitate transcription regulation.

Other (p)ppGpp Binding Proteins

There are several crystal structures of various other functional class of (p)ppGpp binding proteins reported including translation peptide chain release factor 3 (PDB: 3VR1) (Kihira et al., 2012), acetyltransferase A (PDB: 4HNX, 4XPD, 4Y49), PPX/GppA phosphatases (PDB: 2J4R, 6PC1) (Kristensen et al., 2008; Song et al., 2020), DNA primase (PDB: 4EDV, 4EDT) (Rymer et al., 2012), lysine decarboxylase (PDB: 3N75) (Kanjee et al., 2011), aldo-keto reductase (PDB: 6GTM)and RNA pyrophosphohydrolase (PDB: 6VCL) (Gao et al., 2020). The PPX/GppA phosphatases are pppGpp hydrolyzing enzymes that remove the γ-phosphate group from pppGpp to make ppGpp nucleotide, therefore, pppGpp serves as a substrate for these enzymes. DnaG is a DNA dependent RNA polymerase primase, responsible for primer synthesis during DNA replication. DnaG primase binds to various nucleotides including (p)ppGpp nucleotides. Lysine decarboxylase is an acid response protein that catalyzes the decarboxylation of L-lysine. (p)ppGpp binds to Ldcl and inhibits its enzymatic activity. RppH is

Nudix hydrolase enzyme involved in RNA processing. It hydrolyzes various nucleotides including (p)ppGpp alarmone. The detailed interactions analysis and binding pattern of these (p)ppGpp-complexes are given in **Supplementary Figure S2**.

Role of Magnesium Ion in (p)ppGpp and Protein Interactions

Magnesium ion (Mg^{2+}) plays a significant role in the structural stability of nucleic acid and nucleotides by neutralizing highly negative charged phosphate groups (Black et al., 1994; Pechlaner and Sigel, 2012; Leonarski et al., 2017). Interestingly, highly phosphorylated (p)ppGpp has two linear chains of phosphate groups therefore Mg^{2+} ions assist in the specific interaction of (p)ppGpp to their target protein. As shown in the graph (**Figure 6**), we have observed several metal interactions in the structures of (p)ppGpp-protein complexes. In (p)ppGpp synthetases structures, Mg^{2+} ions provide robust physical support to the flexible phosphate chains. In the case of SAS1, one Mg^{2+} ion firmly stabilizes two phosphate chains with the side chain of Lys 32 while in the case of long-form of (p)ppGpp synthetase, Rel_{Tt}, it binds to only one chain of phosphate (Tamman et al., 2020). In addition to physical stability, Mg^{2+} ions assist in the deprotonation of 3′ OH of GDP/GTP by acidic residues in Rel_{Seq} and SAS1 (Hogg et al., 2004; Steinchen et al., 2015). Similarly, in the case of nucleotide metabolic enzymes,

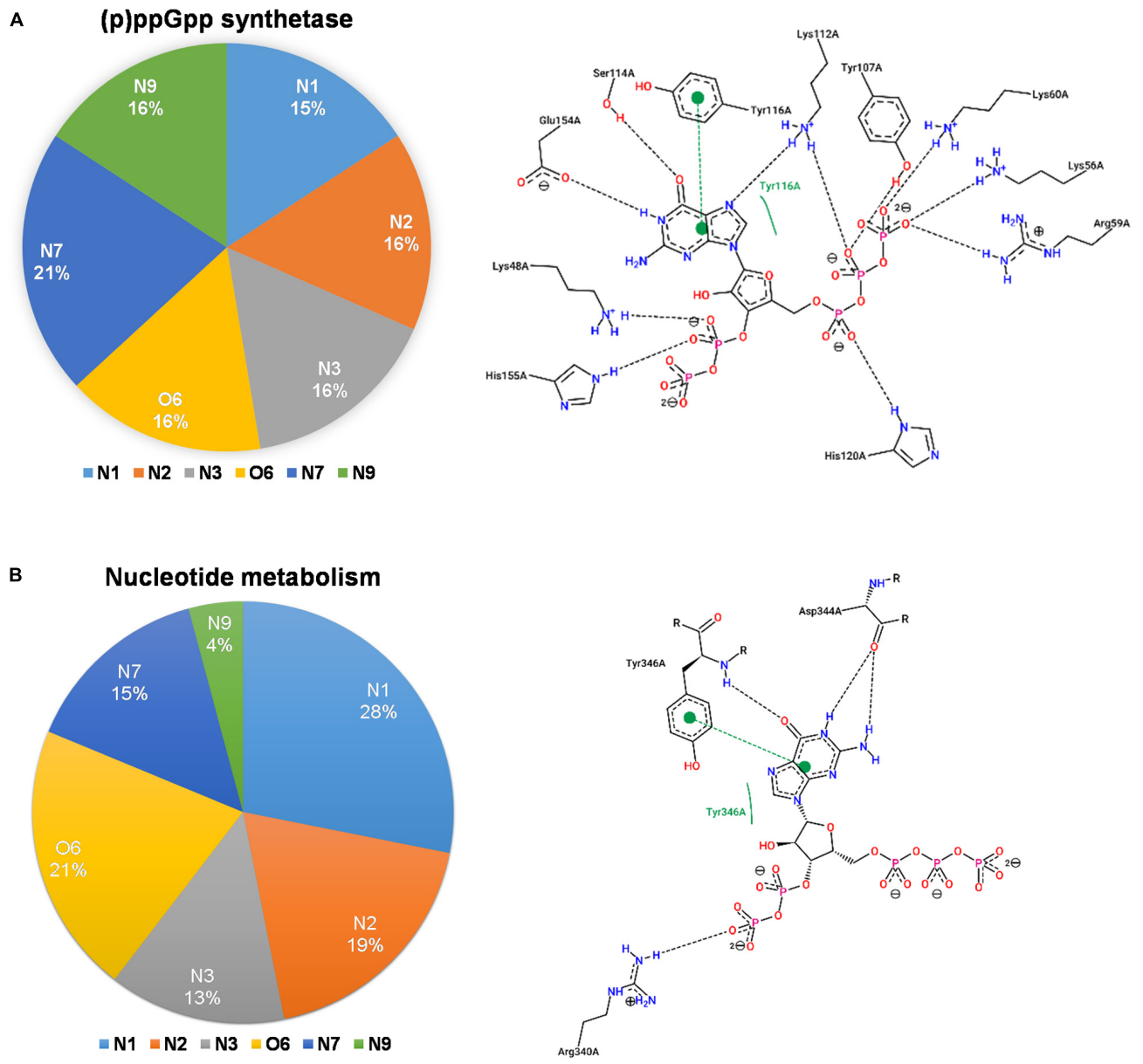

FIGURE 7 | Continued

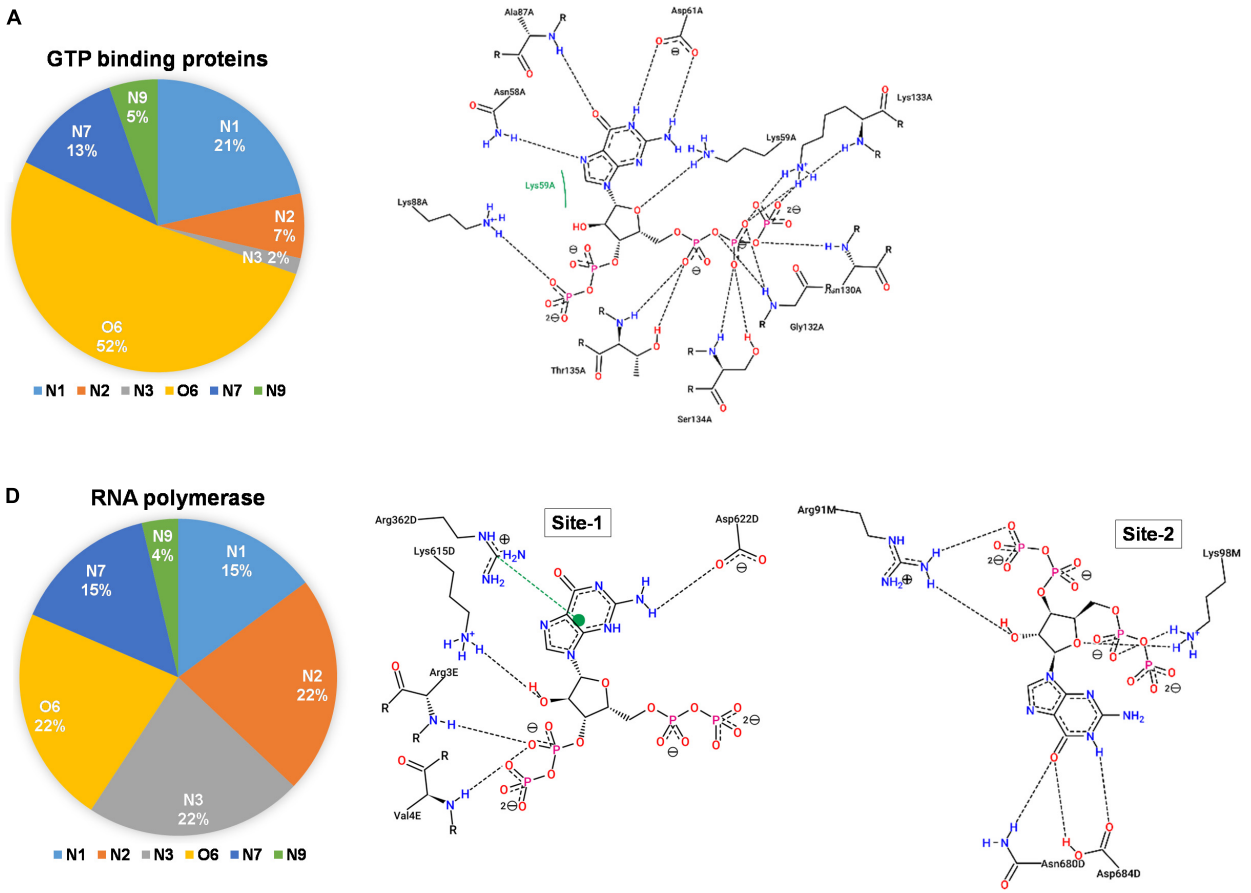

FIGURE 7 | Interactions between (p)ppGpp atoms and protein are identified in the crystal structures of (p)ppGpp-protein complexes. The left panel of each figure displays the frequency distribution of interactions formed by guanine atoms of (p)ppGpp with protein atoms. The right panel of each figure indicates the two-dimensional interaction diagram between (p)ppGpp and protein. The interaction plots, generated by PoseView tool, show hydrogen bonds between (p)ppGpp and protein. **(A)** (p)ppGpp synthetase (5DED), **(B)** nucleotide metabolic enzymes (6GFM), **(C)** GTPase (6G15), and **(D)** RNA polymerase (5VSW).

Mg^{2+} ions provide not only physical stability to one chain of (p)ppGpp but it also mediates interactions between (p)ppGpp and protein side chains. Each phosphate chain of (p)ppGpp is making interactions with one Mg^{2+} ion in the complex of RNA polymerase-(p)ppGpp. Altogether, we have observed Mg^{2+} ions in several other complexes of (p)ppGpp-protein structures except for few complexes which may be the limitation of electron density interpretation as discussed earlier (Leonarski et al., 2017).

CONCLUSION

Secondary messenger nucleotides are key signaling molecules that modulate several cellular functions particularly in response to environmental changes. These nucleotides bind to several enzymes involve in various functional activities. The versatility of the binding mode of secondary nucleotides is facilitated by the conformation flexibility of glycosidic bond, ribose sugar puckering. In contrast to the cyclic nucleotides, (p)ppGpp have linear phosphate chains that provide additional flexibility to adapt various conformations according to the stereochemistry of the binding site of a respective target protein. Overall, our results support the hypothesis that the conformation flexibility of glycosidic bond, ribose sugar puckering, and phosphate groups provide structural plasticity to the (p)ppGpp for binding to the various functional class of proteins. The structures of unbound ppGpp and pppGpp in solution states obtained by MD simulation are similar to that observed in the structures in bound form, hence, these structures resemble biologically active conformations of (p)ppGpp. The gyration conformation profile of glycosidic bond is in agreement with the conformation of (p)ppGpp observed in the bound state. The analysis of (p)ppGpp-protein interactions reveals that the binding pattern of these nucleotides governs the regulation for a particular class of target proteins.

DATA AVAILABILITY STATEMENT

The original contributions presented in the study are included in the article/**Supplementary Material**, further inquiries can be directed to the corresponding author/s.

AUTHOR CONTRIBUTIONS

GK and NB conceptualized the study. GK and AP performed the study. All authors analyzed the data, wrote and edited the manuscript, and agreed on the final version of the manuscript.

FUNDING

This study was supported by Science and Engineering Research Board (SERB), Government of India (SB/YS/LS-176/2014), and ICGEB, New Delhi core funds. GK was supported by grant no. BT/IC-06/003/91-Flagship proposal, from the DBT, Government of India. AP is a recipient of Council of Scientific and Industrial Research (CSIR) Senior Research Fellowship.

SUPPLEMENTARY MATERIAL

The Supplementary Material for this article can be found online at: https://www.frontiersin.org/articles/10.3389/fmicb.2020.575041/full#supplementary-material

REFERENCES

Abranches, J., Martinez, A. R., Kajfasz, J. K., Chávez, V., Garsin, D. A., and Lemos, J. A. (2009). The molecular alarmone (p)ppGpp mediates stress responses, vancomycin tolerance, and virulence in *Enterococcus faecalis*. *J. Bacteriol.* 191, 2248–2256. doi: 10.1128/JB.01726-08

Anderson, B. W., Hao, A., Satyshur, K. A., Keck, J. L., and Wang, J. D. (2020). Molecular mechanism of regulation of the purine salvage enzyme XPRT by the AlarmonespppGpp, ppGpp, and pGpp. *J. Mol. Biol.* 432, 4108–4126. doi: 10.1016/j.jmb.2020.05.013

Anderson, B. W., Liu, K., Wolak, C., Dubiel, K., She, F., Satyshur, K. A., et al. (2019). Evolution of (P)ppGpp-HPRT regulation through diversification of an allosteric oligomeric interaction. *Elife* 8:e47534. doi: 10.7554/eLife.47534

Atkinson, G. C., Tenson, T., and Hauryliuk, V. (2011). The RelA/SpoT Homolog (RSH) superfamily: distribution and functional evolution of ppGppSynthetases and hydrolases across the tree of life. *PLoS One* 6:e23479. doi: 10.1371/journal.pone.0023479

Beljantseva, J., Kudrin, P., Andresen, L., Shingler, V., Atkinson, G. C., Tenson, T., et al. (2017). Negative allosteric regulation of *Enterococcus faecalis* small alarmonesynthetaseRelQ by single-stranded RNA. *Proc. Natl. Acad. Sci. U. S. A.* 114, 3726–3731. doi: 10.1073/pnas.1617868114

Berman, H. M., Westbrook, J., Feng, Z., Gilliland, G., Bhat, T. N., Weissig, H., et al. (2000). The protein data bank. *Nucleic Acids Res.* 28, 235–242. doi: 10.1093/nar/28.1.235

Black, C. B., Huang, H. W., and Cowan, J. A. (1994). Biological coordination chemistry of magnesium, sodium, and potassium ions.Protein and nucleotide binding sites.Coord. *Chem. Rev.* 135–136, 165–202. doi: 10.1016/0010-8545(94)80068-5

Buglino, J., Shen, V., Hakimian, P., and Lima, C. D. (2002). Structural and biochemical analysis of the Obg GTP binding protein. *Structure* 10, 1581–1592. doi: 10.1016/S0969-2126(02)00882-1

Bærentsen, R. L., Brodersen, D. E., and Zhang, Y. E. (2019). Evolution of the bacterial nucleosidasePpnN and its relation to the stringent response. *Microb. Cell* 6, 450–453. doi: 10.15698/mic2019.09.692

Cashel, M., and Gallant, J. (1969). Two compounds implicated in the function of the RC gene of *Escherichia coli*. *Nature* 221, 838–841.

Cashel, M., Gentry, D., Hernandez, V. J., and Vinella, D. (1996). "The stringent response," in *Escherichia coli and Salmonella: Cellular and Molecular Biology*, ed. F. C. Neidhardt (Washington, DC: ASM Press), 1458–1496.

Cassone, G., Kruse, H., and Sponer, J. (2019). Interactions between cyclic nucleotides and common cations: an: ab initio molecular dynamics study. *Phys. Chem. Chem. Phys.* 21, 8121–8132. doi: 10.1039/c8cp07492e

Dalebroux, Z. D., Svensson, S. L., Gaynor, E. C., and Swanson, M. S. (2010). ppGpp conjures bacterial virulence. *Microbiol. Mol. Biol. Rev.* 74, 171–199. doi: 10.1128/MMBR.00046-09

Dalebroux, Z. D., and Swanson, M. S. (2012). ppGpp: magic beyond RNA polymerase. *Nat. Rev. Microbiol.* 10, 203–212. doi: 10.1038/nrmicro2720

Fährrolfes, R., Bietz, S., Flachsenberg, F., Meyder, A., Nittinger, E., Otto, T., et al. (2017). Proteins plus: a web portal for structure analysis of macromolecules. *Nucleic Acids Res.* 45, W337–W343. doi: 10.1093/nar/gkx333

Fan, H., Hahm, J., Diggs, S., Perry, J. J. P., and Blaha, G. (2015). Structural and functional analysis of BipA, a regulator of virulence in enteropathogenic *Escherichia coli*. *J. Biol. Chem.* 290, 20856–20864. doi: 10.1074/jbc.M115.659136

Gao, A., Vasilyev, N., Kaushik, A., Duan, W., and Serganov, A. (2020). Principles of RNA and nucleotide discrimination by the RNA processing enzyme RppH. *Nucleic Acids Res.* 48, 3776–3788. doi: 10.1093/nar/gkaa024

Hauryliuk, V., and Atkinson, G. C. (2017). Small alarmone synthetases as novel bacterial RNA-binding proteins. *RNA Biol.* 14, 1695–1699. doi: 10.1080/15476286.2017.1367889

Hauryliuk, V., Atkinson, G. C., Murakami, K. S., Tenson, T., and Gerdes, K. (2015). Recent functional insights into the role of (p)ppGpp in bacterial physiology. *Nat. Rev. Microbiol.* 13, 298–309. doi: 10.1038/nrmicro3448

He, J., Yin, W., Galperin, M. Y., and Chou, S. H. (2020). Cyclic di-AMP, a second messenger of primary importance: tertiary structures and binding mechanisms. *Nucleic Acids Res.* 48, 2807–2829. doi: 10.1093/nar/gkaa112

Hengge, R., Häussler, S., Pruteanu, M., Stülke, J., Tschowri, N., and Turgay, K. (2019). Recent advances and current trends in nucleotide second messenger signaling in bacteria. *J. Mol. Biol.* 431, 908–927. doi: 10.1016/j.jmb.2019.01.014

Hogg, T., Mechold, U., Malke, H., Cashel, M., and Hilgenfeld, R. (2004). Conformational antagonism between opposing active sites in a bifunctionalRelA/SpoT homolog modulates (p)ppGpp metabolism during the stringent response. *Cell* 117, 57–68. doi: 10.1016/S0092-8674(04)00260-0

Hollingsworth, S. A., and Dror, R. O. (2018). Molecular dynamics simulation for all. *Neuron* 99, 1129–1143. doi: 10.1016/j.neuron.2018.08.011

Jorgensen, W. L., Chandrasekhar, J., Madura, J. D., Impey, R. W., and Klein, M. L. (1983). Comparison of simple potential functions for simulating liquid water. *J. Chem. Phys.* 79, 926–935. doi: 10.1063/1.445869

Jubb, H. C., Higueruelo, A. P., Ochoa-Montaño, B., Pitt, W. R., Ascher, D. B., and Blundell, T. L. (2017). Arpeggio: a web server for calculating and visualising interatomic interactions in protein structures. *J. Mol. Biol.* 429, 365–371. doi: 10.1016/j.jmb.2016.12.004

Kanjee, U., Gutsche, I., Alexopoulos, E., Zhao, B., El Bakkouri, M., Thibault, G., et al. (2011). Linkage between the bacterial acid stress and stringent responses: the structure of the inducible lysine decarboxylase. *EMBO J.* 30, 931–944. doi: 10.1038/emboj.2011.5

Kanjee, U., Ogata, K., and Houry, W. A. (2012). Direct binding targets of the stringent response alarmone (p)ppGpp. *Mol. Microbiol.* 85, 1029–1043. doi: 10.1111/j.1365-2958.2012.08177.x

Karplus, M., and McCammon, J. A. (2002). Molecular dynamics simulations of biomolecules. *Nat. Struct. Biol.* 9, 646–652. doi: 10.1038/nsb0902-646

Karplus, M., and Petsko, G. A. (1990). Molecular dynamics simulations in biology. *Nature* 347, 631–639. doi: 10.1038/347631a0

Kihira, K., Shimizu, Y., Shomura, Y., Shibata, N., Kitamura, M., Nakagawa, A., et al. (2012). Crystal structure analysis of the translation factor RF3 (release factor 3). *FEBS Lett.* 586, 3705–3709. doi: 10.1016/j.febslet.2012.08.029

Kobayashi, E., Yura, K., and Nagai, Y. (2013). Distinct conformation of ATP molecule in solution and on protein. *Biophys.* 9, 1–12. doi: 10.2142/biophysics.9.1

Kriel, A., Bittner, A. N., Kim, S. H., Liu, K., Tehranchi, A. K., Zou, W. Y., et al. (2012). Direct regulation of GTP homeostasis by (p)ppGpp: a critical component of viability and stress resistance. *Mol. Cell* 48, 231–241. doi: 10.1016/j.molcel.2012.08.009

Kristensen, O., Ross, B., and Gajhede, M. (2008). Structure of the PPX/GPPA phosphatase from aquifexaeolicus in complex with the AlarmoneppGpp. *J. Mol. Biol.* 375, 1469–1476. doi: 10.1016/j.jmb.2007.11.073

Kudrin, P., Varik, V., Oliveira, S. R. A., Beljantseva, J., Del Peso Santos, T., Dzhygyr, I., et al. (2017). Subinhibitory concentrations of bacteriostatic antibiotics induce relA -dependent and relA -independent tolerance to β-Lactams. *Antimicrob. Agents Chemother.* 61:e2173-16. doi: 10.1128/AAC.02173-16

Kumar, V., Chen, Y., Ero, R., Ahmed, T., Tan, J., Li, Z., et al. (2015). Structure of BipA in GTP form bound to the ratcheted ribosome. *Proc. Natl. Acad. Sci. U. S. A.* 112, 10944–10949. doi: 10.1073/pnas.1513216112

Kushwaha, G. S., Bange, G., and Bhavesh, N. S. (2019a). Interaction studies on bacterial stringent response protein RelA with uncharged tRNA provide evidence for its prerequisite complex for ribosome binding. *Curr. Genet.* 65, 1173–1184. doi: 10.1007/s00294-019-00966-y

Kushwaha, G. S., Oyeyemi, B. F., and Bhavesh, N. S. (2019b). Stringent response protein as a potential target to intervene persistent bacterial infection. *Biochimie* 165, 67–75. doi: 10.1016/j.biochi.2019.07.006

Leonarski, F., D'Ascenzo, L., and Auffinger, P. (2017). Mg2+ ions: do they bind to nucleobasenitrogens? *Nucleic Acids Res.* 45, 987–1004. doi: 10.1093/nar/gkw1175

Liu, K., Myers, A. R., Pisithkul, T., Claas, K. R., Satyshur, K. A., Amador-Noguez, D., et al. (2015). Molecular mechanism and evolution of guanylate kinase regulation by (p)ppGpp. *Mol. Cell* 57, 735–749. doi: 10.1016/j.molcel.2014.12.037

Manav, M. C., Beljantseva, J., Bojer, M. S., Tenson, T., Ingmer, H., Hauryliuk, V., et al. (2018). Structural basis for (p)ppGpp synthesis by the *Staphylococcus aureus* small alarmonesynthetaseRelP. *J. Biol. Chem.* 293, 3254–3264. doi: 10.1074/jbc.RA117.001374

Marcou, G., and Rognan, D. (2007). Optimizing fragment and scaffold docking by use of molecular interaction fingerprints. *J. Chem. Inf. Model.* 47, 195–207. doi: 10.1021/ci600342e

Mechold, U., Murphy, H., Brown, L., and Cashel, M. (2002). Intramolecular regulation of the opposing (p)ppGpp catalytic activities of Rel(Seq), the Rel/Spo enzyme from *Streptococcus equisimilis*. *J. Bacteriol.* 184, 2878–2888. doi: 10.1128/JB.184.11.2878-2888.2002

Mlýnský, V., and Bussi, G. (2018). Exploring RNA structure and dynamics through enhanced sampling simulations. *Curr. Opin. Struct. Biol.* 49, 63–71. doi: 10.1016/j.sbi.2018.01.004

Molodtsov, V., Sineva, E., Zhang, L., Huang, X., Cashel, M., Ades, S. E., et al. (2018). Allosteric effector ppGppPotentiates the inhibition of transcript initiation by DksA. *Mol. Cell* 69, 828.e5–839.e5. doi: 10.1016/J.MOLCEL.2018.01.035

Moodie, S. L., and Thornton, J. M. (1993). A study into the effects of protein binding on nucleotide conformation. *Nucleic Acids Res.* 21, 1369–1380. doi: 10.1093/nar/21.6.1369

Pausch, P., Steinchen, W., Wieland, M., Klaus, T., Freibert, S. A., Altegoer, F., et al. (2018). Structural basis for (p)ppGpp-mediated inhibition of the GTPaseRbgA. *J. Biol. Chem.* 293, 19699–19709. doi: 10.1074/jbc.RA118.003070

Pechlaner, M., and Sigel, R. K. O. (2012). Characterization of metal ion-nucleic acid interactions in solution. *Met. Ions Life Sci.* 10, 1–42. doi: 10.1007/978-94-007-2172-2-1

Potrykus, K., and Cashel, M. (2008). (p)ppGpp: still magical? *Annu. Rev. Microbiol.* 62, 35–51. doi: 10.1146/annurev.micro.62.081307.162903

Primm, T. P., Andersen, S. J., Mizrahi, V., Avarbock, D., Rubin, H., Barry, C. E., et al. (2000). The stringent response of Mycobacterium tuberculosis is required for long-term survival. *J. Bacteriol.* 182, 4889–4898.

Prusa, J., Zhu, D. X., and Stallings, C. L. (2018). The stringent response and *Mycobacterium tuberculosis* pathogenesis. *Pathog. Dis.* 1:fty054. doi: 10.1093/femspd/fty054

Rojas, A. M., Ehrenberg, M., Andersson, S. G., and Kurland, C. G. (1984). ppGpp inhibition of elongation factors Tu, G and Ts during polypeptide synthesis. *Mol. Gen. Genet.* 197, 36–45.

Ronneau, S., and Hallez, R. (2019). Make and break the alarmone: regulation of (p)ppGppsynthetase/hydrolase enzymes in bacteria. *FEMS Microbiol. Rev.* 43, 389–400. doi: 10.1093/femsre/fuz009

Roos, K., Wu, C., Damm, W., Reboul, M., Stevenson, J. M., Lu, C., et al. (2019). OPLS3e: extending force field coverage for drug-like small molecules. *J. Chem. Theory Comput.* 15, 1863–1874. doi: 10.1021/acs.jctc.8b01026

Ross, W., Vrentas, C. E., Sanchez-Vazquez, P., Gaal, T., and Gourse, R. L. (2013). The magic spot: a ppgpp binding site on *E. coli* RNA polymerase responsible for regulation of transcription initiation. *Mol. Cell* 50, 420–429. doi: 10.1016/J.MOLCEL.2013.03.021

Rymer, R. U., Solorio, F. A., Tehranchi, A. K., Chu, C., Corn, J. E., Keck, J. L., et al. (2012). Binding mechanism of metalšNTP substrates and stringent-response alarmones to bacterial DnaG-type primases. *Structure* 20, 1478–1489. doi: 10.1016/j.str.2012.05.017

Schreyer, A., and Blundell, T. (2009). CREDO: a protein-ligand interaction database for drug discovery. *Chem. Biol. Drug Des.* 73, 157–167. doi: 10.1111/j.1747-0285.2008.00762.x

Shyp, V., Tankov, S., Ermakov, A., Kudrin, P., English, B. P., Ehrenberg, M., et al. (2012). Positive allosteric feedback regulation of the stringent response enzyme RelA by its product. *EMBO Rep.* 13, 835–839. doi: 10.1038/embor.2012.106

Smith, A. K., Lockhart, C., and Klimov, D. K. (2016). Does replica exchange with solute tempering efficiently sample Aβ peptide conformational ensembles? *J. Chem. Theory Comput.* 12, 5201–5214. doi: 10.1021/acs.jctc.6b00660

Song, H., Dharmasena, M. N., Wang, C., Shaw, G. X., Cherry, S., Tropea, J. E., et al. (2020). Structure and activity of PPX/GppA homologs from *Escherichia coli* and *Helicobacter* pylori. *FEBS J.* 287, 1865–1885. doi: 10.1111/febs.15120

Šponer, J., Banáš, P., Jurečka, P., Zgarbová, M., Kührová, P., Havrila, M., et al. (2014). Molecular dynamics simulations of nucleic acids. From Tetranucleotides to the ribosome. *J. Phys. Chem. Lett.* 5, 1771–1782. doi: 10.1021/jz500557y

Srivatsan, A., and Wang, J. D. (2008). Control of bacterial transcription, translation and replication by (p)ppGpp. *Curr. Opin. Microbiol.* 11, 100–105. doi: 10.1016/j.mib.2008.02.001

Steinchen, W., and Bange, G. (2016). The magic dance of the alarmones (p)ppGpp. *Mol. Microbiol.* 101, 531–544. doi: 10.1111/mmi.13412

Steinchen, W., Schuhmacher, J. S., Altegoer, F., Fage, C. D., Srinivasan, V., Linne, U., et al. (2015). Catalytic mechanism and allosteric regulation of an oligomeric (p)ppGppsynthetase by an alarmone. *Proc. Natl. Acad. Sci. U. S. A.* 112, 13348–13353. doi: 10.1073/pnas.1505271112

Stern, N., Major, D. T., Gottlieb, H. E., Weizman, D., and Fischer, B. (2010). What is the conformation of physiologically-activedinucleoside polyphosphates in solution? Conformational analysis of free dinucleoside polyphosphates by NMR and molecular dynamics simulations. *Org. Biomol. Chem.* 8, 4637–4652. doi: 10.1039/c005122e

Stierand, K., Maaß, P. C., and Rarey, M. (2006). Molecular complexes at a glance: automated generation of two-dimensional complex diagrams. *Bioinformatics* 22, 1710–1716. doi: 10.1093/bioinformatics/btl150

Sun, G., Voigt, J. H., Filippov, I. V., Marquez, V. E., and Nicklaus, M. C. (2004). PROSIT: pseudo-rotational online service and interactive tool, applied to a conformational survey of nucleosides and nucleotides. *J. Chem. Inf. Comput. Sci.* 44, 1752–1762. doi: 10.1021/ci049881

Sun, G., Voigt, J. H., Marquez, V. E., and Nicklaus, M. C. (2005). Prosit, an online service to calculate pseudorotational parameters of nucleosides and nucleotides. *Nucleos. Nucleot. Nucleic Acids.* 24, 1029–1032. doi: 10.1081/NCN-200059757

Tamman, H., Van Nerom, K., Takada, H., Vandenberk, N., Scholl, D., Polikanov, Y., et al. (2020). A nucleotide-switch mechanism mediates opposing catalytic activities of Rel enzymes. *Nat. Chem. Biol.* 16, 834–840. doi: 10.1038/s41589-020-0520-2

Wang, B., Dai, P., Ding, D., Del Rosario, A., Grant, R. A., Pentelute, B. L., et al. (2019). Affinity-based capture and identification of protein effectors of the growth regulator ppGpp. *Nat. Chem. Biol.* 15, 141–150. doi: 10.1038/s41589-018-0183-4

Wang, B., Wang, Z., Javornik, U., Xi, Z., and Plavec, J. (2017). Computational and NMR spectroscopy insights into the conformation of cyclic di-nucleotides. *Sci. Rep.* 7:16550. doi: 10.1038/s41598-017-16794-4

Wang, J. D., Sanders, G. M., and Grossman, A. D. (2007). Nutritional control of elongation of DNA replication by (p)ppGpp. *Cell* 128, 865–875. doi: 10.1016/j.cell.2006.12.043

Wang, L., and Berne, B. J. (2018). Efficient sampling of puckering states of monosaccharides through replica exchange with solute tempering and bond softening. *J. Chem. Phys.* 149:072306. doi: 10.1063/1.5024389

Winther, K. S., Roghanian, M., and Gerdes, K. (2018). Activation of the stringent response by loading of RelA-tRNA complexes at the ribosomal a-site. *Mol. Cell* 70, 95.e4–105.e4. doi: 10.1016/j.molcel.2018.02.033

Yang, Y. I., Shao, Q., Zhang, J., Yang, L., and Gao, Y. Q. (2019). Enhanced sampling in molecular dynamics. *J. Chem. Phys.* 151:070902. doi: 10.1063/1.5109531

Zhang, Y., Zbornikova, E., Rejman, D., and Gerdes, K. (2018). Novel (p)ppGpp binding and metabolizing proteins of *Escherichiacoli*. *mBio* 9:e2188-17. doi: 10.1128/mBio.02188-17

Zhang, Y. E., Bærentsen, R. L., Fuhrer, T., Sauer, U., Gerdes, K., and Brodersen, D. E. (2019). (p)ppGpp Regulates a bacterial nucleosidase by an allosteric two-domain switch. *Mol. Cell* 74, 1239.e4–1249.e4. doi: 10.1016/j.molcel.2019.03.035

Zuo, Y., Wang, Y., and Steitz, T. A. (2013). The mechanism of *E. coli* RNA polymerase regulation by ppGppIs suggested by the structure of their complex. *Mol. Cell* 50, 430–436. doi: 10.1016/J.MOLCEL.2013.03.020

Conflict of Interest: The authors declare that the research was conducted in the absence of any commercial or financial relationships that could be construed as a potential conflict of interest.

frontiers in Microbiology

ORIGINAL RESEARCH
published: 05 November 2020
doi: 10.3389/fmicb.2020.587098

Guanosine Tetraphosphate Has a Similar Affinity for Each of Its Two Binding Sites on *Escherichia coli* RNA Polymerase

*Angela R. Myers, Danielle P. Thistle, Wilma Ross and Richard L. Gourse**

Department of Bacteriology, University of Wisconsin-Madison, Madison, WI, United States

During nutrient deprivation, the bacterial cell undergoes a stress response known as the stringent response. This response is characterized by induction of the nucleotide derivative guanosine tetraphosphate (ppGpp) that dramatically modulates the cell's transcriptome. In *Escherichia coli*, ppGpp regulates transcription of as many as 750 genes within 5 min of induction by binding directly to RNA polymerase (RNAP) at two sites ~60 Å apart. One proposal for the presence of two sites is that they have different affinities for ppGpp, expanding the dynamic range over which ppGpp acts. We show here, primarily using the Differential Radial Capillary Action of Ligand Assay (DRaCALA), that ppGpp has a similar affinity for each site, contradicting the proposal. Because the ppGpp binding sites are formed by interactions of the β' subunit of RNAP with two small protein factors, the ω subunit of RNAP which contributes to Site 1 and the transcription factor DksA which contributes to Site 2, variation in the concentrations of ω or DksA potentially could differentially regulate ppGpp occupancy of the two sites. It was shown previously that DksA varies little at different growth rates or growth phases, but little is known about variation of the ω concentration. Therefore, we raised an anti-ω antibody and performed Western blots at different times in growth and during a stringent response. We show here that ω, like DksA, changes little with growth conditions. Together, our data suggest that the two ppGpp binding sites fill in parallel, and occupancy with changing nutritional conditions is determined by variation in the ppGpp concentration, not by variation in ω or DksA.

Keywords: bacterial transcription, RNA polymerase, ppGpp, DksA, omega subunit, stringent response

OPEN ACCESS

Edited by:
Gert Bange,
University of Marburg, Germany

Reviewed by:
Vasili Hauryliuk,
Umeå University, Sweden
Christiane Wolz,
University of Tübingen, Germany

****Correspondence:***
Richard L. Gourse
rgourse@bact.wisc.edu

Specialty section:
This article was submitted to Microbial Physiology and Metabolism, a section of the journal Frontiers in Microbiology

Received: *24 July 2020*
Accepted: *06 October 2020*
Published: *05 November 2020*

Citation:
Myers AR, Thistle DP, Ross W and Gourse RL (2020) Guanosine Tetraphosphate Has a Similar Affinity for Each of Its Two Binding Sites on Escherichia coli RNA Polymerase. Front. Microbiol. 11:587098. doi: 10.3389/fmicb.2020.587098

INTRODUCTION

When nutritional resources change, cells adjust their transcriptional output to match the new environment. In almost all bacterial species, this is accomplished in part by synthesis of the secondary messengers guanosine tetraphosphate (ppGpp; guanosine 5'-diphosphate 3'-diphosphate) and guanosine pentaphosphate (pppGpp; guanosine 5'-triphosphate 3'-diphosphate), respectively, collectively referred to here as ppGpp (reviewed in Hauryliuk et al., 2015; Liu et al., 2015; Irving and Corrigan, 2018). In proteobacteria like *Escherichia coli*, the basal level of ppGpp (from ~1 to 10 μM) only moderately affects gene expression, but induction of RelA in response

to the accumulation of deacylated tRNA(s) increases the ppGpp concentration 100–1,000-fold, dramatically changing gene expression (Ryals et al., 1982; Varik et al., 2017).

In this so-called stringent response, transcription of hundreds of genes, many of which are related to translation, is inhibited within 5 min of ppGpp induction, and transcription of hundreds of other genes, many of which are related to pathways involved in amino acid biosynthesis, is stimulated (Durfee et al., 2008; Traxler et al., 2008; Sanchez-Vazquez et al., 2019). This reprogramming of the transcriptome is accomplished in *E. coli* by direct binding of ppGpp to RNA polymerase (RNAP; Sanchez-Vazquez et al., 2019). ppGpp also binds directly to many proteins other than RNAP, altering their activities and contributing further to the remodeling of cellular metabolism (Zhang et al., 2018; Wang et al., 2019).

Two proteins that are not essential for the catalytic activity of *E. coli* RNAP are nevertheless required for the effects of ppGpp on transcription initiation, the 10.2 kDa RNAP subunit ω and the 17.5 kDa transcription factor DksA (Paul et al., 2004, 2005; Vrentas et al., 2005). Genetic and biochemical evidence indicated that ppGpp binds to two sites on RNAP ~60 Å apart (Ross et al., 2013, 2016), with Site 1 at the interface of the ω and β' subunits of RNAP and Site 2 at the interface of DksA and the secondary channel rim of the β' subunit (**Figure 1**). Crystal structures of the RNAP-ppGpp complex are consistent with the models based on the genetic and biochemical studies, and indicate that at Site 1 the ppGpp phosphates are coordinated by residues 2–5 and other residues in ω, as well as by residues R417, K615 in β'. The guanine base is coordinated by several residues in β', including I619, D622, and R362 (Mechold et al., 2013; Zuo et al., 2013). A strain lacking *rpoZ*, the gene encoding the RNAP ω subunit, (i.e., lacking Site 1) displays a modest lag in recovering from a downshift from a rich to a minimal medium (Gentry et al., 1991; Ross et al., 2013, 2016), while strains lacking *dksA* have more pronounced defects in recovery from a downshift and in transcriptional regulation by ppGpp (Paul et al., 2004; Ross et al., 2016; Sanchez-Vazquez et al., 2019).

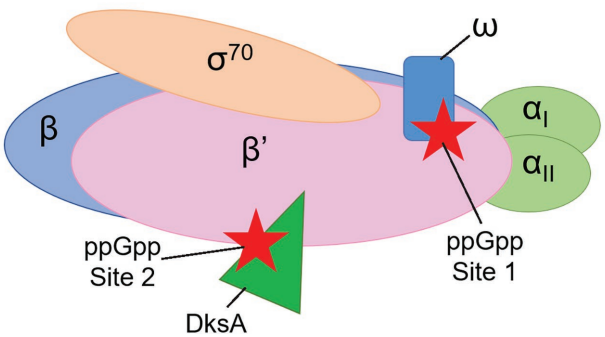

FIGURE 1 | Cartoon representation of *Escherichia coli* RNA polymerase (RNAP) showing the locations of guanosine tetraphosphate (ppGpp) binding Sites 1 and 2. The αI and αII subunits (a homodimer, encoded by the *rpoA* gene) are shown in light green. The β subunit (encoded by the *rpoB* gene) is in blue. The β' subunit (encoded by the *rpoC* gene) is in pink. The ω subunit (encoded by the *rpoZ* gene) is in blue. The σ^{70} subunit (encoded by the *rpoD* gene) is in tan. ppGpp (red stars) binds at the interface of the ω and β' subunits (Site 1) and at the interface of the transcription factor DksA (dark green) and the β' subunit (Site 2).

The two ppGpp binding sites in RNAP are generally conserved among proteobacteria based on conservation of the residues that contribute to binding (Ross et al., 2013, 2016). However, where it has been investigated, the effects of ppGpp on transcription in some evolutionarily distant bacterial phyla do not involve direct binding of ppGpp to RNAP. For example, in *Bacillus subtilis*, ppGpp inhibits transcription by binding to protein targets involved in nucleotide metabolism, leading to reduced levels of GTP, the initiating nucleotide for many promoters (Krasny and Gourse, 2004; Liu et al., 2015).

The identification of a second ppGpp-binding pocket (Site 2) in *E. coli* RNAP provided an explanation for why disruption of Site 1 had only a modest effect on the stringent response. Analysis of the effects of specific mutations in *dksA* or *rpoC* (the gene encoding β') on transcription *in vitro*, crosslinking of 6-thio-ppGpp and binding of ppGpp to the RNAP-DksA complex suggested that Site 2 is at the interface of DksA and the β' subunit rim helices at the entrance to the RNAP secondary channel (Ross et al., 2016). These results and a subsequent crystal structure of an RNAP-DksA-ppGpp complex indicated that residues defined by the mutational studies, including K98, R91, and K139 in DksA, coordinate the phosphates of ppGpp (Molodtsov et al., 2018), and the guanosine base is coordinated by two additional residues implicated by the mutational studies, β' N680 and DksA L95 (Ross et al., 2016; Molodtsov et al., 2018). A recent cryo-EM structure, in which flexible regions of RNAP were not constrained by crystal packing forces, showed that DksA R129 is also in direct contact with ppGpp (Chen, unpublished), consistent with biochemical analysis of effects of DksA substitution variants on ppGpp binding and function at Site 2 (Ross et al., 2016).

Guanosine tetraphosphate binding to Site 1 alone (in the absence of DksA) has a modest inhibitory effect on transcription from the *rrnB* P1 promoter at saturating ω concentrations (~3-fold), and does not activate transcription from amino acid biosynthesis promoters. ppGpp binding to Site 2 alone (i.e., with a near saturating concentration of DksA but in the absence of the ω subunit) has a larger inhibitory effect on *rrnB* P1 (~6-fold) and is sufficient for full activation of amino acid biosynthesis promoters (Vrentas et al., 2005; Ross et al., 2016). When both ppGpp binding sites are present, inhibition of *rrnB* P1 is greater than with either site alone (15–20-fold). These results are consistent with the growth properties of strains lacking ppGpp (Xiao et al., 1991), ω (Gentry and Burgess, 1989; Gentry et al., 1991), or DksA (Paul et al., 2004, 2005), or containing only Site 1 (Ross et al., 2013), only Site 2 (Ross et al., 2016), or both (Ross et al., 2016; Sanchez-Vazquez et al., 2019).

The evolutionary rationale for having two sites is unclear. One model is that the two sites have different affinities for ppGpp, expanding the dynamic range over which ppGpp acts. To test that model, here, we use the Differential Radial Capillary Action of Ligand Assay (DRaCALA; Roelofs et al., 2011), as

modified to measure ppGpp binding to RNAP (Ross et al., 2016), to determine the binding affinities of ppGpp for each of the two sites on *E. coli* RNAP independently as well as together.

We find that both binding sites have similar intrinsic affinities for ppGpp. In addition, we find that the concentrations of ω at different times in cell growth vary only slightly. In conjunction with previous measurements of the concentrations of DksA *in vivo* (Rutherford et al., 2007), our results indicate that the two binding sites fill with ppGpp in parallel and not sequentially as ppGpp concentrations increase. Furthermore, the binding affinities of RNAP for ppGpp that we determined *in vitro* are consistent with the reported effects of ppGpp on transcription even in non-stressed conditions *in vivo*.

MATERIALS AND METHODS

Strains and Plasmids

Strains and plasmids are listed in **Supplementary Table S1** in Supplemental data. To construct the pET23a-His10-SUMO-*rpoZ* plasmid used to purify ω for antibody development, a gene block (Integrated DNA Technologies) of *rpoZ* was inserted into pET23a-His10-SUMO (Invitrogen; RLG14235) at the BamH1 and HindIII sites using HiFi DNA Assembly (NEB) to create RLG15371.

Purification of Proteins

Purification of RNAP [wild-type (WT) or mutant; **Supplementary Figure S1**], the ω subunit of RNAP (**Supplementary Figure S2**), DksA (WT and variants), GreB, and TraR were as described in Expanded Materials and Methods.

Measuring Binding Affinities by DRaCALA

Binding of [^{32}P]-ppGpp to RNAP, RNAP/DksA, RNAP/TraR, or RNAP/GreB complexes was measured by the DRaCALA, adapted from Roelofs et al. (2011). See Expanded Materials and Methods for details.

Mathematical Modeling of ppGpp Binding

The most widely used mathematical model for multisite ligand binding to a protein was first proposed by Hill (1910). By plotting fractional binding of the enzyme as a function of ligand concentration, one can calculate the dissociation constant and the "Hill coefficient," which indicates whether the binding of multiple ligands is positively or negatively cooperative (see Expanded Materials and Methods for details).

Statistical Analysis

All $K_{d,app}$ values for each set of binding experiments were subjected to a rank sum test (Sigma Plot) to determine if the $K_{d,app}$ values in each set were statistically different from other values. Statistically different values were then given a *p*-value.

Western Blots

Polyclonal antibodies were raised by Covance, Inc., following injection of rabbits with purified ω. Quantitative western blots were performed on cells grown in LB as described in Expanded Materials and Methods.

RESULTS

ppGpp Binds With a Similar Affinity to Sites 1 and 2 on RNAP

Our previous studies evaluated the relative roles of Sites 1 and 2 on the transcriptional effects of ppGpp, an indirect indicator of ppGpp binding to RNAP (Ross et al., 2013, 2016). These experiments showed that Site 2 had a much larger effect on both inhibition and activation than Site 1, even though the concentration of ppGpp needed for half-maximal effects on transcription appeared similar, ~12–21 μM for Site 1 at saturating ω and ~19 μM for Site 2 at nearly saturating DksA (Ross et al., 2013, 2016). To measure ppGpp binding more directly, we used DRaCALA (Roelofs et al., 2011; Ross et al., 2016) to determine the affinities of ppGpp for each of the two sites on RNAP independently (**Figure 2**) as well as together (**Figure 3**). The specificity of this assay for ppGpp was established previously using unlabeled nucleotides as competitors (**Supplementary Figure S3A**; Ross et al., 2016). Unlabeled ppGpp competed for binding of ^{32}P-ppGpp to each of the two sites, while GDP partially competed, and ATP did not compete at all. As this is a non-equilibrium binding assay, the K_d values are reported here as apparent K_d ($K_{d,app}$) values. A table summarizing all the apparent K_d values reported here is provided as **Supplementary Table S2**.

For measuring binding of ppGpp to Site 1, wild-type RNAP was purified by concurrent overproduction of the four subunits of core RNAP, α, β, and β' encoded by one plasmid and overproduction of ω encoded by a second plasmid (see Expanded Materials and Methods). DksA was not included in the binding reactions with wild-type RNAP and ppGpp, eliminating binding to Site 2 (Ross et al., 2016). Increasing amounts of RNAP were combined with a fixed low concentration of [^{32}P]-ppGpp (~5 nM). The observed fraction of [^{32}P]-ppGpp bound at each RNAP concentration from each of seven independent experiments was fit to a one site saturation binding curve (see Expanded Materials and Methods for description of curve fitting). The $K_{d,app}$'s for each independent binding curve were then averaged, resulting in a $K_{d,app}$ of 6.1 ± 1.3 μM for ppGpp binding to Site 1 (**Figures 2A,B**).

We ensured that the ω subunit was saturating in the RNAP preparations by adding increasing amounts of purified ω to the binding reaction and measuring the fraction of [^{32}P]-ppGpp bound (**Supplementary Figure S3B**). The additional ω did not increase binding of ppGpp, indicating that ω was already saturating in our RNAP preparation derived from cells overexpressing ω. In contrast, we showed previously that effects of ppGpp on transcription increased slightly when RNAP was purified without concurrent overproduction of ω (Vrentas et al., 2005).

The Site 2 ppGpp binding pocket consists of residues from both DksA and β' (Ross et al., 2016; Molodtsov et al., 2018). For measuring binding of [^{32}P]-ppGpp to Site 2, independent

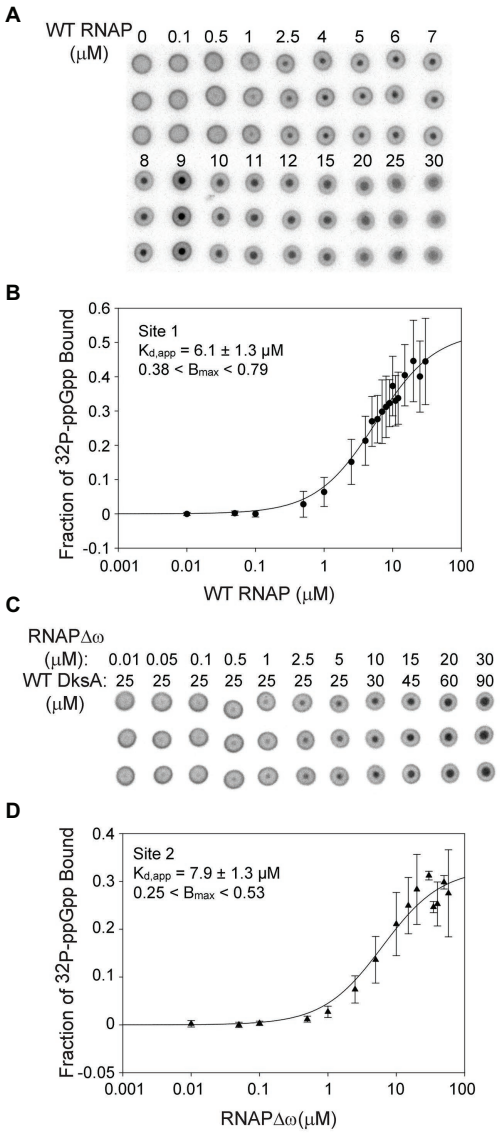

FIGURE 2 | Sites 1 and 2 have similar binding affinities for ppGpp. **(A)** Differential Radial Capillary Action of Ligand Assay (DRaCALA) analysis of [^{32}P]-ppGpp binding to Site 1. Increasing amounts of wild-type (WT) RNAP (without DksA) were equilibrated with a constant amount of [^{32}P]-ppGpp in DRaCALA buffer and spotted on nitrocellulose filters. Triplicate filters from one representative experiment are shown. **(B)** The plot shown is a one-site saturation binding curve using averaged [^{32}P]-ppGpp binding data from seven experiments conducted with five separate preparations of wild-type RNAP. $K_{d,app}$ and B_{max} values were determined by fitting each individual experiment to a one-site saturation ligand binding curve. $K_{d,app}$ and B_{max} values and error shown in the inset were averaged from the values for the seven experiments. See Expanded Materials and Methods for further details. **(C)** Representative DRaCALA analysis of [^{32}P]-ppGpp binding to Site 2. Same as in **(A)** except RNAP lacked the ω subunit (RNAPΔω), and DksA was included. **(D)** Same as **(B)** except the reaction contained RNAPΔω and DksA.

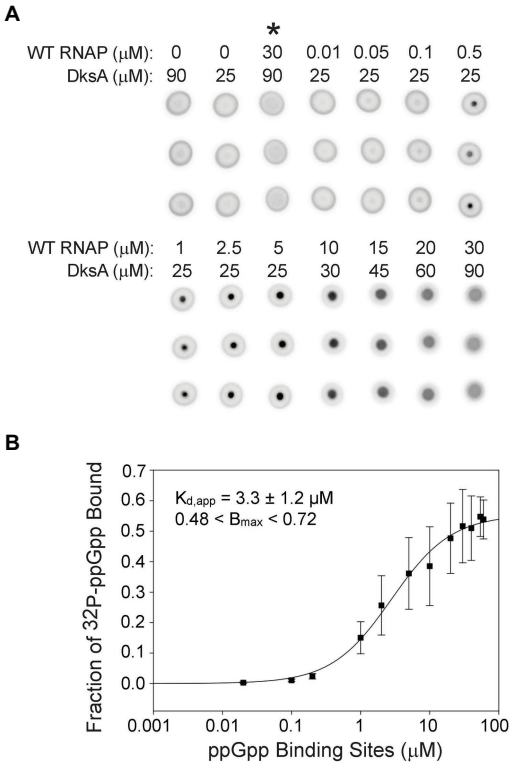

FIGURE 3 | Guanosine tetraphosphate binds with a higher affinity when RNAP contains both ppGpp binding sites. **(A)** [^{32}P]-ppGpp binding to wild-type RNAP in the presence of DksA as measured by DRaCALA. Triplicate filters from one representative experiment are shown. Wild-type RNAP and DksA concentrations are indicated above each column of three filters. Control reactions are in the first three columns. Asterisk above the third column indicates the presence of unlabeled competitor ppGpp (1 mM) in the reaction. **(B)** The plot shown is a one-site saturation binding curve for the average [^{32}P]-ppGpp binding data with the error bars representing one SD from the mean from seven independent experiments conducted with five individually purified preparations of WT RNAP, as described in the legend for **Figure 2**. The $K_{d,app}$, B_{max}, and error shown in the inset were determined by averaging $K_{d,app}$ values from each of the individual experiments, as in **Figure 2**.

of ppGpp binding to Site 1, we used logic similar to that described above, but with purified DksA added to the reactions and using an RNAP lacking ω (RNAPΔω) obtained by purification of RNAP from a strain deleted for *rpoZ* (*ΔrpoZ*). We showed previously that [^{32}P]-ppGpp does not bind to DksA in the absence of RNAP (Ross et al., 2016), and as described above for Site 1, unlabeled ppGpp competed with [^{32}P]-ppGpp for binding to Site 2 (**Supplementary Figure S3A**). The data from each of seven separate experiments measuring ppGpp binding to Site 2 were fit to one-site saturation binding curves, and the $K_{d,app}$ values from each experiment were averaged (**Figures 2C,D**). The $K_{d,app}$ for Site 2 was 7.9 ± 1.3 μM, similar to the ppGpp binding affinity for Site 1.

ppGpp Binds With Very Low Affinity to RNAP Lacking Sites 1 and 2

For comparison with the affinities measured above, we measured binding of [^{32}P]-ppGpp to RNAPs that we had shown previously by *in vitro* transcription did not respond to ppGpp.

The $K_{d,app}$ for an RNAP purified from a strain without ω (Δ*rpoZ*) to which no DksA was added (and thus lacked Sites 1 and 2) was >100 μM (**Supplementary Figure S4A**). Similarly, RNAP purified from a strain without ω (Δ*rpoZ*) overexpressing ωΔ2–5 (RNAPΔω + ωΔ2–5) also had a $K_{d,app}$ >100 μM (**Supplementary Figure S4B**). We define the very weak binding of ppGpp to these two RNAPs as non-specific or background binding, more than an order of magnitude weaker than the affinity of RNAP containing Site 1 or Site 2 for ppGpp.

We also tested ppGpp binding to another RNAP variant that previous work had shown responded very poorly to ppGpp *in vitro* using *in vitro* transcription as an assay (Ross et al., 2013). "RNAP M7" contains a four residue deletion at the N-terminus of ω, ω (Δ2–5), plus three other substitutions in β' residues close to or within the Site 1 binding pocket. Surprisingly, this RNAP bound ppGpp with a $K_{d,app}$ of 16.2 + 4.2 μM, only ~2-fold worse than the RNAPs with wild-type Site 1 or 2 (**Supplementary Figure S4C**). RNAPs containing a subset of the β' substitutions present in M7 (e.g., β'K615A/R417A) were very defective in responding to ppGpp when assayed by *in vitro* transcription and by crosslinking with the zero-length crosslinker 6-thio ppGpp (Ross et al., 2013), yet displayed significant levels of binding in preliminary DRaCALA assays (Ross and Gourse, unpublished data). We suggest that crosslinking and function require very precise positioning of ppGpp in the binding pocket, but DRaCALA assays sometimes can detect binding modes that are non-functional. ppGpp binding to the M7 RNAP may represent such a non-functional binding mode.

ppGpp Binds With Higher Affinity When RNAP Contains Both ppGpp Binding Sites

Even though Sites 1 and 2 are located ~60 Å apart on RNAP (Ross et al., 2016; Molodtsov et al., 2018) and have similar affinities for ppGpp, it was conceivable that having both sites would alter the overall ppGpp binding affinity. Therefore, we compared [^{32}P]-ppGpp binding to RNAPs containing only Site 1 or Site 2 (**Figure 2**) with [^{32}P]-ppGpp binding to an RNAP saturated with both ω and DksA (i.e., containing both sites; **Figure 3A**). For the RNAP with both ppGpp binding sites, we calculated the $K_{d,app}$ from a plot in which the X-axis indicates the concentration of binding sites (twice the RNAP concentration). The data were fit for each of seven separate experiments, and the $K_{d,app}$ values were averaged (**Figure 3B**). For the RNAP with both binding sites, the $K_{d,app}$ was 3.3 ± 1.2 μM, a significant difference from the RNAPs with only one binding site (6.1 or 7.9 μM; $p = 0.006$ for both sites compared to Site 1 or $p = 0.01$ for both sites compared to Site 2). If the nominal concentration of RNAP were used on the X-axis as in **Figure 2**, rather than with the concentration of ppGpp binding sites, the $K_{d,app}$ would be even tighter, 1.7 ± 1.2 μM. Thus, when plotted either way, there was a significant difference in the $K_{d,app}$ of the enzyme for ppGpp with both sites vs. only one site.

The RNAP concentration in the DRaCALA reactions was 100–1,000-fold higher than the ppGpp concentration. Therefore, ppGpp could not fill both binding sites on an RNAP molecule at the same time. The measured binding affinity of the enzyme containing both sites must therefore represent an average of the affinities of ppGpp bound to one site or the other in the population of RNAPs. Nevertheless, we checked for cooperativity by comparing the fits using the equations for one-site and two-site saturation binding curves and the Hill equation. Both resulted in the same $K_{d,app}$. The Hill coefficient was ~1, and the curve was not sigmoidal when the data were plotted on a linear scale (**Supplementary Figure S5**), consistent with a lack of cooperativity.

DksA Binding to RNAP Enhances Binding of ppGpp to Site 1

Although there was no evidence for cooperativity, there was an increase in the affinity of ppGpp for wild-type RNAP containing DksA (both sites) compared to the affinity for RNAP with only one site (3.3 ± 1.2 μM for the RNAP containing both sites, compared to 6.1 ± 1.3 μM or 7.9 ± 1.3 μM for the RNAPs with either Site 1 or Site 2, respectively; **Figures 2, 3**). Since the DksA concentration was saturating in the DRaCALA reactions measuring binding of ppGpp to RNAP with both sites present, DksA was a candidate to explain the increase in affinity. That is, we hypothesized that DksA binding in the RNAP secondary channel might allosterically alter the binding environment of Site 1. To address this hypothesis, we utilized "separation of function" DksA variants, i.e., variants defective for ppGpp binding but competent for RNAP binding. DksA residues K98 and R129 both contact ppGpp directly (Ross et al., 2016; Molodtsov et al., 2018). DksA variants containing alanine substitutions at either of these positions are still able to bind to RNAP and reduce the lifetime of RNAP-promoter complexes (Ross et al., 2016), but they do not support ppGpp binding to Site 2, and they eliminate the effects of ppGpp on transcription by RNAPΔω (Ross et al., 2016). No binding was detected in DRaCALA experiments with RNAPΔω and either DksA-R129A or DksA-K98A, consistent with predictions for a complex lacking both binding sites for ppGpp (**Supplementary Figures S6A**,**B**).

Guanosine tetraphosphate bound to wild-type RNAP in the absence of DksA (i.e., to Site 1) with a $K_{d,app}$ of 6.1 ± 1.3 μM (**Figure 2**). ppGpp bound to Site 1 in wild-type RNAP in the presence of DksA-R129A, with a $K_{d,app}$ of ~1.8 ± 0.5 μM (**Figure 4A**), ~3-fold more tightly than to Site 1 without DksA (a statistically significant difference with a value of $p = 0.001$). In the presence of DksA-K98A, ppGpp bound to Site 1 with a $K_{d,app}$ of ~1.3 ± 0.1 μM (**Figure 4B**), although the significance of this measurement is less certain because of the smaller number of replicates performed. Nevertheless, together these results indicate that ppGpp binds more tightly to Site 1 when DksA is bound to RNAP.

We also tested whether other secondary channel binding proteins increased the affinity of Site 1 for ppGpp. TraR is a distant homolog of DksA that is encoded by the F element (Blankschien et al., 2009). Although TraR is only half the size of DksA, it has an effect on transcription by itself that is as strong as the effect of DksA and ppGpp together (Gopalkrishnan et al., 2017). However, TraR lacks the residues in DksA that interact with ppGpp, and therefore ppGpp does not bind to

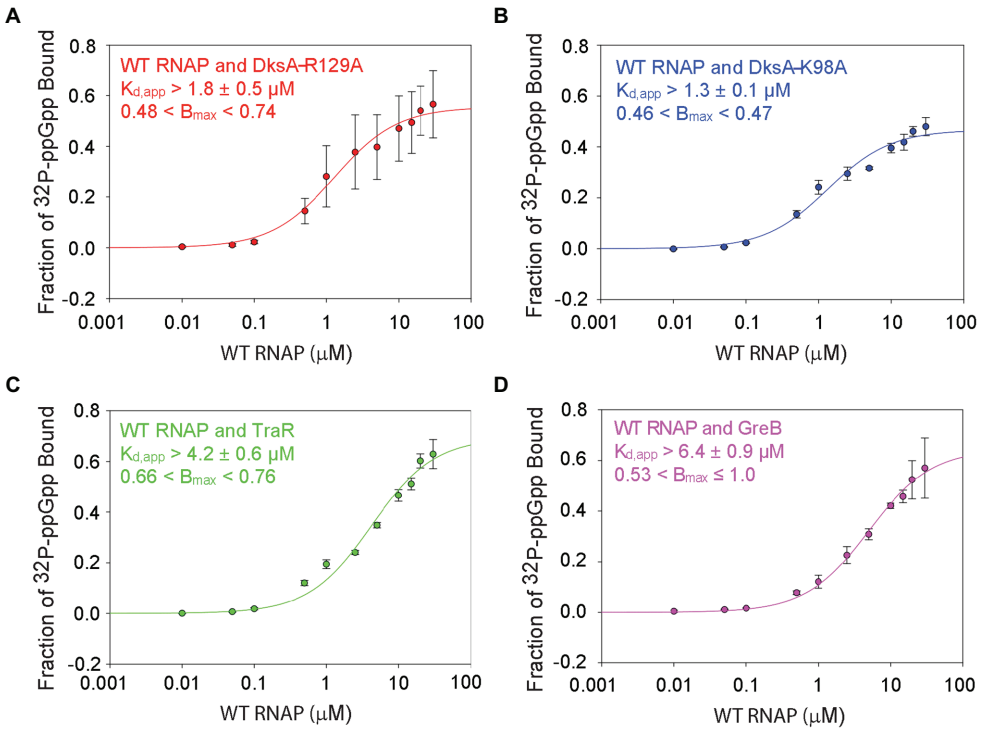

FIGURE 4 | DksA enhances ppGpp binding to Site 1. DRaCALA measurements were performed with wild-type RNAP and the indicated secondary channel binding factors. **(A)** Wild-type RNAP with DksA-R129A. One-site saturation binding curves with data averaged from four independent experiments. $K_{d,app}$ and B_{max} values, and error shown are averages from the values determined for each independent experiment. **(B)** Wild-type RNAP with DksA-K98A. Data from two independent experiments, as described in **(A)**. **(C)** Wild-type RNAP with TraR. Data from three independent experiments, as described in **(A)**. **(D)** Wild-type RNAP with GreB. Data from three independent experiments, as described in **(A)**.

RNAPΔω or increase the effect of TraR on transcription (Gopalkrishnan et al., 2017). The $K_{d,app}$ for ppGpp binding to Site 1 in the wild-type RNAP-TraR complex was at least 4.2 ± 0.6 μM (**Figure 4C**; the curve did not plateau, so the affinity of ppGpp for Site 1 must be considered a lower estimate) vs. 6.1 ± 1.3 μM in the absence of TraR (**Figure 2B**). These $K_{d,app}$ values for binding of ppGpp to Site 1 were not statistically different from each other. The TraR result is discussed further in the next section.

GreB is another secondary channel binding factor that does not function in conjunction with ppGpp (Rutherford et al., 2007; Lee et al., 2012). The $K_{d,app}$ of ppGpp for the wild-type RNAP-GreB complex (i.e., containing Site 1) was ~6.4 ± 0.9 μM (**Figure 4D**), very similar to that in the absence of GreB (**Figure 2**), and ppGpp did not bind to the RNAPΔω-GreB complex (**Supplementary Figure S6C**). In summary, the mutant DksA proteins increased the affinity of ppGpp for Site 1, and these effects were specific, since other secondary channel binding factors did not increase the affinity of ppGpp for Site 1.

Structural Basis for Effects of DksA on ppGpp Binding to Site 1

The crystal structures of the RNAP-DksA-ppGpp complex and the RNAP-TraR complex (Molodtsov et al., 2018) provide a potential explanation for the observed effect of DksA, and not TraR, on ppGpp binding to Site 1. In the structures, DksA residues near its coiled coil tip (D64 and N68) are located 6–10 Å from β' residues K598/K599. β' K598 and K599 are at the N-terminus of a α-helix that extends to ppGpp binding Site 1 (**Figure 5A**). β' residue K615, near the C-terminal end of this α-helix, interacts not only with ppGpp but also with residues in ω that bind to ppGpp. The proximity of DksA to β'-K598/K599 leads us to speculate that a DksA interaction with these residues in β' might allosterically affect residues in Site 1, explaining the effect of DksA on ppGpp binding to Site 1 (**Figure 4**). Consistent with a direct interaction between DksA and K598/K599, an RNAP variant that contains alanine substitutions for K598 and K599 was partially resistant to DksA's ability to shorten the lifetime of RNAP-promoter complexes (Vrentas, 2008).

In contrast, in the structure of the RNAP-TraR complex (**Figure 5B**; Molodtsov et al., 2018; Chen et al., 2019), there is a much greater separation (16–20 Å) between the N-terminus of TraR (corresponding to the coiled-coil tip region of DksA) and β'-K598/K599. We suggest that the increased separation between TraR and K598/K599 might explain the absence of a significant effect of TraR on ppGpp binding to Site 1 (**Figure 4C**). Thus, the structural information supports the

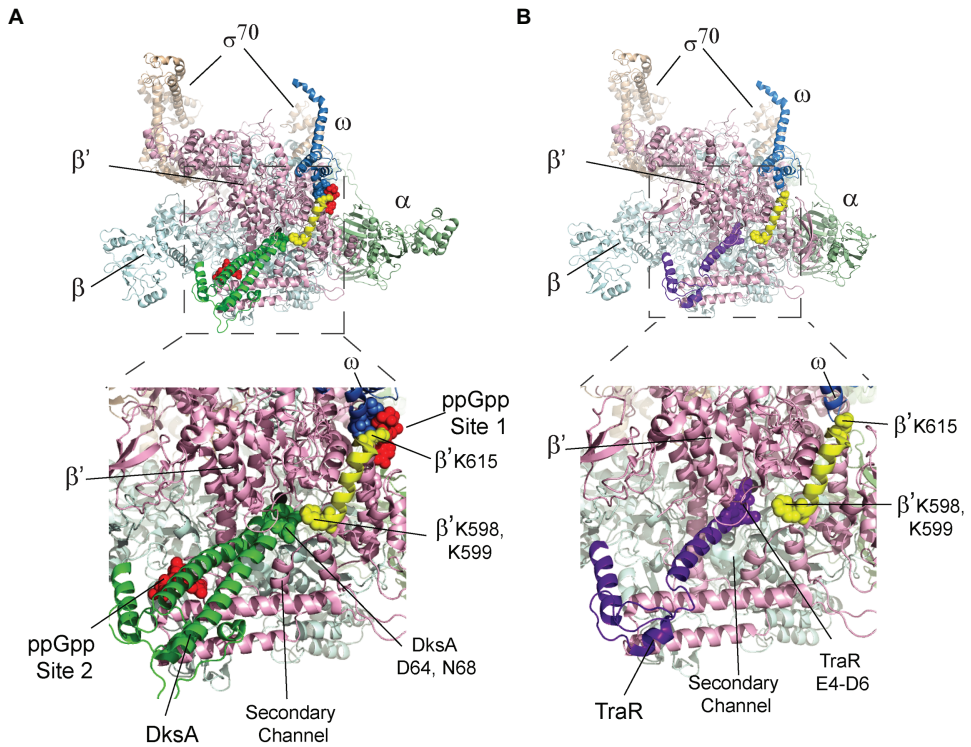

FIGURE 5 | The β' K598-K615 α-helix connects DksA and Site 1. The top image in each panel shows the crystal structure of RNAP with either **(A)** DksA or **(B)** TraR bound in the secondary channel. An expanded view of the boxed region in each panel is shown below the structures of RNAP. **(A)** X-ray crystal structures of wild-type RNAP holoenzyme with DksA and ppGpp soaked into the crystal (PDB 5VSW; Molodtsov et al., 2018). Coloring: α, green; β, cyan; β', light pink; ω, gray; σ, tan; and ppGpp, red spheres. The β' K598-K615 α-helix is yellow with K598, K599, and K615 shown as spheres. DksA is green with D64 and N68 shown as spheres. ω residues A2-T5 are shown as gray spheres. **(B)** RNAP holoenzyme with TraR (PDB 5W1S; Molodtsov et al., 2018). The β' K598-K615 α-helix is yellow, and TraR is dark purple with residues E4, D6, and E7 near the TraR N-terminus shown as spheres.

biochemical data suggesting there is an allosteric effect of DksA on binding of ppGpp to Site 1.

ω Levels Are Relatively Constant

DksA concentrations are constant throughout log phase and decrease only slightly in stationary phase (Rutherford et al., 2007). Therefore, changes in Site 2 binding of ppGpp are more likely a function of changes in ppGpp than DksA concentration, at least during exponential growth. In contrast, there is little information about the concentration of ω at different stages in growth or under different nutritional conditions. We reported previously that the magnitude of the effect of ppGpp on transcription *in vitro* increased slightly when RNAP was purified from cells in which ω was overproduced, suggesting that a small fraction of RNAP lacks ω in cells not overproducing ω (Vrentas et al., 2005).

To determine directly whether ω protein levels vary *in vivo*, we raised an antibody against ω and examined ω protein levels using Western blots. The antibody reacted with a band of the expected size in a strain with wild-type *rpoZ* but not one lacking *rpoZ* (**Supplementary Figure S2B**, compare lanes 1 and 6). Fortuitously, the anti-ω antibody also reacted with σ^{70}. This cross-reactivity was verified using antibody to σ^{70} and ω, and Western blots with purified ω and σ^{70} (**Supplementary Figures S2C,D**).

As with DksA, the ω concentration remained relatively constant in cells growing exponentially in rich medium (LB), but it declined ~2-fold when cells transitioned to stationary phase (~OD_{600} = 1; **Figures 6A,B**). In contrast, the σ^{70} concentration was relatively constant. It is possible that the small decrease in ω levels during stationary phase could decrease the saturation of RNAP with ω and create a subpopulation of RNAP molecules defective in ppGpp binding to Site 1, but the changes in ω concentration are small and unlikely to be a major determinant of regulation by ppGpp during non-starvation conditions.

We also examined ω levels when ppGpp was induced to high concentration. After starvation of cells for serine aminoacyl tRNA by addition of serine hydroxamate (SHX; **Figure 6C**), ω concentrations were stable for at least 60 min, neither increasing nor decreasing well beyond the time needed for a typical stringent response (**Figure 6D**). We conclude that Site 1 occupancy by ppGpp is determined by changes in ppGpp concentration, not by changes in ω concentration, in both starved and unstarved cultures.

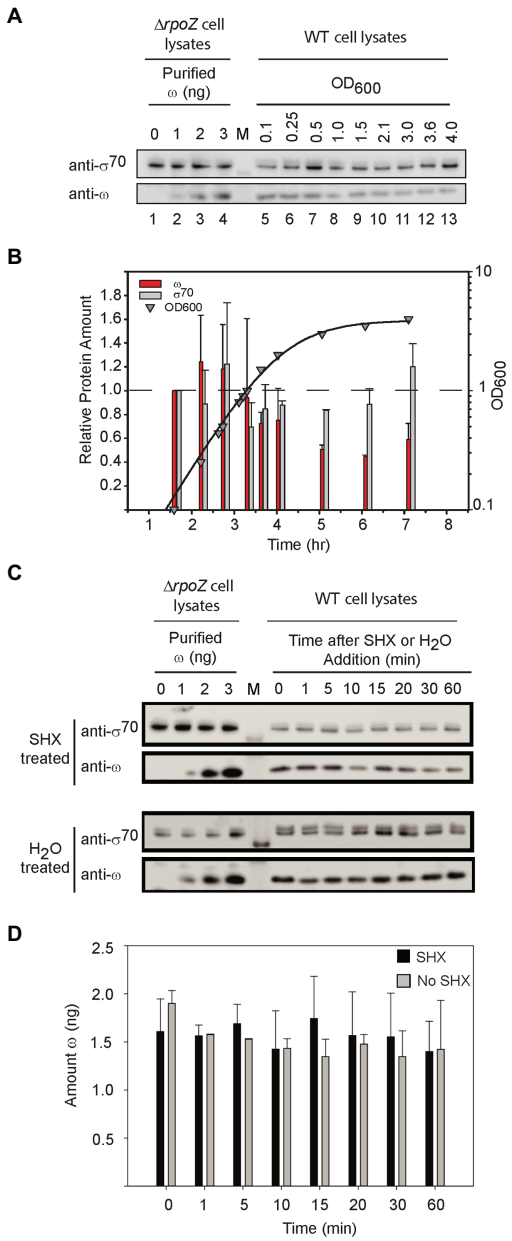

FIGURE 6 | ω levels are relatively constant. **(A)** Representative Western blots using an anti-ω antibody. Purified ω was added to cell lysates from *ΔrpoZ* cells (RLG14044) to create a standard curve for estimation of the amount of ω (lanes 1–4). Wild-type cells were grown in LB, and lysates were collected at different OD_{600} for analysis of ω concentrations using an anti-ω antibody (lanes 5–13). Lane labeled M indicates molecular weight marker. The anti-ω antibody cross-reacted with σ^{70} (see **Supplementary Figure S2**). **(B)** The amounts of ω and σ^{70} at different times in growth were determined from experiments like that in **(A)** and are shown relative to the amounts present at an OD_{600} of 0.1 (first time point, ~1.5 h). Bars indicate the averages of three independent experiments, with error bars representing one SD from the mean. ω bars, red; σ^{70} bars, gray. ω decreased a maximum of ~2-fold, whereas σ^{70} (gray bars) remained relatively constant. **(C)** Representative Western blots with anti-ω antibody and cell lysates following treatment with serine hydroxamate (SHX) which starves cells for serine. Lanes labeled 0–3 indicate amounts of ω added to cell lysates, lane labeled M indicates molecular weight marker, and lanes at right labeled 0–60 indicate minutes after SHX addition. **(D)** Average levels of ω in cells treated with SHX (black bars), compared to untreated cells (gray bars). ω bands in each Western blot were quantified using the ω standard curve derived from the same blot. The bars represent the average ω (in ng) for three separate experiments; error bars represent one SD from the mean.

DISCUSSION

Although the regulatory role of ppGpp during the stringent response has been recognized for more than half a century (Cashel and Gallant, 1969), the mechanistic explanations for the effects of ppGpp on transcription are only now becoming clear. The recent discovery that there are two binding sites for ppGpp on RNAP has shed new light on the mechanisms of transcription regulation by ppGpp (Ross et al., 2016; Molodtsov et al., 2018). Here, we show that the two binding sites on RNAP have very similar intrinsic affinities for ppGpp, contradicting a model in which different affinities of the two sites for ppGpp increase the dynamic range of its effects on transcription during the stringent response. Instead, our data are more consistent with a model in which both binding sites reversibly bind ppGpp, are saturated to approximately the same extent when ppGpp concentrations are low, and become fully occupied at approximately the same time when ppGpp is induced to high levels.

We did not test binding of pppGpp (the pentaphosphate) to the two sites in RNAP. Available data indicate that, in *E. coli*, pppGpp is less abundant than ppGpp *in vivo* and that its effects on transcription *in vivo* and *in vitro*, particularly at Site 2, are less potent than those of ppGpp (Potrykus and Cashel, 2008; Mechold et al., 2013). Structures of the RNAP/DksA/ppGpp complex indicate that ppGpp at each site is partially solvent exposed (Zuo et al., 2013; Molodtsov et al., 2018), suggesting that each site could accommodate the additional phosphate group in pppGpp. However, it is not known whether the additional phosphate group could alter binding affinity.

Guanosine tetraphosphate binding to the two sites on RNAP can affect at least two different steps in transcription, impacting the kinetics of initiation by multiple mechanisms and resulting in different effects on transcriptional output from different promoters (Ross et al., 2016; Sanchez-Vazquez et al., 2019). For example, ppGpp binding to Site 2 can activate transcription from certain promoters whereas binding of ppGpp to Site 1 cannot (Ross et al., 2016; Gourse et al., 2018). In addition, it was also shown long ago that ppGpp affects transcription elongation *in vitro* (Kingston et al., 1981). Since those studies were performed without DksA, the effects on elongation were likely a result of binding to Site 1. Further studies will be needed to understand the mechanism(s) responsible for the effects of ppGpp on elongation, and which other factors play roles in these effects (see for example, Singh et al., 2016).

Given the concentration of ppGpp reported for non-starvation conditions in rich medium (~1–10 μM; Ryals et al., 1982), a concentration of RNAP *in vivo* of ~10 μM (Bremer and Dennis, 2008; Li et al., 2014), and the apparent binding affinities for

ppGpp reported here, in a significant fraction of RNAP molecules it is likely that one or the other site would not be saturated with ppGpp. In the lower range of ppGpp concentrations (i.e., non-starvation conditions), when one site or the other is bound by ppGpp, this could result in some stochastic variation in regulation of transcription by ppGpp in subpopulations of RNAP molecules, creating some "bet-hedging" (Rocha et al., 2002). Stochasticity would be less impactful under starvation conditions when high ppGpp concentrations are present, and both ppGpp binding sites on all RNAP molecules would be saturated.

Depending on which step during transcription is affected, ppGpp function requires the presence of ω or DksA. However, since the concentrations of ω and DksA change little during exponential growth in *E. coli*, and no more than 2-fold in stationary phase, differences in the occupancies of the two ppGpp binding sites over time (and thus the impact of ppGpp on transcription) must result primarily from changes in ppGpp, not ω or DksA concentrations.

Interestingly, our data indicate that DksA increases the affinity of the wild-type RNAP for ppGpp ($K_{d,app}$ = 3.3 ± 1.2 μM average affinity for the two binding sites on wild-type RNAP versus 6.1 ± 1.3 μM or 7.9 ± 1.3 μM, respectively, for RNAPs containing only Site 1 or 2). In addition, the affinity of ppGpp for the RNAPs in complex with the "separation of function" DksA variants is 1.3 ± 0.1–1.8 ± 0.5 μM. These results suggest that the increased affinity of Site 1 for ppGpp in the presence of DksA accounts for the reduced average affinity of wild-type RNAP for ppGpp relative to the affinity for either Site 1 or Site 2 alone. Thus, DksA allosterically enhances binding of ppGpp to Site 1, even though DksA and Site 1 are separated by ~30 Å at their position of closest approach (**Figure 5**). Although a limited number of secondary channel binding proteins was tested, we suggest this enhancement of ppGpp affinity for Site 1 is unique to DksA (**Figure 4**). The physiological consequence, if any, of the enhancement in affinity of Site 1 for ppGpp by DksA remains to be determined.

Finally, the concentrations of ppGpp observed during the stringent response appear to be much higher than needed for full occupancy of the two sites on RNAP. Although the high concentrations undoubtedly evolved in part to increase the kinetics of ppGpp occupancy of RNAP, some 70 proteins in *E. coli* bind ppGpp, only a subset of which bind ppGpp with an affinity as high as RNAP (Pao and Dyess, 1981; Hou et al., 1999; Kanjee et al., 2011a,b; Zhang et al., 2018; Anderson et al., 2019; Wang et al., 2019). We suggest that the high levels of ppGpp produced during severe starvations could be needed for ppGpp to bind to the proteins with lower affinity ppGpp binding sites.

DATA AVAILABILITY STATEMENT

All datasets presented in this study are included in the article/**Supplementary Material**.

AUTHOR CONTRIBUTIONS

AM designed, performed, and analyzed experiments and wrote the paper. WR analyzed experiments and wrote the paper. DT performed and analyzed experiments. RG designed and analyzed experiments and wrote the paper. All authors contributed to the article and approved the submitted version.

FUNDING

This work was supported by a grant to RG from the National Institutes of Health (R01 GM37048). AM was supported in part by predoctoral fellowships from the National Science Foundation and the National Institutes of Health.

ACKNOWLEDGMENTS

We thank J.-H. Lee for purified GreB, S. Gopalkrishnan for purified TraR, and K. Myers, R. Landick, J. Keck, D. Brow, P. Kiley, and T. Record for helpful comments.

SUPPLEMENTARY MATERIAL

The Supplementary Material for this article can be found online at: https://www.frontiersin.org/articles/10.3389/fmicb.2020.587098/full#supplementary-material

REFERENCES

Anderson, B. W., Liu, K., Wolak, C., Dubiel, K., She, F., Satyshur, K. A., et al. (2019). Evolution of (p)ppGpp-HPRT regulation through diversification of an allosteric oligomeric interaction. *Elife* 8:e47534. doi: 10.7554/eLife.47534

Blankschien, M. D., Potrykus, K., Grace, E., Choudhary, A., Vinella, D., Cashel, M., et al. (2009). TraR, a homolog of a RNAP secondary channel interactor, modulates transcription. *PLoS Genet.* 5:e1000345. doi: 10.1371/journal.pgen.1000345

Bremer, H., and Dennis, P. P. (2008). Modulation of chemical composition and other parameters of the cell at different exponential growth rates. *EcoSal Plus* 3. doi: 10.1128/ecosal.5.2.3

Cashel, M., and Gallant, J. (1969). Two compounds implicated in the function of the RC genes of *Escherichia coli*. *Nature* 221, 838–841. doi: 10.1038/221838a0

Chen, J., Gopalkrishnan, S., Chiu, C., Chen, A. Y., Campbell, E. A., Gourse, R. L., et al. (2019). *E. coli* TraR allosterically regulates transcription initiation by altering RNA polymerase conformation. *Elife* 8:e49375. doi: 10.7554/eLife.49375

Durfee, T., Hansen, A. M., Zhi, H., Blattner, F. R., and Jin, D. J. (2008). Transcription profiling of the stringent response in *Escherichia coli*. *J. Bacteriol.* 190, 1084–1096. doi: 10.1128/JB.01092-07

Gentry, D. R., and Burgess, R. R. (1989). *rpoZ*, encoding the omega subunit of *Escherichia coli* RNA polymerase, is in the same operon as spoT. *J. Bacteriol.* 171, 1271–1277. doi: 10.1128/jb.171.3.1271-1277.1989

Gentry, D., Xiao, H., Burgess, R. R., and Cashel, M. (1991). The omega subunit of *Escherichia coli* K-12 RNA polymerase is not required for stringent RNA control in vivo. *J. Bacteriol.* 173, 3901–3903. doi: 10.1128/jb.173.12.3901-3903.1991

Gopalkrishnan, S., Ross, W., Chen, A. Y., and Gourse, R. L. (2017). TraR directly regulates transcription initiations by mimicking the combined effects

of the global regulators DksA and ppGpp. *Proc. Natl. Acad. Sci. U. S. A.* 114, E5539–E5548. doi: 10.1073/pnas.1704105114

Gourse, R. L., Chen, A. Y., Gopalkrishnan, S., Sanchez-Vazquez, P., Myers, A., and Ross, W. (2018). Transcriptional responses to ppGpp and DksA. *Annu. Rev. Microbiol.* 72, 163–184. doi: 10.1146/annurev-micro-090817-062444

Hauryliuk, V., Atkinson, G. C., Murakami, K. S., Tenson, T., and Gerdes, K. (2015). Recent functional insights into the role of (p)ppGpp in bacterial physiology. *Nat. Rev. Microbiol.* 13, 298–309. doi: 10.1038/nrmicro3448

Hill, A. V. (1910). The possible effects of the aggregation of the molecules of haemoglobin on its dissociation curves. *J. Physiol.* 40, iv–vii.

Hou, Z., Cashel, M., Fromm, H. J., and Honzatko, R. B. (1999). Effectors of the stringent response target the active site of *Escherichia coli* adenylosuccinate synthetase. *J. Biol. Chem.* 274, 17505–17510. doi: 10.1074/jbc.274.25.17505

Irving, S. E., and Corrigan, R. M. (2018). Triggering the stringent response: signals responsible for activating (p)ppGpp synthesis in bacteria. *Microbiology* 164, 268–276. doi: 10.1099/mic.0.000621

Kanjee, U., Gutsche, I., Alexopoulos, E., Zhao, B. Y., El Bakkouri, M., Thibault, G., et al. (2011a). Linkage between the bacterial acid stress and stringent responses: the structure of the inducible lysine decarboxylase. *EMBO J.* 30, 931–944. doi: 10.1038/emboj.2011.5

Kanjee, U., Gutsche, I., Ramachandran, S., and Houry, W. A. (2011b). The enzymatic activities of the *Escherichia coli* basic aliphatic amino acid decarboxylases exhibit a pH zone of inhibition. *Biochemistry* 50, 9388–9398. doi: 10.1021/bi201161k

Kingston, R. E., Nierman, W. C., and Chamberlin, M. J. (1981). A direct effect of guanosine tetraphosphate on pausing *Escherichia coli* RNA polymerase during RNA chain elongation. *J. Biol. Chem.* 256, 2787–2797.

Krasny, L., and Gourse, R. L. (2004). An alternative strategy for bacterial ribosome synthesis: *Bacillus subtilis* rRNA transcription regulation. *EMBO J.* 23, 4473–4483. doi: 10.1038/sj.emboj.7600423

Lee, J. -H., Lennon, C. W., Ross, W., and Gourse, R. L. (2012). Role of the coiled-coil tip of *Escherichia coli* DksA in promoter control. *J. Mol. Biol.* 416, 503–517. doi: 10.1016/j.jmb.2011.12.028

Li, G. -W., Burkhardt, D., Gross, C., and Weissman, J. S. (2014). Quantifying absolute protein synthesis rates reveals principles underlying allocation of cellular resources. *Cell* 157, 624–635. doi: 10.1016/j.cell.2014.02.033

Liu, K., Bittner, A. N., and Wang, J. D. (2015). Diversity in (p)ppGpp metabolism and effectors. *Curr. Opin. Microbiol.* 24, 72–79. doi: 10.1016/jmib.2015.01.012

Mechold, U., Potrykus, K., Murphy, H., Murakami, K. S., and Cashel, M. (2013). Differential regulation by ppGpp versus pppGpp in *Escherichia coli*. *Nucleic Acids Res.* 41, 6175–6189. doi: 10.1093/nar/gkt302

Molodtsov, V., Sineva, E., Zhang, L., Huang, X., Cashel, M., Ades, S. E., et al. (2018). Allosteric effector ppGpp potentiates the inhibition of transcript initiation by DksA. *Mol. Cell* 69, 828.e5–839.e5. doi: 10.1016/j.molcel.2018.01.035

Pao, C. C., and Dyess, B. T. (1981). Effect of unusual guanosine nucleotides on the activities of some *Escherichia coli* cellular enzymes. *Biochim. Biophys. Acta* 677, 358–362. doi: 10.1016/0304-4165(81)90247-6

Paul, B. J., Barker, M. M., Ross, W., Schneider, D. A., Webb, C., Foster, J. W., et al. (2004). DksA: a critical component of the transcription initiation machinery that potentiates the regulation of rRNA promoters by ppGpp and the initiating NTP. *Cell* 118, 311–322. doi: 10.1016/j.cell.2004.07.009

Paul, B. J., Berkmen, M. B., and Gourse, R. L. (2005). DksA potentiates direct activation of amino acid promoters by ppGpp. *Proc. Natl. Acad. Sci. U. S. A.* 102, 7823–7828. doi: 10.1073/pnas.0501170102

Potrykus, K., and Cashel, M. (2008). (p)ppGpp: still magical? *Annu. Rev. Microbiol.* 62, 35–51. doi: 10.1146/annurev.micro.62.081307.162903

Rocha, E. P. C., Matic, I., and Taddei, F. (2002). Over-representation of repeats in stress response genes: a strategy to increase versatility under stress conditions? *Nucleic Acids Res.* 30, 1886–1894. doi: 10.1093/nar/30.9.1886

Roelofs, K. G., Wang, J., Sintim, H. O., and Lee, V. T. (2011). Differential radial capillary action of ligand assay for high-through put detection of protein-metabolite interactions. *Proc. Natl. Acad. Sci. U. S. A.* 108, 15528–15533. doi: 10.1073/pnas.1018949108

Ross, W., Sanchez-Vazquez, P., Chen, A. Y., Lee, J. -H., Burgos, H. L., and Gourse, R. L. (2016). ppGpp binding to a site at the RNAP-DksA interface accounts for its dramatic effects on transcription initiation during the stringent response. *Mol. Cell* 62, 811–823. doi: 10.1016/j.molcel.2016.04.029

Ross, W., Vrentas, C. E., Sanchez-Vazquez, P., Gaal, T., and Gourse, R. L. (2013). The magic spot: a ppGpp binding site on *E. coli* RNA polymerase responsible for regulation of transcription initiation. *Mol. Cell* 50, 420–429. doi: 10.1016/j.molcel.2013.03.021

Rutherford, S. T., Lemke, J. J., Vrentas, C. E., Gaal, T., Ross, W., and Gourse, R. L. (2007). Effects of DksA, GreA, and GreB on transcription initiation: insights into the mechanisms of factors that bind in the secondary channel of RNA polymerase. *J. Mol. Biol.* 366, 1243–1257. doi: 10.1016/j.jmb.2006.12.013

Ryals, J., Little, R., and Bremer, H. (1982). Control of RNA synthesis in *Escherichia coli* after a shift to higher temperature. *J. Bacteriol.* 151, 1425–1432. doi: 10.1128/JB.151.3.1425-1432.1982

Sanchez-Vazquez, P., Dewey, C. N., Kitten, N., Ross, W., and Gourse, R. L. (2019). Genome-wide effects on *Escherichia coli* transcription from ppGpp binding to its two sites on RNA polymerase. *Proc. Natl. Acad. Sci. U. S. A.* 116, 8310–8319. doi: 10.1073/pnas.1819682116

Singh, N., Bubunenko, M., Smith, C., Abbott, D. M., Stringer, A. M., Shi, R., et al. (2016). SuhB associates with nus factors to facilitate 30S ribosome biogenesis in *Escherichia coli*. *mBio* 7:e00114. doi: 10.1128/mBio.00114-16

Traxler, M. F., Summer, S. M., Nguyen, H. T., Zacharia, V. M., Hightower, G. A., Smith, J. T., et al. (2008). The global ppGpp-mediated stringent response to amino acid starvation in *Escherichia coli*. *Mol. Microbiol.* 68, 1128–1148. doi: 10.1111/j.1365-2958.2008.06229.x

Varik, V., Oliveira, S. R. A., Hauryliuk, V., and Tenson, T. (2017). HPLC-based quantification of bactgerial housekeeping nucleotides and alarmone messengers ppGpp and pppGpp. *Sci. Rep.* 7:11022. doi: 10.1038/s41598-017-10988-6

Vrentas, C. E. (2008). A study of the requirements for the response of *Escherichia coli* RNA polymerase to guanosine tetraphosphate (ppGpp). University of Wisconsin-Madison.

Vrentas, C. E., Gaal, T., Ross, W., Ebright, R. H., and Gourse, R. L. (2005). Response of RNA polymerase to ppGpp: requirement for the omega subunit and relief of this requirement by DksA. *Genes Dev.* 19, 2378–2387. doi: 10.1101/gad.1340305

Wang, B., Dai, P., Ding, D., Del Rosario, A., Grant, R. A., Pentelute, B. L., et al. (2019). Affinity-based capture and identification of protein effectors of the growth regulator ppGpp. *Nat. Chem. Biol.* 15, 141–150. doi: 10.1038/s41589-018-0183-4

Xiao, H., Kalman, M., Ikehara, K., Zemel, S., Glaser, G., and Cashel, M. (1991). Residual guanosine 3',5'-bispyrophosphate synthetic activity of relA null mutants can be eliminated by spoT null mutations. *J. Biol. Chem.* 266, 5980–5990.

Zhang, Y., Zbornikova, E., Rejman, D., and Gerdes, K. (2018). Novel (p)ppGpp binding and metabolizing proteins in *Escherichia coli*. *mBio* 9, e02188–e02217. doi: 10.1128/mBio.02188-17

Zuo, Y., Wang, Y., and Steitz, T. A. (2013). The mechanism of *E. coli* RNA polymerase regulation by ppGpp is suggested by the structure of their complex. *Mol. Cell* 50, 430–436. doi: 10.1016/j.molcel.2013.03.020

Conflict of Interest: The authors declare that the research was conducted in the absence of any commercial or financial relationships that could be construed as a potential conflict of interest.

frontiers in Microbiology

REVIEW
published: 03 December 2020
doi: 10.3389/fmicb.2020.601417

Survival of the Fittest: The Relationship of (p)ppGpp With Bacterial Virulence

*Shivani Kundra, Cristina Colomer-Winter and José A. Lemos**

Department of Oral Biology, UF College of Dentistry, Gainesville, FL, United States

The signaling nucleotide (p)ppGpp has been the subject of intense research in the past two decades. Initially discovered as the effector molecule of the stringent response, a bacterial stress response that reprograms cell physiology during amino acid starvation, follow-up studies indicated that many effects of (p)ppGpp on cell physiology occur at levels that are lower than those needed to fully activate the stringent response, and that the repertoire of enzymes involved in (p)ppGpp metabolism is more diverse than initially thought. Of particular interest, (p)ppGpp regulation has been consistently linked to bacterial persistence and virulence, such that the scientific pursuit to discover molecules that interfere with (p)ppGpp signaling as a way to develop new antimicrobials has grown substantially in recent years. Here, we highlight contemporary studies that have further supported the intimate relationship of (p)ppGpp with bacterial virulence and studies that provided new insights into the different mechanisms by which (p)ppGpp modulates bacterial virulence.

Keywords: (p)ppGpp, stringent response (SR), bacterial virulence, bacterial stress response, regulatory nucleotides

OPEN ACCESS

Edited by:
Katarzyna Potrykus, University of Gdańsk, Poland

Reviewed by:
Shinji Masuda, Tokyo Institute of Technology, Japan
Robert E. W. Hancock, University of British Columbia, Canada

***Correspondence:**
José A. Lemos
jlemos@dental.ufl.edu

Specialty section:
This article was submitted to Microbial Physiology and Metabolism, a section of the journal Frontiers in Microbiology

Received: *31 August 2020*
Accepted: *16 November 2020*
Published: *03 December 2020*

Citation:
Kundra S, Colomer-Winter C and Lemos JA (2020) Survival of the Fittest: The Relationship of (p)ppGpp With Bacterial Virulence. Front. Microbiol. 11:601417. doi: 10.3389/fmicb.2020.601417

INTRODUCTION

In response to changes in the surrounding environment, bacteria utilize a variety of sophisticated sensory mechanisms that reprogram cell physiology to facilitate adaptation to the new environment. Among those mechanisms are the production of signaling nucleotides such as (i) cAMP, the first regulatory nucleotide ever described, (ii) a growing family of cyclic nucleotides such as c-di-GMP, c-di-AMP, and cAMP-GMP, and (iii) hyperphosphorylated nucleotides, including (p)ppGpp and newly described analogs pGpp and (p)ppApp (Potrykus and Cashel, 2008; Kalia et al., 2013; Gaca et al., 2015b; Yang et al., 2019, 2020; Fung et al., 2020; Jimmy et al., 2020). The commonly used (p)ppGpp abbreviation indicates two guanosine derivatives – ppGpp (GDP, 3′-diphosphate) and pppGpp (GTP, 3′-diphosphate) – initially known as the magic spot or nutritional alarmone (Cashel and Kalbacher, 1970; Potrykus and Cashel, 2008). Seminal studies discovered that in response to stress conditions, (p)ppGpp rapidly accumulates to high levels within the cell and reprograms cell physiology through transcriptional and allosteric mechanisms that ultimately reallocate cellular resources from an active growth state toward a semi-dormant state (Potrykus and Cashel, 2008). When fully active, this process termed the stringent response (SR), has been shown to lower the activity of metabolic pathways associated with rapid cell growth, while activating pathways associated with nutrient uptake, amino acid biosynthesis and stress survival thereby facilitating cell survival under severe adverse conditions (Potrykus and Cashel, 2008;

Kanjee et al., 2012; Gaca et al., 2015a). While initially discovered as a response to amino acid starvation, the SR was also shown to be induced by non-nutritional stresses such as heat stress and antibiotics (Gallant et al., 1977; Glass et al., 1979; Wells and Gaynor, 2006; Hobbs and Boraston, 2019; Schafer et al., 2020). In addition to acting as the effector molecule of the SR, contemporary studies revealed that (p)ppGpp plays a fundamental role in the control of core cellular processes at concentrations that are well below those needed to activate the SR (**Figure 1**). Indeed, during balanced (non-stressed) conditions, relatively small fluctuations in basal (p)ppGpp pools were shown to influence transcription of hundreds of genes, with a complete loss of (p)ppGpp regulation impairing cell fitness even in the absence of stress (Gaca et al., 2013; Colomer-Winter et al., 2019; Sanchez-Vazquez et al., 2019; Fernandez-Coll et al., 2020; Pletzer et al., 2020). Given the critical role of (p)ppGpp in cell physiology, it is not surprising that several studies have implicated (p)ppGpp with bacterial virulence and antibiotic tolerance (**Table 1** and **Figure 2**). Specifically, the production of (p)ppGpp has been associated with expression of virulence traits, which includes but is not limited to adhesion, biofilm formation, toxin production, motility, sporulation, and antibiotic tolerance (Dalebroux et al., 2010). Importantly, several of those studies indicate that the intimate relationship of (p)ppGpp with bacterial persistence and virulence might be more closely linked to basal levels of (p)ppGpp than to those needed to activate the SR. In 2010, Dalebroux and colleagues published a comprehensive review linking (p)ppGpp to bacterial virulence in plants, animals and humans (Dalebroux et al., 2010). Here, we will highlight recent studies that have further supported the intimate relationship of (p)ppGpp with bacterial virulence, with an emphasis on studies that directly tested (p)ppGpp-deficient strains in animal infection models that are relevant to human infectious diseases. For historical and contemporary perspectives of other aspects of the field, we direct the reader to other reviews (Dalebroux and Swanson, 2012; Gaca et al., 2015a; Hauryliuk et al., 2015; Liu et al., 2015; Steinchen and Bange, 2016; Ronneau and Hallez, 2019; Zhu et al., 2019b).

GRAM-POSITIVE PATHOGENS

Most of the Gram-positive bacteria that cause disease in humans belong to the Firmicutes phylum, which is primarily comprised of bacteria with a low-GC content. In Firmicutes, (p)ppGpp metabolism is primarily controlled by the bifunctional synthetase/hydrolase Rel enzyme, also known as RelA or Rsh (for RelA SpoT homolog) (Atkinson et al., 2011). The use of different designations for the (p)ppGpp synthetase/hydrolase of Gram-positive bacteria has created confusion in the field, since the Gram-negative RelA protein (originally described in *Escherichia coli*) is a monofunctional synthetase without hydrolase activity. Though some studies might have originally referred to the bifunctional (p)ppGpp synthetase/hydrolase of Gram-positive bacteria as RelA or Rsh, herein, we will adopt the nomenclature proposed by Atkinson and colleagues (Atkinson et al., 2011) and refer to the bifunctional Gram-positive enzyme as Rel.

While Rel-dependent (p)ppGpp synthesis is primarily responsible for activation of the SR in all Gram-positive bacteria investigated to date, the (p)ppGpp hydrolase activity of this enzyme is essential to some species by avoiding the accumulation of (p)ppGpp to toxic levels (Geiger et al., 2010; Weiss and Stallings, 2013; Gratani et al., 2018; Ronneau and Hallez, 2019). In addition to Rel, Firmicutes express one or two short/small (p)ppGpp synthetases (SASs), termed RelP and RelQ (known as YjbM and YwaC, respectively, in *Bacillus subtilis*) (Atkinson et al., 2011). All SASs appear to be primarily involved in maintainence of basal (p)ppGpp pools during growth, though have been also linked to a timely activation of the SR (Gaca et al., 2012) and to cell envelope stress tolerance (Geiger et al., 2014; Bhawini et al., 2019). While the majority of Firmicutes encode both RelP and RelQ, few species including *Streptococcus pneumoniae*, *Streptococcus suis* and all members of the *Enterococcus* genus only encode RelQ (Atkinson et al., 2011). Below, we review studies that, either through the use of animal models, clinical evidence, or both, provided conclusive evidence of the association of (p)ppGpp with Gram-positive bacterial virulence. When discussing these studies it is important to mention that different than Gram-negative bacteria, (p)ppGpp does not control global gene transcription by physically interacting with the RNAP and by partnering with the transcriptional regulator DksA (Wolz et al., 2010). Instead, (p)ppGpp indirectly affects Gram-positive gene transcription through modulation of intracellular purine concentrations thereby changing the availability of initiating nucleotides of transcription (Krasny and Gourse, 2004; Krasny et al., 2008; Kriel et al., 2012). In addition, the sharp drop in GTP and concomitant increase in ATP directly affects activity of CodY, a nutrient-sensing transcriptional regulator that is widespread in Firmicutes and that controls activation of nutrient-acquisition

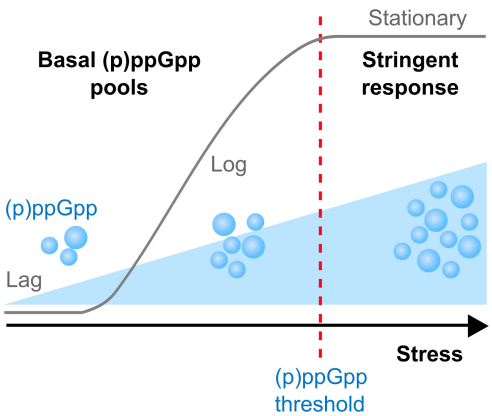

FIGURE 1 | (p)ppGpp modulates bacterial physiology at all growth stages. During adaptation (lag) and exponential (log) growth phases in the absence of stresses, basal levels of (p)ppGpp are important to maintain a balanced metabolism avoiding uncontrolled consumption of energy stores and toxic accumulation of metabolic byproducts. Entry into stationary growth phase or adverse condtions such as nutrient starvation, heat shock or selected antibiotic stresses triggers the accumulation of (p)ppGpp that rapidly reaches the threshold necessary to mount the SR responsible for remodeling cell physiology from a growth mode to a survival mode.

and nutrient biosynthesis pathways and virulence determinants (Sonenshein, 2005). Because CodY is a GTP-responsive regulator, there is an inverse relationship between (p)ppGpp and CodY where the accumulation of (p)ppGpp typically leads to alleviation of CodY regulation (Geiger and Wolz, 2014). As a result, the (p)ppGpp and CodY networks are intertwined, with several reports linking both regulatory networks to bacterial virulence and, in most cases, having an antagonistic relationship (Geiger and Wolz, 2014). In addition to CodY, (p)ppGpp control of bacterial physiology is also exherted through direct interaction with enzymes and riboswitches (Kanjee et al., 2012; Sherlock et al., 2018).

Staphylococcus aureus

A common inhabitant of the human upper respiratory tract, *S. aureus* is also a major threat to public health as they can cause a wide range of opportunistic infections that range from mild skin infections to life-threatening pneumonia, osteomyelitis, endocarditis and sepsis. In *S. aureus*, (p)ppGpp is metabolized by the bifunctional Rel_{Sa} (Rsh_{Sa}) and the monofucntional RelP and RelQ. While the Rel_{Sa} synthetase was dispensable, its hydrolase activity was found to be essential in the presence of functional RelP and RelQ by preventing toxic accumulation of (p)ppGpp due to the activities of SASs (Geiger et al., 2010). The contribution of (p)ppGpp and the SR to staphylococcal virulence was first demonstrated in a synthetase-dead/hydrolase-active Rel mutant strain (rel_{syn}), where loss of Rel_{Sa} synthetase activity significantly attenuated *S. aureus* virulence in a mouse model of kidney infection (Geiger et al., 2010). Follow-up studies testing this mutant confirmed that Rel-dependent (p)ppGpp accumulation was also required for lesion formation in a cutaneous mouse model (Mansour et al., 2016). Notably, virulence of the rel_{syn} mutant was restored by deletion of *codY,* providing clear evidence of the (p)ppGpp-CodY relationship during infection (Geiger et al., 2010). Subsequent studies revealed that most genes activated by (p)ppGpp in *S. aureus* were under CodY control (Geiger et al., 2012), indicating that activation of the SR (i.e., high levels of (p)ppGpp) promotes virulence by, at least in part, alleviation of CodY regulation (Geiger et al., 2010, 2012). In addition to virulence, the SR has been associated to antibiotic tolerance (often referred as antibiotic persistence). For instance, a drug-resistant clinical isolate obtained from a persistent bloodstream infection treated with the protein synthesis inhibitor linezolid was shown to harbor point mutations in the rel_{Sa} gene that led to constitutive activation of the SR (Gao et al., 2010).

In addition to activation of the SR, more recent studies indicated that basal levels of (p)ppGpp (below those needed to activate the SR) contribute to antibiotic tolerance. Specifically, point mutations on the rel_{Sa} gene lowered the (p)ppGpp hydrolase activity of Rel_{Sa} causing a slight increase in basal (p)ppGpp pools that was linked to broad antibiotic tolerance (Mwangi et al., 2013; Bryson et al., 2020). In another study, the $relP_{Sa}$ and $relQ_{Sa}$ genes were shown to be strongly induced upon treatment with cell wall-active antibiotics (ampicillin and vancomycin) and simultaneous inactivation of both genes significantly decreased tolerance of *S. aureus* toward these antibiotics (Geiger et al., 2014). In a more recent study, the association of SASs with antibiotic tolerance was traced to RelQ as inactivation of $relQ_{Sa}$ decreased tolerance to β-lactam antibiotics in methicillin-resistant *S. aureus* (MRSA) by interfering with *mecA* gene expression, which codes for an alternative penicillin-binding protein (Bhawini et al., 2019). Interestingly, the importance of $RelQ_{Sa}$ in β-lactam tolerance could be bypassed by activation of the SR with mupirocin (an isoleucine analog/^{ile}tRNA inhibitor that triggers the SR), suggesting that *mecA* transcription requires a certain (p)ppGpp threshold (Bhawini et al., 2019). Unexpectedly, single inactivation of $relP_{Sa}$ increased β-lactam resistance, which the authors attributed to a sizeable increase in the expression of the $relQ_{Sa}$ promoter in the Δ*relP* strain (Bhawini et al., 2019). MRSA isolates from a clinical case with high tolerance to vancomycin displayed high levels of (p)ppGpp, high expression of cytotoxic PSMs (phenol-soluble modulins), increased PMN lysis and intracellular survival, and enhanced adherence to fibronectin/endothelial cells in *in vitro* assays (Li et al., 2020). Interestingly, transcription activation of PSMs was found to be both (p)ppGpp- and CodY-independent (Geiger et al., 2012). Finally, virulence of the *relP* mutant was not affected in a rabbit infective endocarditis (IE) model but treatment of the heart vegetation colonized by the *relP* mutant with vancomycin reduced spread in the cardiac vegetation and dissemination to other tissues (Li et al., 2020). Collectively, these studies reveal that the SR and CodY mediate *S. aureus* virulence and antibiotic tolerance, but also indicate that basal levels of (p)ppGpp, primarily mediated by RelP and RelQ, play a role in supporting staphylococcal cell attachment, survival to immune cells and antibiotic tolerance. In the future, it will be important to determine the relevance of (p)ppGpp and the SR in other types of infection and evaluate the virulence potential of a triple Δ*rel*Δ*relP*Δ*relQ* mutant [(p)ppGpp^0 strain].

Enterococci

A natural inhabitant of the gastrointestinal tract of animals, enterococci are among the leading causes of life-threatening nosocomial infections (Arias and Murray, 2012). While *E. faecalis* accounts for the majority of enterococcal infections in humans (∼75%), *E. faecium* responds for the majority of vancomycin resistant enterococci (VRE) infections. The genome of *E. faecalis* encodes a bifunctional Rel (Rel_{Ef}) and a single SAS termed $RelQ_{Ef}$. Similar to *S. aureus*, Rel_{Ef} is the major enzyme responsible for (p)ppGpp accumulation and activation of the SR (Abranches et al., 2009; Gaca et al., 2012), an observation that has been confirmed with all other Gram-positive bacteria that have been studied to date. In the past decade, the importance of (p)ppGpp and the SR to *E. faecalis* pathophysiology has been probed to some detail by our group. Collectively, our studies indicate that the association of (p)ppGpp with virulence does not necessarily relate to activation of the SR but to basal levels of (p)ppGpp (Abranches et al., 2009; Gaca et al., 2012, 2013). Specifically, we and others showed that the consequences of single inactivation of rel_{Ef} or $relQ_{Ef}$ to *E. faecalis* pathophysiology are for the

TABLE 1 | Virulence of (p)ppGpp-defective mutants.

Bacterial Pathogen	Strain	Basal (p)ppGpp	Stringent response	Animal Model/Virulence	References
Acinetobacter baumanii	ΔrelA	Yes	No	*G. mellonella*: attenuated	Perez-Varela et al. (2020)
Bacillus anthracis	Δrel	Yes	No	Mouse subcutaneous: ND1	van Schaik et al. (2007)
Borrelia burgdorferi	Δrel	No	No	Mouse intradermal: avirulent	Bugrysheva et al. (2005)
Brucella melitensis	Δrel	No	No	Mouse systemic: attenuated	Dozot et al. (2006)
Burkholderia pseudomallei	ΔrelAΔspoT	No	No	*G. mellonella* and mouse: attenuated	Muller et al. (2012)
Enterococcus faecalis	Δrel	Yes	No	*G. mellonella* or *C. elegans*: ND; Mouse CAUTI: ND; Rabbit abscess: ND; Rabbit endocarditis: attenuated	Abranches et al. (2009); Yan et al. (2009), Gaca et al. (2012); Frank et al. (2014), Colomer-Winter et al. (2018, 2019)
	ΔrelQ	Yes	Yes	*G. mellonella* or *C. elegans*: ND; Mouse CAUTI: ND; Rabbit abscess: ND; Rabbit endocarditis: ND	Abranches et al. (2009); Gaca et al. (2012), Frank et al. (2014); Colomer-Winter et al. (2018)Colomer-Winter et al. (2019)
	ΔrelΔrelQ	No	No	*G. mellonella* or *C. elegans*: attenuated; Mouse CAUTI: attenuated; Rabbit abscess: attenuated; Rabbit endocarditis: ND	Abranches et al. (2009); Gaca et al. (2012), Frank et al. (2014); Colomer-Winter et al. (2018)Colomer-Winter et al. (2019)
Francisella novocida	ΔrelA	Yes	No	Mouse (intranasal): attenuated	Dean et al. (2009)
Francisella tularensis	ΔrelAΔspoT	No	No	Mouse (intranasal): avirulent	Charity et al. (2009); Ma et al. (2019)
Haemophilus ducreyi	ΔrelAΔspoT	No	No	Human pustule: attenuated	Holley et al. (2014)
Listeria monocytogenes	Δrel	Yes	No	Mouse systemic: avirulent	Taylor et al. (2002), Bennett et al. (2007)
	rel:Tn	?	?	Mouse systemic: attenuated	Taylor et al. (2002)
	ΔrelΔrelPΔrelQ	No	No	Mouse systemic: attenuated	Whiteley et al. (2015)
Mycobacterium tuberculosis	relH344Y	Yes	No	Mouse lung: attenuated	Weiss and Stallings (2013)
	relH80A	Yes	Yes	Mouse lung: attenuated	Weiss and Stallings (2013)
	ΔrelΔSAS	No	No	Mouse lung: attenuated	Weiss and Stallings (2013)
	Δrel	Yes	No	Mouse lung and guinea pig lung: attenuated	Dahl et al. (2003); Klinkenberg et al. (2010)
Pseudomonas aeruginosa	ΔrelA	Yes	No	*D. melanogaster*: attenuated; Mouse abscess: ND	Vogt et al. (2011); Pletzer et al. (2017)
	ΔrelAΔspoT	No	No	*D. melanogaster*, Mouse pneumonia: avirulent/attenuated; Mouse abscess/skin: attenuated	Vogt et al. (2011); Xu et al. (2016), Pletzer et al. (2017)
Salmonella Gallinarum	ΔrelAΔspoT	No	No	Chicken (oral): attenuated	Park et al. (2010)
Salmonella Typhi	ΔrelAΔspoT	No	No	Mouse (oral): avirulent	Dasgupta et al. (2019)
Salmonella Typhimurium	ΔrelA	Yes	No	Mouse (intragastric): attenuated	Pizarro-Cerda and Tedin (2004)
	spoT-Δctd	Yes	Yes	Mouse (oral): attenuated	Fitzsimmons et al. (2020)
	ΔrelAΔspoT	No	No	Mouse (intragastric): avirulent	Pizarro-Cerda and Tedin (2004)
Staphylococcus aureus	relSaF128Y	High	Yes	*G. mellonella*: attenuated	Gao et al. (2010)
	relSasyn	Yes	No	Mouse kidney: attenuated; Mouse skin: attenuated	Geiger et al. (2010); Mansour et al. (2016)
	ΔrelP	Yes	Yes	Rabbit endocarditis: ND	Li et al. (2020)
Streptococcus pneumoniae	ΔrelSpn	Yes	No	Mouse pneumonia: attenuated	Kazmierczak et al. (2009)

(Continued)

TABLE 1 | Continued

Bacterial Pathogen	Strain	Basal (p)ppGpp	Stringent response	Animal Model/Virulence	References
Streptococcus suis	ΔrelΔrelQ	No	No	Mouse systemic: avirulent	Zhu et al. (2016)
Vibrio cholerae	ΔrelA	Yes	No	Suckling mouse: attenuated/ND 2; Rabbit ileal loop: attenuated	Haralalka et al. (2003)
	ΔrelAΔspoT	Yes	No	Infant mouse: ND	Oh et al. (2014)
	ΔrelAΔspoTΔrelV	No	No	Infant mouse: attenuated	Oh et al. (2014)
Yersinia pestis	ΔrelA	Yes	No	Mouse: ND	Sun et al. (2009)
	ΔrelAΔspoT	No	Yes	Mouse: attenuated	Sun et al. (2009)

ND, no differences when compared to parent strain. Conflicting data from different laboratories.

most part negligible or fairly modest (Yan et al., 2009; Frank et al., 2014; Colomer-Winter et al., 2018, 2019) whereas a Δ*rel*Δ*relQ* double mutant [(p)ppGpp^0] strain showed multiple phenotypes including impaired survival within the macrophage cell line J774.A1, growth/survival defects in human fluids (blood and urine) *ex vivo*, and attenuated virulence in invertebrate (*Caenorhabditis elegans* and *Galleria mellonella*) and vertebrate [rabbit subdermal abscess and mouse (CAUTI) catheter-associated urinary tract infection] models (Abranches et al., 2009; Gaca et al., 2012; Frank et al., 2014; Colomer-Winter et al., 2019). Through transcriptome and biochemical analyses, the defective phenotypes of the (p)ppGpp^0 strain were traced to a metabolic dysregulation that resulted in toxic accumulation of endogenously produced reactive oxygen species (ROS) and an impaired metal homeostasis (Gaca et al., 2013; Colomer-Winter et al., 2017). In several cases, growth/survival defects of the (p)ppGpp^0 strain could be rescued by addition of glutathione or manganese supplementation, which either directly or indirectly mitigate ROS damage (Colomer-Winter et al., 2017). In agreement with previous findings obtained with other Firmicutes (Bennett et al., 2007; Geiger et al., 2012; Whiteley et al., 2015), inactivation of *codY* restored the virulence of the (p)ppGpp^0 strain in the *G. mellonella* and mouse CAUTI models (Colomer-Winter et al., 2017, 2019). Still, the molecular mechanisms by which (p)ppGpp supports virulence in this species cannot be solely attributed to association of (p)ppGpp with the CodY regulon as (i) basal levels of (p)ppGpp that are unlikely to interfere with CodY activity are more relevant to enterococcal pathogenesis than the SR, and (ii) (p)ppGpp controls several genes in a CodY-independent manner during active growth and during the SR (Gaca et al., 2012; Colomer-Winter et al., 2019).

Similar to clinical observations made with *S. aureus* persistent infections (see text above), whole genome sequencing identified a single missense mutation in the Rel$_{Efm}$ gene of an antibiotic resistant *E. faecium* that was isolated from a bacteremia case (Honsa et al., 2017). This SNP resulted in constitutively high levels of ppGpp directly linking (p)ppGpp to antibiotic tolerance in *E. faecium*. Interesting, this mutation did not change the minimum inhibitory concentration (MIC) for several antibiotics under *in vitro* conditions, including antibiotics that had been administered to the infected patient (Honsa et al., 2017). Collectively, the picture that emerges is that, similarly to staphylococci, increases in (p)ppGpp basal pools can be directly linked to antibiotic tolerance without necessarily conferring antibiotic resistance.

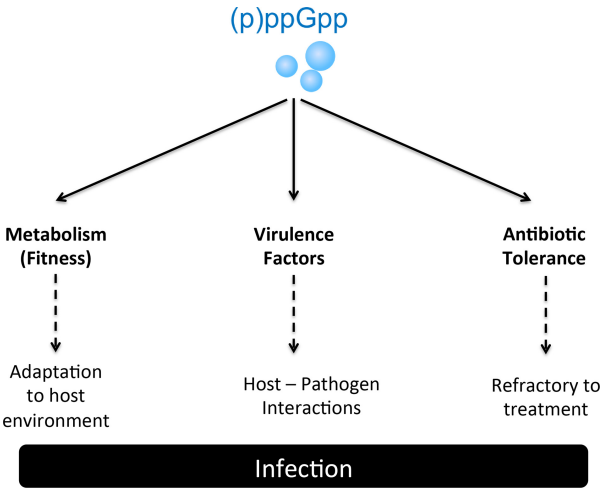

FIGURE 2 | (p)ppGpp participates in the regulation of several processes critical to bacterial pathogenesis. The roles of (p)ppGpp in adaptation to the host environment and antibioric tolerance are likely universal whereas the association with the expression of virulence factors appears to be species-specific.

Streptococci

The genus *Streptococcus* harbors some of the most common human and animal pathogens. Even though seminal studies that helped shape our understanding of how (p)ppGpp is metabolized in Gram-positive bacteria were performed with streptococci, from the first insights into the intramolecular regulation of the two catalytic domains of the Rel enzyme (Mechold et al., 2002; Sajish et al., 2007) to the discovery of SASs (Lemos et al., 2007), very few studies directly probed the significance of (p)ppGpp (and the SR) to streptococcal pathogenesis. In *S. pneumoniae*, which only harbors a single SAS (RelQ$_{Sp}$), inactivation of the bifunctional *rel$_{Sp}$* supported that Rel$_{Sp}$ is the primary source of (p)ppGpp and fully responsible for SR activation (Kazmierczak et al., 2009). Moreover, Rel$_{Sp}$ was shown to play a major role in disease progression in a pneumonia mouse model, and was linked to induction of the *ply*

operon, which encodes the pneumolysin toxin involved in early infection and tissue invasion (Kazmierczak et al., 2009). However, the exact mechanism by which Rel_{Spn}/(p)ppGpp regulates this virulence factor remains to be elucidated. In *S. suis*, an important pathogen of pigs, a (p)ppGpp^0 strain lacking both rel_{Ss} and $relQ_{Ss}$ displayed a number of phenotypic defects that can be linked to *S. suis* pathogenesis including decreased capacity to adhere and invade Hep-2 cells, lower survival in whole blood and decreased anti-phagocytic capacity (Zhu et al., 2016). Not surprisingly, virulence of the *S. suis* (p)ppGpp^0 strain was attenuated in a systemic infection mouse model (Zhu et al., 2016). However, different than *S. aureus*, *E. faecalis,* and *Listeria monocytogenes* (see below), the *S. suis* Δ*rel*Δ*relQ*Δ*codY* triple mutant phenocopied the Δ*rel*Δ*relQ* double mutant in the mouse infection model (Zhu et al., 2019a). Moreover, CodY was shown to interact with the Rel_{Ss} promoter in a GTP-independent manner, suggesting a new mechanism of (p)ppGpp and CodY crosstalk.

Listeria monocytogenes

Listeria monocytogenes is an intracellular foodborne pathogen and the causative agent of human listeriosis (Radoshevich and Cossart, 2018). Similar to *S. aureus* and *Streptococcus mutans*, the genome of *L. monocytogenes* encodes a bifunctional Rel_{Lm} and the SASs $RelP_{Lm}$ and $RelQ_{Lm}$. In one of the first studies to provide direct evidence of the association of (p)ppGpp with bacterial virulence, a transposon insertion library identified rel_{Lm} as an essential gene in a murine model of listeriosis (Taylor et al., 2002). In a study that explored the relationship between (p)ppGpp and CodY, the attenuated virulence of a Δrel_{Lm} strain could be partially linked to continued CodY-dependent repression as inactivation of *codY* in the Δrel_{Lm} background strain (Δrel_{Lm}Δ*codY*) partially restored *L. monocytogenes* virulence (Bennett et al., 2007). However, the reduced survival of the Δrel_{Lm} strain in culture cell lines was not restored in the Δrel_{Lm}Δ*codY* strain (Bennett et al., 2007). Follow up studies demonstrated that virulence of a triple mutant strain lacking all three (p)ppGpp synthetases (Δrel_{Lm}Δ$relP_{Lm}$Δ$relQ_{Lm}$) was severely attenuated in an *in vitro* plaque assay (used as a surrogate for *Listeria* virulence), and in a mouse infection model (Whiteley et al., 2015). Similar to what was observed with the single Δrel_{Lm} strain (Bennett et al., 2007), inactivation of *codY* partially restored virulence of the (p)ppGpp^0 strain (Whiteley et al., 2015) collectively suggesting that (p)ppGpp synthesis promotes virulence in *L. monocytogenes* in a CodY-dependent manner. Of note, *L. monocytogenes* was the first bacterial pathogen to identify a regulatory crosstalk between the (p)ppGpp, CodY, and cyclic diadenosine monophosphate (c-di-AMP) signaling pathways (Whiteley et al., 2015).

Bacillus anthracis

The spore-forming *Bacillus anthracis* is the etiological agent of anthrax (Pilo and Frey, 2018). In *B. anthracis*, activation of the SR, mediated by Rel_{Ba}, was linked to sporulation but did not affect expression of virulence factors or virulence in a subcutaneous infection mouse model (van Schaik et al., 2007). It should be noted that *B. anthracis* as well as other *Bacillus* species also encode RelP and RelQ (YjbM and YwaC, respectively) such that inactivation of rel_{Ba} alone can be anticipated to abolish activation of the SR but not basal production of (p)ppGpp. Based on evidence from other Firmicutes, there is a great likelihood that loss of Rel_{Ba} hydrolase activity in the presence of active RelP and/or RelQ results in a SR-defective strain with high basal levels of (p)ppGpp. Given the mounting evidence that the association of (p)ppGpp with virulence goes beyond activation of the SR, it will be important to assess the virulence potential of a *B. anthracis* triple Δ*rel*Δ*relP*Δ*relQ* mutant [(p)ppGpp^0] strain in future investigations.

GRAM-NEGATIVE PATHOGENS

The textbook description of how (p)ppGpp controls bacterial physiology largely derives from studies conducted with the Gram-negative paradigm *E. coli*. In this group of bacteria, (p)ppGpp regulates transcription through direct interaction with the interface of the β′ and ϖ subunits of the RNAP (Ross et al., 2013). Of note, most transcriptional effects triggered by artificially induced early (p)ppGpp accumulation in the absence of stress were recently shown to be caused by (p)ppGpp-RNAP interaction (Sanchez-Vazquez et al., 2019). Moreover, many of the targets subjected to allosteric regulation by (p)ppGpp including proteins involved in translation, DNA replication and purine biosynthesis were fisrt identified in *E. coli* (Dalebroux and Swanson, 2012). In the absence of clinical reports or *in vivo* studies clearly linking (p)ppGpp regulation to *E. coli* virulence, the bulk of our understanding of the importance of (p)ppGpp to the virulence of Gram-negative pathogens derives from studies conducted with other Gammaproteobacteria such as *Pseudomonas aeruginosa, Salmonella enterica,* and *Vibrio cholerae* (**Table 1**). Different than Firmicutes, (p)ppGpp is metabolized by a monofunctional synthetase (RelA) and a bifunctional synthetase/hydrolase (SpoT) in Gammaproteobacteria (Atkinson et al., 2011). In all organisms with the RelA and SpoT enzyme arrangement, RelA has strong enzymatic activity and is the primary driver of the SR while SpoT has a strong hydrolase activity and weak synthetase activity that is triggered by specific conditions including iron and fatty acid starvation (Vinella et al., 2005; Battesti and Bouveret, 2006). The exception among Gammaproteobacteria, *V. cholerae* encodes a third (p)ppGpp synthetase, which is a SAS-like monofuntional enzyme named RelV (Das et al., 2009). Different than Gammaproteobacteria, Alphaproteobacteria such as *Brucella* sp. and Epsilonproteobacteria such as *Helicobacter pylori* encode a single bifunctional (p)ppGpp synthetase/hydrolase known as Rsh, Rel or SpoT, that seems to be functionally analog to the Gram-positive Rel enzyme as it possess equally strong synthetase and hydrolase activities (Atkinson et al., 2011). While there are numerous studies linking (p)ppGpp to virulence expression in Gram-negative pathogens, many

covered in a previous review (Dalebroux et al., 2010), the sections below will focus on recent studies that have directly linked (p)ppGpp to Gram-negative bacterial virulence using animal infection models.

Salmonella

Salmonella enterica is responsible for a variety of human infections ranging from gastroenteritis to typhoid fever. Early studies with (p)ppGpp^0 strains (Δ*relA*Δ*spoT*) of *S. enterica* serovar Typhimurium, Typhi, and Gallinarum clearly demonstrated the essentiality of (p)ppGpp to *Salmonella* pathogenesis (Pizarro-Cerda and Tedin, 2004; Jeong et al., 2008; Park et al., 2010; Dasgupta et al., 2019). Interestingly, (p)ppGpp was found to regulate the expression of *Salmonella* pathogenicity islands 1 (SPI-1) and 2 (SPI-2), which are required for *Salmonella* virulence (Pizarro-Cerda and Tedin, 2004; Song et al., 2004). Follow up RNA sequencing (RNAseq) analysis revealed that transcription of more than 30% of the *Salmonella* coding regions and approximately 20% of non-coding regions was affected by fluctuations in (p)ppGpp levels (Ramachandran et al., 2012), further confirming the far-reaching scope of (p)ppGpp regulation. To better understand the contributions of RelA and SpoT, a recent study characterized a *spoT* mutant (*spoT*Δctd strain), unable to synthesize (p)ppGpp via SpoT due to the deletion of the *C*-terminal domain (ctd) regulatory element of the enzyme without affectting its hydrolase activity, and revealed that RelA was the primary enzyme responsible for nutrient, nitrosative and oxidative stresses, while (p)ppGpp synthesized by SpoT was important for adaptation and survival within phagocytes (Fitzsimmons et al., 2020). More specifically, the *spoT*Δctd strain failed to induce SPI-2 genes in response to the acidic pH of the phagosome, had a major defect in cation metal uptake, and was highly attenuated in a murine model of acute salmonellosis (Fitzsimmons et al., 2020). Thus, in addition to its well-recognized role in environmental stress adaptation, (p)ppGpp appears to also function as an intracellular signal for *Salmonella* virulence. Finally, single immunization of mice with a live (p)ppGpp^0 strain elicited both systemic and mucosal antibody responses and protected vaccinated animals from a subsequent challenge with a lethal dose of wild-type *S. typhimurium* (Na et al., 2006). Given the high potential of targeting (p)ppGpp metabolism for the development of anti-infective therapies, additional studies are warranted to determine the distinct roles of RelA, SpoT, and of basal (p)ppGpp pools in *Salmonella*.

Pseudomonas aeruginosa

This environmental organism is well known for its remarkable ability to form biofilms on different types of surfaces, intrinsic and acquired tolerance to multiple antibiotics, and association with chronic lung infections in cystic fibrosis patients, burn wound infections and serious nosocomial infections (Gellatly and Hancock, 2013). In the absence of RelA, cells treated with the serine analog serine hydroxamate failed to accumulate (p)ppGpp, confirming previous observations that RelA is responsible for activation of the SR during amino acid starvation (Erickson et al., 2004). While virulence of Δ*relA* and Δ*relA*Δ*spoT* [(p)ppGpp^0] mutant strains was significantly attenuated in a *Drosophila melanogaster* feeding model of infection (Erickson et al., 2004), only the double mutant showed loss of virulence in a rat lung agar bead and in a murine skin infection model (Vogt et al., 2011; Pletzer et al., 2017). Furthermore, basal levels of (p)ppGpp was linked to expression of important virulence determinants such as alginate, type-three secretion system (T3SS), pyocyanin, proteases, siderophores, swarming, twitching and other forms of motility, at least in part due to a crosstalk with the quinolone quorum-sensing system (Vogt et al., 2011). In addition, a *P. aeruginosa* (p)ppGpp^0 strain showed decreased cytotoxicity toward human alveolar adenocarcinoma cell lines and human epithelial cells, reduced hemolytic activity, impaired virulence in a cutaneous abscess model, and reduced mortality, lung edema and inflammatory cell infiltration in a mouse model of acute pneumonia (Xu et al., 2016). In terms of antibiotic tolerance, (p)ppGpp has been associated to *P. aeruginosa* multidrug tolerance upon stationary phase entry through activation of antioxidant defenses. Specifically, lack of (p)ppGpp led to loss of superoxide dismutase (SOD) activity, while genetic or chemical complementation of SOD activity in the Δ*relA*Δ*spoT* strain restored antibiotic tolerance (Martins et al., 2018).

Burkholderia pseudomallei

Burkholderia pseudomallei (formally *Pseudomonas pseudomallei*) is the causative agent of melioidosis, a disease of both humans and animals, classified by the CDC as a category B select agent (Wiersinga et al., 2018). *Burkholderia* spp. are known to be metabolically versatile, to thrive under adverse conditions and to tolerate antibiotic treatment. A *B. pseudomallei* strain lacking the *relA* and *spoT* genes [(p)ppGpp^0], displayed defects in stationary-phase survival, replication within macrophages, and attenuated virulence in the *G. mellonella* invertebrate model as well as acute and chronic mouse models of melioidosis (Muller et al., 2012). Similar to *Salmonella,* vaccination of mice with the (p)ppGpp^0 strain conferred partial protection against subsequent infection with wild-type *B. pseudomallei* (Muller et al., 2012). The distinct roles of RelA and SpoT in the infection process and in antibiotic tolerance, and the extent of the (p)ppGpp regulatory network remain to be explored in *B. pseudomallei* and other pathogenic *Burkholderia* spp.

Vibrio cholerae

A water-borne pathogen and the causative agent of cholera, *V. cholerae* is a versatile pathogen with important virulence factors such as the cholera toxin (CT) and the toxin co-regulated pilus (TCP) (Childers and Klose, 2007). As indicated above, in addition to the canonical RelA and SpoT, the genome of *V. cholerae* encodes a SAS named RelV that is unique to *Vibrio* species (Das et al., 2009). Early studies linked RelA-dependent (p)ppGpp production with optimal expression of CT, TCP, and two major virulence regulators (ToxR and ToxT), and with virulence in rabbit ileal loop and suckling mouse infection

models (Haralalka et al., 2003). However, contradictory findings were subsequently made with a new *relA* mutant that produced normal levels of CT and TCP and displayed no colonization defects in the suckling mouse model (Silva and Benitez, 2006). Later reports using a double Δ*relA*Δ*spoT* mutant strain – an overproducer of basal (p)ppGpp levels due to the activity of RelV – produced higher levels of CT, whereas anaerobic growth via trimethylamine oxide respiration was severely inhibited (Oh et al., 2014). In contrast, a ppGpp^0 strain (Δ*relA*Δ*spoT*Δ*relV*) grew substantially better, but produced no CT, collectively suggesting that CT production and bacterial growth are inversely regulated in response to (p)ppGpp accumulation (Oh et al., 2014). Moreover, virulence of the Δ*relA*Δ*spoT*Δ*relV* strain was significantly attenuated in the infant suckling mouse model (Oh et al., 2014). More recently, (p)ppGpp was also shown to contribute to antibiotic tolerance of *V. cholerae*, possibly by suppressing TCA cycle activity that lowered ROS production (Kim et al., 2018).

Acinetobacter baumannii

An opportunistic pathogen, *Acinetobacter baumannii* has emerged as a leading cause of hospital-acquired infections, in large part due to its stress resilience and multidrug tolerance (Harding et al., 2018). A Δ*relA* strain failed to produce detectable levels of ppGpp during amino acid starvation and was hypermotile while showing reduced tolerance to antibiotics and attenuated virulence in the *G. mellonella* model (Perez-Varela et al., 2020). In a separate study, lack of (p)ppGpp resulted in lower expression of several efflux pump genes, providing a possible explanation for the association of (p)ppGpp with antibiotic tolerance in this organism (Jung et al., 2020). Studies to determine the consequences of a complete loss of (p)ppGpp that should only be achieved in a Δ*relA*Δ*spoT* double mutant strain to the pathophysiology of *A. baumannii* are still warranted.

Haemophilus ducreyi

Haemophilus ducreyi causes the sexually transmitted disease chancroid, a major cause of genital ulceration in developing countries (Lewis and Mitjà, 2016). The conditions encountered in human lesions are thought to resemble those found during stationary phase *in vitro* growth and; in line with this, a (p)ppGpp^0 Δ*relA*Δ*spoT* mutant was attenuated for pustule formation in human volunteers (Holley et al., 2014). However, the (p)ppGpp^0 strain displayed conflicting phenotypes *in vitro* as it was more sensitive to oxidative stress, but showed increased resistance to phagocytosis and prolonged survival in the stationary phase (Holley et al., 2014). RNAseq analysis of *H. ducreyi* grown to stationary phase indicated that loss of (p)ppGpp resulted in the dysregulation of several of its virulence determinants, including reduced production of Flp adhesin proteins (Holley et al., 2015). More recently, the *H. ducreyi* transcriptome in biopsy specimens of human lesions was compared to bacteria grown to mid-log, transition or stationary phases. While many of the genes previously shown to be regulated by (p)ppGpp were not differentially expressed in this study, genes coding for proteins involved in nutrient transport and alternative carbon utilization pathways, which are typically controlled by (p)ppGpp, were upregulated during infection (Gangaiah et al., 2016). Further characterization of the impact of the SR to *H. ducreyi* virulence and antibiotic tolerance by using *relA* and *spoT* single mutants coupled with cellular (p)ppGpp quantifications might shed new light on these findings.

Francisella tularensis

Francisella tularensis is the causative agent of tularemia, which is transmitted to humans upon contact with infected animals (Jones et al., 2014). Because of its high lethality in its pneumonic form and extremely low infectious dose, *F. tularensis* is classified by the United States Center for Disease Control (CDC) as a Category A select agent. Several studies have implicated (p)ppGpp with virulence gene expression of *F. tularensis,* with the most current model indicating that (p)ppGpp promotes virulence in this pathogen by activating transcription of the *Francisella* pathogenicity island (FPI) through interactions with the DNA-binding protein PigR and the MglA-SspA-RNAP complex (Cuthbert et al., 2017; Rohlfing et al., 2018). Indeed, virulence of a double Δ*relA*Δ*spoT* strain was shown to be attenuated in intranasally infected mice (Ma et al., 2019). Similar to observations made with *P. aeruginosa* and *V. cholerae*, (p)ppGpp was shown to govern global transcriptional changes in response to oxidative stress and required for tolerance to oxidants, most likely supporting intraphagocytic survival (Ma et al., 2019). In the closely related *F. novocida* – a laboratory surrogate of *F. tularensis* – survival of a *relA* mutant was impaired in the J774.A macrophage cell line, and its virulence was attenuated in the mouse model of tularemia (Dean et al., 2009). To date, *relA* and *spoT* single mutants of *F. tularensis* have not been characterized and it is unknown how loss of RelA-mediated SR (rather than complete absence of (p)ppGpp of a *relA spoT* double mutant strain) will impact *F. tularensis* virulence. Similar to *Salmonella* and *Burkholderia* (p)ppGpp-deficient strains, infection with the Δ*relA* mutant elicited a protective immune response in mice, further supporting the potential of (p)ppGpp-deficient strains as attenuated live vaccines (Dean et al., 2009).

Brucella

The intracellular pathogen *Brucella melitensis*, the causative agent of brucellosis, possesses a single (p)ppGpp synthetase/hydrolase enzyme known as *rsh*. Inactivation of *rsh* resulted in altered morphology, reduced intracellular growth/survival in HeLa and ovine macrophages, and attenuated virulence in a mouse infection model (Dozot et al., 2006). The attenuated virulence of the (p)ppGpp^0 strain was attributed, at least in part, to (p)ppGpp controlling the expression of the type four secretion system (T4SS) VirB, a major virulence factor of Brucellae (Dozot et al., 2006).

OTHER BACTERIA

Mycobacterium

A distinguishing characteristic of *Mycobacterium* species is the presence of a hydrophobic mycolate layer attached to

the peptidoglycan by an intermediate arabinogalactan layer. The most relevant member of this genus is *M. tuberculosis*, which causes tuberculosis in humans, while some other species are opportunistic animal and human pathogens. The genome of *M. tuberculosis* encodes a bifunctional Rel enzyme and a SAS enzyme which is phylogenetically distinct from the RelP and RelQ enzymes of Firmicutes and the *V. cholerae* RelV (Atkinson et al., 2011).

In *M. tuberculosis*, (p)ppGpp regulates multiple phenotypes, including biofilm formation, latency and antibiotic tolerance (Primm et al., 2000; Dahl et al., 2003; Weiss and Stallings, 2013). Similar to Firmicutes, activation of the SR in *M. tuberculosis* is primarily mediated by Rel_{Mtb}. Inactivation of rel_{Mtb} significantly attenuated *M. tuberculosis* virulence in a mouse model of chronic lung infection (Dahl et al., 2003) and in a guinea pig lung infection model (Klinkenberg et al., 2010). Notably, the pathology of guinea pig lungs infected with the rel_{Mtb} mutant was markedly different showing a delayed hypersensitive response. Collectively, these studies indicate that the SR is not required for initial colonization and growth in the lungs, but essential for chronic infection. In a separate study, a strain harboring a point mutation in rel_{Mtb} that silenced its synthetase activity without disrupting the hydrolase activity phenocopied the rel_{Mtb} deletion strain, as it failed to persist in the lungs of infected mice (Weiss and Stallings, 2013). A double mutant strain lacking both rel_{Mtb} and the SAS-encoding gene, presumably a $(p)ppGpp^0$ strain, also phenocopied the rel_{Mtb} single mutant in this mouse model (Weiss and Stallings, 2013), suggesting that the SR might be more relevant to *M. tuberculosis* pathophysiology than basal levels of (p)ppGpp. In addition to playing an essential role in the latency stage, likely through regulation of central metabolism, transcriptional studies indicate that (p)ppGpp also controls the expression of virulence genes. Specifically, the expression of several polyketide synthases that function as immune modulators and surface proteins important for granuloma formation are regulated in a Rel_{Mtb}-dependent manner (Dahl et al., 2003).

Borrelia burgdorferi

The etiological agent of Lyme disease is a tick-borne obligate intracellular pathogen and a member of the phylum Spirochetes (Steere et al., 2016). The zoonotic life cycle of *Borrelia burgdorferi* involves adapting to a variety of stresses, including nutrient starvation in arthropod hosts. In addition, *B. burgdorferi* must tolerate adverse conditions during infection of the human host. In Spirochetes, a single bifunctional Rel_{Bbu} enzyme (also known as SpoT) is responsible for (p)ppGpp metabolism. Despite conflicting results on whether (p)ppGpp levels increase during conditions that mimic the nutrient-limiting conditions encountered by *B. burgdorferi in vivo* (Bugrysheva et al., 2003; Drecktrah et al., 2015), rel_{Bbu} was required for full virulence in an intradermal infection mouse model (Bugrysheva et al., 2005). Subsequent studies revealed that (p)ppGpp modulates glycerol uptake and utilization, the morphological conversion that occurs during nutrient starvation, and persistence in the tick (Bugrysheva et al., 2015; Drecktrah et al., 2015).

ppGpp SIGNALING AS A THERAPEUTIC TARGET

As the current literature strongly supports that (p)ppGpp is critical for bacterial fitness, virulence and antibiotic tolerance, the identification of molecules that interfere with (p)ppGpp signaling has been actively pursued by investigators around the globe. The first antibiotic to be associated with decreases in alarmone levels was chloramphenicol (Rodionov and Ishiguro, 1995), which was later confirmed and expanded to include other protein synthesis inhibitors (Kudrin et al., 2017). However, the effects of these antibiotics to (p)ppGpp metabolism and activation of the SR were not specific. To date, the lead compounds identified as ppGpp and/or SR inhibitors are classified into two groups: (i) molecules that directly inhibit (p)ppGpp synthesis by interfering with the activity of (p)ppGpp synthetases, and (ii) molecules that promote (p)ppGpp degradation. In the group of (p)ppGpp synthesis inhibitors, the first identified compound was relacin, a synthetic (p)ppGpp analog based on the crystal structure of the *S. equisimilis* Rel (Rel_{Seq}) enzyme (Wexselblatt et al., 2012). While shown to inhibit (p)ppGpp synthetic activity of both the Gram-negative RelA and Gram-positive Rel enzymes *in vitro* (Wexselblatt et al., 2012), relacin does not penetrate the intracellular compartment of Gram-negative bacteria. Thus, the antimicrobial properties of relacin was restricted to Gram-positive pathogens as it was shown to impair cell survival, biofilm formation of *S. pyogenes* and *B. anthracis* and sporulation of *B. anthracis* (Wexselblatt et al., 2012). Based on these promising results, follow up studies modified the relacin structure to develop more potent inhibitors, with two new relacin analogs shown to effectively lower intracellular (p)ppGpp and impair biofilm formation and survival of *Myocobacterium smegmatis* and biofilm formation of *M. tuberculosis* (Wexselblatt et al., 2013; Syal et al., 2017b). Importantly, these compounds were shown to be permeable and non-toxic to human cells (Syal et al., 2017b). However, even the most effective relacin analog showed inhibitory effects in the millimolar range such that further improvements to achieve inhibition in the nanomolar range are deemed necessary prior to testing in human subjects. It should be noted that relacin does not inhibit the activity of the purified *E. faecalis* RelQ enzyme (Gaca et al., 2015b), such that production of (p)ppGpp will most likely not be completely abolished in organisms that encode SASs when treated with relacin or its current analogs.

In addition to relacin, other compounds have been shown to inhibit alarmone synthesis, albeit with low specificity and at even higher concentrations. For example, vitamin C inhibited Rel-dependent (p)ppGpp production in *M. smegmatis* decreasing its long term survival and biofilm formation capacities (Syal et al., 2017a). In another study, a high-throughput screening assay of a library containing ∼2 million compounds against a recombinant Rel_{Mtb} identified one compound with Rel_{Mtb}-specific inhibitory activity that showed synergy with isoniazide in

the treatment of *M. tuberculosis* in a mouse lung infection model (Dutta et al., 2019).

As mentioned above, another useful strategy to interfere with (p)ppGpp signaling is to promote (p)ppGpp hydrolysis rather than interfere with its synthesis. Along this line of thought, the anti-biofilm activity of peptide 1018, a synthetic peptide based on the host defense protein bactenecin, was linked to increased (p)ppGpp degradation (de la Fuente-Nunez et al., 2014) albeit the specific association of peptide 1018 with (p)ppGpp has been challenged with its activity suggested to derive from its general physicochemical properties (Andresen et al., 2016a). Apart from the controversial interpretation of the antimicrobial properties of peptide 1018, the synthetically modified DJK-5 and DJK-6 analogs were found to be more potent than peptide 1018 and to confer protection against *P. aeruginosa* infection in two invertebrate models (de la Fuente-Nunez et al., 2015). Taking a step further, DJK-5 was shown to reduce tissue damage and lesion size caused by either *S. aureus* or *P. aeruginosa* in a murine cutaneous abscess model (Mansour et al., 2016). Finally, this same group showed that *P. aeruginosa spoT* promoter activity was suppressed by treatment with peptides DJK-5 and 1018, and that a peptide-treated *relA* complemented SR double mutant strain exhibited reduced peptide susceptibility in the murine subcutaneous abscess model (Pletzer et al., 2017).

To date, several high-throughput screening assays are in place (Andresen et al., 2016b; Beljantseva et al., 2017) and compounds such as relacin can provide proof-of-principle evidence of the potential of (p)ppGpp signaling as the target for antimicrobial drug development. However, more studies are needed before (p)ppGpp signaling inhibitors can be tested in the clinical setting. For instance, even if more potent compounds are identified, additional studies will be necessary to assess their toxicity to humans, biodistribution and pharmacokinetics. Initially thought to be absent in eukaryotes, studies conducted in the past decade have identified SpoT orthologs in plants, insects, and humans (Sun et al., 2010; Tozawa and Nomura, 2011). While the insect and human genes appear to code for the (p)ppGpp hydrolytic domain with no evidence of functioning as a syhthetase, inactivation of the *D. melanogaster spoT* ortholog led to phenotypes that resemble those found in (p)ppGpp-deficient bacteria (Sun et al., 2010). In addition, one must also take into consideration that the significance of (p)ppGpp signaling and the enzymes responsible for (p)ppGpp metabolism may vary among bacterial groups. Specifically, while in some cases persistence and virulence can be associated with activation of the SR (mediated by RelA/Rel enzymes), in other cases basal (p)ppGpp pools during active growth and below the levels needed to activate the SR, appear to mediate those phenotypes. Thus, the ideal (p)ppGpp inhibitor must be capable of inhibiting the enzymatic activity of the so-called long RSHs (RelA, SpoT, Rel) and of SASs (RelP, RelQ, RelV). Alternatively, an effective antimicrobial might function by tipping the balance of bifunctional enzymes toward (p)ppGpp degradation. Apart from these challenges, the development of antibacterial strategies that target (p)ppGpp signaling have several advantages when compared to the antibiotics that are currently available. First, as non-essential enzymes, (p)ppGpp inhibitors will interfere with bacterial fitness and virulence expression but not cell viability such that drug resistance mechanisms may not arise rapidly or may not be acquired at all. Second, perhaps the most promising strategy, considering accumulating evidence that (p)ppGpp mediates bacterial persistence, (p)ppGpp inhibitors could be used in combination with currently available antibiotics that depend on actively growing cells to be effective.

CONCLUDING REMARKS

In addition to the expression of classic virulence factors such as toxins, capsule and fimbriae, contemporary investigations into the mechanisms of bacterial pathogenesis revealed that core cellular processes associated with metabolism and stress tolerance can be equally or even more critical to bacterial pathogenesis. As a global stress regulator, (p)ppGpp signaling appears to provide bacteria with an "extra edge," increasing cell fitness by controlling central metabolism adjustments in response to environmental fluctuations, activating stress responses, and coordinating expression of classic virulence factors (**Figure 2**). Importantly, the regulatory effects of (p)ppGpp that initially were thought to be linked to the SR activation is now known to occur in an incremental manner as opposed to the on/off switch that is characteristic of the SR (Gaca et al., 2015a). The picture that emerges from recent studies is that the role of either the SR or basal levels of (p)ppGpp to bacterial virulence depends on the lifestyle and metabolic versatility of each organism.

Despite much progress made in recent years, there are still several aspects of (p)ppGpp regulation that are not well understood. In this regard, the relatively recent discovery of a crosstalk between the (p)ppGpp and c-di-AMP signaling networks may provide new clues. c-di-AMP is an essential signaling nucleotide reported to regulate a variety of cellular functions, in particular osmoregulation (Stulke and Kruger, 2020). Parallel studies conducted with *B. subtilis*, *L. monocytogenes,* and *S. aureus* identified a link between the c-di-AMP and (p)ppGpp signaling pathways (Rao et al., 2010; Corrigan et al., 2015; Huynh et al., 2015). It follows that the phosphodiesterases that are responsible for c-di-AMP degradation are subject to allosteric inhibition by ppGpp, such that high levels of (p)ppGpp correlate with high levels of c-di-AMP; studies with *S. aureus* have also shown an overlap between the c-di-AMP and SR transcriptional signatures (Corrigan et al., 2015; Huynh et al., 2015). In *L. monocytogenes*, a diadenylate cyclase (*dacA*) mutant harbored suppressor mutations in the synthetase domain of the bifunctional Rel enzyme, which led to reduced (p)ppGpp levels (Whiteley et al., 2015). Mutational analysis confirmed that *dacA* was essential in wild-type but not in a (p)ppGpp^0 strain (Whiteley et al., 2015). Further studies revealed that c-di-AMP was essential because accumulated (p)ppGpp altered GTP concentrations, thereby affecting CodY activity (Whiteley et al., 2015). While the details of the relationship between c-di-AMP and the (p)ppGpp-CodY networks are not well understood, one can hypothesize that (p)ppGpp acts in concert with c-di-AMP to regulate bacterial activities important for adaptation to new environments.

Therefore, a better understanding of the c-di-AMP regulatory mechanisms and identification of its targets may fill some of the gaps in our current understanding of how (p)ppGpp promote cell fitness and virulence.

AUTHOR CONTRIBUTIONS

SK, CC-W, and JL wrote and reviewed the manuscript. All authors contributed to the article and approved the submitted version.

FUNDING

This study was partially funded by National Institute of Allergy and Infections Diseases.

ACKNOWLEDGMENTS

The work in this field was supported by NIH-NIAID award R21 AI135158. We thank Dr. Marta Monguió-Tortajada for helping with the design of **Figure 1**.

REFERENCES

Abranches, J., Martinez, A. R., Kajfasz, J. K., Chavez, V., Garsin, D. A., and Lemos, J. A. (2009). The molecular alarmone (p)ppGpp mediates stress responses, vancomycin tolerance, and virulence in *Enterococcus faecalis*. *J. Bacteriol.* 191, 2248–2256. doi: 10.1128/jb.01726-08

Andresen, L., Tenson, T., and Hauryliuk, V. (2016a). Cationic bactericidal peptide 1018 does not specifically target the stringent response alarmone (p)ppGpp. *Sci. Rep.* 6:36549.

Andresen, L., Varik, V., Tozawa, Y., Jimmy, S., Lindberg, S., Tenson, T., et al. (2016b). Auxotrophy-based high throughput screening assay for the identification of *Bacillus subtilis* stringent response inhibitors. *Sci. Rep.* 6:35824.

Arias, C. A., and Murray, B. E. (2012). The rise of the *Enterococcus*: beyond vancomycin resistance. *Nat. Rev. Microbiol.* 10, 266–278. doi: 10.1038/nrmicro2761

Atkinson, G. C., Tenson, T., and Hauryliuk, V. (2011). The RelA/SpoT homolog (RSH) superfamily: distribution and functional evolution of ppGpp synthetases and hydrolases across the tree of life. *PLoS One* 6:e23479. doi: 10.1371/journal.pone.0023479

Battesti, A., and Bouveret, E. (2006). Acyl carrier protein/SpoT interaction, the switch linking SpoT-dependent stress response to fatty acid metabolism. *Mol. Microbiol.* 62, 1048–1063. doi: 10.1111/j.1365-2958.2006.05442.x

Beljantseva, J., Kudrin, P., Jimmy, S., Ehn, M., Pohl, R., Varik, V., et al. (2017). Molecular mutagenesis of ppGpp: turning a RelA activator into an inhibitor. *Sci. Rep.* 7:41839.

Bennett, H. J., Pearce, D. M., Glenn, S., Taylor, C. M., Kuhn, M., Sonenshein, A. L., et al. (2007). Characterization of *relA* and *codY* mutants of *Listeria monocytogenes*: identification of the CodY regulon and its role in virulence. *Mol. Microbiol.* 63, 1453–1467. doi: 10.1111/j.1365-2958.2007.05597.x

Bhawini, A., Pandey, P., Dubey, A. P., Zehra, A., Nath, G., and Mishra, M. N. (2019). RelQ mediates the expression of beta-Lactam resistance in methicillin-resistant *Staphylococcus aureus*. *Front. Microbiol.* 10:339. doi: 10.3389/fmicb.2019.00339

Bryson, D., Hettle, A. G., Boraston, A. B., and Hobbs, J. K. (2020). Clinical mutations that partially activate the stringent response confer multidrug tolerance in *Staphylococcus aureus*. *Antimicrob. Agents Chemother.* 64, e2103–e2119.

Bugrysheva, J., Dobrikova, E. Y., Sartakova, M. L., Caimano, M. J., Daniels, T. J., Radolf, J. D., et al. (2003). Characterization of the stringent response and *rel*(Bbu) expression in *Borrelia burgdorferi*. *J. Bacteriol.* 185, 957–965.

Bugrysheva, J. V., Bryksin, A. V., Godfrey, H. P., and Cabello, F. C. (2005). *Borrelia burgdorferi rel* is responsible for generation of guanosine-3'-diphosphate-5'-triphosphate and growth control. *Infect. Immun.* 73, 4972–4981. doi: 10.1128/iai.73.8.4972-4981.2005

Bugrysheva, J. V., Pappas, C. J., Terekhova, D. A., Iyer, R., Godfrey, H. P., Schwartz, I., et al. (2015). Characterization of the RelBbu Regulon in *Borrelia burgdorferi* reveals modulation of glycerol metabolism by (p)ppGpp. *PLoS One* 10:e0118063.doi: 10.1371/journal.pone.0118063

Cashel, M., and Kalbacher, B. (1970). The control of ribonucleic acid synthesis in *Escherichia coli*, V. Characterization of a nucleotide associated with the stringent response. *J. Biol. Chem.* 245, 2309–2318.

Charity, J. C., Blalock, L. T., Costante-Hamm, M. M., Kasper, D. L., and Dove, S. L. (2009). Small molecule control of virulence gene expression in *Francisella tularensis*. *PLoS Pathog.* 5:e1000641. doi: 10.1371/journal.ppat.1000641

Childers, B. M., and Klose, K. E. (2007). Regulation of virulence in *Vibrio cholerae*: the ToxR regulon. *Future Microbiol.* 2, 335–344. doi: 10.2217/17460913.2.3.335

Colomer-Winter, C., Flores-Mireles, A. L., Kundra, S., Hultgren, S. J., and Lemos, J. A. (2019). (p)ppGpp and CodY promote *Enterococcus faecalis* virulence in a Murine model of catheter-associated urinary tract infection. *mSphere* 4:e392-19.

Colomer-Winter, C., Gaca, A. O., Chuang-Smith, O. N., Lemos, J. A., and Frank, K. L. (2018). Basal levels of (p)ppGpp differentially affect the pathogenesis of infective endocarditis in *Enterococcus faecalis*. *Microbiology* 164, 1254–1265. doi: 10.1099/mic.0.000703

Colomer-Winter, C., Gaca, A. O., and Lemos, J. A. (2017). Association of metal homeostasis and (p)ppGpp regulation in the pathophysiology of *Enterococcus faecalis*. *Infect. Immun.* 85:e00260-17.

Corrigan, R. M., Bowman, L., Willis, A. R., Kaever, V., and Grundling, A. (2015). Cross-talk between two nucleotide-signaling pathways in *Staphylococcus aureus*. *J. Biol. Chem.* 290, 5826–5839. doi: 10.1074/jbc.m114.598300

Cuthbert, B. J., Ross, W., Rohlfing, A. E., Dove, S. L., Gourse, R. L., Brennan, R. G., et al. (2017). Dissection of the molecular circuitry controlling virulence in *Francisella tularensis*. *Genes Dev.* 31, 1549–1560. doi: 10.1101/gad.303701.117

Dahl, J. L., Kraus, C. N., Boshoff, H. I., Doan, B., Foley, K., Avarbock, D., et al. (2003). The role of RelMtb-mediated adaptation to stationary phase in long-term persistence of *Mycobacterium tuberculosis* in mice. *Proc. Natl. Acad. Sci. U.S.A.* 100, 10026–10031. doi: 10.1073/pnas.1631248100

Dalebroux, Z. D., Svensson, S. L., Gaynor, E. C., and Swanson, M. S. (2010). ppGpp conjures bacterial virulence. *Microbiol. Mol. Biol. Rev.* 74, 171–199. doi: 10.1128/mmbr.00046-09

Dalebroux, Z. D., and Swanson, M. S. (2012). ppGpp: magic beyond RNA polymerase. *Nat. Rev. Microbiol.* 10, 203–212. doi: 10.1038/nrmicro2720

Das, B., Pal, R. R., Bag, S., and Bhadra, R. K. (2009). Stringent response in *Vibrio cholerae*: genetic analysis of spoT gene function and identification of a novel (p)ppGpp synthetase gene. *Mol. Microbiol.* 72, 380–398. doi: 10.1111/j.1365-2958.2009.06653.x

Dasgupta, S., Das, S., Biswas, A., Bhadra, R. K., and Das, S. (2019). Small alarmones (p)ppGpp regulate virulence associated traits and pathogenesis of *Salmonella enterica* serovar Typhi. *Cell. Microbiol.* 21:e13034.

de la Fuente-Nunez, C., Reffuveille, F., Haney, E. F., Straus, S. K., and Hancock, R. E. (2014). Broad-spectrum anti-biofilm peptide that targets a cellular stress response. *PLoS Pathog.* 10:e1004152.doi: 10.1371/journal.ppat.1004152

de la Fuente-Nunez, C., Reffuveille, F., Mansour, S. C., Reckseidler-Zenteno, S. L., Hernandez, D., Brackman, G., et al. (2015). D-enantiomeric peptides that eradicate wild-type and multidrug-resistant biofilms and protect against lethal *Pseudomonas aeruginosa* infections. *Chem. Biol.* 22, 196–205. doi: 10.1016/j.chembiol.2015.01.002

Dean, R. E., Ireland, P. M., Jordan, J. E., Titball, R. W., and Oyston, P. C. F. (2009). RelA regulates virulence and intracellular survival of *Francisella novicida*. *Microbiology* 155, 4104–4113. doi: 10.1099/mic.0.031021-0

Dozot, M., Boigegrain, R. A., Delrue, R. M., Hallez, R., Ouahrani-Bettache, S., Danese, I., et al. (2006). The stringent response mediator Rsh is required for *Brucella melitensis* and *Brucella suis* virulence, and for expression of the type IV secretion system *virB*. *Cell. Microbiol.* 8, 1791–1802. doi: 10.1111/j.1462-5822.2006.00749.x

Drecktrah, D., Lybecker, M., Popitsch, N., Rescheneder, P., Hall, L. S., and Samuels, D. S. (2015). The *Borrelia burgdorferi* RelA/SpoT homolog and stringent response regulate survival in the tick vector and global gene expression during starvation. *PLoS Pathog.* 11:e1005160.doi: 10.1371/journal.ppat.1005160

Dutta, N. K., Klinkenberg, L. G., Vazquez, M. J., Segura-Carro, D., Colmenarejo, G., Ramon, F., et al. (2019). Inhibiting the stringent response blocks *Mycobacterium tuberculosis* entry into quiescence and reduces persistence. *Sci. Adv.* 5:eaav2104. doi: 10.1126/sciadv.aav2104

Erickson, D. L., Lines, J. L., Pesci, E. C., Venturi, V., and Storey, D. G. (2004). Pseudomonas aeruginosa relA contributes to virulence in *Drosophila melanogaster*. *Infect. Immun.* 72, 5638–5645. doi: 10.1128/iai.72.10.5638-5645.2004

Fernandez-Coll, L., Maciag-Dorszynska, M., Tailor, K., Vadia, S., Levin, P. A., Szalewska-Palasz, A., et al. (2020). The absence of (p)ppGpp renders initiation of *Escherichia coli* chromosomal DNA synthesis independent of growth rates. *mBio* 11:e03223-19.

Fitzsimmons, L. F., Liu, L., Kant, S., Kim, J. S., Till, J. K., Jones-Carson, J., et al. (2020). SpoT induces intracellular *Salmonella* virulence programs in the phagosome. *mBio* 11:e3397-19.

Frank, K. L., Colomer-Winter, C., Grindle, S. M., Lemos, J. A., Schlievert, P. M., and Dunny, G. M. (2014). Transcriptome analysis of *Enterococcus faecalis* during mammalian infection shows cells undergo adaptation and exist in a stringent response state. *PLoS One* 9:e115839.doi: 10.1371/journal.pone.0115839

Fung, D. K., Yang, J., Stevenson, D. M., Amador-Noguez, D., and Wang, J. D. (2020). Small alarmone synthetase SasA expression leads to concomitant accumulation of pGpp, ppApp, and AppppA in *Bacillus subtilis*. *Front. Microbiol.* 11:2083. doi: 10.3389/fmicb.2020.02083

Gaca, A. O., Abranches, J., Kajfasz, J. K., and Lemos, J. A. (2012). Global transcriptional analysis of the stringent response in *Enterococcus faecalis*. *Microbiology* 158, 1994–2004. doi: 10.1099/mic.0.060236-0

Gaca, A. O., Colomer-Winter, C., and Lemos, J. A. (2015a). Many means to a common end: the intricacies of (p)ppGpp metabolism and its control of bacterial homeostasis. *J. Bacteriol.* 197, 1146–1156. doi: 10.1128/jb.02577-14

Gaca, A. O., Kudrin, P., Colomer-Winter, C., Beljantseva, J., Liu, K., Anderson, B., et al. (2015b). From (p)ppGpp to (pp)pGpp: characterization of regulatory effects of pGpp synthesized by the small alarmone synthetase of *Enterococcus faecalis*. *J. Bacteriol.* 197, 2908–2919. doi: 10.1128/jb.00324-15

Gaca, A. O., Kajfasz, J. K., Miller, J. H., Liu, K., Wang, J. D., Abranches, J., et al. (2013). Basal levels of (p)ppGpp in *Enterococcus faecalis*: the magic beyond the stringent response. *mBio* 4:e00646-13.

Gallant, J., Palmer, L., and Pao, C. C. (1977). Anomalous synthesis of ppGpp in growing cells. *Cell* 11, 181–185. doi: 10.1016/0092-8674(77)90329-4

Gangaiah, D., Zhang, X., Baker, B., Fortney, K. R., Gao, H., Holley, C. L., et al. (2016). *Haemophilus ducreyi* seeks alternative carbon sources and adapts to nutrient stress and anaerobiosis during experimental infection of human volunteers. *Infect. Immun.* 84, 1514–1525. doi: 10.1128/iai.00048-16

Gao, W., Chua, K., Davies, J. K., Newton, H. J., Seemann, T., Harrison, P. F., et al. (2010). Two novel point mutations in clinical *Staphylococcus aureus* reduce linezolid susceptibility and switch on the stringent response to promote persistent infection. *PLoS Pathog.* 6:e1000944.doi: 10.1371/journal.ppat.1000944

Geiger, T., Francois, P., Liebeke, M., Fraunholz, M., Goerke, C., Krismer, B., et al. (2012). The stringent response of *Staphylococcus aureus* and its impact on survival after phagocytosis through the induction of intracellular PSMs expression. *PLoS Pathog.* 8:e1003016.doi: 10.1371/journal.ppat.1003016

Geiger, T., Goerke, C., Fritz, M., Schafer, T., Ohlsen, K., Liebeke, M., et al. (2010). Role of the (p)ppGpp synthase RSH, a RelA/SpoT homolog, in stringent response and virulence of *Staphylococcus aureus*. *Infect. Immun.* 78, 1873–1883. doi: 10.1128/iai.01439-09

Geiger, T., Kastle, B., Gratani, F. L., Goerke, C., and Wolz, C. (2014). Two small (p)ppGpp synthases in *Staphylococcus aureus* mediate tolerance against cell envelope stress conditions. *J. Bacteriol.* 196, 894–902. doi: 10.1128/jb.01201-13

Geiger, T., and Wolz, C. (2014). Intersection of the stringent response and the CodY regulon in low GC Gram-positive bacteria. *Int. J. Med. Microbiol.* 304, 150–155. doi: 10.1016/j.ijmm.2013.11.013

Gellatly, S. L., and Hancock, R. E. (2013). *Pseudomonas aeruginosa*: new insights into pathogenesis and host defenses. *Pathog. Dis.* 67, 159–173. doi: 10.1111/2049-632x.12033

Glass, T. L., Holmes, W. M., Hylemon, P. B., and Stellwag, E. J. (1979). Synthesis of guanosine tetra- and pentaphosphates by the obligately anaerobic bacterium *Bacteroides thetaiotaomicron* in response to molecular oxygen. *J. Bacteriol.* 137, 956–962. doi: 10.1128/jb.137.2.956-962.1979

Gratani, F. L., Horvatek, P., Geiger, T., Borisova, M., Mayer, C., Grin, I., et al. (2018). Regulation of the opposing (p)ppGpp synthetase and hydrolase activities in a bifunctional RelA/SpoT homologue from *Staphylococcus aureus*. *PLoS Genet.* 14:e1007514.doi: 10.1371/journal.pgen.1007514

Haralalka, S., Nandi, S., and Bhadra, R. K. (2003). Mutation in the *relA* gene of *Vibrio cholerae* affects *in vitro* and *in vivo* expression of virulence factors. *J. Bacteriol.* 185, 4672–4682. doi: 10.1128/jb.185.16.4672-4682.2003

Harding, C. M., Hennon, S. W., and Feldman, M. F. (2018). Uncovering the mechanisms of *Acinetobacter baumannii* virulence. *Nat. Rev. Microbiol.* 16, 91–102. doi: 10.1038/nrmicro.2017.148

Hauryliuk, V., Atkinson, G. C., Murakami, K. S., Tenson, T., and Gerdes, K. (2015). Recent functional insights into the role of (p)ppGpp in bacterial physiology. *Nat. Rev. Microbiol.* 13, 298–309. doi: 10.1038/nrmicro3448

Hobbs, J. K., and Boraston, A. B. (2019). (p)ppGpp and the stringent response: an emerging threat to antibiotic therapy. *ACS Infect. Dis.* 5, 1505–1517. doi: 10.1021/acsinfecdis.9b00204

Holley, C., Gangaiah, D., Li, W., Fortney, K. R., Janowicz, D. M., Ellinger, S., et al. (2014). A (p)ppGpp-null mutant of *Haemophilus ducreyi* is partially attenuated in humans due to multiple conflicting phenotypes. *Infect. Immun.* 82, 3492–3502. doi: 10.1128/iai.01994-14

Holley, C. L., Zhang, X., Fortney, K. R., Ellinger, S., Johnson, P., Baker, B., et al. (2015). DksA and (p)ppGpp have unique and overlapping contributions to *Haemophilus ducreyi* pathogenesis in humans. *Infect. Immun.* 83, 3281–3292. doi: 10.1128/iai.00692-15

Honsa, E. S., Cooper, V. S., Mhaissen, M. N., Frank, M., Shaker, J., Iverson, A., et al. (2017). RelA mutant *Enterococcus faecium* with multiantibiotic tolerance arising in an immunocompromised host. *mBio* 8:e02124-16.

Huynh, T. N., Luo, S., Pensinger, D., Sauer, J. D., Tong, L., and Woodward, J. J. (2015). An HD-domain phosphodiesterase mediates cooperative hydrolysis of c-di-AMP to affect bacterial growth and virulence. *Proc. Natl. Acad. Sci. U.S.A.* 112, E747–E756.

Jeong, J. H., Song, M., Park, S. I., Cho, K. O., Rhee, J. H., and Choy, H. E. (2008). *Salmonella enterica* serovar *gallinarum* requires ppGpp for internalization and survival in animal cells. *J. Bacteriol.* 190, 6340–6350. doi: 10.1128/jb.00385-08

Jimmy, S., Saha, C. K., Kurata, T., Stavropoulos, C., Oliveira, S. R. A., Koh, A., et al. (2020). A widespread toxin-antitoxin system exploiting growth control via alarmone signaling. *Proc. Natl. Acad. Sci. U.S.A.* 117, 10500–10510. doi: 10.1073/pnas.1916617117

Jones, B. D., Faron, M., Rasmussen, J. A., and Fletcher, J. R. (2014). Uncovering the components of the *Francisella tularensis* virulence stealth strategy. *Front. Cell. Infect. Microbiol.* 7:32. doi: 10.3389/fcimb.2014.00032

Jung, H. W., Kim, K., Islam, M. M., Lee, J. C., and Shin, M. (2020). Role of ppGpp-regulated efflux genes in *Acinetobacter baumannii*. *J. Antimicrob. Chemother.* 75, 1130–1134. doi: 10.1093/jac/dkaa014

Kalia, D., Merey, G., Nakayama, S., Zheng, Y., Zhou, J., Luo, Y., et al. (2013). Nucleotide, c-di-GMP, c-di-AMP, cGMP, cAMP, (p)ppGpp signaling in bacteria and implications in pathogenesis. *Chem. Soc. Rev.* 42, 305–341. doi: 10.1039/c2cs35206k

Kanjee, U., Ogata, K., and Houry, W. A. (2012). Direct binding targets of the stringent response alarmone (p)ppGpp. *Mol. Microbiol.* 85, 1029–1043. doi: 10.1111/j.1365-2958.2012.08177.x

Kazmierczak, K. M., Wayne, K. J., Rechtsteiner, A., and Winkler, M. E. (2009). Roles of rel(Spn) in stringent response, global regulation and virulence of serotype 2 *Streptococcus pneumoniae* D39. *Mol. Microbiol.* 72, 590–611. doi: 10.1111/j.1365-2958.2009.06669.x

Kim, H. Y., Go, J., Lee, K. M., Oh, Y. T., and Yoon, S. S. (2018). Guanosine tetra- and pentaphosphate increase antibiotic tolerance by reducing reactive oxygen species production in *Vibrio cholerae*. *J. Biol. Chem.* 293, 5679–5694. doi: 10.1074/jbc.ra117.000383

Klinkenberg, L. G., Lee, J. H., Bishai, W. R., and Karakousis, P. C. (2010). The stringent response is required for full virulence of *Mycobacterium tuberculosis* in guinea pigs. *J. Infect. Dis.* 202, 1397–1404. doi: 10.1086/656524

Krasny, L., and Gourse, R. L. (2004). An alternative strategy for bacterial ribosome synthesis: *Bacillus subtilis* rRNA transcription regulation. *EMBO J.* 23, 4473–4483. doi: 10.1038/sj.emboj.7600423

Krasny, L., Tiserova, H., Jonak, J., Rejman, D., and Sanderova, H. (2008). The identity of the transcription +1 position is crucial for changes in gene expression in response to amino acid starvation in *Bacillus subtilis*. *Mol. Microbiol.* 69, 42–54. doi: 10.1111/j.1365-2958.2008.06256.x

Kriel, A., Bittner, A. N., Kim, S. H., Liu, K., Tehranchi, A. K., Zou, W. Y., et al. (2012). Direct regulation of GTP homeostasis by (p)ppGpp: a critical component of viability and stress resistance. *Mol. Cell* 48, 231–241. doi: 10.1016/j.molcel.2012.08.009

Kudrin, P., Varik, V., Oliveira, S. R., Beljantseva, J., Del Peso Santos, T., Dzhygyr, I., et al. (2017). Subinhibitory concentrations of bacteriostatic antibiotics induce *relA*-dependent and *relA*-independent tolerance to beta-Lactams. *Antimicrob. Agents Chemother.* 61:e2173-16.

Lemos, J. A., Lin, V. K., Nascimento, M. M., Abranches, J., and Burne, R. A. (2007). Three gene products govern (p)ppGpp production by *Streptococcus mutans*. *Mol. Microbiol.* 65, 1568–1581. doi: 10.1111/j.1365-2958.2007.05897.x

Lewis, D. A., and Mitjà, O. (2016). Haemophilusducreyi: from sexually transmitted infection to skin ulcer pathogen. *Curr. Opin. Infect. Dis.* 29, 52–57. doi: 10.1097/QCO.0000000000000226

Li, L., Bayer, A. S., Cheung, A., Lu, L., Abdelhady, W., Donegan, N. P., et al. (2020). The stringent response contributes to persistent methicillin-resistant *Staphylococcus aureus* endovascular infection through the purine biosynthetic pathway. *J. Infect. Dis.* 222, 1188–1198. doi: 10.1093/infdis/jiaa202

Liu, K., Bittner, A. N., and Wang, J. D. (2015). Diversity in (p)ppGpp metabolism and effectors. *Curr. Opin. Microbiol.* 24, 72–79. doi: 10.1016/j.mib.2015.01.012

Ma, Z., King, K., Alqahtani, M., Worden, M., Muthuraman, P., Cioffi, C. L., et al. (2019). Stringent response governs the oxidative stress resistance and virulence of *Francisella tularensis*. *PLoS One* 14:e0224094.doi: 10.1371/journal.pone.0224094

Mansour, S. C., Pletzer, D., de la Fuente-Nunez, C., Kim, P., Cheung, G. Y. C., Joo, H. S., et al. (2016). Bacterial abscess formation is controlled by the stringent stress response and can be targeted therapeutically. *EBioMedicine* 12, 219–226. doi: 10.1016/j.ebiom.2016.09.015

Martins, D., McKay, G., Sampathkumar, G., Khakimova, M., English, A. M., and Nguyen, D. (2018). Superoxide dismutase activity confers (p)ppGpp-mediated antibiotic tolerance to stationary-phase *Pseudomonas aeruginosa*. *Proc. Natl. Acad. Sci. U.S.A.* 115, 9797–9802. doi: 10.1073/pnas.1804525115

Mechold, U., Murphy, H., Brown, L., and Cashel, M. (2002). Intramolecular regulation of the opposing (p)ppGpp catalytic activities of Rel(Seq), the Rel/Spo enzyme from *Streptococcus equisimilis*. *J. Bacteriol.* 184, 2878–2888. doi: 10.1128/jb.184.11.2878-2888.2002

Muller, C. M., Conejero, L., Spink, N., Wand, M. E., Bancroft, G. J., and Titball, R. W. (2012). Role of RelA and SpoT in *Burkholderia pseudomallei* virulence and immunity. *Infect. Immun.* 80, 3247–3255. doi: 10.1128/iai.00178-12

Mwangi, M. M., Kim, C., Chung, M., Tsai, J., Vijayadamodar, G., Benitez, M., et al. (2013). Whole-genome sequencing reveals a link between beta-lactam resistance and synthetases of the alarmone (p)ppGpp in *Staphylococcus aureus*. *Microb. Drug Resist.* 19, 153–159. doi: 10.1089/mdr.2013.0053

Na, H. S., Kim, H. J., Lee, H. C., Hong, Y., Rhee, J. H., and Choy, H. E. (2006). Immune response induced by *Salmonella typhimurium* defective in ppGpp synthesis. *Vaccine* 24, 2027–2034. doi: 10.1016/j.vaccine.2005.11.031

Oh, Y. T., Park, Y., Yoon, M. Y., Bari, W., Go, J., Min, K. B., et al. (2014). Cholera toxin production during anaerobic trimethylamine N-oxide respiration is mediated by stringent response in *Vibrio cholerae*. *J. Biol. Chem.* 289, 13232–13242. doi: 10.1074/jbc.m113.540088

Park, S. I., Jeong, J. H., Choy, H. E., Rhee, J. H., Na, H. S., Lee, T. H., et al. (2010). Immune response induced by ppGpp-defective *Salmonella enterica* serovar Gallinarum in chickens. *J. Microbiol.* 48, 674–681. doi: 10.1007/s12275-010-0179-6

Perez-Varela, M., Tierney, A. R. P., Kim, J. S., Vazquez-Torres, A., and Rather, P. (2020). Characterization of RelA in *Acinetobacter baumannii*. *J. Bacteriol.* 202:e00045-20.

Pilo, P., and Frey, J. (2018). Pathogenicity, population genetics and dissemination of *Bacillus anthracis*. *Infect. Genet. Evol.* 64, 115–125. doi: 10.1016/j.meegid.2018.06.024

Pizarro-Cerda, J., and Tedin, K. (2004). The bacterial signal molecule, ppGpp, regulates *Salmonella* virulence gene expression. *Mol. Microbiol.* 52, 1827–1844. doi: 10.1111/j.1365-2958.2004.04122.x

Pletzer, D., Blimkie, T. M., Wolfmeier, H., Li, Y., Baghela, A., Lee, A. H. Y., et al. (2020). The stringent stress response controls proteases and global regulators under optimal growth conditions in *Pseudomonas aeruginosa*. *mSystems* 5:e00495-20.

Pletzer, D., Wolfmeier, H., Bains, M., and Hancock, R. E. W. (2017). Synthetic peptides to target stringent response-controlled virulence in a *Pseudomonas aeruginosa* murine cutaneous infection model. *Front. Microbiol.* 8:1867. doi: 10.3389/fmicb.2017.01867

Potrykus, K., and Cashel, M. (2008). (p)ppGpp: still magical? *Annu. Rev. Microbiol.* 62, 35–51. doi: 10.1146/annurev.micro.62.081307.162903

Primm, T. P., Andersen, S. J., Mizrahi, V., Avarbock, D., Rubin, H., and Barry, C. E. III. (2000). The stringent response of *Mycobacterium tuberculosis* is required for long-term survival. *J. Bacteriol.* 182, 4889–4898. doi: 10.1128/jb.182.17.4889-4898.2000

Radoshevich, L., and Cossart, P. (2018). Listeria monocytogenes: towards a complete picture of its physiology and pathogenesis. *Nat. Rev. Microbiol.* 16, 32–46. doi: 10.1038/nrmicro.2017.126

Ramachandran, V. K., Shearer, N., Jacob, J. J., Sharma, C. M., and Thompson, A. (2012). The architecture and ppGpp-dependent expression of the primary transcriptome of *Salmonella* Typhimurium during invasion gene expression. *BMC Genomics* 13:25.doi: 10.1186/1471-2164-13-25

Rao, F., See, R. Y., Zhang, D., Toh, D. C., Ji, Q., and Liang, Z. X. (2010). YybT is a signaling protein that contains a cyclic dinucleotide phosphodiesterase domain and a GGDEF domain with ATPase activity. *J. Biol. Chem.* 285, 473–482. doi: 10.1074/jbc.m109.040238

Rodionov, D. G., and Ishiguro, E. E. (1995). Direct correlation between overproduction of guanosine 3',5'-bispyrophosphate (ppGpp) and penicillin tolerance in *Escherichia coli*. *J. Bacteriol.* 177, 4224–4229. doi: 10.1128/jb.177.15.4224-4229.1995

Rohlfing, A. E., Ramsey, K. M., and Dove, S. L. (2018). Polyphosphate kinase antagonizes virulence gene expression in *Francisella tularensis*. *J. Bacteriol.* 200:e00460-17.

Ronneau, S., and Hallez, R. (2019). Make and break the alarmone: regulation of (p)ppGpp synthetase/hydrolase enzymes in bacteria. *FEMS Microbiol. Rev.* 43, 389–400. doi: 10.1093/femsre/fuz009

Ross, W., Vrentas, C. E., Sanchez-Vazquez, P., Gaal, T., and Gourse, R. L. (2013). The magic spot: a ppGpp binding site on *E. coli* RNA polymerase responsible for regulation of transcription initiation. *Mol. Cell* 50, 420–429. doi: 10.1016/j.molcel.2013.03.021

Sajish, M., Tiwari, D., Rananaware, D., Nandicoori, V. K., and Prakash, B. (2007). A charge reversal differentiates (p)ppGpp synthesis by monofunctional and bifunctional Rel proteins. *J. Biol. Chem.* 282, 34977–34983. doi: 10.1074/jbc.m704828200

Sanchez-Vazquez, P., Dewey, C. N., Kitten, N., Ross, W., and Gourse, R. L. (2019). Genome-wide effects on *Escherichia coli* transcription from ppGpp binding to its two sites on RNA polymerase. *Proc. Natl. Acad. Sci. U.S.A.* 116, 8310–8319. doi: 10.1073/pnas.1819682116

Schafer, H., Beckert, B., Frese, C. K., Steinchen, W., Nuss, A. M., Beckstette, M., et al. (2020). The alarmones (p)ppGpp are part of the heat shock response of *Bacillus subtilis*. *PLoS Genet.* 16:e1008275.doi: 10.1371/journal.pgen.1008275

Sherlock, M. E., Sudarsan, N., and Breaker, R. R. (2018). Riboswitches for the alarmone ppGpp expand the collection of RNA-based signaling systems. *Proc. Natl. Acad. Sci. U.S.A.* 115, 6052–6057. doi: 10.1073/pnas.1720406115

Silva, A. J., and Benitez, J. A. (2006). A *Vibrio cholerae* relaxed (*relA*) mutant expresses major virulence factors, exhibits biofilm formation and motility, and colonizes the suckling mouse intestine. *J. Bacteriol.* 188, 794–800. doi: 10.1128/jb.188.2.794-800.2006

Sonenshein, A. L. (2005). CodY, a global regulator of stationary phase and virulence in Gram-positive bacteria. *Curr. Opin. Microbiol.* 8, 203–207. doi: 10.1016/j.mib.2005.01.001

Song, M., Kim, H. J., Kim, E. Y., Shin, M., Lee, H. C., Hong, Y., et al. (2004). ppGpp-dependent stationary phase induction of genes on *Salmonella* pathogenicity island 1. *J. Biol. Chem.* 279, 34183–34190. doi: 10.1074/jbc.m313491200

Steere, A. C., Strle, F., Wormser, G. P., Hu, L. T., Branda, J. A., Hovius, J. W., et al. (2016). Lyme borreliosis. *Nat. Rev. Dis. Primers* 2:16090.

Steinchen, W., and Bange, G. (2016). The magic dance of the alarmones (p)ppGpp. *Mol. Microbiol.* 101, 531–544. doi: 10.1111/mmi.13412

Stulke, J., and Kruger, L. (2020). Cyclic di-AMP signaling in bacteria. *Annu. Rev. Microbiol.* 74, 159–179. doi: 10.1146/annurev-micro-020518-115943

Sun, D., Lee, G., Lee, J. H., Kim, H. Y., Rhee, H. W., Park, S. Y., et al. (2010). A metazoan ortholog of SpoT hydrolyzes ppGpp and functions in starvation responses. *Nat. Struct. Mol. Biol.* 17, 1188–1194. doi: 10.1038/nsmb.1906

Sun, W., Roland, K. L., Branger, C. G., Kuang, X., and Curtiss, R. III. (2009). The role of *relA* and *spoT* in *Yersinia pestis* KIM5 pathogenicity. *PLoS One* 4:e6720.doi: 10.1371/journal.pone.0006720

Syal, K., Bhardwaj, N., and Chatterji, D. (2017a). Vitamin C targets (p)ppGpp synthesis leading to stalling of long-term survival and biofilm formation in *Mycobacterium smegmatis*. *FEMS Microbiol. Lett.* 364:fnw282. doi: 10.1093/femsle/fnw282

Syal, K., Flentie, K., Bhardwaj, N., Maiti, K., Jayaraman, N., Stallings, C. L., et al. (2017b). Synthetic (p)ppGpp analogue is an inhibitor of stringent response in Mycobacteria. *Antimicrob. Agents Chemother.* 61:e443-17.

Taylor, C. M., Beresford, M., Epton, H. A., Sigee, D. C., Shama, G., Andrew, P. W., et al. (2002). *Listeria monocytogenes relA* and *hpt* mutants are impaired in surface- attached growth and virulence. *J. Bacteriol.* 184, 621–628. doi: 10.1128/jb.184.3.621-628.2002

Tozawa, Y., and Nomura, Y. (2011). Signalling by the global regulatory molecule ppGpp in bacteria and chloroplasts of land plants. *Plant Biol.* 13, 699–709. doi: 10.1111/j.1438-8677.2011.00484.x

van Schaik, W., Prigent, J., and Fouet, A. (2007). The stringent response of *Bacillus anthracis* contributes to sporulation but not to virulence. *Microbiology* 153, 4234–4239. doi: 10.1099/mic.0.2007/010355-0

Vinella, D., Albrecht, C., Cashel, M., and D'Ari, R. (2005). Iron limitation induces SpoT-dependent accumulation of ppGpp in *Escherichia coli*. *Mol. Microbiol.* 56, 958–970. doi: 10.1111/j.1365-2958.2005.04601.x

Vogt, S. L., Green, C., Stevens, K. M., Day, B., Erickson, D. L., Woods, D. E., et al. (2011). The stringent response is essential for *Pseudomonas aeruginosa* virulence in the rat lung agar bead and *Drosophila melanogaster* feeding models of infection. *Infect. Immun.* 79, 4094–4104. doi: 10.1128/iai.00193-11

Weiss, L. A., and Stallings, C. L. (2013). Essential roles for *Mycobacterium tuberculosis* Rel beyond the production of (p)ppGpp. *J. Bacteriol.* 195, 5629–5638. doi: 10.1128/jb.00759-13

Wells, D. H., and Gaynor, E. C. (2006). *Helicobacter pylori* initiates the stringent response upon nutrient and pH downshift. *J. Bacteriol.* 188, 3726–3729. doi: 10.1128/jb.188.10.3726-3729.2006

Wexselblatt, E., Kaspy, I., Glaser, G., Katzhendler, J., and Yavin, E. (2013). Design, synthesis and structure-activity relationship of novel Relacin analogs as inhibitors of Rel proteins. *Eur. J. Med. Chem.* 70, 497–504. doi: 10.1016/j.ejmech.2013.10.036

Wexselblatt, E., Oppenheimer-Shaanan, Y., Kaspy, I., London, N., Schueler-Furman, O., Yavin, E., et al. (2012). Relacin, a novel antibacterial agent targeting the Stringent Response. *PLoS Pathog.* 8:e1002925.doi: 10.1371/journal.ppat.1002925

Whiteley, A. T., Pollock, A. J., and Portnoy, D. A. (2015). The PAMP c-di-AMP is essential for *Listeria monocytogenes* growth in rich but not minimal media due to a toxic increase in (p)ppGpp. *Cell Host Microbe* 17, 788–798. doi: 10.1016/j.chom.2015.05.006

Wiersinga, W. J., Virk, H. S., Torres, A. G., Currie, B. J., Peacock, S. J., Dance, D. A. B., et al. (2018). Melioidosis. *Nat. Rev. Dis. Primers* 4:17107.

Wolz, C., Geiger, T., and Goerke, C. (2010). The synthesis and function of the alarmone (p)ppGpp in firmicutes. *Int. J. Med. Microbiol.* 300, 142–147. doi: 10.1016/j.ijmm.2009.08.017

Xu, X., Yu, H., Zhang, D., Xiong, J., Qiu, J., Xin, R., et al. (2016). Role of ppGpp in *Pseudomonas aeruginosa* acute pulmonary infection and virulence regulation. *Microbiol. Res.* 192, 84–95. doi: 10.1016/j.micres.2016.06.005

Yan, X., Zhao, C., Budin-Verneuil, A., Hartke, A., Rince, A., Gilmore, M. S., et al. (2009). The (p)ppGpp synthetase RelA contributes to stress adaptation and virulence in *Enterococcus faecalis* V583. *Microbiology* 155, 3226–3237. doi: 10.1099/mic.0.026146-0

Yang, J., Anderson, B. W., Turdiev, A., Turdiev, H., Stevenson, D. M., Amador-Noguez, D., et al. (2020). The nucleotide pGpp acts as a third alarmone in *Bacillus*, with functions distinct from those of (p) ppGpp. *Nat. Commun.* 11:5388.

Yang, N., Xie, S., Tang, N. Y., Choi, M. Y., Wang, Y., and Watt, R. M. (2019). The Ps and Qs of alarmone synthesis in *Staphylococcus aureus*. *PLoS One* 14:e0213630.doi: 10.1371/journal.pone.0213630

Zhu, J., Zhang, T., Su, Z., Feng, L., Liu, H., Xu, Z., et al. (2019a). Co-regulation of CodY and (p)ppGpp synthetases on morphology and pathogenesis of *Streptococcus suis*. *Microbiol. Res.* 223, 88–98. doi: 10.1016/j.micres.2019.04.001

Zhu, M., Pan, Y., and Dai, X. (2019b). (p)ppGpp: the magic governor of bacterial growth economy. *Curr. Genet.* 65, 1121–1125. doi: 10.1007/s00294-019-00973-z

Zhu, J., Zhang, T., Su, Z., Li, L., Wang, D., and Xiao, R. (2016). (p)ppGpp synthetases regulate the pathogenesis of zoonotic *Streptococcus suis*. *Microbiol. Res.* 191, 1–11. doi: 10.1016/j.micres.2016.05.007

Conflict of Interest: The authors declare that the research was conducted in the absence of any commercial or financial relationships that could be construed as a potential conflict of interest.

frontiers in Microbiology

ORIGINAL RESEARCH
published: 14 January 2021
doi: 10.3389/fmicb.2020.591802

Induction of the Stringent Response Underlies the Antimicrobial Action of Aliphatic Isothiocyanates

Dariusz Nowicki, Klaudyna Krause, Patrycja Szamborska, Adrianna Żukowska, Grzegorz M. Cech and Agnieszka Szalewska-Pałasz**

Department of Bacterial Molecular Genetics, Faculty of Biology, University of Gdańsk, Gdańsk, Poland

Bacterial resistance to known antibiotics comprises a serious threat to public health. Propagation of multidrug-resistant pathogenic strains is a reason for undertaking a search for new therapeutic strategies, based on newly developed chemical compounds and the agents present in nature. Moreover, antibiotic treatment of infections caused by enterotoxin toxin-bearing strain—enterohemorrhagic *Escherichia coli* (EHEC) is considered hazardous and controversial due to the possibility of induction of bacteriophage-encoded toxin production by the antibiotic-mediated stress. The important source of potentially beneficial compounds are secondary plant metabolites, isothiocyanates (ITC), and phytoncides from the Brassicaceae family. We reported previously that sulforaphane and phenethyl isothiocyanate, already known for their chemopreventive and anticancer features, exhibit significant antibacterial effects against various pathogenic bacteria. The mechanism of their action is based on the induction of the stringent response and accumulation of its alarmones, the guanosine penta- and tetraphosphate. In this process, the amino acid starvation path is employed via the RelA protein, however, the precise mechanism of amino acid limitation in the presence of ITCs is yet unknown. In this work, we asked whether ITCs could act synergistically with each other to increase the antibacterial effect. A set of aliphatic ITCs, such as iberin, iberverin, alyssin, erucin, sulforaphen, erysolin, and cheirolin was tested in combination with sulforaphane against *E. coli*. Our experiments show that all tested ITCs exhibit strong antimicrobial effect individually, and this effect involves the stringent response caused by induction of the amino acid starvation. Interestingly, excess of specific amino acids reversed the antimicrobial effects of ITCs, where the common amino acid for all tested compounds was glycine. The synergistic action observed for iberin, iberverin, and alyssin also led to accumulation of (p)ppGpp, and the minimal inhibitory concentration necessary for the antibacterial effect was four- to eightfold lower than for individual ITCs. Moreover, the unique mode of ITC action is responsible for inhibition of prophage induction and toxin production, in addition to growth inhibition of EHEC strains. Thus, the antimicrobial effect of plant secondary metabolites by the stringent response induction could be employed in potential therapeutic strategies.

Keywords: stringent response, (p)ppGpp, isothiocyanate, sulforaphane, enterohemorrhagic *Escherichia coli*

OPEN ACCESS

Edited by:
Gert Bange,
University of Marburg, Germany

Reviewed by:
Christiane Wolz,
University of Tübingen, Germany
Thomas Keith Wood,
Pennsylvania State University (PSU), United States

****Correspondence:***
Dariusz Nowicki
dariusz.nowicki@ug.edu.pl
Agnieszka Szalewska-Pałasz
agnieszka.szalewska-palasz@ug.edu.pl

Specialty section:
This article was submitted to Microbial Physiology and Metabolism, a section of the journal Frontiers in Microbiology

Received: *11 August 2020*
Accepted: *15 December 2020*
Published: *14 January 2021*

Citation:
Nowicki D, Krause K, Szamborska P, Żukowska A, Cech GM and Szalewska-Pałasz A (2021) Induction of the Stringent Response Underlies the Antimicrobial Action of Aliphatic Isothiocyanates. Front. Microbiol. 11:591802. doi: 10.3389/fmicb.2020.591802

INTRODUCTION

Currently, the great challenges of modern medicine involve increasing resistance to known antimicrobial agents among pathogenic bacteria. This comprises a serious threat of spreading infections due to ineffective treatment leading even to pandemic outbreaks. The extensive and often unnecessary use of antibiotics eventually leads to the occurrence of resistance mechanisms due to bacterial evolution followed by spreading of antibiotic-resistance traits by vertical and, in particular, horizontal gene transfer within and in between bacterial species (Thomas and Nielsen, 2005). The amount of novel antibiotics yearly approved by the U.S. Food and Drug Administration (FDA) is decreasing, which is accompanied by increasing costs of developing new agents (Provenzani et al., 2020). Moreover, these antibiotics usually belong to the already known classes of antimicrobial agents and generally target specific groups of bacteria. This limits their possible usability in the control of infections caused by multidrug-resistant pathogens. Infections caused by antibiotic-resistant bacteria are the cause of at least 25,000 deaths in EU per year, and in addition, these infections are associated with increased costs of health care (Thorpe et al., 2018). This emerging problem creates a gap in the therapeutic agents that are available and leads to the need of extensive search for possible new antimicrobials, preferably differing in their mode of action from those already employed.

Natural products (especially plant-derived) are a promising source of potential compounds with antibacterial effects. As the secondary metabolites of the plants from the Brassicaceae family, isothiocyanates (ITC) gained particular attention due to their broad pro-health effects, including well-studied chemopreventive, anticancer, and antioxidant properties (Singh and Singh, 2012; Wiczk et al., 2012; Pawlik et al., 2013). However, the antibacterial effects of ITCs have not been sufficiently explored. In particular, understanding of ITC mode of antimicrobial action is still quite limited, with proposed underlying mechanisms including such effects as membrane disruption and cell lysis (Abreu et al., 2013; Patel et al., 2020). The unexpected and till recently unexplored mechanism of ITC antibacterial effect involves induction of bacterial stringent response. We have shown that ITCs, such as the widely studied sulforaphane (SFN), phenetyl ITC (PEITC), and benzyl ITC (BITC) inhibit bacterial growth of enterohemorrhagic *Escherichia coli* due to accumulation of the stringent response alarmone (p)ppGpp (Nowicki et al., 2014, 2016). These unusual nucleotides, the guanosine tetra- and pentaphosphate, are synthesized in *E. coli* by two enzymes. One is the RelA synthetase (*relA* gene product), responsive to amino acid starvation, and the other is the SpoT enzyme (*spoT* gene product), which is responsible for (p)ppGpp synthesis during other stresses and limitations, and is also responsible for ppGpp hydrolysis (Potrykus and Cashel, 2008). The ITC treatment interfered with amino acid metabolism, causing amino acid limitation, which in turn triggered RelA-mediated ppGpp accumulation (this effect was absent in the *relA* mutant strain). Moreover, excess of certain, but not all, amino acids, reversed this effect (Nowicki et al., 2014, 2016). Importantly, growth inhibition was accompanied by downregulation of the Shiga toxin synthesis. Expression of *stx* genes (coding for this toxin) is dependent on the lytic development of a lambdoid prophage, and it is the main factor responsible not only for virulence but for the life-threatening complications in humans, such as the hemolytic–uremic syndrome. Notably, the use of some common antibiotics to treat EHEC infections leads to the prophage induction and toxin synthesis, and therefore antibiotic therapy for this infection is disputable and high-risk. Thus, the development of novel methods to inhibit both, the bacterial growth and toxin synthesis, is an important aim in current biomedical research.

Phytoncides are a promising source of biologically active compounds, with various antibacterial activities. In terms of biological effects of ITCs, SNF is one of the best described (Houghton, 2019; Ruhee and Suzuki, 2020). Correlation between the chemical structure and antimicrobial effects of ITCs has been reported for some oral pathogens, where the degrees of these effects were compared for ITCs carrying various chemical groups (Ko et al., 2016). It was shown that the most potent antimicrobial effect was observed for indolyl ITC, followed by aromatic and aliphatic ITCs (Ko et al., 2016). The antimicrobial effects of some of these ITCs, namely, detoxification and anticancer activity, were already evaluated in the eukaryotic models (Munday and Munday, 2004; Milczarek et al., 2018). In this work, we asked what is an antibacterial effect of a set of sulforaphane analogs, also bearing aliphatic groups. Next, we tested the possible synergistic effect of various combinations of aliphatic ITCs and aimed to reveal the mechanism of their action. Our work presents evidence that the basis of the antimicrobial effect of ITCs, also when present in combinations, is accumulation of the stringent response alarmone, (p)ppGpp, induced through the amino acid starvation pathway.

MATERIALS AND METHODS

Bacterial Strains and Growth Conditions

E. coli MG1655 and its *relA*- mutant (Xiao et al., 1991) were employed as standard laboratory strains. Clinical isolates of enterohemorrhagic *E. coli* O157:H7 were from our laboratory collection, EDL 933 and 86-24 Δ*stx*:GFP (Filipiak et al., 2020), and were used to evaluate ITC efficacy on human pathogens. Bacterial susceptibility tests were conducted at 37°C using the Mueller–Hinton (MH) broth (Sigma-Aldrich, Germany) or M9 (Sigma-Aldrich, Germany), with aeration and as indicated in the procedures' description. The isothiocyanates were purchased from LKT Laboratories (United States).

Estimation of Antimicrobial Effects

Antimicrobial activity of ITCs was assessed as described in Nowicki et al. (2019). The MIC values were estimated in accordance with the CLSI guideline M07-A9. Briefly, MICs were assessed by the twofold broth microdilution assay, and ITC concentrations ranged from 0.032 to 32 mM, and were later recalculated for mg/ml as an antibiotic concentration standard. Bacteria were grown in Mueller–Hinton (MH) or M9 medium

on 96-well plates, with a final inoculum of 5×10^5/ml. To determine the minimum bactericidal concentration (MBC), 100 μl of each culture was serially diluted (10^2–10^5) in saline, transferred onto MHA plates, and incubated at 37°C. Colony enumeration was carried out after 24 h. Cell suspensions without a given phytochemical were used as controls. The MBC was taken as the lowest concentration of phytochemicals at which no colony-forming units (CFU) were detected on solid medium. To assess amino acids' impact on ITC antimicrobial effectiveness, 20 mM of each 20 amino acids was supplemented at time zero into M9 medium, and the MICs of ITCs were defined. The 20 mM concentration of amino acids was chosen to achieve their excess over the typical concentrations encountered by bacteria in the human intestines (Adibi and Mercer, 1973; Bener et al., 2006). Zone inhibition tests were assessed by the Kirby Bauer disc diffusion method, using 6 mm membrane discs (Biomaxima, Poland), with 30 μg of chloramphenicol and 50 μg of a given ITC. Cell concentration of the tested microorganisms was adjusted to 0.5 McFarland turbidity standards, inoculated on MHA plates, and diameters of growth inhibition zones were measured after 20 h of incubation at 37°C. All presented results represent at least three independent experiments.

Time-kill assays were performed following the CLSI guidelines. Briefly, overnight bacterial cultures were suspended in MH medium and adjusted to an absorbance of approximately 10^6 CFU/ml. Varying concentrations of the test compounds were added to the inoculum suspensions, with final concentrations corresponding to 1 x, 2 x, and 4 x MIC, and incubated at 37°C with aeration. Aliquots were removed from the inoculum culture after timed intervals of incubation (i.e., 0, 3, 6, 8, and 24 h), and serial 10-fold dilutions were prepared. Samples were plated on MH agar and incubated for 24 h at 37°C. Bacterial cell viability was determined by colony count. The assays were performed in triplicate. Data were analyzed as killing curves by plotting the $\log_{10}$ colony-forming unit per milliliter (CFU/ml) vs. time (hours), and the change in bacterial number was determined. The viable bacterial cell count for the time-kill end point determination, i.e., bactericidal activity, is defined as a reduction of ≥ 3 $\log_{10}$ CFU/ml relative to the initial inoculum, whereas bacteriostatic activity corresponds to < 3 $\log_{10}$ CFU/ml decrease relative to the initial inoculum.

Fractional Inhibitory Concentration Index

The FIC index was used to estimate the synergy between different agents (Kang et al., 2011). Stock solutions and serial twofold dilutions of each drug (made to at least double the MIC) were prepared immediately prior to testing, as described (Bajaksouzian et al., 1996). A total of 50 μl of M9 medium (0.2% glucose) was distributed into each well of the microdilution plates. The first compound of the combination was serially diluted along the ordinate, while the second drug was diluted along the abscissa. An inoculum equal to a 0.5 McFarland turbidity standard was prepared in M9 (for SFN vs. ITC testing). Each microtiter well was inoculated with 100 μl of a bacterial inoculum of 5×10^5 CFU/ml, and the plates were incubated at 37°C for 18–20 h under aerobic conditions. The resulting checkerboard contains each combination of two substances, with wells that contain the highest concentration of each compound at opposite corners, as was presented on isobolograms. The FIC index was calculated as follows:

$$FICI = \left[\frac{MIC_{A(A+B)}}{MIC_{A(alone)}}\right] + \left[\frac{MIC_{B(A+B)}}{MIC_{B(alone)}}\right]$$

The FIC index was calculated on the basis of the abovementioned equation, in which the FIC index = X + Y, and the interactions are defined as: FIC index $\leq$ 0.5, synergy; 0.5 $\leq$ FICI $\leq$ 1.0, additive; 1.1 $\leq$ FICI $\leq$ 2.0, indifferent; and FICI $>$ 2.0, antagonistic (Kang et al., 2011).

Determination of (p)ppGpp Cellular Levels

The cellular levels of the alarmones, i.e., ppGpp and pppGpp, were measured basically as described (Mechold et al., 2002), with minor modifications as in Nowicki et al. (2014). Briefly, overnight bacterial culture grown in MOPS (4-morpholinepropanesulfonic acid) minimal medium was diluted in the same medium, but with a low phosphate concentration (0.4 mM), and then grown to A_{600} of 0.2. Then, bacteria were diluted (1:10) in the same medium with the addition of [^{32}P]orthophosphoric acid (150 μCi/ml) and grown for at least two generations. Next, at time 0, ITCs at 1 × MIC or serine hydroxamate (SHX) at 1 mM were added to induce the stringent response by this amino acid analog. Bacterial samples, collected at specified time points, were lysed with formic acid (13 M) in three cycles of freeze–thaw procedure. After centrifugation, nucleotide extracts were separated by thin-layer chromatography, using PEI cellulose plates (Sigma-Aldrich, Germany) in 1.5 M potassium phosphate buffer (pH 3.4). The chromatograms were then analyzed with a Phosphorimager (Typhoon, GE Healthcare). QuantityOne software was used for densitometry analysis.

Shiga-Toxin Production Analysis by Fluorescence Microscopy

Shiga toxin expression was monitored by GFP fluorescence as described in Nowicki et al. (2019). First, the overnight *E. coli* 86-24Δ*stx*:GFP culture was regrown (1:100 dilution) in fresh MH broth to OD = 0.2. Samples of bacterial cultures (1 ml) were withdrawn to 1.5 ml tubes and washed twice with PBS. Next, bacteria were resuspend in MH broth with or without ITCs (1x MIC). Mitomycin C (0.5 μg/ml) was used as the toxin synthesis inducer and was added to samples at time zero. Cell membranes and phenotypes were visualized by staining for 10 min with the SynaptoRed fluorescent dye (Sigma-Aldrich), at a final concentration of 5 μg/ml. To conduct vital staining and immobilize the culture samples, the thin pads of 1.5% agarose (dissolved in MH medium) were prepared then visualized using a Leica DMI4000B microscope fitted with a DFC365FX camera (Leica). The following Leica filter sets were used: N2.1 (for FM4-64), green fluorescent protein (GFP). Images were collected and processed using LAS AF 3.1 software (Leica).

Phenotype Microarray Analysis

The phenomic analysis of the wild-type strain and *relA* mutant in comparison to strains treated with sulforaphane was carried out using Phenotype MicroArrays for Microbial Cells (Biolog). Duplicate runs of each of the strains were done and pairwise comparisons were created using OmniLog® V.1.5 (Biolog, 178 United States). A reproducibility analysis was performed, and all strains passed the test. This analysis was done commercially by Biolog (Biolog Inc., United States).

Briefly, cellular response was measured for utilization of selected compounds, which led to changes in color development of tetrazolium violet. Here, we selected only plates—testing cells' ability to utilize different nitrogen sources. Sulforaphane was added just before placing the inoculated fluids in the wells of each plate, to ensure there was the same SFN final concentration in each well (0.0625 mM; stock was made as 200 mM in 0.5% DMSO). The kinetic curves are the result of colorimetric measurements taken every 15 min for 48 h. Reproducibility analysis indicates the number of wells where the difference of average height between duplicate runs is above the threshold value—the "average height," which is equivalent to the area under the curve divided by the number of reads (two). Pass/fail is determined by the number of such wells above the threshold value. The same procedure was done for wild-type strain and *relA* mutant. Those values are referred to as relative phenotype strength. Negative values refer to phenotype lost (upon SFN treatment), and positive values refer to phenotype gained (upon SFN treatment). Zero value means that the selected phenotype is not affected (changed) upon SFN treatment.

Statistical Analyses

All experiments were performed independently in triplicates, and the data are presented as mean ± standard deviation. The significance of differences between mean values of two measured parameters was assessed by the *t*-test. Differences were considered significant when *P*-values were < 0.05.

RESULTS

Sulforaphane Analogs Inhibit Bacterial Growth

Isothiocyanates are a broad group of compounds derived from glucosinolates and produced after enzymatic cleavage by myrosinase in plant tissues. To elucidate their antibacterial mechanism of action, we focused here on those produced in nature though one pathway of a glucosinolate precursor, i.e., the aliphatic group of ITCs, which includes sulforaphane (SFN), sulforaphene (SFE), iberverin (IBR), iberin (IBN), alyssin (ALN), erucin (ERU), erysolin (ERY), and cheirolin (CHE) (**Figure 1**). We employed R-sulforaphane, which is naturally present in the plants (in contrary to the chemically synthesized mix of R and S sulforaphane) and its biological activity was reported as more potent than its S enantiomer (Abdull Razis et al., 2011). Initially, we evaluated the antimicrobial effect of these ITCs by the standard disc diffusion assay and microdilution method in order to characterize minimal inhibitory and bactericidal concentrations (**Table 1**). The screening evaluation of growth inhibition zones indicated that all tested compounds exhibit antimicrobial activity against *E. coli* MG1655 laboratory strain. Only ERU caused a lower inhibition of *E. coli* growth in the disc diffusion test (16.6 ± 0.3 mm), while all other ITCs showed ZI > 20 mm. The average inhibition zone of the negative control and the antibiotic chloramphenicol (used as a positive control) against the same target bacteria was 6.0 ± 0.0 mm (diameter of the disk) and 19.67 ± 1.4 mm, respectively. Further examination, employing microdilution assay in the MH medium and plating on solid MHA showed more variety in ITC effectiveness. Namely, among the SFN analogs, the MIC of only SFE was below 100 mg/L (87.7), while MIC values for IBR, IBN, ALN, ERU, ERY, and CHE were approximately twofold higher (147.3, 163.3 191.3, 161.29, 125, and 125 mg/L, respectively) (**Table 1**). SFE showed a potent bactericidal action, similar to SNF, expressed in MBC equal to MI concentration (87.7, 88.6 mg/L, respectively). The MBC of other ITCs were two to fourfold higher than their MIC. Moreover, we demonstrated that the composition of culture medium had an impact on antibacterial effectivity of the tested ITCs. MIC values obtained in M9 medium (+0.2% glucose) were ∼10-fold lower in comparison to the rich MH broth. In the absence of amino acids and peptides in the culture media, SFN, SFE, and IBN exhibited the strongest action (MIC of 5.5, 5.5, 5.1 mg/ml), while for ERU, we observed approximately fourfold MIC decrease (40.3 mg/l). Finally, the MBC assessed in poor nutrient conditions were twofold higher than MIC for ERY and CHE and were equal with MIC for the rest of the tested compounds. The time-kill assay performed with the tested compounds confirmed their bacteriostatic effect (**Figure 2**). Thus, we can conclude that the effectiveness of the antimicrobial effect is correlated with both the type of ITC used and the bacterial growth conditions.

The Stringent Response Induction Underlies Antibacterial Action of Aliphatic Isothiocyanates

Following our previous research (Nowicki et al., 2016, 2019), we tested selected SFN analogs for their potential to elevate the (p)ppGpp alarmones level to reveal the effect of these ITCs on cellular stress response. The results presented here (**Figure 3**), strongly indicate that ITC-mediated bacterial growth inhibition is caused by global metabolism alterations accompanied by enhanced production of the stress alarmones, which is in agreement with the effect reported for SFN. Based on the previous results (Nowicki et al., 2014, 2016), where the involvement of the amino acid starvation pathway was shown as a mechanism responsible for ITC-mediated (p)ppGpp accumulation, we then employed an *E. coli* strain devoid of the *relA* gene. As we did not observe (p)ppGpp accumulation in ITC-treated *relA* mutant, we could conclude that these compounds act by inducing amino acid starvation. However, the actual direct effect of ITCs has an impact on *relA* mutant strain as well, since their sensitivity to the tested compounds is at least at the same level or higher in comparison to the wild-type bacteria (**Supplementary Table S1**). Therefore, in order to explain this phenomenon, we used an excess of

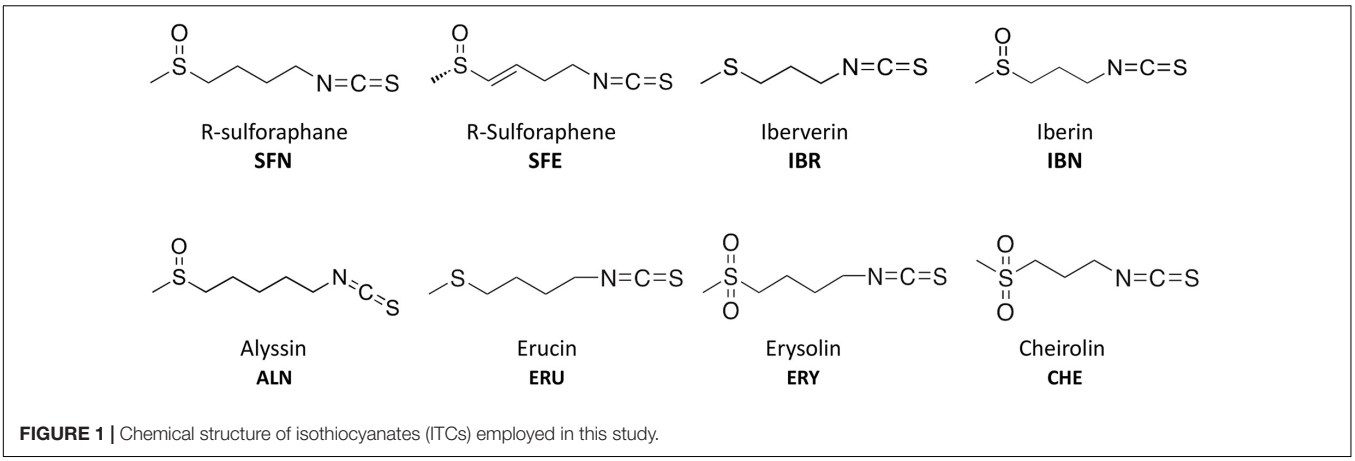

FIGURE 1 | Chemical structure of isothiocyanates (ITCs) employed in this study.

TABLE 1 | Antimicrobial activity of ITCs.

Broth	Mueller–Hinton			M9	
ITC:	MIC mg/L (mM)	MBC mg/L (mM)	ZI mm	MIC mg/L (mM)	MBC mg/L (mM)
SFN	88.6 (0.5)	88.6 (0.5)	22.3 ± 1.0	5.5 (0.03)	5.5 (0.03)
SFE	87.7 (0.5)	87.7 (0.5)	25.8 ± 0.3	5.5 (0.03)	5.5 (0.03)
IBR	147.3 (1.0)	294.6 (2.0)	23.3 ± 0.6	9.2 (0.06)	9.2 (0.06)
IBN	163.3 (1.0)	326.6 (2.0)	24.1 ± 1.6	5.1 (0.03)	5.1 (0.03)
ALN	191.3 (1.0)	382.6 (2.0)	20.8 ± 0.3	11.9 (0.06)	11.9 (0.06)
ERU	161.3 (1.0)	645.2 (4.0)	16.6 ± 0.3	40.3 (0.25)	40.3 (0.25)
ERY	125 (0.65)	500 (2.6)	25.1 ± 1.0	14.8 (0.08)	29.6 (0.15)
CHE	125 (0.7)	500 (2.8)	24.9 ± 1.0	14.8 (0.08)	29.6 (0.17)

Antimicrobial potential against E. coli MG1655 expressed as a minimal inhibitory concentration (MIC) and minimal bactericidal concentration (MBC), as well as zone inhibition (ZI) diameter.

individual free L-amino acids (20 mM) to check whether it affects ITC action. In this analysis, we showed that the antimicrobial action of SFN analogs was impaired by specific amino acids (**Table 2**). The highest reversal effect was observed for SFN and SFE in the presence of glycine and methionine; for other ITCs, glycine was able to increase MIC up to about eightfold. Moreover, some moderate impact of other amino acids was also observed for cultures supplemented with tyrosine, glutamine, cysteine, tryptophan, alanine, and phenylalanine ($\geq$ fourfold MIC increase), while at the same time, none of the amino acids could stimulate ITC antibacterial potential.

The Synergistic Antimicrobial Effect of Isothiocyanate Combinations Results From the Stringent Response Induction

Any effect exerted by an individual compound may vary from the one observed for the combination of various chemicals. This also holds true for the antibacterial agents. Knowing the potential of SFN and its analogs to inhibit bacterial growth, we asked whether the simultaneous action of two ITCs may give a synergistic outcome. For this, we combined SFN with individual ITCs tested previously, and we assessed bacterial growth inhibition by checkerboard titration. In this way, the fractional inhibitory concentration (FIC) index was established for each combination (**Table 3**). The synergistic effects of SFN and IBR, SNF and IBN, and SFN and ALN led to the reduction in MIC for these compounds by four- to eightfold, with the FIC index of ≤ 0.5 indicating synergy. The combinations of SNF with IBR, and IBN and ALN, resulted in the additive effect of the antimicrobial actions (the FIC index value was ≥ 0.5, **Figure 4A**), while others gave additive effects (**Supplementary Figure S1A**). Interestingly, the antibacterial effects of combinations of these ITCs, which acted synergistically with SFN (IBR, IBN, ALN), were synergistic only for the iberin–iberverin mixture, while for the allysin in combination with iberin and iberverin, the effect was additive (**Supplementary Figure S1B**). Thus, these data indicate that some of the combinations of SFN with its analogs can give a synergistic antibacterial effect.

As the bacterial growth inhibition caused by the tested ITCs is straightforwardly related to the induction of the stringent response (**Figure 3**), we assessed the accumulation of (p)ppGpp alarmones upon SNF treatment in combination with those ITCs, which showed the synergistic effect (namely, IBR, IBN, and ALN). The level of accumulated (p)ppGpp in the presence of SFN/ITC combination at the FIC concentrations was comparable to this observed for MIC concentrations of individual compounds (**Figure 4B**). This indicates that the combination of several fold lower concentration of ITCs (FICs) gives a similar effect for the stringent response induction as the much higher

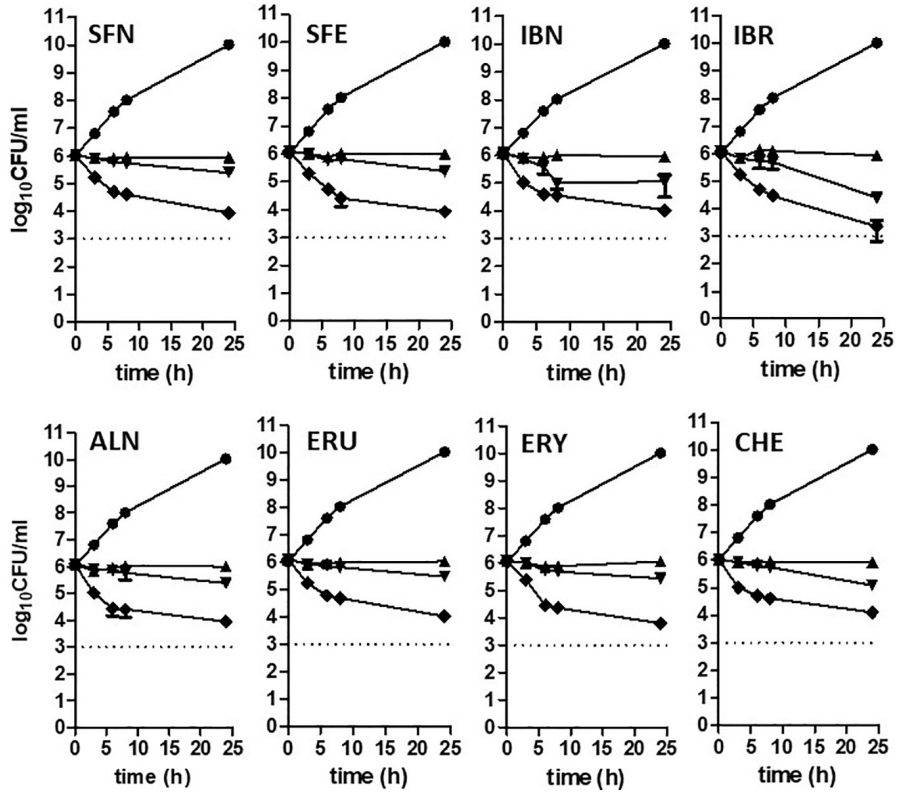

FIGURE 2 | Time-kill kinetics at a range of concentrations of ITCs. *Escherichia coli* MG1655 culture was challenged with compounds at 1 x, 2 x, and 4 x MIC levels and compared to untreated control (triangle, reversed triangle, diamond, and circle, respectively). Bactericidal activity was defined as a reduction of 99.9% (≥ 3 $\log_{10}$) of the total number of CFU/ml in the original inoculum and marked as a dashed line on plots. Data are presented as mean and standard deviation of three independent replicates.

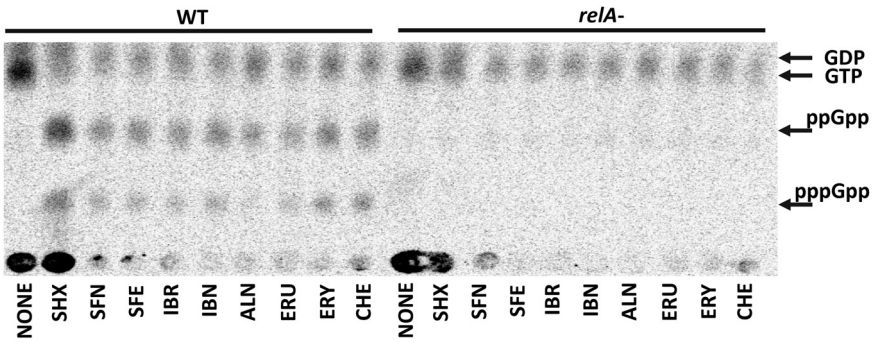

FIGURE 3 | The effect of isothiocyanates on the (p)ppGpp alarmone accumulation in *E. coli*. Bacteria were grown overnight on LB agar plates at 30°C, then collected and washed with PBS buffer, concentrated, and resuspended in low phosphate MOPS labeling medium at OD_{600} = 0.2 density. Cells were labeled with 5 μCi/ml ^{32}P for 20 min. (p)ppGpp synthesis was induced with 1 mg/ml of serine hydroxamate (SHX) for positive control; various isothiocyanates were used at 1 x MIC concentration for 20 min. Samples were spotted on PEI cellulose TLC plates, developed in 1.5 M potassium phosphate buffer and visualized with a Phosphoimager. The positions of guanosine nucleotides (GDP, GTP, ppGpp, and pppGpp) are indicated by arrows.

amounts of individual ITCs (MICs). Interestingly, the kinetics of (p)ppGpp accumulation upon these various treatments showed that the level of the stringent response induction, in terms of amount and time, was similar for the MIC values of SNF and combination of FIC values of SNF and either of three ITC showing synergistic effect (**Figure 4C**). Namely, the levels of accumulated (p)ppGpp expressed as % of pooled guanosine nucleotides were 64.7 [$SFN_{(MIC)}$], 66.6 [$SFN_{(FIC)}$ + $IBR_{(FIC)}$], 66.1 [$SFN_{(FIC)}$ + $IBN_{(FIC)}$], and 63.7 [$SFN_{(FIC)}$ + $ALN_{(FIC)}$] at the end point of the experiment (30 min). Thus, the stress caused by SNF/ITC action is sufficient to achieve cellular (p)ppGpp concentrations inhibiting bacterial growth. Furthermore, we

TABLE 2 | The impact of particular amino acids which can alter ITC antimicrobial action against *E. coli* MG1655.

ITC:	8 x MIC	4 x MIC
SFN	Gly, Met	Tyr, Gln, Trp, Cys, Arg
SFE	Gly, Met	Tyr, Gln, Trp, Phe, Ala
IBR	Gly	Met, Tyr, Gln, Phe
IBN	Gly	Met, Tyr, Gln, Trp, Phe, Ala
ALN	Gly	Met, Tyr, Gln, Phe, Ala
ERU	Gly	Met, Tyr, Gln, Ala
ERY	Gly	Met
CHE	Gly	Met, Asn

The amino acids were assigned into rows according to the strength of their activity, expressed as increased fold change of MIC value for specific ITC (four and eight times, respectively).

TABLE 3 | Estimated FICI values for combinations of ITCs.

ITC combination (A × B)	Combined MIC values (mg/L)	$FIC_A + FIC_B$	FICI
SFN + SFE	1.39 + 2.77	1/4 + 1/2	0.75 ≥ 0.5 ADD
SFN + IBR	0.69 + 1.15	1/8 + 1/8	0.25 ≤ 0.5 SYN
SFN + IBN	1.39 + 0.64	1/4 + 1/8	0.375 ≤ 0.5 SYN
SFN + ALN	1.39 + 1.5	1/4 + 1/8	0.375 ≤ 0.5 SYN
SFN + ERU	1.39 + 20.2	1/4 + 1/2	0.75 ≥ 0.5 ADD
SFN + ERY	1.39 + 7.4	1/4 + 1/2	0.75 ≥ 0.5 ADD
SFN + CHE	0.69 + 7.4	1/8 + 1/2	0.625 ≥ 0.5 ADD
IBR + IBN	1.15 + 0.64	1/8 + 1/8	0.25 ≤ 0.5 SYN
IBR + ALN	2.3 + 5.95	1/4 + 1/2	0.75 ≥ 0.5 ADD
ALN + IBN	1.5 + 2.55	1/8 + 1/2	0.625 ≥ 0.5 ADD

FICI results ≥ 0.5 were considered as additive interactions and ≤ 0.5 as synergistic.

asked how the amino acids Met and Gly, which effectively counteract bacterial growth inhibition, can impair the (p)ppGpp accumulation induced by SFN, IBR, IBN, and ALN. The observed estimated levels of alarmones in the Met and Gly treated cells were significantly reduced (by ∼40%) in comparison to cells treated with an ITC alone ($p < 0.05$) (**Figure 5**). Nevertheless, we also found that Phe and Thr supplementation also acts negatively on the alarmone accumulation, while the impact of other amino acids was moderate and varied depending on a particular ITC.

The Antibacterial Potential of Sulforaphane Analogs Against Enterohemorrhagic *Escherichia coli* Strains

The actual aim of the studies on antimicrobial agents is to assess their effectiveness against pathogenic strains. Therefore, we tested the antibacterial effect of SNF and its analogs on the enterohemorrhagic *E. coli* strains: EDL 933W and 86–24, carrying Shiga toxin-converting prophages. Interestingly, their growth inhibition was at least at the level observed for the wild-type *E. coli* (**Table 3**) for SFN, IBN, ALN, and CHE, while for SFE, IBR, ERU, and ERY, the MIC values were even lower. These results indicate that pathogenic *E. coli* strains are sensitive to the aliphatic ITCs. Because of the specific virulence of EHEC strains, the therapeutic agents should not only stop bacterial growth but, more importantly, inhibit lytic development of *stx*-bearing prophages, preventing Shiga toxin production. The *E. coli* 86–24 Δ*stx*:GFP strain with GFP gene replacing the *stx* gene was used to monitor the ITC effect on prophage induction. The GFP gene expression was mediated by *stx* promoter. In this experiment, mitomycin (0.5 μg/ml) was used to induce phage development (Otsuji et al., 1959), which resulted in the impairment of cell division and subsequent filamentation (**Figure 6F**). At the same time, GFP synthesis was visible as a result of the expression of prophage genes, including the region with the *stx* gene, during phage lytic development (**Figure 6F**). The ITC treatment alleviated both effects of mitomycin: the filamentation phenotype was reversed and GFP synthesis was at an undetectable level; this effect was observed for SNF alone, and for SNF in combination with IBR, IBN, and ALN (**Figures 6G–J**). ITC treatment at FIC concentrations (analogous to the growth inhibition experiments described above) in the absence of mitomycin did not induce prophage induction and *stx* promoter activity (monitored by GFP production) (**Figures 6B–E**), although the stress conditions caused by ITC resulted in decreased cell size (compare **Figure 6A** with **Figures 6B–E**). These results confirmed that ITCs, acting individually or synergistically, decrease growth of EHEC strains without induction of the lambdoid prophage lytic development.

Nitrogen Source Utilization Upon Sulforaphane Treatment

To understand the wide effect of SFN on bacteria, we performed a downstream analysis of bacterial phenotypes due to nitrogen source utilization upon sulforaphane treatment. Many nitrogen-rich (N-rich) compounds that can be transported into a cell and metabolized to produce NADH, will generate a redox potential and flow of electrons to reduce a tetrazolium violet (TV), thereby developing the color change. The more rapid this metabolic flow is, the more quickly the color is formed. The metabolic flow is supressed or unchanged by adding sulforaphane. **Figure 7A** presents the TV reduction kinetics data of wild-type strain and *relA* mutant treated with SFN in comparison to untreated strains (the controls). The curves show the time course (horizontal axis) of the amount of color formed from tetrazolium dye reduction (vertical axis) in each of the 96 wells. Reference (control) is shown in red and Test (compound added) is shown in green (**Figure 7A**). If both curves overlap (the yellow area), it gives an information that there is no difference between the strain tested and not tested with SFN, in the presence of a particular N-source. If the effect of ITC treatment reduces the metabolic flow, the red curves occur (many cases). Measurements that pass the reproducibility test are marked with black box (**Figure 7A**).

The data presented for this experiment strongly suggest that despite SFN treatment, many N-source are metabolized on the same level in the untreated controls. The data show that upon SFN treatment, many amino acids are poorly metabolized as a sole N-source, in both analyzed strains. However, utilization of several N-compounds is not affected upon ITC treatment. Therefore, we have analyzed if are there any correlations between the strength of the phenotype and the physicochemical properties

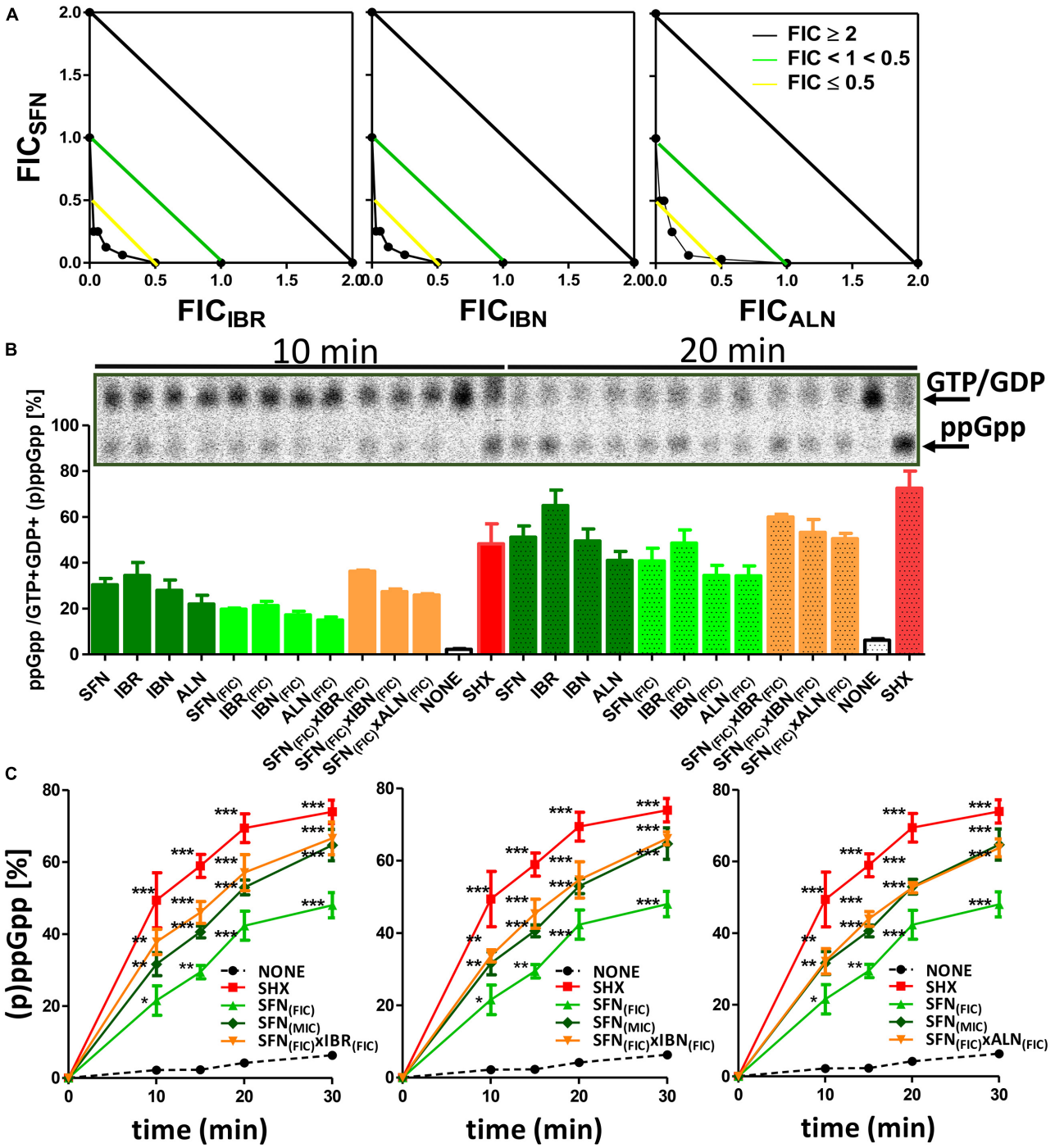

FIGURE 4 | Analysis of synergistic interactions between IBR, IBN, ALN, and SFN. **(A)** Synergistic effects of sulforaphane in mixtures with iberin, iberverin, and alyssin are represented on isobolograms. Estimated FICI values are presented for combinations of SFN with other ITCs. A checkerboard technique was employed to delineate the Fractional Inhibitory Concentration Index (FICI). The treated cultures were screened for visual growth in a microplate reader. The FICI were then calculated as described in section "Materials and Methods" (FICI ≤ 0.5, synergy; 0.5 ≤ FICI ≤ 1.0, additivity; 1.1 ≤ FICI ≤ 2.0, indifference; FICI ≥ 2.0, antagonism) **(B)** ppGpp alarmone accumulation under treatment with synergistic combinations of SFN + ITCs. **(C)** The kinetics of relative ppGpp accumulation in treated cells. Relative ppGpp levels were assessed by densitometry using the QuantityOne Software. The ^{33}P incorporation method was used to evaluate stringent response induction like described previously. (p)ppGpp synthesis was induced with 1 mg/ml of serine hydroxamate (SHX) for positive control; various isothiocyanates were used in 1x MIC or FIC concentration in combination for 10, 15, 20, and 30 min. Samples were spotted on PEI cellulose TLC plates, developed in 1.5 M potassium phosphate buffer and visualized with a Phosphoimager. The results are from at least three independent experiments. The pooled (p)ppGpp and GTP amounts were taken as 100%. The statistical significance of differences in (p)ppGpp amount compared to its basal level of samples at the corresponding time of non-treated control was determined by *t*-test (*$p \leq 0.05$, **$p \leq 0.01$, and ***$p \leq 0.001$) as indicated above or below plots.

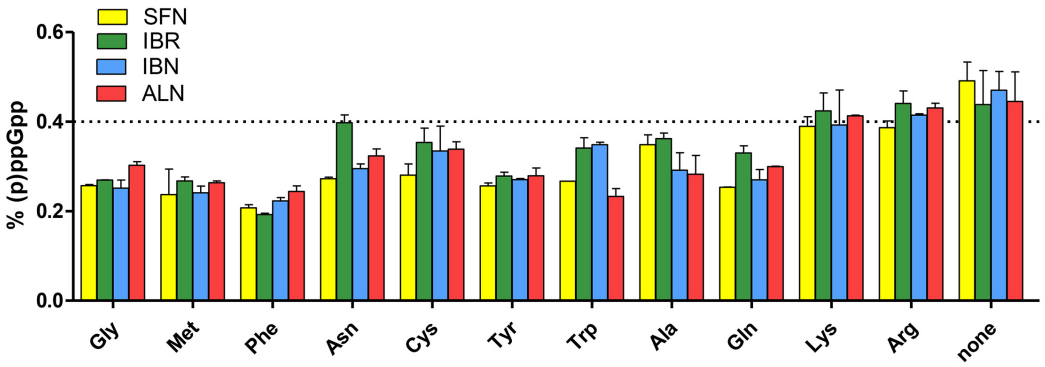

FIGURE 5 | The effect of specific amino acids on the stringent alarmone (p)ppGpp synthesis during SFN, IBR, IBN, and ALN treatment of *E. coli* MG1655. Relative (p)ppGpp accumulation after supplementation with specific amino acids in cultures treated with SFN (yellow), IBR (green), IBN (blue), and ALN (green). The assessment of intracellular level of (p)ppGpp alarmones was determined by [^{32}P]orthophosphoric acid incorporation and developed by TLC on PEI cellulose plates, followed by densitometry. The level of (p)ppGpp represents % of a sum of all G nucleotides visualized on TLC plate. The dotted line represents the mean level of alarmone induction in SFN, IBR, IBN, and ALN treated cells without amino acid supplementation (control). The results are from at least three independent experiments.

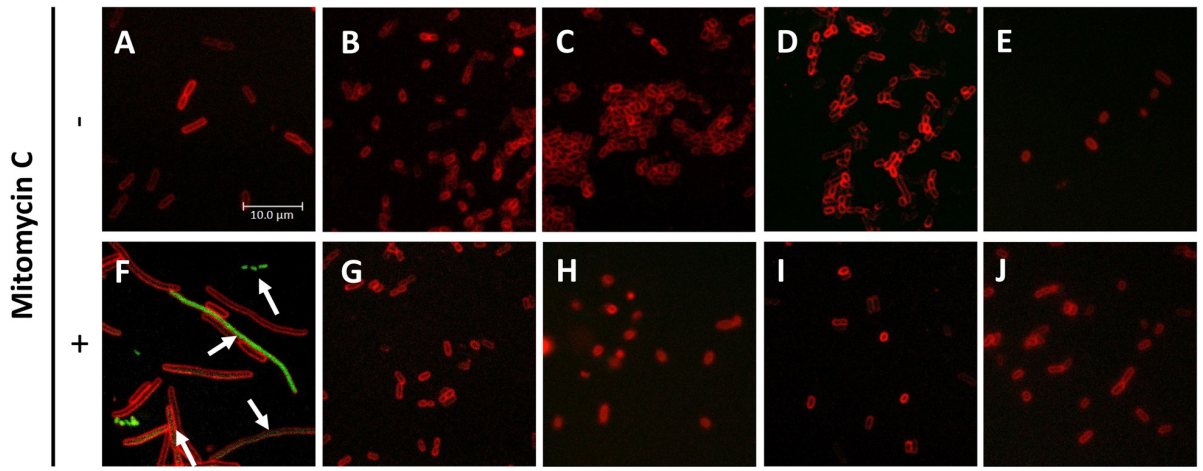

FIGURE 6 | Inhibition of stx_p activity under ITC treatment of *E. coli* 86-24 O157:H7 strain. *E. coli* 86-24 O157:H7 Δ*stx*:GFP was cultivated for 3 h in the presence of **(A)** not-treated control **(B,G)**, SFN added at MIC value, **(C,H)** SFN and IBR at FIC values, **(D,I)** SFN and IBN added at FIC values, **(E,J)** SFN and ALN at FIC values. **(F–J)** Mitomycin C was added as the toxin production inducer. Bacteria were then stained with SynaptoRed to visualize membranes; GFP synthesis was analyzed by fluorescence microscopy. The activity of stx_p:GFP is marked by arrows. Pictures present merged green and red channels; the scale bar is valid for all panels.

of dipeptides (and some tripeptides). We have employed several parameters to the analysis, such us molecular weight, extinction coefficient, iso-electric point, net charge at pH 7, estimated solubility, and hydrophilicity. We found that for a wild-type strain treated with sulforaphane, there is moderate (but significant) negative correlation between estimated solubility of the peptide and the strength of phenotype. Also, we found that there is a low negative correlation between hydrophilicity and the strength of a given phenotype (**Supplementary Table S2**).

DISCUSSION

In this work, we showed that all tested aliphatic ITCs specifically induce stringent control through the amino acid pathway, controlled by RelA. Moreover, the alarmones' accumulation increases in time (**Figure 4C**), which suggests an ongoing stress response. Thus, the antibacterial effect of the ITC treatment is related to the stringent response and to the factors triggering induction of (p)ppGpp accumulation. These factors lead to amino acid starvation, in both, the wild-type and (p)ppGpp-devoid strains; however, in the wt bacteria, the rapid induction of the stringent response results in the subsequent downregulation of the main metabolic processes. Thus, this specific effect of ITCs is responsible for growth arrest, rather than a consequence of bacterial cell disintegration as proposed by others (Borges et al., 2015; Dufour et al., 2015; Romeo et al., 2018). The alterations in bacterial metabolism, resulting from an indirect effect of (p)pGpp accumulation and/or the actual direct action of ITCs related to amino

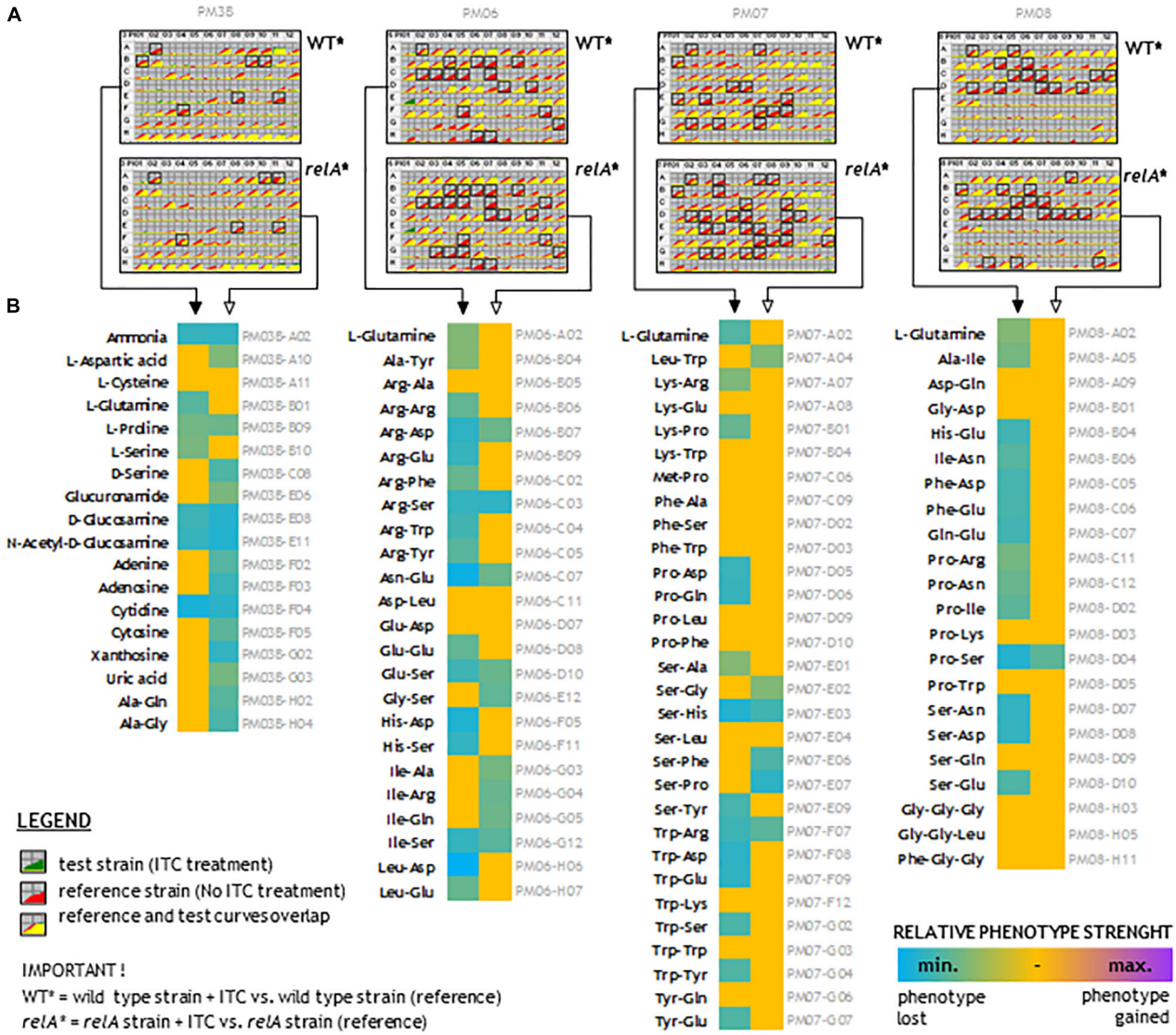

FIGURE 7 | N-source utilization upon sulforaphane treatment. **(A)** Kinetic curves of tetrazolium violet (TV) color development upon 48 h of sulforaphane (ITC) treatment. Each plate shows comparison of treated and untreated strains, as indicated. The yellow color reflects the situation where the tested treated strain utilizes nitrogen-rich compounds at the same level as untreated corresponding strain. The red color reflects reduced metabolic flow in the treated strains (most cases). Black frames indicate scored changes in kinetics that passed the reproducibility test. **(B)** The effect of ITC treatment on the wild-type and *relA* mutant strains. The more turquoise the color, the more ITC treatment suppresses utilization of a given nitrogen compound. Full arrows point to the wild-type strains and open arrows to the *relA* mutants. Descriptions in gray refer to the nitrogen compound plate position.

acid limitation leading to downregulation of protein synthesis, can eventually lead to cellular membrane disruption and cell death. Thus, ITCs can affect both, the wild type and (p)ppGpp-deficient bacteria, which is strongly supported by the sensitivity of *relA* mutant strain to ITCs (**Supplementary Table S1**). The importance of the stringent response induction in the wild-type strain lies in its effect on Shiga toxin production by EHEC strains, as we reported previously (Nowicki et al., 2014, 2016).

The chemical nature of aliphatic ITCs as particularly reactive compounds makes them a subject to nucleophilic attack at the electron-lacking central carbon atom (Wu et al., 2009). In the presence of thiol molecules, this carbon atom is attacked, and dithiocarbamates are formed (Shibata et al., 2011). It has been shown that inhibition of the sulfhydryl enzymes may play a role in the antimicrobial action of ITCs (Luciano and Holley, 2009). Nevertheless, amino acid deficiency is the first observed effect under ITCs treatment, as we showed here and in our previous work (Nowicki et al., 2014, 2016).

The involvement of ITC-mediated effect in the amino acid availability has been already shown for some ITCs (Nowicki et al., 2013, 2016). The potential interaction of ITCs with amino acids was concluded from the observation that excess of specific amino acids reversed antibacterial action of ITCs. Interestingly,

the observed effects were related to the ITCs structure. Selected ITCs, among them those with aliphatic, branched chained, and aromatic groups, exhibit different specificity toward interaction with various amino acids. There were some amino acids common for specific ITCs, such as glycine for SFN, benzyl ITC, and allyl ITC, arginine for SFN, phenyl ITC, and IPRITC, phenylalanine for BITC and AITC, or lysine for PITC and IPRITC. We also noticed that glycine was the most effective in growth arrest recovery (Nowicki et al., 2013, 2016). Here, we aimed to elucidate the possible interactions of amino acids with analogs of SNF. We found here that all aliphatic ITCs tested, seem to effectively interact with Gly and Met, and specifically with other amino acids with different strengths (**Table 2**). It is known that the electron-deficient central carbon of ITCs is susceptible to attack from amino groups, forming thiourea derivatives (Wu et al., 2009). The electrophilic action of AITC was observed while studying reactions between ITCs and proteins (Kawakishi and Kaneko, 1985, 1987). The ability of AITC to initiate disulfide bond oxidative cleavage in cysteine moieties and to react with free amino groups of lysine and arginine was identified (Weerawatanakorn et al., 2015). The interaction of isothiocyanates with cysteine was suggested in their interaction with tubulin (Xiao et al., 2012). Nevertheless, there is no evidence for the microbial proteins as specific targets. Therefore, it is unclear if the same effect would occur *in vivo*. Cejpek and colleagues also postulate that *in vitro*, there are interactions with free amino acids and short peptides (Cejpek et al., 2000). The binding of sulforaphane to a defined peptide sequence was found to be a basis of its interaction with the Hsp90 protein (Li et al., 2012), while the molecular docking modeling indicated the direct interaction of SFN with Asn in NAD(P)H:quinone oxidoreductase (Mazur et al., 2010). To challenge the phenomenon of ITC interaction with amino acids *in vivo*, we extended our investigation by BIOLOG phenotypic arrays analysis (**Figure 7**) for SFN-treated cells employing wt and *relA* strains. Cells were treated with 1/4 MIC value to provoke amino acid starvation without complete shutdown of bacterial growth. This study showed that there are specific interactions where di- and three- peptides and other N-sources can effectively restore bacterial metabolism in the presence of SFN. Specifically, a broad group of short peptides, namely, those containing Gly, Met, Phe, Gln, Trp, and Ala can affect the SFN antimicrobial potential. We even noticed a higher ability to utilize the peptides as a sole N-source in the *relA* strain. We assumed it is a consequence of impaired (p)ppGpp synthesis under amino acid starvation conditions, while due to increased alarmone level in the wt strain, the metabolism and other cellular processes remained altered and generally downregulated upon SFN treatment. However, we do not see any statistically significant correlation between any specific peptide features and the strength of phenotype for the *relA* mutant treated with SFN (**Supplementary Table S2**). There is no clear relationship between the physiochemical properties of N-course compounds and sulforaphane effect. Thus, the molecular mechanism of these interactions remains yet to be solved.

In the search for novel antimicrobials, a possible synergy between compounds is often considered. The phenomenon of synergy occurs when the effect of two compounds in the mixture exceeds the sum of their individual effects. Thus, such interaction results in the increased effectiveness of a given chemical mixture. Importantly, the synergistic effect requires lower concentrations of compounds for comparison with their individual action and decreasing the effective doses usually results in reduction of potential side effects. The synergy of the two components is utilized in, e.g., antibacterial therapy (Kang et al., 2011; Brooks and Brooks, 2014), with the example of a widely used combination of beta-lactam antibiotics and inhibitors of β-lactamases (Neu, 1987). Thus, in fighting antibiotic-resistant pathogens, the important part is not only the finding of novel compounds but also assessment of their effects with the already known agents. The mechanisms underlying the synergistic effects of various compounds involve interactions with different cellular targets, increasing bioavailability and pharmacokinetics of the compounds or activating effectiveness of an otherwise inactive compound (Wagner and Ulrich-Merzenich, 2009). For the antibacterial effects, the synergistic combinations decrease or delay the spread of bacterial resistance to one or both agents (Korcsmáros et al., 2007). For isothiocyanates, the main mechanism of their antibacterial action involves the stringent response induction, which is triggered by the amino acid starvation, as we have shown previously for PEITC, BITC, and SFN (Nowicki et al., 2014, 2016) and, in this work, for the sulforaphane analogs. The synergy in the situation of the same cellular target would seem difficult to envision; however, the effect of amino acid starvation can be attained by depletion of various amino acids. Indeed, the reversal of ITC effects was observed in the presence of various amino acids (**Table 2**), specific for each ITC, indicating possible divergent interaction with amino acids. This effect may involve amino acid transport system, which could be directly or indirectly blocked by ITCs. Therefore, the excess of amino acids would diminish the ITC impact. A possible effect on the aminoacyl tRNA synthetases can be also taken into consideration, as the lack of the specific aminoacyl tRNA would block the ribosomes and activate RelA. The available data on the ITC binding to amino acids and proteins, together with our results on the specificity of amino acid-mediated reversal of ITC effect, suggest that the interaction of isothiocyanates with amino acids (free or present in the proteins) is the basis of pleiotropic effects of ITCs.

TABLE 4 | The determined ITC susceptibility of *E. coli* O157:H7 strains.

***E. coli* O157:H7**	**MIC mg/L (mM)**	
ITC:	**EDL 933W**	**EDL 933W**
SFN	88.6 (0.5)	88.6 (0.5)
SFE	43.9 (0.25)	43.9 (0.25)
IBR	73.7 (0.5)	73.7 (0.5)
IBN	163.3 (1.0)	163.3 (1.0)
ALN	191.3 (1.0)	191.3 (1.0)
ERU	80.6 (0.5)	80.6 (0.5)
ERY	62.5 (0.32)	62.5 (0.32)
CHE	125 (0.7)	125 (0.7)

The observed effects of individual ITCs or their combinations on the model and pathogenic strains of *E. coli* are underlined by the stringent response induction as a main mechanism of their antimicrobial properties. An antibacterial effect of (p)ppGpp accumulation is a very rare mechanism of an antibiotic mode of action. Generally, (p)ppGpp increases bacterial virulence by regulating the expression of pathogenicity island genes, promoting antibiotic resistance (Strugeon et al., 2016) and supporting occurrence of persister cells (Svenningsen et al., 2019) as reported recently, due to ribosome dimerization (Song and Wood, 2020). Thus, studies carried out so far usually focused on developing inhibitors of (p)ppGpp synthesis, e.g., by targeting enzymes responsible for (p)ppGpp synthesis (Wexselblatt et al., 2010, 2012, 2013) or leading to degradation of the alarmone molecules (de la Fuente-Núñez et al., 2014, 2015).

Therefore, the use of ITCs as antibacterial agents can be advantageous, as there are very few examples of bacterial resistance to these compounds, as reported for *Pseudomonas sax* genes related overcoming of host defense mechanisms in *Arabidopsis* (Fan et al., 2011). The bactericidal effect of ITC shown in time-kill assay confirms the antimicrobial effect of these compounds (**Figure 2**). The occurrence of persister cells upon ITC treatment was not reported so far; however, it cannot be excluded because of the increase in (p)ppGpp level, so this problem requires further studies. Our data show promising antibacterial effects of sulforaphane analogs against EHEC strains (**Table 4**). Taking into consideration that, on one hand, these ITCs are a part of normal diet, and their safety for humans is widely investigated for their chemoprevention properties, and on the other hand, the antibiotic treatment of EHEC infections is very limited, this could open broad opportunities to include ITCs as a potential therapeutic strategy based on the stringent response-mediated antimicrobial action.

DATA AVAILABILITY STATEMENT

The raw data supporting the conclusions of this article will be made available by the authors, without undue reservation, to any qualified researcher.

AUTHOR CONTRIBUTIONS

DN and AS-P conceived the study and designed the experimental procedures. DN, KK, PS, AŻ, and GC carried out the experiments. DN, AS-P, and GC analyzed the data and wrote the manuscript. AS-P supervised the project. All authors approved the final manuscript.

FUNDING

This work was supported by the grant from the National Science Centre (Poland) (grant no. UMO-2016/21/B/NZ7/02077) to AS-P and by Foundation for Polish Science, Poland (START 059.2017 *7E9) to DN.

ACKNOWLEDGMENTS

We thank Dr. Katarzyna Potrykus for theoretical and technical support, encouragement to develop the project, and critical reading of the manuscript.

SUPPLEMENTARY MATERIAL

The Supplementary Material for this article can be found online at: https://www.frontiersin.org/articles/10.3389/fmicb.2020.591802/full#supplementary-material

REFERENCES

Abdull Razis, A. F., Iori, R., and Ioannides, C. (2011). The natural chemopreventive phytochemical R-sulforaphane is a far more potent inducer of the carcinogen-detoxifying enzyme systems in rat liver and lung than the S-isomer. *Int. J. Cancer* 128, 2775–2782. doi: 10.1002/ijc.25620

Abreu, A. C., Borges, A., Simões, L. C., Saavedra, M. J., and Simões, M. (2013). Antibacterial activity of phenyl isothiocyanate on *Escherichia coli* and *Staphylococcus aureus*. *Med. Chem.* 9, 756–761. doi: 10.2174/15734064113090050016

Adibi, S. A., and Mercer, D. W. (1973). Protein digestion in human intestine as reflected in luminal, mucosal, and plasma amino acid concentrations after meals. *J. Clin. Invest.* 52, 1586–1594. doi: 10.1172/JCI107335

Bajaksouzian, S., Visalli, M. A., Jacobs, M. R., and Appelbaum, P. C. (1996). Antipneumococcal activities of cefpirome and cefotaxime, alone and in combination with vancomycin and teicoplanin, determined by checkerboard and time-kill methods. *Antimicrob. Agents Chemother.* 40, 1973–1976. doi: 10.1128/AAC.40.9.1973

Bener, A., Dogan, M., Azab, I. A., Rashed, A., and Siddiqui, M. (2006). Amino acid profiles among colorectal cancer patients. *Biomed. Res.* 17, 149–154.

Borges, A., Abreu, A. C., Ferreira, C., Saavedra, M. J., Simões, L. C., and Simões, M. (2015). Antibacterial activity and mode of action of selected glucosinolate hydrolysis products against bacterial pathogens. *J. Food Sci. Technol.* 52, 4737–4748. doi: 10.1007/s13197-014-1533-1

Brooks, B. D., and Brooks, A. E. (2014). Therapeutic strategies to combat antibiotic resistance. *Adv. Drug Deliv. Rev.* 78, 14–27. doi: 10.1016/j.addr.2014.10.027

Cejpek, K., Valusek, J., and Velísek, J. (2000). Reactions of allyl isothiocyanate with alanine, glycine, and several peptides in model systems. *J. Agric. Food Chem.* 48, 3560–3565. doi: 10.1021/jf991019s

de la Fuente-Núñez, C., Reffuveille, F., Haney, E. F., Straus, S. K., and Hancock, R. E. W. (2014). Broad-spectrum anti-biofilm peptide that targets a cellular stress response. *PLoS Pathog.* 10:e1004152. doi: 10.1371/journal.ppat.1004152

de la Fuente-Núñez, C., Reffuveille, F., Mansour, S. C., Reckseidler-Zenteno, S. L., Hernández, D., Brackman, G., et al. (2015). D-enantiomeric peptides that eradicate wild-type and multidrug-resistant biofilms and protect against lethal *Pseudomonas aeruginosa* infections. *Chem. Biol.* 22, 196–205. doi: 10.1016/j.chembiol.2015.01.002

Dufour, V., Stahl, M., and Baysse, C. (2015). The antibacterial properties of isothiocyanates. *Microbiology* 161, 229–243. doi: 10.1099/mic.0.082362-0

Fan, J., Crooks, C., Creissen, G., Hill, L., Fairhurst, S., Doerner, P., et al. (2011). *Pseudomonas* sax genes overcome aliphatic isothiocyanate-mediated non-host resistance in *Arabidopsis*. *Science* 331, 1185–1188. doi: 10.1126/science.1199707

Filipiak, M., Łoś, J. M., and Łoś, M. (2020). Efficiency of induction of Shiga-toxin lambdoid prophages in *Escherichia coli* due to oxidative and antibiotic stress depends on the combination of prophage and the bacterial strain. *J. Appl. Genet.* 61, 131–140. doi: 10.1007/s13353-019-00525-8

Houghton, C. A. (2019). Sulforaphane: its "Coming of age" as a clinically relevant nutraceutical in the prevention and treatment of chronic disease. *Oxid. Med. Cell. Longev.* 2019:2716870. doi: 10.1155/2019/2716870

Kang, H.-K., Kim, H.-Y., and Cha, J.-D. (2011). Synergistic effects between silibinin and antibiotics on methicillin-resistant *Staphylococcus aureus* isolated from clinical specimens. *Biotechnol. J.* 6, 1397–1408. doi: 10.1002/biot.201000422

Kawakishi, S., and Kaneko, T. (1985). Interaction of oxidized glutathione with allyl isothiocyanate. *Phytochemistry* 24, 715–718. doi: 10.1016/S0031-9422(00)84882-7

Kawakishi, S., and Kaneko, T. (1987). Interaction of proteins with allyl isothiocyanate. *J. Agric. Food Chem.* 35, 85–88. doi: 10.1021/jf00073a020

Ko, M.-O., Kim, M.-B., and Lim, S.-B. (2016). Relationship between chemical structure and antimicrobial activities of isothiocyanates from cruciferous vegetables against oral pathogens. *J. Microbiol. Biotechnol.* 26, 2036–2042.

Korcsmáros, T., Szalay, M. S., Böde, C., Kovács, I. A., and Csermely, P. (2007). How to design multi-target drugs. *Expert Opin. Drug. Discov.* 2, 799–808. doi: 10.1517/17460441.2.6.799

Li, Y., Karagöz, G. E., Seo, Y. H., Zhang, T., Jiang, Y., Yu, Y., et al. (2012). Sulforaphane inhibits pancreatic cancer through disrupting Hsp90-p50(Cdc37) complex and direct interactions with amino acids residues of Hsp90. *J. Nutr. Biochem.* 23, 1617–1626. doi: 10.1016/j.jnutbio.2011.11.004

Luciano, F. B., and Holley, R. A. (2009). Enzymatic inhibition by allyl isothiocyanate and factors affecting its antimicrobial action against *Escherichia coli* O157:H7. *Int. J. Food Microbiol.* 131, 240–245. doi: 10.1016/j.ijfoodmicro.2009.03.005

Mazur, P., Magdziarz, T., Bak, A., Chilmonczyk, Z., Kasprzycka-Guttman, T., Misiewicz-Krzemińska, I., et al. (2010). Does molecular docking reveal alternative chemopreventive mechanism of activation of oxidoreductase by sulforaphane isothiocyanates? *J. Mol. Model.* 16, 1205–1212. doi: 10.1007/s00894-009-0628-5

Mechold, U., Murphy, H., Brown, L., and Cashel, M. (2002). Intramolecular regulation of the opposing (p)ppGpp catalytic activities of Rel(Seq), the Rel/Spo enzyme from Streptococcus equisimilis. *J. Bacteriol.* 184, 2878–2888. doi: 10.1128/jb.184.11.2878-2888.2002

Milczarek, M., Mielczarek, L., Lubelska, K., Dąbrowska, A., Chilmonczyk, Z., Matosiuk, D., et al. (2018). In vitro evaluation of sulforaphane and a natural analog as potent inducers of 5-fluorouracil anticancer activity. *Molecules* 23:3040. doi: 10.3390/molecules23113040

Munday, R., and Munday, C. M. (2004). Induction of phase II detoxification enzymes in rats by plant-derived isothiocyanates: comparison of allyl isothiocyanate with sulforaphane and related compounds. *J. Agric. Food Chem.* 52, 1867–1871. doi: 10.1021/jf030549s

Neu, H. C. (1987). Penicillin-binding proteins and beta-lactamases: their effects on the use of cephalosporins and other new beta-lactams. *Curr. Clin. Top. Infect. Dis.* 8, 37–61. doi: 10.1146/annurev.mi.45.100191.000345

Nowicki, D., Kobiela, W., Węgrzyn, A., Wegrzyn, G., and Szalewska-Pałasz, A. (2013). ppGpp-dependent negative control of DNA replication of Shiga toxin-converting bacteriophages in *Escherichia coli*. *J. Bacteriol.* 195, 5007–5015. doi: 10.1128/JB.00592-13

Nowicki, D., Maciąg-Dorszyńska, M., Bogucka, K., Szalewska-Pałasz, A., and Herman-Antosiewicz, A. (2019). Various modes of action of dietary phytochemicals, sulforaphane and phenethyl isothiocyanate, on pathogenic bacteria. *Sci. Rep.* 9:13677. doi: 10.1038/s41598-019-50216-x

Nowicki, D., Maciąg-Dorszyńska, M., Kobiela, W., Herman-Antosiewicz, A., Węgrzyn, A., Szalewska-Pałasz, A., et al. (2014). Phenethyl isothiocyanate inhibits shiga toxin production in enterohemorrhagic *Escherichia coli* by stringent response induction. *Antimicrob. Agents Chemother.* 58, 2304–2315. doi: 10.1128/AAC.02515-13

Nowicki, D., Rodzik, O., Herman-Antosiewicz, A., and Szalewska-Pałasz, A. (2016). Isothiocyanates as effective agents against enterohemorrhagic *Escherichia coli*: insight to the mode of action. *Sci. Rep.* 6:22263. doi: 10.1038/srep22263

Otsuji, N., Sekiguchi, M., Iijima, T., and Takagi, Y. (1959). Induction of phage formation in the lysogenic *Escherichia coli* K-12 by mitomycin C. *Nature* 184, 1079–1080. doi: 10.1038/1841079b0

Patel, J., Yin, H.-B., Bauchan, G., and Mowery, J. (2020). Inhibition of *Escherichia coli* O157:H7 and *Salmonella enterica* virulence factors by benzyl isothiocyanate. *Food Microbiol.* 86:103303. doi: 10.1016/j.fm.2019.103303

Pawlik, A., Wiczk, A., Kaczyńska, A., Antosiewicz, J., and Herman-Antosiewicz, A. (2013). Sulforaphane inhibits growth of phenotypically different breast cancer cells. *Eur. J. Nutr.* 52, 1949–1958. doi: 10.1007/s00394-013-0499-5

Potrykus, K., and Cashel, M. (2008). (p)ppGpp: still magical? *Annu. Rev. Microbiol.* 62, 35–51. doi: 10.1146/annurev.micro.62.081307.162903

Provenzani, A., Hospodar, A. R., Meyer, A. L., Leonardi Vinci, D., Hwang, E. Y., Butrus, C. M., et al. (2020). Multidrug-resistant gram-negative organisms: a review of recently approved antibiotics and novel pipeline agents. *Int. J. Clin. Pharm.* 42, 1016–1025. doi: 10.1007/s11096-020-01089-y

Romeo, L., Iori, R., Rollin, P., Bramanti, P., and Mazzon, E. (2018). Isothiocyanates: an overview of their antimicrobial activity against human infections. *Molecules* 23:624. doi: 10.3390/molecules23030624

Ruhee, R. T., and Suzuki, K. (2020). The integrative role of sulforaphane in preventing inflammation, oxidative stress and fatigue: a review of a potential protective phytochemical. *Antioxidants* 9:521. doi: 10.3390/antiox9060521

Shibata, T., Kimura, Y., Mukai, A., Mori, H., Ito, S., Asaka, Y., et al. (2011). Transthiocarbamoylation of proteins by thiolated isothiocyanates. *J. Biol. Chem.* 286, 42150–42161. doi: 10.1074/jbc.M111.308049

Singh, S. V., and Singh, K. (2012). Cancer chemoprevention with dietary isothiocyanates mature for clinical translational research. *Carcinogenesis* 33, 1833–1842. doi: 10.1093/carcin/bgs216

Song, S., and Wood, T. K. (2020). ppGpp ribosome dimerization model for bacterial persister formation and resuscitation. *Biochem. Biophys. Res. Commun.* 523, 281–286. doi: 10.1016/j.bbrc.2020.01.102

Strugeon, E., Tilloy, V., Ploy, M.-C., and Da Re, S. (2016). The stringent response promotes antibiotic resistance dissemination by regulating integron integrase expression in biofilms. *MBio* 7, e868–e816. doi: 10.1128/mBio.00868-16

Svenningsen, M. S., Veress, A., Harms, A., Mitarai, N., and Semsey, S. (2019). Birth and resuscitation of (p)ppGpp induced antibiotic tolerant persister cells. *Sci. Rep.* 9:6056. doi: 10.1038/s41598-019-42403-7

Thomas, C. M., and Nielsen, K. M. (2005). Mechanisms of, and barriers to, horizontal gene transfer between bacteria. *Nat. Rev. Microbiol.* 3, 711–721. doi: 10.1038/nrmicro1234

Thorpe, K. E., Joski, P., and Johnston, K. J. (2018). Antibiotic-resistant infection treatment costs have doubled since 2002, now exceeding $2 billion annually. *Health Aff.* 37, 662–669. doi: 10.1377/hlthaff.2017.1153

Wagner, H., and Ulrich-Merzenich, G. (2009). Synergy research: approaching a new generation of phytopharmaceuticals. *Phytomedicine* 16, 97–110. doi: 10.1016/j.phymed.2008.12.018

Weerawatanakorn, M., Wu, J.-C., Pan, M.-H., and Ho, C.-T. (2015). Reactivity and stability of selected flavor compounds. *J. Food Drug. Anal.* 23, 176–190. doi: 10.1016/j.jfda.2015.02.001

Wexselblatt, E., Kaspy, I., Glaser, G., Katzhendler, J., and Yavin, E. (2013). Design, synthesis and structure-activity relationship of novel Relacin analogs as inhibitors of Rel proteins. *Eur. J. Med. Chem.* 70, 497–504. doi: 10.1016/j.ejmech.2013.10.036

Wexselblatt, E., Katzhendler, J., Saleem-Batcha, R., Hansen, G., Hilgenfeld, R., Glaser, G., et al. (2010). ppGpp analogues inhibit synthetase activity of Rel proteins from Gram-negative and Gram-positive bacteria. *Bioorg. Med. Chem.* 18, 4485–4497. doi: 10.1016/j.bmc.2010.04.064

Wexselblatt, E., Oppenheimer-Shaanan, Y., Kaspy, I., London, N., Schueler-Furman, O., Yavin, E., et al. (2012). Relacin, a novel antibacterial agent targeting the stringent response. *PLoS Pathog.* 8:e1002925. doi: 10.1371/journal.ppat.1002925

Wiczk, A., Hofman, D., Konopa, G., and Herman-Antosiewicz, A. (2012). Sulforaphane, a cruciferous vegetable-derived isothiocyanate, inhibits protein

synthesis in human prostate cancer cells. *Biochim. Biophys. Acta* 1823, 1295–1305. doi: 10.1016/j.bbamcr.2012.05.020

Wu, X., Zhou, Q., and Xu, K. (2009). Are isothiocyanates potential anti-cancer drugs? *Acta Pharmacol. Sin.* 30, 501–512. doi: 10.1038/aps.2009.50

Xiao, H., Kalman, M., Ikehara, K., Zemel, S., Glaser, G., and Cashel, M. (1991). Residual guanosine 3′,5′-bispyrophosphate synthetic activity of relA null mutants can be eliminated by spoT null mutations. *J. Biol. Chem.* 266, 5980–5990.

Xiao, Z., Mi, L., Chung, F.-L., and Veenstra, T. D. (2012). Proteomic analysis of covalent modifications of tubulins by isothiocyanates. *J. Nutr.* 142, 1377S–1381S. doi: 10.3945/jn.111.152041

Conflict of Interest: The authors declare that the research was conducted in the absence of any commercial or financial relationships that could be construed as a potential conflict of interest.

Advantages of publishing in Frontiers

OPEN ACCESS
Articles are free to read for greatest visibility and readership

FAST PUBLICATION
Around 90 days from submission to decision

HIGH QUALITY PEER-REVIEW
Rigorous, collaborative, and constructive peer-review

TRANSPARENT PEER-REVIEW
Editors and reviewers acknowledged by name on published articles

Frontiers
Avenue du Tribunal-Fédéral 34
1005 Lausanne | Switzerland

Visit us: www.frontiersin.org
Contact us: frontiersin.org/about/contact

REPRODUCIBILITY OF RESEARCH
Support open data and methods to enhance research reproducibility

DIGITAL PUBLISHING
Articles designed for optimal readership across devices

FOLLOW US
@frontiersin

IMPACT METRICS
Advanced article metrics track visibility across digital media

EXTENSIVE PROMOTION
Marketing and promotion of impactful research

LOOP RESEARCH NETWORK
Our network increases your article's readership